1071

A DISTRIBUTED SIMULATION MODEL OF A RECONSTRUCTED ANCIENT WATER HARVESTING SYSTEM IN THE NEGEV DESERT

by

MICHAEL DAVID LEE

DEPARTMENT OF GEOGRAPHY
THE LONDON SCHOOL OF ECONOMICS AND POLITICAL SCIENCE
1989

Thesis submitted for the
Degree of Doctor of Philosphy
in the Faculty of Economics
The London School of Economics and Political Science
University of London

UMI Number: U054409

All rights reserved

INFORMATION TO ALL USERS
The quality of this reproduction is dependent upon the quality of the copy submitted.

In the unlikely event that the author did not send a complete manuscript
and there are missing pages, these will be noted. Also, if material had to be removed,
a note will indicate the deletion.



UMI U054409
Published by ProQuest LLC 2014. Copyright in the Dissertation held by the Author.
Microform Edition © ProQuest LLC.
All rights reserved. This work is protected against
unauthorized copying under Title 17, United States Code.



ProQuest LLC
789 East Eisenhower Parkway
P.O. Box 1346
Ann Arbor, MI 48106-1346

THESES
F
6719



X211087903

ABSTRACT

This thesis addresses the problems of evaluating a water harvesting catchment system in the arid environment of the Negev Desert, Israel. A general interpretation of arid hillslope hydrological response is developed called Contiguous Area Contribution. Whilst agreeing with humid area concepts of partial area contribution, it focusses on the different nature of arid slope contributions to stormflow where frequent and rapid overland flow generation intercepts channels by downslope expansion and extension of flow-lines.

The physical system at Avdat is geometrically represented as a flow net of hillslope and channel cascades for kinematic routing. A survey of the micro-morphology and surface materials enables hillslope areas to be classified into six broad units on the basis of their textural characteristics. These units are used to quasi-distribute process data sampled at locations within them. The process of infiltration is discussed and different mathematical models examined using results from a limited number of field measurements with runon/runoff apparatus. The best-fit is provided by the storage model of Green and Ampt and not the Hortonian models of Philip and Kostiakov. Initial infiltration rates vary from 85 to 18 mm hr^{-1} and steady-state rates from 60 to 6 mm hr^{-1}. The inclusion of detention storage in early time period observations is shown to be a significant problem in modelling. For flow routing, an alternative approach to assuming sheetflow is presented using cross-slope microtopographic profiles to provide an estimate of surface geometry for flow across micro-rough surfaces. Measurements of flow velocity for different discharges are made using the runon/runoff apparatus. By assuming sheetflow, a lower value of Manning's n is predicted if velocity and flow dimensions are known. For a given n, the assumption of sheetflow predicts a lower velocity for a given discharge. The values of n derived at Avdat range from 0.18 to 1.36 with a mean of 0.64 when a micro-rough surface is retained, and 0.12 to 0.62 with a mean of 0.36 if sheetflow is assumed, values considerably higher than those usually adopted from channel studies.

A distributed model is developed to handle surface runoff processes at a range of scales from the small plot to the complete catchment. In a detailed sensitivity analysis, the range of physical and process parameters derived for Avdat show sensitivity of the runoff processes to particular parameters and their combination. For the selected range, flow boundary shape is the most significant influence on the shape of flow hydrographs resulting in quicker, higher peaks if a micro-rough flow geometry is assumed. The model is used at the plot scale to examine the problem of including detention storage in infiltration model parameters, at the cascade scale to show the effect of runoff production enhancing and inhibiting slope areas, and at the sub-catchment scale to assess the predictive ability of the model using the limited process parameter data-set. With three sub-catchments, prediction errors were good volumetrically ranging from 6% to 14% for the high intensity, short duration rainstorm, but deteriorated for the long duration, varied intensity storm with predicting high overestimates. Three sub-catchments consistently under-predicted and one over-predicted. In most, the rising and falling limbs were lagged relative to the observed hydrographs.

ACKNOWLEDGEMENTS

This thesis is dedicated to my Mother and Father, Stanley and Joyce Lee, for their constant encouragement, and to Katherine Rowlands for providing her love and support whenever I needed it.

During the course of this thesis I have good reason to thank many people who have played a part in its development and completion. Each is aware of their own contributions. I would especially like to thank the Natural Environmental Research Council for my Post-Graduate Studentship and fieldwork support, and supervisor Helen Scoging (L.S.E.) and fellow graduate Donald Thompson (R.H.B.N.C.) for all the hours of discussion, fieldwork and proof-reading beyond the call of friendship.

At the L.S.E.:

Geography Department Staff - Alison Aspden, Gary Llewellyn, Jane Pugh, Gavin Allen-Wood, Kate Lantzos. Chris Board, Derek Diamond, Pat Farnsworth, Dan Sinclair, Michael Wise, Craig Whitehead and Susan Horsfall.

The Geography Post-Graduates 1982-89.

Computer Service Staff - Rob Clark, Alma Gibbons, P.Page, Pat Crocker, David Dalby, Jeremy Skelton, Rick Barns, Tracey Mead, Andy Mason, D. Vax, and A. Macintosh.

In Israel:

Mrs. Liesel Evenari.

At the Hebrew University of Jerusalem - Dr. Avi Shmida, Orly Havared, and Simcha Finkelman.

At the Sede Boqer Desert Campus, Ben Gurion University of the Negev - Jiftak Ben-Asher, Arie Issar, Joe Gale, Aaron Yair, Shosh Zahroni, Shosh Zilverbush, Moshe Zilverbush, Ullie Esser, Mike Saller, Wendy Weisner and James Aronson.

At Avdat - Harrie Löewenstein and the Volunteers (Ecke Hahn, Hans Dreyer, Jonathan Heinemann, Michael Moore, Dick Nichols, plus those whose surnames I have now forgotten; David, Mathias, Karola, Jurgen, Wolf, Ben, Moppy, Hutsly, Lady, Blackie, and Jackie).

And Friends in Deed:

Joel Witz, Julie Soranson, Charlie Stewart Cox and Nicholas Miles.

Finally I would like to expressly thank Prof. Michael Evenari, of the Desert Farms Unit of the Ben Gurion University and the Hebrew University of Jerusalem, whose help and encouragement was invaluable to my fieldwork. The gratitude extends to all those at Avdat, past and present, who have made the experiment in reconstructed desert agriculture possible. Toda Raba.

A DISTRIBUTED SIMULATION MODEL OF A RECONSTRUCTED ANCIENT WATER HARVESTING SYSTEM IN THE NEGEV DESERT

MICHAEL DAVID LEE

1989

TABLE OF CONTENTS

	Page
TITLE PAGE	1
ABSTRACT	2
ACKNOWLEDGEMENTS	3
TABLE OF CONTENTS	4
LIST OF FIGURES	12
LIST OF TABLES	15
LIST OF PLATES	18
LIST OF APPENDICES	21
LIST OF SYMBOLS	24
CHAPTER ONE WATER HARVESTING : CONCEPTS AND CONTEXT	29
1.1 INTRODUCTION TO THE THESIS	29
1.1.1 The Hydrological Context	29
1.1.2 Aims and Objectives	30
1.2 WATER HARVESTING AND RUNOFF FARMING	31
1.3 HILLSLOPE HYDROLOGICAL THEORY	34
1.3.1 Runoff Generation and Water Harvesting	34
1.3.2 General Theories on the Pattern of Storm-water Generation	35
1.3.2.a Hortonian Overland Flow	36
1.3.2.b Partial Area Contribution	36
1.3.3 Arid Lands Patterns of Storm-water Generation	38
1.3.3.a Partial Area Contribution and Hortonian Rainfall Excess	38
1.3.3.b A Re-Definition : Contiguous Area Contribution	41
1.4 THE CENTRAL NEGEV HIGHLANDS AND THE AVDAT CATCHMENT	42
1.4.1 Geomorphology and Geology	42
1.4.2 Process Characteristics	43
1.5 THE NEGEV HYDROLOGICAL DEBATE	45
1.5.1 The Role of Loessial Slopes	45
1.5.2 The Role of Rocky Slopes	47
1.5.3 The Negev Runoff Generation Debate and its Significance for Water Harvesting	49

Page

1.5.4 Reconciling the Shanan and Yair Interpretations of Negev Hydrology and Water Harvesting 52
1.5.5 Contiguous Area Contribution and Avdat Water Harvesting 56
1.6 THE DISTRIBUTED MODELLING APPROACH 57
1.6.1 Features of Distributed Models 58
1.6.2 Existing Hydrological Models of Negev Catchment Systems 60
1.6.2.a Shanan's Avdat Runoff Model 60
1.6.2.b The Karnielli *et al* Statistical Approach 61
1.6.2.c The Lavee Theoretical Model 61
1.6.3 The Distributed Approach and the Avdat Catchment 64

CHAPTER TWO REPRESENTING THE PHYSICAL SYSTEM 66

2.1 THE METHODOLOGY 66
2.2 MACRO-MORPHOLOGY - CATCHMENT GEOMETRIC SIMPLIFICATION 67
2.2.1 Flow-line Simplification 67
2.2.2 Some Examples of Surface Discretisation 68
2.2.3 The Method of Discretisation Used for the Avdat Catchment 69
2.2.4 Surveying the Hillslope and Channel Network 69
2.2.5 Processing of the Catchment Topographic Survey Data 70
2.2.5.a Converting the Survey Data to Cartesian Coordinates 70
2.2.5.b Contour Map Production 71
2.2.6.c Flow-net Discretisation 71
2.3 MICRO-MORPHOLOGY - SURFACE CHARACTERISTICS 72
2.3.1 Field Unit Classification 72
2.3.1.a Unit One Slopes 73
2.3.1.b Unit Two Slopes 73
2.3.1.c Unit Three Slopes 74
2.3.1.d Unit Four Slopes 74
2.3.1.e Unit Five Slopes 75
2.3.1.f Unit Six Slopes 76
2.3.2 Quantifying Micro-Morphology 76
2.3.2.a The Sampling Scheme 76
2.3.2.b Theoretical and Practical Significance 77

Page

2.3.3 Surface Material Characteristics 78
2.3.3.a Classifying Surface Materials 78
2.3.3.b Sampling Surface Materials 79
2.3.3.c Processing Surface Material Data 79
2.3.4 Surface Microtopography and Flow-Boundary Dimensions 80
2.3.4.a Sources and Significance of Micro-Topographic Variation 80
2.3.4.b Quantifying Micro-Topography 80
2.3.4.c Processing Hillslope Micro-Topographic Measurements 83
2.3.5 Channel Geometry 88
2.3.6 Testing the Representative Nature of Field Units for Data Distribution 89
2.3.6.a Analysis of Variance Tests and Hypotheses 90
2.3.6.b ANOVA of the Six Major Unit Groups - The Complete Catchment 92
2.3.6.c ANOVA of the Eastern Slopes Unit Groups 93
2.3.6.d ANOVA of the Western Slopes Unit Groups 95
2.3.6.e ANOVA of Unit Groups Across the East-West Division 96
2.3.6.f Conclusions from the ANOVA 97

CHAPTER THREE INFILTRATION 100

3.1 INTRODUCTION TO THE PROCESS 100
3.2 INFILTRATION THEORY 101
3.2.1 The Nature of Infiltration 101
3.2.2 Factors Controlling Infiltration 101
3.2.3 Conceptual Approaches to Infiltration and Runoff Generation 102
3.2.3.a The Hortonian Approach 102
3.2.3.b The Saturation Approach 103
3.2.3.c The Leaky Bottle Approach 103
3.2.4 Infiltration in Arid Environments 104
3.2.4.a Infiltration and Runoff Mechanisms 104
3.2.4.b Factors Affecting the Spatial Patterns of Infiltration and Runoff 106
3.3 MODELLING INFILTRATION 109
3.3.1 The Objectives of an Infiltration Model 109
3.3.2 Models and Their Characteristics 111
3.3.2.a The Hortonian Models 111
3.3.2.b The Non-Hortonian Models 114

Page

3.3.3 Times to Ponding with Hortonian and Storage Models 116
3.3.3.a The Green and Ampt Storage Equation 116
3.3.3.b The Hortonian Equations of Kostiakov and Philip 118
3.3.4 Using Different Models with Temporally Variable Inputs 119
3.3.4.a Time-Variable Input and the Infiltration Model Assumptions 119
3.3.4.b Timing of Ponding and the Infiltration Model Assumptions 120
3.4 FITTING AND TESTING INFILTRATION MODELS 123
3.4.1 Selecting Infiltration Data 123
3.4.2 Model Selection and Fitting 123
3.4.3 The Avdat Field Data 125
3.4.3.a Measuring Infiltration 125
3.4.3.b The Crusting Mechanism 127
3.4.3.c The Flow Method and Initial Infiltration Rates 129
3.4.3.d The Surface Materials and Micro-Topography 130
3.4.3.e The Avdat Data Sets 131
3.4.3.f Results of Model Fitting to the Avdat Data 136
3.4.4 Infiltration Data in the Literature 138
3.4.4.a Literature Sources 138
3.4.4.b Selecting Data-Sets for Direct Comparison with Avdat Field Data 142
3.4.4.c Statistical Analysis 143
3.4.5 Comparisons Between the Avdat Data-Sets and the Literature Data 147

CHAPTER FOUR FLOW ROUTING 152

4.1 INTRODUCTION TO THE FLOW ROUTING PROBLEM 152
4.2 THE EQUATIONS DESCRIBING FLOW MOVEMENT 154
4.2.1 Uniform Flow and the Kinematic Wave Theory 154
4.2.1.a The Kinematic Wave 156
4.2.1.b The Kinematic Cascade 157
4.2.2 Finite Difference Solutions to the Flow Equations 157
4.2.2.a Channel Section Finite Difference Solution 159
4.2.2.b Hillslope Element Finite Difference Solution 161
4.2.2.c Initial and Boundary Conditions 161
4.2.2.d Solution Stability and Accuracy 162

Page

4.3 THE UNIFORM FLOW EQUATION 164
4.3.1 Slope Gradient 165
4.3.1.a Hillslope System Geometry 165
4.3.1.b Specifying Slope Gradients 165
4.3.1.c Hillslope Element Slopes 166
4.3.1.d Channel Element Slopes 167
4.3.2 Flow Dimensions 167
4.3.2.a Channel Flow 167
4.3.2.b Hillslope Flow 170
4.3.3 Flow Resistance 173
4.3.3.a Resistance Theory 173
4.3.3.b Empirical Methods of Defining Mannings n Coefficient 176
4.3.3.c Field Studies of Overland Flow from the Literature 176
4.3.3.d Flow Experiments at Avdat and the Calculation of Resistance 188
4.3.3.e Comparisons Between the Avdat Field Data and the Literature Data 195

CHAPTER FIVE RAINFALL-RUNOFF MODELLING 204

5.1 THE SIMULATIONS AND THEIR OBJECTIVES 204
5.2 THE DISTRIBUTED MODEL 205
5.2.1 The Overall Model Structure 205
5.2.1.a The Model Subroutines 205
5.2.1.b Parameterisation 207
5.2.2 Boundary Conditions 210
5.2.3 Hillslope and Channel Flow Routing 211
5.2.3.a The Approach to Infiltration 211
5.2.3.b The Procedures for Calculating Time to Ponding 211
5.2.3.c Calculating Post-Ponding Infiltration 212
5.2.3.d Net-Storage Change 213
5.2.3.e Discharge Calculations 214
5.2.4 Cumulative Calculations, Stability and Output of Predictions 214
5.2.4.a Avoiding Numerical Instability and Error Calculation 214
5.2.4.b Calculating Predicted Hydrological Response 216
5.2.4.c Calculating Indices of Productivity and Harvesting Efficiency 216
5.2.4.d Hydrograph Output 217

Page

5.3 APPLYING THE MODEL USING A STRUCTURED APPROACH 217

5.3.1 Sensitivity Tests and Hypothetical Simulations 218

5.3.1.a Local Slope Gradient 220

5.3.1.b Slope Resistance Coefficient (Mannings n) 220

5.3.1.c Flow Boundary Shape 221

5.3.1.d Infiltration Regime 221

5.3.1.e Rainfall Intensity/Distribution 222

5.3.1.f Spatial Arrangement 224

5.3.1.g Slope Scale 225

5.3.2 Methods of Results Analysis 225

5.3.3 The Single Plot Cascade Simulations 226

5.3.3.a Parameter Values and Their Hydrological Significance 226

5.3.3.b The Suite of Single Plot Simulations 227

5.3.4 Multiple Cell Cascade Simulations 243

5.3.4.a The Purpose of the Multiple Plot Arrangements 243

5.3.4.b The Parameter Combinations and Their Hydrological Significance 243

5.3.4.c The Effects of Scale 250

5.3.5 Conclusions from the Sensitivity Analysis 255

CHAPTER SIX TESTING THE SIMULATION MODEL 257

6.1 RUN-ON/RUNOFF PLOT SIMULATIONS 257

6.1.1 Purpose of the Plot Simulations 257

6.1.2 Run-on/Runoff Plot Test Conditions and Sources of Error 258

6.1.3 Plot Conditions and the Rainfall-Runoff Process 259

6.1.3.a Times to Run-Out (t_{RO}) 260

6.1.3.b The First Observed Time Increment Volumetric Discharge (Q1) 260

6.1.3.c Intermediate Time Increment Cumulative Discharge (Q3) 260

6.1.3.d Final Observed Time Increment Cumulative Discharge (ΣQ) 261

6.1.4 Initial Simulations 261

6.1.4.a Times to Run-out (t_{RO}) 262

6.1.4.b Discharge Predictions 263

6.1.4.c Interpretation and Evaluation 264

6.1.5 Secondary Simulations Using Modified Plot Parameters 265

6.1.5.a Rationale 265

6.1.5.b Times to Run-out (t_{RO}) 267

6.1.5.c Discharge Predictions 267

6.1.5.d Interpretation and Evaluation 271

Page

6.1.6 Summary and Conclusions 272

6.2 ACTUAL HILLSLOPE CASCADES 273

6.2.1 The Hillslope Cascade 273

6.2.2 Methods of Results Analysis 274

6.2.3 The Simulation Results 277

6.2.3.a Data Output and its Use 277

6.2.3.b The Unaltered Cascade Productivity 280

6.2.3.c The Current Channel Configuration Productivity 283

6.2.3.d Assessing the Efficacy of the Plot Parameters 285

6.3 AVDAT SUB-CATCHMENTS 287

6.3.1 Purpose of the Simulations 287

6.3.2 Predictions and their Significance 288

6.3.3 Method of Results Assessment 289

6.3.4 The Simulation Results and Their Interpretations 290

6.3.4.a Overall Variations in Model Predictions 290

6.3.4.b The Sub-Catchment Groups 292

6.3.4.c Results from Rainstorm 02/03/74 292

6.3.4.d Results from Rainstorm 10/02/74 299

6.3.4.e Significance of the Results and Overall Conclusions 307

6.4 Use of the Model in Applied Studies - Design Evaluation and Management Aspects 311

6.4.1 Using the Cascades to Assess Alternative Channel Configurations 311

6.4.1.a Determining Optimum Channel Configurations 311

6.4.1.b Channel Position, Density and Productivity Relationships 312

6.4.1.c A More Practical Procedure for Channel Siting 313

6.4.1.d Overall Conclusions on the Applied Use of Cascade Simulations 315

6.4.2 The Avdat Water Harvesting System - A Design Evaluation 316

6.4.2.a Channel Siting and Contiguous Area Contribution 316

6.4.2.b Improvements of the Ancient System 318

6.4.3 The Model and Water Harvesting System Design 321

CHAPTER SEVEN SUMMARY AND CONCLUSIONS 322

7.1 SIMULATION RESULTS AND SENSITIVITY 322

7.1.1 Sensitivity to Process Parameters 322

7.1.2 The Importance of the Hillslope Hydrological Context 323

7.1.3 Lessons for Parameter Specification 324

Page

7.2 THE MODEL AS A DESIGN TOOL 324
7.2.1 The Successful Techniques of Routing Modification 325
7.2.2 Evaluating the Ancient Hydro-Engineering Skills 325
7.3 PROBLEMS OF ARID ENVIRONMENT ANALYSIS 326
7.3.1 Rainfall Intensity Variations and their Implications for Infiltration Models 326
7.3.2 Infiltration Parameter Errors and Bias 327
7.3.3 Problems of Measuring Infiltration and Runoff in the Field 328
7.3.4 Weak Links in the Data-Modelling Procedure Chain 328
7.3.5 Strengthening the Routing Link 329
7.4 ARID LANDS HYDROLOGY AND THE NEGEV DEBATE 329
7.4.1 Hortonian Runoff Conditions as a Special Case 330
7.4.2 Resolving the Debate on Key Runoff Producers in the Negev 330
7.4.3 A Storage Model of Infiltration 331
7.5 PROCESS DYNAMICS AND MODELLING PROCEDURES 331
7.5.1 Considering the Complex Nature of Overland Flow Routing at the Intra-Hillslope Scale 331
7.5.2 Orders of Magnitude of Manning's n Coefficient 332

REFERENCES 334
PLATES 343
APPENDICES 362

LIST OF FIGURES

		Page
Chapter One		
1.1.	A Location Map of the Study Area	32
Chapter Two		
2.1	Scoging's Micro-Topographic Dimensions (1985, 1988)	81
2.2	Downslope Micro-Topographic Profile Measurement	82
2.3	Cross-slope Micro-Topographic Profile Measurement	83
2.4	Example of Downslope Micro-Topographic, Rod- and Best-fit Profiles (single profile from sample 23, Unit 3e)	84
2.5	Example of Crosslope Micro-Topographic, Rod- and Best-fit Profiles (single profile from sample 23, Unit 3e adjusted to mean y of zero)	85
2.6	Different Channel Sections Used in the Avdat Model and Their Dimensions	89
2.7	ANOVA Results for the Six Major Unit Groups	93
2.8	ANOVA Results for the Eastern Slopes Unit Groups	94
2.9	ANOVA Results of the Western Slopes Unit Groups	95
2.10	ANOVA Results of the East-West Division of Unit Groups	96
Chapter Three		
3.1	Four Rainfall Conditions Important for Infiltration Models	110
3.2	Rainfall Intensity Distribution and Runoff Predictions for Different Infiltration Models	121
3.3	The Run-on/Run-off Infiltration Apparatus	126
3.4	Plotting Calculated Infiltration Rates	132
3.5	Infiltration Data from the Avdat Run-on/Runoff Plots	134
3.6	Plot Locations on Profile Two	135
3.7	Infiltration Data from the Literature	145
Chapter Four		
4.1	Backward Finite Difference Solution Space-Time Framework	158
4.2	Channel Flow Section	159
4.3	Geometry of a Trapezoidal Channel and Overflow	168
4.4	The Composite Flow Dimensions (vertical scale exaggerated)	172
4.5	Channel Stage-Recorder Apparatus	193

Page

Chapter Five

5.1	WATERH Structural Flow Diagram	206
5.2	WATERH Networking System and Notation	209
5.3	Rainfall Hyetograph for Sensitivity Simulations - High/Short	223
5.4	Rainfall Hyetograph for Sensitivity Simulations - Medium/Long	223
5.5	Rainfall Hyetograph for Sensitivity Simulations - Decreasing	224
5.6	Rainfall Hyetograph for Sensitivity Simulations - Increasing	224
5.7	Sensitivity to Varying Routing Parameters on Micro-Smooth Hillslopes	230
5.8	Sensitivity to Varying Routing Parameters on Micro-Rough Hillslopes	231
5.9	Comparisons of Sensitivity to Varying Routing Parameters on Micro-Smooth and Micro-Rough Hillslopes	232
5.10	Sensitivity to Varying Infiltration Parameters for Different Routing Parameter Combinations on Micro-Smooth Hillslopes	235
5.11	Sensitivity to Varying Infiltration Parameters for Different Routing Parameter Combinations on Micro-Rough Hillslopes	236
5.12	Comparisons of Sensitivity to Varying Infiltration Parameters on Micro-Smooth and Micro-Rough Hillslopes	237
5.13	Sensitivity to Varying Rainfall Intensity Distributions on Impermeable Micro-Smooth and Micro-Rough Hillslopes	240
5.14	Sensitivity to Varying Rainfall Intensity Distributions on Infiltrating Micro-Smooth and Micro-Rough Hillslopes	241
5.15	The Effect of Plot Position on the Hydrological Response from Micro-Smooth Hillslopes	246
5.16	The Effect of Plot Position on the Hydrological Response from Micro-Rough Hillslopes	247
5.17	The Hydrological Response from a Micro-Smooth Hillslope with Different Rainfall Intensity Distributions	252
5.18	The Hydrological Response from a Micro-Rough Hillslope with Different Rainfall Intensity Distributions	253

Page

Chapter Six

6.1	Hyetograph for Rainstorm 02/03/74	276
6.2	Hyetograph for Rainstorm 10/02/74	276
6.3	Observed and Predicted Hydrographs for Sub-Catchment Three (Rainstorm 02/03/74)	294
6.4	Observed and Predicted Hydrographs for Sub-Catchment Four (Rainstorm 02/03/74)	294
6.5	Observed and Predicted Hydrographs for Sub-Catchment Five (Rainstorm 02/03/74)	295
6.6	Observed and Predicted Hydrographs for Sub-Catchment Six (Rainstorm 02/03/74)	295
6.7	Observed and Predicted Hydrographs for Sub-Catchment One (Rainstorm 02/03/74)	296
6.8	Observed and Predicted Hydrographs for Sub-Catchment Two (Rainstorm 02/03/74)	296
6.9	Observed and Predicted Hydrographs for Sub-Catchment Seven (Rainstorm 02/03/74)	297
6.10	Observed and Predicted Hydrographs for Sub-Catchment Three (Rainstorm 10/02/74)	301
6.11	Observed and Predicted Hydrographs for Sub-Catchment Four (Rainstorm 10/02/74)	301
6.12	Observed and Predicted Hydrographs for Sub-Catchment Five (Rainstorm 10/02/74)	302
6.13	Observed and Predicted Hydrographs for Sub-Catchment Six (Rainstorm 10/02/74)	302
6.14	Observed and Predicted Hydrographs for Sub-Catchment One (Rainstorm 10/02/74)	303
6.15	Observed and Predicted Hydrographs for Sub-Catchment Two (Rainstorm 10/02/74)	303
6.16	Observed and Predicted Hydrographs for Sub-Catchment Seven (Rainstorm 10/02/74)	304

LIST OF TABLES

		Page
Chapter One		
1.1	Percentage Annual Runoff on Shanan's Plots	46
1.2	Mean Rainfall Threshold Depth Before Runoff (mm)	46
1.3	Mean Rainy Season Infiltration Rates (mm hr^{-1})	46
1.4	Frequency and Magnitude of Runoff Events at Sede Boqer 1975/76 - 1978/79	48
1.5	Infiltration Rates on Yair's Compartmented Hillslope (mm hr^{-1})	48
1.6	Runoff Yield in Litres Predicted by the Yair and Lavee Simulation Model (Yair and Lavee, 1985)	62
1.7	Runoff Yield in Litres (and mm) per Square Metre of Surface Area Predicted by the Yair and Lavee Simulation Model (Yair and Lavee, 1985)	63
Chapter Two		
2.1	The B.S. 1677 Size Classification Index	79
Chapter Three		
3.1	Best-fit Statistics for Infiltration Models Applied to the Avdat Run-on/Runoff Plots	137
3.2	Predicted Time to Ponding and Depth to Ponding (t_o and V_s) for Different Constant or Mean Rainfall Intensities for the Avdat Run-on/Runoff Plots	139
3.3	Predicted Infiltration Rates at Different Elapsed Times for the Avdat Run-on/Runoff Plots	140
3.4	Raw-Data Infiltration Rates Derived from the Literature	144
3.5	Best-fit Statistics for Infiltration Models Applied to Literature Data	146
3.6	Predicted Time to Ponding and Depth to Ponding (t_o and V_s) for Different Constant or Mean Rainfall Intensities for the Literature Data	148
3.7	Predicted Infiltration Rates at Different Elapsed Times for the Literature Data	149
Chapter Four		
4.1	Roels' Manning's n Values (Roels, 1984)	180
4.2	Emmett's Manning's n Values (Emmett, 1970)	183
4.3	Adjusted Flow Mean Velocities for Plot 23 (3e)	189
4.4	Hillslope Flow Geometry for Plot 23 (3e)	190
4.5	Calculated Manning's n for the Two Flow Assumptions for Plot 23 (3e)	190
4.6	Avdat Hillslope Manning's n	191
4.7	Adjusted Flow Mean Velocities For Stage-Recorder 11	194
4.8	Geometric Characteristics at the Measured Depths for Stage Recorder 11	194
4.9	Calculated Manning's n Values for Observed Stages at Stage Recorder 11	194
4.10	Avdat Channel Manning's n	196

Page

4.11 Summary of Relevant Manning's n Values from the Literature and Field 197
4.12 Emmett's Manning's n (where $q \leq 0.336$ cm^3 s^{-1} for direct comparison with Avdat data) 198
4.13 Roel's Manning's n (where $q \leq 0.336$ cm^3 s^{-1} for direct comparison with Avdat data) 198
4.14 Limerinos' Manning's n Data Set for Gravel Bedded Rivers (1970) 200
4.15 Avdat Channel Manning's n (where $Q \leq 745$ cm^3 s^{-1} for direct comparison with Roels' rilled plots) 202

Chapter Five

5.1 Slope Gradient Sensitivity Parameters 220
5.2 Manning's n Sensitivity Parameters 220
5.3 Flow Boundary Shape Sensitivity Parameters (units of cm) 221
5.4 Infiltration Regime Sensitivity Parameters (units of cm s^{-1}) 221
5.5 Summary Table of Parameters and their Codes 227
5.6 Sensitivity Results for Varying Routing Parameters on Micro-Smooth and Micro-Rough Hillslopes 229
5.7 Sensitivity Results for Varying Routing and Infiltration Parameters on Micro-Smooth and Micro-Rough Hillslopes 234
5.8 Sensitivity Results for Varying Rainfall Intensity Distributions and Infiltration Parameters on Micro-Smooth and Micro-Rough Hillslopes 239
5.9 Parameter Combinations for Simulations of Multiple Plot Cascades 244
5.10 Sensitivity Results for Varying Rainfall Intensity Distributions on Micro-Smooth and Micro-Rough Hillslopes with Different Spatial Distributions of Infiltration and Routing Parameters 245
5.11 Sensitivity Results for Varying Rainfall Intensity Distributions on Micro-Smooth and Micro-Rough Surfaces of Different Length but with Constant Infiltration and Routing Parameters 251

Chapter Six

6.1 Predicted Times to Run-Off and Run-Out (A, B1) 262
6.2 Predicted Summary Discharge Values (A, B1) 263
6.3 Percentage Errors for Predicted Summary Discharge Values (A, B1) 263
6.4 Original and Modified Infiltration Parameters 266
6.5 Predicted Times to Run-Off and Run-Out (A, B2) 267
6.6 Predicted Summary Discharge Values (A, B2) 267
6.7 Percentage Errors for Predicted Summary Discharge Values (A, B2) 268
6.8 Cascade Contributing Area for Different Channels 274

		Page
6.9	Plot and Unit Identification for Each Cascade Element	274
6.10	Matrix of Cascade Productivity (cubic metres) for Rainstorm 02/03/74	278
6.11	Matrix of Cascade Productivity (cubic metres) for Rainstorm 10/02/74	279
6.12	Productivity from an Unaltered Cascade	280
6.13	Cascade Productivity and Per Unit Area Productivity Values for Rainstorm 02/03/74	281
6.14	Cascade Productivity and Per Unit Area Productivity Values for Rainstorm 10/02/74	282
6.15	Predicted Discharges (m^3) into the Existing Man-Made Channel Configuration (02/03/74) Selected from 6.10	283
6.16	Predicted Discharges (m^3) into the Existing Man-Made Channel Configuration (10/02/74) Selected from 6.11	284
6.17	Sub-catchment Dimensions and Unit Type Surface Areas	291
6.18	Catchment Observed and Predicted Runoff for Rainstorm 02/03/74	292
6.19	Catchment Observed and Predicted Runoff for Rainstorm 10/02/74	299
6.20	Errors in Predictions in Depth Terms	309
6.21	Maximum Productivity Channel Configurations	312
6.22	Productivity Using Configurations Determined From Single Cascade	314
6.23	Comparative Characteristics of the Current and Unaltered Catchments	319
6.24	Comparative Productivity of the Current and Unaltered Catchments	319

LIST OF PLATES

Page

C. Plates Showing Views of the Avdat Catchment and its Geomorphological Character

C.1 Aerial photograph of the Avdat Runoff Farm and catchment system. Note terraced fields and man-made drainage channels (see Appendix 3.1) 343

C.2 Oblique view of the northern and southern knolls that form the eastern slope sections of the study catchment. Note the four man-made ditches routing water away from the midslopes and avoiding passage across and into the natural wadi channel network. Note the stage recorders at the inlet to the farm upper terrace 344

C.3 Oblique view from the southern knoll northwards along the line of the man-made ditches collecting from the eastern slope sections 345

A. Plates Showing Hydro-meteorological Instrumentation Used in the Avdat Catchment

A.1 Stage recorder and weir apparatus at one of the seven inlets from the sub-catchments into the farm upper level terraces. Note stilling inlet at base of stand and recording arm marking revolving chart 346

A.2 Large-orifice recording raingauge (B on terrace). Note the revolving chart on which the rising level in the gauge reservoir is marked calibrated to mm rainfall equivalent 346

F. Plates Showing Channel Flow and Terrace Flooding at Avdat 1983-1985

F.1 An upstream view of concentrated rivulet flow discharging from the eastern hillslope unit 3 section into the lower ditch of sub-catchment four 347

F.2 An upstream view of the man-made channel of sub-catchment 6 experiencing rapid flow across the steeply graded bedrock bed 347

F.3 The mid-section of ditch 6 collecting from the unit 4 sections of the eastern hillslope. Note rapid flow past Stage Recorder 11. Note marker in foreground indicating 5 metre distance 348

F.4 The bottom section of the lower ditch of sub-catchment 4 looking downstream to the farm terraces. Contrast the nature of flow with the conditions in the wadi channels at a similar distance upstream 348

F.5 Flow at the confluence of two branches upstream of Stage recorder 14. Bankfull discharge is derived from remote rather than adjacent slopes 349

F.6 Bankfull discharge flowing across the break in slope from the palaeo-terrace into the wadi-bed drainage system. Note extensive channel vegetation and consequent flow dissipation 349

F.7 Discharge along the man-made ditch collecting water from the natural channel flowing down from the terrace area of sub-catchment 2. See Plate F.8 to see its dissipation onto the wadi-bed above the farm 350

F.8 An upstream view back to the previous location showing the ponding and infiltration of outflow onto the wadi before the inlet to the upper terrace. Note vegetation density at exit of man-made ditch 350

F.9 View from the peak of the northern knoll looking north-west to the farm 351

F.10 The flooded terrace supplied by sub-catchment 7. The ancient city of Avdat overlooks from the plateau. 351

I. Plates Showing the Methodology of the Run-on/Runoff Infiltration Plot Tests

I.1 View of infiltration plot - note spreader tube and catching trough 352

I.2 View of wetted area spreading across slope towards trough 352

I.3 Close-up view of wetted plot - note water flowing out tube 352

I.4 View of complete experimental set-up of run-on/runoff infiltration plot. Note constant head device and extent of wetted area from tube to trough 352

P. Photo-Transect Across Sample Profile 2 (Plots 17-48 from the complete set 1-127)

P.17 Profile 2 Sample 1 Unit 1e 353

P.18 Profile 2 Sample 2 Unit 1e (Run-on/Runoff Plot 18/1e) 353

P.19 Profile 2 Sample 3 Unit 2e 353

P.20 Profile 2 Sample 4 Unit 2e (Run-on/Runoff Plot 20/2e) 353

P.21 Profile 2 Sample 5 Unit 2e 354

P.22 Profile 2 Sample 6 Unit 3e 354

P.23 Profile 2 Sample 7 Unit 3e (Run-on/Runoff Plot 23/3e) 354

P.24 Profile 2 Sample 8 Unit 4e 354

P.25 Profile 2 Sample 9 Unit 4e (Run-on/Runoff Plot 25/4e upper) 355

P.26 Profile 2 Sample 10 Unit 4e 355

P.27 Profile 2 Sample 11 Unit 4e 355

P.28 Profile 2 Sample 12 Unit 4e (Run-on/Runoff Plot 28/4e lower) 355

P.29 Profile 2 Sample 13 Unit 4e 356

P.30	Profile 2 Sample 14 Unit 5e	356
P.31	Profile 2 Sample 15 Unit 5e	356
P.32	Profile 2 Sample 16 Unit 5e (Run-on/Runoff Plot 32/5e)	356
P.33	Profile 2 Sample 17 Unit 5w	357
P.34	Profile 2 Sample 18 Unit 5w (Run-on/Runoff Plot 34/5w lower)	357
P.35	Profile 2 Sample 19 Unit 4w	357
P.36	Profile 2 Sample 20 Unit 4w (Run-on/Runoff Plot 36/4w)	357
P.37	Profile 2 Sample 21 Unit 3w	358
P.38	Profile 2 Sample 22 Unit 3w (Run-on/Runoff Plot 38/3w)	358
P.39	Profile 2 Sample 23 Unit 6w	358
P.40	Profile 2 Sample 24 Unit 6w	358
P.41	Profile 2 Sample 25 Unit 6w	359
P.42	Profile 2 Sample 26 Unit 6w (Run-on/Runoff Plot 42/6w)	359
P.43	Profile 2 Sample 27 Unit 6w	359
P.44	Profile 2 Sample 28 Unit 6w	359
P.45	Profile 2 Sample 29 Unit 4w	360
P.46	Profile 2 Sample 30 Unit 4w	360
P.47	Profile 2 Sample 31 Unit 5w (Run-on/Runoff Plot 47/5w upper)	360
P.48	Profile 2 Sample 32 Unit 5w	360

L. Plates Showing Variations in Loessial Crust Surfaces in the Avdat Catchment

L.1	Loessial crust surface on western terrace unit 5w	361
L.2	Loessial crust surface on wadi alluvium at foot of eastern hillslope profile unit 5e	361
L.3	Loessial crust following disturbance by grazing herd	361
L.4	Loessial crust following disturbance by porcupines. Note aggregate formation and depression storage excavation	361

LIST OF APPENDICES

Page

Appendix 1 Avdat Catchment Characteristics and Plot Sampling Scheme

1.1 An Annotated Aerial Photograph Showing the Locations of Sample Flow-Line Profiles and Sample Locations 362

1.2 The Sample Flow-Line Profiles in Cross-Section 363

1.3 Plot Sample Groupings by Overall Catchment Unit, and by Sub-Divided Unit 365

1.4 A Simplified Example of the Methodology of Flow-line Construction and Catchment Discretisation 366

Appendix 2 Plot Sample Data

2.1 Selected Micro-Topographic and Surface Material Characteristics for Each Sample Plot

2.1.1 Selected Surface Material Characteristics for Each Sample Plot 371

2.1.2 Micro-topographic Standard Deviations from the Best-Fit Line for Each Sample Plot (Cross-slope and Downslope) 372

2.1.3 Complex Flow Geometry Regression Results for Each Sample Plot 377

2.2 The Results Matrices from the ANOVA of Micro-Topographic and Surface Material Characteristics for the Different Unit Groupings of Sample Plots 378

2.3 Run-on/Runoff Plot Infiltration Data Sets 381

2.4 Rainfall Recurrence Interval Data Sets 387

Appendix 3 Flow-Net Parameterisation

3.1 Base-map: Avdat Catchment Contour Map
Overlay; Sub-Catchment Divides 388

3.2 Base-map: Catchment Discretisation - Complete Catchment System With Man-Made and Natural Channels
Overlay: Surface Parameter Distribution - Distribution of Surface Conditions Using Sample Sites 1-127 389

3.3 Base-map: Catchment Discretisation - Hypothetical Unaltered Catchment System With Only Natural Channels
Overlay: Surface Parameter Distribution - Distribution of Surface Conditions Using Sample Sites 1-127 390

3.4 Sub-Catchment Geometric and Process Relationship Paramater Sets

3.4.1 Sub-Catchment One Discretised Flow-Net Structure and Channel Data 391

3.4.2 Sub-Catchment One Digitised Coordinate Pairs for Flow Net Elements and Segments 394

Page

3.4.3 Sub-Catchment Two Discretised Flow-Net Structure and Channel Data 398
3.4.4 Sub-Catchment Two Digitised Coordinate Pairs for Flow Net Elements and Segments 400
3.4.5 Sub-Catchment Three Discretised Flow-Net Structure and Channel Data 402
3.4.6 Sub-Catchment Three Digitised Coordinate Pairs for Flow Net Elements and Segments 407
3.4.7 Sub-Catchment Four Discretised Flow-Net Structure and Channel Data 412
3.4.8 Sub-Catchment Four Digitised Coordinate Pairs for Flow Net Elements and Segments 415
3.4.9 Sub-Catchment Five Discretised Flow-Net Structure and Channel Data 419
3.4.10 Sub-Catchment Five Digitised Coordinate Pairs for Flow Net Elements and Segments 421
3.4.11 Sub-Catchment Six Discretised Flow-Net Structure and Channel Data 422
3.4.12 Sub-Catchment Six Digitised Coordinate Pairs for Flow Net Elements and Segments 425
3.4.13 Sub-Catchment Seven Discretised Flow-Net Structure and Channel Data 434
3.4.14 Sub-Catchment Seven Digitised Coordinate Pairs for Flow Net Elements and Segments 436

Appendix 4 The Model Program Notation

4.1 Simulation Model WATERH Program Code 439
4.2 Modified Run-on/Runoff Plot Simulation Model RORO Program Code 475
4.3 Unit and Sample Data Set Used by Model Simulations for Parameter Provision 480

Appendix 5 Model Results

5.1 Results From the Run-on/Runoff Plot Simulations
5.1.1 Results from Plot 18 Unit 1e 481
5.1.2 Results from Plot 20 Unit 2e 485
5.1.3 Results from Plot 23 Unit 3e 489
5.1.4 Results from Plot 25 Unit 4e upper 493
5.1.5 Results from Plot 28 Unit 4e lower 497
5.1.6 Results from Plot 32 Unit 5e 501
5.1.7 Results from Plot 34 Unit 5w lower 505
5.1.8 Results from Plot 36 Unit 4w 509
5.1.9 Results from Plot 38 Unit 3w 513

Page

5.1.10 Results from Plot 42 Unit 6w 517

5.1.11 Results from Plot 47 Unit 5w upper 521

5.2 Model Element and Segment Polygon Framework Used in Choropleth Generation

5.2.1 Current Avdat Flow-Net With Man-Made Channel System 525

5.2.2 Avdat Flow-Net Without Man-Made Channel System 526

5.3 Unit Boundaries for Parameter Provision to Elements and Segments

5.3.1 Current Avdat Catchment With Man-Made Channel System : Unit Distribution 527

5.3.2 Avdat Catchment With Natural Channel System : Unit Distribution 528

5.4 Avdat Runoff Efficiency With Man-Made Channel System (02/03/74) 529

5.5 Avdat Runoff Efficiency With Unaltered Channel System (02/03/74) 530

5.6 Avdat Runoff Efficiency With Man-Made Channel System (10/02/74) 531

5.7 Avdat Runoff Efficiency With Unaltered Channel System (10/02/74) 532

LIST OF SYMBOLS

A	infiltration equation empirical parameter
a	regression equation coefficient
A'	Philip equation transmissivity constant
A(x,t)	flow area
A,A1	infiltration equation empirical parameter
A^	scaled flow-area for substitution into WP-A regression equation derived
Aa	long-axis of particle
AD	infiltration equation empirical parameter applicable to dry conditions
Amax	the maximum normal channel cross-sectional area (bank-full)
Ap	steady-state and/or peak flow cross-sectional area
A_t	instantaneous flow area
AW	infiltration equation empirical parameter applicable to wet conditions
A*	Bork and Rohdenburg equation final infiltration rate
B	infiltration equation empirical parameter
b	regression equation coefficient
B2	modified infiltration empirical parameter
Ba	median-axis of particle
BD	infiltration equation empirical parameter applicable to dry conditions
BW	infiltration equation empirical parameter applicable to wet conditions
Bw	channel bed-width
Ca	short-axis of particle
d	the added depth of water onto Δx resulting from run-on
$d_{\%}$	particle size percentile used in Limerinos equation
d_{50}	Strickler's intermediate bed material particle size of gravel-bed rivers
Di	initial soil moisture deficit
E	left side channel bank-angle
e	the base of natural logarithms 2.718
F	volume of infiltration at time t
f	the Darcy-Weisbach friction factor
F'	Philip equation volume of infiltration at time t
fc	Horton equation minimum infiltration capacity
fo	Horton equation maximum infiltration capacity
f*	Horton equation instantaneous infiltration rate
g	acceleration due to gravity
H	depth of ponded water
h	channel deepest flow depth

hmax	the maximum normal channel flow depth (bank-full stage)
Hr	hydraulic radius of flow
Ht_0	Hortonian predicted time to ponding
i	infiltration
If	Agassi equation final infiltration rate
It	Agassi equation initial infiltration rate
K	coefficient used in Strickler's empirical equation of Manning's n as a function of particle size
k	constant used in Manning's flow equation
k^	coefficient used in Limerinos equation
Kfs	hydraulic conductivity at 'field saturation'
Ks	saturated conductivity
k*	Horton equation soil constant
m	Cowan's Manning's n correction factor for channel sinuosity m
Mcp	cross-slope profile mean y-coordinate
Mdp	downslope profile mean y-coordinate
Mds	plot sample downslope profile mean y-coordinate
Mdu	unit group downslope profile mean y-coordinate
N	runoff efficiency
n	Manning's resistance coefficient
n_0	Cowan's Manning's n value relating to a basic uniform channel of natural materials
n_1	Cowan's Manning's n correction factor for surface irregularities
n_2	Cowan's Manning's n correction factor for shape and size variations in the cross-section
n_3	Cowan's Manning's n correction factor for obstructions
n_4	Cowan's Manning's n correction factor for vegetation and flow conditions
Ns	number of plot samples in unit group
O	observed values
P	predicted value
p	rainfall
Pdp	y-coordinate predicted by the downslope profile best-fit line
Pds	y-coordinate predicted by the plot sample best-fit line
Pdu	y-coordinate predicted by the unit group best-fit line
Pf	capillary pressure at wetting front
Q	discharge
q	discharge per unit width
Q1	lateral inflow discharge into channel from left adjacent hillslope element
q1	lateral inflow dicharge per unit width into channel from left adjacent hillslope element

Q2	lateral inflow discharge into channel from right adjacent hilllslope element
q2	lateral inflow discharge per unit width into channel from right adjacent hillslope element
Q3	discharge volume out of the run-on/runoff plot by the third time period
Qin	the steady-state infiltration volume into a run-on/runoff plot
Ql	lateral inflow from hillslopes into channel
ql	balance between lateral inflow, rainfall and infiltration
Qon	the discharge volume onto a run-on/runoff plot
Qp	steady-state and/or peak discharge
Q_t	instantaneous discharge
RD	the vertical distance measured from the rod to the ground surface
RI	reccurence interval
S	the angle of the rod (in degrees) laid onto the surface
s	slope gradient
S'	Philip equation sorptivity constant
S1	left adjacent hillslope element slope-angle
S2	right adjacent hillslope element slope-angle
Sav	soil water suction at the wetting front
SD	standard deviation
SDcp	standard deviation of a cross-slope profile from the horizontal line y=0
SDcs	standard deviation of the plot sample cross-slope profiles from the horizontal line y=0
SDcu	standard deviation of the unit group cross-slope profiles from the horizontal line y=0
SDdp	standard deviation of a downslope profile from its best-fit line
SDds	standard deviation of the plot sample downslope profiles from the overall plot best-fit line
SDdu	standard deviation of the unit group downslope profiles from the overall unit group best-fit line
Sf	friction slope
So	bedslope gradient
t	time
t_1	time to ponding on final run-on/runoff plot Δx increment
t_2	time to ponding on fourth run-on/runoff plot Δx increment
t_3	time to ponding on third run-on/runoff plot Δx increment
t_4	time to ponding on second run-on/runoff plot Δx increment
t_5	time to ponding on upper run-on/runoff plot Δx increment
t_e	time of runoff cessation
T_1	first observation time
T_2	second observation time

T_n	final observation time
Tep	time to end of steady-state (= Tsp when peak only)
t_o	time to ponding due to the filling of soil storage
t_o'	time to ponding due to rainfall and run-on satisfying storage
t_p	time of rainfall cessation
t_{ro}	time to run-out of flow over the lower boundary of the run-on/runoff plot
Tsp	time to steady-state and/or peak discharge
Tw	channel top-width
v	mean flow velocity
Vc	difference between the cross-slope profile mean y-coordinate and zero
Vdsp	difference between plot sample and downslope profile mean y-coordinates
Vdus	difference between the unit group and plot sample mean y-coordinates
Vp	steady-state and/or peak velocity
V_s	depth of infiltration required to satisfy storage and produce ponding
V_t	instantaneous velocity V_t
W	right side channel bank-angle
wid	plan width of micro-topographic profile
w	width of the channel or hillslope section
w1	width of left adjacent hillslope element
w2	width of right adjacent hillslope element
WA	run-on/runoff plot wetted area
WP	wetted perimeter
WP^	scaled wetted perimeter derived from WP-A regression equation
WPmax	maximum wetted perimeter of micro-topographic profile
X	x-axis coordinate
x	downslope distance or downslope location (in finite difference equations)
Y	y-axis coordiante
y	mean flow depth
yc	standardised cross-slope profile y-coordinate relative to the plot sample mean of zero
yd	standardised downslope profile y-coordinate relative to plot sample mean
ymax	maximum vertical height of a given micro-profile roughness element above the lowest point in the profile
Z	z-axis coordinate
Zf	vertical depth of saturated zone
α	Agassi equation coefficient related to aggregate stability
$\partial A/\partial t$	change in flow area with time
$\partial A/\partial x$	change in flow area with downslope distance
$\partial Q/\partial x$	change in discharge with downslope distance

$\partial v/\partial t$ change in flow velocity with time

$\partial v/\partial x$ change in flow velocity with downslope distance

$\partial y/\partial x$ change in flow depth with downslope distance

ΣQ volumetric discharge from run-on/runoff plot and

ΔA the proportion of predicted flow area A overflowing the normal channel

Δh the height of flow above bank-full stage hmax filling the overflow section

ΔQ discharge in during t_5

$\Delta Q1$ discharge volume out of the run-on/runoff plot in the first time period

Δt finite time increment

$\Delta t1$ first time incrment

ΔWP the wetted perimeter of the overflow section covered by water

Δx finite distance increment

%E percentage error

%V variation between control predicted value and other predicted value

CHAPTER ONE WATER HARVESTING SYSTEMS : CONCEPTS AND CONTEXT

1.1 INTRODUCTION TO THE THESIS

1.1.1 The Hydrological Context

Since the early work of Robert Horton in the 1930s, the subject of arid lands hydrology and its variations from more humid environments has been a topic of debate (Horton, 1933). Some workers have assumed Horton's simple model of a maximum limiting rate of infiltration, instantaneous runoff over the whole catchment and a functional relation between the depth of surface detention and the rate of surface runoff to apply (Freeze, 1972). Others have questioned these concepts, focussing on the highly variable spatial and temporal patterns of runoff generation characterising arid catchments and showing similarities to the partial area contribution concepts that describe the humid area rainfall-runoff response (Lane *et al*, 1978. Lane, 1982). In the Negev Desert, the acceptance that intra-hillslope differences in the infiltration chacteristics of geomorphic units controls local stormwater runoff production frequency and magnitude characteristics has led to a sub-debate on the dominance of particular units, either rocky or loess-crusted surfaces, in determining the stormwater hydrograph (Shanan, 1975. Shanan and Schick, 1979. Yair, 1983. Yair and Lavee, 1985). Whilst both interpretations implicitly accept the notion of partial area contribution, they do so from the opposite ends of a geomorphological spectrum, one focussing on remote mid- and top-slopes and the twin factors of productivity and transmissivity downslope, and the other on the closer slopes and the role of connectivity with the channel network.

The debate centres on the concepts of hydraulic verses geographic remoteness. A hillslope section is hydraulically remote if the productivity and transmissivity conditions downslope are such that stormwater runoff generated at that location is dissipated prior to reaching the catchment outflow although the location may be geographically close. Yair indicates the footslopes favoured by Shanan to be the cause of hydraulic remoteness by dissipating runoff from more geographically remote rocky slopes. Shanan considers the rocky slopes to be relatively poor producers and focuses on the geographical closeness of the footslopes as an indication of the key role they play in stormwater production. The two views are brought together when the subject of this thesis is considered, the reconstructed Avdat water harvesting system in which man-made channels were constructed up from the outflow points of the catchment area and across the hillslopes of the catchment, tapping flow-lines at successively higher elevations and circumventing the footslopes and natural channel network.

From this scenario, the aims and objectives of this thesis can be clearly defined since it is clear that the understanding of water harvesting systems such as Avdat and their functional ability depends on the interpretation of the arid hillslope hydrological conditions in both a broad and local context.

1.1.2 Aims and Objectives

To develop an appropriate arid hillslope hydrological model and to interpret correctly the major controls on water harvesting system efficiency, this thesis analyses and describes the patterns and processes by which runoff is generated, transmitted and consumed within the boundaries of a catchment system in the arid environment at Avdat, in the Negev Desert. The characteristics of downslope variations in runoff productivity and transmissivity, coupled with the connectivity of particular locations to a channel network are considered critical to this understanding. To describe the partial nature of runoff contribution to stormwater flow and the essential differences between the humid and arid models, a new description of the mechanism is defined termed Contiguous Area Contribution. The derivation of this new term and its suitability as a general model of arid conditions is assessed from a review and synthesis of the literature, from fieldwork at the Avdat catchment, and through a structured programme of simulation modelling at a range of scales from small hillslope plots to complete sub-catchment hillslope and channel systems. Contiguous Area Contribution is a version of partial area theory that focusses specifically on hydraulic remoteness and the nature of intra-hillslope and intra-channel variation and their control on stormwater contribution under the limited moisture input conditions in arid catchments.

To undertake this analysis a programme of fieldwork was carried out at Avdat to quantify the critical contributing factors to the control of the catchment hydrological response. Parameters measured include both physical characteristics such as surface geometry and texture, and process characteristics such as infiltration and flow-routing conditions. At a theoretical level, the consequences of selecting different models to represent the infiltration regime and assumptions as to the nature of hillslope overland flow dimensions is tested. The former takes a critical view of the Hortonian procedures for infiltration calculation with respect to storage approaches more commonly used in humid environment modelling and the latter focuses on the assumption of sheetflow and the significance of ignoring microtopographic variation. The physical measurements of surface texture are used for both the analysis of the flow dimensions assumption and for quantifying the spatial variations in surface properties throughout the Avdat catchment area. Key unit areas are defined which can be used for the allocation of parameter values in a distributed model designed to assess the nature of the hillslope hydrology and examine the performance of the water harvesting system introduced to the catchment. The geometric data provides the physical framework across which the parameters are distributed and the rainfall, infiltration and runoff simulated.

A main objective of the thesis is to use the results of the literature review, fieldwork and theoretical dicussions to build a deterministic distributed model of an arid catchment and water harvesting routing system which explains the pattern of water harvesting productivity at Avdat and

which can also be used as a development tool for identifying the runoff efficiency of a given harvesting system. Whilst carrying out these tasks several broad conclusions are drawn as to the sensitivity of both the environment to particular combinations and patterns of process parameters and the data needs of the model for effective simulation of arid environment conditions.

1.2 WATER HARVESTING AND RUNOFF FARMING

Water harvesting is a general term for a range of hydrological techniques that maximise water resources to support people, livestock and crops at suitable locations within a region. It involves a manipulation of the hydrological environment for the collection, concentration, transport and storage of runoff water from natural or man-made surface areas. When water harvesting is used to supply runoff directly onto a farmed area it is called runoff farming.

Water harvesting and runoff farming have been practiced for thousands of years and can be found in one form or another in most dry-land ancient civilisations. In urban locations, runoff from roof-tops was stored in household cisterns and runoff from roads and courtyards stored in communal reservoirs. In rural locations, water was supplied to irrigate crops by diverting channels, piping water underground or channeling water from higher ground down to lower ground where terraced valleys could be flooded.

The purpose of introducing runoff farming systems is that in arid and semi-arid environments, rain-fed agriculture is only marginally feasible without the supply of additional runoff water to supplement rainfall. Consequently, there are periods of surplus and deficit related to annual and seasonal variations in climatic conditions. By developing water harvesting systems, the variations in supply of water can be evened-out and the magnitude of supply increased.

Water harvesting systems can take a variety of forms, using both natural and man-made catchments, but each involves the components of collection, concentration, transport and storage. In many ancient and current traditional runoff farming systems, the episodic flash-floods from natural hillslopes are harnessed by diverting water from its normal course onto an area which would receive insufficient water from rainfall alone, but is otherwise favourable for agricultural production. The systems either divert water from an already concentrated channel source, or prior to concentration by tapping hillslope flow-lines.

The subject of this thesis, the runoff farming and water harvesting systems found in the Negev Desert, and in particular the Avdat runoff farm (Figure 1.1), is a good example of the type of systems that can be introduced to ameliorate conditions sufficiently for agriculture to be carried out. Here, extensive agricultural and urban water harvesting systems were introduced dating back 3,000 years.

FIGURE 1.1 : A LOCATION MAP OF THE STUDY AREA

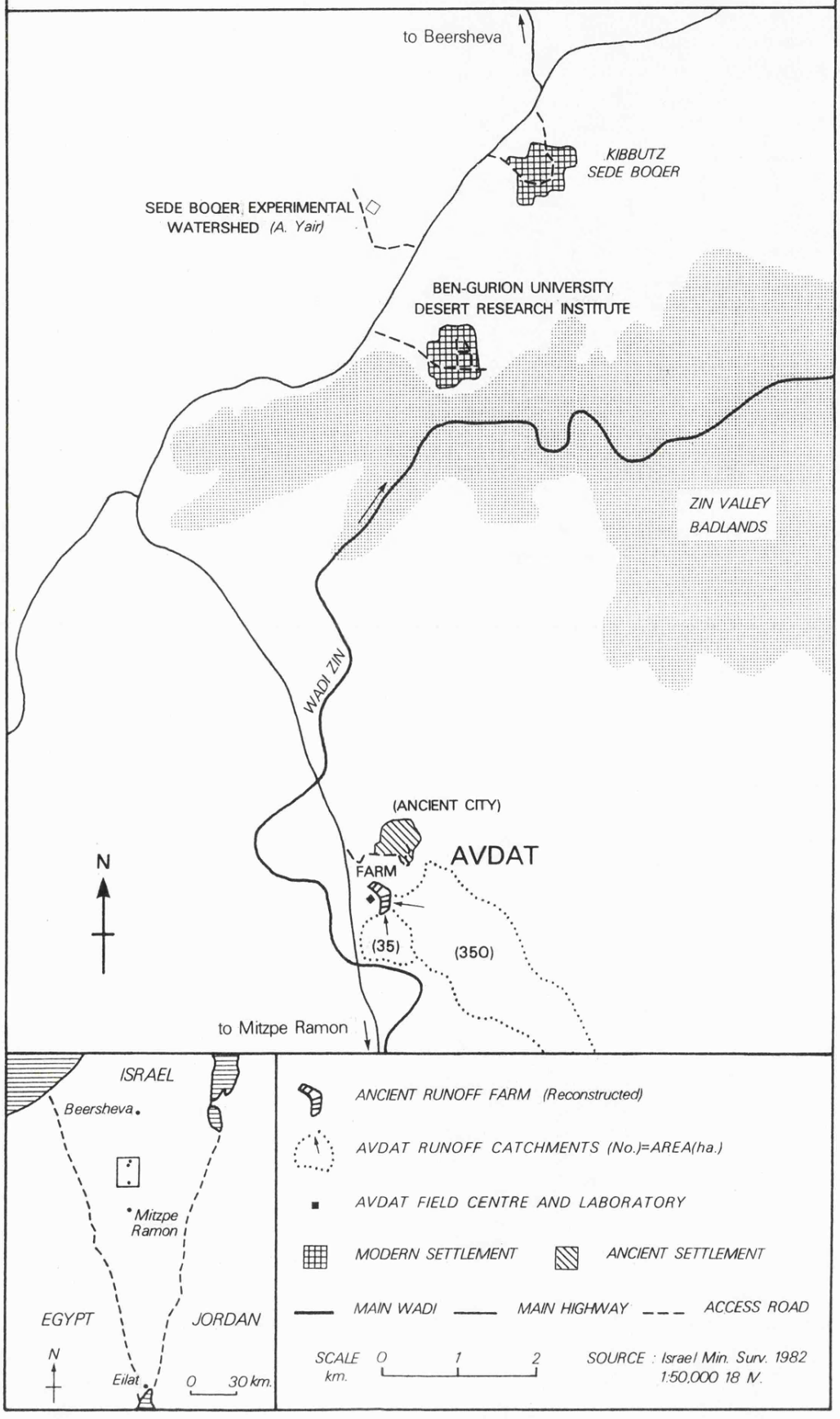

Infrequent rainstorms produced rapid runoff on the rocky hillslopes and stone-built cities. This supported a large population and allowed them to practice agriculture on the shallow-sloping alluvial-valley bottoms using stone-walled terraced-fields. The Avdat runoff farm is a reconstructed ancient system, restored to full working order to examine the ancient practices. Since there is little evidence of climatic change in the region over this period, the current conditions can be considered as representative of the past (Issar *et al*, 1984). Studies carried out on the reconstructed Avdat system are therefore directly relevant to the overall understanding of the water harvesting success of the ancient hydrologists.

There are three basic designs adopted in the Negev for the exploitation of local water resources for agriculture (Evenari *et al*, 1980). The simplest involves the construction of stone-wall checking structures across the alluvium of small valley bottoms. Water draining off the headwater and side-slopes provides direct run-on to the leveled terrace behind each stone-wall. Water ponds and gradually infiltrates the soil column, the storage providing sufficient water for the crops during the cool winter growing season.

The next type of system involves the construction of simple hand-dug ditches across and down the slopes to route water more effectively off the slopes and down to the terraced area, circumventing particular slope areas and reducing the normal flow lengths down to the fields. This increases the density and suitability of the channel spatial distribution, and in some cases enlarges the contributing area to the valley bottom locations. The main advantage of this type of system is where the favourable area for agricultural production, the flat alluvium-filled valley or plain, is separated hydrologically from the contributing slopes by a hillslope environment unsuitable for the generation or transport of surface runoff , and where the majority of the water produced elsewhere would otherwise be consumed on its normal passage through the system. The significance of this characteristic of the natural and the water harvesting system flow patterns is discussed in more detail below.

The third type of runoff farming system is the diversion system which operates at a different scale than the low-order valley systems described previously. It requires a highly concentrated source of runoff which can be partially dammed and diverted onto adjacent land suitable for agriculture, for example the terraces of a floodplain adjacent to a large channel known to flood annually and capable of providing sufficient water in one or more flow-events to satisfy the crops annual moisture requirements.

The system that uses man-made hillslope ditches to improve the natural flow routing is the subject of this thesis and is illustrated in Plates C.1 to C.3. It is the most intensive in terms of man's involvement in the runoff process. The introduction of channels not only taps productivity within the arid catchment system, it changes the pattern of productivity, interrupting flow-lines at particular locations, changing the arrangement and size of contributing area relative to the remote farmed area.

All researchers dealing with the problem of the small runoff farms have agreed that their very existence in the Central Negev Highlands is a result of their effective harvesting of water from the adjoining valley side-slopes. Proper knowledge of the local hillslope hydrology is therefore a primary condition for an understanding of the water harvesting techniques that have been used (Yair, 1983). It is these characteristics that are considered in this research; the relationship between the local arid hillslope hydrology and the man-made routing systems designed to exploit the runoff productivity within a catchment. To evaluate the ability of an existing runoff farming supply system, such as the one introduced at Avdat, and to evaluate other catchment systems for their water harvesting potential, knowledge of the hydrological system at a given location is required, along with a clear understanding of the effects of introducing additional routing elements into the flow system on the overall productivity of the system for a range of input conditions. The general principles and characteristics of arid hillslope hydrology must be analysed and understood. The approach taken here is to develop a numerical model of the hillslope hydrological processes, parameterised from field studies within the water harvesting supply system feeding the Avdat runoff farm. Through manipulation of the model the design considerations and management aspects of water harvesting systems using this type of technology are examined. The productivity of the current system relative to the unaltered catchment illustrates this. The procedures are described in the following chapters but first, an examination of the theory of hillslope hydrology is required and particularly the specific characteristics of the arid catchment hydrological systems.

1.3 HILLSLOPE HYDROLOGICAL THEORY

1.3.1 Runoff Generation and Water Harvesting

The processes responsible for storm runoff generation within catchment systems have been shown to be non-uniform controlled by the variability, often in systematic fashion, of the rainfall receipt, infiltration abstraction and surface and sub-surface flow redistribution. The differing degree to which these processes and their controlling characteristics are responsible for flood generation in a given environment, from humid through to arid, has been the central issue in hydrological debate since the work of Robert Horton in the 1930s first addressed the problem of the origins of storm-water hydrographs. Regardless of the exact mechanism by which hillslopes contribute to channels, and channel flow arrives at the catchment outflow, three critical factors ultimately determine a systems productivity: the patterns and rates of production, transmission and consumption along any route from a point (X, Y, Z) in the system to a pre-determined gauging point (0, 0, 0). Productivity is defined as the proportion of rainfall volume received in a storm event that is discharged as the stormflow hydrograph.

Productivity is a function of catchment size, the complexity of its physiographic conditions and the character of the input through space and time. Productivity is determined by both the magnitude of on-site surface water generation and its continuity, the sequences in which productive, transmissive and consumptive locations occur along a given flow-line. Consumers are hillslope areas or channel sections where discharge in (as opposed to total inputs) exceeds discharge out, rainfall excess is negative and surface water that has been generated at higher locations along the flow-line is consumed. Producers are the opposite. Comparing discharge in to discharge out the balance is positive and surface flow has been added at this location, due to a positive rainfall excess. Transmitters are zones in which input and output are balanced and continuous flow maintained along the flow-line. The longer the flow-line, and the more variable the sequence of producers, transmitters and consumers, the greater the opportunity that rapidly generated surface stormflow will be dissipated before reaching the gauging point. For a water harvesting system based on the construction of artificial channels to intercept natural flow-line sequences within a spatially variable arid catchment, and the use of the harvested rapid stormflow for terrace irrigation at the basin outflow, the ability to recognise and tap into consistently productive and transmissive flow-lines, and to avoid consumptive locations is of critical importance. The superimposed channel network, usually considered a transmitter, but also capable of being a producer or consumer, changes the relative positions of catchment areas in a hydrological, rather than geographical sense, rendering particular areas closer to the outflow point hydrologically by modifying flow-line routings.

The following sections provide the theoretical background to this thesis. They present a brief assessment of the development in hydrological thought that has resulted in the current understanding of storm-water productivity in different catchment systems. Attention is focussed on the special characteristics of arid catchment systems that determine the key differences in the partial area productivity of the arid lands hydrological cycle, and in particular the conditions within the Negev Desert that have given rise to a debate on runoff productivity patterns of relevance to the correct understanding of the Avdat and other Negev water harvesting systems. This is illustrated by a discussion of the diverse character of the Negev landscape, and the likely magnitude and pattern of producer, transmitter, and consumer elements within its flow-line sequences as perceived by two Negev hydrologists, Aaron Yair and Leslie Shanan.

1.3.2 General Theories on the Pattern of Storm-water Generation

Systematic studies in the hydrology of drainage basins have, since the 1930s, demonstrated four different flow processes to be involved in storm channel runoff; Hortonian overland flow, shallow sub-surface flow, saturation overland flow, and groundwater flow (Yair and Lavee, 1985. Hewlett and Hibbert, 1967. Freeze, 1972. Pilgrim and Huff, 1978).

1.3.2.a Hortonian Overland Flow

In the 1930s, working in series of south-western U.S. drainage basins, Robert Horton developed his infiltration theory of runoff (1933, 1938). The theory has three main concepts;

1. there is a maximum limiting rate, the infiltration capacity, at which the soil in a given condition can absorb rainfall,
2. when runoff takes place for a given soil surface, there is a definite functional relation between the depth of surface detention and the rate of surface runoff or channel flow,
3. runoff is instantaneous over the whole catchment.

Horton thus defined the characteristics of rainfall excess, detention and time-lag storage, and the stage-discharge relation. The rainfall excess from intensities higher than the infiltration rate is termed Hortonian Overland Flow and is predicted to begin uniformly across complete hillsides, with discharge increasing in direct proportion to downslope distance from the divide to the channel as flow depths and velocities increase. Hortonian runoff theory requires that most rainfall events exceed infiltration capacities and overland flow is areally widespread. Since this was formulated based mostly on observations in the semi-arid south-west U.S., it has been held to apply most readily to the arid environments (Freeze, 1972). It led to a breed of lumped hydrological models where stormflow is generated uniformly with a surface area equal to basin area (Hewlett and Nutter, 1970).

As the use of hydrological models became more widespread with the development of powerful digital computers, and as the study of basin hydrology became more established, workers began to question the Hortonian theory of runoff generation, and in particular the concept that stormflow is generated from a surface area equal to that of the complete basin. As described below, the Hortonian interpretation is now seen to be the extreme of the runoff production conditions found in arid environments where surface flow down a complete hillslope profile is possible, but is rare, occurring during high magnitude, low-frequency rainfall events, and most often on hillslopes with a small range of hydro-geomorphological variation.

1.3.2.b Partial Area Contribution

In the 1960s the applicability of the traditional Hortonian concept to all catchment systems was first questioned in terms of the pattern (Betson, 1964), and the process (Hewlett, 1961. Hewlett and Hibbert, 1967) of stormflow generation. Dunne and Black (1970) stated that the absence of empirical evidence of sheet-flow on hillsides, and the measurement of high rates of infiltration into the permeable vegetated soils of humid regions casts doubt on the usefulness of Horton's theories. Betson (1964) concluded that although Hortonian rainfall excess occurs across basin slopes, it only occurs from

a small and relatively consistent part of the catchment and not the complete hillslope. In upland forested catchments, overland flow as defined by Horton is seen to occur rarely (Hewlett and Nutter, 1970). According to Hewlett and Nutter, this is due to the fact that infiltration, relative to precipitation receipt, is not limiting, and overland flow, therefore, is exceptional rather than the typical case. They held that the storm-water flow peaks observed, delayed due to soil through-flow time-lag, are faster than those produced by deep-seated base-flow. Their theory suggested that the actual throughflow in the porous soil-mantle contributes rapid flow into the channels. Since flow does not take place over the surface, the source-flow for stream lengths is through the bed and banks from the contributing areas upslope in which soil-water is sufficiently voluminous to be transmitted down and out of the foot-slopes into the channel. The perennial channel system is thus seen to expand as areas of low-storage and high permeability transmit infiltrated water combining with the direct in-channel rainfall to produce the stormflow (Hewlett and Nutter, 1970). The notion of the expanding channel is known as the 'reaching-out' of the network to tap a wider arrangement of ephemeral channels and rills.

Dunne and Black (1970) cast doubt upon the interpretations of Hewlett and Hibbert (1967) and Hewlett and Nutter (1970) that sub-surface through-flow was a direct contributor to storm-water flow in these systems. Freeze (1972) noted that although Hewlett and Hibbert had shown sub-surface flow to be a viable mechanism operating during a rainfall event, doubt existed concerning whether it can provide significant contributions to storm runoff. Although Dunne and Black agreed with Hewlett and Hibbert that saturated areas occur along valley depressions and the lower portions of hillsides, they set out to define whether the mechanisms of storm water flow production operating within a small watershed are sub-surface, or surface dominated, and to measure directly the amounts of flow contributed by each of the forms of runoff encountered. They found that the importance of a hillslope as a contributor to storm-water flow depended on its ability to generate overland flow in the area adjacent to the channel network observing that the water table intersects the land surface at these locations and a small partial area reacts to rainfall essentially as an impervious area. As a result, stormflow hydrographs are extremely sensitive to rainfall intensity fluctuations due to rapid surface flow off these partial areas into the channels. Comparing the response to the likely rates of flow from soil throughflow alone, they conclude that only overland flow on the saturated soils can contribute the large amounts of stormflow runoff due its rapidity combined with short flow-lengths. Antecedent conditioning in the form of groundwater table build-up at the slope foot thus becomes an important factor. Since the overland flow rate is some 100-500 times faster than throughflow, storm-water flow contribution reduces rapidly following rainfall cessation (Dunne and Black, 1970). Betson, the forerunner of this new Partial Area Contribution theory had suggested the overland flow was Hortonian in origin due to rainfall excess. Freeze (1972) and Dunne *et al* (1975) dismissed this process as saturation, rather than Hortonian controlled, due to water tables rising from below, rather than a Hortonian decrease in potential to transmit water due to increasing provision from above. Thus surface flow is storage dominated and a function of the spatial variability of moisture content.

Dunne *et al* (1975) described the control on the partial area productivity exerted by topography. The limit of saturation overland flow spreads first up the previously dry low-order tributary channels, then up the channelled swales and gentle foot-slopes, "reaching out" in the same way as Hewlett and Hibbert described the tapping of through-flow. Dunne *et al* also pointed out that sub-surface concentration of water leads to the formation of saturated overland flow on high conductivity soils in concavities or hollows on a hillside (Dunne and Black, 1970. Anderson and Kneale, 1980), or in locations with impeding layers (Anderson and Burt, 1978) as the product of rising groundwater tables or vertical percolation above an impeding horizon producing return flow and direct precipitation runoff. Since they are often hydrologically remote from the channel system, runoff generated in these locations form part of the partial runoff area, but do not contribute to storm-water outflow due to the lack of connectivity with the channel network. Freeze observed that stormflow hydrographs in the humid regions are dominated only by direct runoff through very short overland flow paths from precipitation on transient near-channel wetlands (1972).

The Partial Area concept is generally accepted. It is clear that humid area basins do not conform to Horton's universal runoff patterns, however, it is widely assumed that arid environments do as indicated by Freeze (1972). However, this thesis argues that given the absolute quantities of water available, and the spatial variability prevalent in arid landscapes, the concept of universal Hortonian flow generation cannot be supported in anything other than the most extreme events and a partial area contribution interpretation is also the most appropriate.

1.3.3 Arid Lands Patterns of Storm-water Generation

1.3.3.a Partial Area Contribution and Hortonian Rainfall Excess

According to Dunne (1983) runoff generation in an arid landscape occurs most frequently as a result of the Hortonian type of overland flow production. It is widely held that in arid areas, scarcity of storms, limited rainfall amounts and durations, shallow patchy soils and low density vegetal cover all conspire to inhibit significant contribution to storm channel runoff by the other three mechanisms (Yair and Lavee, 1985). Under these conditions, watershed runoff may be entirely generated by rainfall rates in excess of infiltration rates (Woolhiser, 1981).

However, the spatial and temporal variability inherent in these characteristics suggest a partial area pattern of contribution to channel flow to be operating here too, rather than the classic Hortonian theory. It seems clear from recent studies undertaken in arid environments that episodic channel flood production corresponds neither to the classical Hortonian theory nor to the more recent Dunne mechanism of overland flow generation represented by the humid Partial Area Contribution theory (Yair

and Lavee, 1981, 1982, 1985. Schick, 1978. Lane *et al*, 1978. Lane, 1982). Spatial variations in hillslope surficial properties and form (Shanan and Schick, 1979. Poesen, 1986), combined with the often characteristic spatial and temporal variability of desert rainstorms (Fogel, 1969. Sharon, 1974, 1980), result in non-uniform patterns of surface water generation and overland flow transmission (Yair and Lavee, 1985). The surface cover proportions of soil, stones and bare rock, and their resultant infiltration characteristics determine the local productivity of surface water under variable rainfall conditions (Yair and Lavee *et seq*. Shanan, 1975). The form of the surface, both the macro-topography of slope gradient change and the micro-topography of slope textural change, determine the productivity of runoff away from a locality through its control on the generative and transmission rates of surface water across the hillslope. Geological conditions play a large part in controlling these characteristics. The resultant effect of these variations is the existence of preferential locations in the catchment where runoff has a higher probability of taking place for a given rainstorm. As in the humid catchments analysed by Dunne *et al* (1975) and Anderson and Burt (1978) these locations may or may not intersect with the channel system, i.e. they may be hydrologically remote from the gauging point. Consequently, the absolute area in which surface water may be generated and overland flow occur can be in excess of the partial area actually contributing to the channel. Whilst the hydrological outcome is a partial area contribution as far as there is lateral inflow from the areas adjacent to the network which do intersect, the mechanism involved does not appear to conform to the normally accepted process controls of the humid Partial Area theory.

In the Dinosaur badlands of Alberta, Bryan *et al* (1978) observed non-uniform runoff generation into a channel system with a pattern virtually identical to the humid-zone case. This is not a function of saturation however, but a response to the spatial variability of surface materials, with layered compacted clays present adjacent to and within the channel depressions. Thus the material properties rather than the moisture regime is seen to be the controlling variable.

Of considerable relevance is the work of Yair and associates who have produced a suite of papers addressing the problems of spatial and temporal variability in slope processes and characteristics in a number of arid environments in Israel (1974, 1976, 1977, 1980, 1981, 1982, 1985). They receive a wider discussion in the debate of the Avdat hydrological system in the following section. Of relevance to the general theory of arid lands hydrology is the observation that overland flow generation through rainfall excess over infiltration can occur in widespread fashion on the shallow and patchy arid-zone soils. However, Yair *et al* have shown generation to be far from uniform and that the classic Hortonian universal flow state is the extreme of arid-zone runoff conditions. On a hillslope section with a high percentage of impermeable bedrock cover in the upper level, and higher permeability colluvial material on the lower level, the combination of short rainstorms, and low measured flow velocities leads to the result that flow generated at the top of the slope does not have enough time to reach the slope base before rainfall cessation and is consumed (Yair *et al*, 1980c). The significance of

this observation for water harvesting systems is obvious. Where man-made channels are introduced to harvest water from the hillslopes, the presence of preferential producing zones along a given flow-line determines where the optimum location of the channels should be and areally, the routes the channels should take from the storage area of the terraced fields, back-up into the supply area to maximise collection from these zones.

Yair's observations are supported by those of Arteaga and Rantz (1971) who suggest that only 26% of a 132 hectare catchment in central Arizona contributes runoff to the outlet. Lane *et al* (1978) attribute this to rainfall and infiltration spatial variability, and the varying hydraulic remoteness of locations from the basin outflow. The term hydraulic remoteness is indicative of the condition observed in Yair's studies, and implies a remoteness in terms of the travel time and character of flow path rather than a purely geographical one. For instance, for a given location, flow paths to the basin outflow may be short but shallow gradients and a large proportion of the length over hillslope surfaces of high infiltrability may render it more hydraulically remote than a distant location with a short steep overland flow path directly into the channel network. The latter will lead to a rapid transmission to the point of outflow, the former will lead to flow dissipation through transmission losses. This is compounded in some locations by the even larger-scale transmission losses within the channel system as identified by Lane and Renard (1972). Thus the concept of consumer, transmitter and producer zones are central to the interpretation of the arid lands hydrological cycle and the operation of the partial area contribution mechanism.

In the Dinosaur badlands of Alberta, Hodges and Bryan (1982) indicate the timing and contributing area for small catchment runoff is governed by the frequency and location of the most actively runoff producing units. The spatial contiguity of the rapidly producing units and non-producing units with a slower response can be influenced by discharge from adjacent upslope 'active' units, for instance promoting surface sealing in crusting soils or reducing times to ponding and detention fill, producing runoff generation where it may not normally occur solely from rainfall. Dunne (1983) highlights the important effect of runoff production loci on downslope areas of higher infiltrability where times to ponding and its variance along the path downslope can be greatly reduced as a consequence of the runon. Thus the characteristic of contiguous runoff production and consumption areas can be seen from two opposing directions;

1. the degree to which the consumers prevent runoff generated upslope at location (X, Y, Z) from contributing to the basin outflow at (0, 0, 0),
2. the degree to which the producers facilitate the consumers reaching the point at which they too can produce Hortonian rainfall excess and contribute stormflow to the channel throughout the remaining portion of the rainstorm.

These characteristics will change with time during the rainfall event. Runoff thresholds vary within any given flow-line, and the arrangement of producers, transmitters and consumers are important factors for all catchment systems, but particularly for the subject of the current research, the Avdat water harvesting system of artificial ditches interrupting normal flow-lines. Dunne's observations on the role of runoff production loci is of central importance to the understanding of water harvesting systems. The consequence of spatial variability in flow production and transmission properties is the selective enhancement and inhibition of runoff production through space and time especially when coupled with variable inputs. Water harvesting systems must tap into consistent producers and avoid consistent consumers to function effectively. The approach adopted in this thesis identifies the important process characteristics through fieldwork and modelling, and develops a method of assessing the operating efficiency of natural catchment systems and the actual and possible water harvesting system configurations introduced to maximise the available water resources for runoff farming.

1.3.3.b A Re-Definition : Contiguous Area Contribution

Dunne *et al* (1975) described the notion of the expanding channel network that represents the Partial Area concept as a "**reaching-out**" mechanism by which the channel sections tap into a wider arrangement of areas experiencing saturated overland flow via a series of ephemeral channels and rills. The driving force is the increase in sub-surface moisture content from soil through-flow. For the partial area contribution characteristic of more arid areas this mechanism must be re-defined as a "**reaching-down**" process by which rapid Hortonian rainfall excess produced at distinct key locations tap into the channel network through the downslope expansion and extension of flow from these points. As upslope areas produce rapid runoff, the consumption into any less-flashy areas eventually may result in their reaching the point of runoff generation also. The Horton-style surface runoff can result from both rainfall intensity and runon intensity relative to infiltration rates, but must become contiguous with other producing sites and the channel network to make any contribution to the stormflow hydrograph. It is therefore more accurately termed Contiguous Area Contribution.

This definition therefore states that for a given rainstorm, the degree to which a particular area is significant in its contribution to basin outflow will depend on its inherent productive capabilities (i.e. its ponding threshold, transmission rates and total surface area), and the relative capabilities of all subsequent locations along the fixed flow-line from the point (X, Y, Z) to the gauging point (0, 0, 0). If they are still in a pre-ponding state, and/or have higher rates of infiltration, water running-on may be consumed in addition to rainfall. Since Hortonian flow can be generated at locations independent of a channel line, and the knock-on **reaching-down** effect of run-on produces a distinct section of hillslope undergoing surface water generation and transmission, when the channel and expanding flow-section intercept and Contiguous Area Contribution occurs, the effect is a pulsed addition of effective contributing area. Up to the point at which a consumptive area is encountered further up the flow-line

towards the watershed divide, the hillslope section is experiencing overland flow in a manner approaching the classical Hortonian concept. In the most extreme case, when rainfall depths or intensity are sufficient for the whole flow-line to be in a state of surface flow, the classic Hortonian state has been obtained. This will be more prevalent the lower the runoff thresholds and the more homogeneous the flow-line conditions, as for instance in an urban watershed. The Horton production is obviously the extreme of the Arid Lands hydrological cycle, with the whole hillslope producing and transporting runoff only when rainfall durations and magnitudes are sufficiently high to exceed infiltration capacities throughout the surface area. It is unlikely that the classic Hortonian condition of discharge increasing in direct proportion to downslope distance will be observed from the top of the flow-line down to the bottom, this only occurring on relatively uniform hillslopes. The spatial variations in roughness, slope gradient and particularly infiltration will operate to reduce or increase discharges regardless of the downslope position with discharge increasing at varying rates.

Although descriptively accurate, the use of the term 'partial area contribution' to describe this kind of dynamic watershed phenomena fails to account for the more spatially varied storm-water generation from arid catchments. Consideration of the Avdat water harvesting system, where the natural flow-line pattern has been significantly altered by the introduction of artificial ditches cutting across hillslope profiles upslope from natural catchment networks, must attempt to directly pin-point and quantify these pulsed additions, in order to determine the efficiency and true character of the system productivity.

1.4 THE CENTRAL NEGEV HIGHLANDS AND THE AVDAT CATCHMENT

1.4.1 Geomorphology and Geology

The Avdat water harvesting system comprises a large terraced alluvial valley fed by two separate catchments. They are located in the Central Negev Highlands, a region of highly variable relief carved out of the sedimentary sequence laid down under the ancient Tethys Ocean that filled the Mediterranean basin (Evenari *et al*, 1982). The current research is concerned with the smaller of the two catchments feeding the upper half of the terrace system which is separated into seven distinct sub-catchments by the arrangement of artificial ditches. These can clearly be seen in the aerial photograph Plate C.1. In addition, the surface morphology is described by the contour map Appendix 3.1 and the sub-catchment divides superimposed on the accompanying overlay.

The Central Negev Highlands are characterised by steep cliffs, coarse debris-covered slopes, badlands, mesas, palaeo-fluvial terraces, channel beds full of coarse materials, and adjacent loessial floodplains. Their form is the result of a complex geomorphological history (Garfunkel and Horowitz, 1966. Yaalon and Dan, 1974). The Avdat catchment is representative of the physiographic conditions

in that it exhibits a range of surface materials with a strong degree of geological control on forms and materials exerted by an undisturbed sedimentary sequence, modified by the super-imposition of aeolian loess and fluviatile loessial sediments.

The small wadi basin is bounded to the north by the runoff farm terraced fields. To the west it is bounded by a short, steep slope leading up to a gently dipping and broad remnant of the larger Wadi Zin terraces. The eastern side is composed of two small mesas with side-slopes exposing the sequence of chalks and limestones. The lower slopes are covered by colluvium and then alluvium except at the southern head-waters of the wadi catchment, where the chalks and limestones grade westwards onto conglomerate capping the Zin terrace. This is clearly seen in Appendix 1.1 and the oblique photographs C.2 and C.3. In addition to the morphological asymmetry of the smaller Avdat catchment, it exhibits an associated fluvial asymmetry, with a more highly developed natural drainage network extending into the colluvial foot-slopes of the east side.

Considering the catchment as a whole, it is clear that the variable morphology and geology ensures that the hillslope profiles comprising the system do not exhibit a simple erosional-depositional sequence. They are complicated by past geomorphological processes and geological influences, particularly the incursion of loess which now mantles different sections of the hillside as colluvium and alluvium. The exact origins of overland flow produced at Avdat depends very much on the spatial variability in the surface form, material characteristics and associated process characteristics of these surfaces. As described previously, the ancient water harvesting system introduced to this non-uniform assemblage of hillslopes and channels involves the positioning of artificial hand-dug ditches across the various hillslope sequences (Plate C.2), expanding the catchment to harvest water from the southern slopes and western terrace that would otherwise drain away from the wadi terraces to the undercutting Zin (as can be seen from a comparison of the flow-net maps in Appendices 3.2 and 3.3 which show a much larger contributing area to the terraced fields resulting from the modifying effects of the artificial routing network). Consequently, the proximity of rapid runoff producing slopes to the natural and artificial channels is of critical importance to the understanding of flood production into the Avdat runoff farm.

1.4.2 Process Characteristics

On an arid hillslope section experiencing uniform rainfall, surface water generation is most likely to be rapid at locations where surficial materials possess one or more of the following characteristics;

1. uniformly low hydraulic conductivities below rainfall intensities (Horton, 1933),
2. high proportions of totally impermeable surface materials (bare rock) with limited storage, whose runoff, added to rainfall, produces precipitation excess on the surface materials with higher hydraulic conductivities (Yair *et al, et seq.*),
3. high initial hydraulic conductivities but with threshold controls producing rapid change to low conductivities (crusting soils) (Ellison, 1944. Hillel, 1960. Farres, 1978. Shanan, 1975. Shanan and Schick, 1979. Hodges and Bryan, 1982),
4. low storage capacities resulting in rapid profile saturation and the inability to absorb additional rainfall or run-on (Scoging, 1988. Scoging and Thornes, 1980. Thornes and Gilman, 1983).

Surface water transmission away from, or across the zone of generation is determined by the arrangement of the rapidly producing zones along a flow-line and the macro- and micro-morphology of the surface; its gradient, size and texture. The first two control the length surface water must traverse and the gravitational forces responsible for its movement. Texture controls the dimensions within which it must move and the resistances opposing its movement. In addition, the combination of the length of the flow-line in the downslope, and the length of the wetted surface in the cross-slope, relative to a given volume of water determine the transmission losses from the water body in combination with the rate of movement. When the combined length is great and the travel times long, opportunity for infiltration increases. When they are both short, this decreases. The most favourable conditions for continuous overland flow therefore must be where infiltration rates decrease or remain constant in a downslope direction, and the combinations of steep gradient and high cross-slope micro-topographic variation combine to produce flow dimensions with generally large hydraulic radii and rapid flow velocities. Since micro-morphology becomes highly significant, especially in catchments exhibiting rough surface conditions, traditional concepts of Hortonian overland flow as a sheetflow approximation are inadequate, given that they have consequence for both the rate of water transmission and the length of the contact zone between the moving water and the surface. With short-duration rainfall events and generally high final infiltration rates, the post-ponding, post-rainfall infiltration phase is likely to account for considerable volumes of runoff water and is a major factor in the observed characteristic that an increase in catchment size and flow-line length is accompanied by a diminishing increase in discharge volume (Yair *et al*, 1980c. Arteaga and Rantz, 1971).

The location of the different productive, transmissive or consumptive areas depends on the pattern of occurrence of different morphological features and the character of surface materials with which they are mantled. The presence of bare-bedrock outcrops, high percentage stone cover, crusting-susceptible clay-rich loess, deep, patchy or shallow soil profiles, and the resultant spatial homo- or heterogeneity of these features determines the exact infiltration and runoff pattern. All may play an important role, with the dominance of any one a function of the relative size of the particular surface type and its position in the flow sequence relative to channels.

1.5 THE NEGEV HYDROLOGICAL DEBATE

As a result of variable down-cutting through sedimentary rock strata and the introduction of aeolian loess (Yaalon and Dan, 1974), the landscape of the Central Negev Highlands contains a whole range of slope environments of considerable hydro-geomorphological complexity. Hydrological work in the Negev has concentrated on two particular geomorphic units with apparent relatively high potential for runoff generation. These dominant units occur at opposite ends of a general downslope erosional-depositional hillslope profile sequence; on the one hand, the high-gradient, high bedrock covered slopes favoured by Aaron Yair and Hanoch Lavee (Yair and Lavee *et seq*); on the other hand, the low gradient, loess-crust covered slopes favoured by Leslie Shanan (Shanan, 1975. Shanan and Schick, 1979).

1.5.1 The Role of Loessial Slopes

Shanan studied small plots, extrapolating results to larger catchment systems using a lumped model (1975). They included;

1. One set of shallow slope micro-plots located in the wadi-bed loessial alluvium, 0.57° (1%) average gradient and stone free,
2. Four sets of medium slope 80 m^2 (4 x 20) plots located on the slope down from the remnant Wadi Zin terrace, south-east facing of varying stone cover and of average gradients; 5.7° (10%), 7.4° (13%), 9.6° (17%) and 11.3° (20%) respectively.

Shanan confined his plots to a single hillslope location, adjacent to the two catchments feeding the Avdat runoff farm terraces (as can be seen in the aerial photograph Plate C.1), and limited their size to ensure homogeneous conditions. The area selected was held to be typical and representative of the stony slopes of the Avdat region in terms of vegetation, the range of slopes (0.57° and 5.7°-11.3°), soil depth, and stone cover. The plots were isolated from the rest of the slope, and altered in four different ways to produce a range of conditions or 'treatments' based on the natural surface, and stone-clearing combined with wet or dry compacting creating the different surface types.

In analysis of daily rainfall and runoff volumes over a roughly ten-year period, Shanan presented the average annual productive efficiencies of his plot environments in terms of the proportion of rainfall converted to runoff (Shanan, 1975). Shanan found an inverse relationship between slope gradient and runoff productivity (Table 1.1). In addition, the analysis of different plot treatments showed runoff to increase significantly with the removal of stone cover (Table 1.2). Infiltration rates were generally higher on the steeper slopes (Table 1.3). From a survey of vegetation types and their

distribution across a hillslope sequence from the wadi up onto the remnant terrace, Shanan found more moist-region plants on the stony steeper slopes indicating a humid soil-moisture regime, a result of the higher infiltration rate and poorer runoff performance. These observations focused attention on the shallow stone-less slopes (generally termed loessial) as major runoff producers under the prevailing climatic regime.

Table 1.1 Percentage Annual Runoff on Shanan's Plots

Plot (% slope)	% Annual Runoff
1	26
10	22
20	11

Table 1.2 Mean Rainfall Threshold Depth Before Runoff (mm)

Plot Type	10%	20%
Stony (40%)	3.0	3.3
Stone-less (0%)	2.4	2.8

Table 1.3 Mean Rainy Season Infiltration Rates ($mmhr^{-1}$)

Plot (% slope)	Initial	Final
1	28	9
10	21	9
20	25	12

To explain his findings, Shanan (1975) defined the infiltration processes operating on stone-free and stony slope surfaces, and contributing to the observed characteristics between cleared (stone-free) and un-cleared plots. Infiltration into a bare surface is said to be determined by the crusting characteristics. Soil aggregates are broken down, a crust is formed with the displacement of trapped soil air prevented. Infiltration drops to a constant relatively small value equal to the hydraulic conductivity of the crust. On the stony soils, stones serve as pressure valves allowing trapped air to escape beneath them. The covered portion of the soil is prevented from sealing, water moves both vertically and horizontally into and around the perimeter of the stones. When the crust becomes more and more saturated, the crust flows and seals the vesicular escape routes around the stones. Shanan assumed this value to be equivalent to 8-10 mm of rainfall. If rainfall continues past this threshold, runoff will be approximately equal to that of the stone-free surface.

Consequently, Shanan identified the loessial slopes as being the most effective surface water and runoff producer within the range of observed plot conditions. Experiments with micro-catchments established on loessial plains of crusted, low-gradient slopes showed the effectiveness of this slope type for runoff production, although the performance depended on the size of the micro-watershed, with

productivity negatively related to size. The importance of the loess was supported by a study of the literature concerning crusting characteristics in clay-rich soils (McIntyre, 1958ab. Hillel, 1960. Farres, 1978). Without directly analysing runoff production on slopes greater than 20% or those outside of the location where his plots are situated, Shanan extended his general findings of negative relationships between runoff productivity and slope gradient and percentage stone-cover to class those steeper, stonier, rougher slopes in the Avdat catchment as poor producers.

1.5.2 The Role of Rocky Slopes

In a series of papers during the 1970s and 1980s, Yair and his main associate author, Hanoch Lavee studied arid hillslope processes of runoff generation and sediment transport in three main locations in Israel; the extremely arid slopes of the Nahal Yael catchment in the Sinai south of Eilat, the badland slopes of the Zin Valley and the first-order drainage basin of the Sede Boqer research watershed, both in the Central Negev Highlands some 8 km north of Avdat (see location map Figure 1.1) (Yair and Lavee, *et seq*). Yair and Lavee specifically focused on the spatial variability in process characteristics and the controlling factors of precipitation intensity and surface material variations.

In the arid extremes of the Sinai, on a debris-block scree-slope environment, Yair and Lavee (1976) observed water rapidly flowing off large blocks, concentrating on small patches of soil in depressions, rapidly exceeding their infiltration capacity. They found a positive relationship between runoff yield and grain size composition of coarse fragments in the stone percentage cover, since larger blocks allowed more concentration of water onto specific limited areas of soils. This was also observed in the relatively moist conditions at Sede Boqer in the Central Negev on the upper compartmented limestone slope section (Yair and Lavee, 1981). Bedrock and stones were seen by experiment with immersion tests to seldom infiltrate more than 1 mm equivalent of water into their surface (Yair and Lavee, 1976).

Yair and Lavee analysed rainfall and runoff relationships on the small compartmented slope sections of resistant rocky slopes, and weathered, loessial-colluvial slopes (Yair and Lavee *et seq*). They contrasted the relative runoff collected from a complete section, the upper resistant rocky slope, and the lower loessial-colluvial slope and concluded that the upper rocky slopes were consistently more productive and more flashy in their runoff generation than the lower soil-covered colluvial slopes.

On the upper slopes of Yair's compartmented plots, massive well-jointed limestones are fissured, with cracks filled with loessial soil of 10 to 15% clay content. The soil has a high absorption capacity, but an overall small surface area and volume. Bedrock cover is 60 - 100%. The addition of direct runoff from the bedrock to the rainfall on these soils resulted in relatively large soil moisture stores and rapid runoff generation. This is illustrated by the large volumes of outflow recorded at the

truncated upper profile compartment foot, and the presence of a plant species distribution characteristic of more humid climatic zones (Yair and Danin, 1980).

On the lower colluvial slopes, the ratio of bedrock and rock fragments to soil cover decreases to between 0-40%. Soil occupies a greater surface area, and with generally deeper profiles, occupies a larger volume. Since the morphology is less rough, compared to the ridges and depressions of the fissured limestone, surface water distribution is more uniform across the surface. Consequently, greater volumes of water were infiltrated although the moisture content per unit volume of soil was relatively low. These conditions were illustrated by the small volumes of outflow recorded at the truncated lower profile compartment foot, and the presence of a plant species distribution characteristics of more arid zones (Yair and Danin, 1980). Flow lines traced with dyes during natural and simulated rainfall events showed flow discontinuity along this hillslope section.

Yair and Lavee (1985) summarised the response from their complete and compartmented hillslope section using the aggregated results from rainstorms during the period 1975 to 1979;

Table 1.4 Frequency and Magnitude of Runoff Events at Sede Boqer 1975/76 - 1978/79

Plot	Plan Area m^2	Length m	Gradient %	Flows	Discharge l	Productivity l m^{-2}
A whole	439	63	27.4	40	5149	11.7
B colluvium	307	34	28.3	36	4084	13.3
C rocky	161	33	27.0	65	5348	33.2

Table 1.5 Infiltration Rates on Yair's Compartmented Hillslope (mm hr^{-1})

Plot	Initial	Final
B colluvium	25	13
C rocky	8	0

The presence of distinct bands of runoff-productive and runoff-consumptive slope units within a hillslope sequence was an inhibiting factor for continuous downslope Hortonian flow generation, and a direct cause of the Contiguous Area Contribution. Citing the Nahal Yael research watershed in the extremely arid Southern Negev, Yair and Lavee (1985) showed the scale effects on generative performance with the runoff-precipitation ratio falling from 36% to 4.4% when considering a 50,000 m^2 watershed compared to the 580,000 m^2 watershed of which it is part. Up to 70% of runoff events measured in the former failed to become outflow of the latter. The response at Nahal Yael was partially explained by infiltration losses increasing downstream as a result of increasing channel and slope width, and alluvial and colluvial thickness. The rainfall and its spatial variation was a major control although the spatial variability in runoff processes was of a greater order of magnitude, mainly controlled by high variability in surface properties (Yair *et al*, 1980c). In the Zin Valley Badlands, the main controls were

said to be the distribution of particular surface materials, and in Sede Boqer, the juxtaposition of productive and consumptive slope units of differing material characteristics.

Yair and Lavee (1981) explained the apparent partial area response characteristics on the arid limestone hillsides of Sede Boqer by the fact that;

1. there were high infiltration losses in the lower colluvial part of the slope,
2. the rain-showers were of short duration and runoff generated upslope did not have enough time to reach the slope base before cessation due to low velocities and shallow depths (Yair and Lavee, 1981b).

Yair focused on the key role of differential infiltration, somewhat ignoring the importance of surface water routing and in particular the shape of surface flow (concentrated or dispersed) and the speed of surface flow. These determine in combination with infiltration the volumetric discharge and transmission losses that can be expected from a particular hillslope or combination of hillslopes as explained below.

Given the variety of controlling influences on runoff generation cited by Yair and Lavee in the above catchments, all of which are sub-sets of the arid zone regional characteristics, from rainfall to surface materials to material-type juxtaposition, the overall picture of conditions within the region is far from homogeneous and requires clarification.

1.5.3 The Negev Runoff Generation Debate and its Significance for Water Harvesting

Leslie Shanan indicated the shallow, loessial slopes to be the most important contributors to storm-channel runoff. From studies at the Avdat Experimental Runoff Farm, Shanan concluded that;

> "daily runoff was found to vary inversely with hillslope angle...related to differences in the mantle factors...on steep slopes, soil cover is only a few centimetres deep and the surface generally covered with large stones...gentler slopes are covered by a continuous soil mantle tens of centimetres deep" (Shanan and Schick, 1979, page 275).

Shanan stressed that the loessial soil slopes were the most productive for runoff, runoff productivity being said to be positively related to the extent and depth of loess soil cover, and negatively related to slope gradient. Rocky slopes were shown to be poor producers in comparison.

Conclusions made by Yair and Lavee cited the steep, rocky slopes as the dominant runoff producer. Yair and Lavee, from their studies at the Sede-Boqer Experimental Watershed eight kilometres further to the north, reported that;

> "runoff frequency and magnitude are positively related to the extent of bedrock outcrops and negatively related to the extent and depth of soil cover...the slope angle and stone cover factors play a minor role" (Yair, 1983, page 298).

Loessial soils in the form of colluvium and alluvium were said to be consumer slopes, particularly when sited downslope of a rocky producer slope section.

These two interpretations of storm-flow generation in the Central Negev Highlands appear to give rise to a dichotomy in the understanding of the local rainfall-runoff relationships. Both support the partial area contribution approach, but from opposite ends of the geomorphological spectrum. Shanan argued that only those areas adjacent to channels that are gentle, continuous loessial crusted slopes will contribute during the majority of rainfall events experienced in the Central Negev Highlands. These tend to be the floodplains adjacent to natural channels subject to alluvial deposition of loessial material, or isolated sections of palaeo-fluvial terraces mantled with aeolian deposits (Shanan, 1975). Yair and Lavee argued that these slopes are in fact barriers to storm-flow contribution having higher infiltration rates and less effective flow transmissivity than the steeper rocky slopes below which they tend to occur (Yair and Lavee, 1985, Yair, 1983). Only where runoff characteristics are sufficiently favourable for the upper slopes to make up the infiltration deficit on the lower slopes through their knock-on effect of run-on (more likely during the higher intensity and longer duration rain events), or where rocky slopes occur directly adjacent to channel sections will contribution to channel storm-flow occur.

This dichotomous situation has both researchers crediting their favoured environments with a quicker response to lower rainfall thresholds, and with more effective transport of overland flow. Shanan dismissed rocky, stony hillslopes as poor producers, Yair dismissed stone-free loessial slopes as poor producers. However, since neither study quantified their terminology of 'rocky' or 'loessial' relative to the other or to the range of environments throughout the various hillslope sequences of the complex Negev catchments, and since each relied heavily on the use of site-specific plot studies held to be 'typical' of the areas geomorphological character, interpreting these results in the light of the relative heterogeneity of the Avdat catchment is difficult. The apparent contradictory nature of the two studies has been strengthened by a recent paper by Aaron Yair, interpreting the ancient water harvesting systems in the light of the Sede Boqer findings, and directly contending the Shanan interpretation.

In his 1983 paper on the areal distribution of ancient agricultural systems in the northern Negev desert, Yair specifically addressed the controlling factors behind the presence of extensive, ancient, sophisticated agricultural systems based on the harnessing of surface runoff water. Yair stated that previous studies by Evenari *et al* (1982) and Shanan (1975) had emphasized, through the development of a nomogram of drainage area, slope angle and stone cover against runoff yield, that runoff yield decreased with slope angle and stone cover, and the effect of clearing stone cover from a surface was to generally increase runoff yield by 24%. From this and other conclusions related to the positive effect of continuous loessial soil cover, Evenari *et al* hypothesized that the crusting character of loess soils enabled the ancient farmer to harvest water from the hillsides under the low rainfall desert conditions. Yair considered the Evenari nomogram to reveal a serious problem since, for example, no runoff should be expected from catchments up to 1.5 ha for annual rainfalls less than 60 mm if slopes exceed a mean of 20%. Lower annual rainfalls than these had been recorded 5 times at Avdat since 1962 and yet runoff had resulted from the steepest sub-catchments.

In his 1975 thesis, Shanan presented the following explanation concerning the design of water harvesting systems using extensive lengths of artificial ditches routing across and down often steeply sloping hillslope sections to the wadi terraces;

> "Areas with moderate slopes have relatively low infiltration rates and are the principal contributor to runoff. These areas lie adjacent to the wadi's or on the high plateaus. This explains why ancient farmers constructed ditches up to 5 km in length to transport runoff from the high plateaus to the terraced fields in the wadis (page 98)"

Yair could not agree with these statements. He pointed to the fact that on the broad sweeping plains of the Hovav plateau 50 km to the north of Avdat and Sede Boqer, where annual rainfall was twice that of the Avdat region, no evidence of the wadi terraces, and hillslope channels that characterise the ancient agriculture could be seen. Presenting plates similar to those of C.2 and C.3 he suggested that rather than harvest from the loessial slopes, the ancient ditches collected water mostly from the very steep slopes, with shallow and stony soils which should, according to the Shanan theory, be poor producers of runoff.

Making the basic statement that the Negev Highlands could be characterised by two major slope units with different hydrological response; the colluvium of the lower profile and the rocky topslopes, Yair presented a case as to which was likely to be the most efficient producer of runoff water using his catchment studies. Plot sprinkler and slope sprinkler experiments, coupled with observations from rainstorms led Yair to conclude for his Sede Boqer slope profiles, that a rocky slope responded more rapidly to rainfall than a colluvial slope. Soils analysis from the upper and lower slopes also showed a reverse trend, with leaching increasing downslope on the bedrock slopes, but decreasing

downslope on the colluvial slopes. Soils on the loessial Hovav plains to the north were less leached than in Sede Boqer, suggesting less surface water enters the soil.

Yair stressed that Shanan failed to credit the determinant role played by massive bare bedrock outcrops and the duration of rain-showers. He criticised Shanan for emphasizing the role of loess and loess crusts. He stated that runoff frequency and magnitude were positively related to the extent of bedrock outcrops and negatively correlated with the extent and depth of soil cover. He supported this with data from Sede Boqer presented in Table 1.4 earlier. He suggested that the ancient farmers apparently preferred to collect from the steeper slopes because of this. Rain-showers were generally short and so runoff generated upslope could not reach the slope base. Thus, in Yair's opinion, most ancient artificial ditches begin on and cross the rocky part of the slope in order to collect the water that was more frequently generated here and not solely to transport water from more remote loessial regions. This was the reason for the existence of extensive agricultural systems based on the harvesting of runoff water only in the Negev Highlands between Sede Boqer and Mitzpe Ramon (see Figure 1.1), and their absence further north where annual rainfall is twice as high but the landscape dominated by sweeping loessial slopes which should, according to Shanan's theory be most suited as supply areas.

1.5.4 Reconciling the Shanan and Yair Interpretations of Negev Hydrology and Water Harvesting

There are two main areas which must be examined;

1. the degree to which Yair's and Shanan's interpretations are in direct conflict,
2. the significance of their findings for the Avdat and other water harvesting systems introduced to the Negev.

The first point that should be made is that the range of slopes analysed by Shanan are not representative of the majority of slopes contained within the catchment. The aerial photograph Plate C.1 shows that the analogous slope areas occupy only a small proportion of the catchment to the west of the wadi drainage network. Shanan concentrated on only a small range of the slope conditions within the Avdat system rather than sample more widely the spatial variability known to occur along catchment flow-lines. Additionally, rather than sample conditions on a slope section of a given type, e.g. stone-free colluvial slopes, Shanan created the surface type by stone-clearing. From these plots, Shanan made wider inferences concerning the relative characteristics of stony and stone-free soils. These inferred results cannot be justified in terms of natural catchment conditions for two reasons. Firstly stone-free slopes of the same gradient and geomorphic position, mid-way down a sequence from terrace to wadi are not naturally occurring and hence the results are not applicable. Secondly, the process of clearing changes significantly the hydrological characteristics of the surface and therefore the

process response only relates to this specific action and cannot be used to infer similar process characteristics for stone-free and stony soils in general.

Shanan derived values of infiltration, soil crust saturation requirements and overland flow losses from best-fit values based on daily rainfall-runoff simulations for the plots. To assess the nature of the catchment response using a deterministic-stochastic model, Shanan applied these results on the basis of a weighting function determined by the proportion of the sub-catchment above or below the 5.7° slope gradient. The percent below 5.7° was equated with the characteristics of that plot, and the percent above was equated with the characteristics of the 11.3° plot. This produced an inappropriate generalisation of the catchment which was further complicated by the adoption of certain assumed frequency distributions of infiltration rates and other hydrological features such as overland flow lengths. Considered in the light of the important role played by spatial variability and the exact positions of one slope type relative to another such a model cannot hope to provide any detailed information about the true internal character of the response, even though observed-predicted correspondence may be high. Applying the best-fit parameters using hydrological values weighted to the assumed 5.7°-11.3° characteristics of the various sub-catchments, Shanan overestimated observed discharge from 30% to 100%. The differences, rather than reflecting the lumped and stochastic nature of the model data were held to have direct physical significance, the un-attributed factor being the channel losses in the natural network and artificial ditches in each sub-catchment. These were calculated to be roughly 0.03 m^3 to 0.06 m^3 per metre length of channel depending on the residual volume between observed and predicted discharge. This was equivalent to the abstraction of 50-100 mm of direct rainfall into the channel perimeter. Since the fits were generally better for sub-catchment five, one of the three sub-catchments that make up the eastern slopes (see Appendix 3.1), an explanation was developed for the difference also using the channels. Since the disparity for sub-catchment five worked out at less than 0.01 m^3 per metre of channel, this was explained as being due to the gradient of the ditch collecting from sub-catchment five being generally greater than 1.7° (3%), and therefore less-prone to losses than the other six sub-catchments whose channels are generally less than 0.57° (1%). Since subcatchments four and six have equal and steeper sloping channel sections than five, and also since the current study has measured bed-gradients in excess of 0.57° at most points in the catchment, this cannot be logically accepted as anything other than a convenient calibration factor designed to improve prediction, but having no acceptable physical basis.

Taking Shanan directly, the combination of assumed channel losses and the explanation for the introduction of channels quoted earlier must be seen as a self-contradiction. If the loss to the channels averages at 0.04 $m^3\ m^{-1}$ then a 5000 m long channel constructed to harvest and transport water from a remote loessial plateau would require 200 m^3 of water just to satisfy the transmission losses. Thus the idea that the midslopes make no significant contribution, with channels designed to just transport water from the distant plateaus cannot be readily accepted in the light of the model results or the plot

inferences, since the plots are not comparable with a large proportion of the hillslopes adjacent to the channels along their course (for instance those on the eastern hillslopes).

It appears that Yair focussed on the terminology of Shanan without considering the differences of that terminology from his own. Yair also generalized broadly from his instrumented hillslope to the whole Central Negev Highlands without a quantifiable basis for these generalizations. He assumed the general form of Central Negev hillslopes to be made up of rocky topslopes and colluvial foot-slopes whereas the picture is more complex than this simple division suggests, as has been shown by other studies he has already undertaken elsewhere in arid Israel, and as is evident in the more spatially variable, morphologically diverse catchment at Avdat.

The concentration of Yair and Shanan on two particular slope environments has failed to explain adequately the response characteristics of a whole series of surface material types and forms that lie between the two possible extremes of bare bedrock scarps on the one hand, and uniform loess crust horizontal planes on the other. Furthermore, they have neglected to define their terms in anything but a loose descriptive manner in that one is left wondering exactly how rocky, or how loessial a particular slope has to be to be categorised according to each theory? The question must be asked, are Shanan and Yair talking about the same types of slopes when they refer to rocky and loessial? The answer must be no if one directly compares the plots of each. Yair's pair of rocky topslope and colluvial foot-slope have average gradients of 15.1° and 15.8° respectively, putting them outside the range of Shanan's plots which are all less than 11.3°. From qualitative observations made by the author at Sede Boqer, and looking at Yair's percentage bedrock cover distribution (Yair, 1985), relative to Shanan's (1975) it is clear that Yair's rocky slopes do not equate with Shanan's. Additionally, Yair's colluvial loessial slopes are not similar to Shanan's stone-free loessial soils which generally refer to wadi-bed or plateau surfaces, both of which are absent from Yair's divided hillslope.

Each picked out different environments as being important for runoff production and the support of continuous downslope flow conditions. The producers are the loess slopes and the rocky slopes. Each gave proof that they both have the potential to contribute. The two interpretations of runoff production appear to show some real variations in runoff productive ability.

Instead of taking Yair and Shanan's work as direct contradictions it must be accepted that they are in fact considering different elements of slope systems that are not mutually exclusive and may indeed occur along the same flow-line depending on the scale and the homogeneity of a given location. For the Avdat system, both sets of slope types are present within the divides, the Yair-type slopes where resistant limestone outcrops, and the Shanan-type slopes in the wadi depression, to the west and on the remnant Zin terrace. This can be seen clearly in the oblique photographs Plates C.2 and C.3.

The theories concerning the relative runoff production are therefore not mutually exclusive when considered for interpretation of the Avdat catchment runoff response to rainfall.

Shanan's findings are to some extent site specific due to his surface treatments and the location of the plots. However, it is likely that he identified some real differences between the narrow range of slopes he considered, and it is generally accepted that crusted loessial soils can be efficient producers of water in particular conditions, as supported in a large number of laboratory and plot studies (Agassi *et al*, 1985 ab, 1986, Morin *et al*, 1981. Zarmi *et al*, 1983. Hillel, 1960).

Although Yair considered a complete hillslope section, the degree to which the results can be generalised into geomorphological principles are somewhat limited. Yair and Lavee (1985) stressed the representative nature of their Sede Boqer instrumeted catchment and in particular the relevance of results for the interpretation of the controlling factors on why runoff farms successfully function in the Central Negev Highlands (Yair, 1983). Many water harvesting systems are associated with much large scale catchment systems which generally have more extensive and complex hillslope profiles. This renders the two-part division into rocky and colluvial slopes obsolete and they become only a small sub-division of a longer flow-line. This is significant in terms of the sequencing of consumptive and productive slopes and the pattern of Contiguous Area Contribution relative to channel lines.

The second of Yair's conclusions as to why ancient agriculture is located solely in the Central Negev Highlands surrounding Avdat is circumstantial. It developed from two main observations, the first concerning the absence of ancient water harvesting in an area in which steeply sloping stony or rocky slope units are not present, the second concerning the apparent processes in that environment. Because the Hovav plateau to the north of the Central Negev Highlands does not contain ancient agricultural remains even though the rainfall is higher, and because the area is dominated by sweeping loessial areas held by Yair to be synonymous with the kind of slopes suggested by Shanan as a requirement for such systems, Yair dismissed the importance of such slope environments. However, this is taking both the loessial slopes described by Shanan, and the ancient agriculture outside their respective contexts. Pedalogically, geomorphologically, and hydrologically, there are significant differences between the loessial slopes of the Central Negev Highlands and those to the north. In the Central Negev, the soils are generally fluvially redistributed loess, hence the term 'loessial' (Yaalon and Dan, 1974), and thus possess different sediment size distributions and mineralogy, with a larger proportion of calcareous fines compared to the more sandy structures to the north. They also tend to be of a smaller scale, incised by ephemeral channel development which results in generally short overland flow paths. Although they may have initially high infiltration rates, once a threshold is reached after which they generate rainfall excess, and once their relatively high detention storage has been overcome, they are likely to be important contributors of runoff due to their often large surface area relative to isolated rocky slopes at the top, or midway down valley side-slopes. The short overland flow paths to

natural and artificial channels compensates for the poor transmission characteristics of these slope environments where runoff is slow and storage is high. This partially explains why such low volumes of runoff will be experienced in the low-drainage density, extensive loess plains elsewhere in the Negev used by Yair to illustrate why loessial valley bottoms or isolated plateaus should not be productive.

The soil observations used by Yair are not substantiated. The evidence of reduced leaching of the Hovav plateau soils relative to those at Sede Boqer took no account of the inherent differences between the two soil types, or their hydrological positions. For instance, a given volume of water infiltrating the stony matrix of the Sede Boqer soils, compared to the more homogeneous loess of Hovav, is distributed through a much smaller soil volume, allowing deeper penetration.

Finally, a purely physiological distinction between areas with water harvesting and without water harvesting remains takes no account of all the additional influences responsible for the concentration of water-harvesters in the Negev Highlands which include political (the presence of distinct 'nations' of people in the densely populated Mediterranean basin), constructional (the ease of availability of building materials), socio-economic (location along direct trade-routes between the Trans-Jordan, the Red Sea and the Mediterranean sea-ports) and historical (the adoption of similar practices by successive Roman and Byzantine settlers in the region following the initial development by the Nabateans) (Evenari *et al*, 1982).

1.5.5 Contiguous Area Contribution and Avdat Water Harvesting

One of the various methods used to supply runoff water to agricultural terraces constructed on wadi floodplains was to modify the natural flood routing system by the construction of hand-dug ditches, positioned at strategic locations down the hillslope profiles to often increase the available drainage area for a given site as shown in Appendix 3.2 and 3.3. The ditches greatly reduced overland flow lengths promoting a shorter channel route down generally steeper gradients into the farm (Lee, 1985). The critical factor controlling the flood generation from a catchment modified in this manner is, as suggested by the term Contiguous Area Contribution, the relationship between the artificial ditches, the natural channels, and the hillslope areas they drain. In the specific context of the Avdat system, this involves a consideration of both the Shanan and the Yair environments. Yair pointed to the existence of artificial ditches constructed up onto the rocky topslopes, Shanan to the ditches harvesting the gentle loessial foot-slopes or loess-mantled remnant wadi terraces. To determine their relative importance, both the local runoff production characteristics of a particular hillslope area (the site conditions) responsible for surface water generation, and the position of the area within the hillslope and channel routing system (the hydrological situation) must be analysed.

It would seem that Yair's rocky hillslopes are only significant for the majority of rainstorms because of the presence of the artificial ditches. Although they may have a knock-on effect, it can be expected that in an unaltered catchment runoff production would be predominantly from the loess-filled wadi-bed and armoured interfluves adjacent to the natural channels.

In terms of the Avdat system, illumination of the true nature of the catchment hydrological characteristics responsible for storm-flow output involves an understanding of the internal mechanisms of runoff production and transmission responsible for the observed relationship between rainfall inputs and runoff outputs. This requires knowledge of the spatial distribution of physical parameters and process variables controlling the generation and movement of surface water across the hillslopes and through the channels and a physically-based modelling approach parameterised from direct field measurements in a distributed manner. Lumping characteristics, in a manner similar to Shanan's runoff model is too restrictive. The critical producer, transmitter and consumer slopes need to be identified and quantified for the catchment as a whole.

1.6 THE DISTRIBUTED MODELLING APPROACH

A distributed model is one in which realistic parameters are allowed to vary in space and time as functions of (x, t) through the use of physically-based measurements within a computational framework designed to represent the original process arrangement and magnitudes as closely as possible. Separate entities are defined within the model and related by process sub-models that simulate the changes in state through time in a dynamic manner. It differs from a lumped model which does not seek to preserve the individual characteristics of particular model components but treats them as generalizations with an assumed statistical distribution of characteristic features.

The distributed, physically based catchment model can account for hydrologically effective changes in catchment characteristics, both natural and man-made, since its parameters can have direct physical interpretation, and their range can be established reasonably well from field and laboratory investigations, as well as with certain remote techniques (Beven and O'Connell, 1982). Its main advantage lies in its ability to allow the determination of the effects of the routing patterns of discharge from the source area on the final distribution of basin outflow (Beven and Kirkby, 1978). By varying fluvial system geometry, system properties, initial conditions and rainfall rates and patterns within a working, distributed model it is possible to demonstrate a whole range of watershed responses. Distributed models can attempt to cope with the non-linear and spatially variable response of catchments, both within and between storms (Beven and O'Connell, 1982).

Since the objective is to identify the dynamic character of likely productive, consumptive and transmissive zones within the water harvesting system controlling the Contiguous Area Contribution,

the ability to identify and quantify the efficiency and productivity of each component is a pre-requisite. Thus specific locations, must be given an identity which allows the calculation, retention and presentation of information directly relevant to these requirements.

It is clear from a knowledge of the arid-lands hydrological cycle and Contiguous Area Contribution that a successful distributed catchment model requires information on the following hydrological and hydraulic parameters and variables;

1. the hillslope surface configuration in the three spatial dimensions of (X, Y, Z) (form factors macro-scale),
2. the channel network configuration in the same (X, Y, Z) coordinate reference (form factors macro-scale),
3. the spatial and temporal characteristics of the inputs to the catchment; the rainfall patterns across (X, Y, Z) and through t (process factors meso-scale),
4. the spatial and temporal distribution of infiltration values throughout the rainfall-runoff duration (process factors meso-scale),
5. the spatial distribution of the physical parameters controlling flow routing; hillslope gradient, micro-topography (form factors micro-scale) and flow resistance (process factors meso-scale), and channel bedslope, cross-sectional dimensions (form factors micro-scale) and flow resistance (process factors meso-scale) at selected locations.

The current approach represents the Avdat water harvesting system through a spatial distribution of the dominant process controls, using a broad unit classification, a direct application of field plot data fine-tuning the unit classes, and a fine time-space mesh of observed flow-lines and variable or constant small time increment steps. This is explained in detail in the following chapters.

1.6.1 Features of Distributed Models

It is the opinion of Beven and O'Connell (1982) that a whole plethora of catchment models exist. Indeed, a perusal of the hydrology journals of the last twenty years shows there is a number of distributed simulation models of one or more components of the basin hydrological cycle. The models vary in size, programming structure and hydrological emphasis, depending on the object of their application and the environment in which they are operational.

Kibler and Woolhiser (1972) state that a distributed model needs the following features;

1. a basis on sound physical reasoning,
2. model parameters of direct physical significance,
3. a solution that is numerically accurate,
4. results that are subject to experimental verification,
5. an uncomplicated computational structure with no difficult programming logic.

Using the most appropriate techniques and by adopting a staged development in which the model is constructed at increasing levels of complexity from the small plot simulation, through to the complete catchment, using a range of input conditions, the numerical techniques are tested before they are applied to the catchment scale, and some of the sensitivities of the model can be determined.

Woolhiser defined a general modelling methodology;

> "In order to apply the equations describing overland flow to complex watersheds to better understand watershed response or to make predictions several decisions must be made. First, a decision must be made regarding the method of spatial representation of the watershed. Then the user must decide on the form of the hydraulic resistance law and the infiltration law and must estimate several key parameters. Finally the user must select appropriate numerical methods for solving the equations"
> (Woolhiser, 1981, page 196)

The difference between the current and former models is the relatively fine spatial resolution with which the model works. This is required to simulate an arid-catchment in which a high degree of spatial variability in form and process characteristics can be identified as the controlling factor on storm-water hydrograph size and shape. Previous models relied on a greater degree of spatial lumping (for example the model discussed by Loague and Freeze, 1985), a smaller number of separate elements, and subject catchments of a markedly lower structural complexity but a more complex hydrological cycle, usually the humid or temperate types. It is only recently that model simulations have been undertaken to answer specific questions concerning the internal operations of the basin hydrological cycle and its component structure.

In the arid environment, where spatial variability in runoff production is great over small distances, it is important that the scale of resolution should be intra-hillslope and intra channel-branch. At Avdat, where the relative positions of particular areas and the channel network to which they drain are critical, the model must be capable of operating at this level. In addition, the temporal resolution of

the model simulation is important, both for the maintenance of computational stability required by the numerical solutions to flow, and for the representation of the processes at the appropriate time-scale.

The more variable the physical character of the catchment, the more detailed the model must become or the lumped nature of the model must be accepted. In view of some intricate site-specific questions asked in this research, the complexities of the physical structure of the subject with widely varying sub-catchment drainage patterns, and the insignificant role played by sub-surface conditions in flood generation an original model for the Avdat system is produced. Before going onto these issues, however, a brief review of some models already developed for hydrological studies in the Negev are presented, in the light of the obvious need for a distributed, physically based approach in this environment.

1.6.2 Existing Hydrological Models of Negev Catchment Systems

This model is the first to adopt a physically-based, geometrically distributed, deterministic approach to Negev catchment hydrology. Previous attempts towards application of results from the Avdat and Sede Boqer studies on a more general basis have been made through the development of three models designed to simulate runoff through the prediction of discharge equal to observed rates (Yair and Lavee, 1985. Lavee unpub., 1985. Karnielli *et al* unpub., 1985. Shanan, 1975).

1.6.2.a Shanan's Avdat Runoff Model

In his 1975 thesis, Shanan applied the results of his plot experiments and thirteen years of Avdat hydrological records to the determination of the effects of several hydrological and geomorphological characteristics on runoff production from basins of various sizes. Using a lumped probability-distributed model (see the definitions of Clarke, 1973) similar to the Stanford Watershed approach (Crawford and Linsley, 1966), Shanan attempted to determine the effects of the areal distribution of rainfall, infiltration rates, slope angle, stone cover, overland flow and channel flow losses on runoff output from different catchments. Using statistical distributions based on the ranges of values from his small plot studies, Shanan applied them to the Avdat catchment on a proportional area basis using the percentages above or below the hillslope gradient of 5.7°. The daily rainfall inputs were then subject to the various loss procedures subtracting crust saturation deficit and the predicted range of infiltration rates to produce a best-fit response between observed and predicted hydrographs.

Shanan simulated daily runoff and rainfall relationships with considerable accuracy. However, as Shanan admits, his model cannot explain the nature of the true hydrological relationship through time and space during a rainstorm that is responsible for the observed output characteristics (Shanan and Schick, 1979). Shanan states that it was not possible to fully understand the hydrological system

comprising the Avdat catchment because the differential effects of hillslope area and hillslope gradient could not be separated out (Shanan and Schick, 1979). The net result is a lumped model which seems to reproduce quite accurately the measured input-output relationship of the Avdat system, but which details little concerning the true internal character of the runoff generative process. Over-estimates of runoff were accounted for by using a calibration factor to represent unattributed channel losses. The inability of Shanan's lumped approach to understand the complexities of the system prevents the management considerations of how well the current system functions, why it functions and how different system configurations might function? from being addressed.

1.6.2.b The Karnielli *et al* Statistical Approach

An unpublished modelling attempt by the Hydrology section of the Desert Research Institute of the Ben-Gurion University of the Negev, used the Avdat hydrological record in an attempt to determine catchment design criteria for water spreading check dams called 'Limans' (Karnielli *et al* unpub., 1985). The model conforms to Clarke's "stochastic-empirical" classification, and considered the partial area contribution phenomena in deciding the size of catchment area required for a given check dam size. It did so by using a lumped approach relating average annual rainfall and catchment area to predict runoff yields per annum using a linear regression function.

$$N = 12.3\ Area^{-0.4} \qquad \text{Equation 1.1}$$

(where N is the runoff efficiency, and Area is the size of contributing area in hectares).

The model has not, to the author's knowledge, been applied in any empirical studies. Again, whilst quite possibly producing a good fit between observed input and output values for known catchment areas such as Avdat, such a model could say little about the temporal and spatial variability characteristic of the runoff generation. Unless the physical characteristics of the sites chosen for suitability tests are the same as the systems used to parameterise the linear function, little benefit can be gained from such an approach in an assessment of system design and performance.

1.6.2.c The Lavee Theoretical Model

Through their more detailed hillslope studies, Yair and Lavee began attempts at process model development using findings from their Sede Boqer experimental watershed. Given an awareness of the limitations of lumped model approaches to a simulation of the nature of rainfall-runoff relationships, Lavee made the first steps towards producing a deterministic, distributed model of runoff response across their two-sector experimental hillside (Lavee unpub, 1985).

The Lavee model used a Hortonian runoff approach to account for the influence of spatial variability of surface properties and rainfall characteristics on runoff generation and flow continuity. The model used a uniform-width cascade of hillslope planes representing an idealised hillslope in which each cell was allowed a different rainfall input, infiltration output and soil moisture storage characteristic. The model had no dynamic flow component in which depth and velocity are calculated from a knowledge of surface resistance and slope gradient. Instead, velocity was held constant at a theoretical rate (3 m min^{-1}, Emmett, 1970), and discharge was purely a function of infiltration excess. The model did not seek to account for the flow routing characteristics across a natural hillslope, but instead concentrated on the effects of slope length and rainfall intensity-duration on runoff generated from the particular slope length. This model was designed to present the field results of Yair and Lavee (*et seq*) who asserted that the spatial arrangement of infiltration values along a hillslope profile determined the partial area contribution in combination with the overland flow length to be covered, and the duration and intensity of rainfall.

Simulations varying slope length, rainfall intensity and duration produced the following table of values of runoff yield converted for convenience into the runoff from the whole plot in units of 1 m^{-2} (equal to the volume in litres divided by the length in metres and the constant width of 10 m).

Table 1.6 Runoff Yield in Litres Predicted by the Yair and Lavee Simulation Model (Yair and Lavee, 1985)

Rate $mmhr^{-1}$	3				6				9				12			
Mins	15	30	45	60	15	30	45	60	15	30	45	60	15	30	45	60
Depth	.75	1.5	2.2	3	1.5	3	4.5	6	2.2	4.5	6.75	9	3	6	9	12
Length																
15 m	0	0	0	0	0	0	0	0.61	0	0	68.6	247.9	0	66.7	322.1	636.3
30 m	0	0	0	0	0	0	0	0.61	0	0	111.4	469.2	0	101.2	610.2	1242.3
45 m	0	0	0	0	0	0	0	0.61	0	0	132.2	664.1	0	110.5	864.6	1818.6
60 m	0	0	0	0	0	0	0	0.61	0	0	136.7	833.0	0	110.5	1085.9	2366.2
75 m	0	0	0	0	0	0	0	0.61	0	0	136.7	976.0	0	110.5	1274.8	2883.6
90 m	0	0	0	0	0	0	0	0.61	0	0	136.7	1093.7	0	110.5	1402.1	3372.4

Table 1.7 Runoff Yield in Litres (and mm) per Square Metre of Surface Area Predicted by the Yair and Lavee Simulation Model (Yair and Lavee, 1985)

Rate $mmhr^{-1}$	3				6				9				12			
Mins	15	30	45	60	15	30	45	60	15	30	45	60	15	30	45	60
Depth	.75	1.5	2.2	3	1.5	3	4.5	6	2.2	4.5	6.75	9	3	6	9	12
Length																
15 m	0	0	0	0	0	0	0	0.004	0	0	0.457	1.650	0	0.445	2.147	4.242
30 m	0	0	0	0	0	0	0	0.002	0	0	0.371	1.564	0	0.337	2.034	4.141
45 m	0	0	0	0	0	0	0	0.001	0	0	0.294	1.476	0	0.245	1.921	4.041
60 m	0	0	0	0	0	0	0	0.001	0	0	0.228	1.388	0	0.184	1.810	3.944
75 m	0	0	0	0	0	0	0	0.001	0	0	0.182	1.301	0	0.147	1.700	3.849
90 m	0	0	0	0	0	0	0	0.001	0	0	0.152	1.215	0	0.123	1.558	3.747

Yair and Lavee's data set is interesting in that it shows there are distinct thresholds before which runoff will not be generated from any part of the hillslope surface, in this case equal to a depth between 4.5 and 6 millimetres. As this depth falls with increasing intensity, the time to runoff appears to reduce, suggesting runoff is intensity controlled, i.e. Hortonian conditions operate. Following ponding, the discharge out of the plot is related to the intensity. In this case it is because the velocity is held constant, therefore the discharge will be directly proportional to the difference between infiltration and rainfall rates, as is shown looking at runoff from the same rainfall depths for different intensities. The data-set shows also that the total discharge increases with the increased length (and hence area) of the plots but at a decreasing rate, as shown by the second table. The differences are not as marked as they might otherwise be since velocity is constant, and the decrease is a result of the proportion of runoff that is infiltrated in its passage downslope once rainfall ceases. This will increase as the length of the slope increases.

The data-set presented by Yair and Lavee, is not as sensitive to rainfall intensity and slope length as it might otherwise be if a more realistic parameter data-set was adopted and proper routing procedures used in which velocity is allowed to vary according to stage. The use of a single variable; infiltration, to account for the complex function between gradient, roughness and infiltration patterns in determining depth, velocity and discharge relationships simplifies the true character of the process. The infiltration curve is a lumped representation of the complete rainfall-runoff-routing process since it is derived from volumetric input, output data-sets from the instrumented hillslope. They neglected to consider that the stage-discharge relationship may be equally as important as varying infiltration in the determination of whether surface water generated at one location becomes runoff output to another, given the often short duration of rain events, and in a purely infiltration-based approach using areal average values, will be an unattributed factor (Wu *et al*, 1982). Since velocity is held constant, the

opportunity for infiltration will be ignored in favour of lumped abstraction volumes. The rate of movement and the volume of infiltration are inherently related and any realistic approach must account for this by modelling them both as dynamic characteristics.

1.6.3 The Distributed Approach and the Avdat Catchment

In an attempt to understand the nature of runoff production in the Avdat catchment and the role of the superimposed water harvesting routing network in providing flood water for the agricultural terraces, it is necessary to get both a clearer picture of the hydrological processes and physical parameters of importance in the catchment system, and to develop a method of analysing their relative contribution to runoff generation in terms of magnitude, space and time variation. Like in other research work to date, a modelling approach is required, but given the objectives of the research outlined in the introduction, none of the approaches so far attempted are really suitable. By adopting a distributed, physically-based deterministic approach, linked to an extensive program of field measurements it ensures a more sensitive and physically realistic selection and quantification of parameters (Dunne, 1983).

In terms of the physical processes contributing to the overall response of a catchment system during a precipitation event, the description of these runoff characteristics at many points in space and time requires complex simulation of interception, infiltration, and flow routing processes since without this, the timing and yield of runoff productivity from any system cannot really be determined (van Liew and Saxton, 1984). It requires knowledge of system geometry; slope length, bed slope, wetted perimeter versus flow area relations, and a suitable computation sequence (the arrangement of slope and channel elements), of infiltration, of flow resistance parameters, of storm characteristics; rain intensity and its areal distribution, and of antecedent conditions (Shen, 1976).

In terms of the hydrological sequence of runoff generation and routing, the model is required to perform a distinct series of process steps. It must determine the infiltration rate firstly from rainfall, then from rainfall and run-on, and finally from run-on alone if the slope and channel areas experience all three phases during the storm simulation. It is necessary to calculate the depths and rates of movement of water for each separate hillslope element or channel segment in a logical downslope and down-catchment sequence (conforming to the laws of gravity and the topological arrangement) for each time period of the simulation, since the inflow from one cell, and the outflow to another (and hence the depth remaining as surface storage) is a direct influence on the hydraulic activity during the subsequent time period. By reproducing these processes at the hillslope and catchment scale, the management and design aspects of water harvesting configurations can be examined by comparing and contrasting patterns and volumes of runoff production from different examples.

The sensitivity of the model to different rainfall, infiltration and flow parameters are examined and the runoff productivity from different catchment configurations are assessed. Hypothetical hillslope cascades, experimental run-on/runoff plots, actual cascades and complete sub-catchments from the Avdat system are simulated to produce a more detailed knowledge of the magnitude and pattern of process response in an arid catchment setting.

CHAPTER TWO REPRESENTING THE PHYSICAL SYSTEM

2.1 THE METHODOLOGY

A physically-based distributed model must tackle the complexity of the drainage basin if it is to represent observed conditions. The dimensions and arrangement of the catchment components must be represented as accurately as possible, since this provides the physical framework on which all processes act. Lumped model types can only deal with areal and temporal averages of hydrological phenomena and so wherever there is significant spatial and temporal variability a distributed model should be used.

For the simulation of a complete catchment model the boundaries of the system must be defined along with the internal arrangement of hillslope and channel components. The first step to building a distributed model is to define the spatial framework of the simulation subject and quantify the physical surface on which the hydrological processes act. This provides the slope gradient along both hillslope and channel flow-lines. The physical dimensions of size, shape, gradient and surface conditions together determine the volume of water input, the gravitational component of the surface flow, the resistances exerted against it and the length the surface flow must travel to the point of outflow. Since not every parameter can be quantified to the same spatial or temporal resolution, a hierarchical approach must be adopted, in which some parameters are distributed more sensitively than others. For those for which only a limited sample can be made, the higher resolution data-set can be used to determine representative areas or 'units' within the system as a basis for quasi-distribution of the more lumped parameters sets (Shen, 1976).

The parameter data-sets can be split into three categories; the macro-morphological, the micro-morphological and the process. The process data-sets are discussed more in the following two chapters, although the morphological characteristics important to the stage-discharge relation; the slope gradient, the flow boundary shape and the flow-length are discussed briefly here. This Chapter primarily illustrates how the physical surface is quantified. It provides a spatial framework with which sample information can be applied on the basis of the distribution of samples and representative units. Each model element is assigned the identity of the sample closest to it, and a unit class based on its position within the representative unit boundaries. The units are used to quasi-distribute parameters sampled at the lowest density; the infiltration and flow characteristics. These are discussed in Chapters Three and Four. The 127 hillslope and 254 channel samples distribute the flow-boundary shape information to the flow-net elements. This is clearly indicated for the hillslopes by the acetate overlays for the two catchment flow-nets in Appendices 3.2 and 3.3. For the channels, the samples are plotted on large flow-net maps and the correct values assigned to the relevant man-made ditch and channel sections. The flow nets provide a routing framework that can illustrate the pattern of runoff production and which can

be manipulated to examine the management and design aspects of water harvesting systems. The methodology is of general relevance to a variety of catchment systems and types but is illustrated with specific reference to the subject of this thesis, the Avdat Catchment and Water Harvesting system.

2.2 MACRO-MORPHOLOGY - CATCHMENT GEOMETRIC SIMPLIFICATION

2.2.1 Flow-line Simplification

Any catchment simplification aims to maintain flow patterns similar to those in the prototype watershed (Woolhiser, 1981). Dingman (1984) stated that in most models, flow paths that are relatively unimportant are simplified by combining them into a smaller number of idealised representative paths. In the literature, the identification and representation of these flow paths has mainly been attempted in three ways; regular gridding methods, kinematic cascade methods, and flow-net methods.

In an early paper, Huggins and Monke (1968) used a grid superimposed over a catchment topographic map, with the hillslope sections represented by the grid-squares within the watershed boundary, and the channel sections corresponding to the grid-lines most closely representing the original channel path. A computer calculated the slope gradients and orientation of each slope and channel unit and water was assumed to flow with the maximum overall slope onto the next unit. This involved a large degree of lumping, with key details ignored such as the presence of defined topographic highs within the grid squares, or a loss of drainage density as smaller channel-lines were excluded by the simple branching allowed by the grid-lines.

The kinematic cascade approach uses a number of planes of varied slope in a sequence of 'n' discrete elements to represent the flow-section parallel to flow-lines (Freeze, 1972). This method generally preserves more surface information, the form of the catchment dictating the arrangement of the elements rather than a uniform arrangement of grid nodes and so the cascade of planes generally has a greater resolution (Kibler and Woolhiser, 1972). Practical experience by Woolhiser (1981) has shown the choice of watershed configuration and manner of simplification to be a somewhat subjective process involving a combination of mathematical and manual manipulation. The geometric procedures and their characteristics were described in detail by Lane et al (1975), Lane and Woolhiser (1977) and Lane and Renard (1979).

A less-subjective simplification is the flow net approach. The surface of the catchment system is defined, measured and discretised using complex mathematical representation of three dimensional surfaces as opposed to the previous techniques which seek to simplify with standard geometric shapes. The catchment is sub-divided into a net of finite, non-uniform elements

interconnected by nodes. This method was adopted in the finite-element approach of Jaywardena and White (1977, 1979). The mesh relies on the fact that overland flow in the catchment is in directions orthogonal to the topographic contours. The flow-net method places no restriction on the number, shape or density of elements.

2.2.2 Some Examples of Surface Discretisation

The choice of discretisation method depends on the level of spatial variability and the level of geometric detail to be preserved along with the size and scale of the problem. This determines the required resolution of the model to accurately address the processes involved. It has been stated in Chapter One, how the scale of interest for water harvesting systems is the intra-hillslope and intra-channel branch variation of processes and their controlling parameters. Consequently, a relatively high level of resolution is required compared to many previous models presented in the literature.

When analysing within catchment characteristics determining the character of spatially variable runoff production, many workers have adopted the kinematic cascade approach. Kibler and Woolhiser (1972) extended the original kinematic routing concepts developed by Wooding and Henderson to handle complex watersheds by linking together strings of varying planes to channel sections as parallel sequences of hillslope cascades linked to sequences of channel cascades. Engman and Rogowski (1974) defined slope strips using pairs of flow lines drawn on a topographic map, splitting them into constant length Δx increments discharging into channel segments at the base of the strip. The increments were delineated by observable changes in bedslope or channel dimensions apparent on topographic maps. Kirkby et al (1976), adopted a similar strip formation as a base for their model using slope orthogonals (flow-lines) and contour intervals to define their flow-net which formed the spatial framework for all model calculations. Concerned with both surface and sub-surface flow-modelling, Freeze adopted the kinematic cascade for surface flow as a sheet across rectangular planes, coupling the surface flow domain to a groundwater domain through their common surface (1972, 1980). Lane and Wallace (1976) and Lane *et al* (1975, 1977, 1978) and his co-workers used a geometrical simplification of cascades and channels but took a more systematic approach to their discretisation of space into modelling elements. The cascades were simple planes and uniform slope channel sections as with the other kinematic cascade approaches, but since they represented the surface at a resolution less than the available topographic data of spot-heights, the discretised surface could be compared against the topographic data to determine a goodness of fit statistic for both channel and hillslope geometry. The coordinates of the known surface were compared against the coordinates of the predicted surface and the residuals used to determine how closely the original characteristics such as area, length, elevation, and so forth are retained. In each case, the modeller conditions the density of the net through the choice of orthogonal frequency and contour interval or other increment definition criteria.

2.2.3 The Method of Discretisation Used for the Avdat Catchment

Woolhiser (1985ab) stated that there is no objective method of selecting the network of planes and channels used to represent the catchment. He suggested the most convenient approach is to mark out the channels on a working map and then sketch lines at right angles to the contours from the ends of the channel segments to the divides. The length, slope and width can subsequently be 'selected' to maintain the area and the length as closely as possible. Although subjective, Kirkby *et al* (1976) suggested that topography is unambiguous, being one of the most accessible parameters controlling fluid flow.

Adopting similar practices to Kirkby (1976), Engman and Rogowski (1974) and Woolhiser (1985) the current method combines graphical and trigonometric procedures to preserve the order of routing patterns in the catchment and the critical dimensions of slope and channel area, length and gradient, necessary to preserve mass continuity and realistic flow conditions. It uses a flow-net of contours and flow-lines to determine non-uniform model 'elements', and then geometrically simplifies each element by transforming it to a planar hillslope section or to a constant gradient channel segment. This approach preserves direct flow-lines instead of the unreasonable simplifications made with many kinematic cascades which, in the case of Wooding's v-shaped catchment discretisation, for instance, could not reproduce steeply rising portions of the hydrograph caused by concentration of runoff (Woolhiser, 1967).

The methodology in constructing this flow-net is described in Appendix 1.4, and the flow-nets produced for the Avdat catchment are presented as the base-maps in Appendix 3.2 and 3.3. There are two flow-nets, one based on the current reconstructed drainage network of natural rills and man-made ditches, and the other assuming that the water harvesting system has not been constructed and the catchment is in its natural, unaltered state. This allows complementary full-catchment simulations to analyse the effect of introducing the water harvesting system on both catchment contributing area, and on the discharge produced from a given input.

2.2.4 Surveying the Hillslope and Channel Network

In order to discretise a catchment system into a flow-net of flow-lines and contours, a topographic survey must be made, and a contour map produced. The approach adopted for this thesis can be briefly described as follows.

A topographic survey was made to provide a relatively detailed set of (X, Y, Z) coordinates (spot-height nodes) across the surface. The spot-height locations were selected by compass-line gridding and marked physically in the field so that the arrangement of spot-heights produces;

a. a regular grid-like distribution when plotted in a horizontal plane, allowing a suitable arrangement for use by contouring programs,
b. a tendency for the density of spot-height nodes to be greatest where slope gradient is plus or minus small values and hence where the slope magnitude and direction is most difficult to identify with certainty,
c. a physical grid for the easy identification of any point within the catchment according to its position along the rows and columns described by the spot-height nodes marked out on the ground surface.

The spot-height nodes were surveyed at regular intervals within the watershed and the seven sub-catchment divides, and along the channels. The nodal spacing produced an approximately 20 m by 20 m surface grid in planar projection over most of the catchment and an incremental spacing of either ten or twenty metres along the channel sections for the purposes of network ordering and gradient calculation. The survey of the Avdat catchment followed conventional practices with the fixing of several principal spot-height nodes and a base node from which forward and backward sightings were made. The principal spot-height nodes comprised the raingauges and discharge recorders within the catchment area.

In all, 1217 spot-heights were surveyed. By marking points in the field arranged in a roughly rectangular grid in the planar projection (established through using the compass-lines) and along the channels, each spot-height node had a reference name for the booking of readings, facilitating the checking of points surveyed from different principal spot-heights. Consequently, multiple readings were easily identified and the range of calculated (X, Y, Z) coordinates and disparate values could be checked.

2.2.5 Processing of the Catchment Topographic Survey Data

2.2.5.a Converting the Survey Data to Cartesian Coordinates

The relative position of each spot-height node was calculated. The (X, Y, Z) values of the principal survey nodes relative to the survey base-node values of (1000, 1000, 100) were calculated first, and then the (X, Y, Z) values of all the field nodes were calculated based on the coordinates of the principal nodes.

Since the base node was not linked into a Survey of Israel triangulation network, the coordinates are relative, bearing no relation to the latitude, longitude or sea level base of existing

topographic maps. However, the theodolite was aligned to compass north. All coordinates refer, therefore, to a grid with the base-node: 1000 m east (X), 1000 m north (Y), 100 m elevation (Z).

2.2.5.b Contour Map Production

To produce the contour map of the catchment, the Surface II Graphics Package was used (Sampson, 1978). Surface II displays spatially distributed data, using a rectangular grid of values which represent the surface by their (Z) variable. To produce a contour map, lines are laced between the grid nodes by linear interpolation. Since this requires a regular grid, and geomorphological data usually takes the form of an irregular distribution, a grid must be estimated from the spot-height data. Surface II performs this gridding function using either 'global' or 'local' fit procedures, depending on the nature of the data, and the degree to which detail can be allowed to be smoothed. Since global fits such as Trend Surface Analysis involve a high degree of spatial smoothing, and since the Avdat catchment contains areas of high morphological complexity (particularly the area of the wadi bottom with its mix of interfluves and channels showing considerable variations in elevation over short distances), a local fit was adopted. This prevented unwanted smoothing and allowed spot-heights of stream beds and interfluves to exert their true influence on the adjacent grid-nodes to achieve a close numerical representation of the surface even with the smoothing of the grid conversion. The regular distribution of points from the original survey combined with the dense channel survey can be expected to have had a positive effect on the accuracy of this representation. These techniques were used to produce a 1:1000 scale, contour map with one metre intervals (scaled-down with catchment divide overlay in Appendix 3.1).

2.2.6.c Flow-net Discretisation

The contour map was used to produce two flow-nets using the combination of one metre contours and flow-lines (contour orthogonals) drawn upslope from channel topographic survey nodes. The net is the discretisation of the catchment and its nodes were digitised to provide the geometric data for the simulation model to simplify the net into cascades of hillslope planes and channel sections. Appendix 3.2 represents the full reconstructed Avdat water harvesting system flow-net of natural channels and artificial ditches, and their contributing hillslope areas. Appendix 3.3 represents the hypothetical unaltered catchment system flow-net, discretised assuming that the ditches have not been made, with flow-lines constructed from the natural channel system only up to the natural watershed.

The model and the discrete flow-net have identical structures in that the logical topological and hydrological order is used. Flow moves down the pathways defined by hillslope and channel flow-lines. The model calculations start from the highest element of the cascade flowing into the uppermost section of the lowest order channel branch. To illustrate this clearly, a simplified, imaginary step-by-

step conversion of a stylised contour map into a digitised set of data points describing a discretised catchment surface is presented in Appendix 1.4. A series of four explanatory figures are presented based on a simple hypothetical catchment with three channel branches, two first order and a second order. They cover the steps of constructing orthogonals, discretisation and ordering of the flow mesh, and digitisation of the nodes. Identical steps to these were followed on a larger scale in the production of Appendices 3.2 and 3.3 and provide the model with data-sets for each flow environment simulated. The model calculations consider each hillslope element, in each hillslope cascade, discharging into each channel segment, in each channel branch, in each sub-catchment.

2.3 MICRO-MORPHOLOGY - SURFACE CHARACTERISTICS

Once the macro-morphological information of the topographic surface, and the spatial arrangement and networking of channel branches is provided, the micro-morphological information and the process variables must be provided. The micro-morphological information has two roles, the first is to help delimit representative areas which can be used for process parameter quasi-distribution and the second is to provide the flow-dimension variables not already accounted for by the macro-morphology, i.e. hillslope and channel flow-boundary shape.

2.3.1 Field Unit Classification

The distribution of lower-resolution parameters through the flow-net is aided by the identification of representative units. The hypothesis adopted is that these can be determined by the distribution of micro-morphological characteristics. During a geomorphological and geological appraisal of the catchment, a field-based classification was made following the land-systems approach (Christian, 1957. Mabbutt and Stewart, 1963). Homogeneous areas represent a geomorphological 'unit' with relatively consistent physical and process characteristics. Adopting a unit classification rationalises the model structure and parameterisation and maximises the use of a limited process field-data set. Parameters can be quasi-distributed based on their association with the units identified from the micro-morphological appraisal. A small number of units is most convenient for modelling although obviously results in a greater lumping of some of the parameters.

The Avdat catchment exhibits a range of hillslope environments as a result of geological and geomorphological process controls as described in Chapter One. Examining Plate C.1 shows the catchment to have four quarters. From east to west there is a transition from the elevated Avdat Plateau surface, capped by the youngest rocks in the Eocene sequence, to the palaeo-fluvial terrace of the Wadi Zin, capped by later Neogene conglomerate. The dividing line east-west is the main channel of the natural drainage network, and a continuation line along its south-north orientation. The dividing line north-south is the edge of the natural channel system incision into the Zin terrace, and the re-

establishment of a continuous profile sequence from the Avdat Plateau down onto the terrace and the eastern edge of the water harvesting system marked by the channel of sub-catchment one (see Appendix 3.1). The edge of the drainage incisions is also the divide of the pre-water harvesting system catchment area because the hillslope flow-lines naturally route runoff onto the terrace and away from the small wadi towards the Wadi Zin. Through skilled hydro-engineering, the ancient harvesters have made it possible to exploit this slope area through the introduction of channels which exploit topographic subtleties and route water across normal flow-lines to the terraced area on the floodplain of the small wadi. This is illustrated clearly by a comparison of the two flow-nets in Appendix 3.2 and 3.3.

Prior to a quantitative appraisal, six distinct units were postulated. Three of the units, (3, 4, and 5) occur on both the east and west sides. Obviously each unit represents only a broadly similar grouping with their boundaries forming a transition zone (although this is considered a distinct line). In the case of units 2 and 3 the boundary is very distinct related to the strong geological influence at a limestone-chalk boundary. The units are hypothesised from geomorphological survey, quadrat sampling, and, the geological literature on local sedimentology and stratigraphy (Arkin *et al*, 1984. Braun, 1967. Garfunkel and Horowitz, 1966. Issar *et al*, 1984). The units are described in the following sub-sections and Appendix 1.2 illustrates the cross-sections of the sample profiles (exaggerated in the vertical scale) showing the positions of the field unit boundaries. In addition, the series of Plates P.17 to P.48 illustrating a photo-transect taken along profile 2 show the sequencing of variation from east to west across the drainage system.

2.3.1.a Unit One Slopes

Unit 1 is confined to the eastern side of the catchment and describes the scarp-face transition from the Avdat Plateau's surface down to the concavo-convex section of unit 2 below. The range of slope conditions contained within this unit grouping are represented for profile 2 by the photographs plates P.17 and P.18. The unit has a high bedrock outcrop up to 100% cover with up to two-metre scarps and debris falls where bands of resistant block-structure limestone weather at zones of weakness. Sheared blocks, debris cones, screes and small loess out-wash fans are found below and intervening the scarps. Overall gradients are generally steep from 12° to 39°.

2.3.1.b Unit Two Slopes

Unit 2 occurs on the eastern slopes directly below unit 1 at a transition from resistant limestone to softer chalk with flint concretions. The range of slope conditions are shown in Plates P.19 to P.21 and gradients vary from 6° to 26°. The chalk is Micite foraminiferal ooze (Braun, 1967) and the slope has a convexo-concavo-convex macro-profile due to its position between two more resistant limestone bands. The upper chalk slope is protected by patches of rock-fall which decrease in

density downslope, and the lower chalk foot-slope grades into the limestone below and is covered by a chalky colluvium comprised of limestone fragments and powdered chalk crusted with loess. The midslope is gullied by runoff from the limestone above and large blocks sit in the rills flowing over the gully bottoms. These are clearly identifiable from the aerial photographs.

Units 1 and 2, exhibiting the highest relative relief at the highest elevations also show the clearest distinction. The other classes become broader and more generalised, as geologic, morphologic, and pedalogic variations combine to show an overall likeness sufficiently different to warrant an apparent distinct grouping relative to adjacent and different slope sections.

2.3.1.c Unit Three Slopes

Unit 3 is recognisable on both sides of the catchment with differences in scale and geology. On the eastern slopes it is a midslope resistant limestone belt of thinly bedded layers broken into a platey structure fragmenting into 20 cm to 40 cm stones. The range of conditions contained in Unit 3e along profile 2 are illustrated in Plates P.22 and P.23 with gradients averaging 10° and varying from 5° to 17°. On the north-facing slope of the eastern hill scarps of 0.5 m to 1.0 m occur, and parallel to the channel system on the eastern slopes the steps are smaller and gradual on the shallower gradients. In the northern quarters, the unit grades into the colluvial-covered foot-slope surrounding the small Avdat wadi. In the south-east quarter, it grades onto the Zin terrace. Bedrock cover is from 25% to 40% although locally it can be higher. The remaining surface is a shallow mantle of loessial colluvium and stones. The soil thickness only locally exceeds 30 cm and is on the whole 10 cm to 20 cm thick.

To the west, unit 3 is a short, relatively steep slope where the Zin terrace conglomerate cap outcrops at the top of the slope. The range of conditions to the west on profile 2 are illustrated in Plates P.37 and P.38. Like to the east, there are broad patches of bedrock cover up to 40% with rounded flint and limestone blocks in a range of sizes from gravel to cobble and above. Loess has settled more readily on this surface and is washed off the terrace. Patchy deposits are up to 20 cm deep.

The east and west slopes are similar although their scale and topological position differ. The eastern slope sections (3e) are a larger feature both in vertical extent and downslope length. From comparisons made at Sede Boqer, it is reasonable to consider unit 3 slopes analogous to the conditions on the upper section of Aaron Yair's study slope (Yair and Lavee, 1985).

2.3.1.d Unit Four Slopes

Unit 4 is a relatively smoothly graded profile of mixed loessial colluvium and stony material, with gradually increasing soil depth downslope. Unit 4 slopes are most analogous to Shanan's rocky

slopes and Yair's colluvial slopes with Shanan the foot-section and Yair the top-section. To the east, unit 4 (4e) forms the upper foot-slope grading into the loessial alluvium of unit 5. The range of surface forms and types for 4e on profile 2 are shown in Plates P.24 to P.29. It increases from a patchy 10 cm soil thickness to a maximum thickness of 30 cm with a large proportion of stone particles comprising 25% to 50% of the surface cover, weathered from the jointed limestone. The foot-slope is bedded by another layer of chalk although this is not exposed. The stone particles have a smaller average size downslope, and the degree of embeddness increases.

To the west, unit 4 is comprised of three slopes, all relatively similar but in different positions. The first is the short slope separating the wadi loess (5w) from the conglomerate outcrop (3w) facing eastwards and northwards into the Avdat wadi. The range of surface conditions are presented in Plates P.35 and P.36. Its surface is similar to the eastern unit 4e. This is the same as the slope section on which Shanan constructed his 5.7° to 11.3° runoff plots.

The second slope the stony section at the southern end of the catchment grading from unit 3e onto the Zin terrace surface (the terrace is a mixture of unit 4w, 5w and 6). The southern 4w is not shown in the photo-transect since it only occurs on profile 5 which runs down the face of the southern mesa (see Appendices 1.1 and 1.2). Profile 5 crosses the area where the limestone of unit 3 and the conglomerate cap juxtapose to form a continual horizontal resistance to the incision of the natural channel network and small wadi which have formed where the resistant conglomerate layer juxtaposes the softer chalky limestone.

The third unit 4w slope is the relatively shallow 5° section representing the far western edge of the terrace before it is cut away by the recently rejuvenated Wadi Zin. The slope conditions of this outer, west-facing edge of the Zin terrace, are shown in Plates P.45 and P.46. The unit is absent at the south and north-west edge where loess covers the terrace as unit 5. Unit 4w adjoins the man-made ditch of sub-catchment one as it follows the western edge of the terrace before its steep incision down to the Zin. The surface characteristics appear similar to the other unit 4 surfaces although the slope gradients are generally shallower.

2.3.1.e Unit Five Slopes

Unit 5 occurs on either side of the east-west divide. Unit 5 is analogous to Shanan's Loessial slope area. Low interfluves occur where the wadi rills incise into the alluvium and colluvium of the foot-slopes and wadi depression. The remaining alluvial floodplain is filled with the redistributed loess from the upper slope elements washed down across a colluvial-alluvial sequence. The loess forms a relatively continuous sheet, decreasing in stone cover percentage as the slope gradient decreases, carrying a dense vegetation along concentrated water lines, or at their dispersal points. The steeper

interfluves can be armoured by a coarse gravel cover, giving it a relatively high percentage stone cover. Unit 5 surfaces on the eastern slopes are shown in the photo-transect by Plates P.30 to P.32.

Unit 5 occurs in two locations in the western sections. The first is the foot of the east-facing slopes of the terrace edge and is shorter than on the east side and slightly steeper due to the marked asymmetry of the Avdat wadi depression. The surface conditions are shown in Plates P.33 to P.34. The second is on the surface of the Zin terrace. The slopes are almost planar, although the surface has a dip parallel to the proto-Zin. The loess fills the undulations in the conglomerate cap through primary wind and secondary fluvial deposition. The surface conditions are shown in Plates P.47 and P.48. The thickness of the terrace loess is variable, not more than 50 cm, but the thickness of the wadi loess can range from 50 cm to more than a metre depending on its proximity to the depression apex, and the height of the interfluves above the wadi-bed. The loess gives way to a bed of soft chalk, as augering showed, undergoing in situ weathering in its top layers. The raised interfluves, in contrast to the adjacent loess, are generally covered with a gravel armour due to rainsplash and particle winnowing under runoff conditions on the relatively steeper slopes. Although the armour cover can reach 75%, stone cover is generally low and dominated by the smaller particles. Slope gradients vary from 1° - 4° for the loess sheet and 3° - 9° for the armoured interfluves.

2.3.1.f Unit Six Slopes

Unit 6 occurs only in the western slope and is not a graduated slope sequence, as the other units tend to represent, with gradually changing conditions downslope. Instead it comprises areas of large stones, often flush with the surface or raised in low piles interspersed with discontinuous patches of stone-free loess. The range of surface characteristics on profile 2 are shown by Plates P.39 to P.44. The stone mounds are weathered from the conglomerate. The intervening lows, showing the variation in the bed morphology of the proto-Zin, are filled with the loessial material, and represent both very shallow drainage lines or areas of large depression storage in times of flood on the terrace (as observed during rainstorms at Avdat). Gradients vary from 1° to 5°. The unit 6 could not be categorised easily as either 4 or 5 since it is a non-uniform mixture of each.

2.3.2 Quantifying Micro-Morphology

2.3.2.a The Sampling Scheme

The gradual changes occurring with a fall in elevation from slope crest to wadi floor leads to a relatively distinct banding and zoning of slope characteristics within the catchment. Since the water harvesting system functions on the basis that channels are constructed to intercept flow-lines by crossing hillsides in a linear fashion, a systematic, stratified sampling pattern was used, locating plots

along flow-line profiles. The position of these profiles are illustrated in the aerial photo and overlay; Appendix 1.1 and their form in the exaggerated cross-sectional profiles in Appendix 1.2.

The sampling followed approximate individual flow-lines as closely as possible. The five profiles crossed the catchment at different distances from the terraced fields towards the southern divide. Starting at the eastern divide and working west, the maximum slope line was followed closely using a hand-held inclinometer until a natural drainage line was encountered, at which point the profile was continued upslope to the next divide and so on. In hindsight, it would have been more convenient and appropriate to start from specific channel nodes and work back upslope to the east and west divides respectively. This was the graphical method adopted in the flow-net discretisation described earlier. Compared with flow-lines that can be traced using the contour map produced from the topographic survey (see Appendices 3.1 to 3.3), the profiles are an adequate representation of the dominant flow direction at a marker spacing of 20 m.

Sample plots were positioned along the profiles with a density of one sample per 20 m of slope length in order to ensure a sampling resolution that would include the frequency of major changes along the slope sections, i.e. within the major geological and morphological zoning identified by the field unit arrangement sketched onto a geomorphological map of the catchment. This sampling approach was successfully adopted for the determination of representative catchment conditions in New South Wales by Bell and Vorst (1980) who state that one must take into account the high spatial variability of relevant factors using a stratified sampling basis if systematic geomorphic variations are observed in initial appraisals.

A total of 127 sample sites were selected. Measurements of textural factors were made at each and of hillslope process characteristics at a sub-set of these as described in Chapters Three and Four. The channels were sampled for their cross-sectional shape and local bed-slope at 254 locations with a spacing of 20 m. These were taken at every second channel spot-height node marked during the survey at 10 m intervals along each natural channel and artificial ditch. Twenty-one of these were selected for process measurements of velocity-stage-discharge. They were distributed subjectively at various positions including the boundaries or mid-points of the field-units or the confluence of sub-catchment sub-sections. They were designed to provide some general characteristics of flow rather than to provide a representative sample.

2.3.2.b Theoretical and Practical Significance

Surface texture is comprised of both the surface materials and the surface-form arrangement they assume across the hillslope or within the channel bed and banks. It is likely to be important for the production, transmission and consumption processes experienced during a storm event for a number

of reasons. Firstly, the nature of the surface materials influences the magnitude of infiltration at a given location. From the literature it can be expected that, depending on the nature of the geology, some bare rock surfaces can have negligible infiltration rates (particularly hard, crystalline limestone), loess crusts can have initially high infiltration rates reducing relatively quickly to a substantially lower level, and mixed loessial and stony colluvium can have infiltration rates that may start and remain high during the course of the event, depending on their exact relative percentage cover and total volume within the soil mass. These are the three main surface environments in the Negev and at Avdat.

Secondly, the shape that these materials assume across the surface can condition the character of production, transmission and consumption by determining the wetted perimeter for a given flow area, and related to this, the resistances to flow it exerts on the surface water once rainfall and/or run-on excess has been generated at a given location. If the surface is highly variable, the total surface in contact with water, as opposed to that exposed to rainfall which will be universal, is lower, up to a given threshold, due to the concentration of flow into micro-channels. The more efficient character of this type of flow-shape, with relatively large hydraulic radius, transmits water more efficiently than a more shallow, sheet-like flow section where total length in contact with the water area is large, and depth small relative to individual surface materials. Water moving over the varied surface has greater velocities, with more rapid throughflow, promoting lower total infiltration volumes since they are a function of both the length and time of contact between the surface and water as well as the character of the surface type.

2.3.3 Surface Material Characteristics

2.3.3.a Classifying Surface Materials

Surface materials can be classified by type, by particle size-distribution and by particle shape and are sampled areally to determine the relative proportions of the surface in particular size classes. The surface materials have a varying hydrological character with differential abilities to transmit water away from the surface, and to store water within and between rainfall events. The surface materials can be divided into three categories;

1. **bedrock**, clearly exposed over one or more m^2 of surface area, and immovable from its position,
2. **stony**, either free-standing, partially buried, or flush with the surface, measured according to length (Aa), width (Ba), and breadth (Ca) axes, and > 2 mm shortest diameter,
3. **soil**, all material smaller than 2 mm shortest diameter, therefore this class includes sands, clays and silts (BS1677 classification).

Table 2.1 The B.S. 1677 Size Classification Index

Class	Range (in mm)	Description
1	Ba ≥ 200.0	Boulder
2	200.0 > Ba ≥ 60.0	Cobble
3	60.0 > Ba ≥ 20.0	Coarse Gravel
4	20.0 > Ba ≥ 6.0	Medium Gravel
5	6.0 > Ba ≥ 2.0	Fine Gravel
soil	2.0 > Ba	Sands, Silts, Clays

The common method for sampling surface material characteristics is the quadrat grid-point approach whereby a grid is placed on the surface, and the material directly below the grid-point selected for examination (Dackombe and Gardener, 1983). The stone particles can then be analysed by size using a variety of classifications. The BS1377 classification is adopted here using the Ba axis. Yair and Lavee in their work in the Negev and Sinai Deserts have shown the positive role played by large boulders on runoff production due to the micro-runoff onto the surrounding soil area. They have also shown how a uniform covering of gravels beneath the large stones has an inhibiting effect on runoff due to the high flow-resistance exerted on runoff water (Yair and Lavee, 1974, 1976, 1981).

2.3.3.b Sampling Surface Materials

For the sampling of hillslope surface materials, a 1 m^2 quadrat was used divided into a 20 cm by 20 cm grid and 25 observations were made per quadrat, 16 quadrats per 4 m by 4 m plot. Thus 400 observations were made per site classifying the material according to rock, stone or soil, and measuring the size of each stone component. The method is analogous to Simanton and Renard (1982) who sampled whether the surface was bare soil, gravel or rock.

2.3.3.c Processing Surface Material Data

For each of the 127 sample field plots, conversion of the surface material types into percentage cover was a simple matter of dividing the total number of observations of each surface type by four. The average Aa, Ba and Ca axial length, the standard deviation of the sample from the average, the skewness, and the kurtosis of the sample were calculated, the last three indicating the range and shape of the distribution. The size distribution of particles can be influential in determining the hillslope infiltration characteristics since a bias in the distribution of stone sizes to the large particle sizes is likely to be favourable to runoff production (Yair and Lavee, 1974, 1976).

2.3.4 Surface Microtopography and Flow-Boundary Dimensions

2.3.4.a Sources and Significance of Micro-Topographic Variation

Micro-topography is a function of the size and spatial arrangement of particles and the nature of the solid geology that may be outcropping. Where particle size distributions are dominated by individual large particles, micro-topography is likely to show distinct topographic highs and lows depending on their position relative to the smaller particles comprising the rest of the surface. If the large particles are situated in topographic lows formed by the arrangement of finer particles such as rills or runnels, they will smooth the overall micro-topographic variation, and if they are situated on topographic highs such as micro-interfluves they will emphasize the topographic variation.

Emmett (1970) considers surface roughness to be a combination of particle roughness, i.e. sand-grain roughness and plant seedling growth, and form roughness, i.e. topographic irregularities. In his definition, texture refers to the individual components of resistance, the particle roughness, and form refers to the nature of the topography they describe, for instance the presence of bedforms such as dunes on a stream bed, or the cross-slope variation in a hillslope surface described by rills and interfluves. Both are important in determining the magnitude of resistance to flow, as discussed in detail in Chapter Four, and the latter is important in determining the cross-sectional shape a given discharge will occupy within a plan width of slope. The spatial arrangement of topographic lows and highs corresponding to rills, hummocks, depressions and large surficial particles is complex and therefore a single standard geometric shape cannot be adopted as with channels, even though flow may well be occurring in defined micro-channels. In many studies of surface runoff, this aspect of micro-topography is ignored in favour of a sheetflow approach in which the surface is assumed planar and water flows with a uniform average flow depth. The hydraulic radius is assumed equal to the average depth and the micro-variations are assumed to be of no great significance in determining the rate of flow and the character of infiltration into the surface. The current approach considers this to be a highly significant assumption made by modellers since for a given flow-volume it will underestimate the flow dimension of hydraulic radius for low-flow states, and overestimate it for high flow-states, depending on the degree of micro-topographic variation. This has implications for both infiltration and routing procedures. The effect of considering overland flow in its complex form is analysed in the following chapters.

2.3.4.b Quantifying Micro-Topography

A review of the literature on this subject shows that several different methods of measuring micro-topographic variations have been adopted. All involve the measurement of the relative heights of the surface over small incremental distances and differ only in terms of equipment sophistication. They

include electronic scanning devices (Schafer and Lovely, 1966), pin-rack profilers (Simanton *et al*, 1978. Burwell *et al*, 1963) and simple measuring rods laid on the surface (Scoging, 1988).

Scoging (1988) attempts to quantify micro-topographic variability on a hillslope surface as a basis for determining an independent roughess value for overland flow routing. Scoging considers microtopographic roughness to be a multi-facetted feature comprising magnitude, frequency, wavelength and periodicity and quantifies it to help describe and distinguish between the observed characteristics at four sites in S.E. Spain where runoff and erosion studies are carried out. The techniques used are an adaptation of Scoging's field methods.

Using a series of microtopographic profiles Scoging measures the spatial variations in the vertical depth of a sequence of 11 surface heights from a rigid rod datum placed on the surface. Derived from these 11 coordinates relative to the rod coordinates vertically above are the length increment between successive surface nodes (roughness length), the area between the surface increment, the rod increment and the two vertical lines between surface and rod (roughness area), and the deviation of the increment from that which could be expected for a straight line surface of no topographic variation (in this case assumed to be the rod length divided by 11).

Figure 2.1 Scoging's Micro-Topographic Dimensions (1985, 1988)

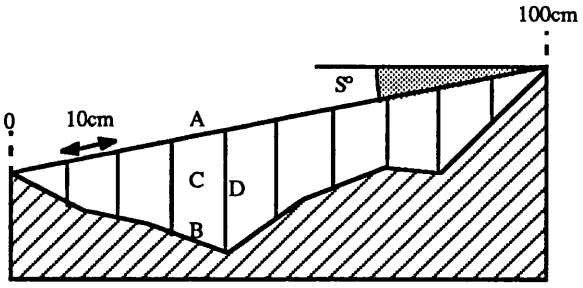

Measured:
S° = ground slope angle
A = rod segment length (10cm)
D = segment depth

Calculated:
B = segment length
C= segment area
E = segment deviation
ΣB = total roughness length
ΣC = total roughness area
ΣD = total roughness deviation

Whilst agreeing with Scoging's analysis and conclusions in interpreting these measurements, a slight flaw exists in each of the indices related to the use of the rod as a datum against which the magnitudes are calculated and compared between plots.

In the current method, as with Scoging's, a rod is laid onto the hillslope and the position it assumes (its angle to the horizontal) is conditioned by the relative heights and arrangement of its contact point with the surface as illustrated in Figure 2.1. The surface below is independent of the rod and sampled at a resolution determined by the number of intervals along the rod-length and their

spacing; in Scoging's case every 10 cm along two 100 cm rods and for the current study every 10 cm for a 190 cm rod length. The vertical depths from the rod to the ground may or may not include the individual roughness elements controlling the position of the rod in space. If the surface exhibits a marked topographic high at one end then the slope of the rod will be conditioned by this large form or grain roughness (depending if it is an individual particle or a collection of particles respectively) and will be at variance with the overall trend of the arrangement of points. Whilst this will not affect the roughness length, it will affect greatly the area calculations which depend on the relative positions of the rod and the surface. It will affect the deviation of the length, since the straight line distance of the surface that should be compared with the actual surface length is not the rod length of 100cm but the best-fit line through the points, a length that will be less than 100cm according to the relative angle of this straight line and the rod angle.

In the rocky, highly rough environment on the Negev slopes, this is an important factor. It is more important on steep slopes or slopes with a large particle size range. Thus the rod is used only as a basis for the calculations of the relative coordinates of the sampled points, and not a basis for the calculation of dimensions categorising their relative roughness characteristics. By considering the distribution of points relative to each other and the dependent 'best-fit' profile passing through them, the statistics derived become independent from any extraneous influences resulting from their method of measurement. This is explained in more detail below.

Figure 2.2 Downslope Micro-Topographic Profile Measurement

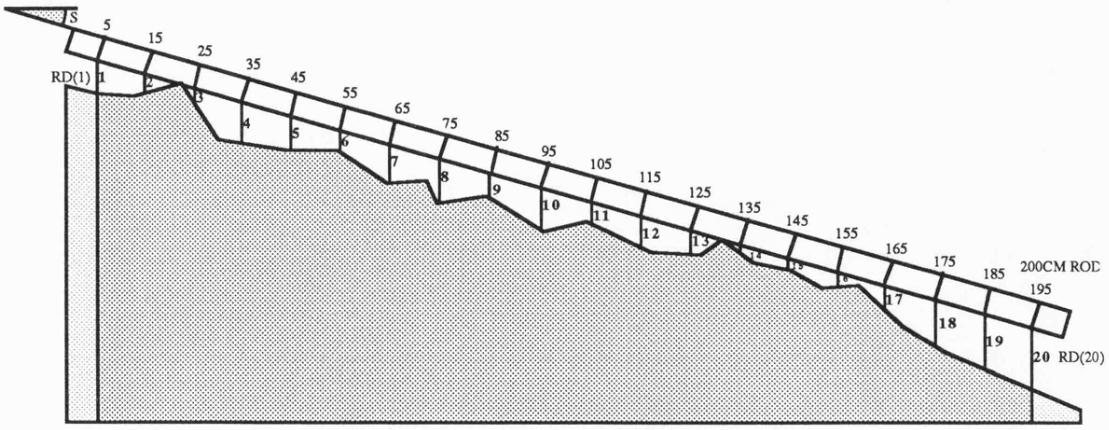

Figure 2.3 Cross-slope Micro-Topographic Profile Measurement

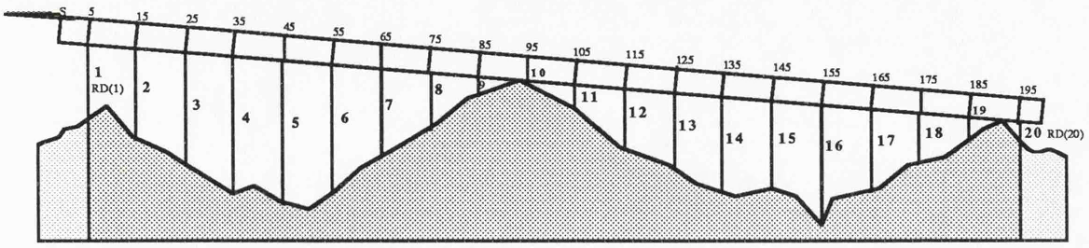

The same 4 m by 4 m, 16 m^2 plot analysed for surface material characteristics was used for micro-topographic analysis by sampling along ten crosslope and ten downslope profile rods. The rods were oriented to be parallel with the maximum slope for the down-slope readings, and perpendicular to the maximum slope for the cross-slope. The gradients of each rod as it lies on the surface was measured by use of an inclinometer placed onto the rod, measured to the nearest 0.25 degree.

Each profile data set was discrete, with two sets of ten microtopographic profiles providing data on the absolute and relative magnitudes and ranges of downslope and cross-slope variations in surface height at the given location.

2.3.4.c Processing Hillslope Micro-Topographic Measurements

The surface points measured relative to the rod were converted into their relative (x, y) coordinates, with x being the horizontal and y the vertical.

The following four formulae (Scoging, 1985) was used to calculate the (x, y) pairing, with Equation 2.2 used to calculate the x coordinate, and depending on whether the rod-datum gradient was negative from observation 1 to 20 (Equation 2.3), zero (Equation 2.4), or positive (Equation 2.5) the other equations to calculate the y coordinate. For the cross-slope the observations 1 to 20 read to the right looking upslope, and for the downslope they read in a downslope direction.

$$x(N) = (N-1) * 10.0 * \cos(S) \qquad \text{Equation 2.2}$$

$$y(N) = - (RD(N) - [(N-1) * 10.0 * \sin(S)]) \qquad \text{Equation 2.3}$$

$$y(N) = -(RD(N)) \qquad \text{Equation 2.4}$$

$$y(N) = (RD(N) - [(N-1) * 10.0 * \sin(S)]) \qquad \text{Equation 2.5}$$

(where N is the number of the observation for 1 to 20, RD(N) is the vertical distance (assumed positive) from the rod to the surface for observation N, S is the angle of the rod laid on the surface, and 10.0 is the constant increment spacing along the rod in centimetres. The coordinate of (1, 1) is therefore [0, -RD(1)]).

For each of the ten crosslope and ten downslope micro-topographic profiles measured at each of the 127 field-plots, the sequence of 20 surface nodes were used in determining three different standard deviations of their positions from a best-fit profile through their distribution. Firstly, the individual profiles were considered as 127 * 20 single groups and the 20 observations per group were considered relative to the best-fit line for that observation group i.e. they were grouped and analysed by profile. Secondly, the observations of the ten cross-slope and ten downslope profiles were grouped separately for each field-plot and considered relative to the best-fit line for that observation group i.e. they were grouped and analysed by field-plot. Thirdly, the groups of profiles were sorted according to whether they occur within the boundaries of each of the field-unit classifications and the observations were considered relative to the best-fit line for that observation group i.e. they were grouped and analysed by field unit. The groupings of the 127 samples are listed in Appendix 1.3. For the downslope sequences, the best-fit profile was assumed to be the linear regression line fitted through the group of observation (x, y) coordinates.

Figure 2.4 Example of Downslope Micro-Topographic, Rod- and Best-fit Profiles (single profile from sample 23, Unit 3e)

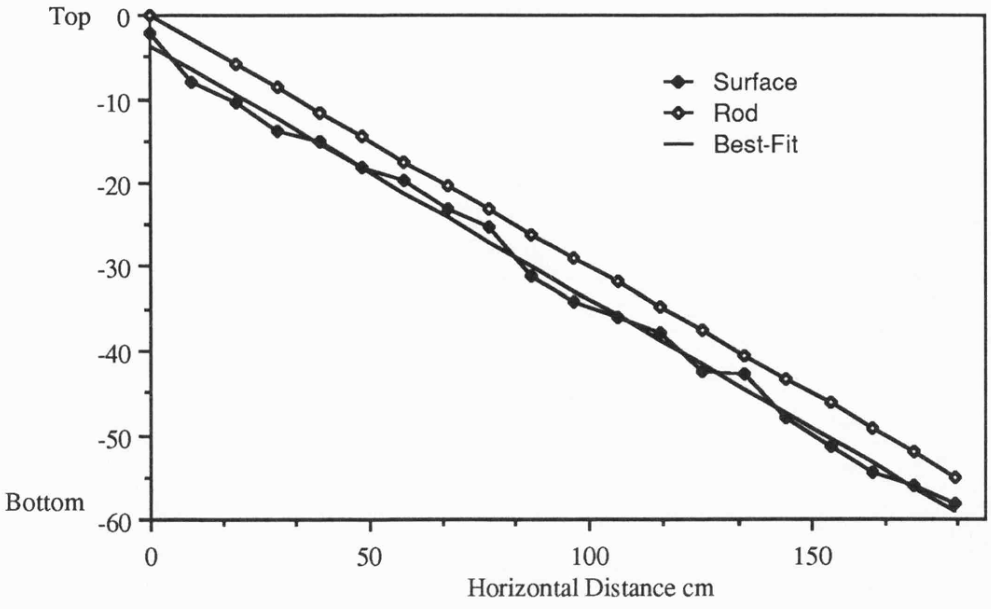

Figure 2.5 Example of Crosslope Micro-Topographic, Rod- and Best-fit Profiles (single profile from sample 23, Unit 3e adjusted to mean y of zero)

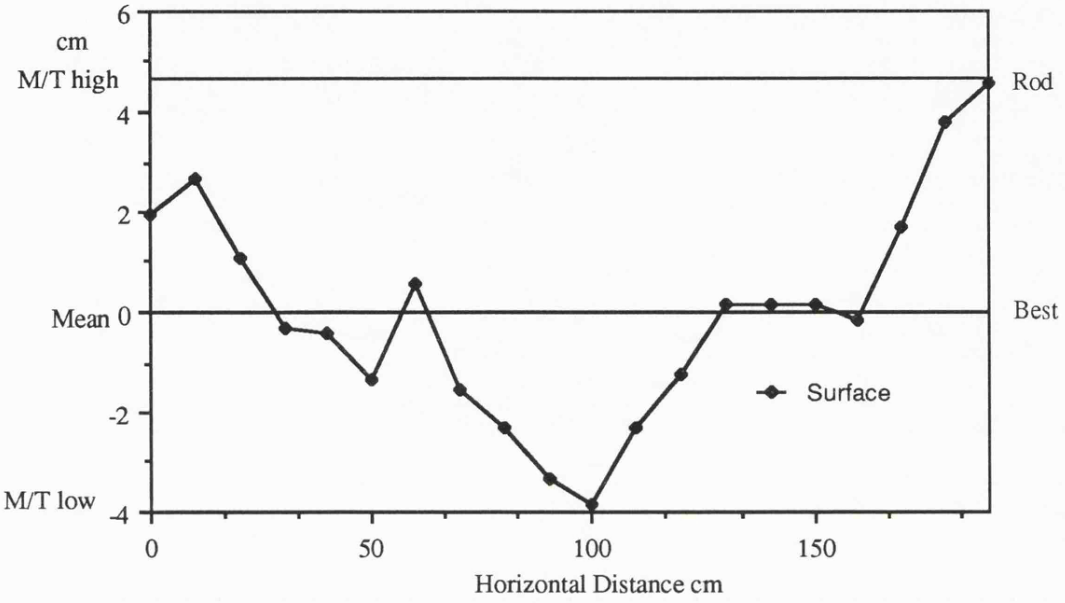

For the cross-slope sequences, the best-fit line was assumed to be the horizontal line passing through the mean of the group, since this represents the case where there is zero topographic variation and the minimum surface length.

In order to standardise the variations for the different levels of aggregation, the individual profiles were adjusted according to the mean of their largest grouping, i.e. for the field-unit group. In the calculation of the standard deviations, all the means for the different unit groupings were identical and their ranges were standardised to prevent additional variation from being introduced. This was accomplished by calculating each downslope profile statistical mean (Mdp) (as opposed to the mean surface described by the regression line) and each plot sample statistical mean (Mds). Each observation point y-value (yd) was then adjusted by the difference between the plot sample mean and the profile mean (Vdsp) to standardise their ranges about the same mean.

$$Mdp = \Sigma_{1,20} (yd) / 20 \qquad \text{Equation 2.6}$$

$$Mds = \Sigma\ 1,10\ [\ \Sigma_{1,20} (yd) / 20\ ] \qquad \text{Equation 2.7}$$

$$Vdsp = Mds - Mdp \qquad \text{Equation 2.8}$$

$$yd = yd + Vdsp \qquad \text{Equation 2.9}$$

Having calculated the sample mean, the unit group mean (Mdu) was calculated as the mean of the sample mean (acceptable since all the sample means have the same number of observations in their group), where Ns is the number of plot samples in the unit group, and the difference between the unit mean and the sample mean (Vdus) was used to adjust each observation point so that each profile group, sample group, and the complete unit group were centred on the same mean.

$$Mdu = \sum 1,Ns \left(Mds / Ns \right) \qquad \text{Equation 2.10}$$

$$Vdus = Mdu - Mds \qquad \text{Equation 2.11}$$

$$yd = yd + Vdus \qquad \text{Equation 2.12}$$

The reason for standardising the mean for each group (either to zero or to the large unit group) was to make the standard deviations directly comparable to determine the degree of additional variation resulting from the aggregation exercise, since this was directly relevant to the analysis of the variation within and between the units.

For the downslope groupings, the standard deviation is the square root of the resultant of the sum of all the observations in the grouping (profile, sample, and unit) minus the observation predicted by the grouping best-fit regression line (Pdp, Pds, and Pdu respectively), divided by the number of observations in the grouping (20, 200 and 200*Ns respectively). This is presented for the profile, sample and unit groups in Equations 2.13 to 2.15 as SDdp, SDds and SDdu respectively.

$$SDdp = \sqrt{ \left[\left\{ \Sigma_{1,20} (yd - Pdp)^2 \right\} / 20 \right] } \qquad \text{Equation 2.13}$$

$$SDds = \sqrt{ \left[\left\{ \Sigma_{1,10} \left(\Sigma_{1,20} (yd - Pds)^2 \right) \right\} / 200 \right] } \qquad \text{Equation 2.14}$$

$$SDdu = \sqrt{ \left[\left\{ \Sigma_{1,Ns} \left(\Sigma_{1,10} \left(\Sigma_{1,20} (yd - Pdu)^2 \right) \right) \right\} / (200 * Ns) \right] } \qquad \text{Equation 2.15}$$

For the crosslope profiles, the coordinates were used in two sets of analyses. Firstly, the standard deviations of the variation of different profile groupings from their best-fit lines were calculated. The least variance profile for each set of 20 coordinates, is the horizontal straight-line passing through the mean of their y coordinates. The y-coordinates were used to calculate the mean y value for the set (Mcp), setting the mean to zero, and adjusting all the yc values so that they retained their original position relative to the mean (by adding the difference of the mean from zero, Vc). This is described by Equations 2.16 to 2.18

$$Mcp = \Sigma_{1,20} (yc) / 20 \qquad \text{Equation 2.16}$$

$$Vc = 0 - Mcp \qquad \text{Equation 2.17}$$

$$yc = yc + Vc \qquad \text{Equation 2.18}$$

Thus every profile had the same mean of zero i.e. the group mean was zero at every level of aggregation. In this case, the range of topographic variation in the cross-profile could easily be calculated, in single profile or multi-profile arrangements relative to the profile with the least variation (shortest length), i.e. the horizontal, which passes through the mean of their group distribution.

Having standardised all of the possible groupings of observations (profile, sample, unit), the standard deviations of the distributions could be calculated as the square root of the sum of all the observations in the group (since the mean is always zero) divided by the number of observations in the group presented for the profile, sample and unit groups (SDcp, SDcs, and SDcu in Equations 2.19 to 2.21 respectively). The predicted observation was zero in all cases.

$$SDcp = \sqrt{ [\{ \Sigma_{1,20} (yc - 0)^2 \} / 20] } \qquad \text{Equation 2.19}$$

$$SDcs = \sqrt{ [\{ \Sigma_{1,10} (\Sigma_{1,20} (yc - 0)^2) \} / 200] } \qquad \text{Equation 2.20}$$

$$SDcu = \sqrt{ [\{ \Sigma_{1,Ns} (\Sigma_{1,10} (\Sigma_{1,20} (yc - 0)^2)) \} / (200 * Ns)] } \qquad \text{Equation 2.21}$$

The calculation of standard deviation of the best-fit profile from the arrangement of points for the two cases of crosslope and downslope microtopography, removed the rod datum from the analysis in the standardisation procedure which considered only the arrangement of each surface point relative to the other points in the group, positioned in a common space on the basis of their distributions. The coordinates were calculated as relative values for each linked set of observations and compared according to the total variance they exhibited in the space around their mean, i.e. the absolute magnitude of their roughness in real terms was measured, at the different levels of aggregation of the different groupings.

The standard deviations are interesting characteristics for the different profiles, samples and unit groups because of their relevance to the question of the kind of flow environment they represent. For the downslope profiles, the smaller the standard deviation, the more closely the surface approaches the best fit straight line passing through the distribution, hence the more favourable the surface is for flow transmission since there will be least resistance offered by topographic highs, and the surface length will be least for a given downslope distance (the minimum length is a perfect straight line) which will reduce infiltration through a smaller wetted perimeter. For the crosslope profiles, the greater the

standard deviation the more variable the surface in the crosslope relative to a horizontal straight line with defined topographic highs and lows leading to the concentration of water into micro-channels. This is more favourable since for a given flow area of water, the greater the area to contact length ratio, and hence the lower the resistance and opportunity for infiltration (up to the point where the wetted length equals the width of the cross-section). The two possible environmental extremes that arise from a comparative analysis of the derived statistics for the downslope and crosslope are the case where the standard deviation is zero in the crosslope and large in the downslope, and zero in the downslope and large in the cross-slope. This would represent the case of downslope rills in the latter and contour furrows in the former.

2.3.5 Channel Geometry

Channels can be assumed to consist of a bed, two banks and an overflow section of greater width to depth ratio. An idealised cross-section can be used. For the Avdat catchment, where channels are generally steep with a small width to depth ratio resulting from their incision into the colluvium or alluvium of the foot-slopes, or their excavation and downslope embankment on the midslopes, a triangular approximation is adopted. The measurement of boundary geometry also used the 200 cm rod aligned horizontally with either end resting on the channel shoulders. Vertical measurements were made from the rod down to the channel perimeter at 5 cm intervals. The assumption was that given the scale of the channels observed in the Avdat network, the cross-section relevant for flow in the majority of runoff events, the normal channel, is contained within a standard 200 cm top-width, with the over-flow geometry assumed to be one of two types. For the artificial ditches banked on the downslope-side with a low wall and/or the excavated material, an asymmetrical overflow section is adopted (Section 1 in Figure 2.6) possessing the angle of the downslope embankment on one side, and the gradient of the hillslope flowing laterally into the channel on the other (see Plates F.1 to F.8 showing different channel locations in flow for a broad illustration of the different channel types and Figure 2.6 below). For the natural channel system, where two lateral inflow slopes contribute, a more symmetrical overflow section is adopted possessing the gradient of the hillslope on either side. Thus the profile provides the normal channel and one overflow bank angle (where relevant) and the model calculations of the characteristics of the lateral inflow element(s) provide one or two overflow bank angles (Sections 2 and 3 respectively in Figure 2.6).

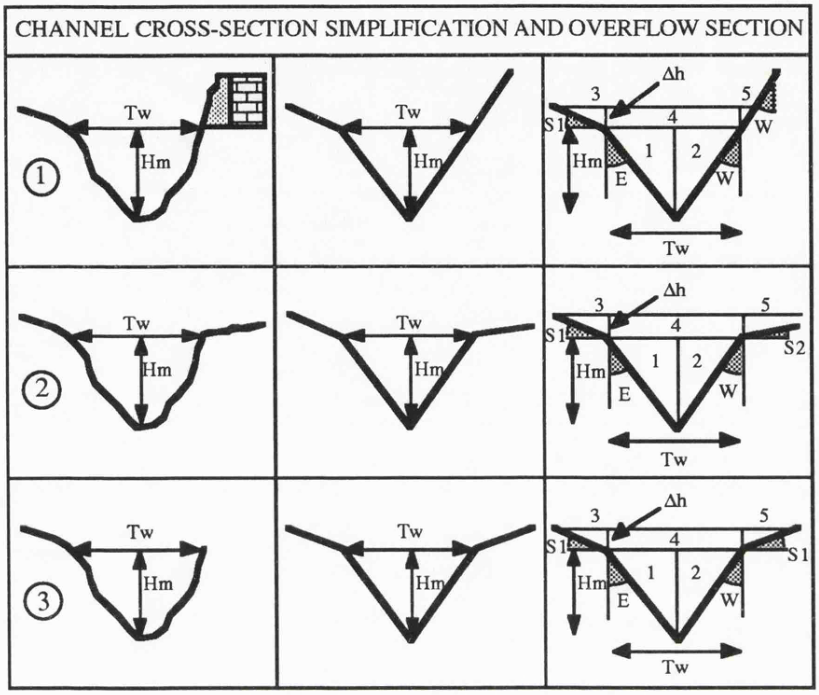

Figure 2.6 Different Channel Sections Used in the Avdat Model and Their Dimensions

A single cross-profile was taken at each of the 254 locations, except for 21 where flow recorders were positioned which had five profiles taken at a spacing of one metre apart. In the far right column of Figure 2.6, the dimensions required for the model to calculate the cross-sectional area and wetted perimiter (using the geometric components) 1-5 for any stage are presented. These calculations are discussed in Chapter Four.

For the purpose of channel flow routing the length, the gradient, and the cross-sectional shape of the channel sections are required. The length and gradient are provided in the model by calculations made using the topographic survey data as explained in Chapter Four. The cross-sectional area and channel perimeter for each depth above the lowest point in the cross-section was calculated from the field measurements. For the stage recorder locations, the average values were determined for each depth for the five cross-sections assuming their lowest points to be equal and zero in each case.

2.3.6 Testing the Representative Nature of Field Units for Data Distribution

As presented in Appendix 1.3 and described in Section 2.3.1, the 127 plot samples were divided into broad unit groupings. To test the efficacy of these groupings, it was necessary to determine the observed degree of heterogeneity or homogeneity present within and between the classificatory groups. This is a direct measure of the spatial variability present within the catchment, and the degree to which a unit classification is appropriate and zones identified which can be assumed representative in terms of their physical character and their hydrological response.

2.3.6.a Analysis of Variance Tests and Hypotheses

Six broad field-categories were identified within the Avdat catchment as described in Section 2.3.1 and logically, units 3, 4 and 5 could be subdivided into their eastern and western sub-groups. The eastern slope sequence is from Avdat plateau surface to wadi bottom (1e to 5e) or onto the edge of the Zin terrace (1e to 3e) and the western slope sequence is from the wadi bottom up the short hillslope section and onto and over the palaeo-fluvial terrace of the proto-Zin (3w to 6w). Statistical analysis was used to determine the efficacy of the field appraised unit classification at the six-unit division, and the sub-divided nine-unit division. If the statistical analysis showed that the unit classifications were not acceptable, the quasi-distribution of parameters could not be made by unit and an alternative methodology would be needed. If the catchment does not possess homogeneous areas in terms of micro-morphological characteristics then it is unlikely that there are homogeneous process domains either and the limited hydrological measurements must be considered site-specific.

Using analysis of variance (ANOVA), a set of techniques for describing and exploring relationships between sets of variables, a pair of null and alternative hypotheses were constructed to test whether sample populations within unit classes are homogeneous relative to the sample population in other unit classes. ANOVA is a parametric test of the difference between three of more samples (Ebdon, 1977) and applied to data measured on interval and ratio scales. It can be applied to an assessment of the textural characteristics; the surface material cover and the micro-topographic profiles. The catchment appeared to exhibit a marked variation in these characteristics. The textural factor was a highly visible and important component in the perception of change and the delimitation of boundaries in the field appraisal. However, balanced against this was the observation that surface materials and micro-topography are interrelated with processes to the geology and macro-form. As such, distinct boundaries are somewhat inappropriate. Consequently, fixing of the six field unit boundaries as described earlier, constituted the allocation of broad groupings, within which the characteristics could be said to be more similar or homogeneous relative to the rest of the group, compared to the character of the other groups. Statistically, the hypothesis states that the observed variation within the field-unit group for any of the surface characteristics chosen for consideration, should be less than the variation between the field groups in order for the broad ranges to be accepted as a single definable entity for the distribution of information from the more limited locational samples of infiltration and resistance.

Null Hypothesis (N):

The field grouping of samples into a classification of units can be rejected on the count that the variation between the populations of each classificatory group, is less than or equal to the variation within the population of each classificatory group for each of the variables tested.

The group samples thus represent samples from statistically similar population groups since there is no significant difference between the unit groups.

Alternative Hypothesis (A):

The field grouping of samples into a unit classification can be accepted on the count that the variation between the populations of each classificatory group is greater than the variation within each classificatory group for each of the variables tested. The group samples thus represent samples from statistically different population groups.

In each ANOVA test, the significance level chosen for the comparison of the F-test statistic against tabulated values was the 0.05% level, which indicated a 95% probability that the condition tested in the analysis could not have occurred by chance in the sampling process, i.e. that the variation is greater between samples than within samples and that this was not a random occurrence but due to some systematic characteristics of the overall population. For the surface materials, separate analyses were performed with the Aa, Ba, and Ca dimensions for all the observations, in each of the 127 field-plot data sets in each unit group. For the micro-topography, the standard deviations from the profile best-fit profile were used in the analysis, ten observations per field-plot for downslope and crosslope directions. Additionally, the standard deviation from the plot best-fit profile was used in a separate ANOVA test showing whether the hypotheses could be accepted using coarser resolution of information. All the statistical analyses were performed using computer programs written to handle the different data-set sizes of the different field unit groupings.

As well as performing ANOVA for the six unit grouping, the east-west sub-groups were compared separately to give a nine unit comparative analysis. Units 3, 4 and 5 were subdivided into units 3e and 3w, 4e and 4w, and 5e and 5w on the basis that they occured to the east and west of the dividing line through the Avdat catchment system. The field-plots were regrouped and a further three ANOVA tests performed; firstly an analysis of the individual groups to the east and west sides respectively, and secondly an analysis of the subdivided units 3, 4 and 5 across the east-west division. The object was to see if there was a statistical basis for the subdivision of the catchment into two halves, one comprising the sequence of unit groups 1e, 2e, 3e, 4e, and 5e down to the wadi bottom, and the other comprising the sequence 5w, 4w, 3w, and 6w up from the wadi bottom and across the Zin terrace. This was accepted if the differences between the units was not weakened by the sub-division (i.e units that previously reject the null hypotheses did not switch to null acceptance) and if the cross-division comparison of common east and west (the subdivided 3, 4, and 5) showed sufficient variation between sample groups to reject the null hypothesis.

Three data sets were used for the ANOVA;

(i) Comparisons of Aa, Ba and Ca axes to assess the difference within and between groups by particle size characteristics,

(ii) Comparisons of downslope and crosslope profile standard deviations (low level of data aggregation) to assess the difference within and between groups on the basis of the variation of the individual profiles from a straight line,

(iii) Comparisons of downslope and crosslope plot standard deviations (high level of data aggregation) to assess the difference within and between groups on the basis of the variation of the individual profiles from a single straight line passing through the mean of the ten profiles in each sample.

The results of the ANOVA tests are summarised below with a matrix showing the group comparisons and the acceptance or rejection of the Null Hypothesis (N) or of the Alternative Hypothesis (A). Some of the data used in the ANOVA are contained in Appendix 2.1 which summarises the micro-topographic conditions and surface material characteristics of the 127 samples. The ANOVA statistics are tabulated in Appendix 2.2.

2.3.6.b ANOVA of the Six Major Unit Groups - The Complete Catchment

Each of the six units were compared against each other unit, with 15 comparisons. The tests examined if there was sufficient homogeneity within the boundaries identified to class the samples as part of six statistically significant groups. This is true if the F-statistic is significant and the Alternative Hypothesis could be accepted for all or the majority of the comparisons. The results are presented in Figure 2.7.

From the consistency with which the Alternative Hypothesis was accepted, the sub-division of the catchment hillslope sections into six major units can be accepted at the 0.05% significance level. Considering comparisons (i) and (ii), the only digressions from this consistent result was with the C-axis of unit 1 and unit 6, which could not be significantly distinguished as different, with the downslope micro-topographic profile standard deviations of unit 4 and unit 6, and with the crosslope micro-topographic profile standard deviations of unit 5 and unit 6. The standard deviations that accepted the null hypothesis showed the units to be more similar than dissimilar in their microtopographic variation from a straight line. This does not mean that they have the same gradient, but that they possess similar variations from their best-fit profiles. Since in 12 out of 15 comparisons, all five characteristics; A, B, C axes, downslope standard deviation, and crosslope deviation at the profile level,

were significantly different from each unit to the next, the unit classification is acceptable. For the other three comparisons, since only one of the five characteristics was not significantly different, the degree to which the unit classification was weakened is minimal.

Figure 2.7 ANOVA Results for the Six Major Unit Groups

(i) Aa,Ba,Ca Axes

Un	1	2	3	4	5	6
1		AAA	AAA	AAA	AAA	AAN
2			AAA	AAA	AAA	AAA
3				AAA	AAA	AAA
4					AAA	AAA
5						AAA

(ii) Downslope S.D. by profile

Un	1	2	3	4	5	6
1		A	A	A	A	A
2			A	A	A	A
3				A	A	A
4					A	N
5						A

(iii) Downslope S.D. by sample

Un	1	2	3	4	5	6
1		A	A	A	A	A
2			N	A	A	A
3				A	A	A
4					A	N
5						A

(ii) Crosslope S.D. by profile

Un	1	2	3	4	5	6
1		A	A	A	A	A
2			A	A	A	A
3				A	A	A
4					A	A
5						N

(iii) Crosslope S.D. by sample

Un	1	2	3	4	5	6
1		A	A	A	A	A
2			N	A	A	A
3				A	A	A
4					N	A
5						N

(where A shows the acceptance of the Alternative Hypothesis, and N acceptance of the Null Hypothesis)

For the set of comparisons (iii), the picture was a little different. At this level of data aggregation, comparing the plot standard deviation, the distinction between unit groups was lost in 4 out of 15 comparisons. In two cases, unit 2 against unit 3, and unit 4 against unit 5, both downslope and crosslope standard deviations accepted the Null Hypothesis, and for cases unit 4 against unit 6 and unit 5 against unit 6 only one of the standard deviations, downslope and crosslope respectively, accepted the Null Hypothesis. This suggested two things. Firstly, that with decreasing resolution accompanying the aggregation of data, the unit groups were shown to be less different than at the more detailed level of the individual profile. Secondly that the aggregation of the data from the profile to the sample variance level resulted in a less sensitive statistic with which to compare the units.

2.3.6.c ANOVA of the Eastern Slopes Unit Groups

A comparison of the samples within unit groups of the eastern slope sections was made; units 1, 2, 3e, 4e, and 5e. The subscript e was used to indicate that the sample group is only part of the total catchment groups 1-6 used above. Each unit was compared against each other unit, with 12

comparisons. The comparison examines whether with the subdivision according to the sample position within the eastern slope sections, there was either an improvement, or no decrease in the ability to class the samples within as distinct statistically significant groups. The ANOVA results are presented in the matrices of Figure 2.8

Figure 2.8 ANOVA Results for the Eastern Slopes Unit Groups

(i) Aa,Ba,Ca Axes

Un	1	2	3e	4e	5e
1		A A A	A A A	A A A	A A A
2			A A A	A A A	A A A
3e				A A A	A A A
4e					A A A

(ii) Downslope S.D. by profile

Un	1	2	3e	4e	5e
1		A	A	A	A
2			N	A	A
3e				A	A
4e					A

(iii) Downslope S.D. by sample

Un	1	2	3e	4e	5e
1		A	A	A	A
2			N	A	A
3e				A	A
4e					A

(ii) Crosslope S.D. by profile

Un	1	2	3e	4e	5e
1		A	A	A	A
2			N	A	A
3e				A	A
4e					N

(iii) Crosslope S.D. by sample

Un	1	2	3e	4e	5e
1		A	A	A	A
2			N	A	A
3e				A	N
4e					N

(where A shows the acceptance of the Alternative Hypothesis, and N acceptance of the Null Hypothesis)

Again, on the basis of comparison (i), there was an unequivocal acceptance of the significant difference between the unit groupings. The strength of the differences between units on the basis of surface materials was not weakened in the subdivision of units 3, 4 and 5. Considering the comparison (ii), this was also true, but two unit comparisons which previously accepted the Alternative Hypothesis at the catchment scale, were unable do so when sub-divided, namely unit 2 against unit 3e for both downslope and crosslope, and unit 4e against unit 5e for the crosslope profile standard deviations. This suggested they are sufficiently alike to be classed as similar sample groups on the basis of their micro-topographic variation. Once again, this did not suggest the gradient is the same, but just that the distribution of topographic highs and lows from a straight line passing through them is similar.

At the aggregated plot deviation scale, the subdivision resulted in another unit comparison accepting the Null Hypothesis; unit 3e against unit 5e. However, with significant ANOVA statistics for all unit comparisons for particle size, and only one out of 12 comparisons failing to accept the Alternative Hypothesis for both downslope and crosslope micro-topography standard deviations, the

unit classification could again be generally supported. It is significant that the comparisons accepting the null hypothesis are generally geographically adjacent (2 and 3, 3 and 4 as shown in Appendix 1.2).

2.3.6.d ANOVA of the Western Slopes Unit Groups

Sub-division produces four western unit groups; unit 5w, 4w, 3w and 6. The comparisons determined whether with the subdivision of the unit groups into western sub-groups, there was either an improvement, or decrease in the ability to class them as statistically significant groups.

Figure 2.9 ANOVA Results of the Western Slopes Unit Groups

(i) Aa,Ba,Ca Axes

Un	3w	4w	5w	6
3w		N N N	A A A	A A A
4w			A A A	A A A
5w				A A A

(ii) Downslope S.D. by profile

Un	3w	4w	5w	6
3w		A	A	A
4w			A	A
5w				A

(iii) Downslope S.D. by sample

Un	3w	4w	5w	6
3w		N	A	N
4w			A	N
5w				A

(ii) Crosslope S.D. by profile

Un	3w	4w	5w	6
3w		A	A	A
4w			A	N
5w				A

(iii) Crosslope S.D. by sample

Un	3w	4w	5w	6
3w		N	A	A
4w			N	N
5w				N

(where A shows the acceptance of the Alternative Hypothesis, and N acceptance of the Null Hypothesis)

The western unit group comparisons all rejected the Null hypothesis and accepted the Alternative except for unit 3w and unit 4w which although dis-similar from units 5w and 6, could not be distinguished on the basis of their tri-axial A, B, C dimensions. The conclusion was that the surface stone materials mantling each are similar in size and shape. Again, the null acceptance was accepted from a comparison of geographically adjacent units.

Considering comparison (ii) in Figure 2.9, all comparisons showed significant differences and Alternative Hypothesis acceptance, apart from unit 4w against unit 6 in the crosslope. Thus although significantly similar in terms of surface materials, unit 3w and 4w showed significant differences in terms of their micro-topographic variability in both downslope and crosslope directions. The Null Hypothesis acceptance of comparisons between unit 4 and unit 6 in the downslope, and unit 5 and unit 6 in the crosslope observed at the catchment scale grouping, were not reproduced at the sub-divided western slope scale, suggesting that the similarities were due to those between the eastern side groupings of unit 4e and unit 5e and unit 6, with the western side groups being significantly different.

Considering comparison (iii) in Figure 2.9, once again at the aggregated plot standard deviations, the degree of differentiation between units was lost, this time in the majority of cases. Only unit 3w against 5w, 4w against 5w, and 5w against 6 for the downslope accepted the Alternative Hypothesis that the samples were significantly different to warrant a separate classification. The others showed statistically similar variations around their best-fit profiles. For the crosslope variations, only unit 3w against unit 5e, and unit 3e against unit 6 showed differences sufficient to warrant acceptance of the Alternative Hypothesis. Those units generally adjacent to each other geographically were shown to be similar.

2.3.6.e ANOVA of Unit Groups Across the East-West Division

The final ANOVA used the unit sub-groups; unit 3e, 4e, and 5e; and 3w, 4w, and 5w. Each unit was compared to each other unit, with 15 comparisons. The comparisons determined whether samples from the same overall catchment unit group were significantly different from, or similar to the same unit on either side of the east-west division, and from the other unit sub-groups.

Figure 2.10 ANOVA Results of the East-West Division of Unit Groups

(i) Aa,Ba,Ca Axes

Un	3e	4e	5e	3w	4w	5w
3e		A A A	A A A	N N A	A A A	A A A
4e			A A A	A A A	A A A	A A A
5e				A A A	A A A	A A A
3w					N N N	A A A
4w						A A A

(ii) Downslope S.D. by profile

Un	3e	4e	5e	3w	4w	5w
3e		A	A	A	A	A
4e			A	A	A	A
5e				A	A	N
3w					A	A
4w						A

(iii) Downslope S.D. by sample

Un	3e	4e	5e	3w	4w	5w
3e		A	A	A	A	A
4e			A	N	N	A
5e				A	A	N
3w					N	A
4w						A

(ii) Crosslope S.D. by profile

Un	3e	4e	5e	3w	4w	5w
3e		A	A	A	A	A
4e			N	A	N	A
5e				A	N	A
3w					A	A
4w						N

(iii) Crosslope S.D. by sample

Un	3e	4e	5e	3w	4w	5w
3e		A	N	N	A	A
4e			N	N	N	N
5e				N	N	N
3w					N	A
4w						N

(where A shows the acceptance of the Alternative Hypothesis, and N acceptance of the Null Hypothesis)

The comparisons of the unit sub-groups was important for determining whether or not the units accepted as different at the catchment scale should encourage a simple six-unit classification, or

whether the additional sub-division of units 3, 4 and 5 into two groups 3e and 3w, 4e and 4w, and 5e and 5w was necessary or justified. Considering comparison (i) it showed that only two comparisons of particle axes lead to the acceptance of the null hypothesis, that of 3e and 3w (B and C only), and 3w and 4w. The 3w-4w similarity was observed in the previous analysis of the western groupings. The comparison of 3e and 3w suggested the overall classificatory group represents a relatively homogeneous unit.

Looking at the comparison (ii) results, the similarities between either 3e and 3w or 3w and 4w were not carried forward for the downslope and crosslope micro-topographic standard deviations from the profile best-fit line. Both resulted in acceptance of the Alternative Hypothesis. For the downslope, only 5e and 5w showed similarity sufficient to accept the Null Hypothesis, whereas in the crosslope, 4e and 5e, 4e and 4w, 5e and 5w, and 4w and 5w showed sufficient similarity to accept the Null Hypothesis. The comparisons between those groups from the same side of the catchment have of course already been considered in the previous two ANOVA.

In comparison (iii) the aggregation of information produced a far lower proportion of unit comparisons accepting the Alternative Hypothesis. As with all the other analyses at this information scale, the whole catchment, the east side, and west side, the crosslope comparisons showed a much higher proportion of Null Hypothesis Acceptances than the downslope. Since this was also true for the profile best-fit standard deviations, it suggested that the downslope standard deviations of profiles from best-fit lines was a more sensitive, or variable characteristics from location to location than the crosslope.

2.3.6.f Conclusions from the ANOVA

By firstly postulating a number of hillslope units on the basis of field observations and measuring the physical characteristics important in defining the field units, ANOVA was used to evaluate the statistical significance of the field classification and whether it could be used as a basis for low resolution parameter distribution. If the variation between the sample populations of the different units was greater than the variation within the units, then the unit sample grouping could be accepted on the basis of its relative homogeniety.

The results show interesting conclusions with respect to the different variables used and the effect of aggregating topographic variation from indivual profiles to the sample level. They show that the textural variables of surface materials and micro-topography can be used to distinguish between different slope environments. The size of the materials from place to place show considerable variation which would appear to vary in systematic fashion related to slope form and geology. This is accepted since the definition of the field units is partly based on form and geology boundaries. The standard-

deviations of the micro-topographic profiles from their best-fit straight lines also show significant differences from unit to unit, although many of the differences are lost as the variation is aggregated from the individual micro-topographic profiles to the sample as a whole. The aggregation destroys the unique relationship between slope gradient, particle size and particle arrangement by aggregating each profile and assessing them relative to some best-fit profile that has no physical meaning. All the profiles are in fact independent and the standard deviation of each sample only gives an idea of the broad range of topographic highs and lows. The downslope profile seems to show more consistent variation between units than the cross-slope, probably due to the influence of slope gradient which dampens the effect of indivdual large particles on the standard deviation and reduces possible within sample variation from random elements. On the cross-slope profiles, indivdual particles can exert their maximum effect relative to the best-fit line of the horizontal.

It is interesting to note that from the analysis of the east versus west units above, only three comparisons out of 45 showed non-significant differences between samples in units from the same overall catchment unit class, and that none showed this characteristic for more than one of the attributes; surface materials, downslope and crosslope variation. The other Null Hypothesis acceptances were all generally between geographically adjacent unit groups (e.g. 3 against 4, 4 against 5). The units are numbered on the basis of a general erosional-depositional sequence continuing down the eastern slopes, and up the western slopes onto the plateau (in which 4w, 5w and 6w intersperse) in the general pattern 1e, 2e, 3e, 4e, 5e, 5w, 4w, 3w, 6w, 4w, 5w (see the profile cross-sections in Appendix 1.2). The groups also represent geographically adjacent units (3w-4w, 4e-5e, 5e-5w, 4w-5w). This suggests that on an overall basis, an east-west division can be accepted, and the classification extended from a six unit to nine unit system. It also suggests that in the areas of lower relative relief, which the environment of units 3, 4, 5 and 6 represent, the fixing of boundaries is by definition a difficult process, as shown by the tendency for at least one of the attributes to accept the Null Hypothesis, suggesting the presence of gradually changing functions and not abrupt, discrete jumps. This is one of the main difficulties facing a distributed model simplified by assuming a discrete number of characteristic types for the provision of parameters; the fixing of boundaries across a continua of parameter change.

This suggests that if the groups were subdivided additionally by profile, or by smaller increments downslope to produce a greater number of groups (for instance classifying unit 2; the chalky convexo-concave slope, as upper, median and lower due to the gradual thinning out of debris-fall and exposure of weathered chalk down the sequence), the number of acceptances of the Null Hypothesis would decrease as definitions became tighter and more exacting. The aggregating effect would decrease. However, the whole object of the exercise is to reduce the number of units adopted to a manageable proportion, in fact the smallest number at which significant differences can still be accepted as distinct groupings. This enables a limited number of process parameter sets to be distributed on the basis of a

small sample within the units identified. The assumption is that observed differences in key physical characteristics such as surface materials and micro-topography, given their significance for the process characteristics, can be used as a basis for quasi-distributing point measurements on a wider areal basis. This has been achieved to a statistically acceptable level.

CHAPTER THREE INFILTRATION

3.1 INTRODUCTION TO THE PROCESS

In 1933, Horton defined infiltration as being the set of physical processes by which water enters the soil. In the context of a water harvesting catchment supply system in an arid environment, infiltration is of interest in terms of the control on runoff generation within the catchment, and runoff transmission through and out of the catchment into the farming area. Infiltration is the key to the timing, the amount and the spatial distribution of runoff generation, since it is responsible for providing a limit to the rate at which water may pass into the soil. Consequently, of most concern is the magnitude of infiltration at each location, its change through time under different input conditions, and its variability through space, particularly the changes that take place along surface water flow lines down a hillslope.

The first step to understanding the rates and patterns of infiltration within an arid catchment is to examine the infiltration literature and determine the major theories concerning the controls on water movement into the soil. The applicability of each to the arid lands hydrological cycle must be evaluated and the processes identified that determine whether rainfall and runoff are consumed or allowed to move as surface flow through the drainage system.

The second step is to consider the methods of representing the infiltration process mathematically so that the likely consumption through time from a given input of rainfall and runoff onto a hillslope area can be reproduced. Infiltration models generally take the form of equations relating the infiltration rate or the cumulative infiltration as a function of time or the moisture content of the soil. There are a number of models, each of which have important implications for the calculation of runoff due to their varying abilities at representing the range of input conditions characteristic of the highly complex rainfall-runoff process. To select the most appropriate model it is necessary to consider their performance both in theoretical terms and practically. From fieldwork at the Avdat water harvesting system and from analysis of relevant data presented in the literature it is possible to parameterise the various models and determine their suitability for representing the observed conditions. The significance of the best-fit models can be examined in the light of the infiltration theory.

3.2 INFILTRATION THEORY

3.2.1 The Nature of Infiltration

Experiments in controlled laboratory and field conditions have shown that when water is applied as a continuous input to a soil surface, infiltration rates are initially high and gradually fall at a decreasing rate to a lower constant value (Collis-George, 1977). When a soil has a low moisture content, the flow process of infiltrating water is governed by the surface tension forces at the air-water interface where films of water around soil particles are separated by partially filled pores (Knapp, 1978). This combines with the force of gravity to pull water into the soil by a suction force. As water begins to fill the voids, the tension forces reduce until gravity controls the movement of water downwards and infiltration approaches the lower relatively constant final value once saturation of the soil profile is reached (Overton and Meadows, 1977).

Under the conditions of continuous water supply, the soil profile characteristically exhibits three zones; the transmission zone where moisture content changes slowly with depth and time, a wetting zone with rapid changes in moisture content with depth, and the wetting front, marking the visible limit to water penetration. For simple soil systems, it is accepted that the flow gradient down to the wetting front becomes constant in the transmission zone, a fact supported by the observation that in most experiments, a steady-state infiltration rate has been attained in measurable time (Collis-George, 1977). The rate of change at which the steady state conditions are approached vary from location to location depending on the physical characteristics of the soils which affects the rates and routes by which water enters the soil.

3.2.2 Factors Controlling Infiltration

According to Horton (1940), the infiltration capacity of a given surface is controlled chiefly by soil texture, soil structure, vegetation cover, biological structures, soil moisture content, and the condition of the soil surface. Infiltration and the resultant soil water profiles depend on the nature of surface entry, transmission and depletion of available storage capacity (Scoging, 1988). Dixon *et al* (1978) identified 9 enhancing and 13 abating factors affecting the magnitude and change of infiltration. Although different combinations of the factors produce different infiltration under a given input condition, it is hard to identify their individual effects under practical conditions.

The enhancement factors leading to higher and more prolonged infiltration rates through time include; increasing flow dimensions with time, eluviation and illuviation leading to micropipe formation, increasing soil wet-ability with depth, decreasing water repellency with depth, increasing ponded water with time, soil water absorption of entrapped air, macropore formation through solution

of soluble salts, increasing ponded surface area with time and melting of soil ice by the infiltrated water.

The abatement factors leading to lower infiltration and more rapid changes to the final constant rates include; decreasing capillary pressure gradient due to deepening wetting front, surface sealing under raindrop impact, decreasing capillary pressure gradient due to increasing moisture content with depth, swelling of clay colloids with corresponding shrinkage of macropores, anaerobic slime formation, rising soil air pressure and the consequent entrapment of soil air in macropores, and freezing of the infiltrated water with consequent blockage of fluid flow routes.

Added to these controls are the characteristics of the infiltrated water itself including its temperature, electrolyte concentration and viscosity. The first two will be important where the chemistry of the soil is an important control on infiltration, in particular in the flocculation of clay minerals. An even more complex and indeterminate control is that of variable rates of water supply at the surface, since the conditions of freely ponded water assumed in the development of most infiltration theory cannot be assumed under natural rainfall-runoff conditions (Scoging, 1988).

3.2.3 Conceptual Approaches to Infiltration and Runoff Generation

Infiltration, therefore, is a complex phenomena which has received considerable attention by hydrologists but for which no universally accepted conceptual model has been produced from the theoretical and practical studies carried out to date. Within the literature, there are three major conceptual approaches towards infiltration and its control on runoff. These are the Hortonian approach, the saturation approach (Hewlett, 1961) and the "leaky bottle" approach (Kirkby, 1978, 1980).

3.2.3.a The Hortonian Approach

The Hortonian approach sees infiltration as being limited by transmission, either at the surface or deeper in the profile. The theory comes from the work of Horton (1933) who proposed that runoff generation occurs universally due to an excess of rainfall intensities over the capacity of the soil to infiltrate the applied water. His concept was that there is a maximum limiting intensity at which rainfall can enter the soil at a given time. Any intensity above this rate will produce runoff, and any intensity below will not. The Hortonian model is often called the Infiltration Mode of surface runoff (Kirkby, 1978) with the maximum infiltration capacity defined by an infiltration curve of infiltration intensities plotted against time Rainfall in excess runs off and rainfall infiltrated is assumed to reduce the rate in subsequent time periods. Infiltration into the surface can be limited by several factors;

1. by the rate of supply which can be less than the infiltration capacity of the soil,
2. by the presence of a significant proportion of impermeable materials such as large stones or bedrock outcrops that prevent the intake of water and result in a larger effective supply onto the remaining soil covered area in excess of infiltration capacity,
3. by the operation of soil crusting properties that result in the gradual sealing of the surface by a layer with low hydraulic conductivities due to the mechanical and chemical forces exerted by the rainfall.

According to Kohler (1963), Horton's infiltration model is strictly applicable only to 'pure surface runoff', where the surface limits water entry or where rainfall intensity is greater than infiltration capacity.

3.2.3.b The Saturation Approach

The saturation approach to infiltration and runoff concentrates on the volumetric storage space within the soil as being the limiting factor for infiltration (Hewlett, 1961). It is incorporated into Dunne's interpretation of catchment area hydrology and the humid partial area contribution theory (Dunne *et al*, 1975. Dunne, 1983). Under conditions of relatively low rainfall intensities, only when the soil is saturated through infiltration and throughflow will runoff occur.

The saturation approach is based on determining a volumetric storage capacity for the soil and calculating a mass balance between the rates of additions to the moisture store and the rates of depletions. The addition comes from both the surface and from within the soil mass by lateral throughflow, a factor which is aided by the presence of sub-surface barriers such as a bedrock or an impervious laterite, clay or caliche layer. Saturation occurs most readily at hollows and at the foot of slope sections. Elsewhere, infiltration capacities remain above rainfall rates for the duration of rainstorms but in the wetter areas, storage can rapidly be filled by quick throughflow and infiltration and subsequent rain runs across the surface along short flow-paths into streams and rivers (Dunne *et al*, 1975). Depletion takes place by deep percolation, lateral throughflow downslope and evapo-transpiration (Dunne *et al*, 1975. Anderson and Burt, 1978. Hewlett and Nutter, 1970). This interpretation was developed to describe the infiltration regime in humid regions where rainfall intensities are relatively low, soils are deep and well-vegetated, and where soil throughflow is prevalent.

3.2.3.c The Leaky Bottle Approach

The third conceptual approach accepts that both of the above are valid in that there are transmission and storage controls on the amount of infiltration and therefore the timing of runoff production for a given pattern of input. The two regimes are not mutually exclusive. Infiltration can

be determined by both the rainfall intensity relative to the capacity for intake, and by the volume of the storage, factors that can be expected to occur even within the same rainfall event. This approach is termed the leaky bottle as presented by Kirkby (1978). Water will enter the soil until one of two limits are reached; either the neck of the bottle is too narrow to accommodate the rate of the supply at the surface, or because the bottle is already full and no storage remains. Recently, Scoging's results from Spain (1988) have thrown doubt on the sub-division of infiltration into the different Hortonian and Saturation models. She presents an interpretation which explicitly allows for a fixed storage volume that is depleted at a rate related to the final infiltration rate and is dependent on profile control once storage has been filled. The time to runoff is dependent on both rainfall intensity and soil storage volume.

3.2.4 Infiltration in Arid Environments

3.2.4.a Infiltration and Runoff Mechanisms

The Hortonian mode of infiltration is often used to explain infiltration conditions in an arid environment. Although research has been carried out into the physics of infiltration and its pattern within a drainage basin, conditions have been largely atypical of arid environments. Unlike in the humid environs, infiltration can be limiting relative to rainfall rates and large quantities of surface water are generated at various locations without the apparent need for complete saturation of the soils. The physical characteristics of the soils exert strong profile controls especially where;

1. infiltration capacities are uniformly low and below rainfall intensities. This is the classic Horton mechanism (Horton, 1933).

This mechanism has long been held to be the dominant cause of runoff generation in arid areas. Horton's theory of widespread, universal runoff has been accepted as the general interpretation and the dominant infiltration-runoff model for arid regions (Dunne, 1983. Freeze. 1972). Where there are universally low infiltration capacities it will be because of the following; limited vegetation cover, poorly aggregated soil surfaces, poor macro- and micro-pore structures worsening with depth, low available moisture storage volume due to poorly weathered regolith and large volumetric percentages of rock in shallow soil profiles.

2. high proportions of totally impermeable surface materials contributing rapid runoff to the remaining materials in excess of their high infiltration capacities (Yair *et seq*). This is the barrier mechanism.

The effects of the varied nature of surface materials on the amount of water infiltrated is that runoff will depend on the relative proportions of infiltrating and non-infiltrating surface components. The proportion is usually more impermeable on steep, rocky areas of the landscape and less so on the lower more shallow colluvial slopes. In the Negev, this has been stated as the dominant control on spatial patterns of infiltration in the work of Yair *et al* (*et seq*), as described in Chapter One.

3. high initial infiltration capacities in excess of rainfall rates, but where a surface crust forms under raindrop impact producing infiltration rates below rainfall intensities (Ellison, 1944. Hillel, 1960. Farres, 1978. Bryan *et al*, 1978. Agassi *et al et seq*). This is the crusting mechanism.

Within the arid environments, the exposure of soil surfaces to the direct impact of raindrops due to limited vegetation cover, and the concentration of fine particles in the surface layer by wind-deposition and infiltration of sediment-carrying overland flow allows crusts to form. With crusting soils, the infiltration capacities depend on the state of the soil prior to rainfall beginning. Stable aggregates, rough soil surfaces and high soil sodicity reduce the effectiveness of crusting and promote higher infiltration values (Agassi *et al*, 1986). Where the surface is aggregated, for instance on tilled ground, infiltration capacities are initially very high depending on the soil and the arrangements of aggregates. All rainfall can infiltrate but the aggregates are gradually broken down by raindrop impact, the tension forces of wetting and the chemical forces of cationic exchange (Ben Hur *et al*, 1985. Agassi *et al*, 1985a. Agassi *et al*, 1986). Desiccation cracks are filled, the aggregates disperse with the formation of a wash-in layer of fines and a thin, dense impact layer on the surface, and the macro- and micro-pore structure is cut-off, reducing infiltration rates dramatically. On already crusted soils, the effect is less dramatic, with lower initial infiltration capacities depending on the density and size of desiccation cracks and a more gradual change through time as the crust is reinforced rather than constructed (Morin and Benyamini, 1977. Agassi *et al*, 1985b).

The result is a thin layer of low hydraulic conductivity where water flow into the soil is inhibited even though high suction forces exist in the soil below the crust. The suction may draw clay particles into the pore structure (Morin *et al*, 1981). According to Hillel (1960), the effect of the over-lying crust is to lower the water intake as a function of the increased bulk density. As indicated in Chapter One, crusting has been presented as the major control on catchment runoff production in the Negev (Shanan, 1975. Shanan and Schick, 1980. Evenari *et al*, 1980) where loessial soil deposits occur on the plains and valley bottoms.

These three mechanisms of runoff generation all conform to the Hortonian approach to runoff generation and infiltration and the traditional view is that the role of saturation of soil storage is relatively unimportant in arid environments. However, recent studies by Scoging (1988), and Scoging

and Thornes (1980) have shown that the storage limitation can also be an important control on runoff generation. They state that many arid soils have a low, fixed storage volume into which all water will initially infiltrate causing a delay until runoff is generated. The saturation is profile controlled with subsequent infiltration rates converging on the saturated conductivity of the soil profile. The profile control may be exerted immediately at the surface by the presence of a crusted layer with low permeability. With higher rainfall intensities, storage is filled more rapidly up to a limiting volume that is independent of any further increases in rainfall intensity. This runoff control can be called the storage mechanism.

3.2.4.b Factors Affecting the Spatial Patterns of Infiltration and Runoff

It is clear that the infiltration process and controls on runoff production are by no means uniform in arid environments. Although large quantities of surface water are produced, they are not produced uniformly, and will move through the system in spatially and temporally variable fashion. The rainstorms themselves are sporadic with spatial and temporal variations in intensity within short distances and times and characterised by bursts of high and low intensities. Times to runoff and opportunity for subsequent infiltration will differ according to which of the mechanisms are dominant within different areas of the catchment system. Where neither crusting or barrier mechanisms operate, and where available moisture storage is not limiting, infiltration will remain consistently higher and no rainfall excess may result. The potential for infiltration remains high.

The implication of this spatial variability in infiltration potential is that runoff can be consumed along particular flow-lines. Where rapid surface water production juxtaposes with areas of high infiltration capabilities, the result may be a discontinuity in the movement of surface water towards the channel system as runoff is consumed on its passage downslope. The passage of water onto the hillslope area with unsatisfied infiltration potential provides the opportunity for infiltration. If infiltration remains constant or decreases down a given flow-line, this opportunity does not exist until rainfall ceases or reduces significantly. Thus as well as considering infiltration as a point process, it is necessary to consider its spatial dimensions and in particular its variations along flow-lines if a clear understanding of arid catchment hydrology is to be achieved. Added to these macro-scale aspects of potential and opportunity are the micro-scale aspects which focus on the surface characteristics that control the proportion of the surface area in contact with runoff water and the rate of movement of the runoff water across the surface. Whilst it may be difficult to measure or model these micro-scale aspects in great detail when considering the rainfall-runoff process at the hillside or catchment scale, it is worth considering them in a descriptive sense as a way of understanding the inter-play between infiltration potential and opportunity and particularly the relative magnitudes for different surfaces and slopes.

In arid environments such as the Negev at Avdat, the hillslopes are characterised by a wide range of slope gradients and cross-slope and downslope micro-topographic profiles. Slope surfaces are seldom planar with the micro-variation a product of both form and materials. Topographic highs may be both the result of large particles lying in the surface layer, or by micro-interfluves caused by an arrangement of smaller particles into rills or furrows, or isolated mounds and depressions. The importance of these microtopographic features have been embodied in the concept of the 'Air-Earth Interface' (AEI) model of infiltration control. Working on shallow sloping agricultural land on methods of controlling infiltration through soil surface management, Dixon (1975) examined ponded water loss on furrowed and un-furrowed plots. In his model, Dixon defines the concepts of inter-facial roughness and openness. Roughness refers to the micro-relief that determines the distribution of ponded water across the surface, and openness refers to the macroporosity that is visible on the surface. The two are closely related. If the surface is rough and open (a furrowed and mulched or aggregated surface), then air and water can be rapidly exchanged between covered and uncovered soil and water moves rapidly inward along short broad routes through the macropore system. If the surface is smooth and closed (a flat and compacted, dense surface), the exchange of air and water is inhibited as the whole surface is covered and as water moves only slowly via the long, tortuous paths of the micropore system. The roughness of the surface determines which macro-pores are covered by water (as for instance in a rilled field) and the density and sizes of macropores determines how quickly this water will infiltrate. In Dixon's studies, the different roughness and openness of the hillslope surface is manufactured by hand furrowing, compacting, mulching and vacuuming of natural soil plots on shallow sloping fields.

A similar concept had been presented by Hickock and Osborn (1969) who make the following analogy of infiltration at the surface; rain entering the soil surface is like water falling on and flowing over the open ends of a closely packed mass of very small diameter vertical tubes or pipes with relatively wide undulating variation in elevation of the surface described by their upper ends. It is apparent that the rate at which water may flow into the pipes depends not only on their size, but also on whether the rate of supply is such as to cause ponding over all or only some of their open ends, as these openings are at various elevations. The role played by the macro-porosity is influenced by the micro-topography. Also the condition of the entrances to the pipes may vary considerably with rainfall intensity and antecedent conditions. This concept was analysed by Beven and Germann (1982) who consider the flows into macro-pipe systems and the effect of their arrangement across the surface.

Dixon's concept of the AEI conforms with the barrier and crusting mechanisms as major determinants of runoff through limiting infiltration capabilities. The crusted soil is an example of Dixon's micro-smooth and closed surface, generally having little micro-topographic variation from the horizontal and a choked micropore and macropore system as a result of surface changes. Prior to the surface changes, however, the infiltration rates would be relatively high. The barrier mechanism usually operates on surfaces that have a high degree of microtopographic roughness, with the large

particles and rock outcrops usually forming the topographic highs, and the intervening soil covered areas the topographic lows. Although soils generally have a coarser texture, the soil covered surface has negligible infiltration capacity relative to the combined rainfall and runoff rates, and hence total infiltration is low. The high degree of roughness, is offset by the absolutely low openness, an observation supported by Yair and Lavee (1976, 1985) and Poesen (1986) through their experimental studies.

On micro-rough surfaces with no barrier effect, it is obvious that infiltration will be relatively high for two reasons. Firstly, in the initial part of a rainfall event, where infiltration is controlled by tension forces, the volume infiltrated will be proportional to the surface area of the ground and not the plan area (the opposite will be true when gravitational forces dominate). Poesen (1984) showed that with increasing rill depth and density, the surface area through which rainwater can enter the soil increases, and infiltrated volumes are higher. Secondly, if ponding occurs and rainfall ceases or falls below rainfall intensities, the avenues for air and water exchange will be left open by the exposure of areas free of ponded water as runoff is concentrated in the rilled sections.

The volume of infiltration will be a direct function of the infiltration rates and the area of contact within a total plan area of hillslope. It will also be a function of the length of time water is available for infiltration and this depends on the rate of movement of water over the surface. Both of these factors are determined by the micro-roughness of the surface, the latter in combination with the slope gradient which determines the potential energy of the water. Microtopography helps determine the length of slope brought into contact with a given runoff discharge, the resistance exerted against its movement and the cross-sectional shape it must occupy in its passage downslope.

Thus the surface of a hillslope; its material composition, micro-topography, and gradient can be seen as major influences on the nature of the infiltration process and the volume of water that will pass into the surface. However, in studies in the literature on modelling infiltration and calculating infiltration rates from field measurements, surfaces are generally simplified and their effects ignored. The assumption is that when water ponds, and then moves across the surface, it does so as a sheet, with rainfall and runoff spread evenly over the plan area. There is no opportunity for partial ponding, and infiltration is assumed to take place over the whole surface. There will only be two states, infiltration from rainfall alone pre-ponding, and infiltration from ponding. Therefore, infiltration rates are calculated on the basis of plan area, even though during the tension dominated early stages of infiltration inflow they will be proportional to surface area, and even though rainfall excess will not be distributed evenly, varying in proportion to the ratio between the volume of water at the surface, and the variation of the microtopography from a plane. This is partly a response to the complexity of the process and our inabilities to produce detailed models accounting for it at the hillslope or catchment scale. However, the surface is the focal point at which the micro and macro features of infiltration

interact. The macro-aspects of spatial variation determine the juxtaposition of flow production and consumption and the micro aspects determine the relative importance of particular phases in determining how much water is actually consumed within the system. Adopting a sheetflow approach has significance for both aspects.

3.3 MODELLING INFILTRATION

Because of the complexity of the process, and because of the fact that most models describe simplified systems through laboratory analysis, a physics-based model of infiltration under arid conditions has not yet been formulated. As described previously, water supply is intermittent and spatially non-uniform in arid zones, and soil conditions are often spatially heterogeneous with a non-uniform vertical structure. Both rainfall and runoff play an important part in determining exactly how much infiltration takes place. These characteristics are not easily simulated under controlled laboratory conditions.

However, it is clear that a variety of mathematical expressions that relate the infiltration capacity to some known state such as elapsed time from water first being supplied, cumulative precipitation, or the amount of water stored in the soil can be applied to the arid environment. These expressions include a number of parameters which are assumed to adequately represent the experience of the soil under a given range of conditions. Both physics-based equations using measurements of soil conditions, and empirical equations using measures of the water infiltrated under given conditions can be used. Whether a single equation, or a number of equations are applied for a particular soil depends on the approach taken to within storm and between storm antecedent conditions, and/or the limitations of the fieldwork data-sets supplying parameters to the model.

3.3.1 The Objectives of an Infiltration Model

Mein and Larson (1973) stated that of the many components of a watershed model, infiltration has the largest influence on the volume of watershed runoff. They suggested that for a hydrologist to properly represent the processes of infiltration, the time to ponding must be predicted, and the subsequent decline in infiltration capacity from this time forecast.

A successful rainfall-runoff modelling exercise depends upon the accurate simulation of the amount, temporal and spatial distribution of lateral inflow to a sequence of physical elements used to describe the system, which to a large degree is determined by the infiltration parameters (Woolhiser, 1981).

Since the objective of this work is to examine the rainfall runoff processes determining the response characteristics of a natural catchment modified for the purposes of runoff farming by the introduction of a water harvesting channel system, the infiltration model seeks to describe rather than explain the soil water movement taking place. It can be argued that as long as the model predicts times to ponding and subsequent infiltration rates adequately it is of little consequence whether it does so because of its underlying physical concepts, or because of its inherent mathematical characteristics. However, this does not mean that models with a strong physics base and developed from a theoretical knowledge of soil water flow processes should not be used. It is generally accepted and desirable that the parameters in an infiltration equation have physical significance (Collis-George, 1977). This is an aid to interpreting the predicted results in the light of the observed conditions.

An infiltration model should ideally be capable of predicting the time to runoff (t_o), and the time distribution of infiltration capacity (i), for a range of inputs. Most models are formulated for the condition where the supply of water is continuous and in excess of the capacity of the soil, i.e. conditions of ponding. Consequently, the ability of the models to reproduce infiltration for conditions of varying input and supply less than infiltration capacity is indeterminate. Each model can be examined to see if it will produce the observed or expected results under the following four rainfall conditions;

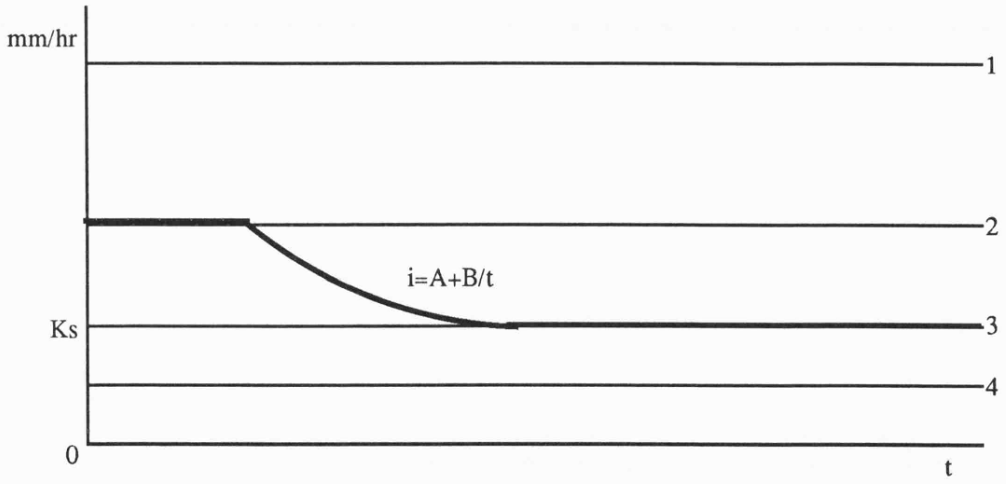

Figure 3.1 Four Rainfall Conditions Important for Infiltration Models

1. where the rainfall intensity p is high and in excess of the infiltration capacity i at all times (the classical Horton runoff condition),
2. where the rainfall intensity p is less than infiltration capacity i at t = 1, but is greater than the saturated conductivity Ks ,
3. where p is equal to the saturated conductivity Ks,

4. where p is less than the saturated conductivity Ks.

Despite the importance of infiltration, most models of the infiltration process have serious deficiencies in their representation of infiltration from rainfall (Mein and Larson, 1973). When infiltration models consider infiltration as a function of time alone then where rainfall intensity is less than the infiltration capacity, 'negative' runoff is predicted rather than accounting for the positive contributions to soil moisture in this pre-runoff phase (Scoging, 1988). This is seen as a disadvantage since to some extent the infiltration model acts independently of the soil state, relying only on the time count to determine the rate of change. By looking at the performance of different models under the above four conditions, the implications of their assumptions for accurate runoff production can be assessed. This is discussed in Section 3.3.3 below. Related to this are the infiltration and flow phases introduced earlier. The input of other water than rainfall plays a major role in the infiltration process and is affected by the assumptions concerning the kind of surface environment assumed, complex or planar.

3.3.2 Models and Their Characteristics

Infiltration has been characterised by hydrologists with only gross simplifications (Smith and Chery, 1973). Where a single time-dependent curve is used, the model conforms to the Hortonian mode of runoff generation, with all water infiltrating until a limiting infiltration capacity is exceeded by rainfall intensity at time $t = t_o$. Time is a surrogate parameter for the physics of the process. The physics-based approach, adopts a model where infiltration rates are not purely functions of time since the onset of rainfall. Under laboratory conditions, independent variables other than time can be measured as to their influence on the eventual shape of the infiltration decay curve and a mathematical expression relating these variables is then developed to predict infiltration at different physical states.

3.3.2.a The Hortonian Models

The Horton Equation

Horton (1933, 1945), fitted an empirical equation to measured data ;

$$f^{\bullet} = fc + (fo-fc)e^{-k^{\bullet}t} \qquad \text{Equation 3.1}$$

(where $f^{\bullet}$ is instantaneous infiltration rate, fc minimum infiltration capacity, fo maximum infiltration capacity, and $k^{\bullet}$ a soil constant, e is the base of natural logarithms 2.718, and t is time from the beginning of the rain).

In terms of the longer duration rainfall events effective in producing floods, the term fc is most important. As indicated, the Horton model is time dependent, and does not change with the nature of the incoming precipitation or the patterns of inflow from other flow-producing slope sections. The term fc will not vary since it is proportional to the saturated conductivity.

The Agassi Infiltration Equation

Agassi *et al* (1986) describe infiltration as a function of cumulative rainfall and some soil parameters. The equation is similar to that of Horton but refers specifically to infiltration into crusting soils by defining the soil constant α from a measure of aggregate stability and including the precipitation intensity in the power term;

$$It = If + (Ii - If)\, e^{-\alpha pt} \qquad \text{Equation 3.2}$$

(where It = initial infiltration, If = final infiltration, t = time from beginning of rain, e is the base of logarithms 2.718, α = coefficient related to aggregate stability and p = rainfall intensity).

In this formula, the infiltration rate decreases sharply with the increase in rainfall intensity since it is related to cumulative rainfall. Derived from their analyses of crusting soils, Agassi *et al* provided a series of values for the various parameters depending on the state of the soil prior to the rainfall event. Un-crusted, aggregated soils have higher parameter values than the already crusted soils.

The Kostiakov Equation

The Kostiakov equation was empirically derived to describe the time-course of infiltration as an initially dry soil absorbs irrigation water (Dixon *et al*, 1978).

$$I = A.t^{B} \qquad \text{Equation 3.3}$$

A is said to have a physical interpretation as the product of the mean conductivity and the driving force gradient for the first time period (Dixon *et al*, 1978). In this formula, the coefficient B is negative, since infiltration decreases with time. Consequently, it is clear that as time tends to infinity then infiltration tends to zero.

It is more easily used in its log10-linearised form;

$$\log i = \log A + B.\log t \qquad \text{Equation 3.4}$$

According to Dixon, large A values are associated with soil surfaces that are micro-rough and macro-porous or with conditions favouring dominance by gravitational forces. Small A values are associated with micro-smooth and micro-porous surfaces where capillary suction forces dominate infiltration rates.

The Philip Equation

The Philip equation (1957) was derived analytically for the downward absorption of water into an initially dry stable porous medium.

$$F' = S't^{1/2} + A't \qquad \text{Equation 3.5}$$

(where F' is volume of infiltration at time t, S' is the sorptivity constant, and A' the transmissivity constant).

A modified Philip equation that accounted for hydrograph shape more closely was derived by Bork and Rohdenburg (1981) from empirical studies in semi-arid southern Spain;

$$i = A^{\bullet} + S'/\sqrt{t} \qquad \text{Equation 3.6}$$

(where i is the instantaneous infiltration rate, $A^{\bullet}$ the final infiltration rate, S' the sorptivity and t time)

For short times, the Philip equation gives satisfactory descriptions for a large range of soils. The S' term gives the infiltration contribution of capillary forces (suction) and the A term gives the contribution from gravitational forces (Dixon *et al*, 1978). Philip remarks (1969) that fitting the curve as a best-fit to field data results in A equal to Ks, the hydraulic conductivity of the soil. It is the most widely used infiltration model, often assumed to be a storage equation. Section 3.3.3 shows this is not the case.

Bloomfield *et al* (1981) recognise that simple equations relating infiltration to time have serious limitations when considering intermittent rainfall, since they cannot cope with soil drainage and subsequent increase in infiltration capacity through time. This concords with the views of Scoging (1988). Where restricted supply conditions are in operation as is the case under most natural, variable storm intensities at some point during the duration of the event, predicting the time to infiltration excess is difficult. Once rainfall ceases or reduces to low intensities below infiltration rates, the condition of ponding may be lost. Calculating infiltration empirically means that all rainfall will infiltrate and that there will be unsatisfied infiltration. If there is no runoff entering the slope area from upstream to make up this deficit, this will mean that the accounting procedures of the model are

predicting negative infiltration rates. In Hortonian models there is no account of storage and so this negative potential is ignored in runoff calculations. By not allowing for the fact that infiltration has been unsatisfied, subsequent infiltration rates will be an underestimate of what they should be. Under these conditions, especially if rainfall stops completely as in the case of a rainstorm characterised by showers it may be desirable to select a separate infiltration curve based on dry and wet infiltration conditions, with a different set of parameters. This allows empirically for the readjustment of the soil's infiltration potential. This approach was adopted by Scoging (1988).

3.3.2.b The Non-Hortonian Models

The non-Hortonian models do not consider infiltration purely as a function of time, but consider it to be controlled by the physical characteristics of the soil which determine the volume of macro and micro-pores available for the intake and storage of water. With this storage approach, the problems of negative runoff predictions are avoided.

The storage approach to infiltration assumes that because of the structural characteristics of the soil profile, there is only a limited volume of water that can be accepted into the soil. This may be controlled by surface layer conditions or by profile characteristics deeper in the column. When all pore spaces are full, then water can be transmitted into the soil at the rate of saturated conductivity. Until then, infiltration rates are assumed to be in excess of the ranfall intensity and all water infiltrates.

The Green and Ampt Equation

The Green and Ampt equation, formulated in 1911 was derived by applying Darcy's law to the situation of infiltration from an excess surface water supply from time zero. As well as for these conditions, Mein and Larson (1973) stated that the model has been successfully applied to non-uniform profiles that become denser with depth, and also to the case of partially sealed surfaces (Hillel and Gardner, 1969). It has been shown to have good to excellent predictive ability for constant rainfall intensity, homogeneous soil, and uniform initial moisture content in the zone of infiltration. It is applicable to events that produce delayed rainfall excess whereas most empirical equations are not (Mein and Larson, 1973).

The Green and Ampt equation has been presented in a variety of forms. Scoging (1988) presents the following equation based on the original Green and Ampt version;

$$i = [Ks (H + Zf - Pf)] / Zf \qquad \text{Equation 3.7}$$

(where i = infiltration rate, H = depth of ponded water, Ks = saturated conductivity, Zf = vertical depth of saturated zone, and Pf = capillary pressure at wetting front).

This can be rearranged to be;

$$i = Ks + [Ks(H - Pf)]/Zf \qquad \text{Equation 3.8}$$

and simplified to;

$$i = A + B/Zf \qquad \text{Equation 3.9}$$

(where A is related to wetting conductivity and B is related to storage volumes).

Mein and Larson (1973) state that;

$$I = Kfs\ [1 + (Di.Sav/F)] \qquad \text{Equation 3.10}$$

(where Sav = soil water suction at the wetting front, Di = the initial soil moisture deficit, Kfs = hydraulic conductivity at 'field saturation' and F = volume of infiltration at time t).

This can be rearranged to;

$$i = Kfs + (Kfs.Di.Sav)/F \qquad \text{Equation 3.11}$$

and simplified again to;

$$i = A + B/F \qquad \text{Equation 3.12}$$

The original formats of the Green and Ampt curve (Equations 3.7 and 3.10), indicate one of the drawbacks of physics-based models. They rely on the specification of soil characteristics such as moisture deficit, or capillary suction, which are seldom measurable in most field studies, and laboratory studies cannot re-create conditions similar to those found in the field to which they must be applied. The key assumptions involved with the derivation of the theory, namely a permanent hydraulic head (ponding) and a uniform and free-draining profile, are seldom satisfied making parameter provision difficult.

However, if the Green and Ampt equation is simplified by assuming the vertical depth of the saturated zone or the volume of infiltration at time t to be a linear function of time, Zf and F can be

substituted with elapsed time t, and the equation used as an empirical equation fitted to measured data, with the parameters having direct physical significance as shown; A being related to the steady state infiltration rate, and B reflecting the storage capacity within the soil mass.

$$i = A + B/t \qquad \text{Equation 3.13}$$

Infiltration occurs under flux control at a rate determined by the rainfall intensity relative to the soil storage requirements until a time t_0 when a fixed moisture store is filled when saturation and runoff occur. Thereafter, the infiltration rate is increasingly controlled by the A parameter (Scoging, 1988). In their analysis of infiltration into soils mantling semi-arid limestone and marl hillslopes in south-east Spain, Scoging and Thornes (1980) developed this simplification of the physically based Green and Ampt equation and apply it to their field data.

3.3.3 Times to Ponding with Hortonian and Storage Models

A key condition for any soil receiving a given rainfall intensity is the time to ponding t_0. This occurs where rainfall rates (and/or supply rates of run-on from locations upslope) are equal to the infiltration capacities predicted by the infiltration equation and for Hortonian models this signifies the point of infiltration excess. For storage models it signifies the point of storage saturation, which may be profile saturation, as in the Dunne mechanism, or surface saturation, as in the Scoging and Thornes analyses (1980). Regardless, at this point p = i and taking the two Hortonian-type equations of Kostiakov and Philip and the storage equation of the modified Green and Ampt, it is possible to see why they each conform to the particular interpretation, and the implications for the way runoff production would be modelled given different input intensities and the predicted infiltration rates through time.

3.3.3.a The Green and Ampt Storage Equation

Where the rainfall intensity is initially less than the infiltration capacity, the infiltration is equal to the precipitation at the time to ponding t_0 when p = i (Scoging, 1988).

$$i = A + {}^{B}/_{t} \qquad \text{Equation 3.13}$$

$$p = A + {}^{B}/_{t_0} \qquad \text{Equation 3.14}$$

$$t_0 = {}^{B}/_{(p-A)} \qquad \text{Equation 3.15}$$

Since V_S, the depth of water infiltrated to the point of ponding, is the product of the constant p and the time t_O then;

$$p.t_O = p.B/(p-A) \qquad \text{Equation 3.16}$$

$$V_S = p.B/(p-A) \qquad \text{Equation 3.17}$$

As the rainfall intensities increase such that (p - A) is almost equal to p, then V_S converges on the constant value of B as p/(p-A) approaches unity. This is to be expected as the B represents the storage parameters in the Green and Ampt equation. Thus there is a constant value to the storage character of the soil which reflects the soil conditions and not the rainfall intensity.

Consequently, it is clear that the condition where rainfall intensity is in excess of infiltration rates from time t = 0, cannot occur if the equation is used in its storage context. Whatever the intensity, the depth V_S must be infiltrated before runoff occurs. Obviously, as intensities increase, t_O falls to a very small time period.

The parameter A represents the saturated conductivity of the soil. If p is equal to A for the duration of the rainstorm no rainfall excess will result because the time to ponding t_O and the storage volume V_S will both be infinity. If p is less than A, then the time t_O will be negative, as will the storage volume V_S. This implies that runoff will not occur and is outside the bounds at which the equation is valid (i.e where $p \geq A$ only). If p is greater than A, then so long as the rainfall duration (t_p) is sufficiently long, runoff will always occur. If t_p is less than the value t_O calculated from Equation 3.15, and hence the total depth of the rainstorm is less than the value of V_S, no runoff will result.

The reason why t_O and V_S varies according to the relative magnitudes of p and A is due to the effect of the saturated conductivity of the soil on the stored volume of infiltrated water in the soil. During the course of the rainstorm, the saturated conductivity, or gravitational percolation rate, will remove water out of the profile controlled store equal to a total depth defined by the product of the parameter A and the time to ponding (at saturation) t_O. This can be seen mathematically by deriving an equation in terms of V_S, B, A and t_O.

$$t_O = B/(p - A) \qquad \text{Equation 3.15}$$

$$V_S = p.t_O \qquad \text{Equation 3.18}$$

$$t_O(p - A) = B \qquad \text{Equation 3.19}$$

$$p.t_o - A.t_o = B \qquad \text{Equation 3.20}$$

$$p.t_o = B + A.t_o \qquad \text{Equation 3.21}$$

$$V_s = B + A.t_o \qquad \text{Equation 3.22}$$

3.3.3.b The Hortonian Equations of Kostiakov and Philip

The Philip Equation

For the Philip equation (Equation 3.6), rearranging to give t_o and V_s when p equals i produces the following formulae:

$$t_o = [B/(p - A)]^2 \qquad \text{Equation 3.23}$$

$$V_s = p.[B/(p - A)]^2 \qquad \text{Equation 3.24}$$

The equations are different from those derived by Kirkby (1978) who uses a different version of the Philip equation. As the rainfall intensities increase, both t_o and V_s converge on zero indicating that the equation is Hortonian. Unlike the Green and Ampt equation, there is no lower constant value for V_s.

The parameter A is said to represent the saturated conductivity of the soil. If p is equal to A for the duration of the rainstorm no rainfall excess will result because the time to ponding t_o and the storage volume V_s will both be infinity. If p is less than A, the times to ponding t_o and the storage V_s will suddenly fall from infinity since although the resultant of B/(p - A) may be negative, its square is positive. The time to ponding t_o will increase again to a maximum as p approaches zero and V_s will change in a manner controlled by the relative magnitude of the squared term and p. V_s varies therefore with rainfall intensity. The effect will also depend on the sign of the A parameter which can be negative because of the curve fitting procedure. If p is greater than A, then so long as the rainfall duration (t_p) is sufficiently long, runoff will always occur.

The Kostiakov Equation

For the Kostiakov equation (Equation 3.3), rearranging to give t_o and V_s when p equals i produces the following formulae:

$$t_o = (p/A)^{1/B} \qquad \text{Equation 3.25}$$

$$V_S = p.\ (p/A)^{1/B} \qquad \text{Equation 3.26}$$

The values of t_o and V_S for the log-linearised Kostiakov equation are identical. As with the Philip equation, as the rainfall intensities increase, both t_o and V_S converge on zero indicating that the equation is a Hortonian one and not storage. In this equation, the parameter A does not represent the saturated conductivity of the soil. The model does not produce a constant final infiltration rate but approaches the asymptote of zero. Runoff will only occur if p is greater than i. Therefore for a given rainfall intensity, so long as the rainfall duration (t_p) is sufficiently long, runoff will always occur.

Unlike the Green and Ampt equation, neither the Philip and Kostiakov equations converge on a fixed total depth. Both predict storage amounts V_S that decrease with increasing rainfall intensity p approaching the limit of zero storage at high rainfall intensities with a time to runoff t_o of zero also. Thus mathematically, it is clear that they present the Hortonian characteristics of infiltration and are thus Hortonian models.

3.3.4 Using Different Models with Temporally Variable Inputs

3.3.4.a Time-Variable Input and the Infiltration Model Assumptions

Bloomfield *et al* (1981) argue that simple equations relating infiltration to time have serious limitations when considering intermittent rainfall, since they cannot cope with soil drainage and any subsequent increase in infiltration capacity with time. Most infiltration equations have been derived under conditions of constant excess supply at the surface. Therefore, the equations predict the maximum potential infiltration rate at a given time or soil moisture state. The storage equations allow for the condition of variable input through time when determining the time to runoff. However, past this time, and with the Hortonian approaches, no account is taken of rainfall intensities that fall below this infiltration potential. It is obvious that this will affect the subsequent path the infiltration equation should take, since by not satisfying potential in the current time period, the potential in the subsequent time period must be increased relative to that predicted by the maximum potential curve derived from conditions of excess supply. Where surface water has been generated previously, the fall of p(t) to below i(t) can be offset such that the potential infiltration rate is satisfied and the path of the curve can be followed. If not, then it is conceptually incorrect to use a single set of parameters to predict subsequent infiltration potential and ideally a second set of parameters should be used once infiltration rates exceed surface supply, and the conditions of ponding are lost. This is the approach that uses a dry curve and a wet curve (for example, Scoging, 1988) with parameters Ad and Bd and Aw and Bw. In any complex rainstorm where several showers occur this can only be an approximation related to the fact that the parameters A(t) and B(t) are not specified.

3.3.4.b Timing of Ponding and the Infiltration Model Assumptions

It is clear that depending on the nature of the time variation of rainfall intensities, the Hortonian approach and the storage approach could result in significantly different predictions of runoff production. To illustrate this it is helpful to use the modified Green and Ampt equation and consider it both in storage terms and in Hortonian terms. The former approach considers the mean precipitation through time to derive a time to ponding t_o when storage can be assumed to be filled, and does not consider the actual instantaneous rainfall intensity and infiltration capacity p(t) and i(t) until after this time. The latter approach considers only p(t) and i(t) from time zero, with runoff occurring as and when p(t) > i(t) irrespective of any concept of storage as defined by the values of t_o and V_s.

Taking a constant rainfall intensity p as the first example. Here, the storage approach states that runoff will occur where p = i and which is at t_o. The Hortonian approach which compares p(t) with i(t) will result in the same time t_o because $p = i(t_o)$ as defined by the infiltration curve. Prior to t_o, $i(t) < p$.

However, when the input is not a constant p, as is usually the case with a natural rainstorm, or when variable runoff is included, there can be a considerable difference in their predictions. Consider a length of hillslope Δx in a given time increment Δt. Taking the storage approach first, the requirement is that the total infiltrated depth of water from both rainfall and water running-on from locations further up the flow-line passing through Δx, must be evaluated at each Δt to determine the average supply intensity p+d over the elapsed time (where p is rainfall and d is the added depth from discharge on to the surface). The time to ponding t_o associated with this average pq must be calculated using Equation 3.15. If the t_o is greater than the elapsed time, then storage has not yet been filled and no surface water produced. If the t_o is equal to the elapsed time, the point of ponding has been reached during the current Δt, and if t_o is less than the elapsed time, then runoff will be produced in the current Δt. Since the Δt steps are generally small in a rainfall-runoff model, this is a relatively accurate calculation. It can be summarised mathematically as follows;

If $p+d \leq A$ ponding not possible

If $p+d > A$ calculate t_o

If $t_o > t$ ponding not achieved since $\Sigma p(t) + \Sigma d(t) < V_s$

If $t_o = t$ ponding is achieved in Δt, next Δt use Hortonian $(p+d)\Delta t$ with $i.\Delta t$ to calculate runoff

If $t_o < t$ ponding and runoff occurs in Δt, use Hortonian $(p+d)\Delta t$ with $i.\Delta t$ to calculate runoff

(where p+d is the sum of $d.\Delta t$ and $p.\Delta t$, d is the depth of water onto Δx resulting from run-on from above).

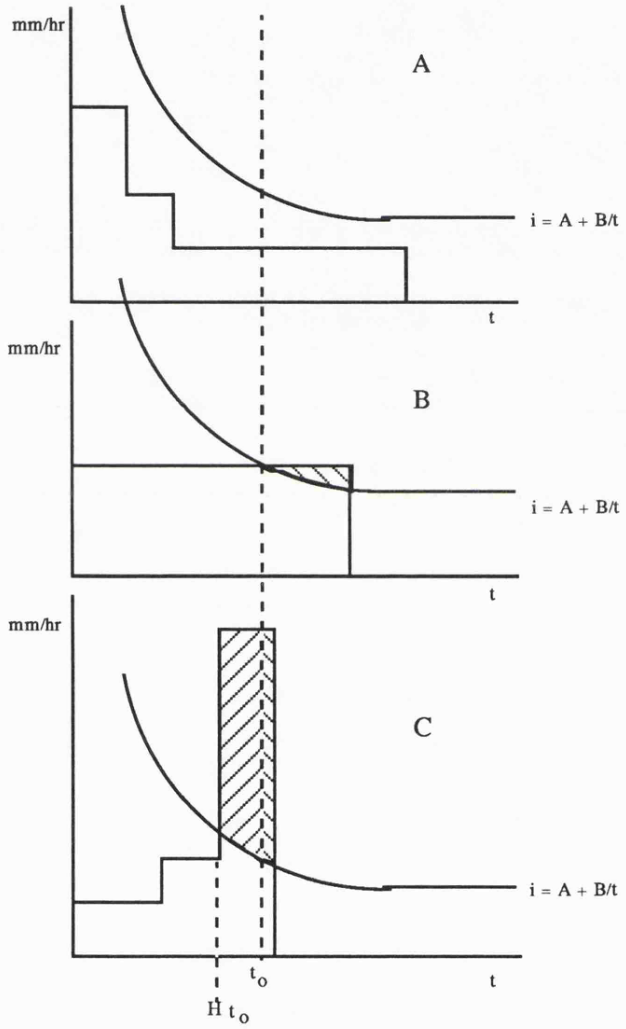

Figure 3.2 Rainfall Intensity Distribution and Runoff Predictions for Different Infiltration Models

What are the effects of using the storage equation in Hortonian fashion comparing the instantaneous supply and infiltration rates? In Figure 3.2, all three of the intensity distributions A-C yield the same depth of rainfall and the infiltration curve is identical for each. If the supply rate is constant, then the point of ponding and runoff production will be the same as predicted using the storage assumptions (see B in Figure 3.2). The right slanting diagonal shaded area signifies the rainfall

excess over infiltration following the Green and Ampt storage t_o. With the gradually decreasing intensity distribution, the average supply is $\Sigma p+d(t)$ (as B). It is quite possible that using a Hortonian approach, because the instantaneous supply rates p+d(t) have always been less than the infiltration capacities i(t), no ponding or runoff would be predicted by the Hortonian approach (see A in Figure 3.3). This difference between the two is due to the fact that the Hortonian approach takes no account of the contributions to storage that supply in excess of the final infiltration rate A will make. With the gradually increasing intensity distribution, assume that the average supply in time t is p+d as before. In this case, it is quite possible that the instantaneous supply rates p+d(t) become greater than the infiltration capacities i(t) as defined by the equation, without the condition of the average supply rate pq producing a time to runoff less than the storage t_o (at time Ht_o in Figure 3.2 C). This difference between the two is due to the fact that the Hortonian approach takes no account of the unsatisfied storage volume that results from conditions of $p+d(t) < i(t)$ in previous time periods. The predicted runoff pre-t_o using the Hortonian approach is the left-sloping shaded section in C, whereas using a storage approach would predict the right sloping shaded section.

From these considerations it is clear that the difference between the timing, and hence the volume of runoff depends greatly on the distribution of precipitation intensities and run-on inputs through time that produce a given total supply relative to the path of the infiltration curve $i = A + B/t$. Another complexity that may be considered for the storage method is the effect of isolated bursts of relatively high intensity that may alone be capable of inducing runoff but which will not do so under certain circumstances. Arid zone rainfall events may be characterised by very low intensities interspersed with very high intensities for short periods. This depends partly on our ability to measure such small time-scale changes. Consider a period of low intensity rainfall. A burst of high intensity rain falls. If the average precipitation for this complete time period is calculated, it may be insufficient to satisfy the storage as calculated from a knowledge of t_o. However, if the single burst on its own was considered resetting the time to zero, the duration would be sufficient to satisfy storage. The parameter B represents the constant fixed storage which must be filled for runoff to occur. With lower rainfall intensities, the amount of infiltrated water required to fill the storage increases as the volume is depleted by percolation. If a single burst of high intensity yields a depth equal to B then it is clear that storage would be filled, irrespective of the supply conditions previously. The problem is one of procedure and how the model, derived for conditions of constant supply, can be used with intermittent supply. This is discussed in more detail in Chapter Five where the infiltration procedures are coupled into a full rainfall-runoff model.

3.4 FITTING AND TESTING INFILTRATION MODELS

3.4.1 Selecting Infiltration Data

As stated, the full rainfall-runoff model (of which the infiltration procedures are an important component) is designed to illustrate and explore the most important aspects of the arid catchment hydrological system in terms of the functioning of a water harvesting system. In particular, the major interest is the relationship between the superimposed channel positions along flow-lines and the pattern of runoff production along that flow-line into the channel and away to the runoff farm. Obviously of importance in such an analysis is data on the spatial distribution of infiltration characteristics within a catchment system and their relative magnitudes.

For the Avdat system, there are two sources of infiltration data, direct field measurement, and relevant data-sets extracted from the literature and applicable to the different slope environments. The objective is to identify the broad characteristics of the spatial variation within the catchment system from different hillslope environments. This can provide parameters for a deterministic analysis of the water harvesting system and a more general consideration of the processes and characteristics important for water harvesting from arid hillslopes using hypothetical examples.

3.4.2 Model Selection and Fitting

There are a variety of infiltration models presented in the literature, both empirical and conceptual. For fitting to an experimental data-set of the change of infiltration through time, empirical time-dependent infiltration curves are required. Dixon *et al* (1978) list a series of evaluation criteria for selection of equations. Those criteria of relevance to the current study include;

1. the equation parameter number should be restricted to two (for linear least-squares regression),
2. infiltration should be expressed as an explicit function of time,
3. equations should have been shown to give consistently accurate fits to data collected under widely varying test conditions,
4. equations should be easily fitted to infiltration data to obtain parameter values,
5. infiltration should easily be calculated using the equation and the parameter estimates,
6. the equation should have the simplest form possible.

Given these criteria and the desire to consider both Hortonian and storage infiltration models, three infiltration equations that conform to these criteria are the Green and Ampt model (Scoging, 1988), the Philip model (Bork and Rhodenburg, 1981) and the linearised version of Kostiakov (Dixon

et al, 1978). Each have two easily defined parameters, each are a function of time, and each have shown considerable accuracy when used in empirical studies of infiltration as shown in the literature.

Green and Ampt	$i = A + B/t$	Equation 3.13
Philip	$i = A + B/\sqrt{t}$	Equation 3.6
Kostiakov	$\log i = \log A + B.\log t$	Equation 3.4

The modified Green and Ampt equation is a widely accepted physics-based model considered universally applicable under a range of conditions (Mein and Larson, 1973) and was successful in predicting infiltration under semi-arid conditions in South-East Spain (Scoging and Thornes, 1980). The Philip equation is widely adopted in rainfall-runoff modelling and has been used in a variety of catchment and hillside routing models (Engman and Rogowski, 1974. Cundy and Tento, 1985. Swartzendruber and Hillel, 1975). The Kostiakov equation performed well over a wide range of rainfall intensities and combinations of infiltration augmenting and abating factors in a detailed analysis by Dixon *et al* (1978).

Dixon *et al* (1978) gave the basic format for a curve fitting procedure;

1. select models to be tested,
2. reduce equations with power terms to their linear form,
3. perform least-squares regression analysis to obtain the parameters,
4. perform correlation and analysis of variance tests on the observed and predicted data points,
5. evaluate the statistics to see which model gives the most accurate representation of the original data characteristics.

The evaluation of the parameters involves examination of their correlation coefficient and the analysis of variance F-statistic of the compared observed and predicted data sets. This shows which of the selected models are the best-fit. Secondly, it involves a consideration of the F-statistic against statistical tables to see if the model fit is statistically significant and can therefore be accepted as an accurate representation of the original data set and used with confidence to reproduce observed conditions. The overall best-fitting equation can be selected for use as the infiltration component of the rainfall runoff model.

The statistical procedure for the comparative tests of these models is as follows. Using the statistical package Minitab, the least squares regression, correlation and analysis of variance (ANOVA) tests are performed and provide the parameters of the regression equation, the correlation coefficient, the r-square values, ANOVA matrix and degrees of freedom. From the last two, the F-statistic can be

calculated and the tabulated statistically significant F-score determined for the pre-set confidence limit of 0.05%.

3.4.3 The Avdat Field Data

3.4.3.a Measuring Infiltration

Infiltration is perhaps the most important of all hillslope parameters to determine, yet it is the most difficult to measure. It is a process operating under constantly changing input conditions and exhibiting variability due to seasonal controls such as vegetation growth and decay, soil moisture variation, soil surface conditions and amount of biotic disturbance. Within an arid catchment system, spatial variations are marked and different process controls can be operating on adjacent areas depending on whether crusting is dominant, soils are shallow and/or with limiting storage, or the proportion of impermeable materials contributes rapidly to satisfying infiltration in surrounding highly infiltrable surfaces. Consequently, with such a large degree of variation, many analyses of infiltration adopt an event-based approach in which attention is directed to sampling spatial variation and not temporal change. The parameters are then used to analyse the effects of infiltration within a limited range of rainfall events where there are no antecedent influences and therefore, no accounting of soil conditions over time are required. According to Loague and Freeze (1985), this event-based approach, when using the infiltration model as a component of a full rainfall-runoff model does not penalise any lack of ability to predict the highly complex antecedent conditions following variable interstorm periods.

The most significant factor for the analysis of water harvesting systems in an arid environment and the Avdat system in particular is the changing conditions along flow-lines. Within the Avdat catchment system supplying the terraced runoff farm, slope gradients vary from the horizontal to the near vertical along individual flow lines. Soil surfaces vary from the micro-smooth loessial slopes prone to the crusting mechanism, to the stone-covered, bedrock out-cropping surfaces prone to the barrier mechanism. In between are a complete range of mixed surfaces which are influenced by both to differing degrees. Testing infiltration on steeply inclined surfaces in remote field locations is a difficult process. Dunne *et al* (1975) state that routine techniques have been developed for quantifying the pattern of infiltration capacities for purposes of predicting runoff, with standard field apparatus. However, the application of these techniques is not routine. Traditionally, infiltration has been measured in the field using ponded head devices (Hills, 1970) or portable rainfall simulators (Morin and Benyamini, 1977. Morin and Cluff, 1980). On steep, rough slopes the former are not realistic or effective. The latter are often impractical due to their size, power and water requirements limiting access to certain sites. Scoging and Thornes (1980) used a small hand-portable simulator in South-East Spain. No small simulator was available for use at Avdat. The Morin rainulator, used to good effect by Agassi *et al* (1985a, 1986) was available and an attempt was made to use it, but access problems

prevented its adoption. The transport of a heavy trailer complete with 200 litre reservoir, simulator, suction pump and electrical generators by four-wheel drive up the steep rocky hillsides, crossing harvesting channels and botanical study areas was not feasible. Whilst manageable on flat land close to access roads or in a laboratory setting, use of the system proved impractical elsewhere.

As an alternative, a non-sprinkling method was developed, involving the controlled run-on of water onto an area of soil surface and measurement of runoff through time, the difference between the two volumes being the losses due to infiltration over the wetted surface area. The method simply involved running a constant, uniformly distributed sheet of water onto the soil surface, allowing it to flow naturally downslope under the force of gravity. The water was then collected in a trough after a uniform distance of one metre and the volume of runoff measured throughout the course of the experiment at frequent time intervals (Figure 3.3 and Plates I.1 to I.4).

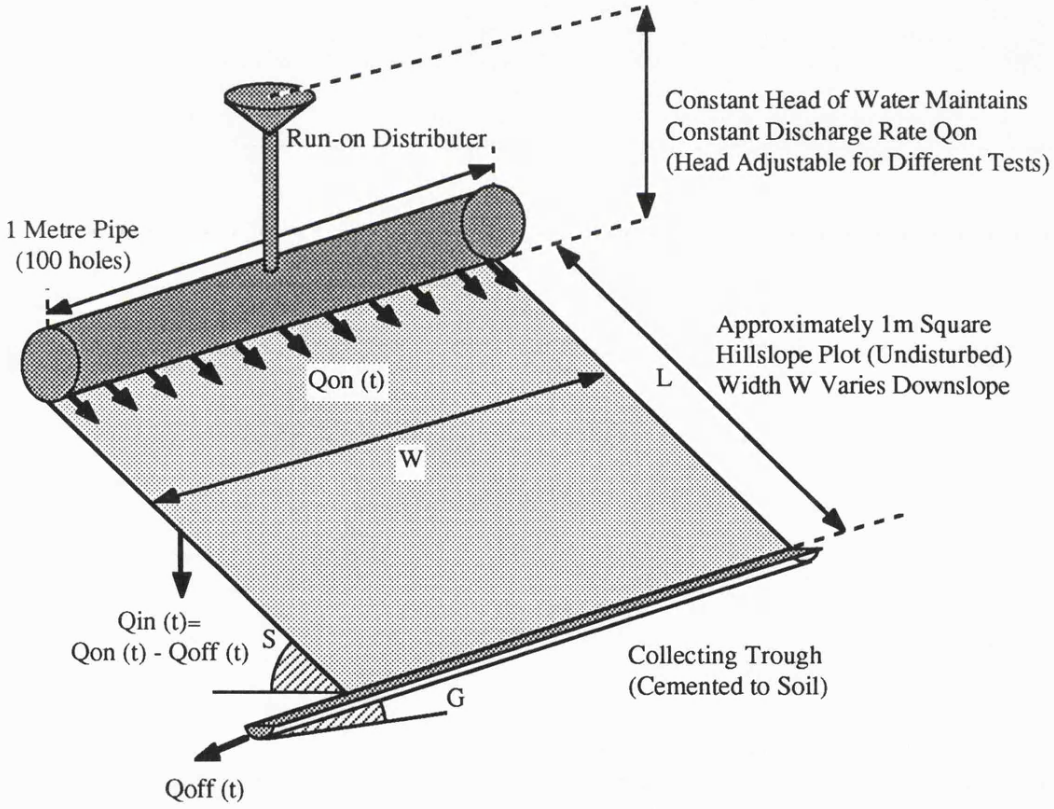

Figure 3.3 The Run-on/Run-off Infiltration Apparatus

The pipe system produced a uniform discharge as the water flowed out of the holes (drilled to be in a horizontal line) and down the circumference of the pipe onto the slope surface. The amount of water flowing out depended on the height of the constant head device supplying the water. This was simply a funnel supported at an adjustable height by a laboratory stand and clamp, with the water in the funnel maintained at a steady height by pouring water from a series of four-litre vessels.

The discharge rate was set up in advance of the test by adjusting the funnel height whilst running the water down a plastic sheet and over the end of the trough onto the slope below the plot. The funnel was pre-set to try and discharge four litres in four minutes. This would be equivalent to 60 mm hr^{-1} rainfall being input as rainfall over a wetted area of one square metre. In reality, the supply rate decreased from a maximum at the top of the plot to a minimum at the bottom of the plot. The pipe was set so the holes were in the horizontal by using a spirit level and observing the level of the miniscus in each hole as the pipe was filled in preparation for the test. After the first four litres were discharged, the time was checked and where it varied from the desired four minutes, an attempt was made to change the discharge rate by lowering or raising the funnel height. By measuring the width of the area wetted during the test, at as many time intervals as possible, the average infiltration rates was calculated by dividing the volumetric loss by the wetted area and the length of time interval.

Eleven infiltration tests were carried out sampling the range of slope environments found along a complete flow-line through the catchment system, from the hilltop down to the wadi-bottom. The different geomorphic zones sampled have been described in more detail in Chapter Two as units one to six, subdivided on the basis of their position to the east and west of the catchment. Although limited, the sample looked at the relative magnitude of infiltration and overland flow velocity for different flow-states on the infiltration plots on different parts of the catchment system. The run-on/run-off method directly addressed the major process being investigated, that of runoff-generation and movement on different sections of hillslopes between channels designed to collect the runoff and deliver it for use on the terraces of the runoff farm. The method could not account for the rainfall phase of the infiltration process where crusting under raindrop impact can be assumed to play a major part on some slope areas. To this end, the literature, especially that of the Israeli authors who have considerable experience of field and laboratory controlled conditions of infiltration on crusting soils, provides the necessary data on the infiltration-crusting process as explained in the following sections.

3.4.3.b The Crusting Mechanism

On certain slope areas, the crusting mechanism is a major control on runoff generation. According to Morin and Cluff (1980), on crust-susceptible soils, the direct impact of raindrops on the surface causes crust formation with a corresponding decrease in the infiltration rate. Raindrops destroy the surface soil aggregates and gradually form a continuous crust with a much lower hydraulic conductivity than that of the original surface (Morin and Benyamini, 1977). If the infiltration tests do not duplicate the natural energy of the falling rain, they do not produce sufficient crust-forming energy so that the resulting infiltration may be less, by an order of magnitude, than the actual infiltration.

As well as the impact of raindrops, crusts are formed by chemical reactions within the soil surface. The infiltration rate of soils is very susceptible to the soils sodicity combined with the

amounts of electrolytes in the applied water. When the electrolyte concentration is high, only physical disintegration of the soil aggregates and mechanical organisation of the upper layer takes place. Therefore applying tap-water, generally more highly electrolytic than rainwater, can result in the maintenance of high infiltration rates. Applying distiled water on the other hand will disperse clay particles which migrate into a clogging zone and reduce the hydraulic conductivity (Agassi *et al*, 1985a). It has been observed that electrolyte concentration has little effect on saline soils, where the dispersive forces are minimised.

The consequence of these considerations are that the Avdat method of flood wetting used on crust-mechanism soils may produce an overestimate of the magnitude and change in infiltration through time because;

a. it involves no impact component of raindrops onto the surface,
b. it uses tap water which has a higher degree of electrolytes than rainwater.

There are several other observations that may balance these consequences. The majority of experiments carried out on crusting soils have been in laboratories on specially prepared soils. They are made up of aggregates, un-crusted prior to testing. When field tests have been made, they have generally been conducted on tilled soils where the natural crust has been broken. Under the impact of simulated rainfall, the process of crust formation is observed showing the change from high to low rates as the crust is formed. A subsequent infiltration test once the crust has dried shows how infiltration has been changed with lower initial and final infiltration rates compared to the un-crusted surface. If further rainstorms are simulated on this already crusted surface, little change can be observed between the infiltration curves produced by those tests relative to the previous tests on the crust. This suggests that once formed, the crust exerts a permanent influence on the infiltration. Agassi *et al* (1985b) looked at infiltration and runoff from wheat fields in the Negev, and found that in a sequence of four simulated storms of 35 mm hr^{-1}, the infiltration of the second storm onto the previously tilled surface was much lower than the first, but in the third and fourth storms, no change in the hydraulic properties took place. In this case the permanent influence of the crust becomes more important than its creation.

Obviously the important question to ask here is to what extent is the crust a quasi-permanent natural feature that exerts its influence in identical fashion regardless of the method with which water is delivered to the surface, or the chemistry of the water? To what extent is the crust re-built with each rainstorm? The chemical influence has already been shown to be determined by relative chemistry of soil and water. The mechanical influence would seem to be only important onto a non-crusted surface. However, since each of the subsequent tests quoted involved an impact component it is not known how important they might be to maintaining the crusting influence rather than rebuilding crusts.

From tests by Hillel (1960), it would suggest that the crust itself is more important than the method of water application. He took loess soil, treated it to produce four different densities of surface from the un-crusted aggregate to the puddled, dense crust and using flood wetting with no impact produced similar orders of magnitude of infiltration into crusted and un-crusted soils as produced by rainfall simulator testers. However, Agassi *et al* (1985b) compared final infiltration rates into crusted soils using both raindrop impact and non-impact wetting. The latter resulted in final infiltration rates of 10 to 40 mm hr^{-1}, which are significantly higher than the impact tests which produced rates of 2 to 8 mm hr^{-1}.

Infiltration tests carried out at Avdat did not involve impact. However, they were carried out at the end of the rainy season when the crust was most complete. It is unclear whether in the alluvial areas and on plain or plateau slope sections where the crust is likely to be a dominant influence, that the observed infiltration rates are unduly affected by the method of testing. A comparison of field results against those from the literature in Section 3.4.5 can indicate whether this is the case.

3.4.3.c The Flow Method and Initial Infiltration Rates

From a description of the run-on/runoff method it is clear that the running of water across the surface rather than sprinkling equally over every point of the wetted area will affect the calculated infiltration values for the early time periods before steady-state flow conditions have been reached. The time intervals for which the volume of water discharge onto the surface and the volume running off are compared vary from three to five minutes for the different plot tests. Within the first four-litre period, the constant discharge of water across the 100 cm wide section moved gradually downslope as a ponded mass of uneven depth and shape in cross-section. Visual observations showed that flow firstly moved down any micro-topographic low in the surface profile, retarded by the surface resistance to flow and the surface tension forces along the wetting front as the dry soil was crossed. As the head was decreased by infiltration, it was increased by the retarding forces. Depression storage was filled and eventually the flow reached the trough one metre downslope and the volume of outflow was recorded. Meanwhile, the wetting front spread laterally with decreasing speed as the steady state conditions were reached and detention storage became constant.

It is clear that not only did the first time period involve infiltration, it also involved the time-lag effect of building up a flow head and the detention storage on the surface. This build up was attributed to infiltration. This problem was recognised by Scoging (1988) for her rainfall/runoff plots. She indicated that from a known input and output, an infiltration rate could be determined, but that this was necessarily a simplification since the value was not only lagged in time but also included the unquantifiable losses mentioned. It is likely, therefore, that the initial infiltration rate is an

overestimate of the actual infiltration rate by a function of the detention storage volume. However, since the detention storage is mostly included in the first time period, the subsequent rates approach the true infiltration rate as steady state conditions are reached and can be accepted with more confidence. In a rainfall sprinkler experiment, a true time to ponding t_o can be measured, from which the B coefficient can be calculated without curve-fitting by rearranging Equation 3.15. In the run-on/runoff plot experiments, the observed time to run-out is not the same as the Green and Ampt time to ponding since it involves a time-lag equivalent to the time required to fill detention storage and for the wetting front to reach the slope base. This is also true of all sprinkler experiments where the time to surface ponding is not noted and instead the time to discharge into a runoff collecting vessel is taken followed by subsequent volumetric measurments. The intial measurements of infiltration will inherently include additions to detention storage unless some explicit attempt is made to account for this in subsequent calculations. Subsequent rates towards steady state will also include a proportion of their depth that is in fact the decreasing additions to surface storage which is maximum when (p - i) is at its maximum.

The problem arises when fitting curves to the data-points and using the parameters in a rainfall-runoff application where smaller time intervals are used compared to the data from which the model is derived. The curve extrapolates to times prior to the first observation time, and extrapolates between subsequent times to provide a continuous function. The initial infiltration rate will therefore have a considerable effect on the nature of the curve and may lead to poor or unreasonable estimates of infiltration in very small time periods. The values of t_o and V_s will most likely be overestimates. Use of the A and B parameters in a deterministic simulation of the run-on/runoff tests should therefore show timing errors in the hydrograph with close prediction of steady-state conditions but a degree of error in the timing of the hydrograph rise, especially in the first few time periods.

3.4.3.d The Surface Materials and Micro-Topography

When water was discharged evenly across a 100 cm section it flowed down the slope in a manner dictated by the cross-slope and downslope micro-topography relative to the head of water produced. The wetting front was uneven, and the depth of water across the slope was varied. This is illustrated in Plates I.1 and I.2. The water spread out or concentrated depending on the slope gradient, the flow resistance, and the micro-topography. It was not a sheet of constant width 100 cm along the one metre length. On the whole, the surface appeared completely wetted as the surface absorption spread water penetration laterally between rivulets. However, water may not actually have been flowing over this portion of the surface. This observation was confirmed by Emmett (1970) and Roels (1984ab) in their field tests. Emmett saw that on hillslope plots in Wyoming subject to simulated rainfall that although the whole surface was glimmering with water, most runoff occurred in concentrations of flow directed downslope rather than the uniform sheetflow. Roels stated that runoff, instead of coalescing as an irregular sheet, concentrated immediately into inter-rill flow paths.

How can these considerations be expected to influence the infiltration rate calculations, particularly the relative magnitudes between different surface types? Where there is significant concentration of water in its passage downslope, the result will be an overestimation of actual infiltration rates by a function of the ratio of actual wetted area to apparent wetted area. If subsequent model simulations use the sheetflow approach and assume even distribution across the slope surface then the average infiltration rates will be acceptable. However, if complex flow is modelled taking account of the micro-profile, it is likely that some of the infiltration models parameterised from the average rates may be underestimates. This is more likely on the rocky steep areas where flow variations from a sheet are most acute.

3.4.3.e The Avdat Data Sets

Infiltration rates were calculated from the measurements of the amount of water entering the plot, the amount of water running off, the wetted surface area and the length of each time period over which each measurement applies. Up until the time that water runs out (t_{ro}), only the amount of water running onto the plot was known. There was no runoff but not all of the water had infiltrated since by this time, some detention storage had been filled and the wetting front had reached the base of the plot where the last micro-increment had reached its time to ponding. After this time, both the amount of water running on, and the amount of water running off were known up to the point T_1, when the first four litre vessel was emptied and an infiltration calculation could be made for the previous time period ($T_1 - t_{ro}$). Subsequently, calculations were made for the periods ($T_2 - T_1$, ..., $T_n - T_{n-1}$). The assumption for the first time period was that since the input was approximately constant for each four litres, the volume running on to the plot from t_{ro} to T_1 was:

$$\text{Volume On} = 4000(T_1 - t_{ro}) / T_1$$

By not including the unknown period up until t_{ro} in the calculation, some of the over-estimate of infiltration due to the inclusion of non-infiltrated detention storage is excluded. The calculation of infiltration rates could then proceed as follows;

$$i = (\text{Volume On} - \text{Volume Off}) / [\,(WA \,.\, \Delta t\,] \qquad \text{Equation 3.27}$$

(where WA is the measured wetted area at time T_n and Δt is the time period to discharge 4000 cm^3, or in the case of the first time increment to T_1, the proportion described above).

The calculated infiltration rates were then plotted against elapsed time since the start of run-on. The chosen plotting times were the mid-point of each time increment since the infiltration rates were

temporally averaged. The mid-point times provide the most appropriate representation of the infiltration time series. The formulae for the plotting times were:

$t = 0 : T_1 \qquad t = t_{ro} + (T_1 - t_{ro})/2$ Equation 3.28

$t = T1 : T_n \qquad t = T_{n-1} + (T_n - T_{n-1})/2$ Equation 3.29

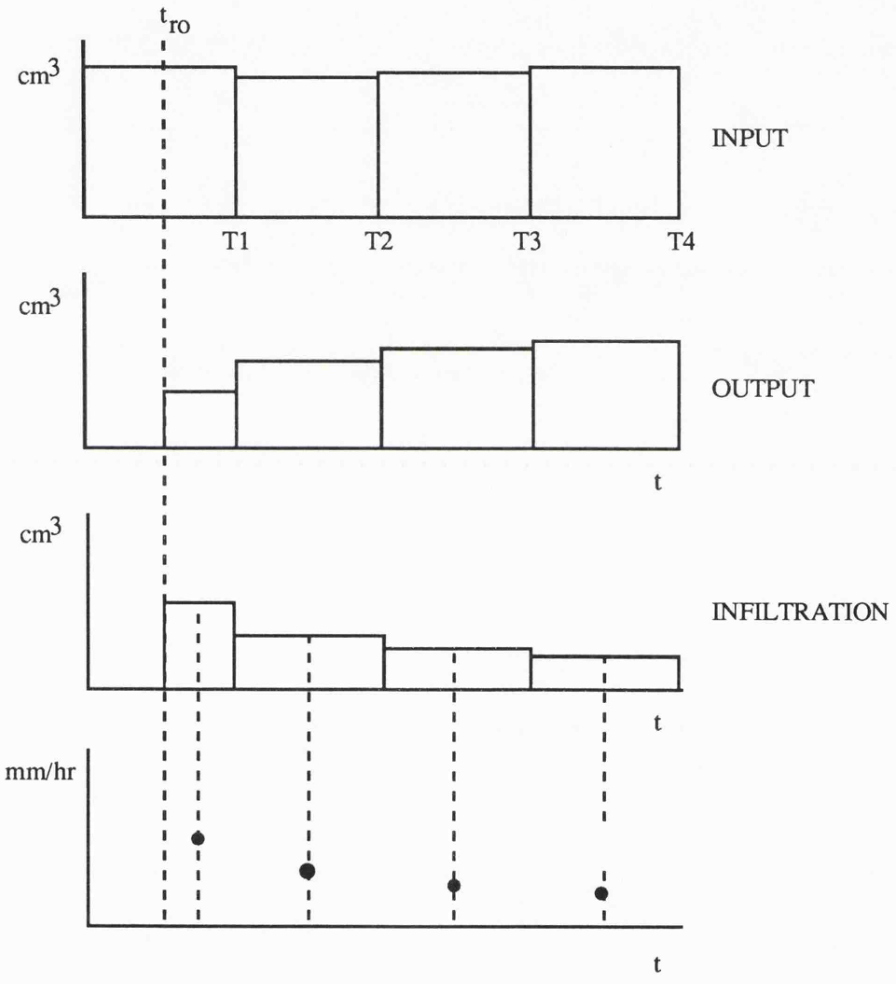

Figure 3.4 Plotting Calculated Infiltration Rates

Considering the time to start run-on as the origin for the time axis has the effect of plotting the infiltration time series to the right of where it should be since this is really only time t = 0 for the top of the plot. The time t = 0 for the bottom of the plot is really $t_{ro} - t_o$ and the average t = 0 is obviously the integral of the different times at which the wetting front flows onto the surface at successive points downslope. However, without an independent t_o for the plot then selecting a true time for the origin (somewhere between 0 and t_{ro}) is indeterminate. For the current analysis, the

absolute time is retained and attempts made to quantify the over-estimation in the B parameter in subsequent simulation tests using a routing model adapted to consider the plot conditions of run-on and runoff.

The method of time-plotting is illustrated graphically in Figure 3.4 and the eleven plot infiltration data-sets are presented in Appendices 2.3.1 to 2.3.11. Plotted on axes of time in minutes against infiltration mm hr^{-1}, they produce the time decay series shown in Figure 3.5. There is clearly a considerable range of infiltration capacities throughout the catchment. The initial infiltration capacities vary from 85 mm hr^{-1} down to 18 mm hr^{-1} with final infiltration capacities ranging from 60 mm hr^{-1} down to 6 mm hr^{-1}. Even allowing for the effects of overestimated first time period infiltration and the likely effects of measurement on the loess-crusted hillslope areas using a non-impact water input method, the variation is considerable. The magnitude of the variation indicates that infiltration will be an important factor in determining the spatial and temporal patterns of runoff production and the functioning of the water harvesting system. If the variation were only slight then infiltration would be a relatively insensitive and insignificant determinant of spatial variation. However, as discussed in Chapter One, the spatial variation and order of magnitude differences are marked in arid catchments and Avdat is no exception to this general observation. If the infiltration curves are assumed representative of the range of infiltration rates to be expected along catchment flow-lines then the order of magnitude difference in observed conditions indicates the critical role that spatial variation is likely to play in runoff production relative to the channel network.

The initial, final and rates of change of infiltration represent the influence of a suite of controlling variables, as described by Dixon *et al* (1978). Whilst it is difficult to identify the roles of particular controls from a small sample, it is possible from the shape of the curves to identify major groups possessing similar characteristics. Variation within the catchment is obviously significant and there does appear to be a systematic division into three groups of plots which have different characteristics from the others, as illustrated in Figure 3.5. The characteristics that were expected from an analysis of infiltration in the Avdat catchment from a knowledge of the physical characteristics of each of the plot sites and the infiltration and runoff mechanisms known to be important which are the barrier mechanism, the crusting mechanism, limited storage and the air-earth interface.

Figure 3.5 Infiltration Data from the Avdat Run-on/Runoff Plots

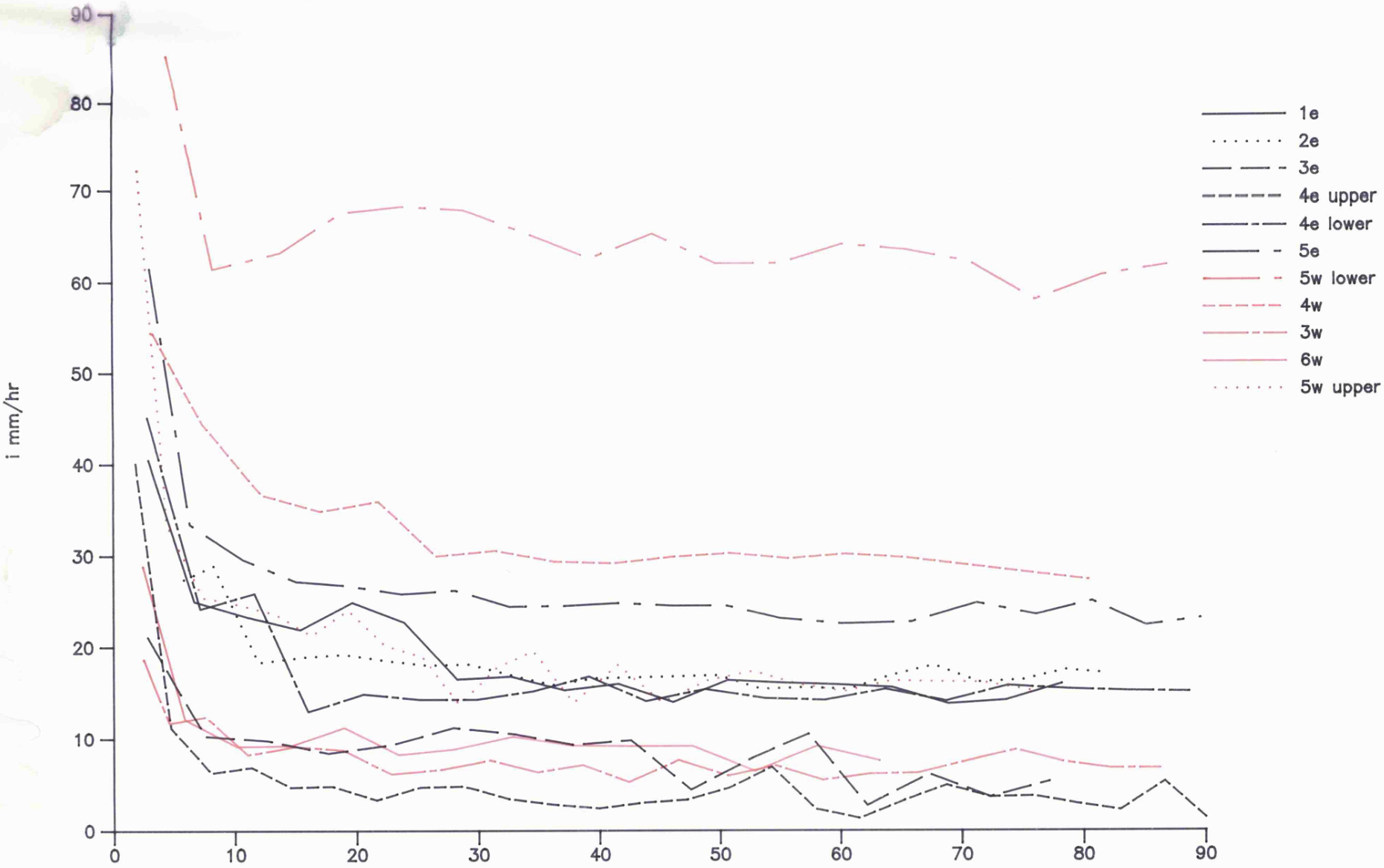

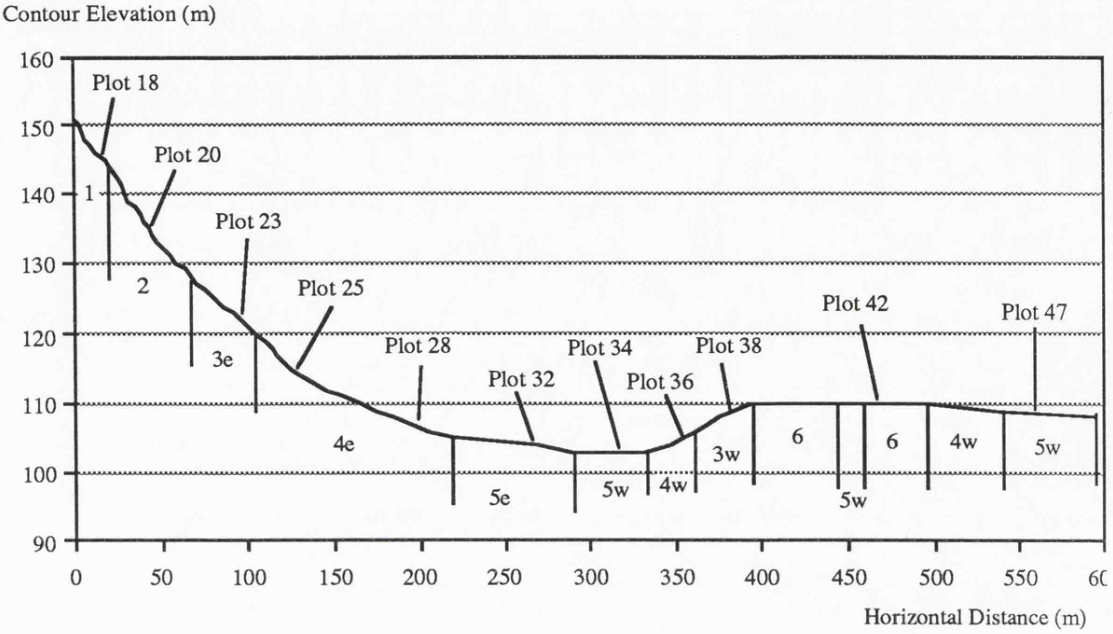

Figure 3.6 Plot Locations on Profile 2

From a consideration of the raw-data infiltration curves presented in Figure 3.5 it is clear that there are broad differences between groups of plots having similar infiltration responses. Whilst it is not necessarily true that they have the same controls that produce this infiltration response, the net effect is that the plots in each group are similar. They are;

1. plots 3e, 4e upper, 3w and 6w which group together as those with the lowest initial and final infiltration capacities ranging from 18 to 40, and 3 to 7 mm hr^{-1} respectively.

2. plots 1e, 2e, 4e lower and 5w upper which group together as those with intermediate initial and final infiltration capacities (with the exception of 5w upper which has an initially high infiltration capacity but comparable subsequent infiltration capacities to the group) ranging from 30 to 45, and 14 to 17 mm hr^{-1} respectively (apart from the initial infiltration of 5w upper at 73 mm hr^{-1}).

3. plots 5e, 5w lower and 4w which are separate from these two groups having higher initial and final infiltration rates that vary widely. This category is not clear as it contains some of the plots that are most likely to be adversely affected by the method of infiltration measurement as explained below.

The grouping includes wide variations in stone, bedrock and soil percentage cover, gradient, and micro-topography. The resultant of these varying characteristics obviously produces a similar response to the test conditions.

Of particular interest in the observed results is the generally relatively high initial, subsequent and final infiltration rates of the loessial soils that theory and the experimental evidence from the literature suggest should produce the lowest final infiltration rates, generally in the order of 5 mm hr^{-1}. In this case the observed infiltration rates are in excess of these values suggesting that the method of experiment adversely effects the results compared to those expected under laboratory conditions. This receives wider discussion in Section 3.4.5.

3.4.3.f Results of Model Fitting to the Avdat Data

The summary statistics from fitting the Green and Ampt, Kostiakov and Philip equations to the Avdat data are presented in Table 3.1. In eight of the plots, the Green and Ampt model provides the best-fit, and in three the Philip curve provides the best. In every case, the Kostiakov equation with its characteristic of converging on the asymptote of zero provides a poorer explanation of the data than the other two equations. In the eight plots where the Green and Ampt is best, the correlation coefficient varies from 0.796 to 0.980 and in each case is significant to the pre-determined 0.05% confidence limit. For the three plots where the Philip equation provides the best-fit, the Green and Ampt is still significant with correlation coefficients of 0.939, 0.827 and 0.971 compared to the Philip equation correlation coefficients of 0.952, 0.833, and 0.982 respectively.

Since the storage model provides the best overall statistical fit, can it be assumed that the process of infiltration into the Avdat catchment surfaces is dominated by storage control, conforming to the physical basis of the Green and Ampt equation? Are the infiltration rates and their change through time limited by both the intake rate of water and the state of the moisture storage independent of the rate of water application? Firstly, without a more detailed data-set it is not possible to answer these questions with certainty. However, it is useful to discuss the implications of these findings both to illustrate some general points facing all empirical analyses of infiltration, regardless of sample size, and to the subsequent use of the parameters in a full rainfall-runoff model. In their work on the enhancing and abating effect of different controls on infiltration, Dixon *et al* (1978) tested a number of different equations. They found that whenever the effect of interacting infiltration processes caused infiltration to reduce by the same gradient as the time parameter of an infiltration equation, the equation would produce the best-fit statistics. However, they state that this fit may well be circumstantial and fortuitous and cannot necessarily be construed as verifying the theory behind or the physical soundness of the equation. Their view is that all infiltration equations are, or become empirical when applied to the complex soil and water conditions found in field situations compared to the simple, ideal conditions

Table 3.1			Best-fit Statistics for Infiltration Models Applied to the Avdat Run-on/Run-off Plots							
Unit	Plot	Test	Equation	A Param	B Param	corr. coeff.	R.square	F.Stat	d.f.	0.05% F
1e	18	9	G and A	0.000414	0.1290	0.939	88.1	117.8	1/16	4.49
			Kostiakov	0.004470	-0.2900	-0.932	86.8	105.1	1/16	4.49
			Philip	0.000237	0.0112	0.952	90.7	154.2	1/16	4.49
2e	20	8	G and A	0.000427	0.1110	0.884	78.2	76.2	1/21	4.32
			Kostiakov	0.001778	-0.1670	-0.819	67.1	42.9	1/21	4.32
			Philip	0.000328	0.0073	0.868	75.4	63.4	1/21	4.32
3e	23	7	G and A	0.000179	0.0686	0.827	68.4	30.5	1/14	4.60
			Kostiakov	0.004260	-0.3960	-0.721	52.0	15.1	1/14	4.60
			Philip	0.000082	0.0061	0.833	69.4	31.6	1/14	4.60
4e	25	6	G and A	0.000047	0.1090	0.968	93.7	349.1	1/24	4.26
upper			Kostiakov	0.007410	-0.5530	-0.779	60.6	36.9	1/24	4.26
			Philip	-0.000109	0.0102	0.892	79.5	93.2	1/24	4.26
4e	28	5	G and A	0.000359	0.1490	0.956	91.5	181.2	1/17	4.45
lower			Kostiakov	0.003160	-0.2540	-0.788	62.1	27.9	1/17	4.45
			Philip	0.000180	0.0122	0.910	82.8	82.0	1/17	4.45
5e	32	10	G and A	0.000592	0.1880	0.975	95.1	350.1	1/18	4.41
			Kostiakov	0.003630	-0.2100	-0.866	75.0	75.0	1/18	4.41
			Philip	0.000387	0.0145	0.916	83.8	83.8	1/18	4.41
5w	34	11	G and A	0.001690	0.1470	0.796	63.4	26.1	1/15	4.54
lower			Kostiakov	0.003020	-0.0693	-0.701	49.1	14.5	1/15	4.54
			Philip	0.001560	0.0099	0.755	57.0	57.0	1/15	4.54
4w	36	1	G and A	0.000777	0.1580	0.971	94.4	254.3	1/15	4.54
			Kostiakov	0.003890	-0.1940	-0.952	90.7	145.9	1/15	4.54
			Philip	0.000581	0.0130	0.982	96.5	408.4	1/15	4.54
3w	38	2	G and A	0.000171	0.0516	0.934	87.3	143.2	1/22	4.30
			Kostiakov	0.001288	-0.2400	-0.808	65.4	41.5	1/22	4.30
			Philip	0.000105	0.0044	0.909	82.6	101.7	1/22	4.30
6w	42	3	G and A	0.000193	0.0820	0.952	90.7	116.6	1/12	4.75
			Kostiakov	0.002344	-0.2970	-0.816	66.6	23.9	1/12	4.75
			Philip	0.000071	0.0074	0.891	79.3	46.0	1/12	4.75
5w	47	4	G and A	0.000381	0.1910	0.980	96.1	513.9	1/21	4.32
upper			Kostiakov	0.007080	-0.3490	-0.903	81.6	92.9	1/21	4.32
			Philip	0.000085	0.0179	0.934	87.3	143.6	1/21	4.32

in which the model was derived and its physical basis established. However, the Green and Ampt equation performed well for Spanish hillslope plot data (Scoging, 1988). It reproduced the rapid observed times to runoff well, with the predicted time to runoff t_o corresponding closely with the observed t_o. This led Scoging to accept the storage interpretation of the infiltration process that underlies this model.

Using the fitted A and B parameters of the Green and Ampt equation for each plot, the predicted t_o and V_s values can be derived for a variety of different input rates. These are presented in Table 3.2. The change in predicted instantaneous infiltration through time is illustrated in Table 3.3 and shows the relative characteristics of the different infiltration regimes. The times to runoff represent the time that ponding occurs when the storage V_s is filled under the point-process conditions of rainfall. The predicted t_o must not be confused with the observed t_{ro}, the time to run-out from the bottom of the plot witnessed during the run-on/runoff test. The time to ponding t_o occurs under conditions of instantaneous, uniform input. The time to run-out t_{ro} occurs after successive small downslope sections of slope reaching ponding as water is supplied from upslope in decreasing volumes. Taking the example of the top 20 cm length down from the onflow pipe which is 100 cm wide. If four litres is discharged in four minutes, the 20 cm section will receive 16.7 cm^3 in one second, equal to a depth of 0.00835 cm and to a rainfall intensity of 300.6 mm hr^{-1}. If the water was distributed by a sprinkler over a 100 cm long by 100 cm wide section, the depth would be 0.00167 cm with an intensity of 60.12 mm hr^{-1}. The former case approaches the point-process conditions more correctly than the latter. The affects of flow resistance prevents the water moving down, creating depression or detention storage and so coupled with infiltration, gradually reduces the rate of input onto successive elements of slope. These characteristics combine to make comparisons of t_o and t_{ro} inappropriate. However, comparisons can be made between the observed time to run-out and the predicted time to runout calculated during model simulations of the run-on/runoff plot response. This shows whether the combined infiltration and routing parameters reproduce the known conditions, and in a manner that adequately represents the point-process prior to use of the parameters as part of a set of larger scale simulations.

3.4.4 Infiltration Data in the Literature

3.4.4.a Literature Sources

A number of infiltration experiments have been carried out in the Negev Desert, the majority concerned with the phenomenon of crusting and its influence on runoff and soil erosion on farmers fields. Some have also been concerned with the rainfall and runoff processes from a range of hillslope environments ranging from loess-covered plains to steep rocky slopes and the various colluvial surfaces in between. Both laboratory and field experiments have been undertaken using flood-wetting, rainfall simulators, hillside sprinkler systems and run-on/runoff tests.

Table 3.2		Predicted Time to Ponding and Depth to Ponding (to and Vs) for Different Constant or Mean Rainfall Intensities for Avdat Run-on/Run-off Plots												
mm/hr			5	5	10	10	20	20	30	30	60	60	120	120
cm/sec			0.00014	0.00014	0.00028	0.00028	0.00056	0.00056	0.00083	0.00083	0.0017	0.0017	0.00333	0.00333
	A	B	To	Vs	To	Vs	To	Vs	To	Vs	To	Vs	To	Vs
1E	0.000414	0.1290	-468.9	-0.0651	-946.98	-0.2631	911.303	0.50628	307.631	0.25636	102.98	0.1716	44.1882	0.14729
2E	0.000427	0.1110	-385.27	-0.0535	-743.86	-0.2066	863.44	0.47969	273.175	0.22765	89.54	0.1492	38.1925	0.12731
3E	0.000179	0.0686	-1710.2	-0.2375	694.488	0.19291	182.178	0.10121	104.84	0.08737	46.112	0.0769	21.7479	0.07249
4E	0.000047	0.1090	1186.22	0.16475	472.316	0.1312	214.333	0.11907	138.618	0.11552	67.298	0.1122	33.1677	0.11056
4E	0.000359	0.1480	-672.39	-0.0934	-1822.2	-0.5062	752.968	0.41832	312.017	0.26001	113.18	0.1886	49.759	0.16586
5E	0.000592	0.1880	-414.91	-0.0576	-598.3	-0.1662	-5158.5	-2.8659	779.006	0.64917	174.94	0.2916	68.5798	0.2286
5W	0.001690	0.1470	-94.771	-0.0132	-104.09	-0.0289	-129.58	-0.072	-171.6	-0.143	-6300	-10.5	89.4523	0.29817
4W	0.000777	0.1580	-247.61	-0.0344	-316.49	-0.0879	-713.5	-0.3964	2804.73	2.33728	177.59	0.296	61.8073	0.20602
3W	0.000171	0.0516	-1606.9	-0.2232	483.247	0.13424	134.181	0.07454	77.9064	0.06492	34.5	0.0575	16.3171	0.05439
6W	0.000193	0.0820	-1515.4	-0.2105	967.235	0.26868	226.172	0.12565	128.058	0.10672	55.644	0.0927	26.1119	0.08704
5W	0.000381	0.1910	-788.89	-0.1096	-1850.4	-0.514	1094.21	0.60789	422.255	0.35188	148.56	0.2476	64.6946	0.21565

Table 3.3 Predicted Infiltration Rates at Different Elapsed Times for the Avdat Run-on/Run-off Plots												
t	1/t (s)	1e	2e	3e	4e upper	4e lower	5e	5w lower	4w	3w	6w	5w upper
1	60	92.30	81.97	47.60	67.09	101.72	134.11	149.04	122.77	37.12	56.15	128.32
2	120	53.60	48.67	27.02	34.39	57.32	77.71	104.94	75.37	21.64	31.55	71.02
3	180	40.70	37.57	20.16	23.49	42.52	58.91	90.24	59.57	16.48	23.35	51.92
4	240	34.25	32.02	16.73	18.04	35.12	49.51	82.89	51.67	13.90	19.25	42.37
5	300	30.38	28.69	14.68	14.77	30.68	43.87	78.48	46.93	12.35	16.79	36.64
6	360	27.80	26.47	13.30	12.59	27.72	40.11	75.54	43.77	11.32	15.15	32.82
7	420	25.96	24.89	12.32	11.03	25.61	37.43	73.44	41.51	10.58	13.98	30.09
8	480	24.58	23.70	11.59	9.87	24.02	35.41	71.87	39.82	10.03	13.10	28.04
9	540	23.50	22.77	11.02	8.96	22.79	33.85	70.64	38.51	9.60	12.41	26.45
10	600	22.64	22.03	10.56	8.23	21.80	32.59	69.66	37.45	9.25	11.87	25.18
12	720	21.35	20.92	9.87	7.14	20.32	30.71	68.19	35.87	8.74	11.05	23.27
16	960	19.74	19.53	9.02	5.78	18.47	28.36	66.35	33.90	8.09	10.02	20.88
20	1200	18.77	18.70	8.50	4.96	17.36	26.95	65.25	32.71	7.70	9.41	19.45
24	1440	18.13	18.15	8.16	4.42	16.62	26.01	64.52	31.92	7.45	9.00	18.49
28	1680	17.67	17.75	7.91	4.03	16.10	25.34	63.99	31.36	7.26	8.71	17.81
32	1920	17.32	17.45	7.73	3.74	15.70	24.84	63.60	30.93	7.12	8.49	17.30
36	2160	17.05	17.22	7.59	3.51	15.39	24.45	63.29	30.61	7.02	8.31	16.90
40	2400	16.84	17.04	7.47	3.33	15.14	24.13	63.05	30.34	6.93	8.18	16.58
44	2640	16.66	16.89	7.38	3.18	14.94	23.88	62.84	30.13	6.86	8.07	16.32
48	2880	16.52	16.76	7.30	3.05	14.77	23.66	62.68	29.95	6.80	7.97	16.10
52	3120	16.39	16.65	7.24	2.95	14.63	23.48	62.54	29.80	6.75	7.89	15.92
56	3360	16.29	16.56	7.18	2.86	14.51	23.33	62.42	29.66	6.71	7.83	15.76
60	3600	16.19	16.48	7.13	2.78	14.40	23.19	62.31	29.55	6.67	7.77	15.63
64	3840	16.11	16.41	7.09	2.71	14.31	23.07	62.22	29.45	6.64	7.72	15.51
68	4080	16.04	16.35	7.05	2.65	14.23	22.97	62.14	29.37	6.61	7.67	15.40
72	4320	15.98	16.30	7.02	2.60	14.16	22.88	62.07	29.29	6.59	7.63	15.31
76	4560	15.92	16.25	6.99	2.55	14.09	22.80	62.00	29.22	6.56	7.60	15.22
80	4800	15.87	16.20	6.96	2.51	14.03	22.72	61.94	29.16	6.54	7.56	15.15
A		0.000414	0.000427	0.000179	0.000047	0.000359	0.000592	0.00169	0.000777	0.000171	0.000193	0.000381
B		0.129	0.111	0.0686	0.109	0.148	0.188	0.147	0.158	0.0516	0.082	0.191

From the literature, 22 relevant experimental infiltration tests are identified in which infiltration rates against time are presented.

Shanan (1975)

The data presented by Shanan (1975) was measured on small plots on hillslopes adjacent to the Avdat catchment. On three different slope gradients; 1% (0.57°), 10% (5.7°) and 20% (11.4°), Shanan measured the infiltration rates prior to the beginning of the winter rainy season and at the end of the rainy season to try and account for the effects of surface conditions and soil moisture stores. The experimental method involved running water down a plot 4 metres long and 20 cm wide with a 2 cm high border preventing lateral flow. The discharge on was 0.05 litres per second which would be equivalent to 225 mm hr^{-1} rainfall intensity over an area of 0.8 m^2. The volume of discharge was measured at increasing intervals of 0.25, 0.5, 1.0, 2.0 and 4.0 hours up to 18 hours. The individual data points were plotted on axes of time against infiltration rate which was calculated as the volumetric difference between input and output divided by the area of 0.8 m^2, and the time interval. Infiltration curves are drawn by hand through these data points.

Yair and Lavee (1985)

Yair and Lavee present data from a number of locations. The colluvial slope sections and the weathered bedrock section were derived from studies on the instrumented hillslopes at the Sede Boqer Experimental Watershed eight kilometres north of Avdat. The loess-crusted slope section data was derived from studies by Morin and Jarosh (1977) using soils from the North-West Negev. The Sede Boqer experiments used a hillside sprinkler system covering a compartmented section; the upper section a rocky stone-covered slope, and the lower section a colluvium mantled slope. The Morin and Jarosh studies used a rainfall simulator over an area of 0.7 m^2.

Yair presents six curves hand-drawn and with no accompanying data-points. Four were calculated from hillslope volumetric input and output through time; the dry and the wet curves for the lower stony colluvial slope used rainfall of 26 mm hr^{-1}, and two dry curves from a weathered limestone and flint rocky slope and a stone-free colluvial slope on weathered chalk used rainfall intensity of 33 mm hr^{-1}. The two curves for loessial soils, one dry and one wet, were derived from the rainfall simulator tests using 56 mm hr^{-1}.

Hillel (1960)

Hillel presents four infiltration curves derived from laboratory studies on fine loess soil taken from the plains near Sede Boqer. The soil was sieved and prepared into four states as overlying layers of uniformly packed soil columns. The loess was laid on top in the following forms; as stable aggregates, as aggregates wetted to produce a thin drying crust, as a lightly puddled crust and as a heavily puddled crust. Water was applied by flooding the soil column and measuring the intake rate through the different toppings through time up to 8 hours.

Agassi *et al* (1986)

Agassi and his co-workers provide infiltration data for a variety of loess soils from both laboratory and field experiments using rainfall simulators. The data set from the laboratory used loess soils from Nahal Oz in the North-West Negev where rainfall conditions are three times as wet as at Avdat and Sede Boqer on average. Loess was taken from the top 30 cm of the soil, dried, screened to provide 0 - 10 mm aggregates and laid as a 2 cm thick layer over 8 cm of coarse sand in a box 0.3 m x 0.5 m angled at 5% (2.85°) to the horizontal. The data set from the field was measured on the loessial soils at Alumim with simulated rainfall at 34 mm hr^{-1}. The three test conditions were as follows; a dry un-crusted (tilled) plot, the same plot seven days later (dry crusted), and the same plot one day later i.e. eight days after the first (wet crusted).

Zarmi *et al* (1983)

Zarmi *et al* present infiltration data from a water harvesting micro-catchment constructed on a gradually sloping loess plain at Sede Boqer. The micro-catchment was subjected to overhead sprinkler rainfall at four different intensities and the times to runoff and final infiltration rates noted. The plot was 125 m^2, 12.5 m long and 10 m wide and had a gradient of 1% (0.57%). The surface was bare crusted loess. The soil was dry when the test was conducted, 2 weeks having elapsed since a previous rain event. The loess is most similar to that at Avdat, both geographically and morphologically.

3.4.4.b Selecting Data-Sets for Direct Comparison with Avdat Field Data

Using the same methods of analysis, some of the data sets were assessed to see which of the three models are the best-fit, and to provide parameters that might be used as comparisons, additions, or alternatives to the Avdat field data parameters. Out of the above sources of data, 12 of the 22 infiltration experiments applicable to the field conditions of Avdat could be used in a comparative discussion. This is because the data points needed to be of a similar time-frequency to remove the added influences on the best-fit statistics from resolution differences. Some of the data-sets were presented in

the literature as curves drawn by hand, or fitted to raw data using some un-specified model. Although biased by the previous fitting procedure, points were read off and treated as a raw data-set. This is the only method of providing comparable model parameters where there are none.

Yair and Lavee, Agassi *et al*, and Zarmi *et al.* data was used. Shanan's sample points were at very wide time intervals relative to the observed nature of the process, carried out for up to 18 hours and as shown in a comparison of Avdat data to the literature, are in contradiction of observed conditions. Hillel also conducted his tests over long time periods, up to eight hours and the resolution is poor. The observations concerning the long times to reach final rates and the gradients of the rates of change conflict with other tests carried out in the laboratory and the field on crusting soils. The data is presented in Table 3.4. The 12 infiltration curves are plotted on the same axes in Figure 3.7.

3.4.4.c Statistical Analysis

The results from the fitting of the three infiltration models to the literature data sets are presented in Table 3.5. In six out of the 12 cases, the Green and Ampt model provided the best-fit of the observed infiltration rates through time. Out of the other five cases, the Philip equation fits three sets best, and the Kostiakov three sets. However, again it is clear that even on those data-sets where the Green and Ampt model is not the best predictor, the parameters are statistically significant in that observed conditions are reproduced within the 0.05% confidence limits of accuracy. With the Green and Ampt, the correlation coefficient for the six best-fits range from 0.968 to 0.997, and the correlation coefficients for the other six range from 0.924 to 0.986. Although the results are varied, they do suggest that the Green and Ampt is a more than adequate model to represent all the experimental observations with confidence. The literatured ata is not ideally suited to model assessment because of the imperfect way secondary data was derived from curves already fitted through subjective (manual) or objective (statistical) procedures prior to publication. However, the generally solid predictions combined with the logic of its physics-base and the observations that the storage approach is appropriate for a wide range of soil types, suggests that the Green and Ampt model can be used with confidence to represent the literature data sets. The fitting of the original curves through the primary data may be one reason why the Kostiakov equation, seen to provide the poorest fit for each of the Avdat plot data sets, provides the best-fit for three of the twelve literature sets. If curves are sketched through a graph-plot of data-points then the final infiltration rate may not be well represented, either by stopping the curve shortly after the final rate is reached, or not drawing an asymptotic section to the curve. In this way, the model which predicts an asymptotic final rate of zero is likely to produce a better fit. Non of the Avdat data-sets have this characteristic, with the infiltration tests carried on well into the steady-state period. This observation is supported by the fact that with all but two of the literature infiltration data-sets, the Philip equation A parameter is negative which means a negative final infiltration rate will be predicted for long time periods. The fact that in all cases the final infiltration

Table 3.4 Raw Data Infiltration Rates Derived from the Literature (see Figure 3.7)															
	Agassi et al.....				Yair and Lavee.....								Shanan		
t mins	Agr Loess	Dry Loess	Wet Loess	Lab Loess	Dry Loess	Wet Loess	Col	St Col	St Col	Wet St Col	Chk Bed	Rocky	% 1 Loess	% 10 Stoneless	% 20 Stony
4		40.0	25.0	39.0	34.0	19.5		23.0	28.0	20.0		8.0	50.0	22.0	27.5
8	40.0	32.0	15.0	25.0	23.0	12.2	35.0	19.0	21.1	15.0	32.0	2.5			
12	37.0	27.5	7.5	12.5	18.0	7.7	24.0	17.5	17.8	11.8	17.5	0.0			
16	32.0	22.0	7.5	9.5	12.7	5.5	20.5	16.0	16.2	10.0	15.0		28.0	16.7	26.0
20	29.0	17.0	6.0	6.9	10.0	5.0	18.0	15.0	15.4	9.1	13.0				
24	25.0	15.0	5.0	5.0	8.1	4.5	16.5	14.5	14.5	8.2	12.0				
28	27.0	14.0	5.0	3.8	6.4	4.5	15.0	14.2	13.6	7.3	11.5				
32	25.0	14.0	6.0	2.9	5.9	1.5	14.0	14.0	13.6	6.4	10.4		20.0	12.6	24.7
36	17.0	12.0	5.0	2.3	5.5	4.5	13.5	13.8	13.6	6.1	10.0				
40	17.0	11.5	5.0	1.9	5.0	4.5	13.0	13.6	13.2	5.9	10.0				
44	16.0	10.0	5.0	1.5	4.5	4.5	12.5	13.5	12.7	5.9	10.0				
48	15.0	10.0		1.5	4.5	4.5		13.4	12.7	5.9			17.0	11.3	22.7
52	15.0	10.0		1.5	4.5	4.5		13.3	12.7	5.9					
56	13.0	9.0		1.5				13.3							
60	12.0	10.0		1.5				13.3							
64	11.0	8.0		1.5				13.3					15.0	10.6	20.7
68	11.5	7.5		1.5											
72	10.0	7.5													
76	10.0	7.5													
80	10.0	7.5													
Agr = Disaggregated			Col = Colluvium		St = Stony			Chk = Chalky		Bed = Bedrock					

Figure 3.7 Infiltration Data from the Literature

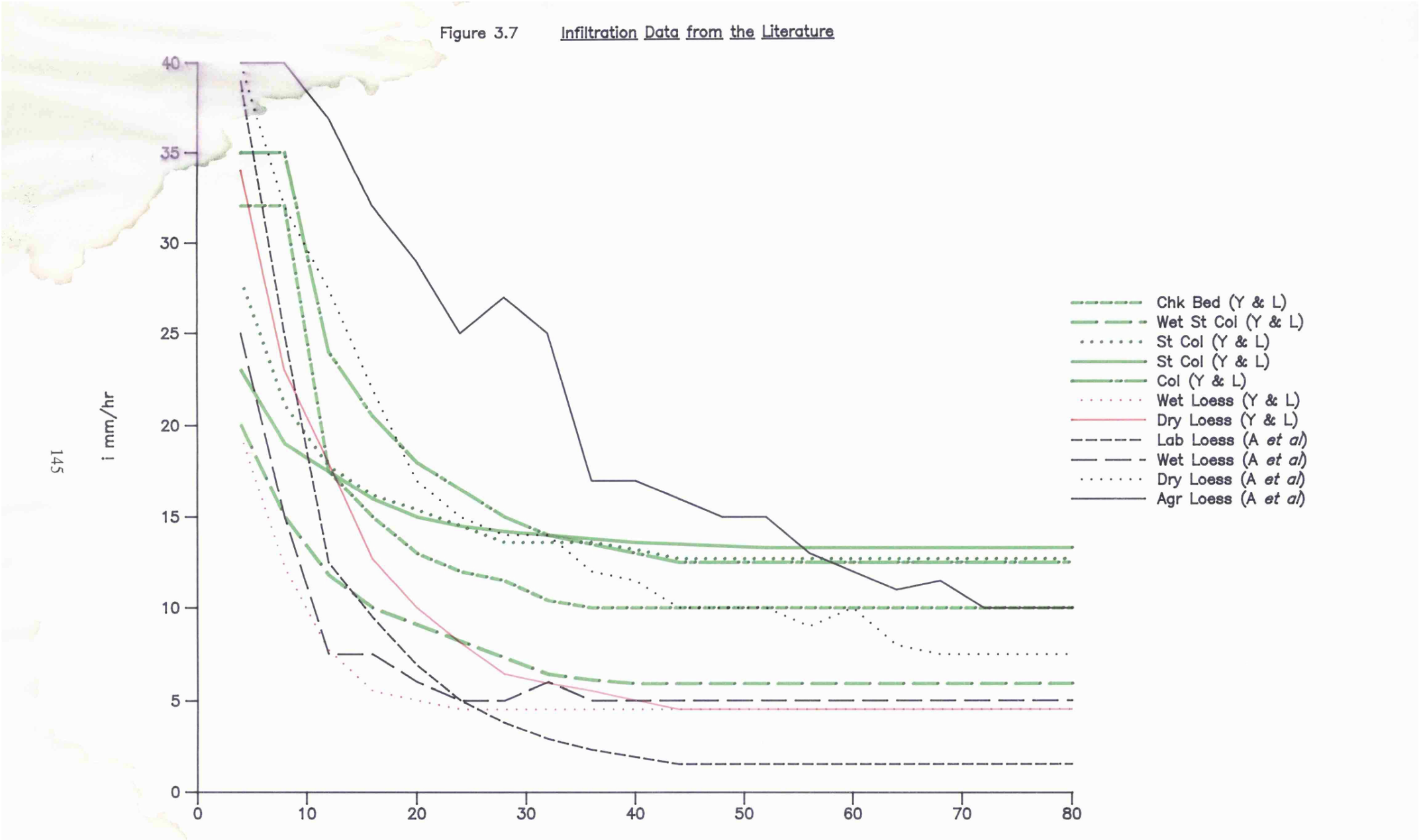

Table 3.5	Best-fit Statistics for Infiltration Models Applied to Literature Data							
Surface	Intensity	Equation	A Param	B Param	corr. coeff.	R.square	F.Stat	D.F.
Agassi	34 mm/h	G and A	0.000253	0.5110	0.924	84.4	98.4	1/17
Alumim		Kostiakov	0.097700	-0.6880	0.971	94.0	283.9	1/17
Agr Loess		Philip	-0.000141	0.0306	0.969	93.5	261.3	1/17
Agassi	34 mm/h	G and A	0.000215	0.2540	0.943	88.4	146.1	1/18
Alumim		Kostiakov	0.038000	-0.6170	0.990	97.8	851.1	1/18
Dry Loess		Philip	-0.000080	0.0198	0.987	97.3	687.2	1/18
Agassi	34 mm/h	G and A	0.000058	0.1520	0.986	96.9	325.1	1/9
Alumim		Kostiakov	0.022900	-0.6730	0.944	88.0	74.4	1/9
Wet Loess		Philip	-0.000151	0.0123	0.962	91.6	111.3	1/9
Agassi	44 mm/h	G and A	-0.000046	0.2860	0.989	97.7	665.6	1/15
Nahal Oz	Σ 70 mm	Kostiakov	2.051200	-1.3300	-0.986	97.0	521.1	1/15
Lab Loess		Philip	-0.000374	0.0217	0.981	96.0	376.9	1/15
Zarmi	Full	G and A	0.000087	0.1710	0.979	95.8	90.7	1/13
Sede B.	Envelope	Kostiakov	0.072440	-0.8120	-0.985	97.1	132.0	1/13
Dry Loess		Philip	-0.000301	0.0191	0.971	94.3	66.2	1/13
Yair	56mm/h	G and A	0.000071	0.2280	0.977	95.0	231.5	1/11
Dry Loess		Kostiakov	0.137700	-0.8810	0.991	98.0	606.1	1/11
nw Neg		Philip	-0.000242	0.0187	0.995	98.9	1063.3	1/11
Yair	56mm/h	G and A	0.000067	0.1140	0.987	97.2	447.5	1/11
Wet Loess		Kostiakov	0.009800	-0.5700	0.930	85.2	69.9	1/11
nw Neg		Philip	-0.000077	0.0089	0.960	91.4	130.1	1/11
Yair	33mm/h	G and A	0.000205	0.3570	0.997	99.3	1663.0	1/8
Colluvium		Kostiakov	0.031600	-0.5800	0.989	97.6	373.2	1/8
		Philip	-0.000126	0.0226	0.984	96.3	231.1	1/8
Yair	26mm/h	G and A	0.000353	0.0735	0.986	97.1	408.5	1/14
Stony		Kostiakov	0.001700	-0.1940	0.974	94.5	260.2	1/14
Colluvium		Philip	0.000264	0.0057	0.995	98.8	831.1	1/14
Yair	26mm/h	G and A	0.000322	0.1140	0.995	98.8	889.5	1/11
Stony		Kostiakov	0.003800	-0.3020	0.983	96.2	310.6	1/11
Colluvium		Philip	0.000171	0.0091	0.995	98.8	889.5	1/11
Yair	26mm/h	G and A	0.000140	0.1090	0.975	94.7	204.6	1/11
Wet Stony		Kostiakov	0.010000	-0.5210	0.993	98.4	734.1	1/11
Colluvium		Philip	-0.000010	0.0089	0.996	99.2	1707.0	1/11
Yair	33mm/h	G and A	0.000109	0.3370	0.968	92.9	118.4	1/8
Chalky		Kostiakov	0.033900	-0.6260	0.951	89.3	76.2	1/8
Bedrock		Philip	-0.000190	0.0209	0.935	85.7	55.2	1/8

rate is not zero or less than zero provides additional support to rejecting the Kostiakov and Philip equations and accepting the Green and Ampt, even though the format of the equation provides marginally poorer best-fit results for six of the twelve data-sets.

The storage parameters of time to ponding (t_o) and storage depth (V_s) for each of these curves are presented in Table 3.6 along with the predicted infiltration capacities in Table 3.7 calculated at the same times as used in Table 3.3 for purposes of comparison of the curves within and between the field and literature models.

3.4.5 Comparisons Between the Avdat Data-Sets and the Literature Data

There are two major points for the comparison of the observed Avdat infiltration data and the literature infiltration data, the first being the overall range of magnitude of the various parameters, and the second being the differences between relatively similar types of slope environment, for instance the shallow loess-covered slopes, or the steeper stone-covered slopes. Both of these types are represented in the literature data, the loess from the laboratory and field studies of Agassi, Zarmi and Yair, and the stoney slopes from the field data of Yair.

Comparisons can be made between several different values. Obviously, the easiest value to compare is the A parameter because this should show clearly whether the orders of magnitude of final infiltration rates are similar. The B parameter is more a function of the testing conditions and the plotting of the raw data-points and there is more opportunity for variation between data-sets depending on the rainfall intensity, the choice of plotting times, the methods of infiltration calculation and whether it involves spatial and temporal averaging. All of these factors control the slope and the position of the recession curve and hence the B parameter. An attempt was made to standardise this by choosing time intervals that are consistent for each infiltration curve. However, as explained for the Avdat field experiments, the first time period infiltration is very important in determining the shape of the overall infiltration curve. Where the experimental procedure involves a runoff component, for instance as with most rainfall simulators in both the laboratory and the hillside, then this can be an overestimate if the build-up of detention storage post-ponding is not excluded from the intial few time-period calculations. With the Green and Ampt method, an indication of true B can be gained by recording both the exact time of surface ponding (t_o) and subsequent infiltration rates from volumetric comparisons as shown by Scoging (1988). In the experimental procedures adopted for both the Avdat field tests and the tests detailed in the literature this time was not noted, the first observation being the time to runoff which involves a detention and routing component.

Firstly, comparing results from the plots on which the crusting mechanism is expected to dominate at Avdat, the wadi-bottom and plateau top, and the laboratory and field tests on crusting soils

Table 3.6	Predicted Time to Ponding and Depth to Ponding (to and Vs) for Different Constant or Mean Rainfall Intensities for the Literature Data														
		p mm/hr		5	5	10	10	20	20	30	30	60	60	120	120
		p cm/sec		0.000139	0.000139	0.00028	0.00028	0.00056	0.00056	0.00083	0.00083	0.0017	0.0017	0.0033	0.0033
Data		A	B	To	Vs	To	Vs	To	Vs	To	Vs	To	Vs	To	Vs
Agassi	Agr Loess	0.000253	0.511	-4478.09	-0.62	20623.32	5.73	1688.95	0.94	880.53	0.73	361.47	0.60	165.89	0.55
	Dry Loess	0.000215	0.254	-3337.23	-0.46	4046.02	1.12	745.84	0.41	410.78	0.34	174.97	0.29	81.45	0.27
	Wet Loess	0.000058	0.152	1879.12	0.26	691.61	0.19	305.49	0.17	196.04	0.16	94.49	0.16	46.41	0.15
	Lab Loess	-0.000046	0.286	1546.88	0.21	883.32	0.25	475.43	0.26	325.25	0.27	166.99	0.28	84.63	0.28
Zarmi	Dry Loess	0.000087	0.171	3295.50	0.46	896.33	0.25	364.95	0.20	229.12	0.19	108.25	0.18	52.67	0.18
Yair	Dry Loess	0.000071	0.228	3358.43	0.47	1102.63	0.31	470.53	0.26	299.08	0.25	142.89	0.24	69.89	0.23
	Wet Loess	0.000067	0.114	1585.78	0.22	540.85	0.15	233.34	0.13	148.76	0.12	71.26	0.12	34.90	0.12
	Colluvium	0.000205	0.357	-5400.00	-0.75	4905.34	1.36	1018.38	0.57	568.17	0.47	244.24	0.41	114.12	0.38
	Stony Col	0.000353	0.074	-343.28	-0.05	-977.10	-0.27	362.86	0.20	153.02	0.13	55.95	0.09	24.66	0.08
	Stony Col	0.000322	0.114	-622.57	-0.09	-2577.89	-0.72	488.11	0.27	222.95	0.19	84.78	0.14	37.86	0.13
	Wet Stony Col	0.000140	0.109	-98100.00	-13.63	791.13	0.22	262.30	0.15	157.21	0.13	71.40	0.12	34.13	0.11
	Chalky Bed	0.000109	0.337	11275.09	1.57	1996.71	0.55	754.67	0.42	465.26	0.39	216.35	0.36	104.52	0.35

Table 3.7 Predicted Infiltration Rates at Different Elapsed Times for the Literature Data													
t (m)	1/t (S)	Agassi.....				Zarmi	Yair and Lavee.....						
		Agr Loess	Dry Loess	Wet Loess	Lab Loess	Dry Loess	Dry Loess	Wet Loess	Colluvium	Stony Col	Stony Col	Wet Stony Col	Chalky Bed
1	0.0167	315.71	160.14	93.29	169.94	105.73	139.36	70.81	221.58	56.81	80.35	70.44	206.12
2	0.0083	162.41	83.94	47.69	84.14	54.43	70.96	36.61	114.48	34.76	46.15	37.74	105.02
3	0.0056	111.31	58.54	32.49	55.54	37.33	48.16	25.21	78.78	27.41	34.75	26.84	71.32
4	0.0042	85.76	45.84	24.89	41.24	28.78	36.76	19.51	60.93	23.73	29.05	21.39	54.47
5	0.0033	70.43	38.22	20.33	32.66	23.65	29.92	16.09	50.22	21.53	25.63	18.12	44.36
6	0.0028	60.21	33.14	17.29	26.94	20.23	25.36	13.81	43.08	20.06	23.35	15.94	37.62
7	0.0024	52.91	29.51	15.12	22.86	17.79	22.10	12.18	37.98	19.01	21.72	14.38	32.81
8	0.0021	47.43	26.79	13.49	19.79	15.96	19.66	10.96	34.16	18.22	20.50	13.22	29.20
9	0.0019	43.17	24.67	12.22	17.41	14.53	17.76	10.01	31.18	17.61	19.55	12.31	26.39
10	0.0017	39.77	22.98	11.21	15.50	13.39	16.24	9.25	28.80	17.12	18.79	11.58	24.14
12	0.0014	34.66	20.44	9.69	12.64	11.68	13.96	8.11	25.23	16.38	17.65	10.49	20.77
16	0.0010	28.27	17.27	7.79	9.07	9.54	11.11	6.69	20.77	15.46	16.23	9.13	16.56
20	0.0008	24.44	15.36	6.65	6.92	8.26	9.40	5.83	18.09	14.91	15.37	8.31	14.03
24	0.0007	21.88	14.09	5.89	5.49	7.41	8.26	5.26	16.31	14.55	14.80	7.77	12.35
28	0.0006	20.06	13.18	5.35	4.47	6.80	7.44	4.85	15.03	14.28	14.39	7.38	11.15
32	0.0005	18.69	12.50	4.94	3.71	6.34	6.83	4.55	14.07	14.09	14.09	7.08	10.24
36	0.0005	17.62	11.97	4.62	3.11	5.98	6.36	4.31	13.33	13.93	13.85	6.86	9.54
40	0.0004	16.77	11.55	4.37	2.63	5.70	5.98	4.12	12.74	13.81	13.66	6.68	8.98
44	0.0004	16.08	11.20	4.16	2.24	5.46	5.67	3.97	12.25	13.71	13.51	6.53	8.52
48	0.0003	15.50	10.92	3.99	1.92	5.27	5.41	3.84	11.84	13.63	13.38	6.40	8.14
52	0.0003	15.00	10.67	3.84	1.64	5.11	5.19	3.73	11.50	13.56	13.27	6.30	7.81
56	0.0003	14.58	10.46	3.72	1.41	4.96	5.00	3.63	11.21	13.50	13.17	6.21	7.53
60	0.0003	14.22	10.28	3.61	1.20	4.84	4.84	3.55	10.95	13.44	13.09	6.13	7.29
64	0.0003	13.90	10.12	3.51	1.03	4.74	4.69	3.48	10.73	13.40	13.02	6.06	7.08
68	0.0002	13.62	9.98	3.43	0.87	4.64	4.57	3.42	10.53	13.36	12.96	6.00	6.90
72	0.0002	13.37	9.86	3.35	0.73	4.56	4.46	3.36	10.36	13.32	12.90	5.95	6.73
76	0.0002	13.14	9.75	3.29	0.60	4.48	4.36	3.31	10.20	13.29	12.85	5.90	6.58
80	0.0002	12.94	9.65	3.23	0.49	4.41	4.27	3.27	10.06	13.26	12.81	5.86	6.45
A		0.000253	0.000215	0.000058	-4.6E-05	0.000087	0.000071	0.000067	0.000205	0.000353	0.000322	0.00014	0.000109
B		0.511	0.254	0.152	0.286	0.171	0.228	0.114	0.357	0.0735	0.114	0.109	0.337

using simulated rainfall indicates whether the discussions of Section 3.4.3.b concerning the quasi-permanent influence of the crust irrespective of the manner of application and the type of water used are correct to assume that the crust exerts its influence without impact. The comparison shows clearly that the field data for the loessial soils (unit 5 plots) are inconsistent with the data presented in the literature being considerably higher both in the initial and subsequent infiltration capacities. Looking at each of the three Avdat loessial field plots, the lowest final capacities are those of the loess soil 5w upper which is on the terrace to the west of the catchment. These are aeolian soils. The highest final infiltration capacities are those of the loess soil in the wadi bed adjacent to the main ephemeral channel 5w lower. The reason for the higher infiltration rates here are probably due to the more coarse fluviatile loessial soil washed into the wadi from the surrounding slopes rather than through wind deposition. The annual flooding results in a heavy growth of annual plants and intense harvester ant activity which means the sub-surface macro-pore structure is likely to be extensive. With each of the loessial soils, if the crusting process is not active, then the access to the underlying macro-pore structure is not cut off by the wash-in layer and impact layer and the final rates will remain high. Of relevance here is the analysis of Agassi *et al* (1986) and particularly the infiltration curve they derived from a field test on an un-crusted tilled loess soil. This shows the highest final infiltration rate of all the literature loess soils although it is still considerably below the final rates of the Avdat plots. Morin *et al* (1981) state that the hydraulic conductivities of loess soils without a crust can be expected to be around 45 mm hr^{-1}, and for crusted soils about 5 mm hr^{-1}. This suggests that under the run-on/runoff test conditions, the loessial soils operate essentially as uncrusted surfaces. It cannot be accepted that the infiltration parameters derived for these surfaces could be applied as spatially distributed parameters in a full routing model in the simulation of a natural rainfall-runoff event. It seems clear that the literature infiltration models should be used in any modelling assessment of the Negev hydrological systems and not the unit 5 field plot data. The most logical set of parameters to use are those derived from the Zarmi *et al* studies of a loessial micro-catchment at Sede Boqer since this is morpohologically and geographically most similar to the Avdat setting and is derived from field experiments.

What about the colluvial or rocky slopes given this poor correspondence between the infiltration rates measured for loessial slopes and the literature data? How well can they be expected to represent true conditions, and how do they compare against relevant tests presented in the literature? It was discussed earlier how the soils on the colluvial slopes and in the rocky areas were likely to be less dependent on the crusting process to control the infiltration capacities and more dependent on the surface stone cover, proportion of bedrock and opportunity for storage within the soil. The field tests on colluvial stony and stoneless soils and on rocky areas presented in Yair's papers are of a similar order of magnitude to the plots measured in the field. The initial capacities in the literature are in the order of 20 to 40 mm hr^{-1} and the final rates vary from 10 to 13 mm hr^{-1} for the colluvium. Yair's bedrock slope, not tested in the statistical analysis due to the limited number of data points, is similar to the results from the unit 3 plot groups, except for the fact that Yair extends his curve qualitatively down to

the zero asymptote instead of leveling off at a low but constant final rate (Yair, 1983). In Shanan's studies, taking the infiltration capacities at 60 minutes the orders of magnitude presented are slight overestimates of Yair's findings. In the tests carried out at the end of the rainy season, after 60 minutes, the rates were 15.0, 10.6 and 20.7 mm hr^{-1} for the 1%. 10% and 20% slopes respectively. The 1% slope represents the same conditions as the unit 5 slopes in the Avdat field tests and therefore has the same overestimation of rates due to the run-on/runoff nature of the tests. The other two represent the higher end of Yair's results, equating with his more highly infiltrable stoneless colluvial slope. The rocky slopes with lower infiltration rates were not sampled in Shanan's studies. The Shanan data represents similar capacities to those observed in the higher of the two groups of Avdat plots.

Where the rainfall-runoff process is characterised by relatively rapid changes in infiltration rates towards steady states, and where rainstorms are generally short with varying intensities, the plotting of infiltration rates and the fixing of initial time period infiltration rates, accounting for detention storage and time-lag effects, are very important in determining the parameters of an infiltration equation. Whilst they will seldom effect the final infiltration rate values, they have considerable effect on the predicted initial infiltration rates and times to ponding when infiltration data is applied in a rainfall-runoff model under different rainfall intensity conditions. This controls the parameters specifying the gradient of the change through time, in the case of the Green and Ampt equation the B parameter. Great attention has been given in past experiments to the achievement of rainfall drop size distributions and terminal velocities which are then discussed in great detail in the experimental methodology (Yair *et al*, 1980. Zarmi *et al*, 1983. Agassi *et al* ,1986). However, few details are given concerning the subsequent observations and calculations of infiltration data and especially the differences between time to runoff and time to ponding, the areal averaging involved in calculating the infiltration rates based on volumetric runoff from the area, and the choice of plotting times for the data since time t=0 when the simulated rainfall began. Each of these relatively simple factors can result in significant effects on the nature of the parameters derived for the infiltration experiment that may be in excess of the influence of differences between simulated and natural rainfall kinetic energies. In deriving A and B parameters for the Avdat infiltration data, the plotting times were seen to be extremely important for the determination of a B coefficient value as was the inclusion of an unquantified detention storage component in the initial infiltration calculations that considered the volumetric input against the recorded output. In each of the literature data sets used in the analysis these important procedures are not detailed. One thing that is clear is that the time to runoff is not the time to ponding but the time until discharge off the surface is recorded for the various experimental procedures used. Thus the initial infiltration calculations, as with the Avdat field tests, are likely to include a significant proportion of surface storage. Therefore, the B coefficients of the Green and Ampt infiltration coefficients fitted through these curves are also likely overestimates.

CHAPTER FOUR FLOW ROUTING

4.1 INTRODUCTION TO THE FLOW ROUTING PROBLEM

Water harvesting systems function by collecting water running off a surface, concentrating it and delivering it to a point at which it is stored for subsequent use. In the case of a runoff farming system like Avdat, the runoff from a natural catchment surface is collected, concentrated and delivered to farm terraces by a series of man-made ditches that intersect hillslope flow-lines. The pattern of generation and movement of surface water is a critical factor in the functioning of the collection system.

The production of surface water in an arid environment due to rainfall excess is both spatially and temporally variable. The movement of water is also a heterogeneous process. Many arid environments such as the Negev, are characterised by considerable variations in surface conditions such as elevation, slope gradient, surface materials and surface micro-topography. Elevation and gradient, in combination with the mass of water input to a given location, provide the forces promoting flow movement. Materials and micro-topography provide the forces opposing movement and dictate how water crosses the surface, whether the flow is concentrated or dispersed, rivulet or sheet-like.

This chapter considers how the highly complex three dimensional processes of hillslope and channel flow can be modelled. For a catchment system, the dynamics of flow must be simplified along with the surface over which it takes place. The former involves a simplification of a three-dimensional, non-uniform, unsteady flow into a one-dimensional, uniform flow. The latter involves a simplification of a hillslope and channel network into a finite number of discrete, inter-connected planes and channel segments, and a method of reproducing the micro-characteristics of flow across them. These simplifications necessarily involve a loss of detail. However, all assumptions are based on the principle that the approximations maintain the most significant characteristics of the original system, retaining the time and space orders of magnitude and rates of change. Any errors compared with the original system, which cannot easily be quantified although known to exist, are not serious enough to limit the predictive or explanatory abilities of the model *vis á vis* the original for those situations simulated.

The first step in the modelling process is to provide the flow equations. They must preserve mass and energy. The simplifications identify the components of flow energy that are most important. The assumption made is that flow is kinematic and uniform. Dynamic components are assumed insignificant with frictional forces balanced by gravitational forces. The second step is to parameterise the flow equation that describes uniform flow by providing a set of parameters for each spatial element within the system. The Manning flow equation is chosen and the parameters are slope gradient, flow

dimensions and resistance to flow. For each of these parameters there is no single, standard technique for considering variations at the intra-hillslope and intra-channel section scale and the role they play in the rainfall-runoff process within arid-land hydrological systems.

Slope gradient is provided from the geometrical simplification of the physical system over which flow takes place. For Avdat, the physical system is an asymmetrical basin with a range of concave, convex, diverging and converging slopes intersected by a number of linear, man-made ditches and a dendritic network of natural rills. To provide appropriate slope gradient parameters, the complex surface is reduced to a finite series of elements of constant slope gradient and known width and length.

Flow dimensions can change with the changing state of flow and the build up of a hydraulic head on the hillslope or in the channel. They are controlled by the geometry of the surface boundary within which the water flows down-slope or down-channel. Boundary shape of a hillslope is often simplified as a uniform plane over which sheetflow occurs because flow is shallow relative to the width of the slope and the hydraulic radius can be approximated by the depth. On a plane surface, water may flow as a thin, fairly uniform film. Topographic irregularities on natural slopes, however, direct most runoff water into lateral concentrations of flow giving the appearance of a wide, shallow, braided channel (Emmett, 1978). Small micro-relief features of only 2.5 cm concentrate the flow paths. Roels (1984b) observed that overland flow should not be considered as sheet-flow but as inter-rill flows. These are permanent flow paths carrying away concentrated runoff but not sufficiently large to be considered rills. Morgan (1980) observed runoff on a partially vegetated surface to consist of numerous, separate, un-channeled water courses in an anastomizing pattern. Although the process can be readily observed, its quantification is more difficult and the use of a sheetflow approach is most likely the source of considerable, so far un-quantified errors in simulating flow over natural slopes. The flow dimensions of depth or hydraulic radius are dependent on the discharge-stage-velocity relationships for a given type of surface. The velocity is dependent on the amount of water, the flow dimensions, slope gradient and resistance and is determined by the flow equation. Parameterising the boundary characteristics accurately is therefore of special importance.

The final parameter, flow resistance, is an important one. Modelling resistance to surface flow presents interesting and complex problems (Scoging, 1988). Li and Simons (1982) state that to evaluate flow-hydraulics, it is essential to determine the resistance to flow. However, recognizing it to be a function of many variables they state that there is no single best method to do this, each having its advantages and disadvantages with the problem not yet adequately solved. This is especially true for the case of surface flow in arid environments where research to date has been limited. Resistance data is most numerous from experiments under laboratory flow conditions or for rivers. Recent field studies presented in the literature and carried out at Avdat show how inappropriate the range and magnitude of parameters are compared to steep, micro-topographically rough hillslope flow.

Although the parameters can be considered independently in theoretical terms, practically they act in unison. Specifying parameters is therefore difficult because of the interdependence of their values and our inability to measure them in isolation, separated from the variables they are required to predict.

4.2 THE EQUATIONS DESCRIBING FLOW MOVEMENT

To study the movement of water through any hydrological system, the basic laws of; conservation of mass, energy and momentum must be applied, which involves some knowledge of or assumptions concerning the physical properties of the water, the physical characteristics of the flow boundaries (fluvial system geometry and the infiltration characteristics at the sequence of locations flow will cross), the initial conditions, and the rates and changes of input through time (Woolhiser, 1981).

Overland and channel flow are unsteady, and spatially varied phenomena. They are supplied by rainfall and depleted by infiltration, both of which are variable in time and space. They can be laminar, turbulent or a combination of both (Emmett, 1970). Three equations are used to consider flow, one defining flow continuity across space and time, a second defining flow momentum, and a third defining a friction law relating the resistance to flow to the properties of the flow. These are the system of partial differential equations that describe one-dimensional, gradually varied, unsteady open-channel flows and were first developed by de Saint-Venant and are called the Saint-Venant equations (Dingman, 1984). Their derivation from first principles is shown in most hydraulic textbooks and is discussed thoroughly in Dingman (1984) and in Miller (1984).

The full Saint-Venant equations can only be solved within limited initial and boundary conditions. Because of this, the current approach makes a number of assumptions to apply them to the complex situation of hillslope and channel flow in a spatially variable environment. These assumptions are that flow is uniform within each individual element considered in calculating routing conditions, that the kinematic wave is appropriate to describe the movement of flow within the hydrological system and that numerical rather than analytical techniques can be used to accurately solve the flow routing equations for a given set of initial and boundary conditions.

4.2.1 Uniform Flow and the Kinematic Wave Theory

By using the uniform flow approximation, acceleration is assumed insignificant and the bed-slope of the channel or hillslope assumed to be equal to the friction slope. Flow can therefore be expressed mathematically using the following general formula;

$$Q = A(x,t).v \qquad \text{Equation 4.1}$$

(where Q is discharge, v is the mean flow velocity through the cross-profile and A(x,t) is the cross-sectional area at location x at time t).

Of importance for the selection of uniform flow assumptions for the consideration of surface flow movement is the nature of the flow and whether it can be considered as laminar or turbulent. This determines the friction law that can be chosen to provide the velocity component. On the basis of the Reynolds numbers associated with shallow surface flow, then the flow should be classified as laminar. However, it is usually considered turbulent in behaviour because of the steep gradients compared to channels, the high degree of surface roughness relative to flow depths, and the effects of raindrop impact onto the surface of the shallow flows.

A commonly used friction law for turbulent flow conditions is the Manning equation, which uses the friction coefficient of n. The general form of the equation is;

$$v = k.\sqrt{s}.Hr^{2/3}/n \qquad \text{Equation 4.2}$$

$$Q = A(x,t).[k.\sqrt{s}.Hr^{2/3}/n] \qquad \text{Equation 4.3}$$

(where s = slope gradient [sine], n is the Manning coefficient, Hr is the hydraulic radius with Hr=y for the sheetflow case, and k is a coefficient used to account for the dimension of $L^{-1/3}$ of the n coefficient which must be adjusted according to the units used. According to Chow, 1959 page 98 and Richards, 1982 page 63, k equals 1.0 for m s^{-1}, 4.64 for cm s^{-1}, and 1.486 for ft s^{-1}).

In order to fully describe open-channel flow (which includes overland flow), the simplified momentum equation (Equation 4.1) must be combined with a continuity equation which is formulated to obey the principle of the conservation of mass.

The continuity equation states that the input to a channel or hillslope section in a given time period minus the output from that section is equal to the change in storage (Miller, 1984).

$$ql - \partial Q/\partial x = \partial A/\partial t \qquad \text{Equation 4.4}$$

$$(p.w + i.WP + Ql/dx) - \partial Q/\partial x = \partial A/\partial t \qquad \text{Equation 4.5}$$

(where ql is the balance between lateral inflow, rainfall and infiltration, ∂Q is the change in discharge, ∂x is the change in downslope distance, ∂A is the change in flow area, ∂t is the change in time, p is

rainfall, w is the width of the channel or hillslope section, i is infiltration, WP is the wetted perimeter, and Ql is the lateral inflow from hillslopes (zero for hillslopes)).

4.2.1.a The Kinematic Wave

The kinematic wave model is an approximation of the dynamic wave model which describes unsteady, gradually-varied, open-channel flow by assuming uniform flow (Miller, 1984). The flow wave is propagated in one direction only downstream. Lighthill and Witham (1955) describe the kinematic wave as a fluid motion whose propagation is specified completely by an equation of continuity for one-dimensional flow and a stage-discharge relation for steady uniform flow, relating depth to discharge through a friction relationship such as Mannings. Discharge Q is assumed to be a function of depth or area alone, thus the bed slope So is assumed to be large enough and the water wave long and flat enough so that the change in depth or area and velocity with respect to distance ($\partial y/\partial x$, $\partial A/\partial x$ and $\partial v/\partial x$) and the change in velocity with respect to time ($\partial v/\partial t$) are negligible. The momentum equation can therefore be represented by Equation 4.1.

The general consensus is that the kinematic approach is most appropriate for overland flow at low rainfall rates over long, rough, steep slopes (Miller and Cunge, 1975) which obviously includes the slopes of the arid environments such as Avdat. In these environments, the change in water-slope, bed-slope and energy-slope can more realistically be assumed to be parallel and the effect of acceleration terms discounted, especially when small incremental, uniform sections are adopted for the solution. Henderson (1963) stated that flood waves on steep slopes are adequately described by the kinematic-wave model. Engman and Rogowski (1974) also support this.

Due to the approximation of the momentum equation by its uniform flow simplification, Miller and Cunge (1975) showed that the kinematic-wave approximations should not be used for highly super-critical flows. These are defined by Chow (1981) to be rapid, shooting or torrential flows, where inertial forces dominate. Most overland flow and channel flows involve sub-critical flows and hence the kinematic approximations can be accepted on the basis of this criteria.

Many applications of kinematic theory have been used in the modelling of complete catchment systems and individual hillsides. The kinematic wave model was first introduced for river floods in the 1950s by Lighthill and Witham (1955). Subsequently it was used by Iwagaki (1955) to model flow through channels with steep slopes, Henderson and Wooding (1964) for simple plane and channel geometries, Brakensiek (1966) for surface runoff from rural watersheds, and Schaake (1965) for runoff from urban watersheds. These have been expanded by the development of the kinematic cascade approach by Brakensiek and its extensive application to arid catchment modelling by Woolhiser (1969, 1981, 1985) and Lane *et al* (1978).

4.2.1.b The Kinematic Cascade

As indicated, Brakensiek (1967) made the essential step from the use of kinematic assumptions for a single flow plane to a series of discrete flow planes and hence produced the kinematic cascade. The uniform flow assumption of kinematic wave theory, as used by Wooding, was not a tenable situation, since flow over a long distance is obviously non-uniform. Where spatial variability in the controlling characteristics on flow generation and transmission occurs along channels and across hillslopes, the assumption that conditions of uniform flow are in operation cannot easily be accepted. By breaking the distance into smaller Δx increments, individual uniform flow conditions can be more readily accepted. In the Manning equation, the parameters are specified for each Δx increment as a finite series of constant, uniform approximations to the non-uniform real conditions.

In order to apply these procedures in a manner that represents natural systems in meaningful ways, individual spatial segments need to be combined in a way that reflects the spatial complexity of the system (Scoging, 1988). This is the purpose of the kinematic cascade which approximates a complex continua by simplification into a number of segments on the basis of some pre-determined criteria such as downslope distance, elevation change, or boundary classification. Where each of these spatial segments is parameterised with process variables the result is a 'distributed model' (Beven and O'Connell, 1982) although obviously depending on the size of the segment, the parameters will represent the lumped conditions within it.

4.2.2 Finite Difference Solutions to the Flow Equations

Rather than treat the problem of flow as one of a continuous process in both time and space, it can be approximated into discrete dimensions by evaluating small incremental changes in flow conditions with respect to Δt and Δx and solving difference as opposed to the more complex differential equations. The differential equations refer to infinitesimally small regions or single points and require an analytical solution. The difference equations refer to a finite, discrete region and and can be solved with a more simple numerical solution.

There are a number of difference solutions and choosing between them depends on which one minimizes storage and execution time on a computer whilst solving to required levels of accuracy and stability. The complete series of differencing schemes is discussed in detail in Miller (1984), Liggett and Woolhiser (1967), Yevjevich and Barnes (1970), Liggett and Cunge (1975) and Abbott (1979). To apply finite-difference techniques, a fixed grid in the x-t plane is usually employed. The boundary conditions are known for each point along the x-direction for $t = 0$ and for each time along the t-direction for $x = 0$. There are two major types of finite difference scheme;

1. explicit schemes which are written so that unknowns at each point in the next time step Δt (t) can be solved individually as an explicit function of the values of the dependent variable at the earlier time step (t - 1),
2. implicit schemes which solve for the unknown dependent variables at a group of advanced points in the space-time frame through the use of as many simultaneous equations as there are unknowns.

According to Liggett and Cunge (1975) the choice of finite difference solutions facing the modeller is not easily made, since there is no definitive 'best' solution for all cases. According to Abbott (1978), the 'best' choice depends on the criteria of;

1. ease of use and computational (storage and execution time) efficiency,
2. optimum accuracy related to choosing $\Delta t/\Delta x$ combinations that keep the solution in the numerically stable regime. This can often impose costs in fieldwork, data preparation and model execution that are themselves constraints.

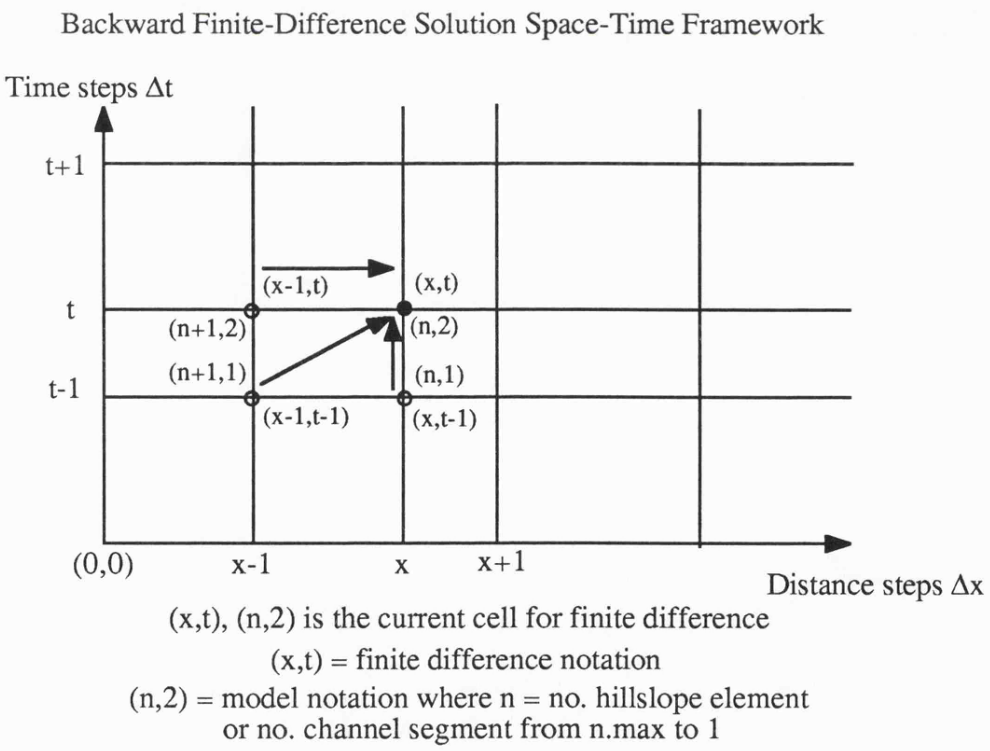

Figure 4.1 Backward Finite Difference Solution Space-Time Framework

The chosen scheme is based on a consideration of the time locations (t) and (t-1), the current and previous time, and the distance locations of (x) and (x-1), the current section and the previous

section upstream. This is a simple backward difference scheme, easily programmed although subject to limiting stability criteria for the choice of Δt increments. The discharge Qin is that coming from (x-1), and the discharge Qout is that leaving (x). Figure 4.1 shows the locations of the known and unknown points in the time-space solution framework. The time steps are variable depending on the stability of the solution (Section 4.2.4.d) and the Δx steps can either be constant or variable, depending on the discretisation of the hillslope or channel lengths (Section 4.3).

4.2.2.a Channel Section Finite Difference Solution

Consider a channel section which receives lateral inflow from two hillslope cascades, one on either side. This is illustrated in Figure 4.2.

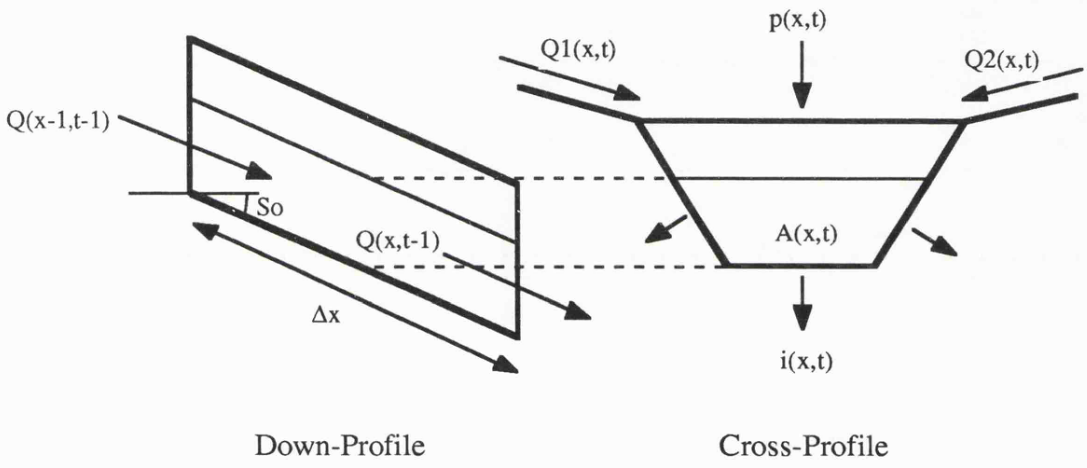

Figure 4.2 Channel Flow Section

As presented previously the continuity equation in flow dimensions of area is;

$$\partial A/\partial t = (p.w - i.WP + Ql/dx) - \partial Q/\partial x \qquad \text{Equation 4.6}$$

Multiplying Equation 4.6 through by ∂t gives the following;

$$\partial A = \partial t.[Ql/dx + (p.w - i.WP) - \partial Q/\partial x] \qquad \text{Equation 4.7}$$

This can be written in finite difference notation if the flow section of length dx (written as Δx) is given the location (x) in the series of increments that comprise the complete channel and the upstream section is given the location (x-1). The continuity equation becomes;

$$A(x,t) - A(x,t-1) = \Delta t.[(Q1(x,t) + Q2(x,t))/\Delta x + (p(x,t).w(x) - i(x,t).WP(x)) - (Q(x,t-1) - Q(x-1,t-1))/\Delta x]$$

Equation 4.8

(where dx and ∂x are the length Δx, Q1 and Q2 are lateral volumetric discharges from the hillslope section on either side, p is rainfall, w is the channel top-width and i is infiltration).

Rearranging to isolate the term required for the solution, the new area A(x,t) in the channel during the current time following the discharge in and out of the channel in the previous time and the additions and subtractions from lateral inflow and rainfall excess, the formula gives A(x,t) to be;

$$A(x,t) = A(x,t-1) + \Delta t/\Delta x.[Q1(x,t) + Q2(x,t) + Q(x-1,t-1) - Q(x,t-1)] + \Delta t[(p(x,t).w(x) - i(x,t).WP(x))]$$

Equation 4.9

Where the hillslope flow is modelled as a sheetflow approximation, as opposed to the area calculations assumed in the above equations, then in this case, since these hillslope sections will discharge laterally into the channel in values of discharge per unit width, the lateral inflow must be multiplied by the width of the inflow element to give the correct discharge and the channel difference equation becomes;

$$A(x,t) = A(x,t-1) + \Delta t/\Delta x.[w1(x).q1(x,t) + w2(x).q2(x,t) + Q(x-1,t-1) - Q(x,t-1)] + \Delta t[(p(x,t).w(x) - i(x,t).WP(x))]$$

Equation 4.10

(where w1(x) and w2(x) is the width of each lateral inflow element into segment x and q1(x,t) and q2(x,t) are the lateral inflow discharges per unit width).

In reality, the rainfall excess component of the equation should be a balance between the area of incoming rainfall, and the area of infiltration from that rainfall into the whole channel perimeter WP(x), and the infiltration from surface flow into the wetted perimeter in contact (which would be WP(x,t)). This allows for the conditions of rainfall pre-ponding, rainfall during ponding, and ponding post rainfall as discussed in the previous chapter Section 3.4. The disputed notation is the term WP(x) which can be both the actual wetted perimeter WP(x,t) for infiltration from the channelised flow, with the total perimeter of the normal channel WP(x) being the factor of importance for infiltration from rainfall. The relationship between channel flow infiltration and channel rainfall infiltration is arbitrary if both are prevailing at a given time (t), but must be separated for the purpose of model calculations.

For the moment, since the current section seeks only to illustrate the general technique, the general form of the difference equation is left as WP(x), infiltration into the total channel perimeter.

4.2.2.b Hillslope Element Finite Difference Solution

For a hillslope surface the finite difference form of the continuity equation is identical to Equation 4.10 except that there is no terms for lateral inflow since flow is considered orthogonal to hillslope contours in the hillslope elements forming the hillslope cascades. Thus the continuity equation becomes;

$$A(x,t) = A(x,t-1) + \Delta t/\Delta x.[Q(x-1,t-1) - Q(x,t-1)] + \Delta t[(p(x,t).w(x) - i(x,t).WP(x)]$$

Equation 4.11

since input is only from rainfall and discharge from the previous hillslope element, with output being outflow discharge to the downslope element, and infiltration into the wetted perimeter (in the case of surface flow), or the complete perimeter (in the case of rainfall) as explained previously.

For overland flow, the assumption is often made that the type of flow to be found, with shallow depths relative to width, can be represented by a rectangular section where width is infinitely large compared to depth and so depth is considered instead of the hydraulic radius. In this case, since the wetted perimeter wp is equal to the total width of the section, the hydraulic radius is equal to the depth y.

$$y(x,t) = y(x,t-1) + \Delta t/\Delta x.[q(x-1,t-1).(w(x)/w(x-1)) - q(x,t-1)] + \Delta t[(p(x,t) - i(x,t)]$$

Equation 4.12

(where w(x)/w(x-1) adjusts the discharge per unit width from the upper element, q(x-1,t-1) by the ratio of the two widths to calculate the correct depth).

4.2.2.c Initial and Boundary Conditions

In the finite difference solution of the flow routing equations, initial conditions are necessarily specified to be a dry surface for time t=0 (Smith and Woolhiser, 1971). Therefore for the initial time period where (t=1) there is no input and output discharge and no depth y(x,t-1) or area A(x,t-1). Thus the new area is equal to the sum of the lateral inflow and the rainfall excess (p - i). The physical dimensions of width and length, and the time increments are all known, and therefore the single unknown A(x,t) can be calculated.

The boundary conditions are that for the upper boundary there is no (x-1), i.e. the boundary is closed. For the lower boundary the assumption is one of unrestricted flow with no backwater effects, i.e. normal flow conditions are operating and the boundary is assumed open. The solution is thus given for all states and updating the time increment with successive iterations marches the routing solution through time.

4.2.2.d Solution Stability and Accuracy

There are two possible sources of errors in the formulation of solutions to the routing equations; those from programming mistakes and numerical errors related to the method of solution. Both lead to the non-preservation of mass continuity with the latter producing numerical instability. For a correct solution that represents the true processes, both numerical stability, and mass continuity must be preserved.

Programming error is minimised by accurate accounting of all the inputs, throughputs and outputs that take place throughout the flow simulation. This requires that equation dimensions balance (i.e. equal ratios of mass, length and time appear either side of each equals sign) and that no stores are neglected as the solution rolls through the time-space framework. Numerical stability is more complex. There are two causes; kinematic shocks which result from the use of kinematic approximations to the full momentum equation; and model instability resulting from the use of the explicit finite difference procedures to solve the kinematic equations.

Kinematic shocks form where abrupt changes in depth occur (Kibler and Woolhiser, 1970) causing successive small waves to travel with greater speed so that waves further downstream are overtaken. Their subsequent coalescence forms the shock. Kinematic waves have only one wave speed and one direction. The kinematic wave does not lengthen or disperse and does not subside as it moves downstream. However, it may distort because $\partial Q/\partial y$ and thus V will increase with y, as described in the stage-discharge relation. The effect of this would be for the wave to form a vertical, and then toppling front if allowed to travel far enough, as described by Henderson (1963, 1966) (in Miller, 1984). This is known as the kinematic shock. By neglecting the inertia and acceleration terms in the full momentum equation which become important where any rapid depth variations occur they effect the solution in a cumulative fashion to produce the shock (Miller, 1984).

Usually, kinematic shocks only occur when the method of characteristics is used to solve the kinematic-wave equation (Miller, 1984). The method of characteristics defines the path of wave propagation. When shock formation does occur, a surge forms with steepening wave structures developing in the passage downstream. However, if a large amount of lateral inflow or channel storage

occurs within the system, the error involved in applying the kinematic-wave model will be small because this helps to gradually attenuate and disperse the wave form leading to smooth depth changes. Thus, in overland and channel flow routing where the routing distances are short, the slopes steep, and the lateral inflow large, the kinematic-wave model should not experience kinematic shocks.

Explicit backward finite difference schemes are subject to a condition that is expressed as a mesh ratio ($\Delta x/\Delta t$) if they are to be stable. They are conditionally stable. Stability refers to the ability of the scheme to prevent numerical errors from growing in an unbounded or uncontrolled manner (Miller, 1984). This limits the size of time step that can be used. Additionally, instabilities can result from the often necessary abrupt changes in slope, roughness and width of successive planes and channels within the kinematic cascades. They may give rise to solution discontinuities in the kinematic equations handling the flow of water (Kibler and Woolhiser, 1972). The physical characteristic of instability is a rising perturbation that forms a roll wave, changing the character of the flow, usually in steep channels leading to bank overflow in its passage down-channel (Liggett, 1975). According to Liggett and Cunge, instability can be avoided in the computation process by asking if a particular part of the solution, perhaps an initially unimportant part, is likely to grow without limit until it destroys the calculation. This is done by considering the mesh ratio as presented in the equation for basic stability; the Courant-Lewy-Friedrichs condition, which requires that Equation 4.13 be observed for explicit finite difference methods.

$$\Delta t/\Delta x \leq 1 / | v \pm \sqrt{gy} | \qquad \text{Equation 4.13}$$

(where Δt is the time increment, Δx is the space increment, v is the mean velocity, g is gravity and y is the mean flow depth).

The full Courant condition applies to the methods of characteristics which specify the directions of disturbances and divide the time-distance plane into a region where the solutions are possible and a region where they are impossible for a given Δt, Δx combination (Yevjevich and Barnes, 1970). The term $(v+\sqrt{gy})$ is the upstream characteristic, and $(v-\sqrt{gy})$ the downstream characteristic (Morgali and Linsley, 1965). The solution must lie within these boundaries to produce hydrographs that dampen oscillations and converge on stable equilibrium flow. Neutral stability occurs where both sides of the condition are equal. Since the kinematic flow approach assumes uniform flow with wave propagation in one direction only, stability requires Equation 4.14 to operate which ensures flow is either critical or sub-critical (Yevjevich and Barnes, 1970).

$$\Delta t/\Delta x \leq 1 / (v + \sqrt{gy}) \qquad \text{Equation 4.14}$$

Since velocities and depths (or hydraulic radii) are calculated internally within the model algorithms as products of the finite difference equations, and the distance increment Δx is a fixed feature of the spatial mesh of the kinematic cascades, the specification of the time increment Δt is critical. In the current model, instability can be prevented by continuously examining the combinations of velocity, flow dimensions (depth or hydraulic radius), and time and space increments to determine if the Courant stability criteria is likely to be violated. If violation is likely in subsequent time increments for one or more of the model spatial elements, the time increment is reduced to prevent it. The time increment change applies for the whole system, and can be increased again if the Courant condition is not in danger of being violated and the likelihood is receding. Reducing the time increment results in a stable solution by dampening the numerical oscillations produced by the solution. The numerical scheme is therefore dispersive which is acceptable and even beneficial since it is analogous to the natural dispersion that occurs in hillslope and channel flow (Morgali and Linsley, 1965).

4.3 THE UNIFORM FLOW EQUATION

The uniform flow equation which approximates the full momentum equation, is central to the modelling of flow movement throughout a hydrological system. It comprises the stage-discharge relation Equation 4.1 and Manning's Equation 4.14 which defines the flow velocity **v** (in units of cm s^{-1});

$$v = (4.64).[s^{-1/2}.Hr^{2/3}/n] \qquad \text{Equation 4.14}$$

There are three components to Manning's equation; the resistance (friction) coefficient **n**, the slope gradient **s**, and the flow dimension **Hr** (which is equal to the average depth **y** for the sheetflow assumption). Their combinations determine the magnitude of velocity and the relationships between velocity and flow dimensions for a given discharge.

The Manning Equation was developed empirically by Robert Manning in 1889. It is the most widely used of all uniform-flow formulae for open-channel computations (Chow, 1981). Although it applies to the case of uniform flow in a turbulent state, it has been used successfully to reproduce hydrographs of flows normally classified as laminar, as well as those produced under turbulent conditions.

The slope gradient **s** is the macro-topographical parameter which determines the potential energy available for movement and according to Manning's equation influences flow velocity in direct relation to the square root of its size. The flow dimensions of hydraulic radius **Hr** is a micro-topographical parameter with the topography ignored in the case of the sheetflow approximation. The hydraulic radius changes with each increase in stage in a manner dictated by the shape of the surface.

The flow dimension parameter influences flow velocity in direct relation to the power 2/3 of its size. Mis-specification has a larger proportional effect on the velocity than the slope gradient. The resistance coefficient of Mannings **n** influences flow velocity in inverse direct proportion to its size.

4.3.1 Slope Gradient

4.3.1.a Hillslope System Geometry

Beven and O'Connell (1982) state that one of the most important characteristics determining the hydrological response of a catchment must be the nature of the catchment topography pointing out that in many lumped models, topographical variations are often completely ignored. Topographical variations are important firstly because they determine the spatial arrangement of the hillslope or catchment surface i.e. the surface areas, lengths and positions, and secondly because they determine the slope gradient.

To deterministically model a catchment or hillslope hydrological system in which surface flow processes are dominant, requires simplification of the system whilst maintaining flow patterns similar to those in the prototype watershed (Woolhiser, 1981). The arrangement and gradients of slopes must be retained. The gradient determines the direction and rate of movement of water, and the spatial arrangement of slope sections and channels determines the sequencing of flow movement which has been termed 'hydraulic remoteness' (Lane *et al*, 1975). The hydraulic remoteness is the total length of hillslope and channel flow-lines that must be traversed by surface water generated at a given location to register at the point of outflow from the system. In the case of a water harvesting system such as Avdat, this is an entrance into the terraced runoff farm at the end of the catchment ditches and channels. Obviously not only the length is important, but the character of the route since this helps dictate whether water will be lost as infiltration along the way. The slope gradient plays a major role in this process of transmission and is important for the hydraulic remoteness. As slope gradient increases, other things remaining equal, velocities will increase as will the capacity to transmit runoff water.

4.3.1.b Specifying Slope Gradients

The provision of slope gradient parameters forms part of the geometric simplification of the flow system in which a simple geometry is substituted for the more complex one of the natural hillsides (Lane and Woolhiser, 1977). In many modelling approaches, the slope gradient is poorly specified either because the spatial arrangement of slopes is not preserved or because the gradient is averaged at a low spatial resolution, for instance using the average gradient for the complete hillslope from divide to channel instead of several distinct sub-sections. An example of this approach would be the Wooding model (1965) which approximates a whole catchment as a single channel section fed

laterally by two flow planes, each representing half of the catchment. Considering such large spatial elements will fail to represent the process at the scale of interest. Where the objective is to consider the spatially variable characteristics along a hillslope in a distributed fashion information on the slope gradients must be provided at the intra-hillslope scale. This is especially true for water harvesting systems where hillslopes are already sub-divided by a pattern of super-imposed collecting ditches and which cross several different hillslope environments along their route from the remote parts of the system to the runoff farm area.

Water moves along a flow-line of maximum slope across a hillside which is the orthogonal to the elevation contours. In the case of a water harvesting system with a sequence of man-made ditches, orthogonals are drawn from the up-slope side of a lower ditch, to the down-slope side of an upper ditch. Where there is considerable variation in the gradient along this flow-line, separate sub-sections must be defined and used in model simulations as discrete Δx increments. The gradient within the Δx is assumed constant and the smaller the Δx increments along a given flow-line, the more accurate the overall gradient becomes. Lane and Renard (1979) use this segmentation procedure in cases where the slope profiles are complex consisting of convex, concave and uniform sections. The hillslope flow-lines coalesce with channel flow-lines. In a natural catchment, the channels are orthogonals whereas in the Avdat system, the man-made ditches are not, modifying the routing system by taking water away along diagonals intercepting flow-lines.

4.3.1.c Hillslope Element Slopes

The flow-lines and contours can be used as the basis for discretizing the hillslope or catchment system and for providing the spatial parameters of length Δx and width w, and the slope gradient parameter s for the routing procedures and the Manning equation. The resolution of the parameters set depends on the spacing of the flow-lines and the relative elevations of the chosen contours compared to the scale of significant slope changes in the system. By fitting planes to a mesh of contour and flow-lines then the gradient and slope length of each mesh element can be preserved along with the total relief and the average elevation. By preserving these characteristics, the potential energy and mass input of the original system is more closely reproduced (Lane *et al*, 1975).

The set of four nodes marking the flow-line and contour-line intersections mark the corners of a trapezium bounded by the lines (see the flow-nets in Appendices 3.2 and 3.3). The shape will vary according to the degree of convergence or divergence of the flow-lines. A reasonable approximation can be made that this surface can be reproduced as a plane of constant width, length and gradient maintaining the area of the trapezium so that the original total surface area will not be distorted. Since the trapezium is bounded by two flow-lines there is no lateral inflow and a string of trapeziums forms a kinematic cascade. The critical features to preserve are surface area, gradient and length as stated by

Lane and Woolhiser (1977) and Lane *et al* (1975). Errors in specifying area will result in a different volumetric input of water and losses to infiltration compared to the original. Errors in slope gradient will produce under or overestimates in velocity of flow. Errors in slope length will change the routing conditions and the distance water must travel over a slope of a given type. Lane and Woolhiser (1977) noted that they got an under-estimated time to peak flow and and overestimated peak discharge by using a uniform channel slope instead of a concave one. Lane *et al* (1975) noted poor estimates from convex surfaces. By approximating the concavity or convexity by splitting the channel into a number of increments each with constant gradients but representing the overall slope shape more closely the estimations were improved. The trigonometry for these calculations is contained in the program code of the simulation model in Appendix 4.

4.3.1.d Channel Element Slopes

For the channel sections, the slope gradient is calculated more easily than the hillslope. Using a contour map, nodes can be selected at discrete intervals down the channel, for instance where topographic survey points were taken and spot-heights exist, and used for the construction of flow-lines from the channel up the slopes to their respective divides. The nodes provide the two (X, Y, Z) coordinates required to calculate the average gradient of the channel and the length using the geometry of a right-angled triangle. Spatially, this channel element corresponds exactly with the final element of the kinematic cascades representing the slopes between the sets of flow-lines draining to the element. This can swiftly be carried out for real channels as part of a simulation models parameterisation routines, calculating the length and gradient and retaining them for each channel segment. The trigonometry for these calculations is contained in the program code of the simulation model in Appendix 4.

4.3.2 Flow Dimensions

Of importance for the characteristics of the flow produced across a hillside or in a channel is the nature of the change in the cross-sectional shape with depth. This determines the relationship between wetted perimeter and depth. The ratio between cross-sectional area and boundary perimeter is the hydraulic radius of the flow section.

4.3.2.a Channel Flow

For channels it is relatively easy to specify an accurate relationship between flow cross-sectional area and boundary length for the complete range of depths in the flow-section above the lowest point on the channel bed. Therefore, it is easy to calculate the hydraulic radius for any flow area A(x,t) produced by the continuity equation. This is because channels tend to have a relatively uniform cross-

sectional shape, especially small hand-dug ditches or natural rills and gullies which are usually approximated as a trapezium. Depending on the shape, the flow dimension parameter can be calculated for a given flow area A(x,t) as long as one or more dimensions such as top-width or bank angle are known. For a trapezoidal channel an equation for cross-sectional area is derived using the knowns of bank-angles and bed-width, and the unknown variable of depth. A flow area A(x,t) can be substituted into the equation and depth can be found, from which the wetted perimeter and hence hydraulic radius can be calculated.

Consider the trapezoidal channel illustrated in Figure 4.3, including the overflow section. The depth h in the main channel can vary from 0 - hmax. The depth in the overflow channel is Δh. The banks of the overland flow channel are the last planes in the kinematic cascades flowing into the channel section. The bank angles (E and W) are considered relative to the vertical, and the hillslope plane angles (S1 and S2) are considered relative to the horizontal. The top width (Tw) can be calculated using the bed-width (Bw), the bank-angles and the maximum depth or else could be measured directly.

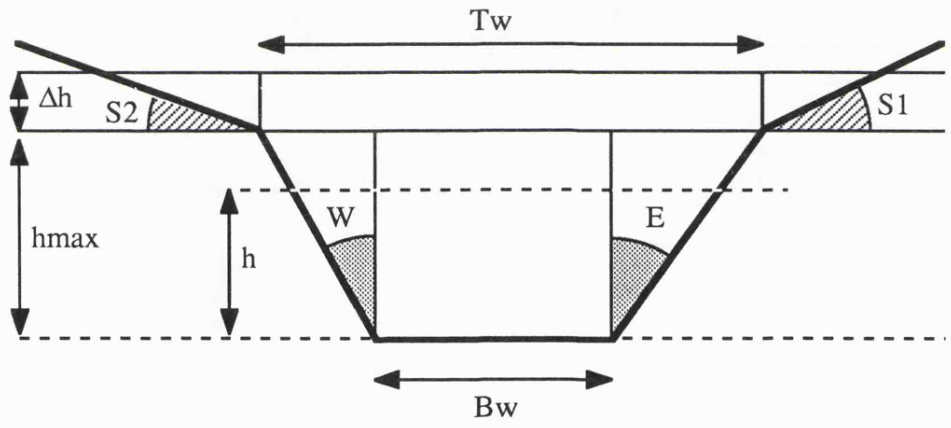

Figure 4.3 Geometry of a Trapezoidal Channel and Overflow

From simple trigonometry the flow area A(x,t) is seen to be;

$$A(x,t) = h.Bw + h.(h.\tan W/2) + h.(h.\tan E/2) \qquad \text{Equation 4.18}$$

Using the formula for the roots of a quadratic equation;

$$0 = h^2.(\tan W + \tan E)/2 + h.Bw + (- A(x,t)) \qquad \text{Equation 4.19}$$

$$h = [- Bw \pm \sqrt{(Bw^2 + 2.\tan W.A(x,t) + 2.\tan E.A(x,t))}]/(\tan W + \tan E)$$

Equation 4.20

The unknown of depth (h) is defined in terms of all the knowns; the channel geometric characteristics of bed-width (Bw) and bank-angles (E and W), and the flow area (A(x,t))provided by the routing finite difference solution. The roots of this equation are identical and opposite in sign. Obviously the positive root is the depth that is associated with the area A(x,t).

The wetted perimeter (WP(x,t)) is;

$$WP(x,t) = Bw + h/\cos E + h/\cos W \qquad \text{Equation 4.21}$$

Using the same trigonometric procedures and the formula for the roots of a quadratic equation, the depth of flow associated with the overflow section area $\Delta A(x,t)$ is;

$$\Delta h = [\, -Tw \pm \sqrt{(Tw^2 + 2.\Delta A(x,t)/\tan S1 + 2.\Delta A(x,t)/\tan S2)}\,].(\tan S1 + \tan S2)$$

Equation 4.22

(where Tw is the top-width, S1 and S2 are the slopes of the adjacent hillslope elements).

For the overflow section the calculation is only necessary if the area A(x,t) is greater than maximum flow area Amax associated with the maximum flow depth hmax. The overflow area $\Delta A(x,t)$ for substitution in the equation is;

$$\Delta A(x,t) = A(x,t) - Amax \qquad \text{Equation 4.23}$$

$$Amax = hmax.Bw + hmax^2.(\tan E + \tan W)/2 \qquad \text{Equation 4.24}$$

The additional wetted perimeter $\Delta WP(x,t)$ to be added to the normal channel maximum wetted perimeter WP(x,t) to give the total normal and overflow wetted perimeter is;

$$\Delta WP(x,t) = \Delta h/\sin S1 + \Delta h/\sin S2 \qquad \text{Equation 4.25}$$

(where Bw is the bed-width, and S1 and S2 the gradients of the adjacent hillslope elements).

4.3.2.b Hillslope Flow

The Sheetflow Approach

Where flow sections are shallow and wide, the assumption is made that hydraulic radius can be considered equal to depth because the boundary perimeter is equal to the width of the section. Where sheetflow is considered surface microtopography is ignored. Only the form of the surface rather than its texture is taken into account. A decrease in gradient or increase in roughness will be manifest by an increase in both depth and velocity. According to Emmett (1970), overland flow resulting from rainfall on natural hillslopes responds to the downslope increase in discharge by increasing its depth and velocity with depth absorbing two-thirds of the increase and velocity one-third.

Limitations of the Sheetflow Approach

In most studies to date, overland flow has been considered as a sheet. The effect of this assumption is that the value (A(x,t)/w(x)) is used in the Manning equation rather than (A(x,t)/wp(x,t)) as used with the channel flow. Depending on the hillslope micro-topography, for a given discharge of water the wetted perimeter of the flow for a given plan width may be less than, greater than or equal to the plan width. This depends on the manner in which the surface varies from a horizontal straight line normal to the line of flow. Studies by fieldworkers including Emmett (1970, 1978), Roels (1984ab) and Morgan (1980) have shown that hillslope overland flow is inaccurately described as sheetflow. In reality flow takes the form of a complex pattern of permanent micro-channels called inter-rills or micro-braids, following an anastomising pattern downslope dictated by the micro-topographic roughness resulting from variations in surface material particle size and particle arrangements.

At low discharge levels it may be that water is concentrated immediately it runs off the whole surface into a number of micro-rills and the total length of contact between moving water and the hillslope is less than the plan width. In this case using mean depth will give an underestimate of the flow dimension and produce a lower velocity than might be expected if the true concentrated character of flow could be represented. At high discharge levels it may be that water covers the complete surface and the total length of contact between the moving water and the slope is greater than the plan width by an order of the difference of the rough surface length and the plan width. In this case, using mean depth will produce an overestimate of the flow dimension and produce a higher velocity than might be expected using the hydraulic radius calculated as the total flow area divided by the surface length. As discharges increase, the hydraulic radius will converge on the depth and the velocities will be similar.

Hillslope Flow Without the Sheetflow Assumption

For the hillslope, where it is clear that flow is not a sheet, it is also clear that no simple geometric shape will reproduce the flow pattern within a given width of slope. The surface is often non-uniform and complex as shown by micro-topographic profiles measuring the change in elevation over small cross-slope or down-slope distances. Depending on the particle sizes of the surface materials and their arrangement into a surface form, the shape over a given plan width may be a smooth horizontal surface, split into a number of rivulets due to micro-topographic highs or lows or take myriad other shapes. These cannot easily be specified in geometric terms by a single standard shape and is partly one of the reasons why there are few attempts in the literature to model overland flow at the hillslope scale using anything other than a sheetflow approximation. Individual micro-rills cannot realistically be modelled separately. Therefore some aggregating relationship between the shape and dimensional parameters are required to specify a total wetted length for a given flow area A(x,t) derived from the continuity equation for each time period Δt. For the purposes of the flow equation, as long as this specification is within acceptable limits of accuracy it does not matter what the actual shape is, just the hydraulic radius. Therefore, a relationship is needed between cross-sectional area and boundary length, for instance a linear regression between the two parameters. This simple observation was first made by Huggins and Monke who commented in 1968 that the relevance of the sheetflow approach to a runoff function of the type needed to describe the actual flow conditions in a watershed is very doubtful. They state that intuitively, a means of quantitatively describing the overall flow conditions of a hillslope element without analysing the rigorous hydrodynamic conditions governing the flow in tiny channels appears to be required.

The Complex Geometry Approach

An approach was made towards this quantitative means of describing the overall flow conditions in an element by considering the notion of the complex flow geometry for a finite width of hillslope. A simple measuring rod marked off at regular intervals and laid on the surface at right-angles to the direction of the flow-line was used to measure a micro-profile of relative elevations of a finite number of points across the surface. Profiles were also measured downslope parallel to the flow-line. They were both used to help characterise the surface according to its micro-topographic roughness and to identify areas sufficiently alike and different from other areas to be classified as representative units. This has previously been discussed in Chapter Two.

The cross-slope profiles, represented by a list of (X,Y) coordinates define the micro-geometry and were transformed using a computer program to show the changes in composite flow geometry resulting from an incremental increase in height Δh above the lowest point in that list of (X,Y) coordinates. The coordinates were considered as nodes and the line passing through them as the surface

of the hillslope. The assumption was that the profile represents the variation either side of the finite slope area, i.e. the profile is replicated, and also that the significant scale for dictating flow occurs within the finite width, for example micro-rills with widths less than the profile measured. By considering the surface profile relative to the lowest point and a horizontal line at a height h above the lowest point (increased by Δh steps) it was possible to calculate the total flow area within the finite horizontal width w (xn - x1) and the length of the surface profile in contact with this flow area as shown in Figure 4.4.

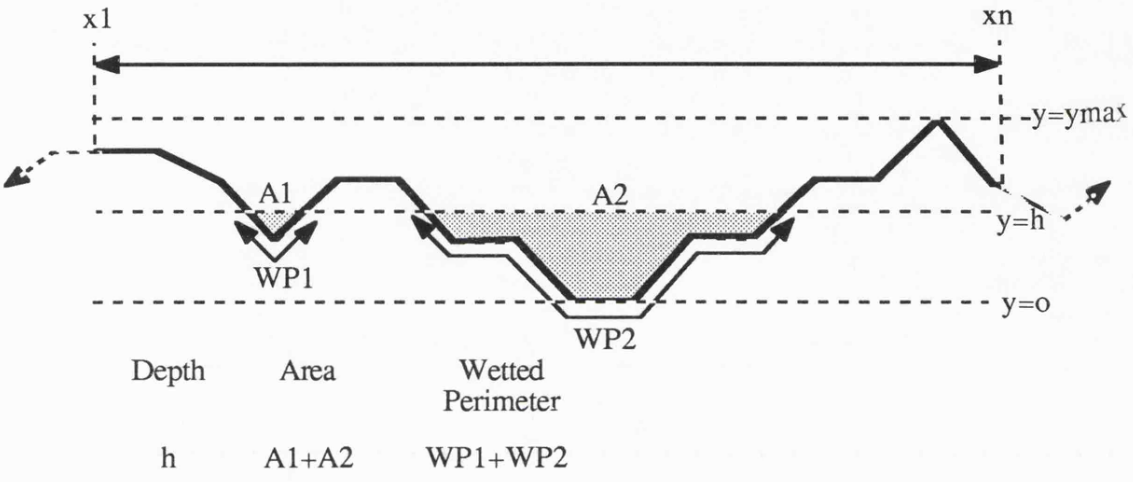

Figure 4.4 The Composite Flow Dimensions (vertical scale exaggerated)

Undertaking this for each height increment Δh, a table of maximum depth, flow area and wetted perimeter was established. Once complete, a numerical relationship was found between flow area and wetted perimeter to allow prediction of wetted perimeter for each computed area to calculate infiltration losses and the hydraulic radius. One micro-topographic profile taken in isolation was unlikely to give a representative picture of the flow dimensions varying according to sampling frequency of the micro-elevations and the character of the chosen line on the surface compared to the rest of the location. A number of profiles were aggregated to give an averaged set of areas and wetted perimeters for given flow depths above the lowest points on the different profiles. The assumption was that since water always seeks to find the lowest point on a surface, that the lowest point on each profile could be equated with Y = 0, and the area and wetted perimeter characteristics at identical depths above this point aggregated to give the representative profile for the location. Where the relative elevations of the profiles taken at a particular location differed between profiles, the range of depths for which areas and wetted perimeters were calculated differed. Those with a lower relative range would reach a maximum wetted perimeter if the whole profile was inundated at lower depths than the profiles with a higher relative range. Since any further depth of water results only in an increase in flow area by (Δh.w) the table of dimensions could be completed for each profile up to the maximum height at which

the profile with the greatest range of elevations would be completely inundated to a depth Δh. This gives a true picture of the overall dimensions when all the profiles are averaged.

Because the relationship derived refers only to a finite width of the surface then when the relationship is applied to a simulation model hillslope element, the value of A(x,t) must be scaled to A^(x,t) for substitution. If the plan width of the profile is pw, and the width of the flow element is W(x),

$$A^{\wedge}(x,t) = A(x,t).(pw/W(x)) \qquad \text{Equation 4.26}$$

Substituting this into the statistical relationship produces the scaled wetted perimeter WP^(x,t). This must be scaled up to give the wetted perimeter of the full model element,

$$WP(x,t) = WP^{\wedge}(x,t).(W(x)/pw) \qquad \text{Equation 4.27}$$

This method was used with micro-topographic data from 127 plots in the Avdat catchment, distributed at regular intervals along 5 flow-line profiles as described earlier in Chapter Two. For each plot there were 10 cross-slope profiles comprised of 20 (X, Y) coordinates over a plan width of approximately 190 cm. A table of maximum depth, flow area, and wetted perimeter was calculated for each profile and aggregated to give the overall conditions for the group of ten profiles representing the plot area. A linear regression between the natural logarithms of the flow area (A) and wetted perimeter (WP) was used (Equation 4.28).

$$\log_{10}WP = a + b.\log_{10}A \qquad \text{Equation 4.28}$$

4.3.3 Flow Resistance

4.3.3.a Resistance Theory

One of the major challenges for distributed, deterministic models of hydrological systems is the correct specification of resistance in the routing of flow. A coefficient of roughness represents the suite of mechanical resistances to motion resulting from friction and encompasses the size of bed and bank materials (static and in motion), shape of bed and bank materials (static and in motion), sediment carried in suspension and vegetation. The friction results from the movement of water particles over and around each other as the body of water moves downslope or down-channel, from the skin friction of the water surface at its air interface, and from the surface drag of the bed materials due to grain roughness and the hydrodynamic forces generated by the micro-topographic features that comprise the flow boundary geometry (Haque and Mahmood, 1983).

Chow (1980) has identified a number of interdependent variables influencing resistance on hillslopes and in channels: surface micro-topographic roughness, vegetation, channel irregularity, channel alignment, silting and scouring, size and shape of channels, stage and discharge, seasonal change, and suspended or bed-load.

The Manning's n coefficient of roughness is the denominator in the Manning flow equation. There are four sources of information on Mannings n for application in models of a given system;

1. the handbook approach of using published values in the literature for analogous site conditions,
2. prior estimates based on an assessment of a pre-flow environmental condition such as micro-topographic roughness or bed and bank material,
3. comparisons between observed hydrographs and those predicted by simulation models using assumed coefficients and selection of the best-fit parameter,
4. calculations from field experiments of the runoff process designed to determine stage-velocity-discharge relationships.

It is clear that the surface micro-topographic roughness plays a major role in the magnitude of flow resistance which must be seen as a dynamic coefficient rather than a constant. However, most studies to date, both theoretical and empirical, have considered the coefficient to be a constant, even though resistance is a phenomena that is inherently related to the size and the shape of the flow medium and the size and the rate of the movement of the flow mass across that medium. To examine the significance of this it is necessary to make a closer examination of the nature of the resistance that might be expected to be exerted by micro-topographic and particle roughness with changing flow dimensions. Whilst it may not be possible to quantify the dynamic nature of roughness sufficiently well to use in a routing model, the significance and implications of conceptualizing resistance to be a variable rather than a constant should be understood.

Miller (1984) indicates that the retarding effect on flow of a particle of a given size is relative in that it will have a greater retarding effect on shallow flow than on deep flow. Since the roughness elements on a channel bed vary in size and shape, they do not all project into the flow by the same amount and some will have a more important effect than others at different flow depths (Bathurst, 1982b). The combined effect of the elements on flow resistance depends of the proportion of the bed material affecting flow. At a site of a given cross-sectional shape, the rate of change of relative roughness with the width/depth ratio should depend on the degree to which both micro-topographic and particle roughness elements project into the flow at any given stage. If the number of elements decreases rapidly with depth then so should resistance. Resistance should therefore be considered a

variable changing with the changing state of flow over a given boundary geometry (Li, Simons and Stevens 1975).

Scoging (1988) conceives of the effects of roughness elements as dispersers and concentrators. She suggests that resistance oscillates with increasing stage reaching a final constant low level at the highest discharge rates for a given distribution of surface particles or a given surface micro-topographic form. The oscillation occurs as different scales of roughness dominate the flow state as water movement switches from being contained by a particular element to covering that element. Of most importance for the surface flow over the micro-topographically rough surface is the cross-sectional characteristics of the flow surface. Where flow is at a low level, roughness elements occupy a significant proportion of the cross-section and water is funnelled between them (Bathurst, 1982b). The greater the degree of funnelling, the higher the average velocity, and depending on the shape, the smaller the length of contact for a given discharge. Thus resistance could decrease with a gradual increase in stage. Where the complete surface is covered, the contact length will be highest and resistance can be expected to have increased. As depth continues to increase resistance will fall, as the effects of the surface is exerted on larger discharges. Where flow is funnelled into rills then it will take the shortest downslope line, reducing travel times and decreasing resistance compared to a more uneven line of flow from depression to depression at angles oblique to the contour orthogonal.

It seems logical, therefore, that a roughness coefficient used in a flow equation should be expected to change under different flow states. It is clear that resistance should vary directly with discharge, since the ratio of water body dimensions to boundary dimensions increases, and therefore the per-unit effect of boundary resistance will decrease. Whether this is oscillatory or not will depend on the boundary conditions. A roughness coefficient that is considered as a constant value for all flow states may mis-represents the true nature of the roughness phenomenon. At low flow-states, bordering on the static ponding or depression storage, resistance is virtually unquantifiable, but can logically be considered to be at its maximum. As the water body gradually increases and flow occurs, resistance will initially possess a large value since the flow dimensions are small relative to the form and textural features constituting boundary roughness. This is likely to reduce rapidly as the flow body increases up to a point where resistance decreases in increasingly smaller amounts as the dimensions of flow relative to the boundary features becomes greater. This is true for all subsequent volumes for the hillslope which can ultimately develop a sheet-like flow of water increasing in depth uniformly across its width. For channels, however, a point will be reached at which over-bank conditions occur, and water flows over onto adjacent land and the ratio of flow area to boundary lengths will decrease with a corresponding increase in resistance to flow. Logically, therefore, an adequate roughness coefficient to represent the process might be expected to change in some kind of overall negative exponential fashion relative to the flow area for the hillslope, and a modified negative exponential for the channel (where the overbank threshold operates).

Having discussed the hypothetical nature of resistance, exactly how can the process-phenomena be realistically and easily quantified for model use, and how can our understanding of the roughness phenomena be represented as a parameter in flow routing procedures? There is no easily reproducible, physically realistic method for determining resistance values for hillslopes and channels at the micro- and meso-scale. Traditionally, methods of quantifying resistance are geared to the needs of engineers concerned with standard form and materials, permanent flows, and large scales when only the range of possible depth-velocities are required or the shape and timing of hydrograph arrival. They have no need to explain the phenomena controlling these factors or to identify their role in the determination of spatial variation in processes. Equifinality, where more than one factor out of a suite of controlling factors can produce a given response from an insufficiently specified model, has contributed to the lack of quantitative consideration of roughness at these small scales. Certainly little attention has been directed at the hillslope scale, and even less to the hillslope and small ephemeral channels found in the semi-arid and arid environments where roughness takes on enormous significance due to its magnitude and spatial variability as discussed in Chapter One.

Since the roughness coefficient n was formulated as a constant could a dynamic n be used in Mannings equation? Manning's n was derived from a variety of studies on artificial channel flow conditions. Its application has been widespread due to its simplicity and ability to reproduce the orders of magnitude of observed flow in many predictive applications. Its original conceptualisation was as a single constant applicable to all states of flow. However, several studies that have measured discharge, flow velocity and flow dimensions have shown n to vary considerably by substituting these parameters into the Manning equation. In reality, resistance helps determine discharge but the substitution of parameters shows that resistance is not constant, generally decreasing with increasing flow dimensions. Some notable studies include Leopold and Maddock (1953), Leopold *et al* (1964), Gregory and Walling (1973) and Dunne and Leopold (1978). Limerinos (1970) presents data for 11 California gravel-bed rivers in which n increases with a decrease in discharge and Johnson (1964) and Dingman (1971) found especially rapid decreases of n with increasing discharge in the small streams they studied. Morgan (1980) states that errors must arise in studies from the assumption of a constant n value because in reality, roughness conditions change not only during a storm but also between storms.

4.3.3.b Empirical Methods of Defining Mannings n Coefficient

Recognising that several primary factors can interact to affect the roughness coefficient, Cowan (1956) developed a procedure for estimating n by the addition of compound values n_0, n_1, n_2, n_3, n_4, and a correction factor for channel sinuosity m;

$$n = (n_0 + n_1 + n_2 + n_3 + n_4)m \qquad \text{Equation 4.29}$$

The variable n_0 applies to a basic uniform channel of natural materials, n_1 corrects for surface irregularities, n_2 for shape and size variations in the cross-section, n_3 for obstructions, and n_4 for vegetation and flow conditions. This is derived from tabulated data, for instance in Chow (1981, page 109). Cowan's approach is typical of the common assumption that a single, constant roughness parameter can be used to represent all flow states at a given location. The most rough flow environment using Cowan's method has an n value of 0.29 and the least rough 0.025. An arid hillslope could be expected to have a value somewhere in the region of 0.1 although the Cowan method is really only appropriate for channels. Field studies carried out on hillslopes in the arid environments have observed n to be in the order of 0.2 to 1.0.

Two other examples of approaches to resistance are the specification of n as some function of particle size of bed and bank materials, or the ratio of particle size to flow stage and dimensions. The former can be termed the 'size-percentile' approach, and the latter the 'relative roughness' approach. Both of these approaches have developed out of studies on the flow hydraulics of gravel-bedded rivers where the flow depth to roughness is relatively low. As such it has some relevance to the flow conditions found for overland flow on rough hillslopes, although the scale of the process is somewhat different.

The size-percentile approach is the basis of Strickler's empirical relationship between Manning's n and the intermediate bed material particle size of gravel-bed rivers.

$$n = K.d_{50}^{1/6} \qquad \text{Equation 4.30}$$

(Bray, 1982 where K depends on the parameter units and is 0.041 for metric)

The technique of using only one size percentile for a comparison between sites relies on the assumption that each percentile has proportionally the same effect at all sites and at all stages of flow. In this case it does not matter that only a single percentile is used because there is a fixed ratio of influence between the percentile and any other percentile. This condition is not met if there are considerable variations in roughness scale, size, shape, orientation and spacing distribution of particles between sites (Bathurst, 1982a). In many arid locations such as Avdat, this variation can be expected and therefore the approach of Strickler is limited.

The relative roughness approach relates the resistance coefficient to the ratio of flow depth or hydraulic radius to some particle size percentile in an empirical equation. This is the basis of the Limerinos (1970) equation.

$$n = k\hat{}.Hr^{1/6}/[a + b.\log10(Hr/d_{\%})] \qquad \text{Equation 4.31}$$

(where $k\hat{} = 0.113$ for $m^3 s^{-1}$, 0.0524 for $cm^3 s^{-1}$ and 0.0926 for $ft^3 s^{-1}$, a and b are regression equation coefficients, $d_{\%}$ is the particle size percentile and Hr = hydraulic radius)

This is developed from boundary theory and confirmed by the observations made by Leopold and Wolman (1957).

$$1/\sqrt{f} = a + b.\log10(Hr/d_{\%}) \qquad \text{Equation 4.32}$$

$$f = 8g.Hr.s/v^2 \qquad \text{Equation 4.33}$$

(where f is the Darcy-Weisbach friction factor and s is the slope gradient).

The Manning flow formula can be substituted for v into the right-hand side of Equation 4.33 and f can be substituted into the left-hand side of Equation 4.32. Solving for the various versions of Mannings equation with different units yields the coefficient values for k in Equation 4.31. The Limerinos equation is said to have an advantage over the Strickler equation because it is stage dependent (n = f{Hr}) (Bray, 1979). The problem with both the particle size percentile and the relative roughness approach to determining resistance is that they cannot easily be applied to conditions where flows are very shallow relative to the roughness features influencing the flow. It has been stated that gravel-bed river studies, from which they are derived, are relevant to the overland flow case. However, this is only true to the degree that they illustrate some of the problems of deriving an effective coefficient of resistance and the considerable simplification that accompanies use of a single constant coefficient for all states of flow, when resistance and the flow state are inter-related. Bray (1982) in fact states that the Limerinos and Strickler equations, amongst others, can only apply to flow situations where the average flow depth is at least three times the chosen particle size percentile. This is agreed by Bathurst (1982b). With the Limerinos equation, if particle size is greater that the depth or hydraulic radius of flow, then the log term will be negative and a negative n predicted with the equation breaking down at this point. The approach seems somewhat limited for the hillslope flow case where flow dimensions are small relative to surface material percentiles, and much of the resistance is exerted by larger particles comprising part of the form roughness that funnels shallow water into micro-rivulets. These provide the boundary resistance but since they exert an effect that is not proportional to their size (which is generally larger than flow depths), but proportional to their arrangement, this cannot be quantified in such a simple way as with the relative roughness approach. The changing nature of the boundary geometry seems, therefore, to be the key to understanding the process. It determines both the changing nature of the flow dimension variable and the likely change in the resistance although its multi-faceted effect is obviously complex.

4.3.3.c Field Studies of Overland Flow from the Literature

A few intensive field tests have been carried out of overland flow across hillslopes which have involved the calculation of resistance coefficient values for micro-topographically rough conditions. Two of the relevant field process studies are those of Roels (1984b) and Emmett (1970).

Roels (1984b) conducted run-on/run-off field tests monitoring flow depths and velocities across a 50 cm by 65 cm surveyed plot. Roels picked two locations in the Ardeche Rangelands, one a hillslope of 7.8° and the other a hillslope of 10.25° and on each selected three sites that were either rilled or pre-rilled. Rills were defined as micro-channels having a mean width of 50 cm and a depth from 10 to 60 cm, and pre-rills were at an earlier stage of development and can be described as permanent flow paths which carry away concentrated runoff but do not yet appear to be rills. The micro-topography was surveyed on a 5 cm grid system with seven transverse and 13 downslope intervals. Ten velocity measurements were averaged to give the mean surface velocity using dye tracing. Ten to 30 depth readings were averaged to give the mean flow depth.

Roels stated that the resistance of the flow surface was partly determined by the number of stones on and in the surface. The partial incorporation of stones into the soil matrix meant that resistance could not be simply expressed by the total number of stones on the bed surface however. To do this would require a consideration of micro-topographic variation (the boundary geometry) and not just particle size since the latter would not accurately account for the projection of particles through the flow profile. Roels considered hydraulic radius to be proportional to depth and used it in the Manning equation along with velocity to derive values of n for the 12 plots in his study. For the pre-rill conditions on the 7.8° slope the average n was 0.216 and on the 10.25° slope it is 0.13. For the rilled conditions on the 7.8° slope the average n was 0.177 and on the 10.25° slope it is 0.079. The results for each of the twelve plots are included in Table 4.1.

Emmett (1970, 1978) conducted hillslope sprinkler experiments on field plots 2.1 m wide and 14 m long, comparing results to laboratory flume studies. The rainfall intensity was 200 mm hr^{-1} with runoff rates estimated as 100 mm hr^{-1}. Emmett chose seven field sites with slope gradients varying from 1.66° to 18.4°. The micro-topography was surveyed on a 30 cm grid. Dye was poured over the ground surface at the upper end and the time to cover each 30 cm downslope recorded. Micro-relief features of only 2.5 cm were seen to dictate the paths of flow concentrations that formed. Overland flow as a uniform sheet of water was not observed. However, the topographic maps of the surface have insufficient detail to illustrate these micro-concentrations as shown by Emmett's superimposed dye flow-lines and the 6 cm contours prepared from the survey. The data from these experiments are presented in Table 4.2. The mean roughness calculated from 146 separate observations

Table 4.1 Roels' Manning's n Values (Roels, 1984)

Plot	Hr	V	v cm/s	Q cm3/s	q cm3/s	n	Plot	Hr	V	v cm/s	Q cm3/s	q cm3/s	n
	cm	cm/s						cm	cm/s				
pre-rill							rilled						
No. 1	0.24	4.3	1.72	20.64	0.41	0.384	No. 4	0.12	2.7	1.08	6.48	0.13	0.385
s=0.136	0.10	1.8	0.72	3.60	0.07	0.512	s=0.136	0.16	4.0	1.60	12.80	0.26	0.315
	0.24	2.0	0.80	9.60	0.19	0.826		0.21	5.0	2.00	21.00	0.42	0.302
	0.27	3.0	1.20	16.20	0.32	0.596		0.27	6.0	2.40	32.40	0.65	0.298
	0.33	5.1	2.04	33.66	0.67	0.401		0.34	7.7	3.08	52.36	1.05	0.271
	0.37	9.0	3.60	66.60	1.33	0.245		0.34	7.2	2.88	48.96	0.98	0.289
	0.37	3.9	1.56	28.86	0.58	0.565		0.39	11.4	4.56	88.92	1.78	0.200
	0.41	6.3	2.52	51.66	1.03	0.375		0.45	10.2	4.08	91.80	1.84	0.246
	0.36	4.9	1.96	35.28	0.71	0.442		0.50	10.8	4.32	108.00	2.16	0.250
	0.46	13.7	5.48	126.04	2.52	0.186		0.52	10.9	4.36	113.36	2.27	0.254
	0.46	9.5	3.80	87.40	1.75	0.268		0.55	16.9	6.76	185.90	3.72	0.170
	0.52	8.3	3.32	86.32	1.73	0.333		0.62	19.6	7.84	243.04	4.86	0.159
	0.59	17.6	7.04	207.68	4.15	0.171		0.60	21.7	8.68	260.40	5.21	0.140
	0.46	11.0	4.40	101.20	2.02	0.232		0.67	24.9	9.96	333.66	6.67	0.132
	0.52	11.7	4.68	121.68	2.43	0.236		0.70	24.2	9.68	338.80	6.78	0.139
	0.57	14.3	5.72	163.02	3.26	0.206		0.65	22.2	8.88	288.60	5.77	0.145
n=17	0.56	21.3	8.52	238.56	4.77	0.136		0.60	17.8	7.12	213.60	4.27	0.171
					av n=	0.358		0.73	37.6	15.04	548.96	10.98	0.092
					s.d. n=	0.184	n=19	1.06	35.6	14.24	754.72	15.09	0.125
												av n=	0.21
												s.d. n=	0.08

Plot	Hr	V	v cm/s	Q cm3/s	q cm3/s	n	Plot	Hr	V	v cm/s	Q cm3/s	q cm3/s	n
	cm	cm/s						cm	cm/s				
pre-rill							rilled						
No. 2	0.15	3.6	1.44	10.80	0.22	0.335	No. 5	0.07	4.2	1.68	5.88	0.12	0.173
s=0.136	0.12	3.1	1.24	7.44	0.15	0.336	s=0.136	0.13	5.9	2.36	15.34	0.31	0.186
	0.23	10.2	4.08	46.92	0.94	0.157		0.17	9.5	3.80	32.30	0.65	0.138
	0.27	23.0	9.20	124.20	2.48	0.078		0.22	10.4	4.16	45.76	0.92	0.150
	0.27	13.5	5.40	72.90	1.46	0.132		0.26	15.3	6.12	79.56	1.59	0.114
	0.35	17.7	7.08	123.90	2.48	0.120		0.33	10.3	4.12	67.98	1.36	0.198
	0.41	15.6	6.24	127.92	2.56	0.151		0.36	12.3	4.92	88.56	1.77	0.176
	0.38	19.0	7.60	144.40	2.89	0.118		0.39	15.6	6.24	121.68	2.43	0.146
	0.43	21.9	8.76	188.34	3.77	0.111		0.42	17.8	7.12	149.52	2.99	0.135
	0.51	19.3	7.72	196.86	3.94	0.141		0.49	17.2	6.88	168.56	3.37	0.155
	0.54	26.3	10.52	284.04	5.68	0.108		0.51	18.4	7.36	187.68	3.75	0.148
	0.58	26.9	10.76	312.04	6.24	0.111		0.53	21.7	8.68	230.02	4.60	0.129
	0.56	28.6	11.44	320.32	6.41	0.102		0.57	18.2	7.28	207.48	4.15	0.162
	0.62	39.0	15.60	483.60	9.67	0.080		0.61	19.2	7.68	234.24	4.68	0.160
	0.59	35.0	14.00	413.00	8.26	0.086		0.64	22.0	8.80	281.60	5.63	0.144
n=16	0.68	52.0	20.80	707.20	14.14	0.064		0.70	23.5	9.40	329.00	6.58	0.144
					av n =	0.139	n=17	0.67	20.3	8.12	272.02	5.44	0.161
					s.d. n=	0.081						av n =	0.15
												s.d. n=	0.02

Table 4.1 Roels' Manning's n Values (Roels, 1984)

Plot	Hr	V	v cm/s	Q cm3/s	q cm3/s	n	Plot	Hr	V	v cm/s	Q cm3/s	q cm3/s	n
	cm	cm/s						cm	cm/s				
pre-rill							rilled						
No. 3	0.14	6.1	2.44	17.08	0.34	0.189	No. 6	0.06	3.1	1.24	3.72	0.07	0.211
s=0.136	0.19	9.0	3.60	34.20	0.68	0.157	s=0.136	0.10	4.5	1.80	9.00	0.18	0.205
	0.24	10.0	4.00	48.00	0.96	0.165		0.18	7.3	2.92	26.28	0.53	0.187
	0.27	9.9	3.96	53.46	1.07	0.181		0.21	8.9	3.56	37.38	0.75	0.170
	0.29	14.2	5.68	82.36	1.65	0.132		0.26	11.4	4.56	59.28	1.19	0.153
	0.32	16.9	6.76	108.16	2.16	0.118		0.27	12.9	5.16	69.66	1.39	0.139
	0.37	13.9	5.56	102.86	2.06	0.159		0.33	13.0	5.20	85.80	1.72	0.157
	0.38	15.3	6.12	116.28	2.33	0.147		0.34	15.9	6.36	108.12	2.16	0.131
	0.40	14.9	5.96	119.20	2.38	0.156		0.39	13.6	5.44	106.08	2.12	0.168
	0.43	18.2	7.28	156.52	3.13	0.134		0.40	13.7	5.48	109.60	2.19	0.170
	0.45	20.0	8.00	180.00	3.60	0.126		0.45	17.0	6.80	153.00	3.06	0.148
	0.48	21.7	8.68	208.32	4.17	0.121		0.48	19.0	7.60	182.40	3.65	0.138
	0.49	20.6	8.24	201.88	4.04	0.129		0.52	21.3	8.52	221.52	4.43	0.130
	0.53	24.8	9.92	262.88	5.26	0.113		0.55	21.3	8.52	234.30	4.69	0.135
	0.60	27.1	10.84	325.20	6.50	0.112		0.58	21.1	8.44	244.76	4.90	0.141
n = 16	0.63	34.5	13.80	434.70	8.69	0.091	n = 16	0.65	26.8	10.72	348.40	6.97	0.120
					av n =	0.139						av n =	0.16
					s.d. n =	0.027						s.d. n =	0.03
pre-rills					av n =	0.216	rilled					av n =	0.18
s=0.136						0.157	s=0.136					s.d. n =	0.06
n=49							n=52						

Plot	Hr	V	v cm/s	Q cm3/s	q cm3/s	n	Plot	Hr	V	v cm/s	Q cm3/s	q cm3/s	n
	cm	cm/s						cm	cm/s				
pre-rill							rilled						
No. 7	0.08	2.4	0.96	3.84	0.08	0.331	No. 10	0.05	8.7	3.48	8.70	0.17	0.067
s=0.178	0.12	4.1	1.64	9.84	0.20	0.254	s=0.178	0.11	10.3	4.12	22.66	0.45	0.095
	0.13	6.3	2.52	16.38	0.33	0.174		0.13	13.7	5.48	35.62	0.71	0.080
	0.25	8.9	3.56	44.50	0.89	0.191		0.15	19.2	7.68	57.60	1.15	0.063
	0.28	9.4	3.76	52.64	1.05	0.195		0.18	19.1	7.64	68.76	1.38	0.071
	0.34	9.5	3.80	64.60	1.29	0.219		0.24	21.1	8.44	101.28	2.03	0.078
	0.36	9.3	3.72	66.96	1.34	0.233		0.28	22.9	9.16	128.24	2.56	0.080
	0.39	14.2	5.68	110.76	2.22	0.161		0.30	21.2	8.48	127.20	2.54	0.090
	0.44	14.5	5.80	127.60	2.55	0.171		0.31	22.1	8.84	137.02	2.74	0.089
	0.49	19.0	7.60	186.20	3.72	0.140		0.36	18.8	7.52	135.36	2.71	0.115
	0.43	19.9	7.96	171.14	3.42	0.122		0.37	28.3	11.32	209.42	4.19	0.078
	0.50	15.2	6.08	152.00	3.04	0.177		0.43	26.4	10.56	227.04	4.54	0.092
	0.52	14.8	5.92	153.92	3.08	0.187		0.43	30.8	12.32	264.88	5.30	0.079
	0.54	18.7	7.48	201.96	4.04	0.152		0.50	36.3	14.52	363.00	7.26	0.074
	0.55	17.2	6.88	189.20	3.78	0.167		0.48	40.0	16.00	384.00	7.68	0.066
	0.65	27.9	11.16	362.70	7.25	0.115	n = 16	0.59	40.5	16.20	477.90	9.56	0.074
n = 17	0.66	29.5	11.80	389.40	7.79	0.110						av n =	0.08
					av n =	0.173						s.d. n =	0.01
					s.d. n =	0.055							

Table 4.1 Roels' Manning's n Values (Roels, 1984)

Plot	Hr	V	v cm/s	Q cm3/s	q cm3/s	n	Plot	Hr	V	v cm/s	Q cm3/s	q cm3/s	n
	cm	cm/s						cm	cm/s				
pre-rill							rilled						
No. 8	0.06	4.9	1.96	5.88	0.12	0.134	No. 11	0.08	6.5	2.60	10.40	0.21	0.122
s=0.178	0.09	7.6	3.04	13.68	0.27	0.113	s=0.178	0.13	8.4	3.36	21.84	0.44	0.131
	0.12	14.2	5.68	34.08	0.68	0.073		0.20	12.5	5.00	50.00	1.00	0.117
	0.13	10.0	4.00	26.00	0.52	0.110		0.23	14.8	5.92	68.08	1.36	0.109
	0.18	15.2	6.08	54.72	1.09	0.090		0.27	14.8	5.92	79.92	1.60	0.121
	0.22	15.2	6.08	66.88	1.34	0.103		0.33	20.6	8.24	135.96	2.72	0.099
	0.26	22.6	9.04	117.52	2.35	0.077		0.37	18.5	7.40	136.90	2.74	0.119
	0.29	19.1	7.64	110.78	2.22	0.098		0.40	26.2	10.48	209.60	4.19	0.089
	0.32	27.6	11.04	176.64	3.53	0.073		0.46	24.1	9.64	221.72	4.43	0.106
	0.37	26.3	10.52	194.62	3.89	0.084		0.44	21.7	8.68	190.96	3.82	0.114
	0.45	37.3	14.92	335.70	6.71	0.067		0.51	22.4	8.96	228.48	4.57	0.122
	0.42	26.2	10.48	220.08	4.40	0.092		0.52	22.7	9.08	236.08	4.72	0.122
	0.51	31.5	12.60	321.30	6.43	0.087		0.59	28.4	11.36	335.12	6.70	0.106
	0.57	30.4	12.16	346.56	6.93	0.097		0.64	27.7	11.08	354.56	7.09	0.115
	0.65	32.5	13.00	422.50	8.45	0.099		0.61	27.4	10.96	334.28	6.69	0.112
n = 16	0.71	43.5	17.40	617.70	12.35	0.078	n = 16	0.81	31.6	12.64	511.92	10.24	0.118
					av n =	0.092						av n =	0.11
					s.d. n =	0.017						s.d. n =	0.01
Plot	Hr	V	v cm/s	Q cm3/s	q cm3/s	n	Plot	Hr	V	v cm/s	Q cm3/s	q cm3/s	n
	cm	cm/s						cm	cm/s				
pre-rill							rilled						
No. 9	0.05	5.9	2.36	5.90	0.12	0.098	No. 12	0.12	24.6	9.84	59.04	1.18	0.042
s=0.178	0.09	9.0	3.60	16.20	0.32	0.095	s=0.178	0.16	29.0	11.60	92.80	1.86	0.043
	0.14	11.0	4.40	30.80	0.62	0.105		0.19	25.2	10.08	95.76	1.92	0.056
	0.20	13.6	5.44	54.40	1.09	0.108		0.20	38.0	15.20	152.00	3.04	0.039
	0.23	17.3	6.92	79.58	1.59	0.093		0.20	23.8	9.52	95.20	1.90	0.061
	0.27	16.9	6.76	91.26	1.83	0.106		0.20	34.0	13.60	136.00	2.72	0.043
	0.30	17.9	7.16	107.40	2.15	0.107		0.20	50.9	20.36	203.60	4.07	0.029
	0.36	19.1	7.64	137.52	2.75	0.113		0.20	37.9	15.16	151.60	3.03	0.039
	0.40	20.8	8.32	166.40	3.33	0.112		0.20	41.2	16.48	164.80	3.30	0.036
	0.45	21.3	8.52	191.70	3.83	0.118		0.21	42.9	17.16	180.18	3.60	0.035
	0.51	20.5	8.20	209.10	4.18	0.133		0.20	47.0	18.80	188.00	3.76	0.031
	0.57	24.2	9.68	275.88	5.52	0.122		0.20	59.9	23.96	239.60	4.79	0.024
	0.59	25.0	10.00	295.00	5.90	0.120		0.20	52.9	21.16	211.60	4.23	0.028
	0.63	25.3	10.12	318.78	6.38	0.124	n = 14	0.24	59.5	23.80	285.60	5.71	0.028
n = 15	0.65	26.0	10.40	338.00	6.76	0.123						av n =	0.04
					av n =	0.112						s.d. n =	0.01
					s.d. n =	0.012							
pre-rills	s=0.178		n = 48		av n =	0.130	rilled	s=0.178		n = 46		av n =	0.08
					s.d. n =	0.052						s.d. n =	0.03
pre-rills	all		n = 97		av n =	0.173	rilled	all		n = 98		av n =	0.13
					s.d. n =	0.125						s.d. n =	0.07
All	n = 195				av n =	0.152							
					s.d. n =	0.103							

Table 4.2 Emmett's Manning's n Values (Emmett, 1970)

Site	ΣΔx ft	Y ft	v ft/s	q cfs	n (fps)	Y cm	v cm/s	q cm3/s	n (cgs)
New Fork	1	0.0155	0.006	0.00009	2.60	0.47	0.18	0.086	2.62
River 2	3	0.0114	0.025	0.00028	0.51	0.35	0.76	0.264	0.51
s=1.66°	5	0.0155	0.031	0.00047	0.51	0.47	0.94	0.446	0.51
s=0.029	7	0.0341	0.020	0.00066	1.37	1.04	0.61	0.633	1.33
	9	0.0111	0.077	0.00085	0.16	0.34	2.35	0.793	0.16
	11	0.0124	0.084	0.00104	0.16	0.38	2.56	0.966	0.16
	13	0.0148	0.083	0.00123	0.18	0.45	2.53	1.139	0.18
	15	0.0280	0.051	0.00142	0.46	0.85	1.55	1.325	0.46
	17	0.0164	0.098	0.00161	0.16	0.50	2.98	1.491	0.17
	19	0.0234	0.077	0.00180	0.27	0.71	2.35	1.671	0.27
	21	0.0294	0.068	0.00199	0.35	0.90	2.07	1.854	0.35
	23	0.0296	0.074	0.00218	0.33	0.90	2.25	2.032	0.33
	25	0.0154	0.154	0.00237	0.10	0.47	4.69	2.200	0.10
	27	0.0664	0.039	0.00256	1.08	2.02	1.19	2.402	1.06
	29	0.0398	0.069	0.00275	0.43	1.21	2.10	2.547	0.43
	31	0.0250	0.118	0.00294	0.18	0.76	3.59	2.736	0.18
	33	0.0418	0.075	0.00313	0.41	1.27	2.28	2.908	0.41
	35	0.0706	0.047	0.00332	0.92	2.15	1.43	3.078	0.92
	37	0.0945	0.037	0.00351	1.42	2.88	1.13	3.243	1.42
	39	0.0941	0.039	0.00370	1.34	2.87	1.19	3.404	1.34
	41	0.0486	0.080	0.00389	0.42	1.48	2.44	3.607	0.42
n = 22	43	0.0905	0.045	0.00408	1.14	2.76	1.37	3.778	1.13
								av n =	0.66
								s.d. n =	0.61
Site	ΣΔx ft	Y ft	v ft/s	q cfs	n (fps)	Y cm	v cm/s	q cm3/s	n (cgs)
Pole Creek	1	0.0004	0.174	0.00007	0.01	0.01	5.30	0.065	0.01
Site 1	3	0.0066	0.032	0.00021	0.52	0.20	0.97	0.196	0.51
s=5.51°	5	0.0071	0.049	0.00035	0.35	0.22	1.49	0.323	0.35
s=0.096	7	0.0081	0.060	0.00049	0.31	0.25	1.83	0.451	0.31
	9	0.0046	0.136	0.00062	0.09	0.14	4.14	0.580	0.09
	11	0.0106	0.072	0.00076	0.31	0.32	2.19	0.708	0.31
	13	0.0143	0.063	0.00090	0.43	0.44	1.92	0.836	0.43
	15	0.0214	0.049	0.00104	0.74	0.65	1.49	0.973	0.72
	17	0.0180	0.066	0.00118	0.49	0.55	2.01	1.102	0.48
	19	0.0204	0.065	0.00132	0.54	0.62	1.98	1.230	0.53
	21	0.0176	0.083	0.00146	0.38	0.54	2.53	1.355	0.38
	23	0.0136	0.117	0.00160	0.23	0.41	3.56	1.476	0.22
	25	0.0151	0.115	0.00173	0.25	0.46	3.50	1.611	0.24
	27	0.0265	0.071	0.00187	0.58	0.81	2.16	1.745	0.58
	29	0.0249	0.081	0.00201	0.49	0.76	2.47	1.871	0.48
	31	0.0246	0.088	0.00215	0.24	0.75	2.68	2.008	0.44
	33	0.0189	0.121	0.00229	0.27	0.58	3.69	2.121	0.27
	35	0.0209	0.116	0.00243	0.30	0.64	3.53	2.249	0.30
	37	0.0361	0.071	0.00257	0.71	1.10	2.16	2.378	0.71
	39	0.0280	0.097	0.00271	0.44	0.85	2.95	2.519	0.44
	41	0.0380	0.075	0.00285	0.70	1.16	2.28	2.644	0.69
n = 22	43	0.0486	0.061	0.00298	1.01	1.48	1.86	2.750	1.01
								av n =	0.43
								s.d. n =	0.22

Table 4.2 Emmett's Manning's n Values (Emmett, 1970)

Site	ΣΔx ft	Y ft	v ft/s	q cfs	n (fps)	Y cm	v cm/s	q cm3/s	n (cgs)
New Fork	1	0.0018	0.058	0.00010	0.12	0.05	1.77	0.097	0.12
River 1	3	0.0070	0.045	0.00031	0.39	0.21	1.37	0.292	0.38
s=5.71°	5	0.0104	0.050	0.00052	0.45	0.32	1.52	0.482	0.45
s=0.0995	7	0.0139	0.052	0.00073	0.52	0.42	1.58	0.670	0.52
	9	0.0138	0.068	0.00094	0.40	0.42	2.07	0.870	0.40
	11	0.0178	0.064	0.00115	0.50	0.54	1.95	1.057	0.50
	13	0.0176	0.077	0.00135	0.42	0.54	2.35	1.257	0.41
	15	0.0255	0.061	0.00156	0.67	0.78	1.86	1.443	0.67
	17	0.0203	0.077	0.00177	0.46	0.62	2.35	1.450	0.45
	19	0.0195	0.102	0.00198	0.34	0.59	3.11	1.845	0.33
	21	0.0209	0.105	0.00219	0.34	0.64	3.20	2.036	0.34
	23	0.0233	0.103	0.00240	0.38	0.71	3.14	2.226	0.37
	25	0.0269	0.097	0.00261	0.44	0.82	2.95	2.420	0.43
	27	0.0221	0.133	0.00281	0.27	0.67	4.05	2.727	0.28
	29	0.0233	0.13	0.00302	0.30	0.71	3.96	2.810	0.29
	31	0.0215	0.150	0.00323	0.24	0.65	4.57	2.992	0.24
	33	0.0283	0.122	0.00334	0.36	0.86	3.72	3.203	0.36
	35	0.0385	0.095	0.00365	0.57	1.17	2.89	3.393	0.56
	37	0.0200	0.193	0.00386	0.18	0.61	5.88	3.581	0.18
	39	0.0219	0.186	0.00406	0.20	0.67	5.66	3.779	0.20
	41	0.0263	0.162	0.00427	0.26	0.80	4.93	3.952	0.26
n = 22	43	0.0214	0.209	0.00449	0.17	0.65	6.37	4.149	0.17
								av n =	0.36
								s.d. =	0.14
Site	ΣΔx ft	Y ft	v ft/s	q cfs	n (fps)	Y cm	v cm/s	q cm3/s	n (cgs)
Boulder	1	0.0026	0.040	0.00010	0.31	0.08	1.22	0.096	0.30
Lake 1	3	0.0144	0.022	0.00031	1.77	0.44	0.67	0.294	1.72
s=10.65°	5	0.0025	0.208	0.00052	0.06	0.08	6.34	0.482	0.06
s=0.185	7	0.0164	0.045	0.00073	0.94	0.50	1.37	0.685	0.92
	9	0.0188	0.050	0.00094	0.92	0.57	1.52	0.872	0.90
	11	0.0206	0.056	0.00115	0.88	0.63	1.71	1.070	0.86
	13	0.0146	0.093	0.00135	0.42	0.44	2.83	1.260	0.41
	15	0.0103	0.152	0.00156	0.20	0.31	4.63	1.452	0.20
	17	0.0055	0.322	0.00177	0.06	0.17	9.81	1.643	0.06
	19	0.0125	0.158	0.00198	0.22	0.38	4.81	1.832	0.22
	21	0.0195	0.112	0.00219	0.42	0.59	3.41	2.026	0.41
	23	0.0180	0.133	0.00240	0.34	0.55	4.05	2.221	0.33
	25	0.0148	0.176	0.00261	0.22	0.45	5.36	2.416	0.22
	27	0.0343	0.082	0.00281	0.84	1.04	2.50	2.609	0.82
	29	0.0191	0.158	0.00302	0.29	0.58	4.81	2.799	0.29
	31	0.0310	0.104	0.00323	0.62	0.94	3.17	2.991	0.61
	33	0.0204	0.169	0.00344	0.29	0.62	5.15	3.198	0.28
	35	0.0389	0.094	0.00365	0.80	1.18	2.86	3.392	0.78
	37	0.0293	0.132	0.00386	0.47	0.89	4.02	3.588	0.46
	39	0.0349	0.116	0.00406	0.60	1.06	3.53	3.755	0.59
	41	0.0422	0.101	0.00427	0.78	1.29	3.08	3.954	0.77
n = 22	43	0.0281	0.160	0.00448	0.38	0.86	4.87	4.171	0.37
								av n =	0.53
								s.d. n =	0.38

Table 4.2 Emmett's Manning's n Values (Emmett, 1970)

Site	ΣΔx ft	Y ft	v ft/s	q cfs	n (fps)	Y cm	v cm/s	q cm3/s	n (cgs)
Pole Creek	1	0.0051	0.020	0.00010	0.99	0.16	0.61	0.095	0.99
Site 3	3	0.0093	0.034	0.00031	0.90	0.28	1.04	0.293	0.87
s=11.75°	5	0.0083	0.063	0.00052	0.45	0.25	1.92	0.485	0.44
s=0.204	7	0.0128	0.057	0.00073	0.66	0.39	1.74	0.677	0.64
	9	0.0103	0.091	0.00094	0.36	0.31	2.77	0.869	0.35
	11	0.0243	0.047	0.00115	1.54	0.74	1.43	1.059	1.20
	13	0.0151	0.090	0.00135	0.47	0.46	2.74	1.261	0.46
	15	0.0200	0.078	0.00156	0.64	0.61	2.38	1.447	0.63
	17	0.0142	0.125	0.00177	0.32	0.43	3.81	1.647	0.31
	19	0.0329	0.060	0.00198	1.17	1.00	1.83	1.831	1.15
	21	0.0193	0.113	0.00219	0.43	0.59	3.44	2.023	0.43
	23	0.0350	0.069	0.00240	1.07	1.07	2.10	2.240	1.04
	25	0.0313	0.083	0.00261	0.82	0.95	2.53	2.410	0.80
	27	0.0235	0.120	0.00281	0.47	0.72	3.65	2.616	0.46
	29	0.0356	0.085	0.00302	0.87	1.08	2.59	2.807	0.85
	31	0.0338	0.096	0.00323	0.75	1.03	2.92	3.010	0.73
	33	0.0299	0.115	0.00344	0.57	0.91	3.50	3.190	0.56
	35	0.0428	0.085	0.00365	0.98	1.30	2.59	3.375	0.97
	37	0.0433	0.089	0.00386	0.95	1.32	2.71	3.575	0.93
	39	0.0436	0.093	0.00406	0.91	1.33	2.83	3.761	0.89
	41	0.0400	0.107	0.00427	0.75	1.22	3.26	3.970	0.73
	43	0.0556	0.081	0.00448	1.24	1.69	2.47	4.178	1.21
	45	0.0475	0.099	0.00469	0.91	1.45	3.02	4.362	0.89
n = 24	47	0.0441	0.111	0.00490	0.77	1.34	3.38	4.541	0.75
								av n =	0.76
								s.d. n =	0.27
Site	ΣΔx ft	Y ft	v ft/s	q cfs	n (fps)	Y cm	v cm/s	q cm3/s	n (cgs)
Boulder	1	0.0008	0.119	0.00009	0.06	0.02	3.62	0.088	0.06
Lake 2	3	0.0026	0.110	0.00028	0.15	0.08	3.35	0.265	0.14
s=18.34°	5	0.0051	0.093	0.00047	0.28	0.16	2.83	0.440	0.27
s=0.315	7	0.0041	0.162	0.00066	0.14	0.12	4.93	0.616	0.13
	9	0.0139	0.061	0.00085	0.81	0.42	1.86	0.787	0.79
	11	0.0123	0.085	0.00104	0.54	0.37	2.59	0.970	0.52
	13	0.0128	0.096	0.00123	0.50	0.39	2.92	1.140	0.48
	15	0.0144	0.099	0.00142	0.52	0.44	3.02	1.322	0.50
	17	0.0139	0.116	0.00161	0.43	0.42	3.53	1.496	0.42
	19	0.0178	0.101	0.00180	0.58	0.54	3.08	1.668	0.56
	21	0.0215	0.093	0.00199	0.72	0.65	2.83	1.855	0.69
	23	0.0129	0.169	0.00218	0.28	0.39	5.15	2.022	0.27
n = 13	25	0.0185	0.128	0.00237	0.24	0.56	3.90	2.197	0.46
								av n =	0.41
								s.d. =	0.22

Table 4.2 Emmett's Manning's n Values (Emmett, 1970)

Site	ΣΔx ft	Y ft	v ft/s	q cfs	n (fps)	Y cm	v cm/s	q cm3/s	n (cgs)
Pole Creek	1	0.0011	0.072	0.00008	0.13	0.03	2.19	0.073	0.12
Site 2	3	0.0006	0.394	0.00024	0.02	0.02	12.00	0.219	0.02
s=18.37°	5	0.0052	0.076	0.00039	0.34	0.16	2.31	0.367	0.33
s=0.315	7	0.0182	0.030	0.00055	1.97	0.55	0.91	0.506	1.92
	9	0.0095	0.075	0.00071	0.52	0.29	2.28	0.661	0.50
	11	0.0184	0.047	0.00087	1.28	0.56	1.43	0.802	1.24
	13	0.0119	0.086	0.00102	0.52	0.36	2.62	0.949	0.51
	15	0.0199	0.059	0.00118	1.07	0.61	1.80	1.089	1.04
	17	0.0160	0.084	0.00134	0.66	0.49	2.56	1.247	0.63
	19	0.0201	0.074	0.00150	0.86	0.61	2.25	1.380	0.83
	21	0.0098	0.169	0.00165	0.58	0.30	5.15	1.536	0.23
	23	0.0249	0.073	0.00181	1.01	0.76	2.22	1.686	0.97
	25	0.0266	0.074	0.00197	1.04	0.81	2.25	1.826	1.00
	27	0.0203	0.105	0.00212	0.61	0.62	3.20	1.977	0.59
	29	0.0295	0.077	0.00228	1.07	0.90	2.35	2.107	1.03
	31	0.0230	0.106	0.00244	0.66	0.70	3.23	2.262	0.64
	33	0.0228	0.114	0.00260	0.47	0.69	3.47	2.411	0.59
	35	0.0299	0.092	0.00275	0.90	0.91	2.80	2.552	0.87
	37	0.0240	0.121	0.00292	0.59	0.73	3.69	2.694	0.57
	39	0.0284	0.108	0.00307	0.74	0.86	3.29	2.845	0.72
n = 21	41	0.0206	0.157	0.00323	0.41	0.63	4.78	3.000	0.40
								av n =	0.70
								s.d. n =	0.42
All 7 Sites		n = 146						av n =	0.55
								s.d. n =	0.41

of depth and velocity for the seven different plots was 0.57 with a standard deviation of 0.395. Emmett's laboratory analyses of roughness observed flow over a smooth 1.2 m wide by 4.9 m long flume and one covered with 0.5 mm grain sand-paper. The range of n for slopes from 0.2° to 4.4° is 0.008 to 0.04 with average flow depths from 1.2 cm to 0.1 cm.

From the field experiments, Emmett described overland flow resulting from rainfall on natural slopes as being characterised by several lateral downslope concentrations of flow rather than the uniform sheetflow. In fact he observed flow moved rarely as a sheet traveling mostly in several lateral concentrations unique to each site. These concentrations of flow were dictated by the resistance to flow developed on each slope. He also observed depths increasing to a greater degree downslope on the field plots than in flume tests as a function of the greatly increased and more complex resistance factors. Runoff was generally shallow, ranging from 0.1 cm to 1.5 cm with the shallowest flow-depths recorded on the steepest slope sections. A drawback with Emmett's data is that the series of observations at each plot were only collected for a single discharge at each location downslope. Although a range of n values were presented for the same plot for a series of increasing discharges, the observations were made at regular intervals downslope as discharge increased. They are not comparable because the conditions change from location to location in an unspecified manner. The observations are therefore discrete.

As with Roels' experiments, Emmett substituted measured velocities (adjusted by 0.4 to give the mean velocity compared to the measured maximum velocity) and depths of overland flow into the Manning flow equation to derive n. Roels did not make these adjustments and so the data presented in his 1984 paper have been modified by 0.4 to give the results presented in Table 4.1.

Other relevant studies include those of Pearce (1976) who analysed runoff on 2 m long field plots subjected to simulated rainfall. The mean gradient of the plots was 4° and in an optimisation of observed and predicted flow hydrographs yielded a best-fit value of 0.35 for Mannings n. The range of n values produced for the plots was 0.05 to 0.5. Working in the semi-arid environment of Southern Spain, Scoging (1988) examined the resistance to flow on rough, steep hillslopes though computer simulation using observed hydrographs of overland flow. The optimum n value was 0.2 with a range of values from 0.05 to 0.4. The values of Mannings n given for all of these hillslope studies are considerably in excess of the values presented for channels in hydraulic texts such as Chow (1980) or Dingman (1984). They are in general agreement and are logically expected given the different conditions of hillslope flow compared with channels.

4.3.3.d Flow Experiments at Avdat and the Calculation of Resistance

As shown by the experiments of Emmett and Roels, if plot measurements are made of velocity and flow dimensions, and the gradient of the plot is known, a series of calculations can be made to provide values of n using Mannings equation. By rearranging the Equation 4.2;

$$n = k.\sqrt{s}.Hr^{2/3}/v \qquad \text{Equation 4.34}$$

(where k is 4.64 for $cm^3\ s^{-1}$, s is the sine of the slope gradient, v is the mean velocity through the flow profile in cm s^{-1}, Hr is the hydraulic radius in cm which is equal to the average depth y for the sheetflow).

Two sets of measurements were carried out at the Avdat field site in order to calculate Mannings n. The first set measured overland flow characteristics using the run-on/runoff apparatus after completion of the infiltration tests. Using three different rates of discharge onto the plots, tracer-dye was used to time the movement of water over the one-metre downslope distance from pipe to trough. The second set measured channel flow at various locations along the natural channels and the man-made ditches. During actual rainfall-runoff events in the 1984/85 rainy season, depth and velocity tests were taken systematically from 19 locations in the catchment system where simple stage-recorders were located and where detailed cross-profile measurements were made. Measuring the maximum stage at different times during an event, and using tracer-dyes to track the time of water flow over a distance of five metres provided a sample of flow conditions during the passage of the flood at each location. The number of measurements depend on the frequency and timing of floods in the different channels.

Overland Flow Resistance

For the hillslope plots, the travel time represented the time for the leading edge of the tracer to traverse the one metre downslope under the three input rates which are roughly in the order of magnitude 1, 2 and 4. Since the flow cross-sections are complex both in cross-slope and downslope directions, measurement of the movement of the leading edge of a tracer cloud during the infiltration plot overland flow simulation produced a velocity that represented both the maximum cross-sectional rate and the shortest downslope path. Thus the velocity was an over-estimation of the average flow velocity across and down the hillslope flow profile on two counts and Emmett's adjustment factor of 0.4 was used to convert this maximum velocity into the mean flow through the complete profile. This is lower than the 0.6 used for the channel velocity and represents the more diverse profile of the overland flow situation in which boundary effects from large roughness elements produce a non-uniform distribution of velocities throughout the cross-section.

This gave a small data-set covering a broad range of overland flow conditions at each site. No measurements of depths were made, unlike Roels' studies in the Ardeche rangelands (Roels, 1984a, 1984b). Instead, the discharge across the surface was divided by the product of the average width and the velocity to give the average flow depth. Additionally, the discharge was divided by the velocity alone to give the average flow cross-sectional area. The two alternative values were used to illustrate the effect of assuming flow is a sheet or trying to quantify the complex overland flow profile. From a knowledge of the micro-topography the wetted perimeter could be calculated to give an indication of complex flow conditions.

Table 4.3 Adjusted Flow Mean Velocities for Plot 23 (3e)

Discharge Across ($cm^3\ s^{-1}$)	Max. Velocity ($cm\ s^{-1}$)	Mean Velocity ($cm\ s^{-1}$)
37.24	5.00	2.00
12.01	3.45	1.38
7.31	2.63	1.05

Looking first at the sheetflow assumption using average depth over the whole plot;.

$$y = (Qon - Qin) / [(A/100)*v] \qquad \text{Equation 4.35}$$

(where Qon is the discharge volume onto the plot, Qin is the steady-state infiltration volume into the plot, A is the wetted area and v is the measured velocity)

The second assumption was distinct channelised flow represented by the complex flow geometry. By calculating the flow-area on the plot at the time of velocity measurement, the log-log relationship between flow area and wetted perimeter provided the hydraulic radius. The flow-area (A) was the discharge across the plot divided by the velocity;

$$A = (Qon - Qin) / v \qquad \text{Equation 4.36}$$

$$\log_{10}A = a + b.\log_{10}WP \qquad \text{Equation 4.37}$$

$$10 ** [(\log_{10}A - a) / b] = WP \qquad \text{Equation 4.38}$$

(where a and b are regression equation coefficients).

Dividing A by wetted perimeter WP gave the hydraulic radius for the particular discharge level. Using Plot 23 as the example once more;

Table 4.4 Hillslope Flow Geometry for Plot 23 (3e)

Discharge Across ($cm^3\ s^{-1}$)	Mean Depth (cm)	Cross-Sectional Area (cm^2)	Wetted Perimeter (cm)	Hydraulic Radius (cm)
37.24	0.168	18.55	50.9	0.36
12.01	0.090	8.62	34.7	0.25
7.31	0.086	6.86	28.4	0.24

For the example Plot 23, the results from substitution of the values into Equations 4.55.a and 4.55.b are;

Table 4.5 Calculated Manning's n for the Two Flow Assumptions for Plot 23 (3e)

	Hillslope Gradient	Mean Depth (cm)	Mean Velocity ($cm\ s^{-1}$)	Manning's n
Sheetflow	0.255	0.168	2.00	0.36
	0.255	0.090	1.38	0.34
	0.255	0.086	1.05	0.44

	Hillslope Gradient	Hydraulic Radius (cm)	Mean Velocity ($cm\ s^{-1}$)	Manning's n
Complex	0.255	0.36	2.00	0.60
	0.255	0.25	1.38	0.67
	0.255	0.24	1.05	0.86

The full data sets are presented in Table 4.6. From the 11 different plots there are a total of 32 separate stage-discharge observations . For the sheetflow assumptions, the range of calculated Mannings n values are from 0.12 to 0.61 with an overall mean of 0.35 and a standard deviation of 0.13. These accord well with the calculations derived from other field studies as discussed below.

For the rivulet flow assumptions, the opposite of what logically might be expected occurs in that the calculated values of Mannings n are all in excess of those for the sheetflow assumption with a range from 0.18 to 1.32 and an overall mean of 0.63 and standard deviation 0.28. From a consideration of discussions earlier in this chapter it was suggested that concentrated flow, due to the more efficient

Table 4.6 Avdat Hillslope Manning's n (Full Data)

Plot	I A	I B	I const	Δt per l	Q1	QI	Q2	Area	AvA	Av D	MT A	MT B	WP	Hr	Sine G	Av V	Sh n	Ar n	Mean	Mean
18 (1e)	0.000353	0.265	0.000397	0.55	30.30	4.49	25.82	11300	16.13	0.143	1.31	0.406	46.4	0.35	0.4	1.60	0.51	0.93	Sh n	Ar n
	0.000353	0.265	0.000397	1.09	15.29	4.13	11.16	10410	6.97	0.067	1.31	0.406	31.4	0.22	0.4	1.60	0.31	0.69		
	0.000353	0.265	0.000397	2.27	7.35	3.18	4.17	8000	5.22	0.065	1.31	0.406	23.9	0.22	0.4	0.80	0.61	1.37	0.48	1.00
20 (2e)	0.000406	0.163	0.000433	0.55	30.30	5.66	24.65	13060	12.84	0.098	1.37	0.380	49.0	0.26	0.3	1.92	0.29	0.55		
	0.000406	0.163	0.000433	0.85	19.61	5.54	14.06	12800	10.56	0.082	1.37	0.380	44.9	0.23	0.3	1.33	0.37	0.74		
	0.000406	0.163	0.000433	1.98	8.44	4.23	4.21	9770	6.30	0.064	1.37	0.380	31.2	0.20	0.3	0.67	0.62	1.33	0.43	0.88
23 (3e)	0.000154	0.145	0.000178	0.43	39.22	1.97	37.24	11070	18.62	0.168	1.37	0.380	51.0	0.37	0.3	2.00	0.36	0.60		
	0.000154	0.145	0.000178	1.22	13.72	1.70	12.01	9560	8.71	0.091	1.37	0.380	34.8	0.25	0.3	1.38	0.34	0.67		
	0.000154	0.145	0.000178	1.91	8.73	1.42	7.31	7950	6.95	0.087	1.37	0.380	28.5	0.24	0.3	1.05	0.44	0.87	0.38	0.71
25 (4e	0.000010	0.196	0.000043	0.43	38.76	0.57	38.19	13440	22.89	0.170	1.37	0.386	63.5	0.36	0.2	1.67	0.38	0.63		
upper)	0.000010	0.196	0.000043	0.88	18.88	0.50	18.37	11800	16.06	0.136	1.37	0.386	51.1	0.31	0.2	1.14	0.48	0.84		
	0.000010	0.196	0.000043	1.87	8.93	0.42	8.51	9800	10.64	0.109	1.37	0.386	38.9	0.27	0.2	0.80	0.59	1.10	0.49	0.86
28 (4e	0.000298	0.300	0.000348	0.60	27.78	4.56	23.22	13100	13.04	0.100	1.39	0.358	48.5	0.27	0.1	1.78	0.14	0.26		
lower)	0.000298	0.300	0.000348	1.20	13.89	3.78	10.11	10870	9.36	0.086	1.39	0.358	38.2	0.25	0.1	1.08	0.20	0.41		
	0.000298	0.300	0.000348	1.83	9.13	3.63	5.50	10440	5.98	0.057	1.39	0.358	31.7	0.19	0.1	0.92	0.18	0.40	0.17	0.36
32 (5e)	0.000564	0.278	0.000610	0.48	34.72	8.11	26.62	13280	24.92	0.188	1.30	0.578	110.0	0.23	0.1	1.07	0.44	0.49		
	0.000564	0.278	0.000610	1.18	14.09	6.37	7.72	10440	8.69	0.083	1.30	0.578	54.1	0.16	0.1	0.89	0.31	0.47		
	0.000564	0.278	0.000610	2.08	8.00	5.07	2.93	8310	6.00	0.072	1.30	0.578	39.7	0.15	0.1	0.49	0.51	0.83	0.42	0.60
34 (5w	0.001670	0.217	0.001706	0.45	37.04	16.72	20.32	9800	19.54	0.199	1.35	0.520	76.4	0.26	0.0	1.04	0.32	0.38		
lower)	0.001670	0.217	0.001706	1.33	12.58	10.27	2.31	6020	5.06	0.084	1.35	0.520	30.0	0.17	0.0	0.46	0.41	0.65	0.36	0.51
36 (4w)	0.000714	0.266	0.000758	0.61	27.32	7.58	19.74	10000	14.95	0.150	1.34	0.462	54.0	0.28	0.1	1.32	0.38	0.57		
	0.000714	0.266	0.000758	1.14	14.62	6.67	7.95	8800	7.95	0.090	1.34	0.462	37.7	0.21	0.1	1.00	0.36	0.63		
	0.000714	0.266	0.000758	2.10	7.94	5.69	2.25	7500	3.51	0.047	1.34	0.462	23.7	0.15	0.1	0.64	0.36	0.78	0.37	0.66
38 (3w)	0.000131	0.136	0.000154	0.63	26.46	2.83	23.62	18440	14.87	0.081	1.42	0.344	65.3	0.23	0.1	1.59	0.15	0.30		
	0.000131	0.136	0.000154	1.33	12.53	2.60	9.93	16950	11.82	0.070	1.42	0.344	57.1	0.21	0.1	0.84	0.26	0.53		
	0.000131	0.136	0.000154	2.50	6.67	2.34	4.32	15240	9.24	0.061	1.42	0.344	48.9	0.19	0.1	0.47	0.42	0.89	0.27	0.57
42 (6w)	0.000135	0.190	0.000167	0.53	31.27	1.65	29.62	9870	21.47	0.217	1.48	0.337	55.0	0.39	0.1	1.38	0.27	0.40		
	0.000135	0.190	0.000167	1.25	13.33	1.60	11.74	9590	10.87	0.113	1.48	0.337	42.9	0.25	0.1	1.08	0.23	0.39		
	0.000135	0.190	0.000167	2.00	8.33	1.25	7.08	7510	8.51	0.113	1.48	0.337	33.6	0.25	0.1	0.83	0.29	0.50	0.26	0.43
47 (5w	0.000305	0.358	0.000365	0.47	35.46	4.71	30.75	12910	17.32	0.134	1.54	0.352	73.7	0.24	0.0	1.78	0.12	0.18		
upper)	0.000305	0.358	0.000365	1.00	16.67	3.67	13.00	10060	14.25	0.142	1.54	0.352	58.5	0.24	0.0	0.91	0.25	0.36		
	0.000305	0.358	0.000365	1.93	8.64	2.71	5.92	7440	11.84	0.159	1.54	0.352	45.1	0.26	0.0	0.50	0.50	0.69	0.29	0.41
								Mean	11.91	0.110			47.5	0.25		1.13	0.36	0.64	Mean	
								s.d.	5.55	0.045			17.7	0.06		0.44	0.13	0.28	s.d.	

IA = infiltration A; IB = infiltration B; Δt per l = time taken to discharge one litre; Q1 = run-on discharge; QI = discharge lost to infiltration

Q2 = run-off discharge; Area = wetted plot area; AvA = average flow area; Av D = average flow depth; MT A and MT B = WP-A regression coefficients

WP = wetted perimeter; Hr = hydraulic radius; Sine G = sine of the slope angle; Av V = adjusted average velocity; Sh n = sheetflow Manning's n

Ar n = complex flow Manning's n

flow section and the lower contact ratio between the surface and the water body will have higher velocities for a given discharge due to the lower resistance exerted against movement. However, these calculations have shown resistance to be higher for concentrated flows. The reason for this is that we are not considering two different flow situations but two ways of considering flow. The mean velocity for each is the same because they are the same test. However, by conceiving of flow as either a sheetflow or as a complex flow, the resistance associated with this assumption differs because the velocity is the same but the other parameters vary. By assuming sheetflow the parameter for flow dimension is changed and therefore the value of n will change based on the difference between average depth and hydraulic radius. The effect of the sheetflow assumption has seldom been analysed because there is usually no alternative dimension data-set against which to compare it. By developing a relationship between flow area and boundary length for a micro-topographically rough surface the effect of the sheetflow assumption can be assessed. In this case, assuming sheetflow produces a lower estimate of n for a given discharge.

Channel Flow Resistance

Specific locations within the channel network were fitted with simple stage-recorders and detailed cross-sectional profiles were measured. They provided an average cross-section data-set for the five metre long flow section detailing the change in flow area, wetted perimeter, top-width and hydraulic radius with each stage increase above the lowest point in the cross-section. The fleld technique involved measuring the height of flow above the lowest point in the centre of the five profiles on the tube-gauge dipstick, and then injecting tracer slightly upstream from the first profile marker, beginning the travel time as the leading edge passed this point, and recording the time the leading edge reached the 5m mark downstream. This time and distance combination provided the velocity of flow, and the stage above the lowest profile point can be compared to the tabulated values of cross-sectional geometry derived for the section. The tube-gauge is illustrated below in Figure 4.5 along with an annotation of its main components.

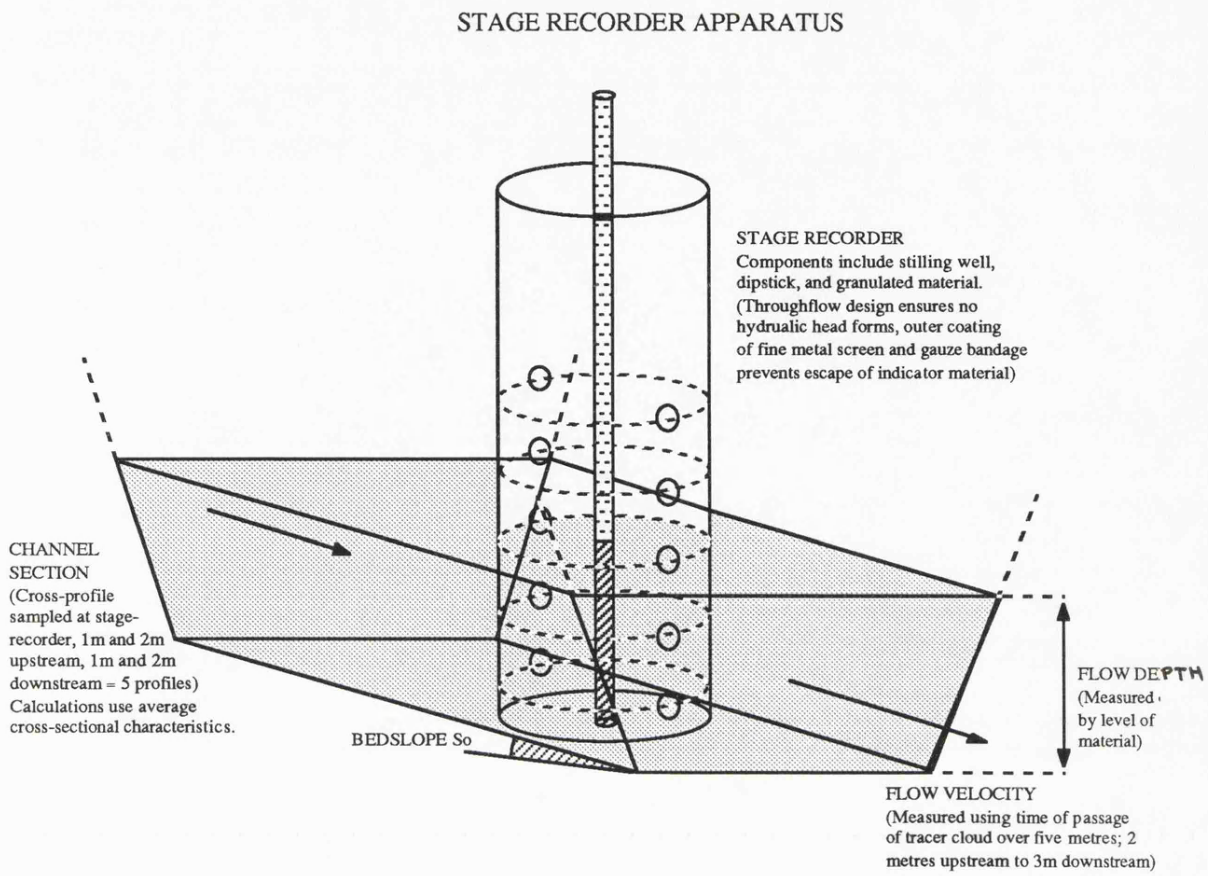

Figure 4.5 Channel Stage-Recorder Apparatus

A body of water flowing through a constrained area does not possess a uniform velocity distribution (Chow, 1981. Dingman, 1984). The measurements taken in the field provide the maximum, or near maximum velocities through the cross-section, due to the movement of the tracer in the near-surface, central portion of the flow body, and through measurement of the fastest, leading edge of the tracer cloud. Consequently, measured velocities must be adjusted to account for this over-estimation. For the channel flow measurements, the maximum measured rates have been multiplied by 0.6 to give an approximation of the mean velocity. This value is derived from theoretical and empirical studies showing velocity throughout a profile to follow a log distribution (Chow, 1981). This reflects the balance between the twin retarding influences of bed and bank friction and air-surface skin friction, and also accounts somewhat for the balance between laminar and turbulent flow resulting from the presence of boundary layers throughout the profile (Dingman, 1984).

Table 4.7 Adjusted Flow Mean Velocities For Stage-Recorder 11

Max. Depth (cm)	Max. Velocity ($cm\ s^{-1}$)	Mean Velocity ($cm\ s^{-1}$)
13.5	100.0	60.0
7.1	26.3	15.8
5.0	8.6	5.2
4.8	5.6	3.4

For the channels, at the same time velocity was measured, the maximum flow depth in the channel section was measured against the permanent stage-recorder. From this depth, the flow cross-sectional area and wetted perimeter and the hydraulic radius can be selected. As explained previously in Section 4.3.2, the channels were measured by taking a micro-profile of vertical depths to the bed from a horizontal datum aligned from bank-top to bank-top. This profile provides the means for calculating the geometric relationships for a given depth above the lowest point in the channel cross-section. For use in the model, these flow-sections are approximated as triangular cross-sections with known bank-angles and maximum depth to bank over-topping.

Table 4.8 Geometric Characteristics at the Measured Depths for Stage Recorder 11

Max. Depth (cm)	Cross-Sectional Area (cm^2)	Wetted Perimeter (cm)	Hydraulic Radius (cm)
13.5	765.0	103.3	7.4
7.1	253.0	72.2	3.5
5.0	136.0	51.8	2.6
4.8	136.0	51.8	2.6

Table 4.9 Calculated Manning's n Values for Observed Stages at Stage Recorder 11

Discharge ($cm^3\ s^{-1}$)	Gradient	Hydraulic Radius (cm)	Mean Velocity ($cm\ s^{-1}$)	Manning's n
45900.0	0.07	7.41	60.0	0.08
3997.4	0.07	3.51	15.8	0.18
707.2	0.07	2.63	5.2	0.45
448.8	0.07	2.63	3.3	0.70

For each stage-recorder location, determining Manning's n for each observed flow depth simply involved substituting the calculated hydraulic radius and the adjusted mean velocity into the rearranged

Manning equation along with the local slope gradient (sine S) calculated from the spot-heights surveyed along the channel system.

The full data sets from each of the channel locations are presented in Table 4.10 and their locations within the Avdat catchment system shown in Appendix 1.1. Out of the 76 separate observations, the range of values for n is from 0.044 to 0.70 with the higher values representing the lower discharge rates at each individual location. Although there is only a poor general relationship between n and the discharge for the whole data-set, the individual channel locations themselves, for which 1 to 6 observations are available for the rainy season 1984/85 show a general increase in n with decrease in Q.

The overall mean for the 76 stage observations is 0.156 with a standard deviation of 0.103. The slope gradient of all the channels ranges from 4.6° to 1.0° with a mean of 3.0° and a standard deviation of 1.1°. These values accord with the observations of Roels' rilled plots described earlier which produce n values with means of 0.131 and 0.069 for the two different gradients of rills as shown in Table 4.1.

4.3.3.e Comparisons Between the Avdat Field Data and the Literature Data

In order to make correct comparisons between the Avdat field data and those presented in the literature, particularly from the field studies of Emmett and Roels, all the relevant data-sets have been converted into cgs units as explained previously allowing comparisons of the broad characteristics of the data-sets including the orders of magnitude and range of values.

Firstly considering Table 4.11. All the data sets are applicable to a range of poorly vegetated hillslope surfaces, the conditions from which they were derived, or in the case of the handbook approach of Cowan, to which they are most relevant. For comparison with these hillslope examples, the values of Limerinos are presented from his study of gravel-bed rivers. The Avdat field data falls in line comfortably with the data collected from the literature both in terms of the order of magnitude of the Mannings coefficient and the range of values. Using depth as the flow dimension the Avdat hillslopes exhibit a mean value of Mannings n of 0.35 with a minimum and maximum of 0.12 and 0.62 respectively. This contrasts favourably with the mean field value of n produced by Pearce of 0.35, by Emmett of 0.55, and by Roels of 0.173 (for the pre-rilled plots that are most relevant to the Avdat hillslopes as explained previously). The last two mean values are calculated for a range of discharges far in excess of those used at Avdat. The limited data-sets for Emmett and Roels using only the range of discharges used on the Avdat plots (where unit discharge $q \leq 0.336\ cm^3\ s^{-1}$) are presented in Tables 4.12 and 4.13 respectively for comparison with the Avdat data in Table 4.6. The handbook method of

Table 4.10 Avdat Channel Manning's n

Stage Rec.	Sine Slope	Max depth	Max velocity	Average velocity	Area	Discharge	Wetted Perimiter	Hydraulic radius	Manning's n	Mean n
1	0.033	9.6	62.5	37.5	830.0	31125.0	139.0	5.99	0.074	
	0.033	5.7	26.3	15.8	359.4	5671.3	105.0	3.42	0.121	0.098
2	0.021	9.5	71.4	42.8	637.8	27323.4	131.0	4.86	0.044	
	0.021	5.0	38.5	23.1	191.6	4426.0	77.9	2.46	0.052	0.048
3	0.017	7.5	50.0	30.0	458.2	13746.0	134.0	3.41	0.046	
	0.017	5.0	38.5	23.1	187.8	4338.2	83.8	2.24	0.045	
	0.017	3.0	21.7	13.0	65.0	846.3	48.7	1.34	0.057	0.049
4	0.020	5.0	26.3	15.8	240.0	3787.2	79.4	3.02	0.086	
	0.020	4.4	31.3	18.8	203.0	3806.3	76.0	2.67	0.067	
	0.020	3.2	8.9	5.3	103.2	551.1	59.0	1.75	0.176	0.110
5	0.045	1.3	6.7	4.0	18.6	74.8	18.9	0.99	0.243	
	0.045	1.3	6.9	4.1	18.6	76.4	18.9	0.99	0.238	0.241
6	0.050	11.6	76.9	46.1	332.8	15355.4	57.5	5.79	0.072	
	0.050	10.7	62.5	37.5	285.2	10695.0	52.8	5.41	0.085	
	0.050	4.9	18.5	11.1	81.8	908.0	30.5	2.68	0.181	0.113
8	0.072	8.0	50.0	30.0	311.8	9354.0	69.5	4.49	0.113	
	0.072	7.8	51.3	30.8	311.8	9597.2	69.5	4.49	0.110	
	0.072	4.9	17.3	10.4	137.4	1426.2	52.4	2.62	0.228	
	0.072	4.5	13.5	8.1	113.0	915.3	49.6	2.28	0.266	
	0.072	4.2	15.6	9.4	90.4	846.1	46.3	1.95	0.208	
	0.072	3.8	13.5	8.1	90.4	732.2	46.3	1.95	0.240	0.194
9	0.040	9.5	91.0	54.6	271.8	14840.3	58.8	4.62	0.047	
	0.040	7.5	62.5	37.5	176.8	6630.0	49.5	3.57	0.058	
	0.040	4.5	20.8	12.5	69.2	863.6	32.6	2.13	0.123	
	0.040	3.8	14.7	8.8	55.8	492.2	29.4	1.90	0.161	0.097
10	0.067	8.0	50.0	30.0	305.4	9162.0	71.9	4.25	0.105	
	0.067	5.0	31.3	18.8	125.0	2343.8	55.6	2.25	0.110	
	0.067	2.1	10.0	6.0	23.2	139.2	20.5	1.13	0.217	
	0.067	1.4	6.9	4.1	14.0	57.5	17.5	0.80	0.251	0.171
11	0.070	13.5	100.0	60.0	765.0	45900.0	103.3	7.41	0.080	
	0.070	7.1	26.3	15.8	253.0	3992.3	72.2	3.51	0.180	
	0.070	5.0	8.6	5.2	136.0	701.8	51.8	2.63	0.450	
	0.070	4.8	5.6	3.3	136.0	452.9	51.8	2.63	0.700	0.353
12	0.038	6.4	58.8	35.3	197.0	6950.2	49.3	3.98	0.060	
	0.038	5.0	45.4	27.2	132.0	3595.7	42.2	3.12	0.070	
	0.038	2.1	20.8	12.5	32.0	399.4	25.2	1.27	0.090	
	0.038	1.5	11.6	7.0	20.0	139.2	21.8	0.93	0.120	0.085
14	0.053	14.5	91.0	54.6	1165.0	63609.0	156.3	7.46	0.070	
	0.053	5.9	31.3	18.8	266.0	4987.5	94.4	2.82	0.110	
	0.053	5.0	29.4	17.6	182.0	3210.5	63.2	2.88	0.120	
	0.053	4.9	19.2	11.5	182.0	2096.6	63.2	2.88	0.190	
	0.053	4.8	10.4	6.2	182.0	1135.7	63.2	2.88	0.350	0.168
15	0.057	2.5	37.1	22.3	59.0	1313.3	46.8	1.27	0.060	
	0.057	1.5	19.2	11.5	22.0	253.4	28.3	0.78	0.080	
	0.057	1.3	21.7	13.0	22.0	286.4	28.3	0.78	0.070	0.070
A	0.064	8.9	50.0	30.0	820.0	24600.0	209.2	3.92	0.100	
	0.064	7.3	29.4	17.6	659.0	11624.8	193.8	3.40	0.150	
	0.064	4.9	16.7	10.0	353.0	3537.1	156.4	2.26	0.200	
	0.064	2.4	13.2	7.9	78.0	617.8	58.6	1.33	0.180	0.158
B	0.073	10.5	66.7	40.0	553.0	22131.1	107.5	5.15	0.090	
	0.073	4.0	20.0	12.0	85.0	1020.0	40.5	2.10	0.170	
	0.073	3.7	27.8	16.7	67.0	1117.6	33.9	1.96	0.120	
	0.073	2.8	16.7	10.0	52.0	521.0	29.0	1.78	0.180	
	0.073	1.8	12.8	7.7	24.0	184.3	21.9	1.10	0.170	0.146
C	0.071	3.7	20.8	12.5	94.0	1173.1	47.3	1.99	0.160	
	0.071	3.7	33.3	20.0	94.0	1878.1	47.3	1.99	0.100	
	0.071	2.7	21.7	13.0	35.0	455.7	36.1	0.96	0.090	
	0.071	2.3	19.2	11.5	35.0	403.2	36.1	0.96	0.100	
	0.071	2.0	11.6	7.0	38.0	264.5	30.4	1.24	0.210	
	0.071	2.0	16.7	10.0	38.0	380.8	30.4	1.24	0.140	0.133
D	0.080	6.0	52.6	31.6	168.0	5302.1	51.6	3.25	0.091	
	0.080	3.8	29.4	17.6	83.0	1464.1	36.7	2.26	0.128	
	0.080	3.0	16.7	10.0	52.0	521.0	30.4	1.71	0.187	
	0.080	2.5	7.1	4.3	39.0	166.1	27.9	1.40	0.385	
	0.080	1.6	7.1	4.3	17.0	72.4	18.5	0.90	0.287	
	0.080	1.0	7.2	4.3	9.0	38.9	11.9	0.73	0.245	0.221
E	0.033	3.5	22.7	13.6	77.0	1048.7	38.9	1.97	0.098	
	0.033	2.4	12.8	7.7	44.0	337.9	29.2	1.51	0.145	
	0.033	1.9	5.8	3.5	31.0	107.9	24.8	1.26	0.284	0.176
F	0.055	2.5	18.5	11.1	38.0	421.8	25.4	1.49	0.128	
	0.055	1.8	13.9	8.3	36.0	300.2	22.1	1.63	0.181	0.155
G	0.070	12.0	91.0	54.6	624.0	34070.4	89.1	7.00	0.082	
	0.070	7.4	25.0	15.0	287.0	4305.0	72.2	3.97	0.205	
	0.070	6.8	20.8	12.5	254.0	3169.9	70.1	3.62	0.232	
	0.070	5.8	17.2	10.3	192.0	1981.4	61.8	3.10	0.253	0.193

Table 4.11 Summary of Relevant Manning's n Values

Author	Type of Data Set	Description	Min n	Max n	Mean n	s.d. n
Cowan	Hand-book set for use with channel flow	Composite	0.025	0.290	0.11[a]	n.a.
[1956]	[a] this value represents a bare hillslope					
Emmett	Field plot studies using simulated rainfall on	1.66°	0.100	2.620	0.660	0.610
[1970]	a range of slopes from 1.66° to 18.4°. The	5.51°	0.010	1.010	0.430	0.220
	plots are 2.1 by 14 m and the n values	5.71°	0.120	0.670	0.360	0.140
	calculated using Emmett's depth and velocity	10.65°	0.060	1.720	0.530	0.380
	converted into cgs units. Poorly vegetated	11.75°	0.310	1.210	0.760	0.270
	slopes in Wyoming.	18.34°	0.060	0.790	0.410	0.220
		18.37°	0.020	1.920	0.700	0.420
		All plots	0.010	2.620	0.550	0.410
Roels	Field plot studies using run-on/runoff on	7.8° pre-rill	0.064	0.826	0.216	0.157
[1984]	two slopes, 7.8° and 10.2° both pre-rilled	10.2° pre-rill	0.067	0.331	0.130	0.052
	and rilled. The plots are 0.5 x 0.65 m and	7.8° rilled	0.092	0.385	0.177	0.060
	the n values are calculated using Roels'	10.2° rilled	0.024	0.131	0.079	0.033
	hydraulic radius and velocity converted into	All pre-rilled	0.064	0.826	0.173	0.125
	cgs units. Ardeche rangelands.	All rilled	0.024	0.385	0.131	0.069
		All	0.024	0.826	0.152	0.103
Scoging	Field plot studies using rainfall simulation	16.4° sd 4.3°	0.050	0.300	0.100	0.060
[1988]	and run-on/runoff at four locations. The	22.6° sd 3.4°	0.100	0.250	0.250	0.000
	rain plot is 0.7 m diameter and the run-on	24.5° sd 9.5°	0.050	0.100	0.070	0.020
	plot 1.0 m long by 0.5 m wide. The n	16.0° sd 3.2°	0.100	0.400	0.260	0.100
	values are derived from best-fit of observed	All plots				
	and simulated hydrographs. Semi-arid	19.5° sd 6.8°	0.050	0.400	0.160	0.110
	S.E. Spanish hillsides. Units of cgs.					
Pearce	Field plot studies using rainfall simulation.	4°	0.050	0.500	0.350	n.a.
[1976]	Plots are 2 m long.					
Limerinos	Field studies of flow at stations on 11	All stations	0.020	0.107	0.053	0.021
[1970]	California gravel-bedded rivers. Units fps?					
Lee	Field studies using run-on/runoff plots at 11	Using mean				
[1984/85]	sites in arid catchment. The plots are 1.0	depth Y	0.125	0.624	0.356	0.134
	by 1.0 m and the full results presented in	Using Hr from				
	Table 4.6. The n values are	microtopog.	0.181	1.365	0.639	0.282
	calculated using measured velocity and					
	depth, and hydraulic radius calculated from	Channels	0.044	0.450	0.156	0.103
	discharge and flow area. Channel n is					
	calculated using same from instrumented					
	locations. Units of cgs. Negev Desert.					

Table 4.12	Emmett's Manning's n (where q≤0.336 cm3/s for direct comparison with Avdat data)										
Site	s	y cm	v cm/s	q cm3/s	n	Site	s	y cm	v cm/s	q cm3/s	n
New Fork	0.029	0.47	0.18	0.086	2.620	Pole Creek 3	0.204	0.16	0.61	0.095	0.990
River 2		0.35	0.76	0.264	0.510			0.28	1.04	0.293	0.870
Pole Creek 1	0.096	0.01	5.30	0.065	0.010	Boulder Lake 2	0.315	0.02	3.62	0.088	0.060
		0.20	0.97	0.196	0.510			0.08	3.35	0.265	0.140
		0.22	1.49	0.323	0.350						
						Pole Creek 2	0.315	0.03	2.19	0.073	0.120
New Fork	0.100	0.05	1.77	0.097	0.120			0.02	12.00	0.219	0.020
River 1		0.21	1.37	0.292	0.380						
						Mean of all 7 sites		0.18	2.44		0.581
Boulder Lake 1	0.185	0.08	1.22	0.096	0.300		s.d.	0.15	2.88		0.703
		0.44	0.67	0.294	1.720						

Table 4.13	Roels' Mannings n (where q≤0.336 cm3/s for direct comparison with Avdat Data)										
Site	s	Hr cm	v cm/s	q cm3/s	n	Site	s	Hr cm	v cm/s	q cm3/s	n
Pre-rill 1	0.136	0.10	0.72	0.07	0.512	Rilled 4	0.136	0.12	1.08	0.13	0.385
		0.24	0.80	0.19	0.826			0.16	1.60	0.26	0.315
		0.27	1.20	0.32	0.596						
Pre-rill 2	0.136	0.12	1.24	0.15	0.336	Rilled 5	0.136	0.07	1.68	0.12	0.173
		0.15	1.44	0.22	0.335			0.13	2.36	0.31	0.186
Pre-rill 3	0.136	0.14	2.44	0.34	0.189	Rilled 6	0.136	0.06	1.24	0.07	0.211
								0.10	1.80	0.18	0.205
Pre-rill 7	0.178	0.08	0.96	0.08	0.331	Rilled 10	0.178	0.05	3.48	0.17	0.067
		0.12	1.64	0.20	0.254						
		0.13	2.52	0.33	0.174						
Pre-rill 8	0.178	0.06	1.96	0.12	0.134	Rilled 11	0.178	0.08	2.60	0.21	0.122
		0.09	3.04	0.27	0.113						
Pre-rill 9	0.178	0.05	2.36	0.12	0.098	Rilled 12	none	none	none	none	none
		0.09	3.60	0.32	0.095						
All pre-rill	mean	0.13	1.84		0.307	All Rilled	mean	0.10	1.98		0.208
	s.d.	0.06	0.86		0.213		s.d.	0.04	0.74		0.095
All plots	mean	0.11	1.89		0.269						
	s.d.	0.05	0.82		0.184						

Cowan produces lower estimates compared to the Avdat field data and all the other data sets when it comes to the maximum predicted Mannings n for the very roughest surface.

In contrast it is interesting to note the values produced for various gravel-bed rivers by Limerinos (1970) presented in Table 4.14. These are often held to be most relevant to the overland flow case of micro-topographically rough vegetation-free hillsides but as shown, they have n values that are an order of magnitude lower. This observation is supported by Morgan (1980) who argues that in modelling hillslope flow, larger values should be used than those normally adopted for channels. He illustrates this by showing that the value of 0.02 commonly used for channels on bare soil are an order of magnitude lower than values appropriate for partially vegetated hillslope surfaces which vary from 0.125 to 1.7 with the best predictor for overland flow and sediment erosion being 0.2 (Morgan, 1980), an observation that accords with the findings of Scoging (1988).

Roels' Data Sets

It is clear from the summarised data sets in Table 4.11 that a broad range of Mannings n values have been observed and predicted in terms of their minimum, maximum, and mean, and their standard deviations. Roels' plot data seems to suggest a positive relation between n and slope gradient and micro-topographic variation (rilled and pre-rilled). Both Scoging and Emmett show the range of n and the mean n to vary widely between plots of similar and different gradient. Roels' data set samples a range of discharges mostly in excess of those experienced over the Avdat field plots. Only those process observations and calculations of n for Roels' plots that are within the range of magnitude of discharge conditions used at Avdat ($q \leq 0.336$ cm^3 s^{-1}) are presented in Table 4.13. As with the Avdat data-set there are only a maximum of three observations for each plot within this reduced range of discharges and for some plots only one. The aggregated characteristics of this more comparable group of observations correlate much more closely with the Avdat plot characteristics. Whereas previously for the pre-rilled plots the mean and standard deviation was 0.173 and 0.125, for those where $q \leq 0.336$ cm^3 s^{-1} the mean is 0.307 and the standard deviation 0.213. This compares favourably to the Avdat values of 0.35 and 0.13 particularly considering the wider range of slope gradients sampled in the Avdat study.

From Roels' descriptions of his rilled plots, they are similar morphologically to the Avdat channel system rather than the hillslopes. Consequently, the characteristics of the two data-sets should be more closely comparable. In Roels' studies the maximum discharge was 754 cm^3 s^{-1} calculated on the assumption that Roels' has equated mean depth with mean hydraulic radius. To make comparisons between the Avdat channel characteristics independent of any discharge effects, only the 28 observations where discharge is less than this amount are used in the calculations. These are presented in Table 4.15.

Table 4.14 Limerinos' Manning's n Data Set for Gravel Bedded Rivers (1970)

Site	Q cfs º	Q cm3/s	q cm3/s	n
Austin Creek	5050	143000075.3	4691603.52	0.036
	11375	322104130.0	10567720.80	0.036
	853	24154270.1	792462.93	0.036
	672	19028920.9	624308.43	0.038
Cache Creek	2180	61730725.6	2025286.27	0.020
	944	26731103.2	877004.70	0.022
	277	7843766.5	257341.42	0.023
Eel River	9000	254851619.3	8361273.60	0.035
	1350	38227742.9	1254191.04	0.043
Kaweah River	1050	29732688.9	975481.92	0.071
	869	24607339.7	807327.42	0.067
	405	11468322.9	376257.31	0.083
Kings River	3690	104489163.9	3428122.18	0.064
	3660	103639658.5	3400251.26	0.059
	3200	90613909.1	2972897.28	0.064
	2440	69093105.7	2266834.18	0.066
Merced River	1840	52102997.7	1709415.94	0.035
	1650	46722796.9	1532900.16	0.036
	1340	37944574.4	1244900.74	0.044
	1170	33130710.5	1086965.57	0.050
	983	27835460.2	913236.88	0.052
	666	18859019.8	618734.25	0.068
	622	17613078.6	577856.91	0.064
Outlet Creek	15200	430416068.2	14121262.08	0.033
	5640	159707014.8	5239731.46	0.035
	4420	125160461.9	4106314.37	0.036
	1610	45590123.0	1495738.94	0.028
	1210	34263384.4	1124126.78	0.028
	1200	33980215.9	1114836.48	0.029
	1130	31998036.6	1049804.35	0.025
	542	15347730.9	503534.48	0.036
	348	9854262.6	323302.58	0.038
Smith River	3000	84950539.8	2787091.20	0.042
	1950	55217850.9	1811609.28	0.044
	1570	44457449.1	1458577.73	0.047
Van Duzen River	1840	52102997.7	1709415.94	0.039
Van Duzen River	5310	150362455.4	4933151.42	0.088
	3570	101091142.3	3316638.53	0.107
	2510	71075284.9	2331866.30	0.098
º assumed cfs units				
			mean	0.053
			s.d.	0.021

The mean value of Mannings n for the Avdat channels is 0.212 with a minimum of 0.07 and a maximum of 0.7 as illustrated in Table 4.15. Roels' rilled plots produce a mean n of 0.131 with a minimum of 0.024 and a maximum of 0.385 as shown in Table 4.1. Although Roels' plots are in the order of two to three times steeper than the Avdat channels, the velocities are similar with the two means being 7.93 cm s^{-1} and 8.42 cm s^{-1} for Avdat and the Ardeche respectively. The standard deviations of the velocities are similar also. The two data sets therefore show a relatively close correspondence suggesting that the Avdat field data provide n values of an acceptable order of magnitude and range for these types of small, incised vegetation-free channels. The difference between these values and handbook or tabulated values presented in the literature and usually assumed for channels is quite striking.

Limerinos presents Mannings n values calculated for a number of gravel-bed rivers in California, the mean value for all locations being 0.053 with a standard deviation of 0.021 as shown in Table 4.14. The difference in magnitude reflects both the increased scale of the channel and the considerably larger discharges passing through the sections. The small, micro-rough rill-like channels at Avdat and in the Ardeche rangelands have mean roughnesses 2.5 to 4.0 times as large as the gravel-bed rivers. The tabulated values presented in the literature (Chow, 1980) suggest mean n's to be around 0.04 for excavated cobble-bottomed and clean-sided channels which most accurately describe some of the Avdat channels. Using the handbook method of Cowan would yield an appropriate n of 0.065. The rilled plots and Avdat channels therefore have considerably higher n values than those conventionally predicted for channelised flow. Use of the literature values in the Avdat catchment as parameters for a simulation of channel flow would seriously overestimate velocity relative to observed conditions and would not reproduce hydrograph shape. This would have important implications for the determination of partial area productivity and the amount of water harvested from a given location through time.

Emmett's Data Sets

Emmett's data-set, unlike Roels' and the Avdat field data, does not provide observations for different discharges at the same location, but provides single observations for a series of locations for which different steady-state discharges are observed under the conditions of a Horton-type increase in discharge with downslope distance. Since conditions vary in an unknown manner between locations, the Manning's n values cannot be compared for the different discharge rates nor between the different locations. Emmett's data is therefore only suitable for a consideration of the range of resistance coefficients within a plot length of a given overall slope gradient. Since neither the physical or the discharge variables are constant, any systematic downslope changes in n, should they exist, are masked by the increase in discharge. Any changes in n with discharge will be masked by the different conditions at successive locations.

Table 4.15 Avdat Channel Manning's n (where Q≤745cm3/s for direct comparison with Roels' rilled plots)

Site	Hr cm	v cm/s	Q cm3/s	n
4	1.75	5.34	551.09	0.176
5	0.99	4.02	74.77	0.243
	0.99	4.11	76.44	0.238
8	1.95	8.10	732.24	0.240
9	1.90	8.82	492.16	0.161
10	1.13	6.00	139.20	0.217
	0.80	4.11	57.54	0.251
11	2.63	5.16	701.76	0.450
	2.63	3.33	452.88	0.700
12	1.27	12.48	399.36	0.090
	0.93	6.96	139.20	0.120
15	0.78	13.02	286.44	0.070
	0.78	11.52	253.44	0.080
A	1.33	7.92	617.76	0.180
B	1.78	10.02	521.04	0.180
	1.10	7.68	184.32	0.170
C	0.96	13.02	455.70	0.090
	1.99	19.98	403.20	0.100
	1.24	10.02	380.76	0.140
	1.24	6.96	264.48	0.210
D	1.71	10.02	521.04	0.187
	1.40	4.26	166.14	0.385
	0.90	4.26	72.42	0.287
	0.73	4.32	38.88	0.245
E	1.51	7.68	337.92	0.145
	1.26	3.48	107.88	0.284
F	1.49	11.10	421.80	0.128
	1.63	8.34	300.24	0.181
Mean	1.72	4.64		0.351
s.d.	1.29	0.74		0.141
no. = 28				

The complete data-set for Emmett's plots are presented in Table 4.2. For direct comparison with the Avdat plot data, only the observations for unit width discharge of $q \leq 0.336$ cm^3 s^{-1} must be used. This limits the observations to the first two metres of the Emmett's plots where under the approximately 100 mm hr^{-1} runoff rates, discharges rapidly increase downslope to values in excess of those produced in the run-on/runoff tests at Avdat. Emmett's plots yield a much wider range of depths, velocities and n values for similar discharges compared to the Avdat plots as illustrated by a comparison of Table 4.6 and 4.12. The mean n for the limited data set is higher at 0.58, dominated by several particularly high and low values outside the range of the Avdat n values and contributing to the high standard deviation recorded by Emmett. It is possible that the generally higher values are due to the influence of raindrop impact which would be expected to increase resistance compared to runoff-only conditions, and also to the fact that Emmett's plots are more highly vegetated than those at Avdat.

CHAPTER FIVE RAINFALL-RUNOFF MODELLING

This chapter has three parts. Firstly it discusses the objectives of the simulation model for the analysis of arid lands hillslope hydrology and water harvesting systems introduced for the collection of runoff water. Secondly, it describes the computer simulation model itself and how it handles the different types and scales of system including the run-on/runoff plots, sections of hillslope, complete flow-lines or sub-catchments. The most important characteristics of the model are described in some detail, particularly where they illustrate certain procedural problems related to representing sequentially the contemporaneous processes of rainfall, infiltration, inflow and outflow. Thirdly, the model is used with a range of parameters derived from the Avdat field surveys to illustrate the sensitivity of the rainfall-runoff process to particular parameters and parameter combinations and the significance of these sensitivities for water harvesting system design. Additionally, the sensitivity simulations examine the importance of adopting sheetflow assumptions for the calculation of infiltration and routing rather than attempting to approximate the more complex micro-flow conditions on rough arid-slope hillsides.

5.1 THE SIMULATIONS AND THEIR OBJECTIVES

The full rainfall-runoff model requires a coupling of the routing model procedures with the infiltration modelling procedures. The objective is to simulate rainfall, infiltration and runoff in hypothetical and actual catchment situations paying particular attention to the relationship between hillslope and channel positions and how their respective characteristics influence productivity. The routing procedures and data-sets are used in four levels of simulation;

1. Sensitivity - hypothetical consideration of the sensitivity of the routing process to particular parameters and parameter combinations and their arrangements for idealised hillslope cascades of different lengths and complexity,
2. Run-on/Runoff Plots - prediction of the run-on/runoff plot observed flow using the data derived for each plot,
3. Actual Flow-Profile Cascades - theoretical modelling of actual hillslope cascade flow-profiles from the Avdat catchment system to look at the effect of interrupting flow-lines on downslope runoff patterns and water harvesting productivity,
4. Sub-Catchments - simulation of complete hydrological systems of hillslope and channel cascades in the Avdat catchment using observed input hyetographs and output hydrographs. Two sets of simulations are made: the current system (see Appendix 3.2) and the hypothetical unaltered system (see Appendix 3.3).

By simulating rainfall, infiltration and runoff under hypothetical slope conditions using process parameters measured in the field or taken from the literature, the sensitivity of the changes in runoff production to particular parameters can be identified. Increasing the complexity shows how suites of variables combine to produce significant differences in productivity patterns. In particular, the way these patterns effect water harvesting functions are of key interest.

For actual simulations, the parameters derived for the Avdat hillslopes are used to address relevant questions for water harvesting in the context of the Avdat system, and in particular the design considerations facing the positioning of the man-made channel system amidst the pattern of producing, transporting and consuming slope sections. Simulating the observed conditions for the Avdat catchment provides information on an actual water harvesting system and can identify the controls on efficiency and productivity. Manipulating the model shows the management aspects of water harvesting system development, and in particular how the current system functions relative to the same catchment in its unaltered state, or to a possible alternative design.

5.2 THE DISTRIBUTED MODEL

5.2.1 The Overall Model Structure

5.2.1.a The Model Subroutines

The rainfall-runoff model WATERH is structured as a series of sub-routines controlled by a main routine. The approach is similar to that of Kirkby *et al* (1976), who organise their model into subroutines, corresponding to sub-processes of the system, controlled by a master routine which determines the sequence of action of the subroutines and supplies them with relevant data. The main routine calls on a series of internal subroutines that handle geometric and precipitation parameter provision, the attribution of parameters to the various entities defined in the system, the routing of water throughout the course of the event in the correct sequencing, the calculation and storage of predicted output, and the maintenance of numerical stability and mass continuity (Figure 5.1). The various sub-routine FORTRAN codes are contained in Appendix 4.1 (and 4.2 for the modified run-on/runoff plot program RORO) along with relevant input and output data-sets in Appendices 3.4.1 to 3.4.17 (the flow-net digitisation and element and segment arrangement data-sets) and Appendix 4.3 (the unit and sample data set).

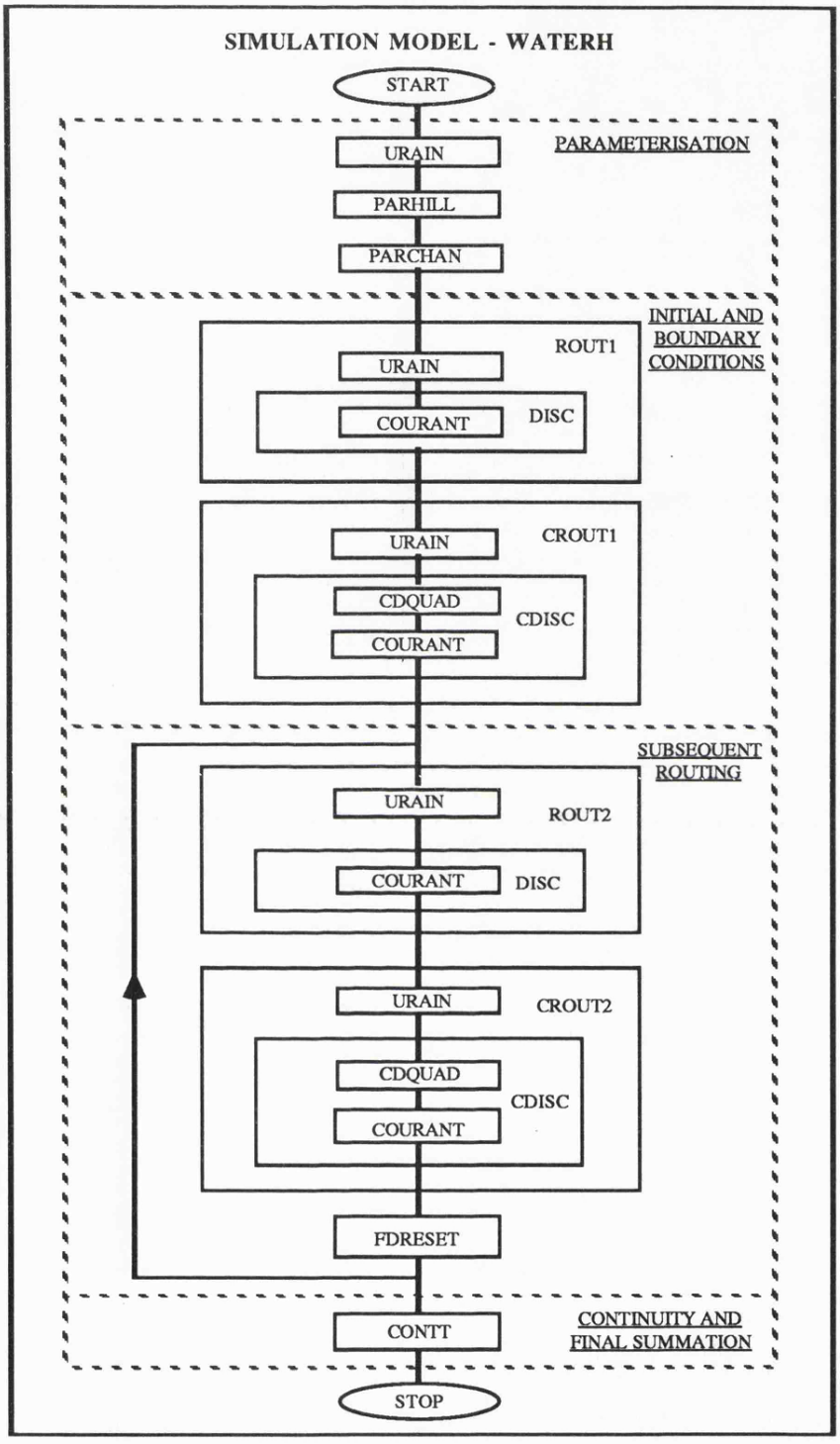

Figure 5.1 WATERH Structural Flow Diagram

The flow diagram (Figure 5.1) shows the flow of information in the main routine of WATERH and the calls to subroutines for the case of a full catchment with both hillslope and channel components. Where only cascades are simulated, the subroutines CROUT1 and CROUT2 are ignored. The structure mirrors the topological arrangement of a natural catchment system. It identifies the main

catchment, sub-catchments, sub-catchment channel branches, channel segments, lateral inflow hillslope cascades, and hillslope elements as shown in Figure 5.2. The segments and elements are the model entities and are assigned process and dimensional parameters. To provide flexibility and universality, dummy channel branches are used for varied branching patterns. The number of time stores are limited to two, the current and the previous, minimizing demands on computer memory during simulation.

The main routine of WATERH controls the complete simulation and contains two main sections, a parameter and data-input section, and an execution section. Each subroutine is described in more detail below, but briefly, the subroutine URAIN handles the reading in of hyetograph data and the provision of rainfall intensities for each time period. PARHILL and PARCHAN read in and provide parameters to the hillslope elements and channel segments in each sub-catchment and calculate the character and size of contributing area to each location. ROUT1 and ROUT2 handle the infiltration and routing of water for the hillslope elements and call on URAIN to provide rainfall intensity and DISC to calculate flow-velocity and discharge. The subroutine COURANT is called to maintain the numerical stability of the solutions to the finite difference equations. CROUT1 and CROUT2 handle the infiltration and routing of water for the channel segments and call on URAIN to provide rainfall intensity and CDISC to calculate flow-velocity and discharge. The subroutine CDQUAD is called to calculate the depth of flow appropriate to a given flow area provided by the solutions to the routing equations and COURANT is called to maintain the numerical stability of the solutions to the finite difference equations. Once each time increment is complete and each hillslope element and channel segment have been considered, FDRESET is called to update the two time stores and send flow and infiltration data to various output files. Subroutine CONTT is called once the simulation is finished to produce summary statistics used to evaluate the performance of the model and provide relevant values for the analysis of harvesting efficiency and Contiguous Area Contribution.

5.2.1.b Parameterisation

The first step in the model execution is to initialise the execution structure and provide a series of values that will determine which data sets are selected for input and output and the simulation characteristics. These include the names of the input and output files, the type of rainfall, the number of hyetographs, the type of raingauge inclination, the time increment, the number of sub-catchments, the type of hillslope dimensional data (digitised, measured off maps, or pre-calculated), the type of channel segment dimensional data (digitised, measured off maps, or pre-calculated), the number of field units used for parameter provision, the number of field samples used, and the channel infiltration assumption. For each of the units the infiltration parameters (Green and Ampt A and B) and the mean Manning's n calculated from the run-on/runoff tests are supplied. For each of the samples, the wetted-perimeter/flow-area relationship parameters (logA and B), the maximum perimeter to top-width ratio and the field unit group are supplied. Other initialisation values include the total simulation time in

seconds and the maximum iterations permissible to achieve this time for use when the time increment is variable.

Following initialisation, the model enters its parameter allocation phase. The rainfall subroutine URAIN is called to provide steady, unsteady, uniform or non-uniform rainfall. Rainfall is simulated as discrete constant intensity blocks with a procedure capable of supplying an average intensity block, should a time increment fall between two digitised intensities. A predicted set of hydrograph data and observation times are provided for the subcatchments, and/or the complete catchment (if more than one sub-catchment is simulated). The observation times are in seconds from the time of first runoff and not from the start of the rainstorm, due to the lack of synchronisation between the historical meteorological and hydrologic records available for Avdat. Additionally, intermediate hydrographs and cumulative data about the contributing area are collected at any predetermined location by providing the array subscripts of those channel segments or hillslope elements. This is used to specifically address the question of spatial variability of runoff characteristics in the catchment area.

To allocate the macro-topographic dimensions of the channel branches, branch segments, segment contributing hillslope cascades, and hillslope cascade elements, a looping structure is adopted based on the topological/gravitational ordering of the set of branches, the sub-set of segments, the sub-sub-set of cascades, and the sub-sub-sub-set of elements. The subroutines PARHILL and PARCHAN are called during these procedures to perform the parameter provision.

Firstly, each sub-catchment is considered separately (since they are not dependent on each other for their flow conditions). Secondly, the number of branches is supplied which is based on a symmetrical network using a Strahler bifurcation (two first orders equal a second order, two-second orders equal a third order, etc.), with an asymmetrical structure handled by using dummy branches. The parameters ensure the model automatically assigns dummy elements with zero characteristics and ignores them during routing.

For each branch the number of segments are given, for each segment the number of hillslope cascades, and for each cascade the number of hillslope elements. An option is available to consider cascades that do not discharge into a channel. This is required for simulating single hillslope cascades. Where a branch is allocated zero segments, it is a dummy. Where a segment has only one cascade, it has a raised bank on the downslope side (man-made ditch) or else the contributing hillslope is too short for a cascade to be outlined on the flow-net as explained in Chapter Two. When there are no channel branches specified, the procedures for a single cascade are used and all the channel calculations are ignored.

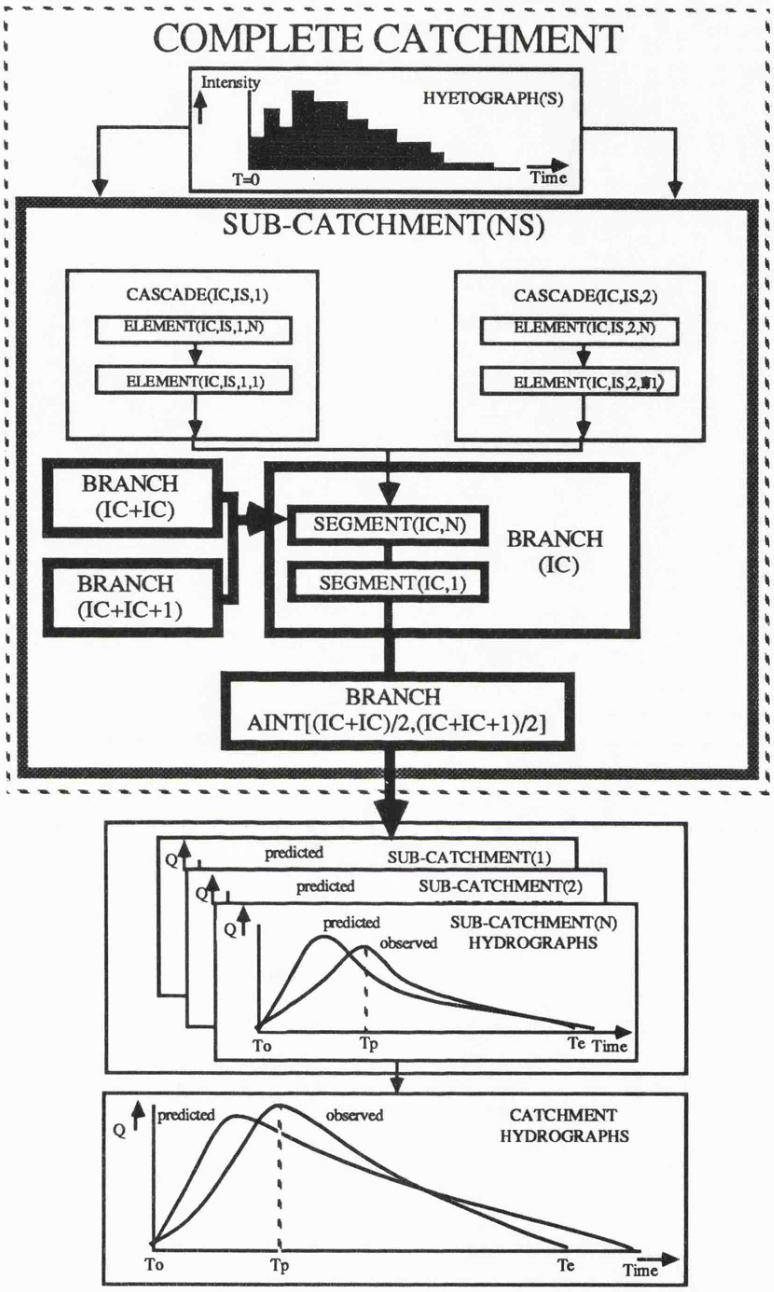

Figure 5.2 WATERH Networking System and Notation

The appropriate hyetograph, field sample and unit identifiers are assigned to each element and section from detailed maps prepared prior to simulation and their characteristics are entered into the relevant stores during the initialisation. The flow net can be supplied as follows;

1. in digitised form as pairs of nodal (X, Y, Z) coordinates,
2. the plan lengths of the boundaries of each entity plus the diagonal for the hillslope element, the plan length of the channel and the contour heights of the lower and upper boundaries measured from the flow-net,

3. in pre-calculated form as length, width (for hillslopes) and slope gradient.

In the current study, option one is used. For the individual channel sections the mean Manning's n applicable to the section, the bed-width (zero for a triangle), the east and west bank angles, the maximum depth and the type of overflow section are supplied.

For the hillslope elements, using the trigonometry of the shape described by the four points, a geometric simplification represents the surface between them as a rectilinear plane with a length and gradient equal to the average of the two orthogonals, and an area equal to the trapezium described by the four points, preserved by varying width. For the channel segments, the last pair of (X, Y, Z) coordinates of the nodes of the cascades (the channel line and the flow-line intersections) are used to geometrically simplify the segment as the straight line length and gradient between the two nodes. By keeping a cumulative account of the surface area of each element and each upstream element(s), the changing nature of the contributing area is known. This is significant for the interpretation of the productivity of a given location in per unit area terms and in the determination of Contiguous Area Contribution characteristics. The character of the surface area largely determines the kinds of productivity and transmissivity observed.

5.2.2 Boundary Conditions

Since the finite differencing technique is a backward single-step variety, only process stores for two time iterations are needed, the current elapsed time (t) and the previous elapsed time (t-1), since only these are relevant for the hydrological state at any time. The updating of the time stores is made at the end of each time iteration by subroutine FDRESET, the finite difference reset routine. If required, a variable time increment can be selected to help preserve continuity.

Subroutine ROUT1 is called by the master program to handle the boundary conditions for hillslope routing for the first time iteration from time equals zero. Subroutine ROUT1 calls on URAIN, DISC and COURANT and controls the input of water to the hillslope element, its infiltration, and its movement for the first time period. The boundary conditions are that the surface is initially dry in all elements, and there is no discharge in or out during this period. In addition, the upper physical boundary condition states that if a hillslope element is the uppermost in a given cascade, or if a channel segment is the uppermost in a first-order channel branch, then there is no discharge inflow from the previous element or segment (x-1, t-1) at any time state. For the channel segments the initial boundary conditions are slightly different than for the hillslope elements. Conditions are initially dry with no pre-existing surface storage, and no inflow from the upstream channel segment(s), or outflow to the downstream segment occurs during this time period. However, there is lateral inflow from the contributing hillslope cascades as determined by the continuity equation.

The subroutines ROUT2 and CROUT2 handle the infiltration from rainfall and surface water and its routing down the hillslope elements for the time periods from time increment 2 to the final time. They account for inflow from upstream or upslope, and outflow to downstream or downslope, calculated as the balance between the discharge inflow (x-1, t-1) and outflow (x, t-1).

5.2.3 Hillslope and Channel Flow Routing

For each time step, a call to URAIN provides the rainfall input, adjusted to the correct intensity if the raingauge measures in the vertical plane as opposed to normal to the slope. Subsequently, infiltration must be calculated and the continuity balance made to determine the rainfall excess for the time period. This requires a consideration of the temporal sequencing of contemporaneous processes and how to procedurise the chosen conceptual approach to infiltration.

5.2.3.a The Approach to Infiltration

There can be two components of surface water input into the element; rainfall and discharge in from upstream or upslope. This is complicated by the fact that surface runoff may not be assumed to occur as a uniform sheet over all surfaces, but its flow shape and contact area as it moves over the surface are conditioned by the micro-topographic profile. Rainfall is uniformly distributed over the complete surface area, whereas surface runoff may only cover a proportion of the surface. In this case, it is logical therefore to consider infiltration from rainfall into the whole surface, and infiltration from runoff (run-in pre-ponding, run-in and runoff post-ponding, or run-in post rainfall) into the partial surface. This has been discussed in Chapter Three.

One of two assumptions can be made concerning channel infiltration. Since no field tests are undertaken of bank infiltrability, it is assumed that the infiltration rate is identical to that of the adjacent hillslope surface, or alternatively, that the infiltration in the channels compared to that on the slopes is minimal and therefore can be assumed zero. This is analogous to Woolhiser's approach in the model KINEROS 85 (Woolhiser, pers.comm. 1985). For the full Avdat sub-catchment simulations the zero option is selected.

5.2.3.b The Procedures for Calculating Time to Ponding

The time to ponding and runoff generation is calculated using the Green and Ampt equation storage approach. No runoff is assumed to occur until a storage depth is filled calculated by substituting a constant input rate p into the equation and deriving t_o, the time to ponding, and V_s, the depth required for ponding. Where t_o is less than the elapsed time since the start of input, then runoff

is allowed to begin. On the assumption that rainfall does not fall to zero during the rainfall event, runoff can be considered Hortonian once storage is filled. This is valid when the same intensity is maintained since rainfall is always in excess of infiltration capacity, or when runoff passes through the system maintaining water availability at a high level. Where rainfall and runoff fall below infiltration capacities then there is unfulfilled infiltration and subsequent infiltration rates should be adjusted to prevent underestimation. However, this is difficult to procedurise both in terms of the model and in terms of the data-sets used. Ideally, what is required is a series of infiltration equations in which the coefficients A and B are not constants, or in the case of Scoging (1988), wet or dry (AD, BD or AW, BW) but are a function of the applied water and the timing of application (A,B = f{p,t}). This is beyond most field studies and model applications and so approximations are made. In the case of the storage model, the approximation is that post-ponding ($t \geq t_0$), infiltration operates in a Hortonian sense.

However, this does not tackle the problem of how to procedurise situations where rainfall intensity is not constant from time t_0. In her testing of the storage approach, Scoging adopts first minute rainfall rates guaranteed to produce runoff rapidly (i.e produce a t_0 less than 60 seconds). Under actual conditions precipitation is variable, for instance for catchment simulations at Avdat. In the model WATERH, the input of water to an element, both from precipitation and run-on, is calculated as a rate (cm s^{-1}). Where this is less than the infiltration parameter A, it is not assumed to contribute to an increase in the soil storage as shown in Chapter Three. Where it is greater than A, a cumulative store is calculated from which the average rate is derived for use in calculating the time to storage filling (Equations 3.15 and 3.17 are used to give t_0 and V_S). The time t_0 is compared to the individual time counter (the elapsed time since the input exceeded the rate A) and ponding is predicted once this time counter is greater than or equal to the time t_0. The assumption is made that the infiltration potential into the whole surface must be satisfied so that in the case of run-on prior to ponding, the water is added to the general store and an average depth over the surface length is calculated. Once the predicted t_0 is positive, and less than or equal to the elapsed time (as explained in Chapter Three) then ponding occurs and the rest of the infiltration regime is considered Hortonian with predicted infiltration capacities compared against instantaneous input.

5.2.3.c Calculating Post-Ponding Infiltration

The potential infiltration loss into the complete perimeter is calculated as the product of the infiltration rate at time t and the maximum perimeter. In the case of the channel this is the normal flow section described by the geometry parameters, and in the case of the hillslope it is the length multiplied by the ratio of perimeter length and the plan width established from plot micro-topographic profiles. Infiltration is assumed to act perpendicular to the surface rather than in the vertical. This is most appropriate for the short duration, low magnitude rainfall events where infiltration rates are not at

their steady-state and suction forces are dominant. For longer duration events with greater depths, it would be more appropriate to consider infiltration as operating vertically and proportional to plan width, since gravitational forces dominate. However, the former case is considered acceptable for each of the rainstorms simulated.

Since the continuity equation works in the dimensions of flow-area as shown in Chapter Four, the product of the surface length and the infiltration rate is multiplied by the time increment to give the total area of water that could be infiltrated over the surface in the model time step. The rainfall depth in this time increment is multiplied by the plan width to give the equivalent rainfall area. If this is greater than the potential infiltration loss then rainfall excess is created which can be routed downslope or down-channel (this is considered a positive infiltration area). If this is less, then there is still potential infiltration unfulfilled (a negative infiltration area). If there is no surface water storage in the element from earlier ponding and if there was no storage in the contributing element(s) in the previous time period (and hence no discharge in during the current time period as dictated by the continuity equation) then the infiltration remains unfulfilled (as with the Hortonian approach). If there is storage and/or a positive inflow/outflow residual then infiltration is abstracted from this area of water.

5.2.3.d Net-Storage Change

To achieve the input-output-storage balance, the continuity equation is accounted firstly for just existing detention storage A(x, t-1), inflow Q(x-1, t-1) and outflow Q(x, t-1). This gives the storage balance. If this is positive and the potential infiltration is also positive then the two are added to give the total storage from inflow/outflow and rainfall excess. If the potential infiltration is negative then this must be subtracted from the storage balance. The current approach allows for both sheetflow and complex flow situations and therefore differs from most other approaches. For the channel geometry or the complex flow approach, a relationship is established between boundary length and flow area and so provides the wetted surface length to go with any calculated area. The assumption is made that infiltration will only take place through this wetted length. Therefore the potential unfulfilled infiltration, calculated for the complete surface length, must be adjusted by the ratio of the actual wetted length and the total surface length. Although this is obviously an integral process, with the wetted length decreasing in proportion to the infiltration subtracted, it is assumed that the wetted length for the storage area prior to infiltration is a sufficient approximation. This is calculated by substituting the scaled area into the logWP-logA relationship for the hillslopes, and the full area into a series of quadratic equations contained in subroutine CDQUAD for the channels. This checks to see if the area is greater or less than the maximum that can be held by the normal channel and then calculates the maximum depth associated with this area. This can then be used to calculate the wetted boundary length in the normal channel and/or the overflow section.

5.2.3.e Discharge Calculations

The residual of the storage area and adjusted potential area infiltrated provides the outcome of the continuity equation A(x, t). This can then be used to produce the discharge for the hillslope or channel that will be used as the outflow (and inflow to the elements it contributes to) in the subsequent time period (current for hillslopes to channel inflow). This is accomplished using Mannings flow equation in subroutines DISC and CDISC which are called from the ROUT and CROUT subroutines as shown in Figure 5.1. The hydraulic radius is calculated using either CDQUAD for the channels or the hillslope WP-A(x,t) regression equation scaled according to the ratio of the element plan width and the micro-topographic width of 190 cm. Manning's coefficient of resistance n is supplied from field tests as discussed earlier and the slope gradient is calculated for each element by the model. The adjustment of 4.64 is used in calculating discharge since all units are in cgs as explained in Chapter Four.

5.2.4 Cumulative Calculations, Stability and Output of Predictions

5.2.4.a Avoiding Numerical Instability and Error Calculation

During each call to the subroutines DISC and CDISC the numerical stability of the explicit finite difference solution is considered. The solution must be kept in the stable domain as defined by the Courant stability criterion;

$$\Delta t/\Delta x \leq 1/[v+\sqrt{(g.y)}] \qquad \text{Equation 5.1}$$

(where g is gravity 981 cm s^{-1} s^{-1}, v is velocity cm s^{-1}, y is depth cm, Δt is time increment seconds, and Δx is distance increment cm).

There are two approaches that can be taken to ensure that the criterion is never violated. The first is to set the time increment at a very small constant value, and the second is to alter the time period during the simulation so that the criteria is never violated but that the time increment can be as large as possible to facilitate efficient computation. This is particularly relevant for the pre-ponding phase, the initial rising limb and on the recession limb of the hydrograph. A constant time increment structured to produce stability at the most critical point, the rapid discharge state at flow peak, is unnecessary and wasteful, since the early rising limb, and the recession limb of the hydrograph require markedly lower resolution. In a complex model, the choice of time step is very important for overall stability as was observed by Rogers *et al* (1985) who adopt a shorter time step for finer grid spacings as required by the Courant condition.

The approach selected depends on the type of simulation being undertaken, sensitivity analysis or real simulation. For the real simulations, the smallest time increment is set at one second. This is small enough to be below the critical Δt calculated for all the hillslope and channel Δx increments with a sufficient safety margin. If the computed minimum Δx for stability is in excess of the current model time-step by a sufficient amount (a factor of ten), the time step is increased to allow more rapid execution of the computations and a lower cpu-time for the program execution. The opposite occurs if Δt is ten seconds or larger and the computed critical Δt falls to between ten and twenty times below this. The model time-step is then decreased to one-tenth of its previous size (down to a minimum of one second). The time increment is the only denominator/numerator in the Courant stability criteria that is independent and flexible in the value it assumes. If only one entity is susceptible to numerical instability the time must be changed since the program is only as strong as its weakest link, and the formation of a kinematic shock at one location may be enough to crash the program if the new flow area or depth calculated by the continuity equation fluctuates between positive and negative with the passage of the wave (as explained in Chapter Four).

The situation is different for the assessment of sensitivity to a variety of parameter combinations. Models are sensitive to the time step itself, most importantly for calculating infiltration. The time increment is therefore kept constant at one second to prevent the introduction of an uncontrolled source of variation independent of the effects of the controlled variation in slope length and configuration on patterns of downslope discharge.

Once each sub-catchment calculation is complete, subroutine CONTT checks to determine whether the law of mass-continuity has been obeyed. The total rainfall into the sub-catchment is set to the cumulative rainfall volume into the outflow segment contributing area, the total infiltration into the sub-catchment is set to the cumulative infiltration volume into the outflow segment contributing area, and the total residual storage volume is set to the sum of the hillslope and channel residual volume running totals. The sub-catchment volumetric error in the mass continuity equation becomes;

Error = Rainfall - Infiltration - Discharge - Residual volume Equation 5.2

This is converted into a percentage error by dividing the volumetric error by the volumetric rainfall input and multiplying by one hundred. The percentage error is checked to see if it is within acceptable bounds of rounding errors, or reflects a mis-calculation resulting from program bugs or the development of a stability problem that results in unreal stage discharges at certain susceptible locations in the catchment (identified in calls to subroutine COURANT).

5.2.4.b Calculating Predicted Hydrological Response

The subroutine FDRESET resets the current time increment (t), to the previous time increment (t-1) for all the relevant stores. It calculates predicted hydrographs at comparable observation times to the observed, and calculates additional intermediate hydrographs at other locations. On each entry the elapsed time is compared against several time counters. This looks to see if the simulation should be terminated, whether the time at which predicted hydrographs should be calculated for direct comparison against observed for the sub-catchment or complete catchment, or whether a pre-determined time has elapsed after which intermediate hydrological results are recorded for specific locations pre-assigned in the simulation initialisation. These pre-determined locations are important for illustrating and understanding the nature of the water harvesting system relative to the spatial variability within the system. By comparing the array identities of each hillslope element and channel location against the identities supplied during the initialisation the correct calculation can be made for the correct location at the correct time.

5.2.4.c Calculating Indices of Productivity and Harvesting Efficiency

The model takes the final cumulative rainfall, runoff and infiltration values along with any residual storage remaining, for each of the channel segments and hillslope elements in each branch (excluding the dummy branches) and segment hillslope cascade, respectively, and calculates two indices of productivity. These are designed to address the questions central to the model application for the current research, namely the spatial distribution of runoff productivity and efficiency within the routing network. By determining the ratio between total volumetric inputs and total volumetric outputs, the percentage runoff efficiency of the entity can be shown as a measure of its relative ability to produce runoff water. In addition, by determining the net balance between the volume of water entering the entity from its contributing area, and the volume exiting the entity, the productivity and transmissivity of the entity can be established per unit area, with the most important net producers and net consumers of runoff water identified in volumetric terms along with their importance to the absolute production and loss of water.

The percentage runoff efficiency establishes the relative abilities of different locations to convert incoming water to out-going runoff. The productive index is calculated to illustrate the order of magnitude of the productivity and transmissivity of each element, i.e. the absolute additions or subtractions to flow generation produced by the element in cubic centimetres per square metre. This identifies the consumers and producers within the system since the discharge coming in is compared to the discharge going out during the course of the simulation to determine the net difference in volumetric terms. Dividing this by the element area (calculated by subtracting the previous contributing area from the current) standardises for the effect of different element sizes on the calculated volumes. If the

productive index is negative, the element is a net consumer of surface flow, if the value is zero the element is a transporter of surface flow, a conveyor in which no additions to the total flow are made, and if the value is positive, the element is a net producer of surface flow.

The subroutine CONTT takes the final cumulative calculations for the sub-catchment and establishes the spatial variability in runoff productivity per square metre, and runoff production efficiency for each entity comprising the catchment to illustrate the objectives of the modelling exercise for the Avdat water harvesting system.

5.2.4.d Hydrograph Output

The simulation is finished when the cumulative sum of Δt increments equals the pre-set elapsed time at which the simulation should stop. This is equal to the known duration of the observed flood event with a convenient addition designed to ensure that any model lags between observed and predicted runoff hydrographs, and also any synchonisation errors in the original data set will not terminate the simulation until the predicted flood event is complete. For the final stage of the Avdat analysis and model evaluation, the sub-catchment predicted hydrograph information is calculated and converted to the time units of hours, and volumes of m^3 adopted in the observed hydrographs from the model internal units of seconds and cm^3. The two are then directly comparable. Additionally, if more than one sub-catchment has been considered during the simulation and a predicted hydrograph required for the complete catchment this is calculated during each subsequent simulation of the remaining sub-catchments and prior to termination of the complete catchment simulation. Predicted data sets can then be used in MINITAB, or in micro-computer spread-sheet programs for statistical analysis and graphical presentation of hydrological characteristics and observed-predicted relationships.

5.3 APPLYING THE MODEL USING A STRUCTURED APPROACH

A suite of simulations have been structured so that the nature of hillslope hydrological response on Avdat catchment hillslopes can be examined and some general principles of arid-land hillslope hydrology under spatially and temporally variable conditions can be identified. From this, the key characteristics and influences on the productivity of a catchment water harvesting system can be determined. Not only do these simulations provide indications and some explanations of the character of the hydrological systems in the Central Negev Highlands, they also provide a rigorous examination of the ability to both conceive and model the processes responsible at the intra-hillslope and intra-channel branch scale, and ultimately the ability to reproduce the resultant catchment scale response. Whether the differences between predicted and observed values result from the problems of modelling the complex system or providing the parameters in a sufficiently representative manner are apparent.

The first phase is a suite of hypothetical simulations designed to determine the robustness of the model under a range of input conditions, and to evaluate, through sensitivity analysis, the relative impact on the results of the model of individual parameters under controlled conditions. This also illustrates key principles important for determining the known characteristics of arid-lands hillslope hydrological response. The suite of simulations and their results are presented in the following sections. The second phase simulates the run-on/runoff plots, the third phase simulates full flow-line cascades from the Avdat eastern sub-catchments and the final phase simulates the Avdat sub-catchments and the unaltered catchment. These last three phases are discussed in Chapter Six.

5.3.1 Sensitivity Tests and Hypothetical Simulations

These sensitivity tests are designed to accomplish three things;

1. to analyse the affects of different parameters on hillslope runoff response to rainfall,
2. to focus on the factors significant for controlling water harvesting system productivity, namely the scale of and distribution of flow parameters along a flow-line,
3. to test the affect of certain routing assumptions related to the use of sheetflow or complex flow, particularly on the interaction of the infiltration and routing components.

A discussion of approaches to sensitivity discussed in the literature is relevant, showing which parameters have been the focus in previous studies. Bathurst (1986b) assessed the sensitivity of the SHE distributed model to structural parameters such as time and space steps as opposed to catchment parameters such as soil conductivity and flow resistance. He sought to identify which catchment parameters were the most significant and how accurately they should be defined for adequate predictions. He used two rainstorms and analysed the predicted hydrographs relative to a calibrated optimum parameter set derived from previous simulations using a wider range of five hydrographs. The difference between the observed, the best-fit (using the calibrated set) and the predicted using the sensitivity data-set illustrate the effect of using particular parameters. He found that the model was as sensitive to the structural parameters as the catchment ones. One of the major conclusions was that the time and space steps of the simulation should be small in comparison with the scales of spatial and temporal variations they are used to represent. Bathurst's method of sensitivity analysis, however is at variance with the requirements at Avdat where optimisation procedures are not warranted. As Bathurst noted, there are several equally satisfactory calibrations based on different combinations of structural and catchment parameters and so the problem of equifinality blurs the picture of true sensitivity to single influences. Working at a smaller and less complex flow-scale and increasing complexity would allow a greater understanding of the process-response of the system in question.

Rogers *et al* (1985) considered the humid-zone Institute of Hydrology Distributed catchment model. They performed their sensitivity analysis to determine which parameters had the greatest control on the predicted output from their distributed model. They used five storms and looked at the effect of the changes of parameters on the overall storm hydrograph from the complete catchment system. Both the model parameters (saturated conductivity Ks, and Chézy's flow resistance coefficient C) and the process parameters (grid spacing and time step) were selected for examination. The best-fit predictions were used in subsequent simulations as 'optimum' parameters. The parameters were calibrated on the basis of this sensitivity analysis.

Scoging (1988) focused her sensitivity tests on the assessment of the influence of specific variables on the character of flow under constant space-time and variable space-time conditions at the intra-hillslope scale. Scoging looked at the variables of Manning's n, rainfall intensity, infiltration, spatial arrangement of infiltration, and spatial dimensions and performed 23 different simulation runs. Scoging's approach is the most relevant to the current study since the resolution of the process is very important and lumped sensitivity tests such as Rogers *et al*, followed by calibration are not warranted when considering water harvesting productivity using distributed, physically based procedures. Since the individual flow-line responses are critical for the catchment-wide response and since the pattern of spatial variation that results from downslope arrangement of parameters is a likely major control, the sensitivity analysis must be at the appropriate scale. To understand the flow-line response requires an understanding of the role of individual parameters and their spatial arrangement and combinations. The influence of flow-line length must also be understood. To develop this understanding, a small set of parameters representing the range of conditions on the Negev hillslopes and within the Avdat water harvesting system are required. The sensitivity to variations in single or combinations of the following characteristics are examined; slope gradient, slope resistance coefficient (Mannings n), flow boundary shape, infiltration regime, rainfall intensity and distribution, spatial arrangement and hillslope scale. For sensitivity assessments, only the hillslope flow is considered, the assumption being that the character of the channels will only modify the timing of the catchment hydrographs, contributing a limited volume of water through direct runoff due to the small proportion of surface area. The role played by the channels can be determined in actual simulations of Avdat sub-catchments.

The benefits of selecting parameters using the range of conditions found at Avdat and based on statistical selection criteria include the following;

1. the values are within the orders of magnitude found within the catchment,
2. they are systematically selected using consistent criteria,
3. they can be directly related to actual simulations carried out using the full data-sets.

The following sections describe the nature of each of the parameters selected and how they can be used to illustrate the sensitivities. Of greatest interest is the significance of the parameters for flow generation, transmission and consumption and on a relative scale, the parameters are classed according to whether they will be a relative enhancement to runoff production and transmission or an inhibition. Each of the parameters are in cgs units throughout.

5.3.1.a Local Slope Gradient

In the field survey, 127 plots were sampled for micro-topography and the best-fit line through the profiles obtained. The slope of this line approximates the local hillslope gradient which can be used to represent the range of slope gradients found at across the Avdat flow-lines. The mean and the standard deviation are 8.28° and 6.88° respectively and provide the parameters in Table 5.1

Table 5.1 Slope Gradient Sensitivity Parameters

Code	Significance	Source	Degrees	Sine
1	Control	Mean	8.28°	0.1440
2	Flow Inhibiting	Mean - 1 SD	1.40°	0.0244
3	Flow Enhancing	Mean + 1 SD	15.16°	0.2615

5.3.1.b Slope Resistance Coefficient (Mannings n)

From the Avdat run-on/runoff plots, a series of Mannings n values were calculated for the two flow assumptions of sheetflow and complex flow as explained in Chapter Four. The mean and standard deviation for the 32 observations are 0.356 and 0.134 for the sheetflow approach, and 0.639 and 0.282 for the complex approach respectively. In order to isolate the effect of single variables, only one set of Mannings n is required for use under both boundary shape assumptions, since then the effect of boundary shape alone can be identified. The sheetflow n values are selected for the sensitivity tests and are presented in Table 5.2.

Table 5.2 Mannings n Sensitivity Parameters

Code	Significance	Source	Value
1	Control	Mean	0.348
2	Flow Enhancing	Mean - 1 SD	0.218
3	Flow Inhibiting	Mean + 1 SD	0.478

5.3.1.c Flow Boundary Shape

Choosing two flow boundary shapes tests the sensitivity of runoff productivity and routing to;

1. micro-topography,
2. adopting the sheetflow assumption or the complex flow assumption in flow modelling.

This is done by considering flow over a plane (sheetflow and micro-topographically smooth flow routing surface) and flow over a micro-rilled surface (complex flow and micro-topographically rough surface). Flow shape is handled by the relationship between wetted perimeter and cross-sectional area discussed in Chapter Four (Table 5.3). An idealised micro-topography is used that has the same ratio of maximum wetted perimeter (WPmax) to plan width (wid) as all composite profiles of the 127 Avdat sample plots (Equation 5.3). The relationship applies to 190 cm wide section of hillslope and must be used with scaled flow areas based on the actual plan width of model cells.

$$WPmax = 1.025\ wid \qquad \text{Equation 5.3}$$

Table 5.3 Flow Boundary Shape Sensitivity Parameters (units of cm)

Code	Significance	Flow Assumption	Relationship	WP/w Max
1	Flow Inhibiting	Sheetflow (smooth)	log WP = 2.28	1.000
2	Flow Enhancing	Complex Flow (rilled)	logWP = 0.84 + 0.496 logA	1.025

5.3.1.d Infiltration Regime

For the purposes of illustrating the effects of different infiltration conditions, three infiltration A and B parameter sets are used. The first, the control, is an impermeable surface with infiltration set to zero throughout. The others are represented by two of the original plot infiltration curves. The three are used to parameterise the plot conditions for different roughness and gradient combinations, hyetographs and spatial configurations. One set of parameters represents a surface with a low final infiltration rate and relatively shallow curve, the other represents a high final infiltration rate with a steeper rate of change through time. The A and B parameters are derived from the run-on/runoff plots through the fitting of the Green and Ampt equation to the field data.

Table 5.4 Infiltration Regime Sensitivity Parameters (units of cm s^{-1})

Code	Significance	Equation
1	Impermeable (control)	i = 0.0
2	High Productivity	i = 0.000047 + 0.109/t
3	Low Productivity	i = 0.000359 + 0.149/t

5.3.1.e Rainfall Intensity/Distribution

From the literature (Button and Ben-Asher, 1983) and from an analysis of the Avdat rainfall record since 1961, it can be seen that the maximum rainstorm depth with a one year recurrence interval (RI) is 14.0 mm (Appendix 1.6). For the simulations, a constant total depth of 10 mm is selected which has an RI of 0.55, i.e. will occur on average almost twice annually and which is generally above the total depth threshold at which runoff will be generated from Negev hillslopes and the Avdat system. This of course depends on the intensity and its timing.

To contrast the sensitivity to different rainfalls, the total yield is kept constant at 10 mm but the intensity and intensity distribution varied to produce four types of hypothetical rainstorms. They are;

1. a high intensity, short-duration event (40 mm hr^{-1} for 0.25 hours with a 20.0 recurrence interval). This is assumed the control,
2. a lower intensity, longer-duration event (10 mm hr^{-1} for 1.0 hours with an 8.0 recurrence interval),
3. a decreasing intensity distribution event with each intensity-duration increment having a 1.5 recurrence interval (see Figure 5.5),
4. an increasing intensity distribution event with each intensity-duration increment having a 1.5 recurrence interval (see Figure 5.6).

These are illustrated in Figures 5.3 to 5.6. The recurrence intervals are calculated by Button and Ben-Asher (1983) from 7 years of Avdat data, and relate to the maximum durations of different intensities from an annual extreme series. This shows that although a 10 mm rainstorm may occur twice a year, one produced by intensities averaging higher than 40 mm hr^{-1} will only occur every 20 years. It is therefore an extreme example.

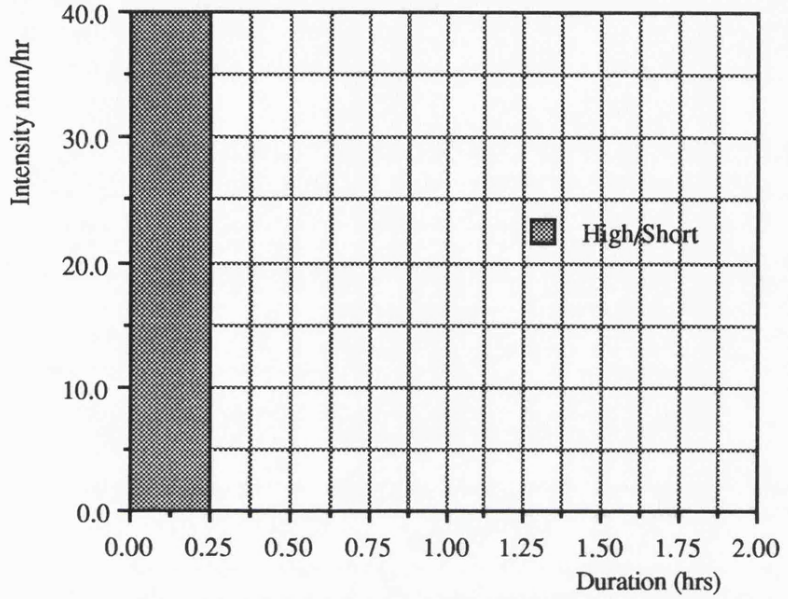

Figure 5.3 Rainfall Hyetograph for Sensitivity Simulations - High/Short

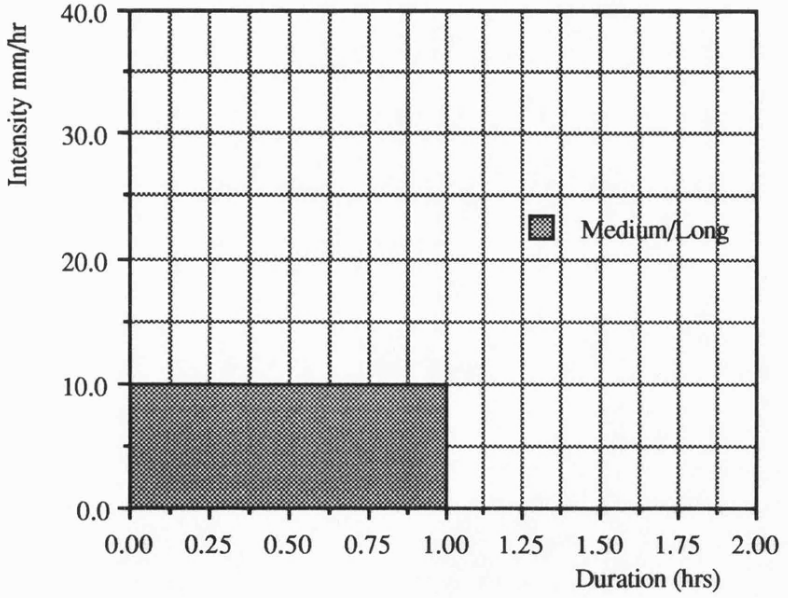

Figure 5.4 Rainfall Hyetograph for Sensitivity Simulations - Medium/Long

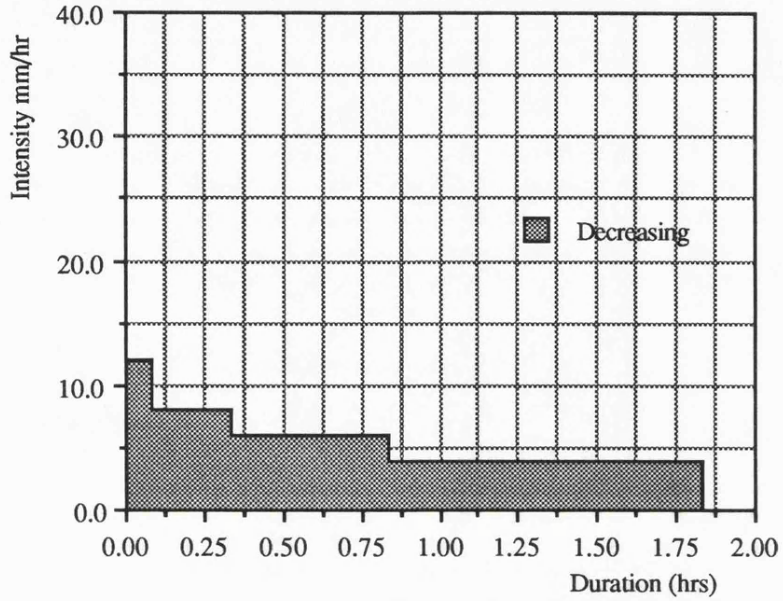

Figure 5.5 Rainfall Hyetograph for Sensitivity Simulations - Decreasing

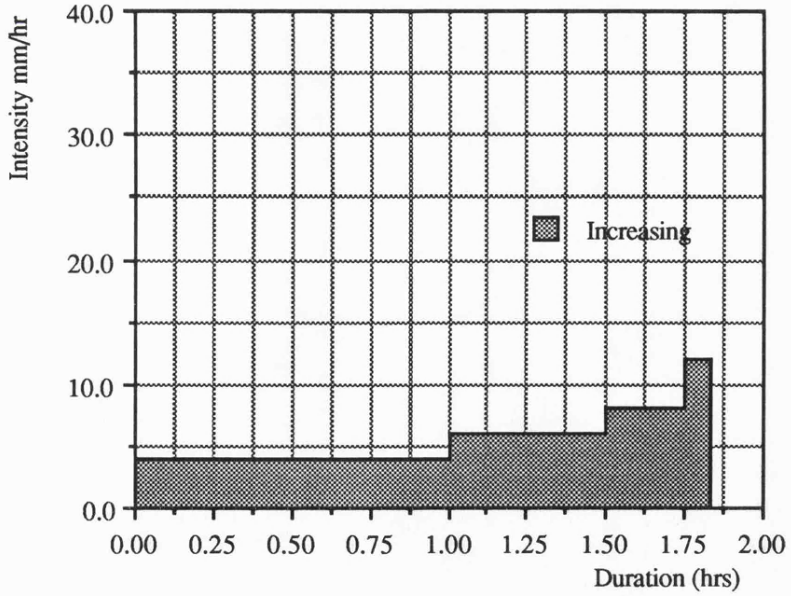

Figure 5.6 Rainfall Hyetograph for Sensitivity Simulations - Increasing

5.3.1.f Spatial Arrangement

Both single and multiple cells are used to show the effect of slopes in isolation and as part of a complex cascade. A simple square hillslope is used, ten metres by ten metres and sub-divided into ten

constant width Δx increments, each one metre long. The coordinates of the left and right nodes of each upper and lower boundary is calculated for each slope gradient, and each spatial arrangement of slope gradient (constant, increasing and decreasing as described below). For the single slope cells there are 11 pairs of nodes describing the cell. The hydrological data is recorded for the last one-metre increment of the cell (element 1).

Two plots are used in a cascade to show the effects of spatial arrangement. The different types of spatial arrangements relate to the attributes of an upper and lower group of cells in a flow sequence. Each cell is subdivided into one-metre increments, giving a total slope length of 20 metres with 21 pairs of nodes. Of importance is the sensitivity of runoff production to conditions where flow productivity and transmissivity increases downslope (Improving), decreases downslope (Worsening) or are constant (Control). This shows a small range of the effects of spatial variation and illustrates the knock-on, productive effects of upper slopes, and the stopper, consumptive effects of lower slopes in particular conditions. The hydrological data is recorded for the tenth (element 11) and twentieth (element 1) one-metre increment in the cascade.

5.3.1.g Slope Scale

The sensitivity of runoff production to the length of the slope illustrates the Contiguous Area Contribution concepts and the characteristic of arid areas that an increasing basin size, all things remaining equal, will result in increasing discharge at a decreasing rate. How this changes with different parameter characteristics is an important indicator showing the role of re-infiltration which controls the development and suppression of Contiguous Area Contribution. Four ten-metre cells are linked in a cascade and the productivity change downslope at elements 31, 21, 11 and 1 assessed.

5.3.2 Methods of Results Analysis

For each simulation the following characteristics are recorded;

Qp = steady-state and/or peak discharge in $cm^3\ s^{-1}$,
Vp = steady-state and/or peak velocity in $cm\ s^{-1}$,
Ap = steady-state and/or peak flow cross-sectional area in cm^2,
Tsp = time to steady-state and/or peak discharge in s,
Tep = time to end of steady-state (= Tsp when peak only) in s,
ΣQ = volumetric discharge in m^3.

The time distribution of instantaneous discharge Q_t, velocity V_t and flow area A_t are plotted based on an observation frequency of 50 or 100 seconds depending on the total simulation time. This

produces a smooth hydrograph shape in each simulation and highlights the major differences between simulations in terms of the gradients of the rising and recession curves and the length of the steady-state discharge, if reached, or the height of the peak if not. The overall differences in terms of the timing, the rising and the falling limb show the sensitivity of flow conditions to parameters.

The variations in these parameters and the hydrographs can be used for consideration of the relative characteristics resulting from any parameter combinations. A control parameter combination is selected as a base against which the responses of other parameter combinations are assessed in relative terms. For comparisons to the control, the percentage variation (%V) is calculated between the control value and the other values for Qp, Vp, Ap, and ΣQ.

$$\%V = [(\text{Control} - \text{Other})/\text{Control}] * 100 \qquad \text{Equation 5.1}$$

A negative %V shows the other value is greater than the control and vice versa. The largest positive percent is 100 because peak discharge, velocity, area or time to peak cannot be negative. The negative percent size depends on the degree to which the other simulation exceeds the control in relative terms. The direction and the magnitude of the variation are the indicators of sensitivity. Additionally, the hydrographs are compared visually by plotting to provide the overall picture of variation between different parameter combinations.

5.3.3 The Single Plot Cascade Simulations

5.3.3.a Parameter Values and Their Hydrological Significance

The control simulation, against which the relative characteristics of all the other simulations are compared is that representing the intermediate parameter conditions for flow routing using data collected in the Avdat catchment area. The mean roughness coefficient n, and the mean slope gradient S are used with the sheetflow, micro-smooth surface dimensions (for which the roughness coefficients were derived) and zero infiltration. The input is the high-intensity short-duration rainfall producing ten millimetres in 15 minutes as described in Section 5.3. Because the simulations involve modelling rainfall and runoff on hillslopes possessing complex combinations of five different parameters, a simple code is used to allow the identification of each of the parameters associated with each simulation.

Code = R I n G D

(where R is the rainfall, I infiltration, n Mannings roughness coefficient, G gradient, and D flow dimensions)

Referring to Tables 5.1 to 5.4, the control is therefore coded '11111'. To help with understanding these code numbers and their significance in terms of parameter combinations the parameter code and code number, control or effect and value or type is summarised in Table 5.5. The control allows quantitative and qualitative comparisons of the effects of changing different parameters whilst keeping others constant, the range of observed responses showing the sensitivity of the routing process and the model simulations to particular parameters. For the single cells, with four rainfall parameter sets, three infiltration, three roughness, three gradient, and two surface dimensions, the full matrix has 216 combinations. The objective however is only to look at specific combinations that illustrate the basic relationships between parameters.

Table 5.5 Summary Table of Parameters and their Codes

Code	No.	Effect or Control	Values or Type
R	1	Control	High Intensity
R	2		Low Intensity
R	3		Decreasing Intensity
R	4		Increasing Intensity
I	1	Control-Impermeable	i = 0.0
I	2	High Productivity	i = 0.000047 + 0.109/t
I	3	Low Productivity	i = 0.000359 + 0.149/t
n	1	Control	0.348
n	2	Flow Enhancing	0.218
n	3	Flow Inhibiting	0.478
G	1	Control	0.1440
G	2	Flow Inhibiting	0.0244
G	3	Flow Enhancing	0.2615
D	1	Control-Flow Inhibiting	Sheetflow
D	2	Flow Enhancing	Complex Flow

5.3.3.b The Suite of Single Plot Simulations

The total number of simulations carried out is 50. They show the most important sensitivities of the process model and provide a foundation for the interpretation of the flow environment on the Avdat hillslopes, illustrating the key features of specific slopes in terms of their potential for runoff generation and transportation.

1. the role of the routing parameters; roughness, gradient and dimensions, without the influence of rainfall inputs or infiltration losses on the hydrograph.

This group of 14 simulations keeps rainfall constant at 40 mm hr^{-1} for 15 minutes onto an impermeable surface. Firstly, the three roughness parameters are combined with the intermediate slope

gradient. Secondly, the other two slope gradients are combined with the intermediate roughness parameter. Thirdly, the combinations theoretically most favourable and unfavourable for flow are simulated, that of lowest roughness and highest slope gradient, and highest roughness and lowest slope gradient respectively. These are repeated for the complex flow surface.

The sensitivity results presented in Table 5.6 show that as roughness is increased and the gradient decreased, then the gradient of the rising curve and falling curve become less steep, with a decrease in mean velocity and increase in cross-sectional flow area as the same steady-state discharge moves more slowly across the surface. The opposite occurs where roughness is decreased and slope gradient is increased. This is shown in the Figures 5.7 and 5.8. Compare for instance the worst parameter combination 11321, the control 11111 and the most favourable combination 11231. In terms of the enhancement of flow, the slope roughness parameter is most important, a decrease in roughness producing a greater than proportional effect than an increase in gradient. In terms of flow inhibition, the opposite is true. The difference between the best and worse roughness values and the control are more similar (but obviously opposite) than the differences between the two slope gradients and the control. The reduction in gradient produces a much higher relative change. This is to be expected since the square root of the gradient is used in the flow equation and so an increase does not produce an equal change in magnitude to a decrease.

These characteristics are repeated for both sets of simulations using the smooth and varied surface boundary shape as shown by a comparison of both Figure 5.7 and 5.8 hydrographs. Comparing the sets of results produced for each boundary shape shows that the variations relative to the control are more sensitive to shape than to the roughness or gradient. Comparing the hydrographs in Figures 5.7 and 5.8 to the solid red line representing the control shows how five of the seven simulations produces greater transmissivity than the control, compared with three with the same smooth surface (sheetflow). For the same slope and roughness parameter combinations, the complex flow case produces a much reduced time to steady-state discharge and a considerable increase in steady-state velocity and decrease in steady-state flow-area compared to the sheetflow case. For example, for the optimum slope-roughness combination (11231-2), with the complex flow case (11232) the flow velocity is four times that of the control steady-state velocity compared to the two times increase for the sheetflow case (11231). They are 8.78, 4.37 and 2.76 cm s^{-1} respectively. The differences between the hydrographs for the same parameter pairing but different dimension assumption can be seen in the set of hydrographs of Figure 5.9 where the control, best and worst combination responses are plotted on the same axis.

With each flow-boundary shape, the effect of decreasing slope gradient whilst increasing slope roughness is to attenuate both the rising limb and the falling limb, reducing flow velocity and increasing flow area and producing a lower discharge for the same observation time. The reverse is true when the best parameter combination is made. This is clear from Figures 5.7 to 5.9 and Table 5.6.

Table 5.6 Sensitivity Results for Varying Routing Parameters on Micro-Rough and Micro-Smooth Hillslopes

R	I	n	G	D	Qp	Vp	Ap	Tsp	Tep	ΣQ	%V Qp	%V Vp	%V Ap	%V ΣQ
1	1	1	1	1	1111	2.76	402.7	750	900	0.997	0.0	0.0	0.0	0.0
1	1	2	1	1	1111	3.65	304.2	550	900	0.999	0.0	-32.2	24.5	-0.2
1	1	3	1	1	1111	2.28	487.2	900	900	0.996	0.0	17.4	-21.0	0.1
1	1	1	2	1	1098	1.60	684.4	900	900	0.999	1.2	42.0	-70.0	-0.2
1	1	1	3	1	1111	3.30	336.8	600	900	0.998	0.0	-19.6	16.4	-0.1
1	1	2	3	1	1111	4.37	254.4	550	900	0.999	0.0	-58.3	36.8	-0.2
1	1	3	2	1	1053	1.30	807.6	900	900	0.985	5.2	52.9	-100.5	1.2
1	1	1	1	2	1111	4.92	225.6	450	900	1.000	0.0	-78.3	44.0	-0.3
1	1	2	1	2	1111	6.99	158.9	300	900	1.000	0.0	-153.3	60.5	-0.3
1	1	3	1	2	1111	3.88	286.0	550	900	1.000	0.0	-40.6	29.0	-0.3
1	1	1	2	2	1111	2.52	441.0	850	900	1.000	0.0	8.7	-9.5	-0.3
1	1	1	3	2	1111	6.15	180.5	350	900	1.000	0.0	-122.8	55.2	-0.3
1	1	2	3	2	1111	8.78	127.2	250	900	1.000	0.0	-218.1	68.4	-0.3
1	1	3	2	2	1109	1.98	558.6	900	900	1.000	0.2	28.3	-38.7	-0.3

R = rainfall
I = infiltration
n = resistance
G = gradient
D = dimensions (see Table 5.5)

Qp = peak discharge (cm3/s)
Vp = peak flow velocity (cm/s)
Ap = peak flow area (cm2)
Tsp = time to reach Qp (s)
Tep = time when Q falls below Qp (s)
ΣQ = total discharge (m3)

%V Qp = % variation from 11111
%V Vp = % variation from 11111
%V Ap = % variation from 11111
%V ΣQ = % variation from 11111

Figure 5.7 Sensitivity to Varying Routing Parameters on Micro-Smooth Hillslopes

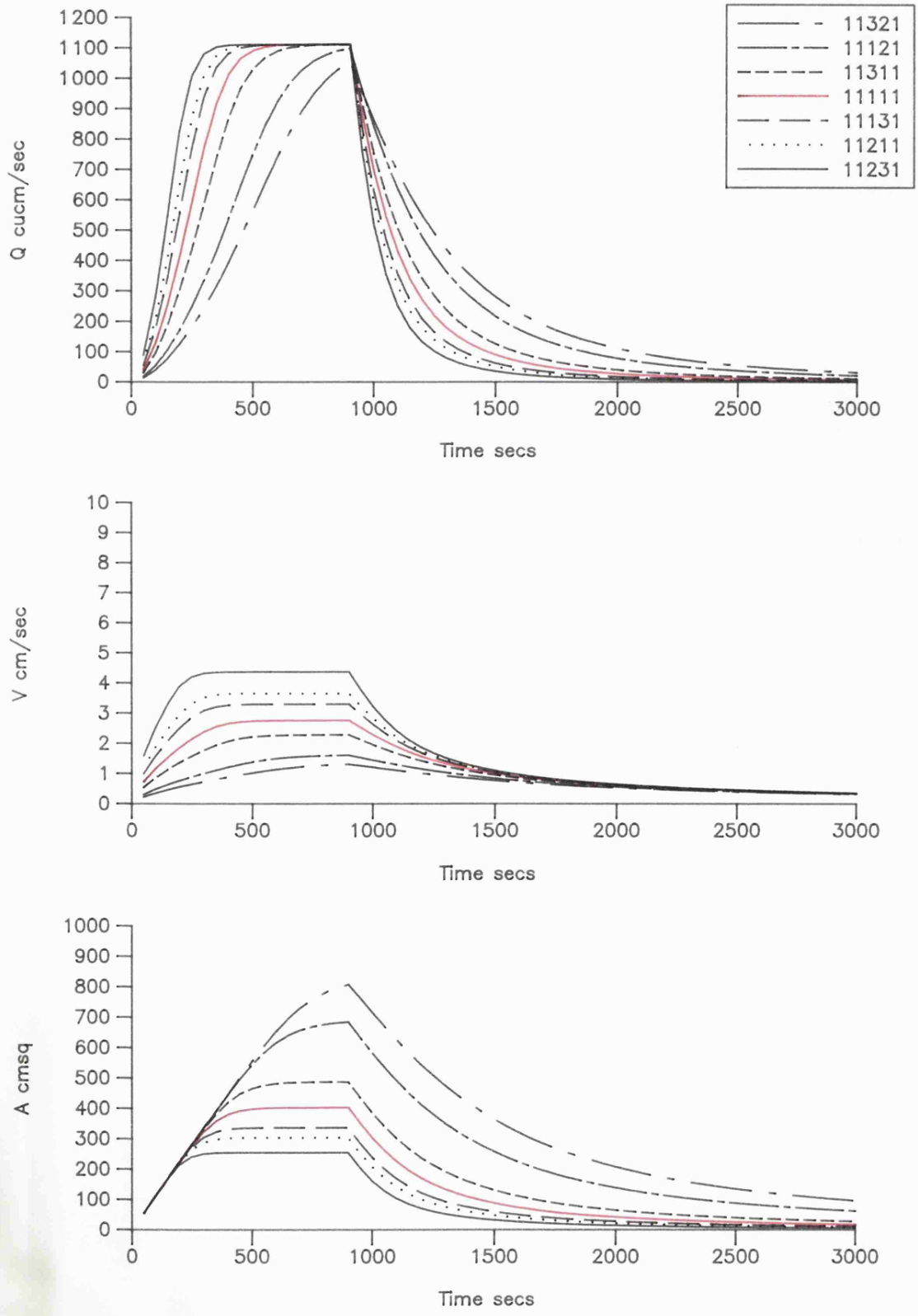

Figure 5.8 Sensitivity to Varying Routing Parameters on Micro-Rough Hillslopes

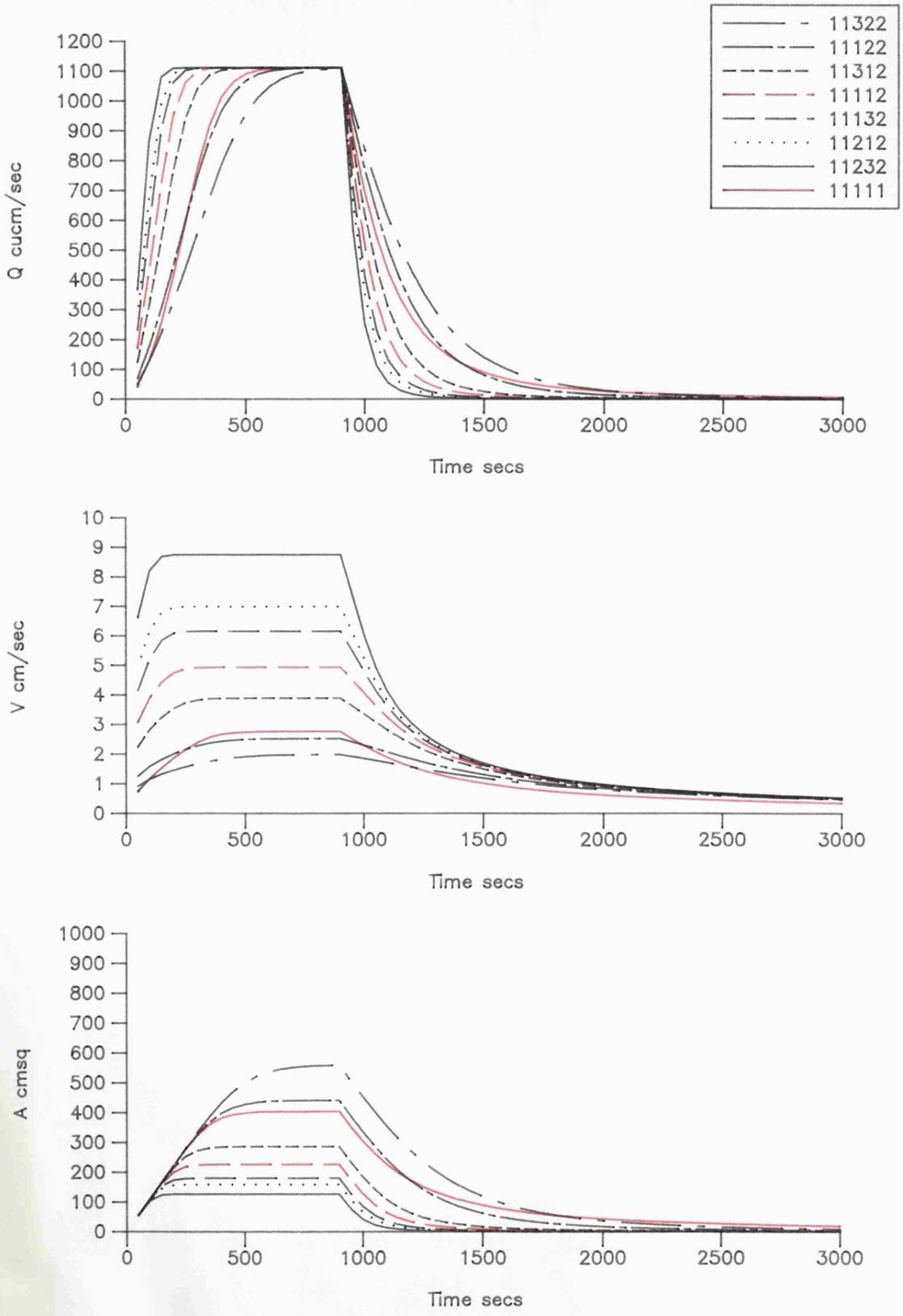

Figure 5.9 Comparisons of Sensitivity to Varying Routing Parameters on Micro–Smooth and Micro–Rough Hillslopes

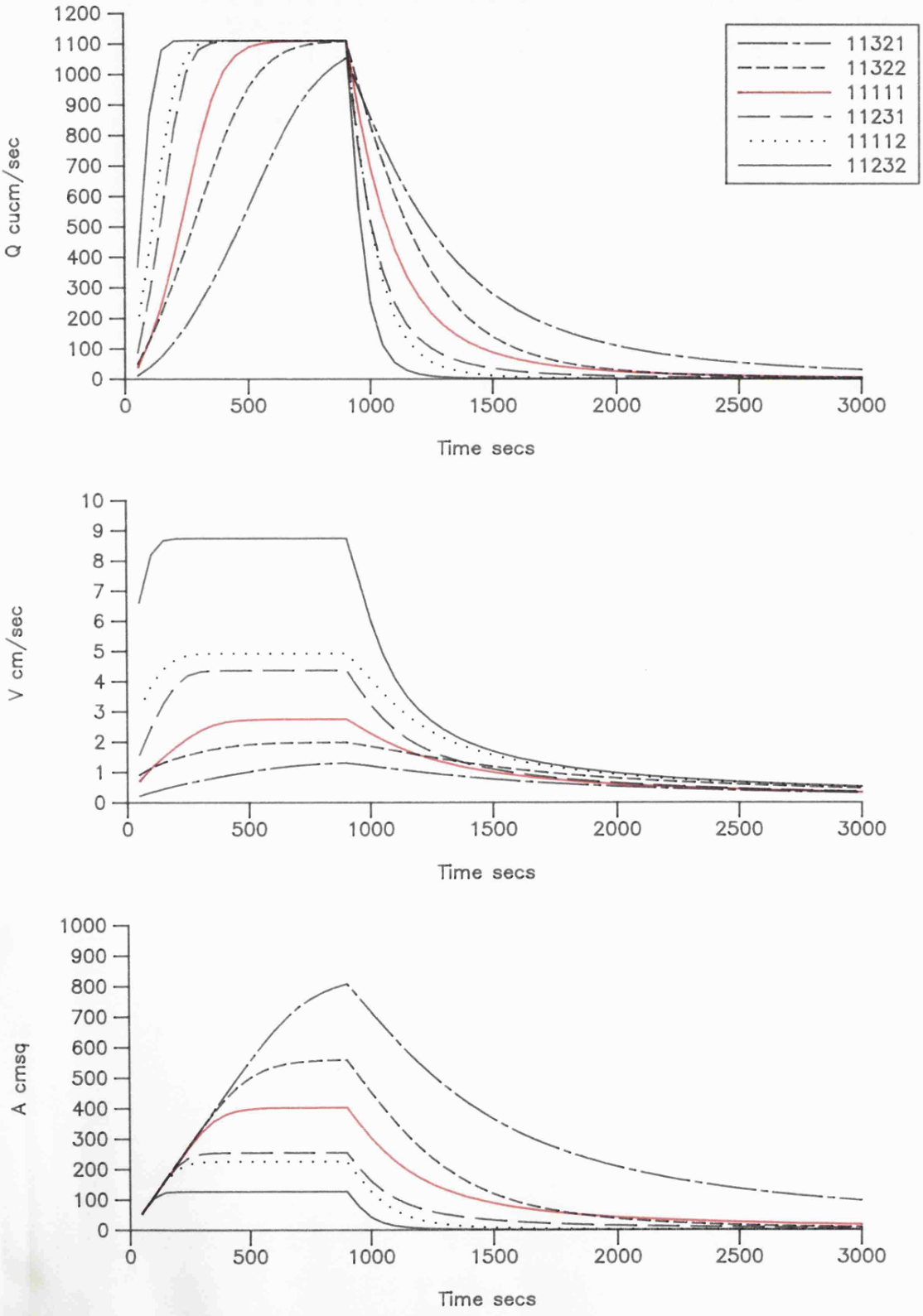

2. the effect of infiltration and routing parameter variations without the influence of varying rainfall inputs. This uses the optimum, intermediate and least favourable combinations of roughness and gradient to examine the relationship between flow routing and the infiltration regime for the two flow dimensions parameters since these effect potential infiltration parameters.

This involves another 12 simulations using the two infiltration A and B parameter sets 2 and 3 and the intermediate, optimum and least favourable combinations of roughness and slope gradient parameters with the two flow dimension assumptions. The effect of the particular parameter combinations for the same and different infiltration regimes are visible.

As expected from a knowledge of hillslope hydrology, the hydrographs produced show distinct differences in terms of the absolute and relative effects of infiltration on the volume and timing of the runoff response. This reflects the combined effects of productivity and transmissivity. The transmissivity relationships were identified in the previous sensitivity analyses. The summary data is presented in Table 5.7 and in the hydrographs of Figures 5.10 to 5.11. An important characteristic determining how much water is produced for a given infiltration is the rapidity of water movement across the surface and off the plot, particularly in the post-rainfall period. Additionally the length of contact between the slope surface and the moving water is important since it determines the magnitude of infiltration losses once rainfall ceases. This explains the increased productivity for the same rainstorm and infiltration when complex flow is assumed rather than sheetflow. The results of these simulations show that in each case, there is a greater infiltrated volume of water for the sheetflow surface compared to the complex flow surface, i.e. for a smooth rather than a micro-rough plot with the same infiltration, gradient and roughness coefficient. This variation increases with an increase in the competence to transmit flow, i.e. the steeper the slope, and the lower the roughness, the lower the total infiltration. For the worst parameter combination, Table 5.6 shows that for the low infiltration regime, runoff productivity is 0.455 for sheetflow and 0.585 for complex flow, an increase of 29%. For the high infiltration the increase is 176%. This compares with the two percentage increases for the best parameter combination of 7% and 25% respectively. Comparing the hydrographs in Figures 5.10 and 5.11, the complex flow response can be seen to produce a steeper rising curve and higher peak discharge, with a steeper falling limb. The faster throughflow (higher discharges for a given time) means that water remains on the surface for a shorter period, a factor that is very important in the post-rainfall recession flow period. Additionally, the cross-sectional area associated with a discharge is lower (due to a higher velocity) and hence in the case of complex flow, the wetted perimeter in contact with the surface will be smaller and the total infiltration lower. Once rainfall ceases, the more rapid the throughflow, the less opportunity for subsequent infiltration of surface water. Thus parameter combinations that produce high peak velocities and steep falling limbs produce proportionally more

Table 5.7				Sensitivity Results for Varying Routing and Infiltration Parameters on Micro-Rough and Micro-Smooth Hillslopes										
R	I	n	G	D	Qp	Vp	Ap	Tsp	Tep	ΣQ	%V Qp	%V Vp	%V Ap	%V ΣQ
1	1	1	1	1	1111	2.76	402.7	750	900	0.997	0.0	0.0	0.0	0.0
1	1	2	3	1	1111	4.37	254.4	550	900	0.999	0.0	-58.3	36.8	-0.2
1	1	3	2	1	1053	1.30	807.6	900	900	0.985	5.2	52.9	-100.5	1.2
1	2	1	1	1	911	2.55	357.4	900	900	0.531	18.0	7.6	11.2	46.7
1	2	2	3	1	927	4.06	228.2	900	900	0.560	16.6	-47.1	43.3	43.8
1	2	3	2	1	632	1.06	594.5	900	900	0.455	43.1	61.6	-47.6	54.4
1	3	1	1	1	504	2.01	250.5	900	900	0.184	54.6	27.2	37.8	81.5
1	3	2	3	1	557	3.31	168.1	900	900	0.227	49.9	-19.9	58.3	77.2
1	3	3	2	1	206	0.68	303.7	900	900	0.088	81.5	75.4	24.6	91.2
1	1	1	1	2	1111	4.92	225.6	450	900	1.000	0.0	-78.3	44.0	-0.3
1	1	2	3	2	1111	8.78	127.2	250	900	1.000	0.0	-218.1	68.4	-0.3
1	1	3	2	2	1109	1.98	558.6	900	900	1.000	0.2	28.3	-38.7	-0.3
1	2	1	1	2	922	4.70	196.3	900	900	0.599	17.0	-70.3	51.3	39.9
1	2	2	3	2	930	8.35	111.4	900	900	0.603	16.3	-202.5	72.3	39.5
1	2	3	2	2	855	1.86	460.0	900	900	0.585	23.0	32.6	-14.2	41.3
1	3	1	1	2	547	4.12	132.7	900	900	0.276	50.8	-49.3	67.0	72.3
1	3	2	3	2	560	7.35	76.2	900	900	0.284	49.6	-166.3	81.1	71.5
1	3	3	2	2	418	1.55	269.3	900	900	0.243	62.4	43.8	33.1	75.6
R = rainfall				Qp = peak discharge (cm3/s)							%V Qp = % variation from 11111			
I = infiltration				Vp = peak flow velocity (cm/s)							%V Vp = % variation from 11111			
n = resistance				Ap = peak flow area (cm2)							%V Ap = % variation from 11111			
G = gradient				Tsp = time to reach Qp (s)										
D = dimensions				Tep = time when Q falls below Qp (s)										
(see Table 5.5)				ΣQ = total discharge (m3)							%V ΣQ = % variation from 11111			

Figure 5.10 Sensitivity to Varying Infiltration Parameters for Different Routing Parameter Combinations on Micro–Smooth Hillslopes

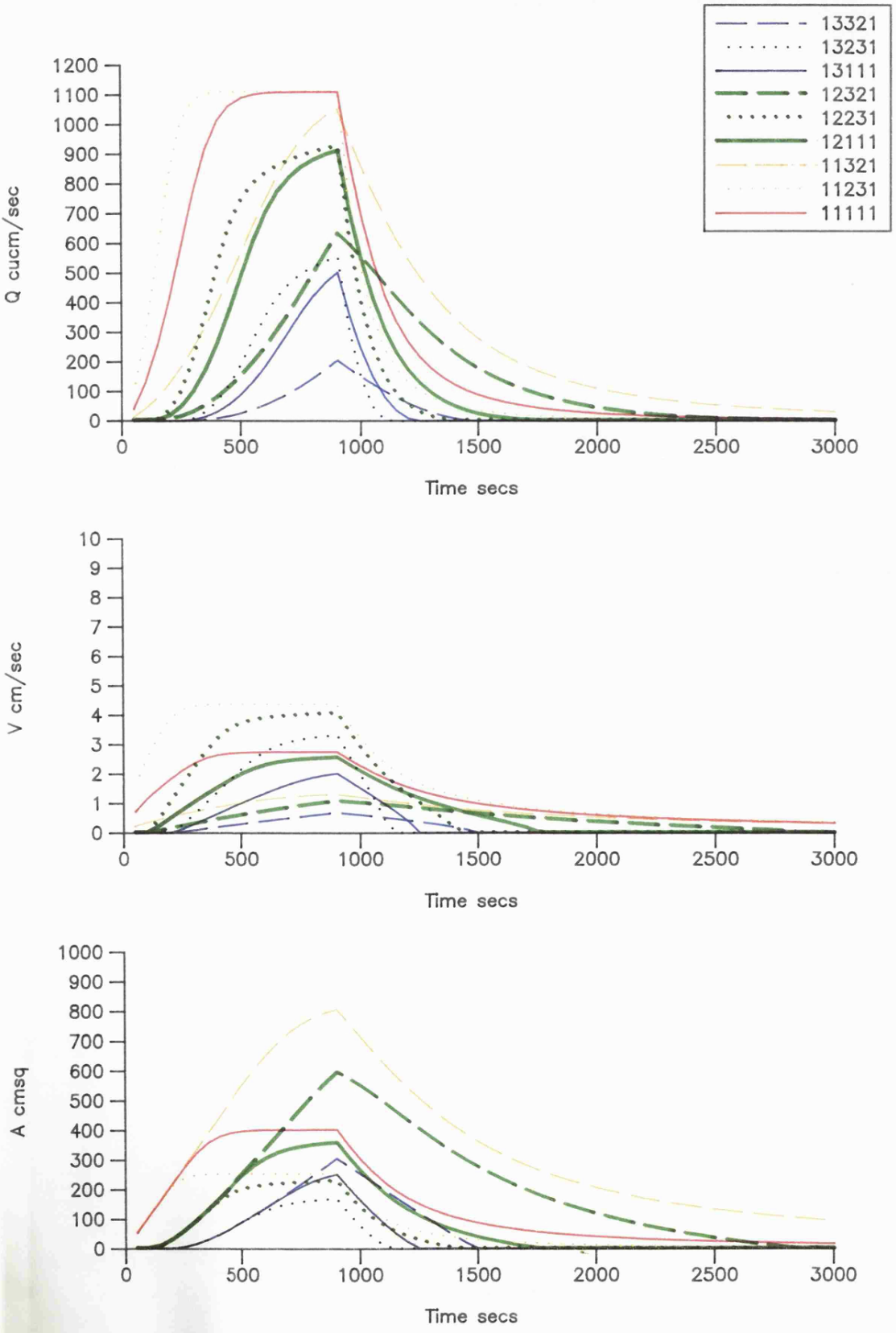

Figure 5.11 Sensitivity to Varying Infiltration Parameters for Different Routing Parameter Combinations on Micro-Rough Hillslopes

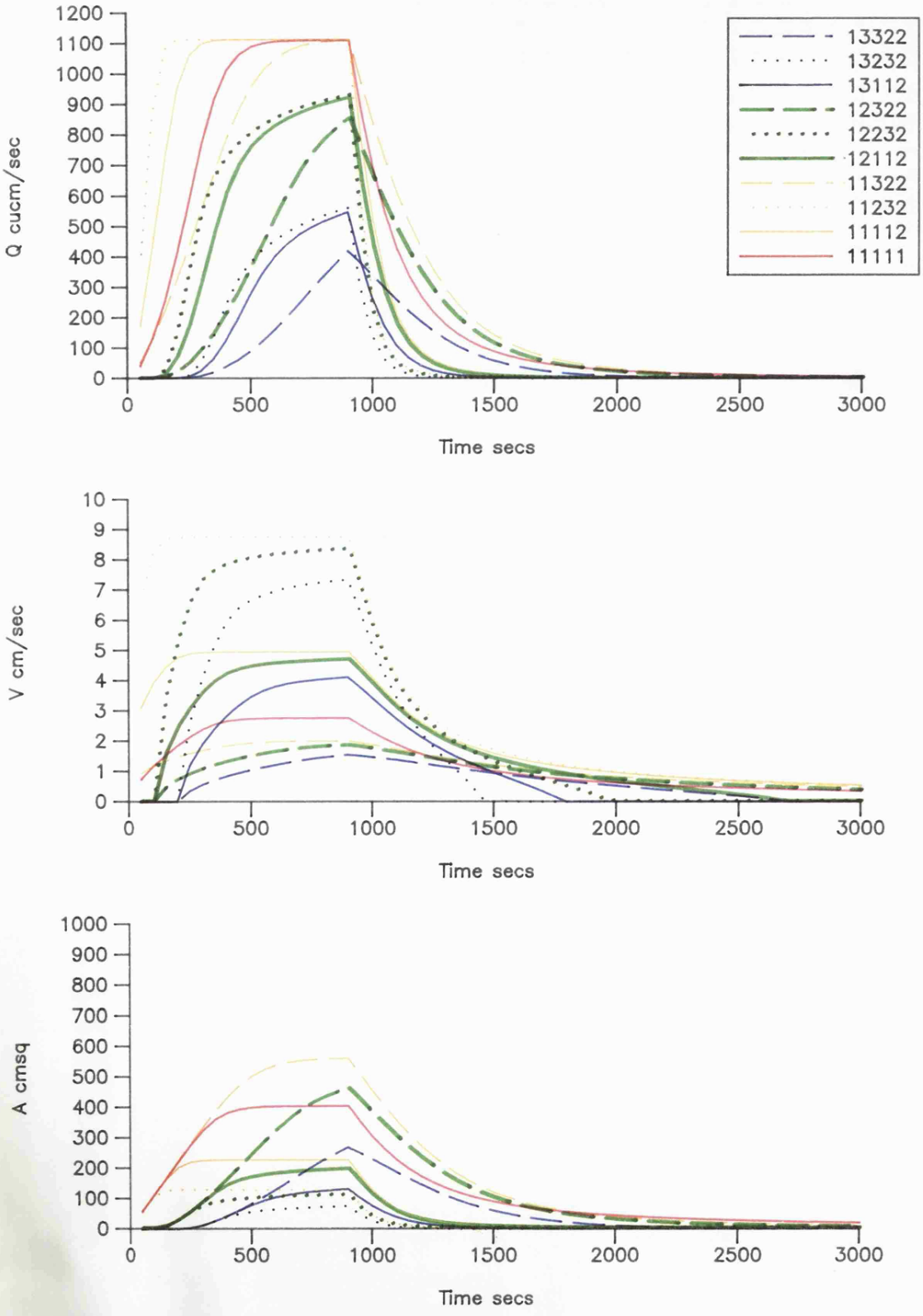

Figure 5.12 Comparisons of Sensitivity to Varying Infiltration Parameters on Micro–Smooth and Micro–Rough Hillslopes

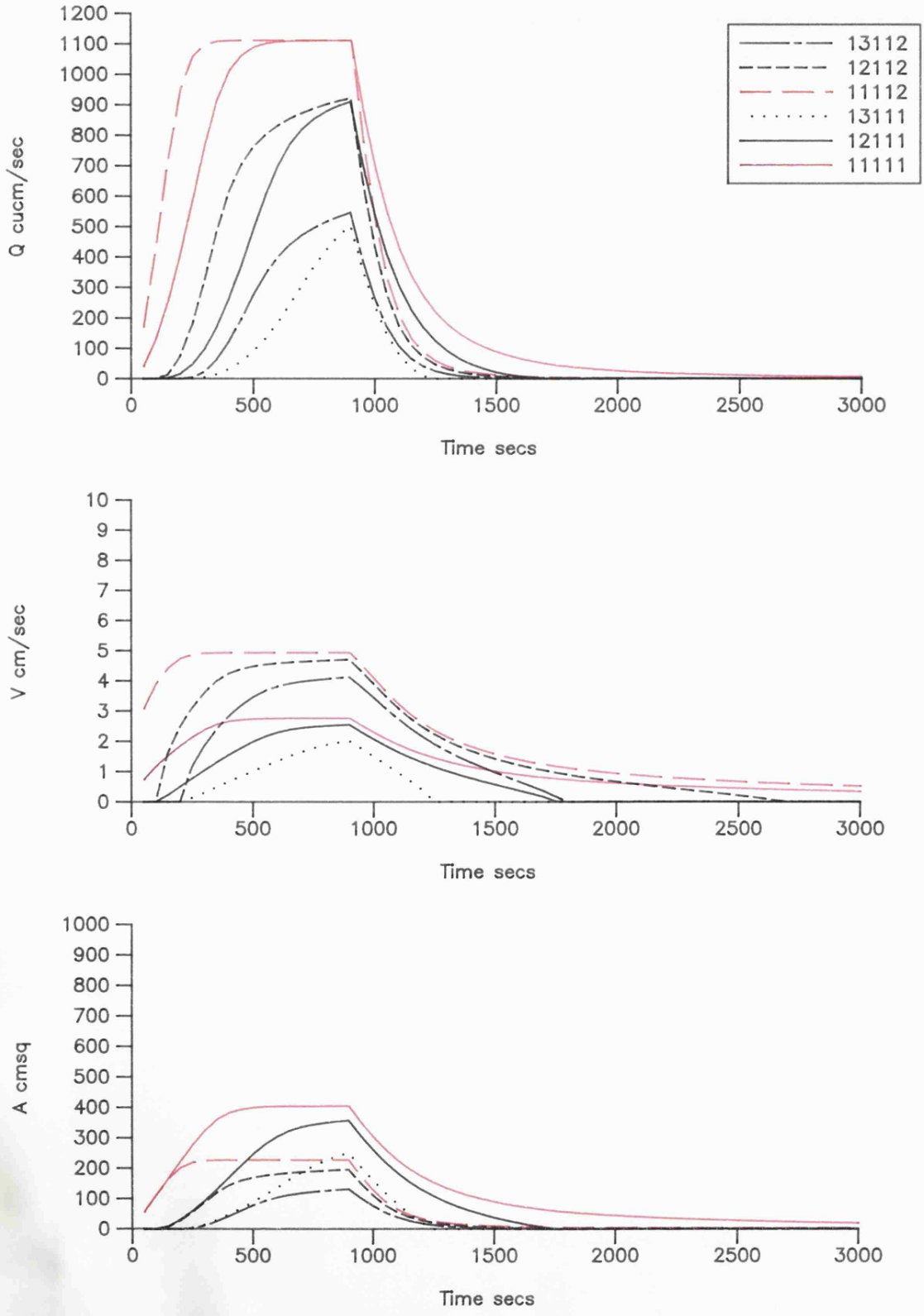

runoff under a given infiltration regime. The improved routing capability of the surface somewhat compensates for the increase in infiltration rates.

The critical role played by boundary shape, and hence by the flow assumption of sheetflow or complex flow is illustrated by an examination of the hydrographs for the intermediate flow parameter combination in Figure 5.12. Comparing the pairs of hydrographs 11111 and 11112, 12111 and 12112 and 13111 and 13112 shows clearly the more rapid rise times associated with the micro-rough surface. This has an important determination on the total volume of water produced because it controls the amount of runoff leaving the plot whilst rainfall excess is still occurring. The infiltration into the plot whilst rainfall is occurring is marginally higher for the complex flow due to the total surface perimeter being longer than the surface width. Once rainfall ceases, water flowing across the surface can be rapidly infiltrated as shown by the steep recession curves for the two black sets of hydrographs, although in greater volumes on the sheetflow surface due to the wetting of the total surface area. The surface water held in detention is therefore infiltrated more readily on its passage downslope, and the recession curves of the hydrographs are more similar. The effects of infiltration are clear in that no plots reach steady-state discharge during the 900 seconds of rainfall, whereas on the impermeable surface, this is reached rapidly. The greater the infiltration, the shallower the rising curve and the lower the peak discharges. In each case the effect of infiltration is dampened by assuming complex flow conditions. This shows some of the practical implications for using a sheetflow approach to routing surface flow, a fact which has received insufficient attention in the literature to date.

3. the effects of rainfall and infiltration parameters on flow routing without the influence of routing parameters of roughness and gradient, but for both the flow dimension parameters since these effect potential infiltration volumes.

These 24 simulations are designed to determine the sensitivity of the combination of infiltration parameters and the rainfall intensity distribution and duration of rainfall. The total yield of the rainstorms are identical at 10 mm, and the flow-routing parameters of roughness and gradient are kept constant set to the median conditions. The flow dimensions are varied with both the smooth and the varied flow profile (sheet and complex flow) situations modelled. The effect of the distribution of rainfall intensities for different infiltration regimes in terms of volumetric output and the shape of the hydrograph and flow characteristics is visible from a consideration of Table 5.8 and the hydrographs plotted in Figures 5.13 to 5.14.

The simulations show that the intensity distribution of the rainfall is an important factor in determining the runoff productivity from the cell surface. This can be seen by comparing the hydrographs produced for the impermeable surface, which show the effect of distribution and peak rainfall intensities on hydrograph shape and peak flow characteristics and then looking at the variation

Table 5.8				Sensitivity Results for Varying Rainfall Intensity Distributions and Infiltration Parameters on Micro-Rough and Micro-Smooth Hillslopes											
R	I	n	G	D	Qp	Vp	Ap	Tsp	Tep	ΣQ	%V Qp	%V Vp	%V Ap	%V ΣQ
1	1	1	1	1	1111	2.76	402.7	750	900	0.997	0.0	0.0	0.0	0.0
2	1	1	1	1	278	1.58	175.2	1150	3600	0.993	75.0	42.8	56.5	0.4
3	1	1	1	1	226	1.46	155.0	900	900	0.993	79.7	47.1	61.5	0.4
4	1	1	1	1	293	1.62	181.2	6600	6600	0.992	73.6	41.3	55.0	0.5
1	2	1	1	1	911	2.55	357.4	900	900	0.531	18.0	7.6	11.2	46.7
2	2	1	1	1	198	1.38	143.0	3600	3600	0.453	82.2	50.0	64.5	54.6
3	2	1	1	1	76	0.94	80.7	3000	3000	0.260	93.2	65.9	80.0	73.9
4	2	1	1	1	223	1.45	153.5	6600	6600	0.387	79.9	47.5	61.9	61.2
1	3	1	1	1	504	2.01	250.5	900	900	0.184	54.6	27.2	37.8	81.5
2	3	1	1	1	0	0.00	0.0	0	0	0.000	100.0	100.0	100.0	100.0
3	3	1	1	1	0	0.00	0.0	0	0	0.000	100.0	100.0	100.0	100.0
4	3	1	1	1	0	0.00	0.0	0	0	0.000	100.0	100.0	100.0	100.0
1	1	1	1	2	1111	4.92	225.6	400	900	1.000	0.0	-78.3	44.0	-0.3
2	1	1	1	2	278	3.47	79.9	600	3600	1.000	75.0	-25.7	80.2	-0.3
3	1	1	1	2	303	3.55	85.3	300	300	1.000	72.7	-28.6	78.8	-0.3
4	1	1	1	2	327	3.62	90.4	6600	6600	1.000	70.6	-31.2	77.6	-0.3
1	2	1	1	2	922	4.70	196.3	900	900	0.599	17.0	-70.3	51.3	39.9
2	2	1	1	2	197	3.19	61.8	3600	3600	0.489	82.3	-15.6	84.7	51.0
3	2	1	1	2	79	2.53	31.1	3000	3000	0.275	92.9	8.3	92.3	72.4
4	2	1	1	2	260	3.42	76.0	6600	6600	0.421	76.6	-23.9	81.1	57.8
1	3	1	1	2	547	4.12	132.7	900	900	0.276	50.8	-49.3	67.0	72.3
2	3	1	1	2	0	0.00	0.0	0	0	0.000	100.0	100.0	100.0	100.0
3	3	1	1	2	0	0.00	0.0	0	0	0.000	100.0	100.0	100.0	100.0
4	3	1	1	2	0	0.00	0.0	0	0	0.000	100.0	100.0	100.0	100.0

R = rainfall
I = infiltration
n = resistance
G = gradient
D = dimensions
(see Table 5.5)

Qp = peak discharge (cm3/s)
Vp = peak flow velocity (cm/s)
Ap = peak flow area (cm2)
Tsp = time to reach Qp (s)
Tep = time when Q falls below Qp (s)
ΣQ = total discharge (m3)

%V Qp = % variation from 11111
%V Vp = % variation from 11111
%V Ap = % variation from 11111
%V ΣQ = % variation from 11111

Figure 5.13 Sensitivity to Varying Rainfall Intensity Distributions on Impermeable Micro-Smooth and Micro-Rough Hillslopes

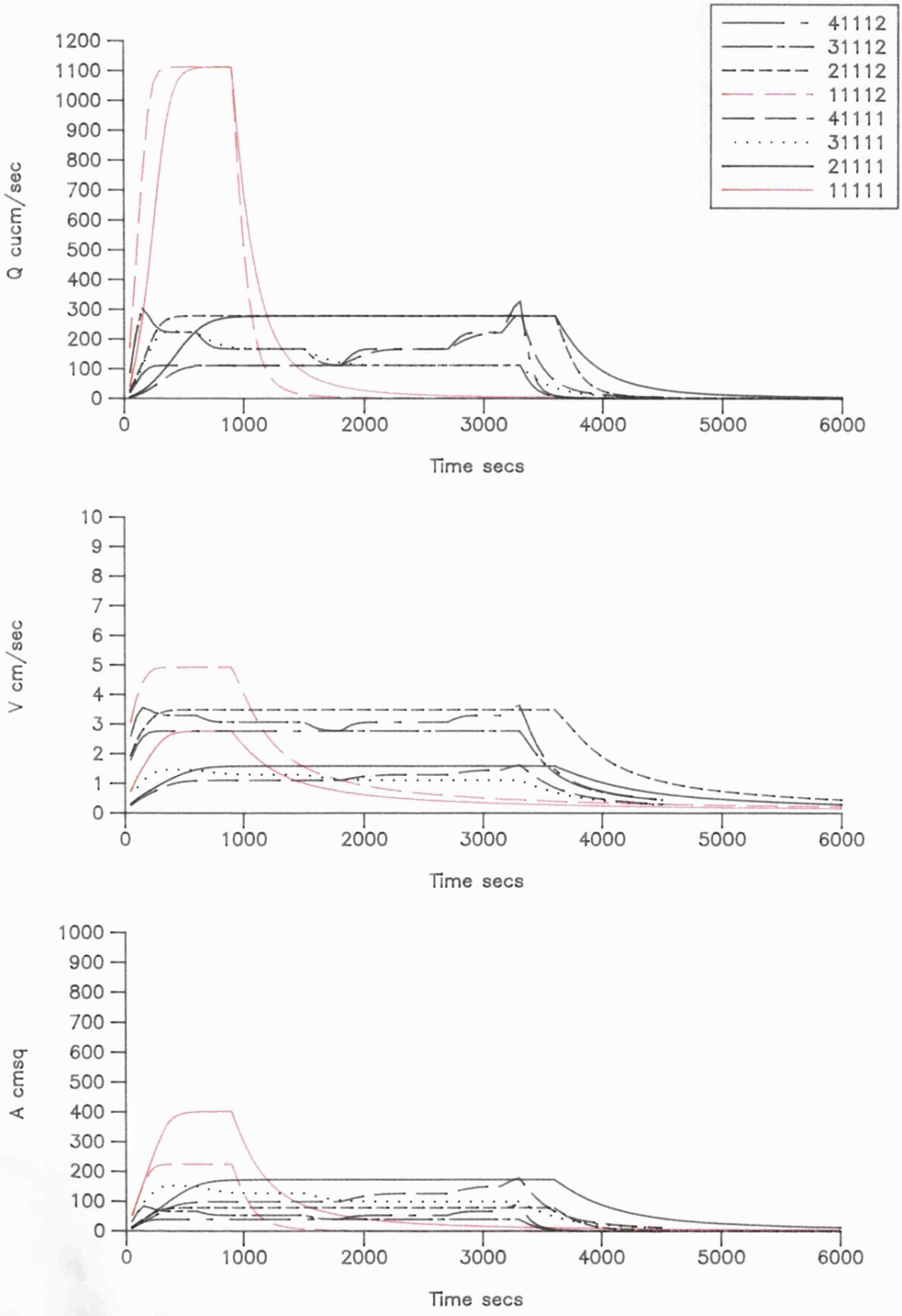

Figure 5.14 Sensitivity to Varying Rainfall Intensity Distributions on Infiltrating Micro–Smooth and Micro–Rough Hillslopes

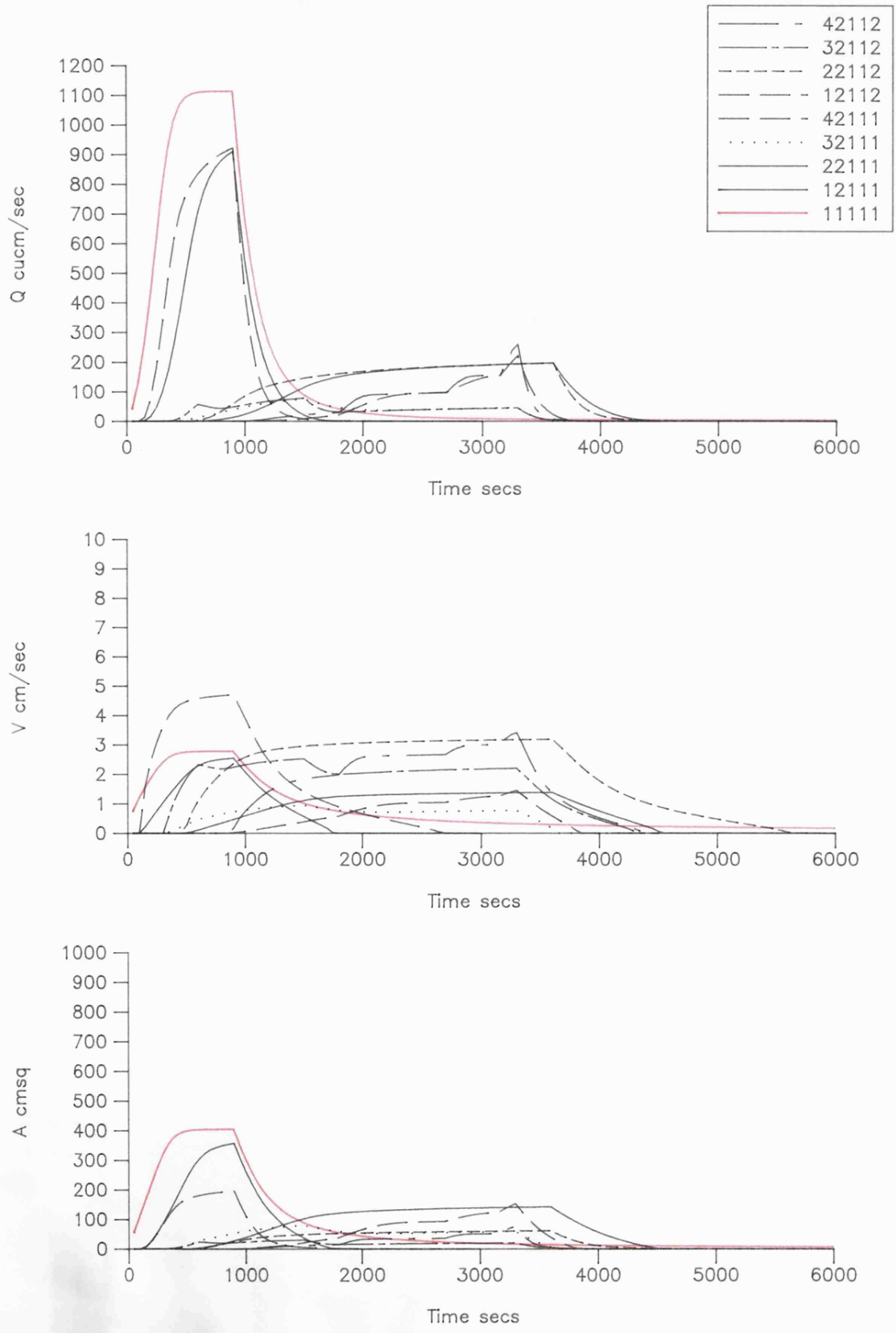

in production between each infiltration regime for the different rainfalls. All the variations within this final set of simulations are the result of variations in infiltration and rainfall and the flow-shape assumption, the other routing parameters being kept constant at their intermediate values.

The first observation for the impermeable surface is how important rainfall intensity is in determining peak discharge. Rainfall regime 1 (40 mm hr^{-1}) produces four times the peak discharge of rainfall regime 2 (10 mm hr^{-1}. For 1111D it is 1111 cm^3 s^{-1} and for 2111D it is 278 cm^3 s^{-1}. However, there is not the same correspondence between peak rainfall and peak discharge in the case of rainfalls 3 and 4; the decreasing and increasing intensities respectively. Here timing is important. The increasing intensity results in a higher peak discharge, since rain falls at the highest intensity (12 mm hr^{-1}) once flow is already established on the surface, and approaches steady-state conditions more rapidly before the rainfall ceases. The decreasing intensity falls onto a previously dry-surface and achieves a lower discharge before the highest intensity block ceases and a lower intensity starts. Additionally, there are variations between the peak discharges for the two flow conditions of sheetflow and complex flow due to the fact that the steady-state conditions have not been reached. For example, compare 31111 to 31112 or 42111 to 42112. Their relative peak discharges are 226 and 303 cm^3 s^{-1} and 293 and 327 cm^3 s^{-1} respectively. This effect is a result of the transmissivity between the two different flow shapes. The complex flow assumption results in greater velocities for the same flow area due to the use of hydraulic radius rather than average depth, which for all flow states up to the point where the wetted perimeter is equal to or greater than the plan width will be larger. Thus the timing of the hydrographs is different and for any time prior to steady-state discharge for the less-responsive combination, the discharge of the more responsive combination will be higher. These results were also experienced in the distributed model analysis of Bathurst (1986 b) who finds that the magnitude of the roughness coefficient determines the rapidity of response of the surface runoff. By affecting the time for which the surface runoff remains on the surface, the coefficient also partially determines the volume of water which can infiltrate into the soil. Lower resistance coefficients enables overland flow to reach channels faster, with steeper rises and recessions of the hydrographs. The opposite effect results from increasing the magnitude of resistance.

Comparing the productivity from different rainfall amounts for the different rainfall regimes shows clearly the key role played by intensity and by transmissivity. For the low constant intensity and the two low, varying intensity events there is no runoff produced at all for the highest infiltration regime. The lowest infiltration regime shows the effect that varying intensity can have on the runoff productivity. For the sheetflow, smooth surface, the largest production results from the high/short intensity storm, followed by the medium/long intensity and the increasing intensity. The smallest amount of runoff results from the decreasing intensity hyetograph. Their respective volumes are 0.531, 0.453, 0.387 and 0.260 m^3. The storage depth will be filled at different times for the different rainfall intensities since V_s equals $(B + A.t_o)$ as shown in Chapter Three. Once it is filled, the volume of

runoff will be dependent on the relative intensities of the rainfall and infiltration. Obviously, as long as ponding does occur, the runoff from an increasing intensity distribution is likely to be greater than a decreasing intensity distribution. This helps explain the different volumes of water produced for the same infiltration combinations for the different rainfall regimes.

The results confirm that infiltration is a key factor in determining the hydrological response but also show the complex relationship between it and the rainfall intensity and temporal distribution. Where rainfall intensities are initially low, runoff production is delayed with longer times to runoff. The role of transmissivity post-ponding shows how the effects of both infiltration and intensity can be modified by flow states where velocity of flow is increased, area decreased, and in the case of complex flow, surface wetted length reduced for infiltration calculations post-rainfall.

5.3.4 Multiple Cell Cascade Simulations

5.3.4.a The Purpose of the Multiple Plot Arrangements

An additional series of simulations analyse the effects of spatial arrangement and scale. Parameter combinations are selected to occupy the upper and lower positions in a two-plot cascade. Each plot is subdivided into ten one metre long elements to give a total of twenty elements in sequence. The effect of the spatial variation in parameters has significance for the positioning of channels to intercept productive sections along flow-lines. The influence of producer and consumer slopes on total productivity can be determined hypothetically by considering the two recorded hydrographs of outflow from the lowest element of each plot. For the top plot this is elements 11 and for the bottom plot this is element 1. Comparing these against the discharge recorded for a single plot (with only ten elements) shows any knock-on effect from plots positioned upslope, and comparing the total productivity from the two plots in sequence compared to the cumulative productivity from separate plots shows the quantitative effect of introducing channels to a hillslope.

5.3.4.b The Parameter Combinations and Their Hydrological Significance

The combinations of values used to parameterise the top and bottom plot elements are grouped in Table 5.9. They are arranged to give constant, improving and worsening conditions. There are four sets of parameters in total, best constant, improving, worsening and worst constant allowing a complete comparison. The improving conditions refer to flow productivity and transmissivity improving in a downslope direction.

Table 5.9 Parameter Combinations for Simulations of Multiple Plot Cascades

		Top	Bottom
(1) Best Constant	Gradient	15.16°	15.16°
	Manning's n	0.222	0.222
	Infiltration (cm s^{-1})	I=0.000047 + 0.109/t	I=0.000047 + 0.109/t
(2) Improving	Gradient	1.40°	15.16°
	Manning's n	0.478	0.222
	Infiltration	i=0.000359 + 0.149/t	I=0.000047 + 0.109/t
(3) Worsening	Gradient	15.16°	1.40°
	Manning's n	0.222	0.478
	Infiltration (cm s^{-1})	I=0.000047 + 0.109/t	i=0.000359 + 0.149/t
(4) Worst Constant	Gradient	1.40°	1.40°
	Manning's n	0.478	0.478
	Infiltration (cm s^{-1})	i=0.000359 + 0.149/t	i=0.000359 + 0.149/t

Both flow boundary shapes (1-2) are simulated for the same four rainfall regimes (1-4). The hydrograph pairs for the different two-plot combinations are presented in Figures 5.15 to 5.16 where the blue curves are best constant, green curves improving, yellow curves worsening and red curves worst constant conditions. In Table 5.10, the pairs of plots are listed on consecutive lines. Comparing the results from each in volumetric terms and the shape of the hydrographs shows the effects of stopper and enhancer slope sections and the sensitivity to the different parameters such as rainfall intensity distribution and flow boundary shape.

The results of the 32 simulations are compared most usefully in terms of volumetric production, and through a comparison of the bottom cell hydrographs in Figures 5.15 to 5.16. The first observation, is that the presence of a poor runoff producer and transmitter below a more productive slope has the effect of dissipating the runoff productivity on its passage across the lower area. With the chosen parameter sets, this results in no runoff at all for three rainstorms as expected from the previous sensitivity simulations for the sheetflow assumption. Here, the production from the upper slope is consumed along with the rainfall onto the lower slope, and is insufficient to bring the whole length of slope to the point of ponding, although it does result in the upper increments of the lower plot reaching a flow-state. However, the effects of worsening conditions are not so extreme where complex flow is assumed. Here, the water runs off the upper plot with a more favourable timing and in large quantities such that all the lower slope increments can reach their time to runoff and both plots can transmit runoff down and eventually out of the slope boundary. This is seen clearly in Table 5.10 for rainstorms 2 and 4 and is consistent with the discussions of the characteristics of arid zone hillslope hydrology in Chapter Two. If runoff is not sufficiently rapid from upper slopes, or if lower slopes have higher infiltration rates and are poor transmitters, then downslope continuity of runoff generation and

Table 5.10 Sensitivity Results for Varying Rainfall Intensity Distributions on Micro-Smooth and Micro-Rough Hillslopes with Different Spatial Distributions of Infiltration and Routing Parameters

R	I	n	G	D		Qp	Vp	Ap	Tsp	Tep	ΣQ	R	I	n	G	D		Qp	Vp	Ap	Tsp	Tep	ΣQ
1	2	2	3	1	Top	927	4.06	228.2	900	900	0.560	1	2	2	3	2	Top	930	8.35	111.4	900	900	0.603
1	2	2	3	1	Bot	1832	5.33	343.6	900	900	1.081	1	2	2	3	2	Bot	1849	9.92	186.3	900	900	1.201
2	2	2	3	1	Top	199	2.19	90.6	3600	3600	0.471	2	2	2	3	2	Top	198	5.66	35.0	3600	3600	0.490
2	2	2	3	1	Bot	396	2.89	137.0	3600	3600	0.916	2	2	2	3	2	Bot	395	6.73	58.6	3600	3600	0.979
3	2	2	3	1	Top	80	1.52	52.3	3000	3000	0.271	3	2	2	3	2	Top	80	4.50	17.7	3000	3000	0.276
3	2	2	3	1	Bot	154	1.98	77.8	3000	3000	0.526	3	2	2	3	2	Bot	158	5.35	29.5	3000	3000	0.551
4	2	2	3	1	Top	250	2.40	104.0	6600	6600	0.404	4	2	2	3	2	Top	268	6.11	43.9	6600	6600	0.423
4	2	2	3	1	Bot	452	3.04	148.3	6600	6600	0.784	4	2	2	3	2	Bot	529	7.24	73.0	6600	6600	0.844
1	2	2	3	1	Top	927	4.06	228.2	900	900	0.560	1	2	2	3	2	Top	930	8.35	111.4	900	900	0.603
1	3	3	2	1	Bot	342	0.84	406.1	0	0	0.432	1	3	3	2	2	Bot	1260	2.08	605.2	900	900	0.794
2	2	2	3	1	Top	199	2.19	90.6	3600	3600	0.471	2	2	2	3	2	Top	198	5.66	35.0	3600	3600	0.490
2	3	3	2	1	Bot	0	0.00	0.0	0	0	0.000	2	3	3	2	2	Bot	155	1.23	125.2	3600	3600	0.186
3	2	2	3	1	Top	80	1.52	52.3	3000	3000	0.271	3	2	2	3	2	Top	80	4.50	17.7	3000	3000	0.276
3	3	3	2	1	Bot	0	0.00	0.0	0	0	0.000	3	3	3	2	2	Bot	0	0.00	0.0	0	0	0.000
4	2	2	3	1	Top	250	2.40	104.0	6600	6600	0.404	4	2	2	3	2	Top	268	6.10	43.9	6600	6600	0.423
4	3	3	2	1	Bot	0	0.00	0.0	0	0	0.000	4	3	3	2	2	Bot	131	1.18	111.5	7000	7000	0.073
1	3	3	2	1	Top	206	0.68	303.8	900	900	0.088	1	3	3	2	2	Top	418	1.55	269.3	900	900	0.243
1	2	2	3	1	Bot	1030	4.23	243.2	900	900	0.610	1	2	2	3	2	Bot	1273	9.03	140.9	900	900	0.836
2	3	3	2	1	Top	0	0.00	0.0	0	0	0.000	2	3	3	2	2	Top	0	0.00	0.0	0	0	0.000
2	2	2	3	1	Bot	199	2.19	90.6	3600	3600	0.471	2	2	2	3	2	Bot	198	5.65	35.0	3600	3600	0.490
3	3	3	2	1	Top	0	0.00	0.0	0	0	0.000	3	3	3	2	2	Top	0	0.00	0.0	0	0	0.000
3	2	2	3	1	Bot	79.5	1.52	52.3	3000	3000	0.211	3	2	2	3	2	Bot	79.9	4.50	17.7	3000	3000	0.276
4	3	3	2	1	Top	0	0.00	0.0	0	0	0.000	4	3	3	2	2	Top	0	0.00	0.0	0	0	0.000
4	2	2	3	1	Bot	250	2.40	104.0	6600	6600	0.404	4	2	2	3	2	Bot	268	6.10	43.9	6600	6600	0.423
1	3	3	2	1	Top	206	0.68	303.7	900	900	0.088	1	3	3	2	2	Top	418	1.55	269.3	900	900	0.243
1	3	3	2	1	Bot	207	0.69	300.9	900	900	0.090	1	3	3	2	2	Bot	468	1.62	288.4	900	900	0.419
2	3	3	2	1	Top	0	0	0	0	0	0	2	3	3	2	2	Top	0	0	0	0	0	0
2	3	3	2	1	Bot	0	0	0	0	0	0	2	3	3	2	2	Bot	0	0	0	0	0	0
3	3	3	2	1	Top	0	0	0	0	0	0	3	3	3	2	2	Top	0	0	0	0	0	0
3	3	3	2	1	Bot	0	0	0	0	0	0	3	3	3	2	2	Bot	0	0	0	0	0	0
4	3	3	2	1	Top	0	0	0	0	0	0	4	3	3	2	2	Top	0	0	0	0	0	0
4	3	3	2	1	Bot	0	0	0	0	0	0	4	3	3	2	2	Bot	0	0	0	0	0	0

R = rainfall	Qp = peak discharge (cm3/s)	R = rainfall	Qp = peak discharge (cm3/s)
I = infiltration	Vp = peak flow velocity (cm/s)	I = infiltration	Vp = peak flow velocity (cm/s)
n = resistance	Ap = peak flow area (cm2)	n = resistance	Ap = peak flow area (cm2)
G = gradient	Tsp = time to reach Qp (s)	G = gradient	Tsp = time to reach Qp (s)
D = dimensions	Tep = time when Q falls below Qp (s)	D = dimensions	Tep = time when Q falls below Qp (s)
(see Table 5.5)	ΣQ = total discharge (m3)	(see Table 5.5)	ΣQ = total discharge (m3)

Figure 5.15 The Effect of Plot Position on the Hydrological Response from Micro-Smooth Hillslopes

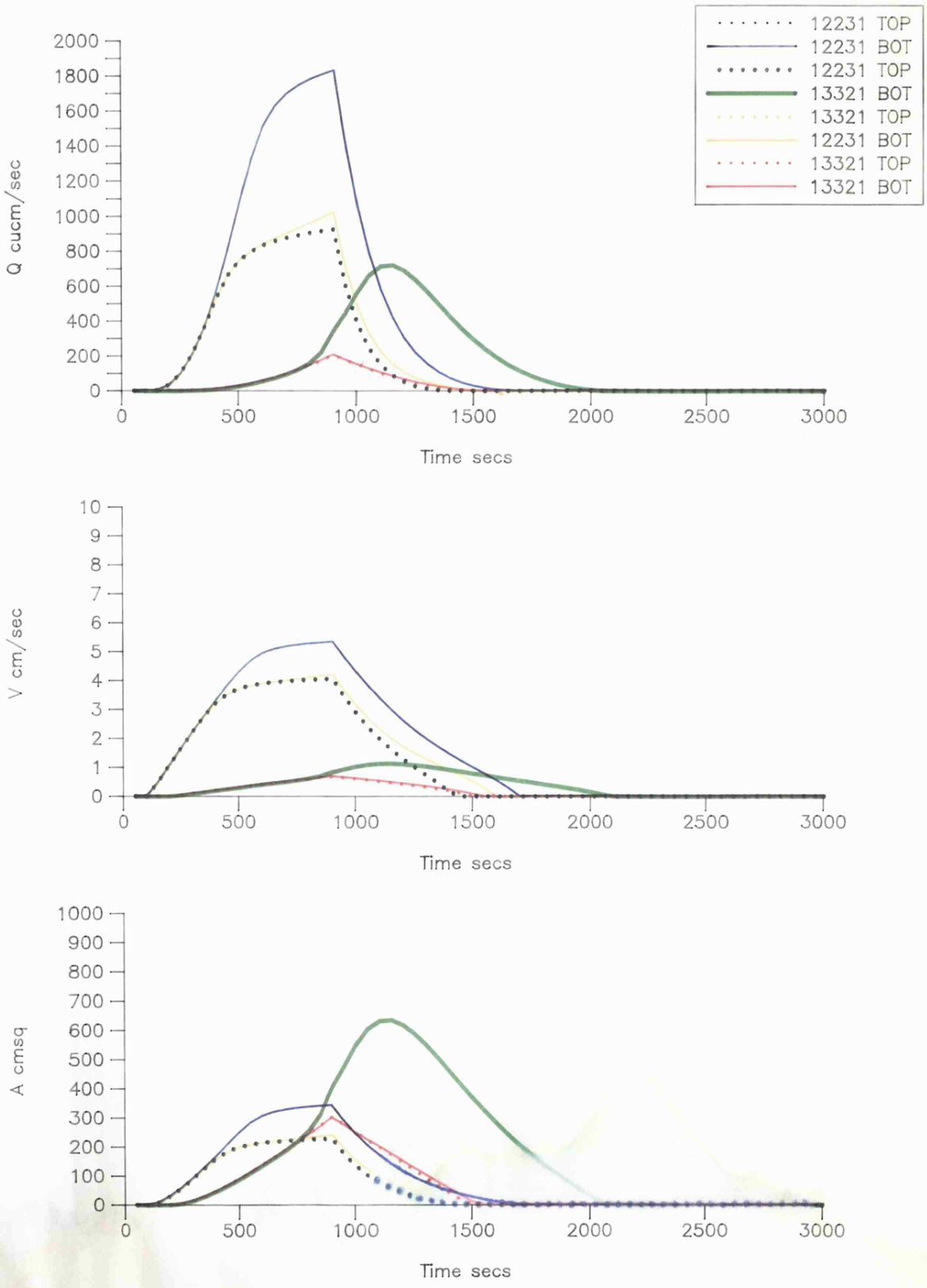

Figure 5.16 The Effect of Plot Position on the Hydrological Response from Micro-Rough Hillslopes

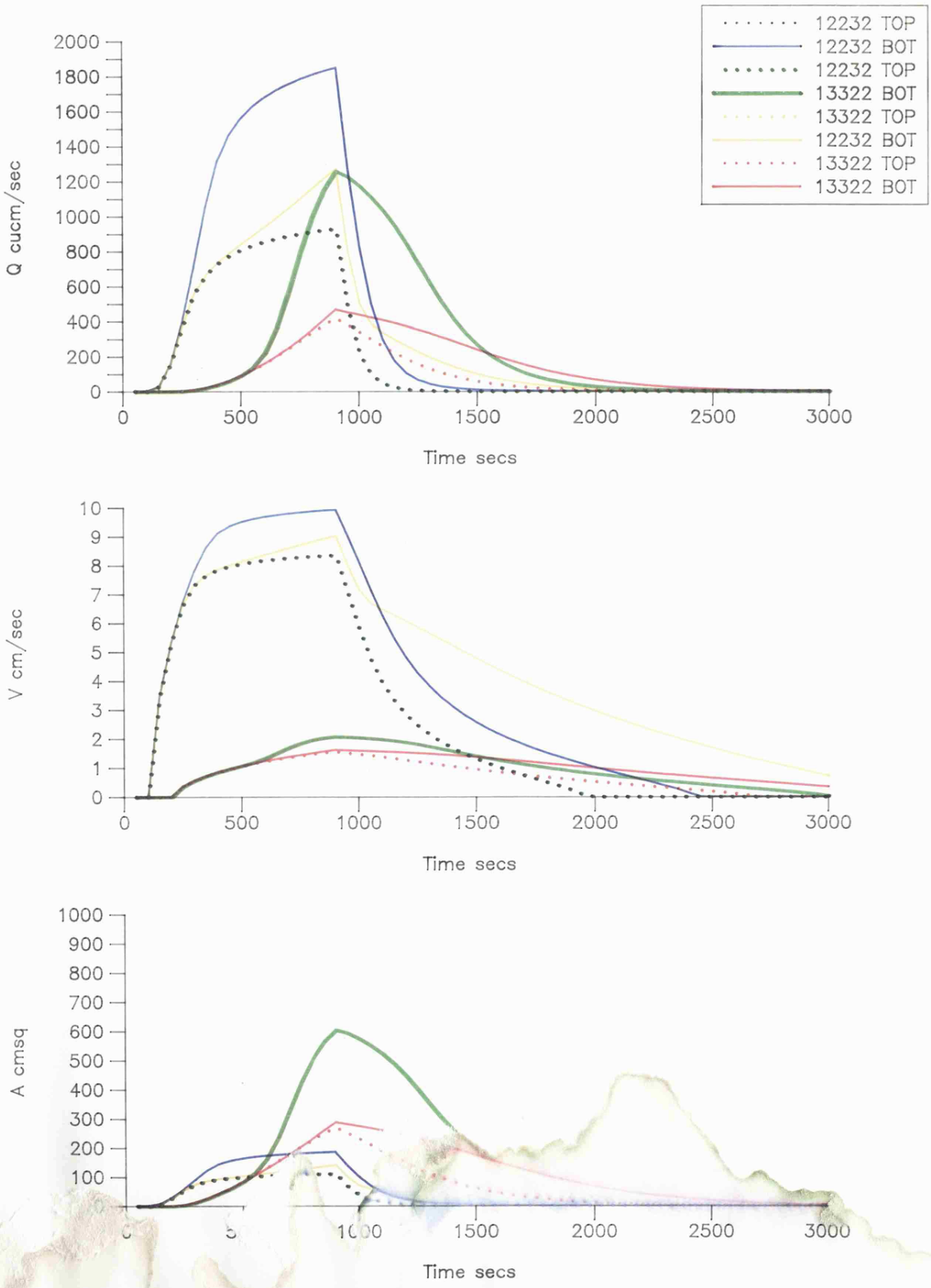

transmission will not be maintained. In the most extreme cases, runoff production will be lost completely. The only way to prevent this natural waste of productive potential is to tap the flow-line at higher elevations, for instance, at the boundary between the upper and the lower cells. On an improving slope, this has little effect on productivity. In the case of rainfall one, the high intensity rainstorm, the increase in harvest would be from 0.610 to 0.648 m^3 for the sheetflow conditions and from 0.836 to 0.846 m^3 for the complex flow. However, on a worsening slope, the increased productivity would be from 0.088 to 0.648 m^3 for the sheetflow, and from 0.243 to 0.846 m^3 for the complex flow as productivity from two separate lengths of slope is tapped and the effects of infiltration of run-off reduced.

Of interest in this hydrological assessment, is the shape of upslope and downslope hydrographs, particularly in the case of the complex flow, where the consumptive effects of the lower slope are overcome by the knock-on effect of the upper slopes. With the sheetflow, the consumptive or 'stopper' effects are generally dominant, whereas with the complex flow, the knock-on effects can prevail due to the more rapid and effective routing of water. The knock-on effect on the downslope hydrograph is three-fold. Firstly it affects timing of runoff generation. By inflow from above, the lower slope can be made to produce runoff earlier than it would otherwise under rainfall alone. With the storage approach to infiltration, runoff is calculated to occur when equations 3.15 and 3.17 are satisfied. Where runoff is added from above, p becomes (p+Q/A) and therefore t_o and V_s are reduced. Following this, the transmission effect creates a gradually steepening rising limb with larger depths and discharges as rainfall and run-in combines. The predicted hydrograph diverges from that experienced by the single plot as discharge increases directly with downslope distance. The final recession effect depends on the relative difference between any two plots and whether water is input at a sufficient rate post-rainfall to maintain flow conditions above the infiltration rate of the lower plot. This is observed in the length and gradient of the recession curve which becomes attenuated by the inflow of water from above. Where an asymmetrical hydrograph (skewed to the post-peak side) is experienced then the recession effect is in operation and will help increase the total productivity.

Considering the high intensity rainstorm and the sheetflow conditions. In Figure 5.15 there is only one red hydrograph (13321 top and 13321 bottom) because the runoff production from the upper slope, and the high infiltration and poor routing conditions in the lower slope are insufficient to significantly effect the flow conditions of the lower slope. There is no appreciable knock-on effect recorded at element 1 from the elements 20 to 11. Of great interest is the comparison between the yellow and the green hydrographs. This shows graphically the effect of spatial location on a cells productivity. The two upper cells are the green dotted line (worsening 12231 top) and the yellow dotted line (13321 top) which is identical to and masked by the red hydrograph (improving). The two lower cells are the solid lines. Comparing the green dotted line (12231 top) to the yellow solid line (12231 bottom) shows the effect of having a poor producer and transmitter above a good producer and

transmitter. The result is that the latter experiences only marginal effects with identical rising limb, a slightly increased peak and a shallower recession limb as the production from above attenuates this flow stage. Comparing the green solid line (13321 bottom) to the yellow dotted line (red hydrograph 13321 top) shows a more striking difference. The effects of discharge from upslope is clear as a bell-shaped hydrograph is produced. Again the same rising curve is experienced, but soon the run-on from above raises discharge to a much higher level although the upslope hydrograph is somewhat dissipated by infiltration into the lower plot. For the best constant conditions, the effect of the upslope productivity is to cause rapid divergence of the lower from the upper plot hydrograph as the discharge increases directly with distance downslope. A higher peak is reached and the recession curve is attenuated as flow from the upper plot continues to add to the residual flow in the lower slope post-rainfall. This can be seen by comparing the green dotted hydrograph (which masks the blue 12232 top) and the blue solid hydrograph. The peak of the latter is 1832 $cm^3 s^{-1}$ compared to 927 $cm^3 s^{-1}$ for the upper plot.

Making the same comparisons for the complex flow case for the high intensity rainstorm, the conclusion is that the downslope stopper effect of the worsening conditions can be suppressed by the more rapid and effective routing associated with this flow assumption. The runoff production is greater from the upper slope, the peak of the lower slope is higher and earlier, and the volume of lower slope production increased. With the constant slope conditions this is observed by comparing the blue dotted hydrograph 12232 top (same as the green dotted hydrograph) with the blue solid hydrograph for the best conditions, and the red dotted hydrograph with the red solid hydrograph for the worst conditions. In both cases, the effect of run-on from upslope is to raise the peak discharge and attenuate the falling limb as runoff from above makes its way across the lower slope and out of element 1. The response for the worst conditions are markedly different from the sheetflow assumption, showing the key role of transmissivity in overcoming the consumptive effects of infiltration by its effect on runoff routing timing. Comparing the improving conditions with the worsening conditions again shows the knock-on and stopper effects of spatial variation. The flow peak is transmitted downslope more rapidly so that the hydrograph of the lower slope for the worsening conditions is shifted to the left, and a larger proportion of the flow takes place within the rainfall period. With higher peak discharges, this explains the increased volumetric production between the two plots for the high intensity rainfall. With the improving conditions, the poor top slope producer still has an affect on the flow experienced out of element 1 by adding to the peak discharge and extending the rising limb to a higher and steeper peak whilst also attenuating the falling curve. This is attributable to the greater and more rapid discharge experienced from the upper plot when complex flow is assumed.

The effects of varying rainfall intensity through time also show some interesting characteristics. In the case of the worst parameter combination cells, the reduction in intensity is sufficient to result in no runoff being produced at all for each of the sheetflow simulations, as previously observed in single cell simulations. Coupled with the more productive cells, the knock-on

effect of inflow from above is capable of producing increased runoff for two of the additional rainstorms, the only one not producing runoff from element 1 in the cascade being the decreasing intensity rainfall. There is a permanent state of moisture deficit on the lower slope, and water produced upslope does not make it to the bottom. Looking at the decreasing intensity rainstorm and the predicted output for the best constant conditions (for which runoff is predicted for each), the presence of early peaks in rainfall are largely masked by the infiltration process on both the upper and lower plots. For the increasing intensity, some knock on effect is observed as the two hydrographs diverge and a higher, more sustained peak is reached. This is shown in Figures 5.17 for the micro-smooth, sheetflow case and Figure 5.18 for the micro-rough, complex flow case. This is observed for all the rainstorms for this parameter combination with total runoff production almost twice the runoff production from a single cell. The fact that it is slightly less than twice reflects the effects of spatial scale, and particularly downslope length on run-off productivity. It is more pronounced for sheetflow assumed conditions than complex flow as explained below.

The most obvious conclusion is that the presence of a highly productive, quick-responding plot above a less productive, slowly-responding plot can have an enhancing effect on the runoff productivity of the lower plot relative to that produced by the lower plot in isolation. However, the combination of increased flow-line length, or worsening flow productivity and transmissivity can combine to consume runoff water generated upslope before it reaches the foot of the cascade. The results for the worsening spatial arrangement are a direct illustration of the nature of Contiguous Area Contribution, with runoff productivity expanding downslope, **reaching-down** from key rapid producers to a channel at the foot of the sequence as explained in Chapter One.

5.3.4.c The Effects of Scale

To illustrate the effects of scale on the amount of runoff collected at the foot of different lengths of slope, a cascade of four ten metre cells was simulated for each of the four rainstorms. The cells were provided either with the best or worst parameters, and simulated for both sheetflow and complex flow conditions. Since the worst parameter combinations would not produce any runoff from rainstorms 2-4, these were not simulated and the results from rainstorm 1 only are listed in Table 5.11 along with the results for the best parameter combinations. To show the effect on downslope productivity of increasing slope length and hence increasing contributing area, the flow characteristics through time were recorded at the end of each ten metre plot at elements 31, 21, 11 and 1 in the cascade as listed in Table 5.11.

Studies of runoff production from hillslopes in the Negev have shown the effect of increasing slope length to be a significant determinant of the total productivity and hence the productivity per unit area (Yair and Lavee, *et seq*). This was shown hypothetically by Yair and Lavee (1985) in their

Table 5.11	Sensitivity Results for Varying Rainfall Intensity Distributions on Micro-Smooth and Micro-Rough Hillslopes of Different Length but with Constant Infiltration and Routing Parameters																					
R	I	n	G	D		Qp	Vp	Ap	Tsp	Tep	ΣQ		R	I	n	G	D		Qp	Vp	Ap	Tsp	Tep	ΣQ
1	2	2	3	1	31	927	4.06	228.2	900	900	0.560		1	2	2	3	2	31	930	8.35	111.4	900	900	0.603
1	2	2	3	1	21	1832	5.33	343.6	900	900	1.081		1	2	2	3	2	21	1849	9.92	186.3	900	900	1.201
1	2	2	3	1	11	2712	6.24	434.6	900	900	1.570		1	2	2	3	2	11	2754	10.97	251.0	900	900	1.790
1	2	2	3	1	1	3548	6.95	510.6	900	900	2.040		1	2	2	3	2	1	3646	11.78	309.6	900	900	2.380
2	2	2	3	1	31	199	2.19	90.6	3600	3600	0.470		2	2	2	3	2	31	198	5.66	35.0	3600	3600	0.490
2	2	2	3	1	21	396	2.89	137.0	3600	3600	0.920		2	2	2	3	2	21	395	6.73	58.6	3600	3600	0.980
2	2	2	3	1	11	591	3.39	174.3	3600	3600	1.340		2	2	2	3	2	11	591	7.45	79.3	3600	3600	1.460
2	2	2	3	1	1	786	3.80	206.6	3600	3600	1.750		2	2	2	3	2	1	786	8.01	98.2	3600	3600	1.950
3	2	2	3	1	31	80	1.52	52.3	3000	3000	0.270		3	2	2	3	2	31	80	4.50	17.7	3000	3000	0.280
3	2	2	3	1	21	154	1.98	77.8	3000	3000	0.530		3	2	2	3	2	21	158	5.35	29.5	3000	3000	0.550
3	2	2	3	1	11	224	2.30	97.3	3000	3000	0.770		3	2	2	3	2	11	234	5.91	39.7	3000	3000	0.820
3	2	2	3	1	1	289	2.55	113.3	3000	3000	1.000		3	2	2	3	2	1	309	6.33	48.8	3000	3000	1.100
4	2	2	3	1	31	250	2.40	104.0	6600	6600	0.410		4	2	2	3	2	31	268	6.11	43.9	6600	6600	0.420
4	2	2	3	1	21	451.7	3.05	148.3	6600	6600	0.780		4	2	2	3	2	21	529.1	7.25	73.0	6600	6600	0.840
4	2	2	3	1	11	636	3.49	182.1	6600	6600	1.150		4	2	2	3	2	11	753	7.92	95.1	6600	6600	1.260
4	2	2	3	1	1	813	3.85	210.9	6600	6600	1.490		4	2	2	3	2	1	944	8.38	112.5	6600	6600	1.680
1	3	3	2	1	31	206	0.68	303.7	900	900	0.088		1	3	3	2	2	31	418	1.55	269.3	900	900	0.243
1	3	3	2	1	21	207	0.69	300.9	900	900	0.090		1	3	3	2	2	21	468	1.62	288.4	900	900	0.419
2	3	3	2	1	11	207	0.69	300.6	900	900	0.090		2	3	3	2	2	11	468	1.62	288.4	900	900	0.419
2	3	3	2	1	1	207	0.69	300.6	900	900	0.090		2	3	3	2	2	1	468	1.62	288.4	900	900	0.419

R = rainfall	Qp = peak discharge (cm3/s)	R = rainfall	Qp = peak discharge (cm3/s)
I = infiltration	Vp = peak flow velocity (cm/s)	I = infiltration	Vp = peak flow velocity (cm/s)
n = resistance	Ap = peak flow area (cm2)	n = resistance	Ap = peak flow area (cm2)
G = gradient	Tsp = time to reach Qp (s)	G = gradient	Tsp = time to reach Qp (s)
D = dimensions	Tep = time when Q falls below Qp (s)	D = dimensions	Tep = time when Q falls below Qp (s)
(see Table 5.5)	ΣQ = total discharge (m3)	(see Table 5.5)	ΣQ = total discharge (m3)

Figure 5.17 The Hydrological Response from a Micro-Smooth Hillslope with Different Rainfall Intensity Distributions

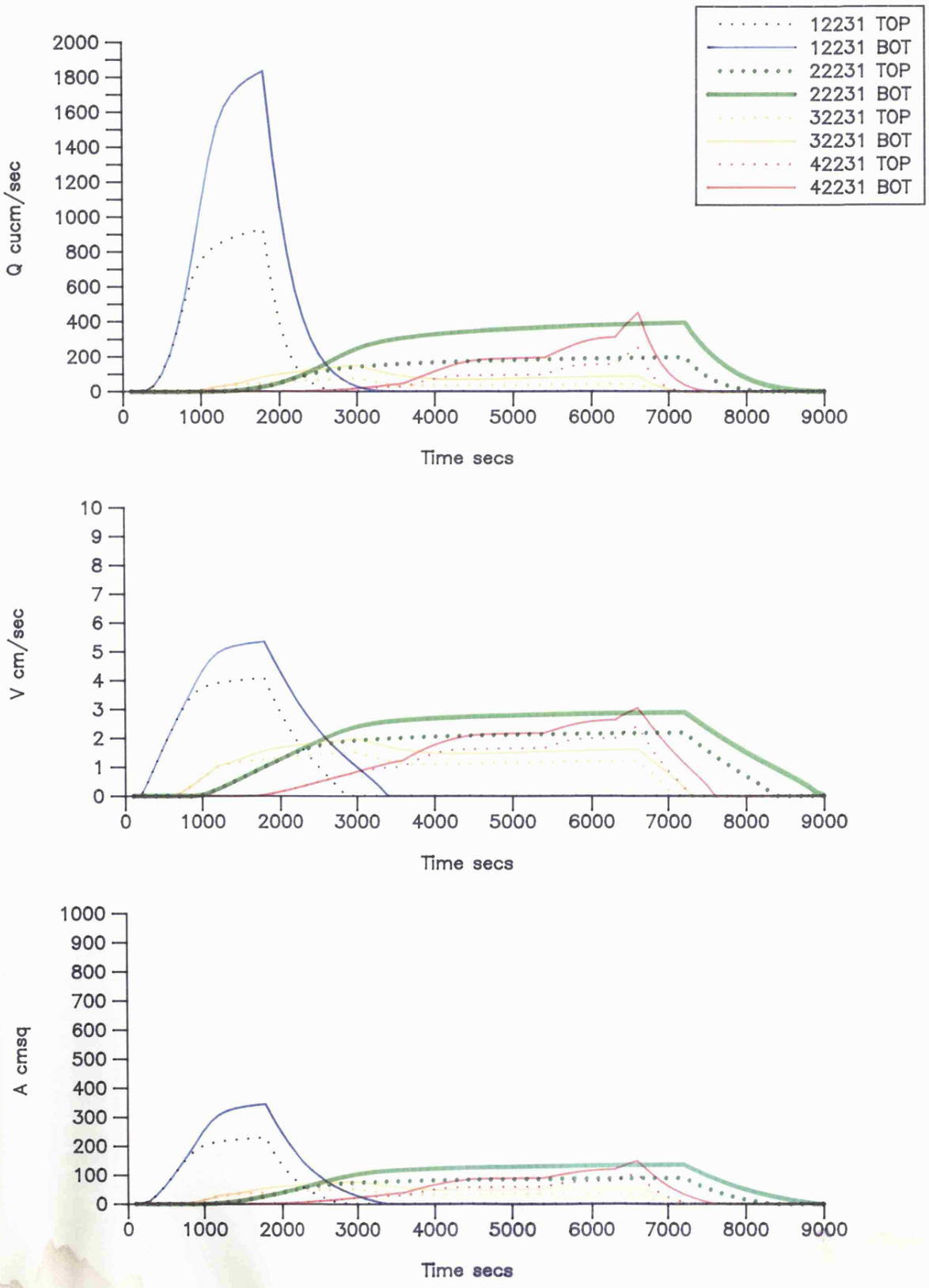

Figure 5.18 The Hydrological Response from a Micro-Rough Hillslope with Different Rainfall Intensity Distributions

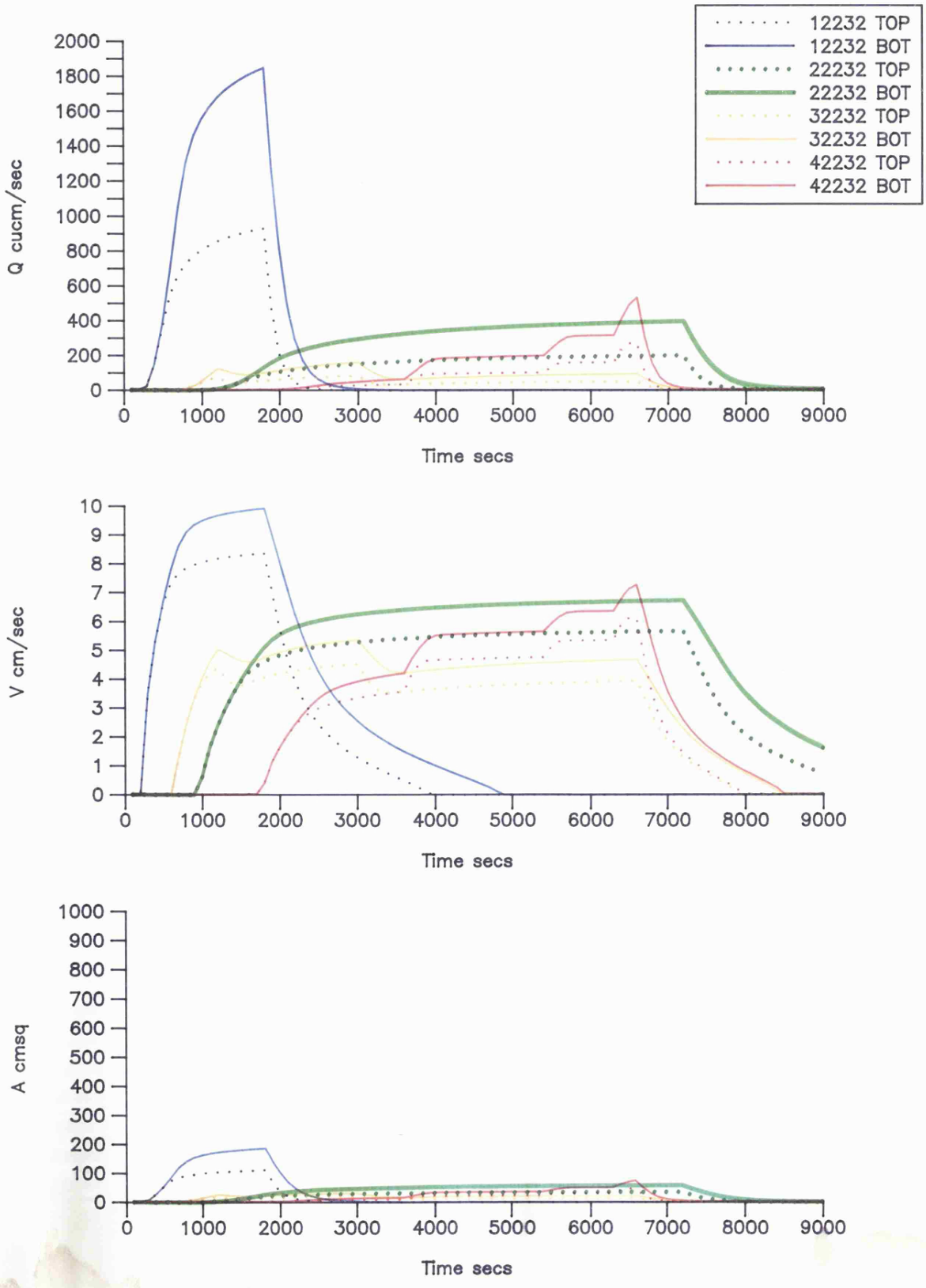

simplified hillslope runoff model as well as though a range of instrumented catchment field experiments. Assessing first the best parameter combination cascade, it is clear that with slope conditions held constant downslope, there is a general increase in peak discharge levels downslope as expected from earlier discussions in Chapter One, although not a uniform one, as steady-state conditions are not reached. The major effect of increasing downslope length is felt in the total discharge produced from the cascade and the losses experienced once rainfall ceases. There are marked variations between the experiences of a micro-smooth surface (sheetflow assumption), and a micro-rough surface (complex flow assumption) for the range of rainstorms simulated for the best parameter combination cascade.

To look at the effect of slope length the productivity from 'j' plots in a cascade must be compared to the productivity from 'j' single plots in isolation. Considering the productivity from the upper cell (element 31) for each rainstorm. The predicted runoff out of 1 m^3 input of rainfall is 0.560 m^3 for the 40 mm hr^{-1} intensity and 0.470 m^3 for the 10 mm hr^{-1} intensity for the sheetflow, smooth surface. For the varied complex surface the productivity is 0.603 m^3 and 0.490 m^3 for the two rainfalls. As explained, this shows how intensity is important in determining runoff productivity. It also shows how the variation in the surface profile from a plane helps increase productivity. The productivity from a single cell for the decreasing and increasing rainfall intensities is 0.270 and 0.410 m3 respectively. Again this shows the effect of intensity distribution and how increasing rainfall intensities following runoff production yield a higher total runoff than decreasing intensities due to the relative magnitude of infiltration rates and intensities.

From a consideration of the relative productivities from slopes of different lengths, it is clear that for the parameter sets chosen and the length of hillslope considered, the runoff productivity is relatively insensitive to slope length compared to the sensitivity to slope spatial variation. Where complex flow is assumed, then for the best parameter combination cascade, the percentage productivity remains more or less the same for each location downslope. The volumetric discharge increases in direct proportion to the downslope length maintaining the per unit area productivity. This is due to the fact that the routing of runoff is very effective, and the losses to infiltration post-rainfall minimal with a steep, short falling limb as most of the water is routed over and off the surface during or soon after the rainfall period. The proportion of water held in detention is small compared to the total discharge and hence the productivity figures are unaffected. This is not true for the sheetflow assumption where productivity decreases from 56%, 47%, 27% and 41% for the four rainstorms onto a single plot to 51%, 44%, 25% and 37% respectively. This is still not a great change and shows how for constant conditions on a highly productive and transmissive slope, the effect of length is less important than the effect of rainfall intensity on runoff productivity for a given rainfall input depth. Taking the alternative cascade which has been assigned the worst combination of routing and infiltration parameters, this is not the case. For three of the rainstorms, no runoff is forecast due to high infiltration rates and the

large Vs associated with the infiltration parameters. For the high intensity rainstorm, there is runoff, but the poor routing and the high infiltration means that the knock-on effect downslope is inhibited as rainfall ceases soon after runoff begins and surface water is soon consumed. Insufficient time elapses to allow the flood wave generated on one cell to pass downslope and build up discharge levels on subsequent cells. Consequently, the productivity reduces with an increase in contributing area as total discharge recorded remains constant. In the case of the sheetflow, the productivity decreases from 8.8% of total inputs to 2.0% and for the complex flow, from 24% to 10.5% as slope length is increased from 10 to 40 metres. Where complex flow is assumed it seems that the duration of the flow event is sufficient for the flood wave to pass from one cell to the next, but not from the top of the plot to the bottom as with the best parameter combination. This is shown by the way there is an increase in discharge between the first and second cells, but the remaining cells 2-4 have equal discharge characteristics.

The results of the simulations with varying flow length are interesting because they show that for the range of parameters used, the interplay between rainfall intensity and distribution and infiltration rates are most important in determining productivity than the length of slope. Additionally the effect of juxtaposing two different slope sections is also a more important control on productivity than scale and the modifying effect of assuming either sheetflow or complex flow can have considerable effects with different parameter combinations. Concentrating on scale alone without giving sufficient attention to the routing components controlling flow velocity and discharge is likely therefore to mask true sensitivity.

5.3.5 Conclusions from the Sensitivity Analysis

The results of changing contributing slope length coupled with the observations of the effects of changing slope conditions along a flow-line are important for the understanding of partial area productivity and the functioning of water harvesting systems. The major conclusions are summarised in the following points;

1. Slope length becomes more important at controlling total productivity as flow routing and infiltration conditions worsen. Water generated on the slope moves more slowly and the potential for post-rainfall infiltration remains high relative to the volumes of water on the surface,

2. Where routing is more effective (in the case of complex flow for instance), then for a given infiltration, productivity increases and the effect of slope length is suppressed,

3. Where spatial variation exists along a flow-line then the characteristics of partial area contribution can be seen and the knock-on, reaching-down conditions described in Chapter One are experienced,

4. Where a good producer is situated above a poor producer, then depending on their relative characteristics and the amount and timing of rainfall, the poor producer can act as a consumer, totally dissipating the high discharge running on from above, or the good producer can reach-down over the poor producer and help it to reach ponding more quickly and both generate and transmit runoff out of the slope and into a channel assumed to be located at its base,

5. Where the consuming effect is high, by locating a channel immediately below the good producer, the consumptive effects of the poor producer could be avoided and the total productivity of the slope enhanced,

6. Point (5.) is not true for slopes which show no variation in conditions and are uniformly good producers and transmitters. Introduction of additional channels would not appreciably increase the amount of water harvested from this kind of slope section. This has obvious relevance to the design and functioning of water harvesting systems. Since the effect of allowing water to flow un-obstructed over long consumptive sections of hillslopes is to dissipate potential productivity, then where water volumes supplied to a runoff farm are insufficient, channels must be introduced at selected points within the flow-line to increase productivity,

7. A final conclusion of considerable theoretical relevance can be made from the predicted responses using the two different flow dimensions assumptions, that of micro-smooth (sheetflow) and micro-rough (complex flow) surfaces. They show the result of assuming sheetflow when it is known that the surface varies significantly from a plane. Depending on how the infiltration parameters are calculated, as discussed in Chapter Three, the assumption of sheetflow may lead both to underestimates of productivity from a given location and to an overestimate of the transmission losses on the recession limb of the hydrograph post-rainfall.

CHAPTER SIX TESTING THE SIMULATION MODEL

In addition to theoretical simulations using the rainfall-runoff model WATERH designed to show the sensitivity of both the model and the arid hillslope hydrological regime to particular parameters and parameter combinations, the model is tested through application to a number of real situations at a variety of scales and levels of complexity. These are designed to fulfil several functions. Firstly, there are the modelling considerations which illustrate the versatility of the programming procedures and concepts in addressing key questions concerning the process environment at a range of scales, and the subject of this thesis, the technology of runoff harvesting from arid catchment systems. Secondly, there are the data considerations which concern the advantages and limitations of the techniques adopted for the provision of model parameters and their ability to reproduce observed conditions. This illustrates a perennial problem for deterministic modelling, that of reconciling plot experiments and areal sampling with wider scale application to represent a more complex and dynamic system. Thirdly, there are the applied aspects of the simulations; the use of the model as an analytical and design tool to assess the design considerations for effective water harvesting in a particular context. Irrespective of any of the other considerations, the applied aspects of the model use at the intra-hillslope and intra-catchment scale to illustrate the principles of water harvesting and its relation to the hydrological concepts of hydraulic remoteness and contiguous area contribution are inherently important.

Through the rigorous, systematic programme of plot, hillslope cascade, and complete sub-catchment modelling described in this chapter, the requirements, limitations and successes of the use of distributed models in the applied study of an arid environment can be determined. This focuses on the interpretation of the processes, the measurement of those processes, their modelling and the applied use of the model.

6.1 RUN-ON/RUNOFF PLOT SIMULATIONS

6.1.1 Purpose of the Plot Simulations

The purpose of the run-on/runoff plot simulations is to assess the sensitivity of the process parameters in predicting the observed infiltration and runoff response under field test-conditions. They are used to parameterise a simple routing model of the plots. The predictions help to evaluate the parameters and their suitability for application in additional larger-scale simulations under rainfall-routing conditions.

The field experiments of run-on and runoff yield uniquely determined parameters compared with rainfall simulations used to parameterise the storage infiltration model in its original conceptualisation.

It must be assessed whether the parameter concepts lend themselves to a wider application outside the plot conditions where input is supplied from rainfall rather than run-on. It is clear from discussions in Chapter Three that the experimental conditions do not lend themselves to wider application if used directly due to the probable over-estimation of initial rates from the dual effects of routing and detention storage. Steps must be taken to get beneath these values and determine how the experimental design can be used to maximise parameter generality. This can be accomplished by considering how useful the parameters are at predicting runoff response under the unique plot conditions and through recognising that the simulation results depend upon a number of factors including:

1. how the plot experiment was conceptualised in terms of the method of run-on and runoff, and the timing of observations,
2. the specification of infiltration values for the fitting of curve parameters,
3. the role played by routing and the resistance coefficient and its affect on hydrograph shape,
4. the slope gradient of the plot.

Each of these play a role in determining the sensitivity of the simulated flow conditions to the observed. The first three factors relate to the fact that the experimental design operates at a larger temporal scale than is required by the simulation model, both for the plot simulations, and for wider applications. Initial infiltration and rising curve routing is significantly controlled by conditions observed during later phases. This section adopts a methodology that investigates this temporal gap and explores the possibility of filling it through an assessment of the infiltration parameters. Whilst it is true that the overall emphasis of the plot run-on/runoff experimentation is on the steady-state conditions the importance of approximating the conditions in the more dynamic rising phase is recognised and attempted.

6.1.2 Run-on/Runoff Plot Test Conditions and Sources of Error

Water is run-on to an initially dry surface and must pass over a length of one-metre as a wetting-front, satisfying infiltration and building up a hydraulic head as detention storage rises. The first observed output discharge from which infiltration is calculated as input minus output also reflects a significant amount of water that is in detention storage. However, the additions to storage decrease through time towards the steady state conditions which can be expected to represent closely the actual infiltration. Data is sampled at a relatively coarse time resolution.

In the earliest time periods, calculated infiltration rates are clearly over-estimates resulting from the combined effects of:

1. areally and temporally averaging input as a single average depth equivalent. In the early phases, infiltration estimates from input minus output are affected by routing flow, detention storage and averaging,
2. the assumption that the infiltration process starts at time t=0 for all points on the surface whereas this is only true for the very top of the plot. In reality, the infiltration process starts at t=0 for the first micro-increment and t_{ro} (time to run-out) minus t_o (time to runoff) for the last micro-increment,
3. the inclusion of additions to surface storage in the volumes of water attributed to infiltration. This will logically decrease towards steady state conditions where the infiltration rate is controlled by the A parameter. This is the routing time-lag as surface water is generated but is restrained from flowing off the plot by the forces of friction (defined by Mannings n).

A probable source of error in the simulations is the need to predict infiltration rates at smaller time increments than the original data set used in the curve-fitting procedures. This is especially important within the first observed time period in which the infiltration predictions may be least sensitive.

The routing parameters of slope gradient and Manning's n roughness include areal and temporal averaging which could be expected to affect sensitivity. The slope gradient represents the average over the 16 m^2 field sample area in which the run-on/runoff plot is sited and hence may vary slightly from the local slope of the plot. The resistance coefficient was calculated from the flow-data established once steady-state conditions were achieved during the field tests at each plot, measuring the velocity of flow and calculating the mean depth across the wetted surface. This is used to quantify the resistance for the complete duration of the field test, on both the rising stage and at steady-state.

6.1.3 Plot Conditions and the Rainfall-Runoff Process

The method of calculating the infiltration time series by temporal and areal averaging means that the B parameter of the Green and Ampt infiltration model is unlikely to be representative of the rainfall-runoff process, a fact that can be tested by modelling the routing across the plot in a fashion that represents rainfall-equivalent conditions. The effects of the averaging and adjustment of parameters must be assessed. As explained in Chapter Three, errors between the predicted and observed conditions will result predominantly from over-estimations of the B-parameter. Whilst the predicted final infiltration rates (increasingly controlled by the A-parameter) can be accepted as a close estimation of the true final infiltration rates, the initial infiltration rates, as controlled by the B-parameter, reflect all the non-point, non-instantaneous aspects of the infiltration calculations. How these affect the predictive ability can be seen from the simulation results.

In a consideration of the results of the simulation, the objective is to determine clear and meaningful measures of the differences and similarities between observed and predicted flow and infiltration conditions during the course of the tests. Both numerical and graphical measures can be used to provide a qualitative and quantitative assessment of the predictions. The most relevant values are the time to run-out from the bottom of the plot, the first time period volumetric discharge, some intermediate time period volumetric discharge, and the total volumetric discharge. Each reflect important aspects of the parameter performance. In addition, the shape of the rising and steady-state portions of the predicted hydrograph can be compared to assess the overall goodness of fit of the predictions and whether there is a systematic basis to the errors, i.e. whether the predictions vary with time and in particular whether they are confined to the initial rising curve.

6.1.3.a Times to Run-Out (t_{ro})

The predicted time to run-out of water across the lower boundary of each run-on/runoff plot is the summation of the initial times to runoff for each downslope increment. Water is input into the upper increment as a depth and once the time t_o has been reached when the storage V_s is full as defined by Equations 3.15 and 3.17, water is routed out of the increment using the flow and finite difference equations.

6.1.3.b The First Observed Time Increment Volumetric Discharge ($\Delta Q1$)

For each of the run-on/runoff plots, the first time increment (Δt_1) contains the observed time to run-out. The predicted discharge for this first time increment shows the ability of the infiltration and routing components of the simulation model to reproduce the time to run-off and initial flow conditions on the plot with the given parameters.

6.1.3.c Intermediate Time Increment Cumulative Discharge (Q3)

This is used to indicate two major characteristics of the predicted response. Firstly, when compared with the first time period infiltration, it shows the degree to which the predictions have adjusted to the observed during the sensitive initial rising-curve period of roughly nine to 12 minutes. Secondly, when compared with $\Delta Q1$ and the total predicted discharge ΣQ, it shows the degree to which the error distribution is skewed towards the initial time periods or whether there are also considerable differences during the later steady-state period.

6.1.3.d Final Observed Time Increment Cumulative Discharge (ΣQ)

This represents the overall performance of the model and parameters at predicting the total output from the run-on/runoff plot. Where there is a general under- or over-prediction of rising curve discharge but the errors in total discharge are small, it means the steady-state discharges have compensated by their own over- or under-predictions.

6.1.4 Initial Simulations

The simulation model used is a truncated version of the full simulation model designed to handle the special case of the run-on/runoff plot simulations in which an input hydrograph enters over the upper boundary and the output hydrograph exits over the lower boundary. The total length of the plot is 100 cm and the widths of individual increments are defined by the shape of the wetted area measured at intervals during the field tests. The simplified model couples the Green and Ampt equation, Mannings flow equation and the finite difference routing equation (as presented in Chapters Three and Four) to form a kinematic cascade routing model. The flow assumption is that of sheetflow, since the infiltration data is derived from field plots whose resolution does not allow calculation of the series of wetted lengths associated with each observation time. This could only realistically be carried out in controlled laboratory studies or more rigorous, instrumented field plot experiments. The theoretical implications of assuming sheetflow have been discussed in Chapter Three and in the previous sensitivity analysis.

The cascade configuration chosen to represent the run-on/runoff plot is a series of five 20 cm long slope increments. Any length and number of increments could have been simulated by the runoff model. However, a balance was necessary between the following considerations. If the number of increments was too few, and the length of the increments too long, the approximation of the actual conditions of a decreasing head of water moving down over successive locations would be lost in favour of a spatially averaged, lumped input. This would neither be a test of the routing characteristics of the model, nor a representation of the conditions experienced in wider applications of the parameter sets. However, if the number of increments were too many, the opportunity for the compounding of errors caused by routing and time to runoff calculations would increase. Five 20 cm cells were considered to be an appropriate balance between these two considerations, given that the resolution of the gradient, resistance and infiltration data set applies to the whole one metre length of the plot or larger, and the wetted width of the plot was measured at 10 cm intervals from the top of the plot to the bottom to provide the wetted area used to define the surface configuration.

Table 6.1 Predicted Times to Run-Off and Run-Out (A, B1)

6.1.4.a Times to Run-out (t_{ro})

Plot	Unit	t_5	t_4	t_3	t_2	t_1	t_{ro}	Obs t_{ro}
18	1e	18	48	46	50	51	215	85
20	2e	24	84	110	153	91	462	215
23	3e	11	38	35	40	49	173	37
25	4e up	11	37	39	46	52	185	37
28	4e lo	21	54	46	41	39	201	48
32	5e	25	74	80	109	196	484	120
34	5w lo	28	108	107	151	438	832	222
36	4w	26	83	97	112	123	441	107
38	3w	6	29	33	39	45	152	116
42	6w	10	34	33	39	47	165	66
47	5w up	17	51	47	47	48	210	68

(where t_5 - t_1 are the predicted times following inflow at which ponding occurs for the five spatial increments and t_{ro} is the predicted time for runoff to discharge from the bottom of the complete plot i.e the sum of t_5 - t_1. This must be compared to Obs t_{ro}, the observed time to runoff out of the plot)

Use of the basic infiltration and routing parameters in the simulations of the plot response to flow input results in consistently higher predictions of the time to run-out than those observed. This shows under-predicted runoff productivity due to the inclusion of non-infiltration components in the definition of the infiltration B parameter. The hydraulic head build-up is essentially included twice in the calculations, firstly in the fitting of the B-parameter to the calculated infiltration time-series, and secondly in the routing procedures using the B-parameter. Times to run-off are higher than might be expected for each Δx increment 5 to 1 due to the initial infiltration values being infiltration plus storage, and then for the routing routines, the discharge is determined by the proportion of post-ponding surface water retained as detention storage (A(x+1, t-1)) in each increment. Whilst the latter may well be an accurate representation of the actual detention storage build-up, when coupled with over-estimated infiltration, the time to run-out is poorly specified. The seriousness of these over-estimates of infiltration is such that in some plots (20, 32, 34, 36 and 47), no run-out is predicted at all in the first observed time increment $\Delta t1$, as discussed below.

6.1.4.b Discharge Predictions

Table 6.2 Predicted Summary Discharge Values (A, B1)

Plot	Unit	O ΔQ1	P ΔQ1	O Q3	P Q3	O ΣQ	P ΣQ
18	1e	1190	165	6440	5143	47928	46714
20	2e	248	0	4600	3022	59296	57782
23	3e	2032	716	8422	6791	52638	50992
25	4e up	1262	0	8110	5370	94086	91639
28	4e lo	1669	437	6878	6020	49783	48590
32	5e	244	0	3466	934	34144	31571
34	5w lo	68	0	1724	148	15858	14354
36	4w	286	0	2882	1788	28776	26468
38	3w	905	105	6865	5645	74555	73274
42	6w	1600	312	8160	6231	44590	43016
47	5w up	870	0	5930	4036	63870	62696

Table 6.3 Percentage Errors for Predicted Summary Discharge Values (A, B1)

Plot	Unit	%E ΔQ1	%E Q3	%E ΣQ
18	1e	86	20	2
20	2e	100	34	2
23	3e	65	19	3
25	4e up	100	34	3
28	4e lo	74	12	2
32	5e	100	73	7
34	5w lo	100	91	9
36	4w	100	38	8
38	3w	88	18	2
42	6w	80	24	3
47	5w up	100	32	2

The summary discharge values listed in Table 6.2 shows that overall, the basic parameters under-predict the observed discharges during the rising curve period, variously under or over-predict the discharges on the approach to steady-state, and predict extremely well the final, steady-state discharges in all plots. This is borne out by an examination of the hydrographs in Appendices 5.1.1 to 5.1.11 which show a close correspondence in all cases between the steady-state predicted hydrograph and the steady-state observed hydrograph. The under-prediction in the first time periods is serious as shown by the third and fourth columns of the percentage error Table 6.3 above in which the minimum error for all the plots for the first three observation times (%E Q3) is 12% and the mean 36%. Examining the distribution of errors presented with the observed and predicted hydrographs in Appendices 5.1.1 to 5.1.11 shows how generally these start high and then converge on and fluctuate around zero until the end of the test following the first four or five observations. This is supported by the total discharge errors which reduce to a mean of 4%, with the highest being 9%. The source of these early timing errors is clearly not due to mis-specification of the infiltration model vis á vis the observed data because, as shown by the graphs of the observed data, infiltration curve, and distribution of variations between the model predictions and the observed data, the model performs well. Therefore, the error lies within the estimated infiltration values themselves for these early time periods. This is exactly what was expected from the descriptions of the experimental design and model structure as described earlier

and supports the conclusion that the observed infiltration rates are over-estimates by a function of the routing time-lag included in the infiltration rate calculations.

Having said that the infiltration model performs well, what is also obvious from the graphs of discharge and infiltration, is that where the model generalises the time-series of infiltration rates this affects subsequent predicted discharges. This is very clear for plots 18 and 28 and shows the importance of correctly specifying infiltration parameters in a rainfall runoff model. These effects are expected since the infiltration model is only an idealised representation of the observed conditions.

6.1.4.c Interpretation and Evaluation

Because the predictions of discharge from the run-on/runoff plots converge closely on the final observed values it can be accepted, as stated in Chapter Three, that a problem is encountered with the initial infiltration rates which is a consequence of the experimental method chosen for measurement and the inclusion of detention storage in initial infiltration rate calculations. Initial infiltration values are overestimated although the final value is relatively accurate. The steady state-discharge shows that the routing function is adequate as expected since the resistance parameter is derived from steady-state conditions.

The over-estimation of the B-parameter is clearly a problem. Due to the use of an explicit finite difference procedure in defining the routing equations, smaller time increments must be used to model flow than were used to measure infiltration. The model is therefore required to work at a resolution smaller than the original data. The model relies on subsequent time periods for its parameters and although the general form of the equation is obviously correct, as shown by the goodness of fit to the observed data, the sensitivity to these early time periods is the weakest.

If the B coefficient used in these simulations were to be used for wider applications outside the plots without addressing the over-estimation, the parameters could not be expected to produce the orders of magnitude of observed runoff response at the larger catchment scale. Poor forecasts of time to runoff might possibly prevent runoff occurring altogether at the hillslope scale for the slope areas that have the highest over-estimates of initial infiltration rates such as units 2e, 5e, 4w and 5w (although the unit 5 infiltration in the catchment simulations is represented by literature values due to the problems of accounting for crusting with a run-on/runoff set of parameters as explained in Chapter Three).

6.1.5 Secondary Simulations Using Modified Plot Parameters

6.1.5.a Rationale

To use the field infiltration data to parameterise a full rainfall-runoff model application to the wider Avdat catchment, it is necessary to get behind the parameters and the effects of the unique experimental conditions from which they were derived. This applies to the B parameter which because of the spatial and temporal averaging in the calculation of the infiltration rate time series, limits the ability to predict the important initial time to runoff period and the rising portion of the hydrograph when applied at a smaller temporal and spatial resolution. The B parameter must therefore be modified so that the new curve helps predict the observed character of the run-off downslope across the plot. The effects of changing the B-parameter can be examined by re-simulation keeping all other parameters constant. Whilst it is accepted that there are other possible sources of error in the predictions, specifically Manning's n which also plays a key role in the dynamics of this phase, only the infiltration parameters can be modified due to data constraints

The methodology for getting behind the spatial and temporal averaging in B parameter specification is to concentrate on the first Δx increment (increment 5) as a surrogate for the complete plot for the period t=0 to t_o. In terms of the plot configuration, the only increment for which the input conditions are known is the uppermost slope increment. This receives a known volume of water in a given time, whereas subsequent increments receive an amount determined by prior segment predicted infiltration and the routing procedures. The depth input to the increment depends on the increment size. Conceptually, the infiltration model requires that the time to runoff be predicted for a given surface when the soil storage V_s is full and flow can begin. For the plot as a whole, the time to run-out (t_{ro}) is the nearest measurement to this given the experimental method. However, it is not the same as the time to run-off (t_o). Having split the plot into smaller increments to approach more closely the rainfall-runoff conditions, it can be assumed that the time to runoff of the first increment provides a closer approximation to the true time to runoff of the whole plot than does the time to run-out. It is the only one of the five in the cascade whose input and time to runoff are not affected by the routing parameters.

The stages in B parameter modification are:

1. calculate infiltration by subtracting output from input,
2. fit best-fit curve A and B parameters to data, where B includes the effects of spatial and temporal averaging and detention storage,
3. run the simulation model using these parameters to predict times to runoff for each increment, and subsequent runoff for the duration of the test (the initial predictions are poor),

4. modify the parameters using the predicted time to runoff (t_5) for increment 5 to concentrate on the first Δx increment rather than the whole plot for which only the time to run-out (t_{TO}) is known.

Substituting the predicted time to runoff of the upper increment into the Equation 6.1 with the average rainfall intensity equivalent for the complete plot and the original A parameter gives a modified B-parameter (B2) designed to account for the over-estimates of infiltration by spatial and temporal averaging.

$$B2 = t_5 (\Delta Q/(t_5.WA) - A) \qquad \text{Equation 6.1}$$

(t_5 is time to ponding on the uppermost element, ΔQ is the discharge in during t_5 and WA is the run-on/runoff plot wetted area).

By taking the small section time to runoff prediction, the problem of double accounting of the routing and detention storage errors does not occur. By using the average rainfall depth equivalent of the discharge into the small plot, an attempt is made to compensate for the over-estimates in the original data-set through the inherent spatial and temporal averaging. As shown in Table 6.4, the B2 value is smaller than the B1 value derived by curve-fitting through the original data. It represents a change in the gradient of the curve since the final infiltration rates are controlled by the A-parameter and the initial rates by the B. This is conceptually correct, but its sensitivity at reproducing the observed discharge conditions when applied in a set of run-on/runoff simulations must be determined. Comparing the B1 and B2 infiltration curves presented for each plot in Appendices 5.1.1 to 5.1.11 it is clear that the modification of B1 to B2 results in a much steeper approach to steady-state conditions at an earlier time as expected. The changes in predictions of times to run-out, initial, intermediate, and final cumulative discharges and an examination of the observed and predicted hydrographs examines the appropriateness of this assumption.

Table 6.4 Original and Modified Infiltration Parameters

Plot	Unit	A	B1	B2
18	1e	0.000414	0.1290	0.0274
20	2e	0.000427	0.1110	0.0106
23	3e	0.000179	0.0686	0.0133
25	4e up	0.000047	0.1090	0.0188
28	4e lo	0.000359	0.1490	0.0438
32	5e	0.000592	0.1880	0.0328
34	5w lo	0.001690	0.1470	0.0228
36	4w	0.000777	0.1580	0.0233
38	3w	0.000171	0.0516	0.0065
42	6w	0.000193	0.0820	0.0156
47	5w up	0.000381	0.1910	0.0457

6.1.5.b Times to Run-out (t_{ro})

Table 6.5 Predicted Times to Run-Off and Run-Out (A, B2)

Plot	Unit	t_5	t_4	t_3	t_2	t_1	B2 t_{ro}	Obs t_{ro}	B1 t_{ro}
18	1e	4	17	18	19	18	76	85	215
20	2e	3	20	29	36	46	134	215	462
23	3e	3	14	17	19	22	75	37	173
25	4e up	2	13	18	21	22	76	37	185
28	4e lo	6	25	23	21	19	94	48	201
32	5e	5	24	29	31	31	120	120	484
34	5w lo	5	43	47	47	50	192	222	832
36	4w	4	26	32	35	35	132	107	441
38	3w	1	9	16	18	19	63	116	152
42	6w	2	14	18	20	22	76	66	165
47	5w up	4	22	23	23	23	95	68	210

Use of the modified B2 parameter in simulations keeping all the other characteristics of the previous B1 simulations constant produces much closer predictions of the observed times to run-out. Previously each time to run-out was over-estimated, but with these simulations there are both over and under estimates. These results compared with the previous indicate that adjusting the B1 coefficient has the effect of significantly increasing the rate at which the water input over the upper boundary of the plot moves across the previously dry surface. Whilst there are still variations between the observed and predicted values, the new B2 parameter would appear to better represent the wetting front transmission and hence is more appropriate for wider use under rainfall conditions.

6.1.5.c Discharge Predictions

Table 6.6 Predicted Summary Discharge Values (A, B2)

Plot	Unit	O $\Delta Q1$	P $\Delta Q1$	O Q3	P Q3	O ΣQ	P ΣQ
18	1e	1190	1754	6440	7874	47928	51264
20	2e	248	960	4600	6197	59296	63571
23	3e	2032	2116	8422	8927	52638	54055
25	4e up	1262	1452	8110	9004	94086	97855
28	4e lo	1669	1755	6878	8394	49783	53324
32	5e	244	910	3466	5371	34144	40097
34	5w lo	68	298	1724	1928	15858	17555
36	4w	286	791	2882	4870	28776	31901
38	3w	905	1654	6865	8438	74555	77955
42	6w	1600	1745	8160	8699	44590	46622
47	5w up	870	893	5930	7631	63870	69970

Table 6.7 Percentage Errors for Predicted Summary Discharge Values (A, B2)

Plot	Unit	%E ΔQ1	%E Q3	%E ΣQ
18	1e	-47	-22	-7
20	2e	-287	-35	-7
23	3e	-4	-6	-3
25	4e up	-15	-11	-4
28	4e lo	-6	-22	-7
32	5e	-273	-55	-17
34	5w lo	-338	-12	-11
36	4w	-177	-69	-11
38	3w	-83	-23	-5
42	6w	-9	-7	-5
47	5w up	-3	-29	-9

These summary indicators illustrate that the use of the modified B2 parameter in simulations of the run-on/runoff plot response results in over-estimates of discharge from the plot during the rising curve, but again, the final steady-state discharges are closely predicted as shown by comparisons of the observed and predicted hydrographs in Appendices 5.1.1 to 5.1.11. Examining the steady-state phase of the infiltration curves in the figures for each plot and comparing this with the steady state hydrographs shows that there is a close correspondence between the two. This suggests that both the infiltration and the routing parameters function very well in this flow phase.

During the rising phase, however, there are universal over-estimates of runoff production out of the base of the plot. These decrease towards the steady-state conditions which as shown, produce generally close estimates. The degree of overestimation varies between plots but the error distribution is generally skewed to the start of the simulation as shown in Appendices 5.1.1 to 5.1.11. In each, the cumulative discharge errors decrease as convergence with the observed values reduces the overall error through the course of the simulation.

For the first three time periods, the over-estimates of run-out volume average 26%. What degree of this is due to changing the infiltration parameter, the general fit of the infiltration curve, or the routing effects of the slope gradient and particularly the resistance coefficient is difficult to determine. However, an examination of each plot response can allow some broad conclusions to be drawn.

Plot 18 (1e)

The original estimates of runoff showed that although the infiltration model fitted almost exactly the first two time period observed rates, the predicted runoff was considerably lower, suggesting the infiltration rates for these time periods to be over-estimated. By changing the B1 parameter to B2, the effect has been to increase the predicted runoff in the rising phase, and over-estimate runoff in the intermediate phase (Appendix 5.1.1).

Plot 20 (2e)

The use of parameters A and B1 produced a very close prediction of observed runoff after the first four time periods but an under-prediction of the rising curve. With B2, the error distribution changes to over-prediction in the first four time periods and a similar, slightly lower set of values subsequently. The rising curve errors are opposite to the previous simulations although of a similar magnitude (Appendix 5.1.2).

Plot 23 (3e)

There is a very close prediction to the observed conditions in the rising, intermediate, and in the steady-state phases and the B2 parameter accounts very well for the previous errors in predictions (Appendix 5.1.3).

Plot 25 (4e upper)

The B2 parameter produces a close prediction of observed conditions throughout the whole run-on/runoff response. The rising curve is slightly over-predicted although the errors are relatively consistent throughout the duration of the test. This may be a result of a slight under-estimation of the A-parameter in the original curve-fitting which results in reduced steady-state discharge when coupled with a smaller B2 (Appendix 5.1.4).

Plot 28 (4e lower)

There is an over-estimation of runoff production for the second and third time periods but subsequently and for the first time period the predictions are very close to observed. The intermediate incremental predictions of runoff are improved considerably over the previous although the steady-state predictions are consistently slight overestimates. The over-predictions in the second and third time periods are a result of the original infiltration curve-fitting, further emphasised by the reduction in B1 to B2. The two error outliers are sufficiently large to maintain a higher error statistic for the complete simulation (Appendix 5.1.5).

Plot 32 (5e)

A considerable portion of the 17% total over-prediction is due to the final rate infiltration. Since the B1 parameter is large, it plays a relatively more important part in determining the infiltration rates in the intermediate and steady-state periods of the infiltration. The original parameters reproduced the steady-state conditions, only underestimating the initial rates. By reducing B1 to B2 the steady-state

predicted infiltration falls below the observed and so the B2 parameter over-compensates for the assumed detention storage error and influences predictions by its affect on steady-state (Appendix 5.1.6).

Plot 34 (5w lower)

Plot 34 provides a generally good prediction of the observed hydrograph as shown in Appendix 5.1.7. The very large over-prediction in the initial runoff is large in percentage terms, but small in absolute terms. The runoff production from this plot is the lowest of all. The rising curve is otherwise well predicted with a total over-prediction of only 12%. The over-predictions contribute to maintaining a relatively high over-prediction for the cumulative discharge at 11%.

Plot 36 (4w)

Although runoff is now forecast to occur in the first time period, there are over-predictions in the rising and intermediate phase. The steady-state runoff predictions converge very closely on the actual values although the initial errors are sufficiently high to maintain a complete over-estimate of 11%. The modification of the B1 parameter to B2 would seem to underestimate the infiltration to a greater degree than the previous set over-estimated it. However, part of the over-prediction may be attributable to the routing components and particularly the resistance parameter (Appendix 5.1.8).

Plot 38 (3w)

There is a relatively good fit to the observed infiltration data, although again, the errors in over-prediction for the early time periods, are of a similar order of magnitude as the errors in under-prediction with the B1 parameter. There are a series of fluctuating errors related to the fact that the original infiltration time series is a scattered one and the curve a generalised fit as shown in Appendices 5.1.9. With B2, there is an over-estimate of the rising curve sufficient to predict discharge in excess of the steady-state. This suggests that the routing potential is over-estimated and greater velocities are predicted for a given depth, raising discharge rates over those expected. The predictions gradually settle with small errors and the total cumulative discharge is finally only 5% greater than the observed.

Plot 42 (6w)

The predictions from this plot are good for the whole duration of the run-on/runoff response. The previous over-predictions of infiltration on the rising stage have been replaced by close predictions with only a 9% over-estimate which reduces as the simulation proceeds into the steady-state phase (Appendix 5.1.10).

Plot 47 (5w upper)

The first part of the rising curve is well reproduced with a better estimate of time to run-out and first time period discharge (3% over-prediction) but then the prediction worsens as the rest of the rising and intermediate hydrograph is over-predicted until the predictions again converge closely to the observed during steady-state. Modification of the B-parameter results in the probable over-compensation of the already generalised curve-fitting (Appendix 5.1.11).

6.1.5.d Interpretation and Evaluation

It is clear that there are problems with the infiltration parameters and that they conform to the explanations earlier in this chapter and in Chapter Three. This is shown by the generally encouraging, but mixed results from the modification of the B1 parameter to B2 using the surrogate times to runoff from the first small sub-section of the plot. By modifying B, the serious problems of underestimating the critical time to runoff period and the rising-limb of the hydrograph have been addressed and partially solved. However, since the parameter set is weighted towards steady-state conditions by the experimental procedures and use of the steady-state Manning's n values, the rising curve remains a difficult phase to reproduce. It is clear from the switch to over-predictions that the cause of errors are more complex and the issue of parameter modification is highly dynamic. For a completely satisfactory solution, a more detailed and sophisticated set of measures would be required than is warranted by the data set and proposed application in which a small number of plot data sets are used to provide the order of magnitude of responses within a larger catchment system.

From discussions of the nature of arid zone hillslope hydrology in Chapter One and flow routing in Chapter Four, the most likely source of the rising curve over-predictions can be attributed to the flow velocities and depths associated with the early flow stages. In the theoretical sensitivity analysis described in Chapter Five, the effects of varying resistance and slope gradient with and without the added influence of infiltration were analysed. The influence of both resistance and gradient on the timing of the hydrograph was considerable for the range of values derived from the Avdat catchment. At low gradients, a given variation in slope has a greater than proportional effect than for a larger slope. Thus the plots with low slope gradients such as 28, 32, 34, 36, 42 and 47, the unit 4, 5 and 6 areas, are more likely to be sensitive to the use of an average slope to describe the plot than the others. Mannings n has a direct influence on predicted velocities in proportion to its relative size, a decrease in n by 50% causing an increase in velocity by two and hence a steeper rising curve as discharge increases for a given excess of run-on over infiltration. When combined with infiltration, the effect of reducing resistance or increasing gradient is to route water more quickly over the surface and hence reduce overall values of infiltration as shown in Chapter Five. In the particular case of the run-on/runoff plots, the effect of any over-specified routing capability would be to reduce the time taken for each increment to

reach its full storage condition and hence for every observed time, the infiltration rates would be less than that experienced on the plot. More runoff would therefore be predicted. This may be compounded by any infiltration under-estimates.

6.1.6 Summary and Conclusions

The effect of reducing the B2 parameter and the generally improved predictions of times to run-out and overall hydrograph shape, show that the character of the infiltration curve is a rapid fall towards the final infiltration rate in a short period of time after the input of water onto the soil surface. The chosen method of infiltration measurement using a run-on/runoff configuration did not sensitively reproduce this characteristic. The time period chosen for calculating the individual times and rates was relatively coarse and the duration of the tests meant that the steady-state phase dominated the infiltration model rather than the initial rate conditions. This is appropriate for longer duration events in which the steady-state infiltration rates dominate the overall response from the surface both during rainfall and following rainfall cessation as transmission of surface water across the slope and through channels continues.

It is likely that the overestimation of infiltration in the first-stage simulations using the original B parameters (B1) masked the expected effects of under-estimation of resistance for the rising curve that accompanies the use of a single constant Manning's n. By reducing the overestimates of infiltration through double-accounting of detention effects and the process of areal and temporal averaging, the effects of the resistance parameters are felt in the second-stage simulations. However, without more rigorous field experimentation designed specifically to focus on the routing aspects of overland flow and the resistance phenomena, these issues cannot be addressed.

Considering the potential influences on model predictive ability and the spatial and temporal averaging in deriving infiltration model parameters, then the results of the simulations are very encouraging and the errors presented in Table 6.7 are within acceptable levels. Not all of the run-on/runoff plots are to be used in a wider simulation of the Avdat catchment area. The unit 5 plots 32, 34 and 47 which have three of the highest overall error figures are unsuited regardless for use in the catchment due to the variation between the observed infiltration rates and the infiltration rates presented in the literature for loessial surfaces. They are replaced by an infiltration curve from the literature assumed to be representative of loessial soils in the area which has been derived under conditions of rainfall. Out of the remaining nine, eight are used to represent units 1e, 2e, 3e, 4e, 4w, 3w, and 6w. Using 4e upper rather than 4e lower means that the mean overall error of these plots is 5%, and the mean intermediate cumulative discharge error (%E Q3) is 22%. These errors are well within the bounds achieved by other deterministic models particularly those using spatially averaged or temporally averaged values. Since much of the error may relate to timing rather than any inherent infiltration

parameter problem the use of these parameters to represent the orders of magnitude of infiltration in the wider Avdat catchment, distributed on the basis of the units they represent should enable a good picture of the functioning of the water harvesting system to be gained. Additionally, the importance of the spatial variations in infiltration conditions at the within hillslope and within catchment scale can be assessed, a factor of general importance for the interpretation of arid hillslope hydrology.

6.2 ACTUAL HILLSLOPE CASCADES

The purpose of simulating runoff productivity along a hillslope cascade selected from the flow net of the Avdat catchment is to provide an intermediate analysis of the run-off response to rainfall of a complete hillslope section with a range of parameter combinations along its length. This has two roles, to assess the efficacy of the various field data sets at reproducing the expected order of magnitude of runoff from a wider scale of system, and to examine the characteristics of hillslope hydrology discussed in Chapter One as important for the successful operation of the type of water harvesting system practiced at Avdat. This requires consideration of the relative characteristics of runoff production from complete and sub-divided flow lines, since this illustrates the role played by channel location on exploitation of runoff potential through drainage manipulation. The spatial variation in runoff production and transmission properties within the contributing area combined with slope length determines partial area productivity into a particular channel. The characteristics of this Contiguous Area Contribution can be examined by simulating flow on a complete profile and then theoretically super-imposing an arrangement of channels and calculating the difference in the amount of water harvested from each. This requires working backwards. In the case of the Avdat catchment, a network of channels already exists. To assess the effects of channels in a controlled manner, a cascade must be selected from the hypothetical flow-net produced for Avdat (Appendix 3.3) and then the equivalent locations of the current channel system can be determined (through overlay on Appendix 3.1) and the production from that same cascade calculated in its un-interrupted state.

6.2.1 The Hillslope Cascade

The selected cascade extends from the eastern boundary of the catchment down to the wadi-depression and most closely follows sample Profile 2 along which the run-on/runoff plots 1e to 5w lower and sample plots 17 to 34 are positioned (see Plates P.17 to P.34). The elements of the cascade corresponding to the current channel positions and the section of the cascade contributing to each channel are listed in Table 6.8.

Table 6.8 Cascade Contributing Area for Different Channels

Channel	Element	Section
6	13	54-13
5	10	12-10
4 upper	8	9-8
4 lower	7	7
natural	1	6-1

The 54 elements use the infiltration and routing parameters listed in Table 6.9. The slope gradient, element length and width is calculated internally by the simulation model from the coordinate data defining the digitised flow-cascade.

Table 6.9 Plot and Unit Identification for Each Cascade Element

Elements	Plot	Unit	Infiltration A	Infiltration B2	Manning's n
54-48	17	1e	0.000414	0.0274	0.460
47-42	18	1e	0.000414	0.0274	0.460
41-38	19	2e	0.000427	0.0106	0.420
37-33	20	2e	0.000427	0.0106	0.420
32-29	21	2e	0.000427	0.0106	0.420
28-25	22	3e	0.000179	0.0133	0.380
24-20	23	3e	0.000179	0.0133	0.380
19-17	24	4e	0.000047	0.0188	0.480
16-14	25	4e	0.000047	0.0188	0.480
13-12	26	4e	0.000047	0.0188	0.480
11-10	27	4e	0.000047	0.0188	0.480
9-8	28	4e	0.000047	0.0188	0.480
7	29	4e	0.000047	0.0188	0.480
6	30	5e	0.000087	0.1710	0.410
5	31	5e	0.000087	0.1710	0.410
4	32	5e	0.000087	0.1710	0.410
3-1	33	5w	0.000087	0.1710	0.280

6.2.2 Methods of Results Analysis

There are no observed data-sets for individual cascades, only for the whole sub-catchments which are fitted with automatic stage-recorders (as shown in Plate A.1). However, as a rough guide, the percentage productivity of the sub-catchments over which the cascade crosses can be calculated for different rainfall events. This gives a productivity range that might be expected from simulating a given rainstorm and so provides a measure of whether the plot data applied to the full cascade reproduces the order of magnitude response of the sub-catchments along all or part of its length. The results provide a wider context for the consideration of the observations made in the sensitivity tests and in simulations of the plot run-on/runoff responses. However, it is clear that all responses at the hillslope scale are the net results of parameter interaction and the effects of individual components are difficult to isolate.

Two rainstorms are selected from the historical record for Avdat. A full analysis of the record is presented in Appendix 1.6 and establishes the recurrence intervals of both annual and daily storm

totals. In 1985, Ben-Asher digitised the Avdat hyetographs and hydrographs for the years 1971/72 to 1982/83 (Ben-Asher pers.comm.). An examination of this data-set reveals that very few individual runoff events have a complete record and so only a limited number can be considered for use in simulations of the Avdat system. Rather than use a quantitative method of selecting hyetographs for testing, a qualitative selection process was made on the basis that the storms selected;

1. produce runoff in each sub-catchment,
2. have a magnitude less than 14 mm so that they are annually occurring (and therefore critical for the base level performance of the runoff farming system, given that its success depends on its ability to provide sufficient water resources annually),
3. are preceded by at least seven dry days to ensure no antecedent conditioning and an initially dry surface (corresponding with infiltration test conditions),
4. possess features desirable to illustrate the sensitivity of the catchment to particular rainstorm characteristics. This relates to the intensity distribution.

The first of the two rainstorms is that of 02/03/74 which is digitised from the recording raingauge record by Ben-Asher as three intensity blocks. It has a single peak flanked by two low-intensity periods as illustrated in Figure 6.1. The previous 6.5 days were dry-days. The magnitude is 7.43 mm with a recurrence interval of approximately 0.34 showing that this depth or greater occurs on average three times every year. However, the peak intensity of 41.6 mm hr^{-1} for 0.15 hours has a recurrence interval of approximately 6 years showing that although the depth is common, the intensity is not. The storm is likely to produce considerably more runoff because of this than might otherwise be expected from a longer duration, lower intensity event.

To contrast this, the second rainstorm is that of 10/02/74 which is digitised by Ben-Asher into the hyetograph illustrated in Figure 6.2. The previous 10 days were dry days. The magnitude is 10.96 mm with a recurrence interval of approximately 0.58 showing that it can be expected to be equaled or exceeded almost twice each year. The peak intensity block of 25.65 mm hr^{-1} for 0.11 hours has a recurrence interval of 2 years and shows the rainstorm is more typical of that which can be expected to occur on a regular basis. The two rainstorms present an interesting contrast; the single-peaked high intensity short-duration event, and the multi-peaked intensity longer-duration event with a dominant first peak.

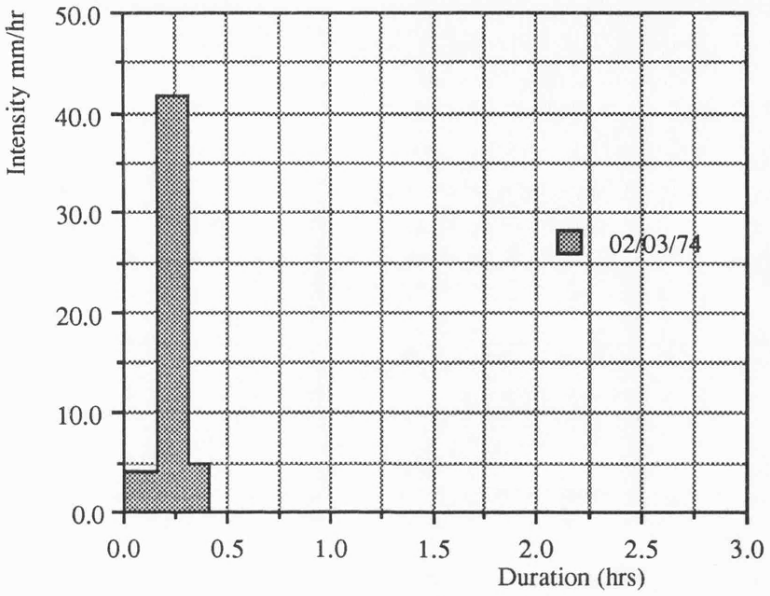

Figure 6.1 Hyetograph for Rainstorm 02/03/74

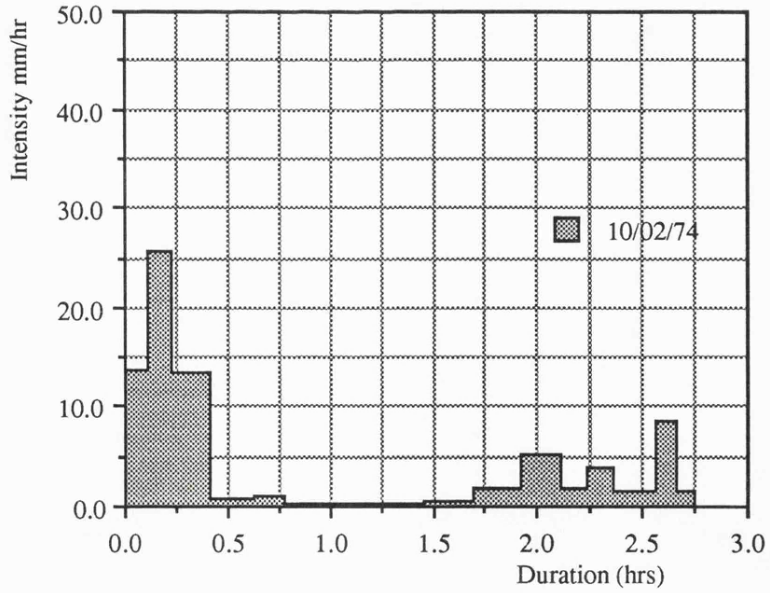

Figure 6.2 Hyetograph for Rainstorm 10/02/74

Comparisons can be made between the volumetric runoff productivity from different flow-line lengths showing the effect of positioning a channel at a given location and reducing the length of flow-line contributing runoff to subsequent locations downslope. The first aim is to show the performance of the current channel configuration compared to an unaltered hillslope profile. This is followed at a

later stage by simulations to show where the flow-cascade should be tapped with the least number of channels to give the maximum volumetric production, and how these locations could be identified by distributed simulation modelling (Section 6.4). These objectives are independent of any assessment of the efficacy of parameters at reproducing observed conditions since they have their own inherent theoretical significance. The simulations show the effect of slope length, spatial diversity, and input character on the full-scale operation of the Contiguous Area Contribution principle and the ability of the model to be used as a design tool.

6.2.3 The Simulation Results

6.2.3.a Data Output and its Use

The cascade is simulated using the full working model WATERH. As explained in Chapter Five, this model has a series of sub-routine conditional statements that allows just a single cascade to be simulated. Requests can be made to store predicted information of a variety of types, in a variety of formats for a number of pre-determined locations in the catchment. When considering a cascade, the locations would be the elements at which channels interrupt the flow-line. Simulating different lengths of cascades down to these elements shows the effect of truncating the flow upslope by positioning of a man-made channel. For instance, to show the relative effects of positioning a channel at the outflow of element four, the productivity of section 54-1 can be compared with the productivity of sections 54-4, and 3-1. Section 54-4 would be the length of cascade contributing to the man-made channel, and section 3-1 to the natural channel at the slope foot.

The approach taken is to simulate the runoff productivity through time for each element for the full matrix of possible contributing slope lengths. A channel could theoretically be positioned at the base of any element from 1 to 54. By repeating the simulation for 54 different cascade lengths, each time omitting to include the uppermost element in the cascade (54 then 53, 52, etc.), the full matrix of possible productivity from any configuration of channel positions can be calculated by working through the matrix combinations (Tables 6.10 and 6.11). The cascade begins at the divide which is the upper boundary of element 54. By tracing down the column headed by 54 this shows the productivity of any cell with this uppermost boundary to its contributing length. Assuming a channel is positioned at 13 (in this case the man-made channel of sub-catchment 6) the figure in row 13 of column 54 represents the amount of runoff that can be expected for a given rainstorm for the channel with the contributing length of elements 13 to 54. Assuming the next channel is at the lower boundary of element 10, the runoff production from this section is found by following row 13 across until the column 12 is reached. Going down column 12 to row 10 shows the runoff production into this channel (in this case, the man-made channel of sub-catchment 5) from the contributing section 10-12. This process could be carried out for any combination of possible channel configurations taking

Table 6.10 Matrix of Cascade Productivity (cubic metres) for Rainstorm 02/03/74

Unit	Element	Divide at..... 54	53	52	51	50	49	48	47	46	45	44	43	42	41	40	39	38	37	36	35	34	33	32	31	30	29	28	27	26	25	24	23	22	21	20	19	18	17	16	15	14	13	12	11	10	9	8	7	6	5	4	3	2	1
1	54	0.03																																																				
1	53	0.07	0.05																																																				
1	52	0.14	0.13	0.09																																																		
1	51	0.20	0.19	0.16	0.09																																																	
1	50	0.26	0.26	0.23	0.18	0.10																																																
1	49	0.32	0.32	0.30	0.26	0.20	0.11																																															
1	48	0.39	0.39	0.38	0.35	0.29	0.22	0.13																																														
1	47	0.47	0.46	0.46	0.43	0.39	0.32	0.24	0.14																																													
1	46	0.53	0.53	0.52	0.50	0.47	0.42	0.35	0.26	0.14																																												
1	45	0.58	0.58	0.58	0.56	0.53	0.49	0.43	0.35	0.25	0.12																																											
1	44	0.63	0.63	0.63	0.61	0.59	0.55	0.50	0.43	0.34	0.24	0.13																																										
1	43	0.67	0.67	0.67	0.66	0.64	0.61	0.57	0.51	0.43	0.33	0.24	0.12																																									
1	42	0.72	0.72	0.71	0.71	0.69	0.67	0.63	0.57	0.51	0.42	0.33	0.23	0.12																																								
2	41	0.80	0.80	0.79	0.79	0.78	0.76	0.73	0.68	0.62	0.55	0.47	0.38	0.28	0.17																																								
2	40	0.91	0.91	0.91	0.90	0.90	0.88	0.86	0.82	0.77	0.71	0.65	0.57	0.48	0.38	0.23																																							
2	39	1.01	1.01	1.01	1.01	1.00	0.99	0.97	0.95	0.91	0.86	0.80	0.75	0.65	0.57	0.43	0.23																																							
2	38	1.12	1.12	1.12	1.11	1.11	1.10	1.09	1.07	1.04	1.00	0.95	0.90	0.83	0.75	0.63	0.45	0.25																																						
2	37	1.23	1.23	1.23	1.23	1.23	1.23	1.22	1.20	1.18	1.15	1.11	1.07	1.01	0.95	0.84	0.68	0.50	0.29																																					
2	36	1.33	1.33	1.33	1.33	1.33	1.33	1.32	1.31	1.29	1.27	1.24	1.20	1.15	1.10	1.00	0.86	0.71	0.51	0.26																																				
2	35	1.43	1.43	1.43	1.43	1.43	1.43	1.43	1.42	1.41	1.39	1.36	1.33	1.29	1.25	1.17	1.04	0.91	0.74	0.51	0.28																																				
2	34	1.54	1.54	1.54	1.54	1.54	1.54	1.54	1.53	1.52	1.51	1.49	1.47	1.44	1.40	1.33	1.23	1.12	0.97	0.77	0.57	0.33																																			
2	33	1.64	1.64	1.64	1.64	1.64	1.64	1.64	1.64	1.63	1.62	1.61	1.59	1.57	1.54	1.48	1.38	1.30	1.17	1.00	0.83	0.61	0.32																																			
2	32	1.75	1.75	1.75	1.75	1.75	1.75	1.75	1.75	1.75	1.74	1.73	1.72	1.70	1.68	1.64	1.58	1.50	1.40	1.27	1.12	0.94	0.70	0.43																																			
2	31	1.85	1.85	1.85	1.85	1.85	1.85	1.85	1.85	1.85	1.84	1.84	1.83	1.82	1.81	1.78	1.73	1.68	1.60	1.50	1.39	1.24	1.05	0.83	0.49																																			
2	30	1.96	1.96	1.96	1.96	1.96	1.96	1.96	1.96	1.96	1.96	1.95	1.95	1.95	1.94	0.92	1.89	1.86	1.81	1.74	1.66	1.56	1.42	1.25	0.99	0.62																																			
2	29	2.03	2.03	2.03	2.03	2.03	2.03	2.03	2.03	2.03	2.03	2.03	2.03	2.02	2.02	2.01	2.00	1.98	1.95	1.90	1.85	1.78	1.68	1.56	1.37	1.09	0.62																																			
3	28	2.81	2.81	2.81	2.81	2.81	2.81	2.81	2.81	2.81	2.81	2.81	2.82	2.81	2.81	2.80	2.79	2.77	2.75	2.71	2.67	2.61	2.52	2.42	2.25	2.00	1.57	1.00																																			
3	27	3.54	3.54	3.54	3.54	3.54	3.54	3.54	3.54	3.54	3.54	3.54	3.54	3.54	3.54	3.53	3.52	3.51	3.49	3.46	3.42	3.37	3.30	3.21	3.06	2.83	2.45	1.92	1.00																																			
3	26	4.27	4.27	4.27	4.27	4.27	4.27	4.27	4.27	4.27	4.27	4.27	4.27	4.27	4.27	4.27	4.26	4.25	4.23	4.21	4.18	4.13	4.07	3.99	3.86	3.66	3.32	2.84	2.00	1.08																																			
3	25	4.97	4.97	4.97	4.97	4.97	4.97	4.97	4.97	4.97	4.97	4.97	4.97	4.96	4.96	4.96	4.95	4.95	4.93	4.91	4.89	4.85	4.80	4.74	4.62	4.44	4.13	3.69	2.92	2.07	1.09																																			
3	24	5.69	5.69	5.69	5.69	5.69	5.69	5.69	5.69	5.69	5.69	5.69	5.69	5.69	5.68	5.68	5.68	5.67	5.66	5.65	5.63	5.60	5.56	5.50	5.40	5.24	4.97	4.57	3.86	3.00	2.19	1.20																																			
3	23	6.38	6.38	6.38	6.38	6.38	6.38	6.38	6.38	6.38	6.38	6.38	6.38	6.38	6.38	6.37	6.37	6.37	6.36	6.35	6.33	6.31	6.27	6.23	6.14	6.01	5.78	5.40	4.76	4.05	3.22	2.32	1.24																																			
3	22	7.07	7.07	7.07	7.07	7.07	7.07	7.07	7.07	7.07	7.07	7.07	7.07	7.07	7.07	7.07	7.06	7.06	7.05	7.05	7.03	7.01	6.99	6.95	6.88	6.76	6.54	6.22	5.64	4.99	4.25	3.42	2.44	1.32																																			
3	21	7.69	7.69	7.69	7.69	7.69	7.69	7.69	7.69	7.69	7.69	7.69	7.69	7.69	7.69	7.69	7.68	7.69	7.68	7.68	7.67	7.65	7.63	7.60	7.54	7.44	7.25	6.96	6.43	5.84	5.16	4.41	3.51	2.49	1.29																																			
3	20	8.19	8.19	8.19	8.19	8.19	8.19	8.19	8.19	8.19	8.19	8.19	8.19	8.19	8.19	8.19	8.19	8.19	8.18	8.18	8.17	8.16	8.14	8.11	8.06	7.97	7.80	7.54	7.05	6.51	5.88	5.18	4.34	3.39	2.29	1.10																																			
4	19	9.58	9.58	9.58	9.58	9.58	9.58	9.58	9.58	9.58	9.58	9.58	9.58	9.58	9.58	9.58	9.58	9.58	9.57	9.57	9.56	9.55	9.53	9.50	9.45	9.37	9.21	8.95	8.48	7.95	7.33	6.64	5.82	4.89	3.81	2.64	1.57																																			
4	18	10.85	10.85	10.85	10.85	10.85	10.85	10.85	10.85	10.85	10.85	10.85	10.85	10.85	10.85	10.85	10.85	10.85	10.85	10.84	10.83	10.82	10.80	10.78	10.73	10.65	10.49	10.24	9.78	9.26	8.65	7.98	7.18	6.27	5.20	4.06	3.01	1.49																																			
4	17	12.46	12.46	12.46	12.46	12.46	12.46	12.46	12.46	12.46	12.46	12.46	12.46	12.46	12.46	12.46	12.46	12.46	12.46	12.45	12.44	12.43	12.42	12.39	12.35	12.27	12.12	11.88	11.43	10.92	10.33	9.68	8.90	8.01	6.97	5.85	4.82	3.35	1.91																																			
4	16	14.15	14.15	14.15	14.15	14.15	14.15	14.15	14.15	14.15	14.15	14.15	14.15	14.15	14.15	14.15	14.15	14.15	14.15	14.14	14.14	14.13	14.11	14.09	14.05	13.97	13.83	13.59	13.16	12.67	12.10	11.46	10.70	9.83	8.82	7.73	6.73	5.30	3.90	2.07																																		
4	15	15.64	15.64	15.64	15.64	15.64	15.64	15.64	15.64	15.64	15.64	15.64	15.64	15.64	15.64	15.64	15.64	15.63	15.63	15.63	15.62	15.61	15.60	15.58	15.54	15.46	15.32	15.10	14.68	14.20	13.64	13.02	12.28	11.43	10.44	9.38	8.40	7.00	5.65	3.87	1.89																																		
4	14	17.24	17.24	17.24	17.24	17.24	17.24	17.24	17.24	17.24	17.24	17.24	17.24	17.24	17.24	17.24	17.24	17.24	17.23	17.23	17.22	17.22	17.20	17.18	17.14	17.08	16.94	16.72	16.31	15.85	15.31	14.71	13.99	13.16	12.19	11.16	10.02	8.84	7.52	5.81	3.91	2.10																																	
4	13	18.91	18.91	18.91	18.91	18.91	18.91	18.91	18.91	18.91	18.91	18.91	18.91	18.91	18.91	18.91	18.91	18.91	18.91	18.90	18.90	18.89	18.88	18.86	18.82	18.76	18.63	18.42	18.03	17.58	17.06	16.47	15.77	14.97	14.03	13.02	12.09	10.77	9.49	7.83	6.01	4.27	2.28																																	
4	12	20.59	20.59	20.59	20.59	20.59	20.59	20.59	20.59	20.59	20.59	20.59	20.59	20.59	20.59	20.59	20.59	20.59	20.59	20.59	20.58	20.57	20.56	20.54	20.51	20.45	20.33	20.13	19.75	19.32	18.81	18.25	17.57	16.79	15.87	14.89	13.99	12.71	11.46	9.87	8.11	6.44	4.54	2.39																																	
4	11	22.36	22.36	22.36	22.36	22.36	22.36	22.36	22.36	22.36	22.36	22.36	22.36	22.36	22.36	22.36	22.36	22.36	22.36	22.36	22.35	22.34	22.33	22.32	22.28	22.23	22.11	21.92	21.56	21.14	20.66	20.11	19.46	18.70	17.82	16.87	15.99	14.75	13.55	12.01	10.33	8.73	6.92	4.89	2.65																																	
4	10	23.94	23.94	23.94	23.94	23.94	23.94	23.94	23.94	23.94	23.94	23.94	23.94	23.94	23.94	23.94	23.94	23.94	23.94	23.94	23.93	23.93	23.91	23.90	23.87	23.81	23.78	23.52	23.17	22.78	22.31	21.78	21.15	20.42	19.56	18.64	17.79	16.58	15.42	13.94	12.32	10.78	9.05	7.12	5.00	2.54																																	
4	9	25.42	25.42	25.42	25.42	25.42	25.42	25.42	25.42	25.42	25.42	25.42	25.42	25.42	25.42	25.42	25.42	25.42	25.42	25.42	25.42	25.41	25.40	25.39	25.36	25.31	25.28	25.03	24.69	24.31	23.86	23.35	22.74	22.03	21.20	20.31	19.48	18.02	17.19	15.76	14.20	12.72	11.07	9.23	7.22	4.91	2.54																																	
4	8	27.13	27.13	27.13	27.13	27.13	27.13	27.13	27.13	27.13	27.13	27.13	27.13	27.13	27.13	27.13	27.13	27.13	27.13	27.13	27.13	27.12	27.11	27.10	27.07	27.02	26.92	26.76	26.44	26.08	25.65	25.17	24.58	23.90	23.10	22.24	21.44	20.33	19.24	17.88	16.39	14.99	13.42	11.69	9.81	7.66	5.46	3.11																																	
4	7	29.07	29.07	29.07	29.07	29.07	29.07	29.07	29.07	29.07	29.07	29.07	29.07	29.07	29.07	29.06	29.06	29.06	29.06	29.06	29.06	29.05	29.05	29.03	29.01	28.97	28.88	28.72	28.43	28.09	27.69	27.23	26.68	26.04	25.28	24.47	23.71	22.65	21.63	20.35	18.95	17.64	16.19	14.59	12.86	10.89	8.87	6.73	3.94																																	
5	6	23.46	23.46	23.46	23.46	23.46	23.46	23.46	23.46	23.46	23.46	23.46	23.46	23.46	23.46	23.46	23.46	23.46	23.46	23.46	23.45	23.65	23.44	23.44	23.42	23.38	23.31	23.19	22.94	22.66	22.32	21.94	21.47	20.92	20.27	19.57	18.92	18.02	17.15	16.08	14.93	13.86	12.69	11.42	10.08	8.57	7.06	5.49	3.58	1.30																																	
5	5	19.75	19.75	19.75	19.75	19.75	19.75	19.75	19.75	19.75	19.75	19.75	19.75	19.75	19.75	19.75	19.75	19.75	19.75	19.75	19.75	19.75	19.74	19.73	19.72	19.69	19.63	19.52	19.31	19.06	18.77	18.42	18.01	17.52	16.94	16.32	15.74	14.94	14.18	13.24	12.26	11.34	10.36	9.31	8.21	7.00	5.81	4.61	3.24	1.76	0.96																																	
5	4	14.97	14.97	14.97	14.97	14.97	14.97	14.97	14.97	14.97	14.97	14.97	14.97	14.97	14.97	14.97	14.97	14.97	14.97	14.97	14.96	14.96	14.96	14.95	14.94	14.92	14.87	14.78	14.60	14.40	14.14	13.86	13.50	13.09	12.60	12.07	11.58	10.91	10.28	9.52	8.73	8.01	7.26	6.47	5.68	4.83	4.05	3.30	2.53	1.76	1.34	0.85																																	
6	3	10.00	10.00	10.00	10.00	10.00	10.00	10.00	10.00	10.00	10.00	10.00	10.00	10.00	10.00	10.00	10.00	10.00	10.00	10.00	10.00	10.00	9.99	9.99	9.98	9.96	9.93	9.86	9.72	9.56	9.36	9.13	8.84	8.51	8.11	7.69	7.30	6.77	6.28	5.72	5.15	4.66	4.16	3.67	3.21	2.77	2.39	2.07	1.77	1.47	1.30	1.08	0.69																																	
6	2	6.91	6.91	6.91	6.91	6.91	6.91	6.91	6.91	6.91	6.91	6.91	6.91	6.91	6.91	6.91	6.19	6.19	6.19	6.19	6.19	6.19	6.19	6.18	6.18	6.17	6.14	6.09	5.99	5.86	5.71	5.54	5.32	5.07	4.77	4.45	4.15	3.76	3.41	3.00	2.64	2.34	2.06	1.82	1.63	1.46	1.33	1.23	1.13	1.03	0.96	0.86	0.69	0.39																																	
6	1	4.87	4.87	4.87	4.87	4.87	4.87	4.87	4.87	4.87	4.87	4.87	4.87	4.87	4.87	4.87	4.87	4.87	4.87	4.87	4.86	4.86	4.86	4.86	4.85	4.84	4.82	4.78	4.69	4.58	4.45	4.30	4.11	3.89	3.63	3.35	3.09	2.76	2.46	2.13	1.82	1.59	1.40	1.25	1.14	1.06	1.00	0.95	0.89	0.83	0.79	0.73	0.62	0.42	0.19
Volume p (m3)		108.86	108.75	108.50	108.11	107.79	107.43	107.06	106.64	106.17	105.69	105.29	104.88	104.49	104.12	103.67	103.02	102.39	101.70	100.86	100.13	99.35	98.39	97.46	96.07	94.48	92.32	90.08	88.15	86.24	84.17	82.10	79.75	77.35	74.76	72.27	70.23	68.19	66.26	63.72	60.91	58.38	55.50	52.32	48.94	45.06	41.38	36.70	32.08	26.48	19.29	14.61	9.18	4.15	0.97

Table 6.11 Matrix of Cascade Productivity (cubic metres) for Reinstorm 18/02/74

Unit	Element	Divide at..... 54	53	52	51	50	49	48	47	46	45	44	43	42	41	40	39	38	37	36	35	34	33	32	31	30	29	28	27	26	25	24	23	22	21	20	19	18	17	16	15	14	13	12	11	10	9	8	7	6	5	4	3	2	1
1	54	0.00																																																				
1	53	0.00	0.00																																																				
1	52	0.01	0.01	0.01																																																		
1	51	0.01	0.01	0.01	0.01																																																	
1	50	0.01	0.01	0.01	0.01	0.01																																																	
1	49	0.02	0.02	0.02	0.02	0.01	0.01																																																
1	48	0.02	0.02	0.02	0.02	0.02	0.02	0.01																																															
1	47	0.02	0.02	0.02	0.02	0.02	0.02	0.02	0.01																																														
1	46	0.02	0.02	0.02	0.02	0.02	0.02	0.02	0.02	0.01																																												
1	45	0.02	0.02	0.02	0.02	0.02	0.02	0.02	0.02	0.02	0.01																																											
1	44	0.03	0.03	0.03	0.03	0.03	0.03	0.03	0.02	0.02	0.02	0.01																																										
1	43	0.03	0.03	0.03	0.03	0.03	0.03	0.03	0.03	0.03	0.02	0.02	0.01																																										
1	42	0.03	0.03	0.03	0.03	0.03	0.03	0.03	0.03	0.03	0.03	0.03	0.02	0.01																																									
2	41	0.50	0.50	0.05	0.05	0.05	0.05	0.05	0.05	0.05	0.05	0.05	0.04	0.04	0.03																																									
2	40	0.07	0.07	0.07	0.07	0.07	0.07	0.07	0.07	0.07	0.07	0.07	0.07	0.07	0.06	0.04																																								
2	39	0.09	0.09	0.09	0.09	0.09	0.09	0.09	0.09	0.09	0.09	0.09	0.09	0.09	0.08	0.06	0.04																																								
2	38	0.11	0.11	0.11	0.11	0.11	0.11	0.11	0.11	0.11	0.11	0.11	0.10	0.10	0.10	0.09	0.07	0.04																																							
2	37	0.12	0.12	0.12	0.12	0.12	0.12	0.12	0.12	0.12	0.12	0.12	0.12	0.12	0.11	0.11	0.09	0.07	0.04																																							
2	36	0.12	0.12	0.12	0.12	0.12	0.12	0.12	0.12	0.12	0.12	0.12	0.12	0.12	0.12	0.12	0.11	0.10	0.08	0.04																																						
2	35	0.13	0.13	0.13	0.13	0.13	0.13	0.13	0.13	0.13	0.13	0.13	0.13	0.13	0.13	0.13	0.12	0.12	0.10	0.08	0.05																																						
2	34	0.14	0.14	0.14	0.14	0.14	0.14	0.14	0.14	0.14	0.14	0.14	0.14	0.14	0.14	0.14	0.13	0.13	0.12	0.11	0.08	0.05																																					
2	33	0.14	0.14	0.14	0.14	0.14	0.14	0.14	0.14	0.14	0.14	0.14	0.14	0.14	0.14	0.14	0.14	0.14	0.14	0.13	0.11	0.09	0.05																																					
2	32	0.15	0.15	0.15	0.15	0.15	0.15	0.15	0.15	0.15	0.15	0.15	0.15	0.15	0.15	0.15	0.15	0.15	0.14	0.14	0.14	0.13	0.12	0.10	0.06																																					
2	31	0.15	0.15	0.15	0.15	0.15	0.15	0.15	0.15	0.15	0.15	0.15	0.15	0.15	0.15	0.15	0.15	0.15	0.15	0.15	0.14	0.14	0.12	0.11	0.07																																					
2	30	0.15	0.15	0.15	0.15	0.15	0.15	0.15	0.15	0.15	0.15	0.15	0.15	0.15	0.15	0.15	0.15	0.15	0.15	0.15	0.15	0.15	0.15	0.14	0.12	0.08																																					
2	29	0.15	0.15	0.15	0.15	0.15	0.15	0.15	0.15	0.15	0.15	0.15	0.15	0.15	0.15	0.15	0.15	0.15	0.15	0.15	0.15	0.15	0.15	0.15	0.14	0.13	0.08																																					
3	28	0.93	0.93	0.93	0.93	0.93	0.93	0.93	0.93	0.93	0.93	0.93	0.93	0.93	0.93	0.93	0.93	0.93	0.93	0.93	0.93	0.93	0.93	0.93	0.92	0.91	0.87	0.79																																					
3	27	1.64	1.64	1.64	1.64	1.64	1.64	1.64	1.64	1.64	1.64	1.64	1.64	1.64	1.64	1.64	1.64	1.64	1.64	1.64	1.64	1.64	1.64	1.63	1.63	1.62	1.58	1.51	0.79																																					
3	26	2.33	2.33	2.33	2.33	2.33	2.33	2.33	2.33	2.33	2.33	2.33	2.33	2.33	2.33	2.33	2.33	2.33	2.33	2.33	2.33	2.33	2.33	2.33	2.33	2.32	2.29	2.22	1.56	0.85																																					
3	25	2.98	2.98	2.98	2.98	2.98	2.98	2.98	2.98	2.98	2.98	2.98	2.98	2.98	2.98	2.98	2.98	2.98	2.98	2.98	2.98	2.98	2.98	2.98	2.98	2.97	2.94	2.88	2.28	1.63	0.86																																					
3	24	3.64	3.64	3.64	3.64	3.64	3.64	3.64	3.64	3.64	3.64	3.64	3.64	3.64	3.64	3.64	3.64	3.64	3.64	3.64	3.64	3.64	3.64	3.64	3.64	3.63	3.61	3.55	3.01	2.41	1.72	0.95																																					
3	23	4.27	4.27	4.27	4.27	4.27	4.27	4.27	4.27	4.27	4.27	4.27	4.27	4.27	4.27	4.27	4.27	4.27	4.27	4.27	4.27	4.27	4.27	4.27	4.27	4.26	4.24	4.19	3.70	3.15	2.52	1.82	0.97																																				
3	22	4.89	4.89	4.89	4.89	4.89	4.89	4.89	4.89	4.89	4.89	4.89	4.89	4.89	4.89	4.89	4.89	4.89	4.89	4.89	4.89	4.89	4.89	4.89	4.88	4.88	4.86	4.81	4.37	3.88	3.31	2.68	1.91	1.84																																				
3	21	5.44	5.44	5.44	5.44	5.44	5.44	5.44	5.44	5.44	5.44	5.44	5.44	5.44	5.44	5.44	5.44	5.44	5.44	5.44	5.44	5.44	5.44	5.44	5.44	5.43	5.42	5.38	4.98	4.53	4.01	3.44	2.74	1.95	1.82																																				
3	20	5.87	5.87	5.87	5.87	5.87	5.87	5.87	5.87	5.87	5.87	5.87	5.87	5.87	5.87	5.87	5.87	5.87	5.87	5.87	5.87	5.87	5.87	5.87	5.87	5.86	5.85	5.81	5.45	5.04	4.56	4.03	3.39	2.66	1.79	0.87																																				
4	19	7.48	7.48	7.48	7.48	7.48	7.48	7.48	7.48	7.48	7.48	7.48	7.48	7.48	7.48	7.48	7.48	7.48	7.48	7.48	7.48	7.48	7.48	7.48	7.48	7.48	7.46	7.43	7.07	6.67	6.20	5.68	5.05	4.32	3.47	2.56	1.71																																				
4	18	8.94	8.94	8.94	8.94	8.94	8.94	8.94	8.94	8.94	8.94	8.94	8.94	8.94	8.94	8.94	8.94	8.94	8.94	8.94	8.94	8.94	8.94	8.94	8.94	8.93	8.92	8.89	8.54	8.14	7.68	7.17	6.55	5.83	5.00	4.09	3.26	1.62																																				
4	17	10.74	10.74	10.74	10.74	10.74	10.74	10.74	10.74	10.74	10.74	10.74	10.74	10.74	10.74	10.74	10.74	10.74	10.74	10.74	10.74	10.74	10.74	10.74	10.74	10.73	10.73	10.72	10.49	10.35	9.96	9.51	9.01	8.48	7.79	6.89	6.00	5.18	3.61	2.87																																				
4	16	12.58	12.58	12.58	12.58	12.58	12.58	12.58	12.58	12.58	12.58	12.58	12.58	12.58	12.58	12.58	12.58	12.58	12.58	12.58	12.58	12.58	12.58	12.58	12.58	12.58	12.56	12.53	12.20	11.83	11.39	10.90	10.31	9.63	8.82	7.96	7.16	5.66	4.19	2.24																																				
4	15	14.17	14.17	14.17	14.17	14.17	14.17	14.17	14.17	14.17	14.17	14.17	14.17	14.17	14.17	14.17	14.17	14.17	14.17	14.17	14.17	14.17	14.17	14.17	14.17	14.17	14.15	14.12	13.80	13.44	13.01	12.53	11.95	11.29	10.56	9.65	8.86	7.43	6.82	4.16	2.05																																				
4	14	15.84	15.84	15.84	15.84	15.84	15.84	15.84	15.84	15.84	15.84	15.84	15.84	15.84	15.84	15.84	15.84	15.84	15.84	15.84	15.84	15.84	15.84	15.84	15.84	15.84	15.84	15.83	15.80	15.49	15.13	14.72	14.25	13.68	13.03	12.26	11.44	10.47	9.29	7.94	6.18	4.19	2.27																																				
4	13	17.55	17.55	17.55	17.55	17.55	17.55	17.55	17.55	17.55	17.55	17.55	17.55	17.55	17.55	17.55	17.55	17.55	17.55	17.55	17.55	17.55	17.55	17.55	17.55	17.55	17.54	17.51	17.20	16.86	16.45	16.00	15.45	14.81	14.06	13.25	12.50	11.19	9.91	8.24	6.36	4.55	2.45																																				
4	12	19.31	19.31	19.31	19.31	19.31	19.31	19.31	19.31	19.31	19.31	19.31	19.31	19.31	19.31	19.31	19.31	19.31	19.31	19.31	19.31	19.31	19.31	19.31	19.31	19.31	19.31	19.27	18.96	18.62	18.21	17.76	17.20	16.57	15.82	15.03	14.30	13.05	11.83	10.25	8.48	6.78	4.83	2.57																																				
4	11	21.23	21.23	21.23	21.23	21.23	21.23	21.23	21.23	21.23	21.23	21.23	21.23	21.23	21.23	21.23	21.23	21.23	21.23	21.23	21.23	21.23	21.23	21.23	21.23	21.22	21.21	21.18	20.88	20.53	20.13	19.68	19.12	18.49	17.74	16.95	16.22	15.00	13.81	12.29	10.64	9.05	7.24	5.16	2.83																																				
4	10	23.00	23.00	23.00	23.00	23.00	23.00	23.00	23.00	23.00	23.00	23.00	23.00	23.00	23.00	23.00	23.00	23.00	23.00	23.00	23.00	23.00	23.00	23.00	23.00	23.00	22.99	22.96	22.65	22.31	21.91	21.45	20.98	20.27	19.52	18.73	18.00	16.81	15.64	14.16	12.55	11.04	9.35	7.42	5.28	2.72																																				
4	9	24.75	24.75	24.75	24.75	24.75	24.75	24.75	24.75	24.75	24.75	24.75	24.75	24.75	24.75	24.75	24.75	24.75	24.75	24.75	24.75	24.75	24.75	24.75	24.75	24.74	24.73	24.70	24.40	24.00	23.65	23.20	22.65	22.01	21.27	20.48	19.75	18.58	17.44	15.99	14.41	12.94	11.29	9.56	7.52	5.19	2.72																																				
4	8	26.90	26.90	26.90	26.90	26.90	26.90	26.90	26.90	26.90	26.90	26.90	26.90	26.90	26.90	26.90	26.90	26.90	26.90	26.90	26.90	26.90	26.90	26.90	26.90	26.90	26.89	26.86	26.55	26.22	25.82	25.37	24.82	24.19	23.44	22.66	21.95	20.78	19.67	18.25	16.72	15.29	13.69	11.95	10.04	7.93	5.72	3.38																																				
4	7	29.68	29.68	29.68	29.68	29.68	29.68	29.68	29.68	29.68	29.68	29.68	29.68	29.68	29.68	29.68	29.68	29.68	29.68	29.68	29.68	29.68	29.68	29.68	29.68	29.67	29.66	29.63	29.34	29.01	28.61	28.17	27.63	27.01	26.28	25.50	24.78	23.66	22.58	21.21	19.72	18.33	16.78	14.11	13.27	11.25	9.15	6.94	4.12																																				
5	6	22.47	22.47	22.47	22.47	22.47	22.47	22.47	22.47	22.47	22.47	22.47	22.47	22.47	22.47	22.47	22.47	22.47	22.47	22.47	22.47	22.47	22.47	22.47	22.47	22.47	22.46	22.43	22.16	21.85	21.48	21.06	20.56	19.98	19.29	18.56	17.87	16.83	15.84	14.58	13.22	11.96	10.59	9.19	7.92	6.56	5.23	3.89	2.31	0.59																																				
5	5	18.01	18.01	18.01	18.01	18.01	18.01	18.01	18.01	18.01	18.01	18.01	18.01	18.01	18.01	18.01	18.01	18.01	18.01	18.01	18.01	18.01	18.01	18.01	18.01	18.01	18.00	17.96	17.72	17.44	17.09	16.70	16.25	15.68	15.04	14.35	13.71	12.74	11.82	10.68	9.46	8.37	7.24	6.27	5.36	4.37	3.43	2.52	1.57	0.71	0.45																																				
5	4	12.72	12.72	12.72	12.72	12.72	12.72	12.72	12.72	12.72	12.72	12.72	12.72	12.72	12.72	12.72	12.72	12.72	12.72	12.72	12.72	12.72	12.72	12.72	12.72	12.71	12.71	12.69	12.46	12.21	11.90	11.56	11.14	10.65	10.08	9.46	8.90	8.06	7.28	6.33	5.36	4.54	3.75	3.08	2.52	1.98	1.53	1.17	0.86	0.61	0.52	0.37																																				
6	3	7.58	7.58	7.58	7.58	7.58	7.58	7.58	7.58	7.58	7.58	7.58	7.58	7.58	7.58	7.58	7.58	7.58	7.58	7.58	7.58	7.58	7.58	7.58	7.58	7.58	7.57	7.56	7.37	7.15	6.89	6.59	6.23	5.82	5.33	4.82	4.35	3.67	3.05	2.34	1.67	1.17	0.88	0.74	0.66	0.66	0.56	0.53	0.50	0.46	0.44	0.48	0.29																																				
6	2	4.09	4.09	4.09	4.09	4.09	4.09	4.09	4.09	4.09	4.09	4.09	4.09	4.09	4.09	4.09	4.09	4.09	4.09	4.09	4.09	4.09	4.09	4.09	4.09	4.08	4.08	4.06	3.90	3.72	3.50	3.25	2.95	2.60	2.21	1.81	1.45	0.99	0.65	0.43	0.32	0.30	0.29	0.29	0.29	0.29	0.29	0.29	0.29	0.28	0.28	0.27	0.24	0.16																																				
6	1	3.23	3.23	3.23	3.23	3.23	3.23	3.23	3.23	3.23	3.23	3.23	3.23	3.23	3.23	3.23	3.23	3.23	3.23	3.23	3.23	3.23	3.23	3.23	3.23	3.23	3.23	3.21	3.06	2.89	2.69	2.46	2.19	1.88	1.53	1.18	0.89	0.53	0.31	0.22	0.21	0.21	0.21	0.21	0.21	0.21	0.21	0.21	0.20	0.20	0.20	0.20	0.19	0.15	0.08																																				
Volume p (m3)		160.65	160.49	160.13	159.55	159.01	158.54	158.01	157.39	156.68	155.98	155.38	154.78	154.20	153.66	153.08	152.84	151.11	150.01	148.84	147.78	146.61	145.20	143.85	141.78	139.43	136.25	132.94	130.10	127.28	124.22	121.16	117.70	114.15	110.53	106.66	103.64	100.63	97.79	94.84	89.90	86.15	81.90	77.22	72.22	66.58	61.07	55.63	48.66	39.08	28.46	21.56	13.54	6.13	1.43

the uppermost channel first. Each channel location then becomes the divide for the next channel's contributing section and so forth.

As with the simulation of the runoff plots, and as explained in Chapter Three, the flow assumption adopted for the cascade simulations is that of sheetflow. The infiltration parameters are calculated on this basis and their use with the complex flow assumption would be inappropriate. The infiltration rates predicted by the infiltration models assume that the whole surface is infiltrating as is the case when rainfall is occurring or sheetflow covers the complete width of the slope element. Complex flow calculates the actual wetted length for any stage and thus infiltration rates based on full wetting would under-predict actual infiltration in the post-rainfall, or run-on phases.

6.2.3.b The Unaltered Cascade Productivity

Simulating runoff production from the two rainstorms for the full 54 elements along the Profile 2 cascade shows hypothetically the productivity that could be expected if the Avdat water harvesting system had not been constructed. Therefore, no channels sub-divide the hillslope as they do in reality. Surface water is generated at different times across the hillslope depending on the relative infiltration regimes (defined by the sets of A and B2 parameters associated with a given unit) and could be routed from the top of the cascade uninterrupted down to the bottom controlled by the resistance parameter and local slope gradient of each element. The last is derived from the topographic survey of the catchment used to produce the contour map and cascade network of flow-lines as explained in Chapter Two.

Table 6.12 Productivity from an Unaltered Cascade

Rainstorm	Elements	Area	ΣQ m^3	% of Input
02/03/74	54-1	14652.5	4.87	4.5
10/02/74	54-1	14652.5	3.23	2.0

(where Q is discharge).

The productivity from the cascade in volumetric (m^3) and percentage of input terms is presented in Table 6.12. Clearly it is a very low percentage and on its own suggests that runoff production is minimal from these two storms. However, from a consideration of column 54 in Tables 6.10 and 6.11 it is clear that for both rainstorms, there is considerably more water being produced and transmitted down sections of the profile than that which finds its way over the lower boundary of the cascade into the natural wadi channel. The slope section above the channel acts as a stopper, a consumer slope that absorbs runoff from elsewhere due to having relatively high infiltration rates and

Table 6.13 Cascade Productivity and Per Unit Area Productivity Values for Rainstorm 02/03/74

EL	UN	% PROD	PROD/A $cm^3\ m^{-2}$	SUM A m^2
54	1	26.155	1943.09	14.57
53	1	27.348	1404.20	47.33
52	1	29.965	1241.80	100.20
51	1	42.723	1312.52	143.27
50	1	46.245	1299.26	192.71
49	1	51.932	1275.23	241.24
48	1	53.058	1264.07	297.79
47	1	53.352	1102.24	362.04
46	1	56.154	997.94	426.27
45	1	62.367	947.93	480.29
44	1	63.327	863.15	535.68
43	1	66.220	859.07	587.93
42	1	68.741	860.92	637.47
41	2	68.464	1330.18	697.55
40	2	62.773	1279.71	785.06
39	2	65.516	1194.12	870.26
38	2	65.599	1149.44	963.49
37	2	62.981	1036.03	1076.93
36	2	67.982	996.69	1174.39
35	2	67.668	959.40	1280.19
34	2	64.491	844.56	1409.08
33	2	66.483	797.65	1533.82
32	2	57.805	591.78	1720.82
31	2	55.357	462.57	1935.06
30	2	48.861	373.62	2225.69
29	2	48.327	237.60	2527.65
28	3	71.150	3023.81	2786.69
27	3	74.928	2823.35	3043.91
26	3	76.187	2631.17	3322.26
25	3	78.198	2477.62	3601.86
24	3	77.782	2283.62	3917.54
23	3	78.817	2133.69	4241.19
22	3	78.866	1984.43	4589.03
21	3	80.471	1866.46	4924.71
20	3	84.132	1804.67	5199.33
19	4	93.603	5049.76	5474.43
18	4	94.347	4917.35	5733.30
17	4	93.022	4700.00	6075.80
16	4	92.719	4483.91	6453.18
15	4	93.679	4341.42	6794.89
14	4	93.101	4132.15	7182.34
13	4	92.649	3916.76	7609.54
12	4	92.350	3688.50	8065.60
11	4	91.403	3393.44	8586.74
10	4	91.914	3183.51	9082.80
9	4	92.043	2993.44	9578.33
8	4	90.002	2687.94	10214.04
7	4	86.806	2351.34	11087.73
6	5	64.693	-5785.41	12056.59
5	5	70.211	-5889.10	12685.87
4	5	59.916	-6373.94	13417.31
3	6	53.301	-6373.83	14093.68
2	6	55.126	-6373.93	14522.34
1	6	74.903	-6373.87	14652.50

El = element
UN = unit
% PROD = % runoff productivity
PROD/A = productivity per unit area
SUM A = cascade contributing area

Table 6.14 Cascade Productivity and Per Unit Area Productivity Values for Rainstorm 10/02/74

EL	UN	% PROD	PROD/A cm3 m-2	SUM A m2
54	1	1.346	147.56	14.57
53	1	1.143	60.48	47.33
52	1	1.214	55.89	100.20
51	1	2.182	78.27	143.27
50	1	2.504	68.29	192.71
49	1	3.080	61.39	241.24
48	1	3.192	62.19	297.79
47	1	3.035	25.92	362.04
46	1	3.205	19.96	426.27
45	1	4.020	27.15	480.29
44	1	4.098	20.97	535.68
43	1	4.637	35.61	587.93
42	1	5.260	45.74	637.47
41	2	7.345	342.25	697.55
40	2	7.387	274.49	785.06
39	2	9.125	204.57	870.26
38	2	9.582	157.80	963.49
37	2	8.713	96.22	1076.93
36	2	10.588	81.41	1174.39
35	2	10.388	74.96	1280.19
34	2	9.010	45.20	1409.08
33	2	9.649	48.52	1533.82
32	2	6.657	4.07	1720.82
31	2	5.906	5.53	1935.06
30	2	4.595	20.14	2225.69
29	2	4.449	2.96	2527.65
28	3	31.107	3000.80	2786.69
27	3	43.610	2739.28	3043.91
26	3	49.776	2505.31	3322.26
25	3	55.247	2322.08	3601.86
24	3	56.576	2100.24	3917.54
23	3	59.374	1933.10	4241.19
22	3	60.443	1769.31	4589.03
21	3	63.476	1642.34	4924.71
20	3	69.481	1574.65	5199.33
19	4	84.199	5860.32	5474.43
18	4	86.604	5623.58	5733.30
17	4	84.583	5249.43	6075.80
16	4	84.580	4887.03	6453.18
15	4	86.792	4652.95	6794.89
14	4	86.007	4312.22	7182.34
13	4	85.511	4003.08	7609.54
12	4	85.628	3857.66	8065.60
11	4	84.835	3682.21	8586.74
10	4	86.268	3582.39	9082.80
9	4	87.016	3512.17	9578.33
8	4	84.826	3392.99	10214.04
7	4	81.346	3174.71	11087.73
6	5	55.759	-7438.28	12056.59
5	5	61.331	-7084.65	12685.87
4	5	48.850	-7240.40	13417.31
3	6	37.655	-7593.58	14093.68
2	6	33.275	-8152.06	14522.34
1	6	58.629	-6560.60	14652.50

El = element
UN = unit
% PROD = % runoff productivity
PROD/A = productivity per unit area
SUM A = cascade contributing area

poor transmissivity. The latter is a function of their low slope gradient as the hillslope is mantled by deposits of colluvium as part of the overall erosional-depositional sequence as described in Chapter Two and illustrated in Plates P.17 to P.34. This stopper effect is clearly illustrated in Tables 6.13 and 6.14 which contain the productivity percentage and per unit area productivity values of each element. For the last six elements in the cascade, the former is very small and the latter negative. The significance of these indices were discussed in Chapter Five and show the ratio of the volume of water entering the cascade element and the volume exiting as run-off, and the net balance between the two in per unit area terms. Where the percentage efficiency is high then the cascade is a good transmitter of runoff and when the productivity is positive, it is a good producer. On the basis of their given parameters, the elements at the base of the cascade are neither whereas the elements along the rest of the cascade are both.

6.2.3.c The Current Channel Configuration Productivity

The matrix of volumetric productions can be used to show the performance of the man-made channel system reconstructed to form the current Avdat water harvesting system. The results of these simulations provide a control for assessing the relative productivity from different catchment configurations, and for the assessment of whether the selected parameters from the plot samples and the run-on/runoff plots reproduce the expected orders of magnitude of runoff production observed from the various sub-catchments for a particular rainstorm.

Table 6.15 Predicted Discharges (m^3) into the Existing Man-Made Channel Configuration (02/03/74) Selected from Table 6.10

	Divide At				
	54	12	9	7	6
Channel At					
13	18.91				
10	23.94	7.12			
8	27.13	11.69	5.46		
7	29.07	14.59	8.87	3.94	
1	4.87	1.25	1.00	0.89	0.83

Table 6.16 Predicted Discharges (m^3) into the Existing Man-Made Channel Configuration (10/02/74) Selected from Table 6.11

	Divide At				
	54	12	9	7	6
Channel At					
13	17.55				
10	23.00	7.42			
8	26.90	11.95	5.72		
7	29.68	14.11	9.15	3.30	
1	3.23	0.21	0.21	0.21	0.20

The total productivity from superimposing the current channel configuration on this cascade is the sum of the upper value in each of the columns 54, 12, 9, 7 and 6. The man-made channels are located approximately at the lower boundaries of elements 7, 8, 10 and 13. The natural channel is situated below element 1. For rainstorm 02/03/74 productivity is 36.27 m^3, which is 33.3% of the total rainfall input to the elements 1-54 of 108.86 m^3. This can be compared to the predicted discharge from the complete unaltered cascade of 4.87 m^3 which is only 4.47% and shows the effect of partial area productivity clearly. For rainstorm 10/02/74 productivity is 34.19 m^3, which is 21.3% of the total rainfall input of 160.65 m^3. This can be compared to the predicted discharge from the complete unaltered cascade of 3.23 m^3 which is only 2%.

The causes of such radical differences in production are due to the reduction in the length of individual flow-sections contributing to channels (a rise in drainage density), and the prevention of water running on to slope areas with less favourable transmissivity and higher potential infiltrability, i.e. the unit five slope sections. Firstly, for early time periods they are predicted to have high infiltration rates due to their large B coefficients. With a short duration, high intensity rainstorm, these slopes maintain relatively high infiltration rates even though their final infiltration rates may be low. Secondly, the slope gradients are very small and water flowing rapidly down higher slope sections slows down over this section and can infiltrate during the flow recession following rainfall cessation. Large amounts of detention storage are retained and flow velocities are very low. The result is consumption of water from upslope, especially once rainfall has stopped.

It is possible to see the influence of intensity, timing and amount of rainfall. Rainstorm 02/03/74 has a smaller magnitude (7.43 mm) and the higher peak intensity (41.6 mm hr^{-1} for 9 minutes) and rainstorm 10/02/74 a larger magnitude (10.44 mm) and lower peak intensity (25.65 mm hr^{-1} for 6.6 minutes). The productivity from the slopes are such that the higher intensity, shorter duration event produces the largest volumetric discharge, with higher peak discharges for each element.

The importance of rainfall intensity was already observed in the sensitivity analysis described in Chapter Five. The results from these cascade simulations indicate that the role of intensity is more important than the magnitude of the rainstorm, an observation that concurs with field data from Yair and Lavee elsewhere in the Negev (*et seq*).

There are several things to examine from these results. Firstly, there is the question of whether the parameters are producing the expected values of runoff productivity. Secondly, whether the differences in productivity from the superimposed man-made channels and the hypothetical unaltered cascade represent the true benefits of water harvesting system construction. This specifically relates to the doubts expressed earlier concerning the magnitude of the B parameter produced for the unit 5 loess slopes from curve-fitting to the Zarmi *et al* micro-catchment test data. In Chapter Three the possible over-estimation of the initial infiltration due to the inclusion of detention storage was discussed. If the infiltration rates of this slope section are poorly represented, the apparent stopper effect exerted by unit 5 slope sections would not be realistic and the relative productivity from the man-made and unaltered slope would not be so extreme.

6.2.3.d Assessing the Efficacy of the Plot Parameters

Observed Results and Expected Productivity Percentages

According to the digitised flood records, the mean runoff percentage for rainfall 02/03/74 for the eastern hillslope sub-catchments 3-6 which the profile crosses is 34.5%, varying from 23.3% to 55.6%. This accords well with the order of magnitude of predicted runoff from the current channel configuration for this rainstorm which is 33.3%. For rainstorm 10/02/74, the mean runoff percentage is 8.2% for these four sub-catchments, varying from 4.7% to 14.1%. The predicted runoff percentage from the input of 160.65 m^3 is 21.3%, somewhat higher than expected for the eastern slope profiles. There are two likely main reasons for this over-prediction which results from the combined character of the rainstorm, and the procedures representing the infiltration component of the rainfall-routing model. The first probable reason is that the initial infiltration rates predicted by the run-on/runoff plot derived infiltration parameters are under-estimates compared with the actual infiltration rates. The significance of this is explained in more detail in a discussion of the sub-catchment simulations but is more important for the lower intensity rainstorm of 10/02/74 than the high intensity storm of 02/03/74. The second reason is that the infiltration parameters are not designed to handle rainfall and runoff conditions in which intensities fall below saturated conductivities and the surface dries up prior to rainfall intensities increasing again to levels above the saturated conductivities. From the data output recorded from the simulation of the cascade response for rainstorm 10/02/74, it can be seen that the fall in intensity to a low level is of sufficient duration to allow the detention storage on the surface of the slope to totally infiltrate as both the additions from runoff and the rainfall are insufficient to exceed the

infiltration capacity of the surface of each element. The cascade therefore loses its ponding state, the first element (54) after 1238 seconds, and 41 of the 54 elements after 5000 seconds. Because of the use of a single set of infiltration parameters, and the fact that infiltration in each element is assumed to be Hortonian once the storage is satisfied and the time to runoff passed, the infiltration rate continues to decrease towards A even though there is unsatisfied potential for each time period post-runoff. When the rainfall intensity increases again, runoff occurs immediately when p and run-on q exceeds i. The total runoff volume will therefore be over-estimated. This is a limitation of the infiltration model since if the amount of water available is less than the potential infiltration, the storage in the soil will empty and the potential for infiltration will increase rather than decrease in Hortonian fashion. At 5000 seconds, the predicted output of runoff for the five channel configuration (13, 10, 8, 7 and 1) is 30.34 m^3 which is 18.8% of the total input to the catchment during the rainstorm. Because of the generally low subsequent rainfall intensities (1 to 8 mm hr^{-1}), if a second set of infiltration parameters were to be used to allow for the increase in infiltration potential during the period of low intensity, little runoff would be forecast across the dried-up cells and the total productivity would remain at about the 5000 second level. This influence of this factor is discussed in Section 6.3 for the sub-catchment simulations.

The Role of the Foot-Slopes

It is difficult to assess the role of unit five foot-slopes on the forecast runoff productivity of the slope due to the fact that this unit occupies only a small proportion of the total percentage area of the cascade and contributes to only one of the five channels from which the total productivity is calculated. The orders of magnitude of the predicted response appear well within the range expected for these surfaces showing both the infiltration and the routing components of the model to be parameterised acceptably well. However, the difference between the productive efficiency percentages and per unit area productivity of the unit 5 slopes and all the other slopes is quite striking. Is this expected given a knowledge of the hydrological environment? Firstly, the accepted characteristic of crusting soils is that they have initially high infiltration rates that fall rapidly to a low final rate of 3 to 6 mm/hr following the crusting process which takes place when several millimetres of rainfall have fallen. This explains the relatively high B coefficient from the best-fit curve. It would be expected that the productivity from a short duration rainfall event would therefore result in quite considerable infiltration, although this is not so for a longer duration event, especially one with high initial rainfall intensities like 10/02/74.

If there is an overestimate of infiltration for unit 5 slopes, the most probable reason would be an unintentional overestimation of infiltration from the inclusion of a detention storage component in determining the times to runoff used to provide the infiltration envelope. In the paper of Zarmi *et al*, the authors refer to the time to runoff beginning, but seem to indicate that this is the time that runoff is

recorded from the micro-catchment surface. Since this involves a component of hydraulic head build-up and routing off the surface and into the collection trough, it may be that the times to runoff are slight overestimates, and hence the infiltration curve is shifted slightly towards the right. This was previously discussed in Chapter Three. This inclusion of routing and detention storage was seen to be major cause of infiltration overestimation in simulations of the Avdat run-on/runoff plot response. Whether this is the case for the Zarmi parameters is uncertain. However, it may be a factor.

Probably of more importance is the observation that the slope gradient decreases considerably over this slope section, and hence the competence to transmit surface water decreases accordingly. The mean gradient of the last six cascades is 2.47°. At these low slope gradients, any errors in specifying the gradient become extremely important as the result can be a relatively large change in the value of the sine used in Mannings flow formula to calculate velocity. Flow across shallow slopes is difficult to reproduce with accuracy. An error in the gradient of one degree, i.e. 1° instead of 2°, results in a difference in predicted velocity by a factor of 2, the same magnitude error at 20° resulting in a difference in velocity by a factor of only 1.05. If the routing components are poorly represented for slope sections of low gradient, then sub-catchments with a large proportion of low slopes, especially where they are located between long hillslope sections and the harvesting channels, should produce the poorest estimates of runoff production vis á vis the observed in the wider scale simulations. This can be assessed from an analysis of predictions from the seven complete Avdat sub-catchments.

6.3 AVDAT SUB-CATCHMENTS

6.3.1 Purpose of the Simulations

The purpose of the sub-catchment simulations is to apply the runoff-routing model developed in this thesis is to assess the runoff productivity and harvesting potential of complete hydrological systems. In this case, the systems are the sub-catchments supplying the Avdat runoff farm and for purposes of comparison, an additional hypothetical catchment configuration. As explained in Chapter Two, this represents the catchment area that would supply the runoff farm if the harvesting system had not been introduced. Observed hydrographs exist for each of the seven sub-catchments and parameters are supplied from plot studies and topographic surveys as described in previous chapters. There is no observed hydrograph for the hypothetical catchment, and instead, volumetric production and the spatial pattern of runoff generation and transmission are compared with the conditions predicted for the seven sub-catchments. This is carried out in Section 6.4.

The sub-catchment boundaries of the reconstructed Avdat water harvesting system are shown on the overlay of the catchment contour map in Appendix 3.1. The flow-nets used by the model as a geometric and hydrological framework for flow calculation and routing are shown in Appendix 3.2.

The unaltered catchment flow-net is shown in Appendix 3.3. The catchment area contributing to the runoff farm is clearly increased by the man-made drainage network. Areas of the catchment that would drain to other locations are brought within the grasp of the terraced fields by the reaching out of channels to exploit topographic subtleties. By routing water across flow lines at an angle rather than allowing water to flow down them, the channels can cross lateral sub-divides of hillside sections. The size of each of the catchment areas is calculated by the model as part of the parameterisation sub-routines.

6.3.2 Predictions and their Significance

The model predicts the runoff response of each hillslope and channel element in the various catchment area flow-nets for the two rainstorms shown earlier in Figures 6.1 and 6.2, 02/03/74 and 10/02/74. The former is a high intensity, single peak, short duration rainstorm. The latter is a medium and low intensity, multiple peak, long duration rainstorm. How the model performs under both situations is a rigorous test of the parameter characteristics and the model procedures, and conclusions can be drawn from the observed and predicted results as to the sensitivity of the two and the sources of any error encountered.

A complete range of hydrological variables could be calculated by the model for any pre-determined element within the system. This capability has been of considerable benefit in the previous three stages of simulation of smaller systems. However, in these wider scale simulations of catchments and sub-catchments, as compared with plots or individual cascades, only summary variables are used to interpret the response, along with the predicted hydrographs. The main variables are volumetric productivity and the two key indices of the productivity percentage, and the net productivity/transmissivity per unit area. The former is the percentage of input from rainfall and run-on converted to runoff output for the particular element or segment. The latter is the per unit area additions or subtractions to flow and is a balance between the rainfall excess produced out of the element and the infiltration of water running into the element. This figure shows up the degree to which a slope is a producer or consumer. Consumptive slopes can consume in both the pre-ponding phase and the post-rainfall phase as they experience the knock-on effect of water from above helping them reach their ponding point (this effect has been described by Dunne, 1983) and as they exert a stopper effect once rainfall ceases and their relatively high infiltration rates or poor routing characteristics rapidly deplete surface storage and dissipate water entering in from more productive upslope locations.

6.3.3 Method of Results Assessment

There are two main thrusts in the assessment of the predictions from simulations of the sub-catchments and unaltered catchment system. The first is to examine the quantitative ability of the model and its parameters to reproduce sensitively observed conditions and suggest logical reasons for any errors observed. The second is to examine the qualitative ability to assess the key characteristics of the catchment hydrology controlling the harvesting efficiency of an artificial channel network. This is done through largely graphical methods, assessing the spatial distribution of runoff production and consumption relative to the channel arrangement and through a consideration of volumetric production from the different catchment components. This can be used in explanations of the predictive abilities of the model and also in theoretical terms to show the principles of partial area productivity and spatial variation of runoff potential regardless of the goodness of fit of predictions. Accepting the given characteristics of the different units used to provide the catchment parameters, the effects of their distribution relative to each other along particular flow-lines and to man-made and natural channels can be assessed in the light of the discussions on arid hillslope hydrology in Chapter One. Comparing productivity from the current water harvesting system and from the catchment in its hypothetical unaltered state focuses on the key concepts of hydraulic remoteness and contiguous area contribution. This comparison and qualitative assessments are made in Section 6.4.2 of this chapter.

The quantitative analysis of the results is similar to that adopted for the run-on/runoff plots. The percentage error between observed and predicted values is calculated (Equation 6.1) for summary variables such as total discharge volume. Hydrographs are not compared by goodness of fit. The observed hydrograph is not synchronised on the same time scale as the rainfall hyetograph and hence the correspondences between observed and predicted instantaneous discharges are not known. Instead, a largely visual comparison of observed and predicted hydrograph shape is made by equating start of runoff and plotting the graphs on identical axes. The disadvantage of this relates to the fact that in reality, discharge from the channel system will not register on the flood recorder (and hence the digitised observed hydrograph) until depression storage in the channel system and the stilling well outside the v-notch weir has filled. The simulation model does not consider these delays. Therefore, the two hydrographs are likely to be offset, the predicted hydrograph plotted at later elapsed times that the observed by a function of this time-lag. It may be in the order of tens of minutes. Consequently, the visual appraisal of the hydrographs should take into account hydrograph position and look more at shape rather than synchronicity. Analysis of the predicted results vis á vis the observed shows whether the parameters are effective in reproducing known conditions and whether they have been successfully applied from the small to the large scale as part of a distributed rainfall-runoff model.

For the qualitative analysis, choropleth maps are provided of the distribution of productivity percentages in Appendices 5.4 to 5.7. The pattern of this runoff efficiency identifies the producers and

consumers and the most important locations for the positioning of channels. It is the juxtaposition of good and bad producers to each other and to the channel system that shows the degree to which a given channel configuration effectively exploits potential, and the presence of un-tapped producers within the hillslope system shows an under-utilised resource. The spatial arrangement of the productivity percentages are mapped using the computer package *Mapics*. They can be used to compare the patterns of production from different rainstorms, within separate sub-catchments and between the man-made and unaltered catchment systems. The last comparison is particularly interesting and encompasses several aspects, for instance, whether the introduction of extra channels has any observable effect on the patterns of productivity along hillslopes, and the likely volumetric improvements resulting from the introduction of man-made channels. Interpretation of the spatial distribution of productivity vis á vis collecting channels can help explain any systematic differences between observed and predicted results for the various sub-catchments. For convenience, catchment flow-nets have been plotted at the same scale as the choropleth maps, and maps of the unit distribution are included to show their spatial pattern. The characteristics of the sub-catchments, the complete catchment and the unaltered catchment including total area, channel length, drainage density and proportion of area in each unit class are summarised in Table 6.17. This is critical to the understanding of the catchment productivity and the control that each unit type and its spatial location exerts on the character of runoff from the whole catchment.

6.3.4 The Simulation Results and Their Interpretations

6.3.4.a Overall Variations in Model Predictions

It is clear from the results of the simulations presented in Tables 6.18 and 6.19 below that the use of the model and parameters derived from fieldwork at Avdat and from the literature in the case of the infiltration regime on Units 5e and 5w, results in both good and poor predictions for the two rainstorms for different groups of sub-catchments. For the first group (sub-catchments 3, 4, 5 and 6) the model and parameters produce generally good predictions for one rainstorm (02/03/74) but not for the other. For the second group (sub-catchments 1, 2 and 7), predictions are poor for both rainstorms. From an examination of these different groups and the nature of the predictions for the two rainstorms it is possible to identify and explain some of the problems and sources of error encountered when simulating complex systems at a larger scale. These problems are important because they show the limits of the routing and infiltration components of the model, particularly in relation to parameter provision.

	Table 6.17 Sub-Catchment Dimensions and Unit Type Surface Areas								
Catchment	1	2	3	4	5	6	7	Current	Unaltered
Area m2	77760.7	49558.4	49921.5	32443.2	8737.6	46641.6	30171.9	295234.9	180202.4
Channels m	928.9	351.7	1230.3	1032.5	429.7	733.5	293.0	4999.6	1126.8
Density m2/m	83.7	140.9	40.6	31.4	20.3	63.6	103.0	59.1	159.9
Area by Unit m2									
1-1e	0.0	0.0	0.0	1748.7	0.0	0.0	31.6	1780.3	5718.6
2-2e	0.0	0.0	556.4	3488.3	0.0	7617.7	491.2	12153.6	12674.0
3-3e	1977.9	0.0	9192.9	13640.7	1204.3	15505.6	1330.4	42851.8	27088.8
4-4e	0.0	0.0	10260.9	9135.8	5266.4	9891.5	6218.1	40772.7	38660.8
5-5e	0.0	0.0	15384.2	4429.8	2266.9	10895.8	22100.6	55077.3	32675.9
6-5w	23015.7	16038.9	6124.9	0.0	0.0	2731.1	0.0	47910.6	26517.0
7-4w	20389.7	9559.2	3515.5	0.0	0.0	0.0	0.0	33464.4	11349.3
8-3w	5746.2	7446.0	4503.7	0.0	0.0	0.0	0.0	17695.9	11567.1
9-6w	26631.1	16514.2	383.1	0.0	0.0	0.0	0.0	43528.4	13951.0
Area by Unit %									
1-1e	0.0	0.0	0.0	5.4	0.0	0.0	0.1	0.6	3.2
2-2e	0.0	0.0	1.1	10.8	0.0	16.3	1.6	4.1	7.0
3-3e	2.5	0.0	18.4	42.0	13.8	33.2	4.4	14.5	15.0
4-4e	0.0	0.0	20.6	28.2	60.3	21.2	20.6	13.8	21.5
5-5e	0.0	0.0	30.8	13.7	25.9	23.4	73.2	18.7	18.1
6-5w	29.6	32.4	12.3	0.0	0.0	5.9	0.0	16.2	14.7
7-4w	26.2	19.3	7.0	0.0	0.0	0.0	0.0	11.3	6.3
8-3w	7.4	15.0	9.0	0.0	0.0	0.0	0.0	6.0	6.4
9-6w	34.2	33.3	0.8	0.0	0.0	0.0	0.0	14.7	7.7

6.3.4.b The Sub-Catchment Groups

Each of the two groups of sub-catchments have similar geomorphological characteristics as well as having similar predictive abilities. The first group, sub-catchments 3, 4, 5 and 6, can be classed as high drainage density (20 - 64 m^2m^{-1}), low percentage shallow sloping surface sub-catchments (14 % of the hillslope elements are below 5°) each of which has channels juxtaposing a range of different slope unit types and steepness. Flow-lines are intercepted at different positions in the downslope sequence of slope types and not predominantly at the end of the erosional depositional sequence which would involve them passing across a very shallow, soil covered area such as the wadi depression or the raised proto-Zin terrace (as shown clearly in Appendix 3.1 and Plates C.1 to C.3). Individual flow-line cascades are generally short as shown by the drainage density figures in Table 6.17 and the flow-net Appendix 3.2.

The second group, sub-catchments 1, 2 and 7, are the low drainage density (84 - 141 m^2m^{-1}), high percentage shallow sloping surface sub-catchments (49 % of the hillslope elements are below 5°) each of which has a particular spatial distribution of slope types adjacent to the majority of the length of harvesting channels. Flow-lines are generally intercepted after they have passed over very shallow-sloping areas such as the unit 5e and 5w, and unit 6w slopes. The unit 5e and 5w slopes have infiltration parameters derived from the literature and for which the B parameter might be overestimated as explained in Section 6.2. Individual flow-line cascades are generally long in comparison to the former group of sub-catchments 3, 4, 5 and 6.

6.3.4.c Results from Rainstorm 02/03/74

Table 6.18 Catchment Observed and Predicted Runoff for Rainstorm 02/03/74

	Sub-Catchment							
Value	1	2	3	4	5	6	7	Σ All
Observed Input m^3	577.7	368.2	370.9	241.0	64.9	346.5	224.1	2193.3
Observed Output m^3	141.7	215.3	118.7	56.1	36.1	94.4	129.5	791.8
Predicted Output m^3	37.4	21.6	102.2	84.2	30.9	88.0	18.0	382.3
%E [(O-P)*100/P]	73.6	90.0	13.9	-50.0	14.3	6.7	86.1	51.7
Obs Qp $m^3 s^{-1}$	340.0	504.3	444.7	285.5	160.6	392.5	278.4	
Pred. Qp $m^3 s^{-1}$	29.3	28.6	166.7	104.5	51.9	142.3	40.2	

(where O is observed, P is predicted and Qp is peak discharge)

Good Predictions

As shown in Table 6.18, the good predictions for rainstorm 02/03/74 are recorded for sub-catchments 3, 4, 5, and 6. Whilst for each, the peak discharge rates are underestimated by a consistent factor averaging at 2.8, the total discharge predicted for the sub-catchments varies between an under-prediction of 14% and an over-prediction of 50%. This shows that the volume of runoff predicted is on the whole good, but the timing of hydrograph arrival is less so, with predicted hydrographs attenuated in the rising and falling stages as shown in Figures 6.3 to 6.6.

Looking more closely at the individual sub-catchments through an examination of Plates C.1 to C.3, and Appendix 3.1 and 5.2.1, shows how the channels in these sub-catchments harvest directly from a range of slope types and unit characteristics. In particular many of these are relatively steep and flow-lines down to the channels are relatively short. Sub-catchment three harvests from the wadi bottom but also taps into a number of steeper sloping sections fringing the wadi, through which the natural and man-made network of channels pass. The predicted hydrograph is attenuated, with a lower peak and a longer duration although the predicted volume is only 13% below the observed (Figure 6.3). Sub-catchment four produces a highly attenuated hydrograph compared to the observed (Figure 6.4) and an over-prediction of total discharge by 50%. Sub-catchment five is a very small catchment area wholly contained on the eastern hillsides and sandwiched between the channels of sub-catchments four and six. The volumetric runoff production for rainstorm 02/03/74 is 86% of the observed although once again, as with sub-catchments three and four, the hydrograph is attenuated with a lower peak and longer, shallower recession curve (Figure 6.5). In sub-catchment six, the majority of the slope area is comprised of the steep upper-level slope units 2e to 4e and the prediction of total discharge for 02/03/74 is closest at 93% although once more the peak is under-estimated and the whole response attenuated as shown in Figure 6.6.

Poor Predictions

For rainstorm 02/03/74, the grouping of 1, 2 and 7 produce large under-predictions of runoff as shown by the summary values in Table 6.18 and the observed and predicted hydrographs in Figures 6.7 to 6.9. Both the size and shape of the hydrographs predicted are poor compared with the observed, although the duration of runoff is similar. For sub-catchment one only 26% of the observed runoff is predicted, 10% for sub-catchment two and 14% for sub-catchment seven. The predicted peak discharges vary from 6% to 14% of the observed.

Figure 6.3 Observed and Predicted Hydrographs for Sub-Catchment Three (Rainstorm 02/03/74)

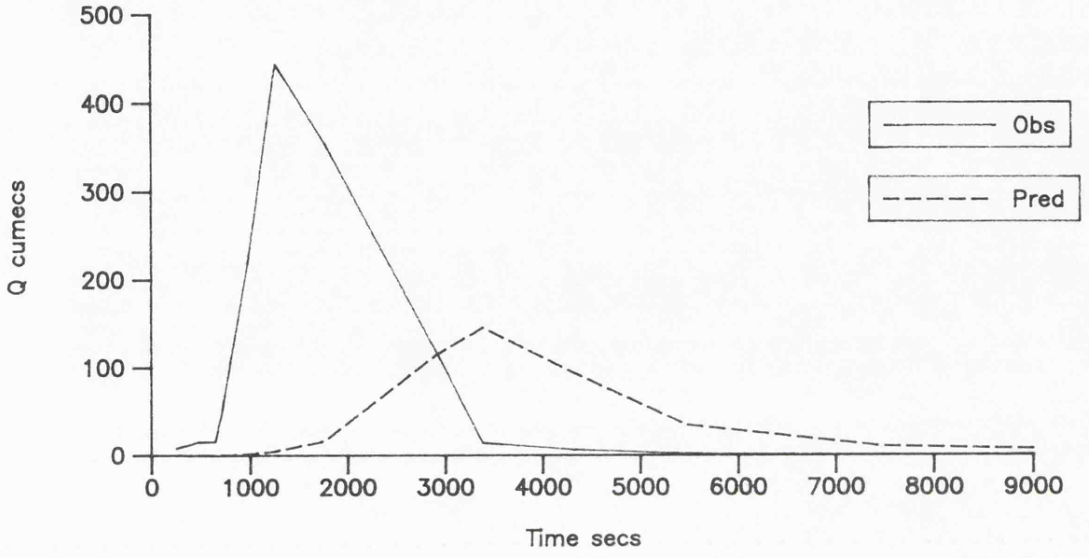

Figure 6.4 Observed and Predicted Hydrographs for Sub-Catchment Four (Rainstorm 02/03/74)

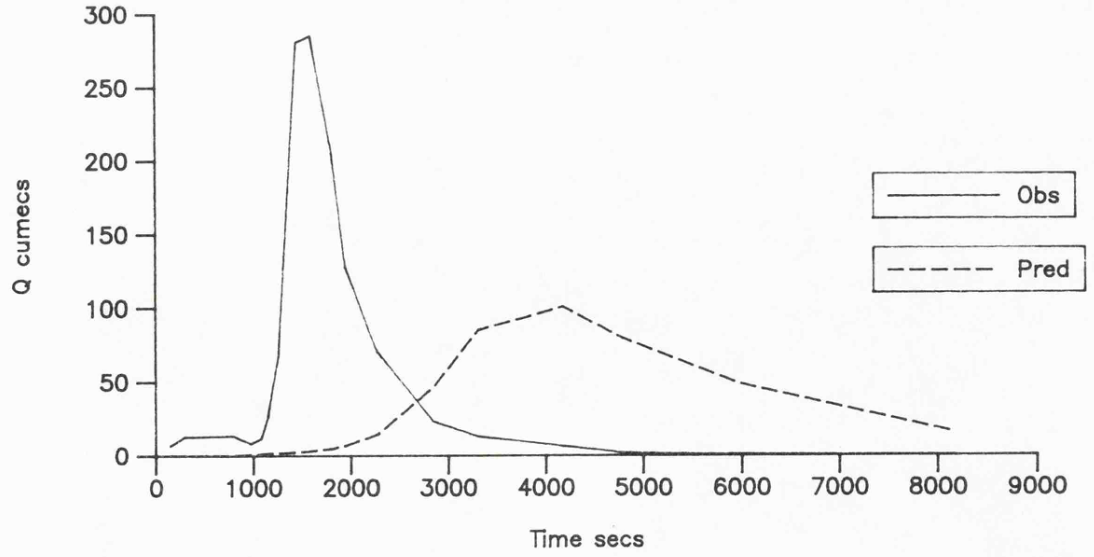

Figure 6.5 Observed and Predicted Hydrographs for Sub-Catchment Five (Rainstorm 02/03/74)

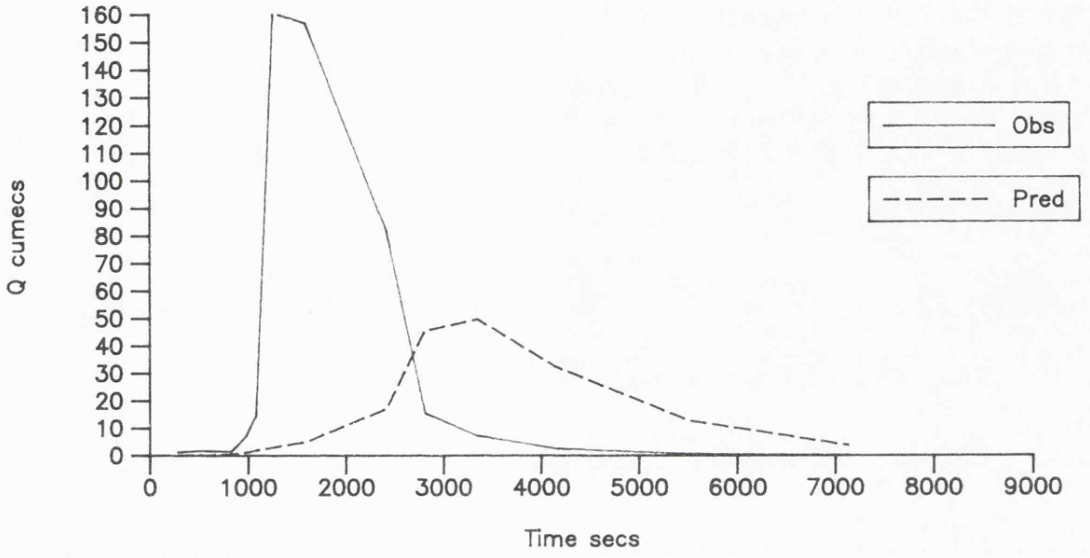

Figure 6.6 Observed and Predicted Hydrographs for Sub-Catchment Six (Rainstorm 02/03/74)

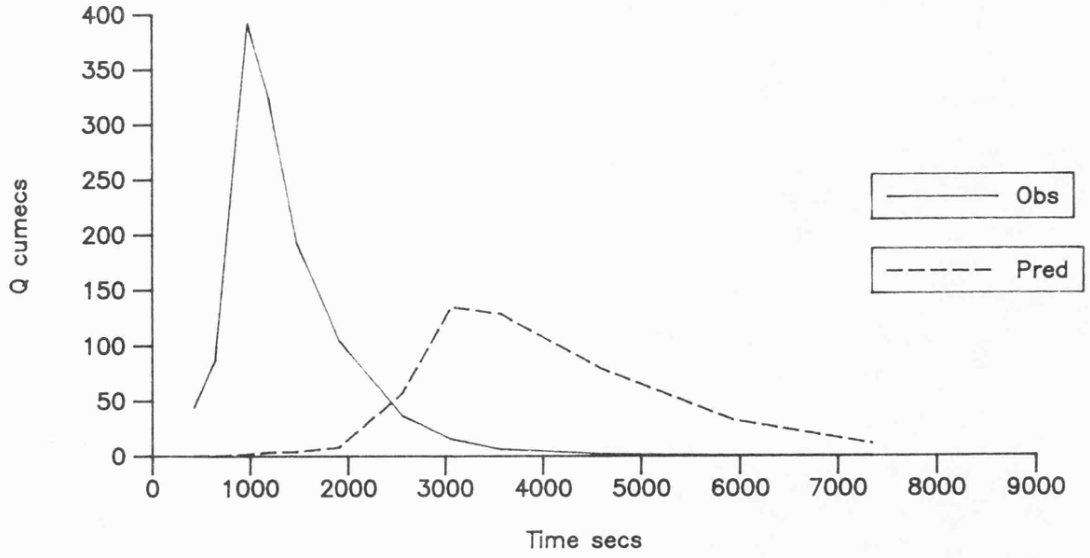

Figure 6.7 Observed and Predicted Hydrographs for Sub-Catchment One (Rainstorm 02/03/74)

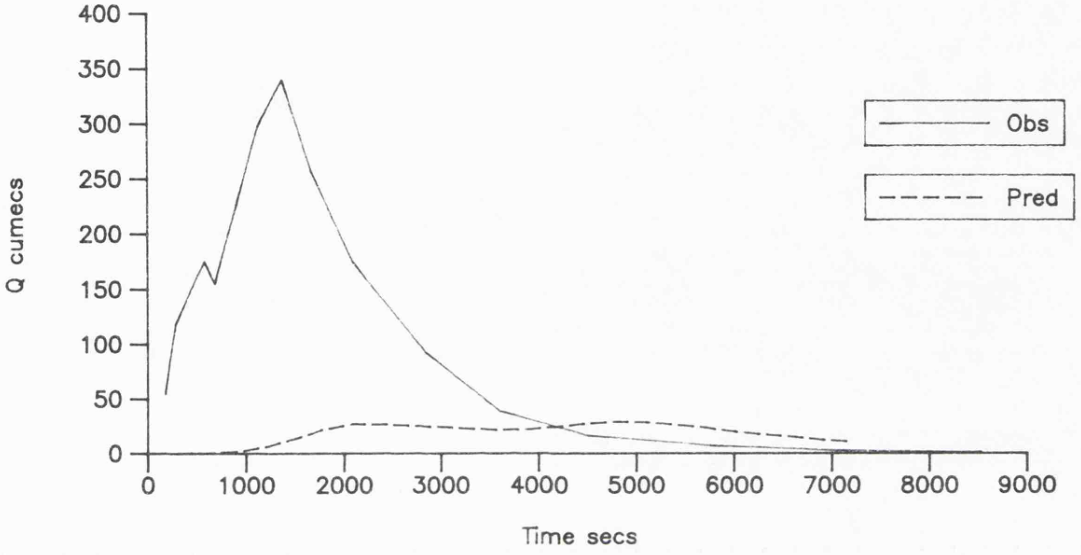

Figure 6.8 Observed and Predicted Hydrographs for Sub-Catchment Two (Rainstorm 02/03/74)

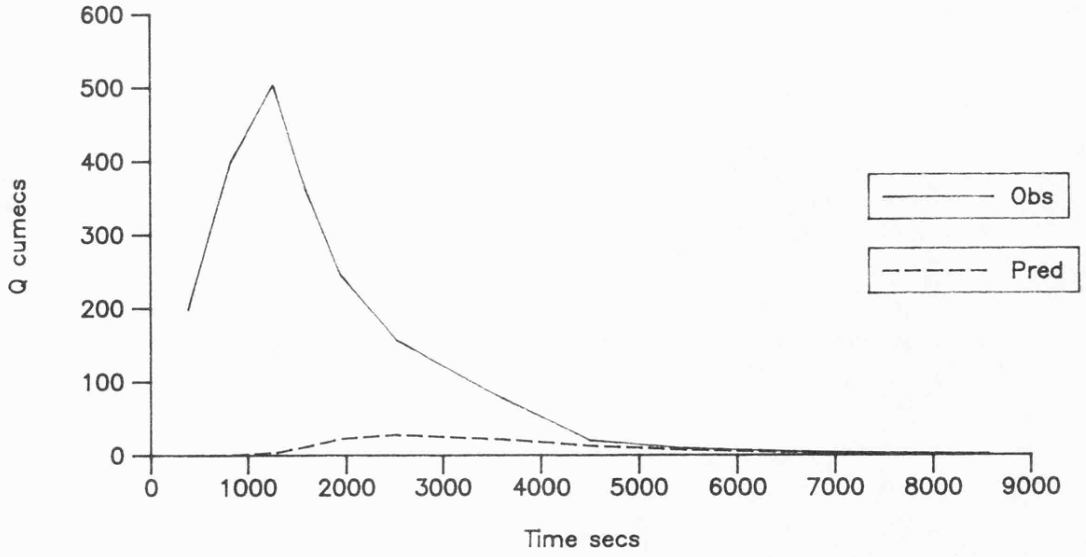

Figure 6.9 Observed and Predicted Hydrographs for Sub-Catchment Seven (Rainstorm 02/03/74)

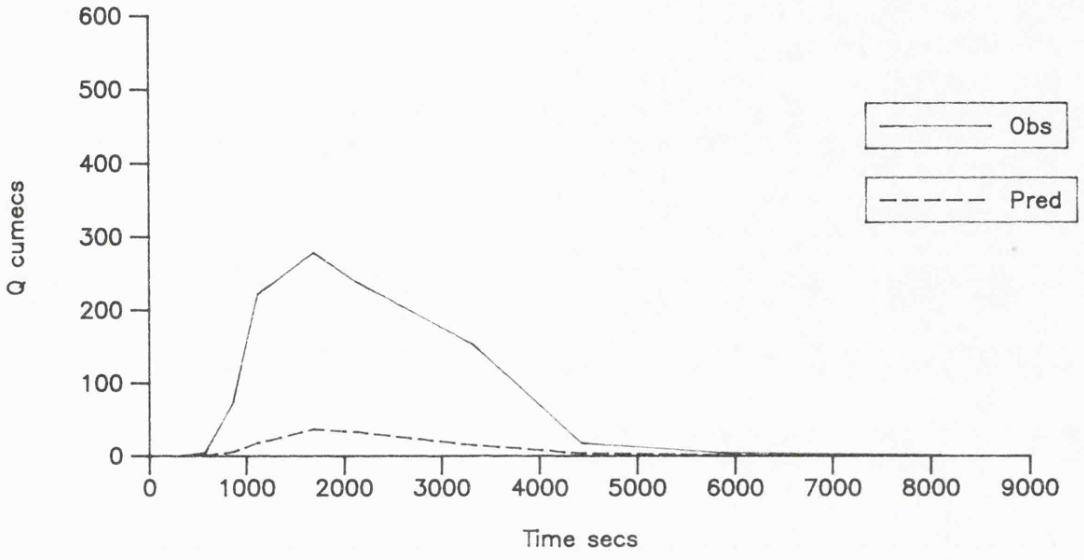

Conclusions and Interpretations

The differences between the two groups in terms of their predictive abilities are wide and require explanation given that the same parameter sets and model routines are used for each. The explanation must therefore come from a consideration of the physical character of the sub-catchments and the context in which the different parameter sets are distributed and the role they play in the Contiguous Area Contribution in the different sub-catchments. Given the character of the rainstorm, which is a single high-intensity peak, the character of the predicted hydrograph variations from the observed can also be understood by assessing the role of the physical characteristics.

The cascade simulated in the previous modelling exercises passes through the four sub-catchments of 3, 4, 5 and 6 from the upper divide of six through to the channel of three. Productivity was seen to vary within the hillslope profile. Since the majority of water harvested by the channels occurs where they are contiguous with the most productive cascade sections then the character of the hydrograph depends on the relative timing of the productivity from locations up and down-stream and the routing of flow along the channel length to the farm inlet. If the routing characteristics off all or part of the slope sections and through the channels are not closely reproduced, then the hydrograph shape is unlikely to be similar to the observed. If the peak runoff from the closer slopes was not predicted to coincide with the peak runoff from the more geographically remote slopes, then hydrographs would be attenuated and peaks reduced. If the flood wave in the channel were to be dispersed this would also cause the rising and falling limb to be attenuated. Both of these seem a likely explanation for the difference in observed and predicted hydrograph shapes. Channel routing does not affect the total productivity from the sub-catchments because they are assumed impermeable.

With the group of sub-catchments 1, 2 and 7 most flow-lines cross or end in a broad swath of shallow-sloping unit 5e or 5w slopes. This brings into play two characteristics, firstly that the infiltration parameters derived for this unit from the literature on loessial crusted slopes in the Negev may result in an uncontrollable source of under-prediction of runoff. Secondly, that the model routing procedures and the geometric simplification of the Avdat catchment surface is not sensitive to the routing conditions on very shallow slopes, under-predicting the stage-discharge relationship, leading to increased detention storage and for the hillslopes, to over-predictions of infiltration once rainfall ceases and runoff dissipates. Small magnitude differences in slope gradient at low slopes result in considerable differences in the stage-discharge relation predicted by Mannings flow equation compared to the same differences at greater slope gradients. Retention of larger detention stores and less rapid routing of surface water between two points increase potential for transmission loss compared with that which might be expected if the slope gradient were more sensitively specified in these shallow surface areas such as the wadi-bed, footslopes or proto-Zin terrace area. This apparent inability to accurately reproduce shallow gradient routing and detention storage, coupled with infiltration parameter

insensitivity would effectively limit the predictive ability of the model for catchments in which these slope conditions are dominant and in which the insensitive infiltration parameters play a critical role. Whereas on a hillslope cascade, or at a small plot scale, these limitations were seen to be relatively unimportant, at the larger, more complex scale, they can become controlling characteristics as shown with the poor predicting group of sub-catchments 1, 2 and 7. For the channels, insensitivity to shallow-gradient routing conditions could significantly affect hydrograph shape, leading to lower flow-peaks and hydrograph attenuation. A rapidly arriving flood wave from further upstream would dissipate on entry to the final sections of channels which decrease as they approach the farm inlets as they cross the wadi bed or footslopes.

This explanation is supported quite well by the predictions for rainstorm 02/03/74. The lowest proportions of unit 5e and 5w, and 6w slopes are encountered in sub-catchments 3, 4, 5 and 6 and in particular, the lowest proportion of flow-lines that end in these shallow slopes. In sub-catchment four, the unit 5e slopes occupy only 14% of the area and this is the only sub-catchment to over-predict runoff generation The highest proportions of the shallow slopes comprised of units 5e, 5w and 6w and fringing each of the channels are found in sub-catchments 1, 2 and 7 and these universally produce poor predictions. The two sub-catchments 1 and 2 are of similar character, as shown in Appendix 3.1 and 3.2, occupying the same western side of the catchment system, harvesting from across the top and the side-slopes of the now remnant proto-Zin terrace. The proportions of shallow unit 5 and unit 6 slopes are almost identical, comprising 65% of the catchment (Table 6.17), and the unit 5 slopes are interspersed between the rest of the catchment and the channels. Sub-catchment seven, like one and two, contains a large proportion of unit five slopes, all of which occur at the end of long, unbroken flow-lines and intersperse between the channels and the rest of the sub-catchment. This is visible from the unit distribution choropleth maps in Appendix 5.3.1.

6.3.4.d Results from Rainstorm 10/02/74

Table 6.19 Catchment Observed and Predicted Runoff for Rainstorm 10/02/74

	Sub-Catchment							
Value	1	2	3	4	5	6	7	All
Observed Input m^3	852.6	543.4	547.3	355.7	95.8	511.3	330.8	3236.9
Observed Output m^3	159.1	85.5	25.6	25.1	13.5	36.1	21.0	365.8
Predicted Output m^3	37.3	16.7	95.0	84.5	33.6	76.0	11.5	354.6
%E [(O-P)*100/P]	76.6	80.5	-271.1	-236.7	-149.4	-110.3	45.1	3.1
Obs Qp $m^3 s^{-1}$	133.4	87.8	47.3	53.8	34.1	81.9	43.9	
Pred. Qp $m^3 s^{-1}$	18.2	14.0	112.0	74.9	39.9	91.2	17.6	

The second rainstorm of 10/02/74 can be used to assess the suitability of the interpretations of prediction results for rainstorm 02/03/74. They are of a different character as shown in Figures 6.1 and 6.2. Whereas in rainstorm 02/03/74, one group of sub-catchments performed well, and the other poorly, for rainstorm 10/02/74, although consistent in their collective performance, both groups now perform poorly as shown in Table 6.19 and Figures 6.10 to 6.16. The group 3, 4, 5 and 6 producing good predictions for 02/03/74 have switched to uniformly over-predicting both total volumetric production and peak discharge whereas the poor predictors 1, 2, and 7 remain consistent and again produce under-predictions.

Over-Predictions

As shown in Table 6.19 and Figures 6.10 to 6.13, the hydrographs for sub-catchments 3, 4, 5, and 6, whilst a good shape compared to the observed, are poor in terms of the magnitude, being generally larger by a factor of 100 to 270%. Peak discharge is also overestimated, more so for sub-catchments 3 and 4 than for 5 and 6. The hydrographs for the predicted discharge are lagged compared to the observed, although this is expected as explained earlier by the fact that the simulations do not allow for any filling of depression storage in the channels. The over-predictions of runoff from these sub-catchments were expected given the results already achieved in the simulations of the hillslope cascade (Section 6.2). For the four sub-catchments, the observed proportion of rainfall discharged as stormwater runoff was 8%. In the cascade simulations the predicted discharge into the channels sub-dividing the cascade was 21%. In the sub-catchment simulations, the proportion of runoff predicted from the four is 19%. Because the peak discharge is over-estimated, and the rising curves and falling limbs are attenuated, this suggests both routing and productivity differences from the observed. A similar conclusion was drawn from the predictions for rainstorm 02/03/74.

Under-Predictions

There is consistency in the predictions for the second group of sub-catchments 1, 2 and 7 where once again, both volumetric and peak discharge are underestimated. The hydrographs show good timing, but clearly there is an overestimate of the amount of rainfall retained within each of the sub-catchment boundaries. This could be through an overestimation of infiltration by one or more of the unit parameter sets, either in the initial phase (delaying the start of runoff during the immediately high intensities that characterise this rainstorm) or during the final rates since this rainstorm continues for a longer duration. The predictions could also be due to the poor routing of runoff from significant areas of the catchment as explained for these sub-catchments for rainstorm 02/03/74.

Figure 6.10 Observed and Predicted Hydrographs for Sub-Catchment Three (Rainstorm 10/02/74)

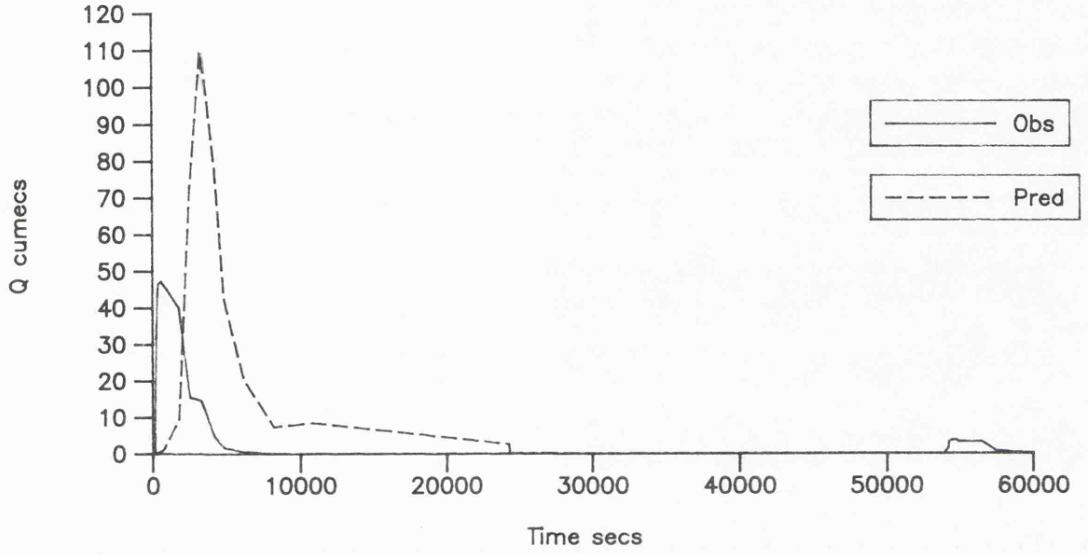

Figure 6.11 Observed and Predicted Hydrographs for Sub-Catchment Four (Rainstorm 10/02/74)

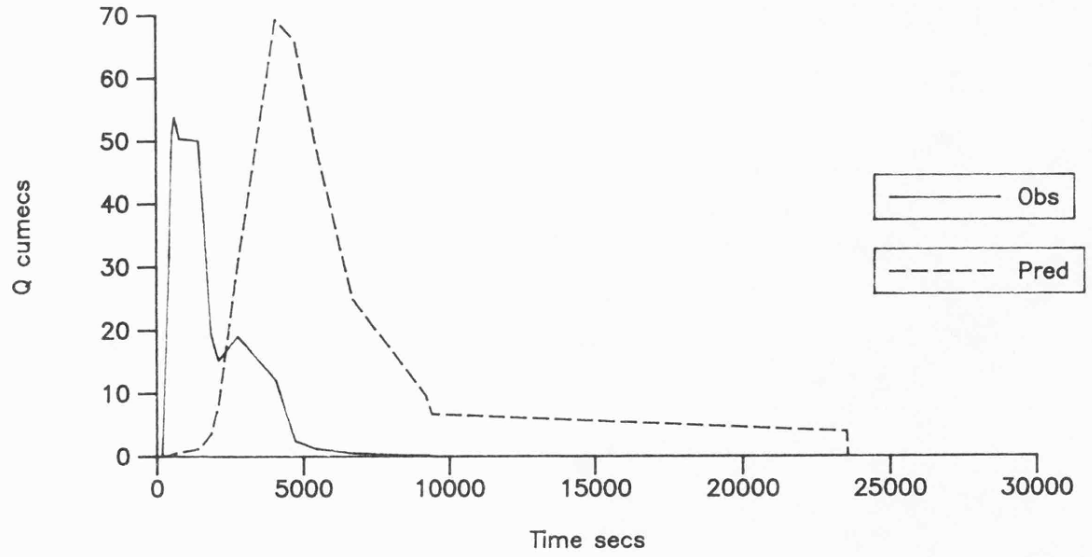

Figure 6.12 Observed and Predicted Hydrographs for Sub-Catchment Five (Rainstorm 10/02/74)

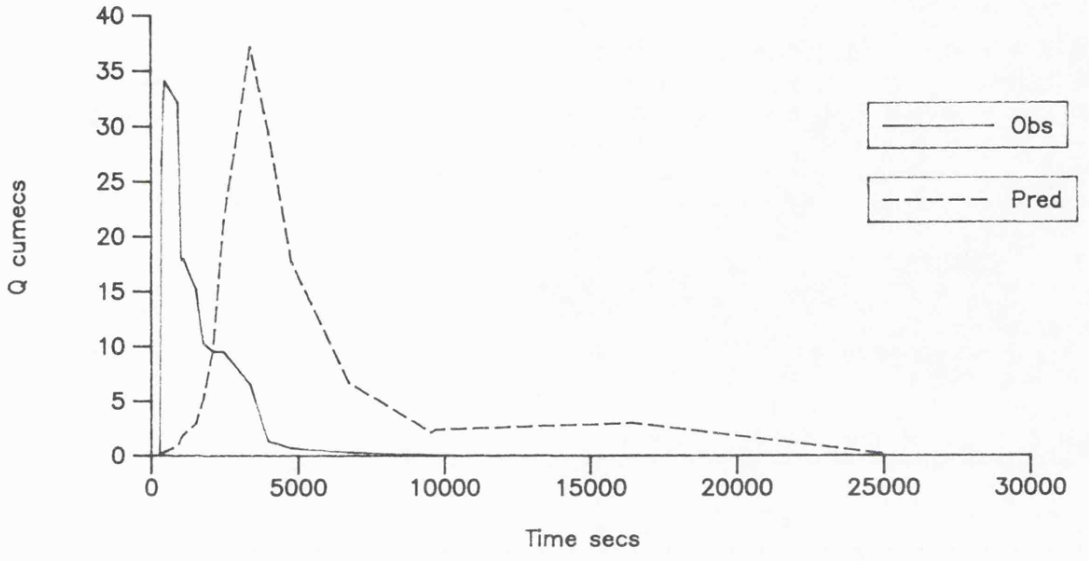

Figure 6.13 Observed and Predicted Hydrographs for Sub-Catchment Six (Rainstorm 10/02/74)

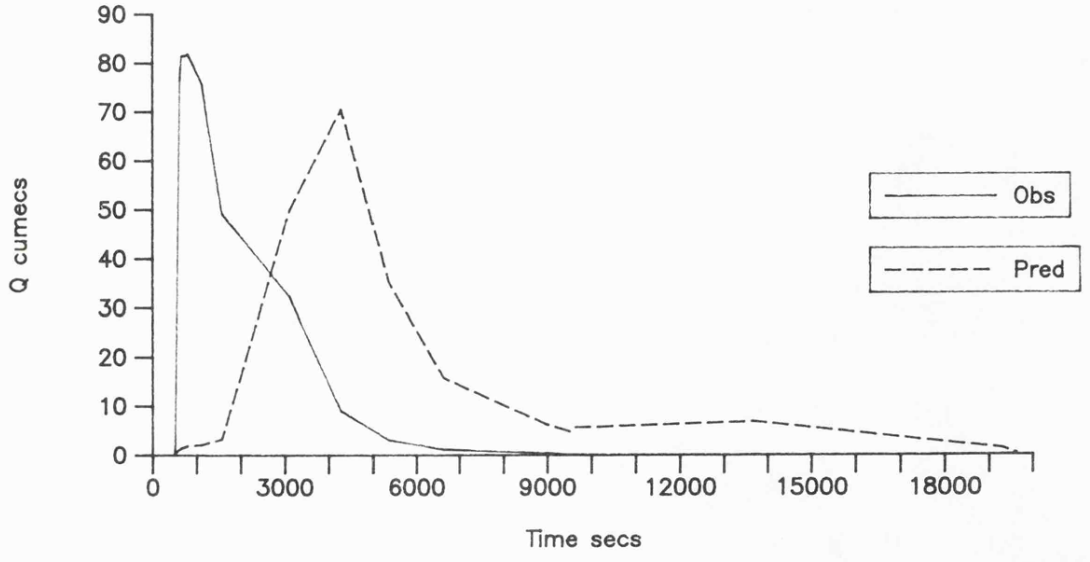

Figure 6.14 Observed and Predicted Hydrographs for Sub-Catchment One (Rainstorm 10/02/74)

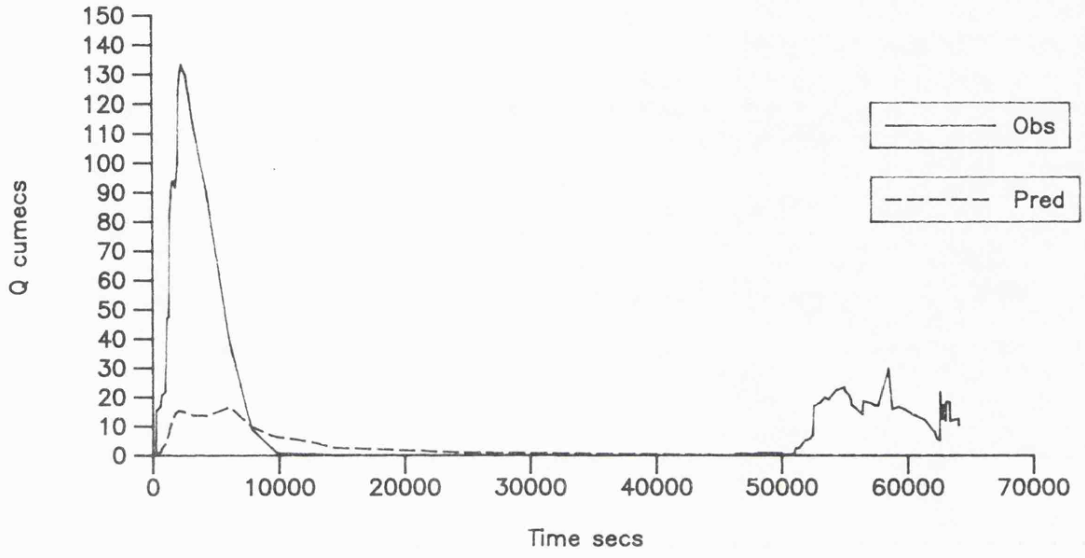

Figure 6.15 Observed and Predicted Hydrographs for Sub-Catchment Two (Rainstorm 10/02/74)

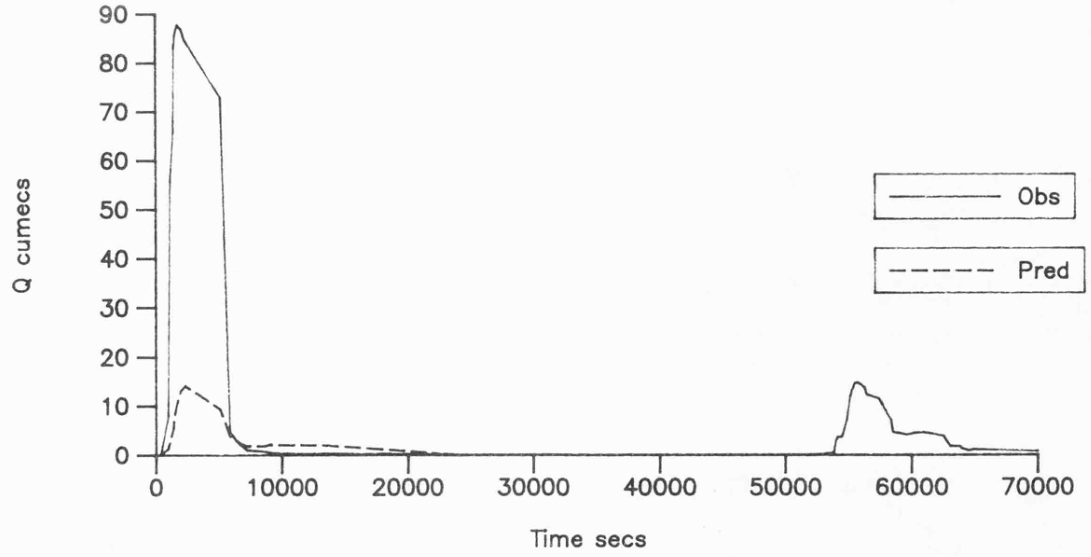

Figure 6.16 Observed and Predicted Hydrographs for Sub-Catchment Seven (Rainstorm 10/02/74)

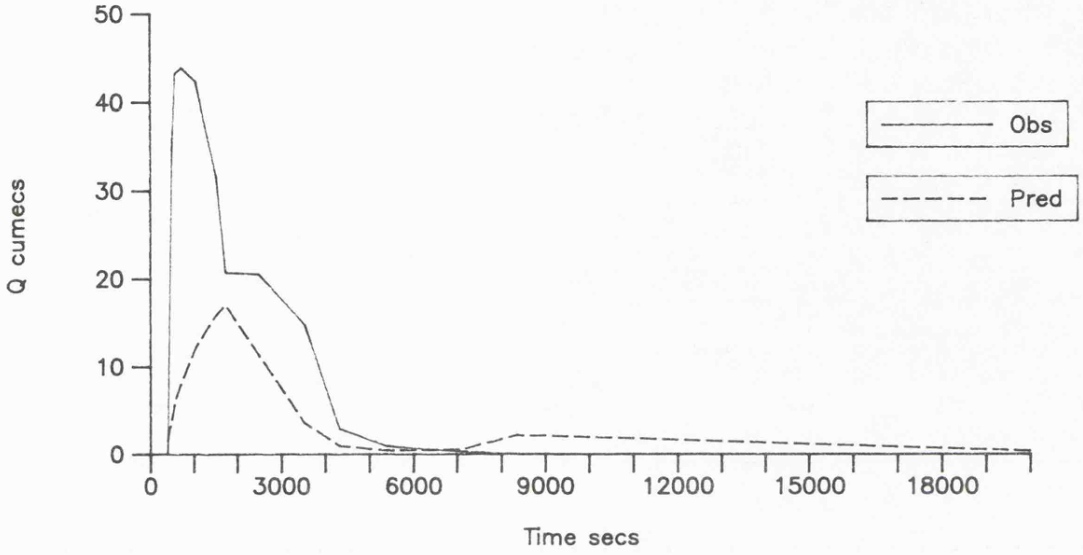

Conclusions and Interpretations

Referring back to the run-on/runoff plot simulations and comparing the responses from the two different rainstorms provides a useful basis for concluding which are the main controls on the predictions achieved during the simulations and the variation between the performance of the two groups for the two selected rainstorms. In the simulations of the run-on/runoff plots with the modified B2 infiltration parameter, the predicted runoff hydrographs were consistently over-estimates of the observed hydrograph in the rising portion, although the final rates were generally very accurate. This suggested that the initial infiltration curve overestimated the fall in infiltration rates towards steady state. How would this affect the predictions of runoff for the two rainstorms?

For rainstorm 02/03/74, the rainfall intensity is high and the duration short. Rainstorm 10/02/74 has lower rainfall intensities for a longer period, although both produce roughly the same depth. Rainstorm 02/03/74 produces roughly 6.2 mm in a 540 second period with an intensity of 42 m hr^{-1} following a brief intensity increment of 4 mm. Rainstorm 10/02/74 produces 6.9 mm in the first 1500 seconds with intensities from 13 to 25 mm hr^{-1}. The effect of underestimates of initial infiltration would be greatest in relative terms for the rainstorm with the lowest intensities since by predicting an earlier time to run-off and lower subsequent rates towards the final infiltration rate, the amount of runoff predicted would be relatively high compared to the observed. To use a numerical example, by under-predicting infiltration by 2 mm hr^{-1} (10 instead of 12) for a rainfall intensity of 20 mm hr^{-1} would result in an over-prediction of 25% compared with an over-prediction for a rainfall intensity of 40 mmhr^{-1} of 7%. Since the rainfall intensities for rainstorm 10/02/74 are lower and of longer duration than 02/03/74 and the same infiltration parameters are used for each simulation, then if the initial infiltration rates are under-predictions, the effect on the predictions of the former rainstorm would be greatest. This seems to be borne out by the performances of the sub-catchment group 3, 4, 5 and 6. Because the final infiltration rates predicted by the infiltration parameters were seen to produce good steady-state predictions in the run-on/runoff plot analysis, then the difference between the two sets of performances of group 3, 4, 5, and 6 can be explained by the sensitivity of the infiltration parameters to the different types of rainstorm intensity distributions.

The shape of the hydrograph for 10/02/74 can be explained by the rainfall intensity distribution coupled with the likely under-prediction of early time-period infiltration rates. There is rapid runoff generation producing a rapid peak of discharge into the channel system followed by a swift drop-off as intensities fall to below 1 mm and infiltration on the hillslope causes runoff water to dissipate. Some of the overestimates of runoff productivity result from the significant proportion of the runoff volume that originates after the early rainfall peak and would appear to be response to the second peak of rainfall that falls at around 7000 and 9000 seconds (as shown in Figures 6.10 to 6.13). Infiltration is calculated using the Hortonian notion of rainfall excess once the storage ponding

condition has been satisfied. Prior to the onset of the second major period of rainfall, most elements infiltrate all surface water as indicated by the times to drying-up printed to the output data-files. However, infiltration is assumed to remain at its final rate and no allowance is made for the change in state of soil moisture. The model is therefore inappropriate for this type of rainfall. No runoff is expected for this time period, as shown by the observed hydrograph. The slight resurgence of runoff predicted, and the attenuation of the hydrograph to these later times is clearly a function of the model's inability to forecast correct infiltration conditions during highly variable rainstorm intensity distributions. Whilst the results from the simulations would still be over-predictions, the error statistics would be less severe, resulting only from initial period parameter sensitivity and not the modelling procedures themselves.

But what about the consistently poor predictor group of sub-catchments 1, 2 and 7? It would seem clear that since the major difference between the two groups is the position and proportion of unit 5e and 5w slopes with respect to channel distribution, then this explains the variation in prediction between the two groups. The consistent poor prediction from sub-catchments 1, 2 and 7 compared with the varying prediction from sub-catchments 3, 4, 5 and 6 points to the role of shallow slopes (routing) and the unit 5 infiltration parameters as the major controls on model performance. The infiltration parameters used for this unit are not derived from the run-on/runoff plots. The degree to which they are affected by the methods of measurement and the non-allowance for the double-inclusion of detention storage in initial infiltration calculations is not known and can only be speculated. Since both rainstorms are characterised by initial intensities that provide the significant proportion of total inputs and therefore, in volumetric terms are affected greatly by the timing of time to runoff (t_o) forecasts and subsequent infiltration rates, then over-estimates of infiltration would clearly lead to significant differences between observed and predicted responses. This is the most logical explanation for the performance of sub-catchments 1, 2 and 7 combined with the knowledge from the sensitivity analysis of the role of slope gradient in flow routing predictions. Because of the special positions of the unit 5 slopes (for their infiltration parameters) and the unit 5e, 5w and 6w slopes (for their geomorphological character) at the end of flow-lines adjacent to the majority of the channel length (as shown in Appendix 5.3.1), these sub-catchments are most prone to their influence on overall catchment performance whereas sub-catchments 3, 4, 5 and 6 are only prone to their control on hydrograph shape. Thus the variations in predictive ability depends not only on the parameters themselves, but the complexity of the sub-catchment. Recognising the differences highlights both a problem for and a benefit of distributed models. Using a lumped model of the Avdat catchments would neither show up the role of individual parameters, nor the need for individual parameter sensitivity improvements. The added advantages of being able to explore the nature of hillslope hydrology of actual and theoretical significance are discussed in the following section.

6.3.4.e Significance of the Results and Overall Conclusions

Confidence Limits of the Model at Different Scales

As overall conclusions it is clear that the performance of the model at this scale is mixed. At a lumped level, the total runoff volume predicted collectively for the seven sub-catchments for rainstorm 02/03/74 is 52% of the observed volume, and for rainstorm 10/02/74 it is 97% of the observed volume. These statistics, like most lumped hydrological results for complex catchment systems, mask the range of individual performances by sub-catchments that indicates marked sensitivity variations in simulation predictions. The source of these sensitivity variations are as complex as the catchment itself and may only be identified through attempts, such as the current modelling approach, to consider the process at a significant scale, i.e intra-hillslope flow-line and intra-channel branch.

It would seem that the model routing parameters, and or the parameters provided by the discretisation procedure, are not sensitive to predicting runoff from shallow sloping areas and especially those in which these areas are juxtaposed with the channels in a manner in which they are allowed to inhibit Contiguous Area Contribution. The combination of poor routing, and apparent over-estimation of initial infiltration by parameters derived from literature values for loess-crusted micro-catchments conspires to effectively limit the predictive ability of the model regardless of the aptness of the other surface areas and parameter values at reproducing local conditions. The natural role of spatially variable conditions in determining hydraulic remoteness and controlling Contiguous Area Contribution is intensified by the unwanted effects of selective parameter insensitivity. However, by simulating the catchment system at a lower resolution, the role of these conditions and the affects of individual parameters would not be visible.

Under certain conditions identified from these full sub-catchment simulations, the model is limited both by the need to use small plot parameters applied to a much wider scale, and in the sensitivity of the procedures to cope with important local conditions. Under other conditions these limitations are of little significance and model and parameters work well. Other specific limitations relate to the fact that the infiltration procedures have difficulty coping with the time-varying input, as expected in discussions in Chapter Three. This has been seen to affect the predictions differently for different rainstorms. The geometric simplification does not adequately specify the important local slope gradient controlling routing from areas with low average slope but locally significant variations. This problem is one of resolution and was discussed in Chapter Four as a possible problem in specifying individual flow parameters for the Mannings flow equation. These conclusions are important in that they can be expected to occur in most applications of physically-based models to conditions more complex than those in which the individual procedures such as infiltration and flow-routing were conceived and the parameters derived.

The Bias of Error Statistics in Evaluating Model Performance in Arid Environments

To put the model performance and observed-predicted variations into their true context it is necessary to consider the environment of application and the harsh nature of error statistics. The methodology chosen to evaluate predictive performance is the same as that used in most modelling applications to date, that of percentage errors. This provides a ratio of observed and predicted values. The statistics refer to the relative magnitudes of values and so little account is taken of the absolute variations. Consider two applications of the same infiltration and routing models, one in an arid environment characterised by short duration, low magnitude rainstorms, and one in a humid environment characterised by long duration, high magnitude rainstorms. Consider the errors to be the result of under-estimation of initial infiltration rates and also poor routing such that detention storage is over-estimated leading to post-rainfall transmission losses. For the humid environment, the poor initial predictions would result in a relatively smaller increase in total productivity even if the errors were the same absolute magnitude as in the arid environment. With accurate specification of the final infiltration rates, the longer the total duration of the runoff period, the more chance the majority of the runoff has of leaving the catchment irrespective of routing differences between observed and predicted conditions. The post-rainfall period would therefore also have less significance in volumetric terms when compared to the total runoff than for the arid environment when the surface flow is generated and dissipated relatively quickly and the conditions of maximum or steady-state discharge (if reached) is for a short period only.

The conclusion from this discussion is that in the interpretation of arid environments, the problems of parameter sensitivity take on a greater significance simply because with the same modelling tools, the parameters must be that more closely specified to produce the same levels of performance when judged in relative terms. In absolute terms, errors in predictions may be small (for instance the over- or under-estimation of infiltration in depth per unit area). However, in relative terms they may be very high leading to large percentage errors when assessing simulation results. In more humid environments, the same order of magnitude of error would appear more acceptable since in relative terms, percentage differences between observed and predicted values would be smaller. These evaluation considerations have not been given sufficient attention simply because only recently have attempts been made to get to grips with the small-scale processes in each of the environments and to dispense with the lumped or calibrated models that have previously been use to represent hydrological systems. The more attempts that are made to explore hydrological systems at the critical scales for the processes, the more the advantages and limitations of current modelling tools and methods of parameter specification will become apparent. By modelling process responses at a variety of scales for the Avdat catchment, hillslopes and plots, the varying strengths and weaknesses of these tools and methods have been illustrated very well.

To stress the significance of these conclusions for an evaluation of the predictive success or failure of the sub-catchment modelling carried out in the previous section the absolute, rather than the relative magnitude of errors can be examined. Table 6.20 contains the values of the volumetric difference between observed and predicted total runoff, and the depth this represents over the whole sub-catchment area for each of the two rainstorms simulated. The depth is calculated by dividing the volumetric error by the total surface area. It shows to what degree the model and parameters over- or under-estimate the depth of water retained within the catchment boundaries and quite clearly shows that in most cases, in absolute terms this is very small. If the same absolute error were to be experienced in the modelling of a humid area catchment response, the error statistics would not be as harsh as they seem for the current set of simulations.

Table 6.20 Errors in Predictions in Depth Terms

	02/03/74						
	1	2	3	4	5	6	7
Volume O ΣQ - P ΣQ (m^3)	104.3	193.7	16.5	-28.1	5.2	6.4	111.5
Depth Equivalent (mm)	1.3	3.9	0.3	-0.9	0.6	0.1	3.7

	10/02/74						
	1	2	3	4	5	6	7
Volume O ΣQ - P ΣQ (m^3)	121.8	68.8	-69.4	-59.4	-20.1	-39.9	9.5
Depth Equivalent (mm)	1.6	1.4	-1.4	-1.8	-2.3	-0.8	0.3

A Summary of Probable and Possible Sources of Variations in Predictions

From the previous discussion the conclusion must be drawn that there are a number of sources of differences between observed and predicted responses at the sub-catchment level and which determine the variations of these differences between sub-catchments and between rainstorm types. Of course there are other possible uncontrolled sources of error in predictions that could also play a part in predictions mostly related to the observed data itself and its accuracy and sensitivity to the process domain being modelled. Those relevant or likely in the case of the Avdat catchment are included in the following summary.

The main problems and limitations relate to the extrapolation of parameters from small plot studies to larger areas where the individual variables such as slope gradient cannot be so closely specified or data of different resolution are combined. In particular this relates to the use of a set of infiltration parameters taken from the literature which are assumed to represent an important proportion

of the catchment for which the field methods used to test infiltration were inappropriate, and to the combination of only a small number of field infiltration data samples with routing parameters provided at a greater detail. The model itself is not parameterised to be sensitive to variable rainfall and the presence of distinct peaks and would require not only more infiltration parameter sets to be more sensitive on a spatial scale, but multiple parameter sets that could allow prediction of infiltration rates from dry and wet starting conditions. This was previously discussed in Chapters Three and Five.

The additional sources of variations not discussed so far can now be briefly listed. One is the effect of assuming channels to be impermeable. For rainstorm 02/03/74 which is of short duration, the effects of assuming no channel infiltration are likely to be relatively insignificant in volumetric terms. However, for the rainstorm 10/02/74 in which low rainfall intensities occur and the rainfall is distributed over a long period of time, the effect of assuming no channel infiltration might be to increase the predicted volume of runoff for the total catchment area.

There are several possible sources of variations between predicted runoff response and the observed hydrographs that might result from the characteristics of the observed data-set and their measurement irrespective of the model procedures or parameters. The first source is from the digitisation of the rainfall hyetographs at a relatively coarse resolution. It is clear from the sensitivity, cascade and sub-catchment simulations how the runoff generation process is highly sensitive to rainfall intensity. Large quantities of water can be produced from very short bursts of high intensity, which will move proportionally more quickly through the system and with lower proportional losses than for the smaller, slower flows. The smoothing of the intensities into longer, lower intensity blocks could significantly reduce sensitivity of the model vis á vis the observed response.

The second source is from the sub-catchment hydrographs. According to Shanan (1975) the stage-recorders are calibrated using theoretical formulae that may give rise to three sources of error that have not been quantified. They include the use of a non-standard weir-shape, estimation rather than measurement of discharge coefficients, and submergence at high-stages. The weirs are not designed so that they have a constant width, slope and direction (perpendicular) of channel approach and the magnitude of errors have not been quantified. Therefore, there is no guarantee that the volumes and discharge rates for each sub-catchment represent the true flow experience accurately.

The final source relates to the fact that the routing characteristics of the catchment measured to date, may not be the same as those in 1972. This specifically relates to the channel cross-sectional dimensions. When the farm was originally reconstructed in 1959, the channels were all cleared of vegetation and dredged of accumulated debris and silt. The man-made channels in the wadi depression were excavated into broad, deep ditches. Since then, little maintenance work has been carried out in the catchment and channels, particularly those in the wadi have become extensively re-vegetated and their

cross-sectional shape altered by deposition of sediments. The effect of this on sub-catchments 2 and 3 can be seen from Plates F.5 to F.8. Water discharging into the wadi section is dissipated prior to reaching the farm, as witnessed in several rainfall events over the 1983-85 period. Poor specification of the routing dimensions will obviously affect the predictions of hydraulic radius for a given cross-sectional area of water and hence in turn affect predictions of flow velocity and the stage-discharge relationship. This may help explain some of the variation between observed and predicted shapes of hydrographs since the shallow-sloping sections of channels adjacent to the farm inlets are most likely to have changed character through deposition of sediments since 1972. These can exert considerable influence on the shape of flood-wave arrival.

6.4 Use of the Model in Applied Studies - Design Evaluation and Management Aspects

Section 6.3 has shown the potential for variations in predictions at the wide sub-catchment scale to occur from a wide range of sources both dependently and independently of the influences of the model procedures and parameters. The predictions achieved, though mixed between the sub-catchments and for the two rainstorms show the general robustness of the model and the efficacy of its performance as an analytical tool to examine such a sensitive and complex process environment. With a slight increase in the spatial and temporal resolution of model parameters its use as a tool would be significantly enhanced in a deterministic sense. However, regardless of these variations, in a wider, practical sense it has great potential for illustrating the key controls on arid lands runoff productivity and the applied use of such a model for the assessment of water harvesting systems. Knowing the characteristics of the parameters and their obvious effect on runoff production and transmission and using the model as an evaluation tool provides a clear insight into the critical nature of hydraulic remoteness and Contiguous Area Contribution. The predictions of runoff from the hillslope cascade and the Avdat sub-catchments described in Sections 6.2 and 6.3, combined with a theoretical assessment of runoff production from the same flow systems in an unaltered state, can now be used to examine both the nature of runoff generation from different hillslope and channel configurations, and to look at complete catchment areas and assess the performance of a water harvesting catchment system design.

6.4.1 Using the Cascades to Assess Alternative Channel Configurations

6.4.1.a Determining Optimum Channel Configurations

By recording the production of runoff and the transmissivity of different hillslope elements, the model can quite clearly be used as a design tool for determining whether there is an optimum channel configuration that will maximise collected volumes for a minimum of channels. One possible method of optimally siting channels based on the rainstorm predictions for the selected cascade is to use the

matrices of productivity values presented in Tables 6.10 and 6.11. The optimum positions for different numbers of channels are found by scanning the matrix and finding the combinations of sections producing the greatest cumulative discharge. For a single man-made channel, this location is found by looking down column 54 to find the largest single volume. This is element 7 for both rainstorms, which produces 29.07 m^3 for 02/03/74 and 29.68 m^3 for 10/02/74. To this must be added the discharge received by the natural channel which is found by following row 7 across to column 6 and adding the value at the base. This is 0.833 m^3, giving a total of 29.90 m^3 (27.5%) for 02/03/74 and 0.20 m^3, also giving a total of 29.90 m^3 (18.6%) for 10/02/74.

From an assessment of the cascade, the maximum productivity from the two rainstorms for a natural channel and one to four additional channels are listed in Table 6.21.

Table 6.21 Maximum Productivity Channel Configurations

Rainstorm	Productivity	Channels
02/03/74	4.87	1
	29.90	7,1
	34.33	13,7,1
	36.20	16,11,7,1
	37.17	19,13,10,7,1
	36.27	current (13,10,8,7,1)
Rainstorm	Productivity	Channels
10/02/74	3.23	1
	29.90	7,1
	32.51	16,7,1
	34.67	15,11,7,1
	35.75	17,13,10,7,1
	34.19	current (13,10,8,7,1)

6.4.1.b Channel Position, Density and Productivity Relationships

The conclusions from this assessment are that compared with an unaltered cascade flow section, the addition of one or more channels significantly increases the volume of runoff water harvested from the hillslope. However, as the number of channels is increased, the increase in water harvested is at a decreasing rate. It also shows that when taking this profile in isolation, the existing channel locations are close to producing the optimum runoff harvest, since they are concentrated across a slope section that is one of the most productive and transmissive on the whole profile. If the

channels were located too far down the slope, then there would be a consumptive area between the producer section and the channels (as is the case with the single channel). If they were located above the major producer, then their contribution would be minimal. Where a slope section is a consistently good producer it is clear from both rainstorms that a single well-placed channel can harvest close to the maximum amount capable of being harvested without the need for additional channels. It would seem then from an analysis of a single cascade that the presence of four man-made channels on the eastern hillslopes is inefficient, since the extra channels increase the harvest by an average of 7% each. However, this takes the sequence of channels out of their physical context and their overall position across the wide valley sides of the Avdat catchment. The significance of this is discussed following an assessment of how channel positions might be designed without the need to resort to such repetitive and time-consuming simulation and matrix scanning.

The productivity in volumetric terms is also a function of the contributing area of each element. As flow-lines diverge or converge in their path downslope, then the element areas vary accordingly. The runoff production from the element will therefore depend on the combined area and productive potential. If a highly productive slope section covers only a small total area or downslope length, then it may be less effective to tap this than a less productive section comprising a greater total area and hence providing a greater total discharge over a range of rainstorms.

6.4.1.c A More Practical Procedure for Channel Siting

An alternative method of determining the most appropriate channel positions without scouring the matrices is to use the indices of productivity and transmissivity calculated by the model. They identify the spatial pattern of net producers and net consumers in volumetric terms and illustrate the relative importance of different locations to the production and loss of water within the contributing area. When designing a complete water harvesting system, it would be necessary to consider productivity across a whole slope system, both downslope and laterally. However, to illustrate the principle, the single cascade can be used.

As illustrated by the sensitivity analysis described in Chapter Five, channels should wherever possible be placed above locations where the runoff productivity falls considerably, and especially where it drops to zero or even negative values. Above this section, transmissivity is favourable and there is still a volumetric increase in discharge with downslope distance. Once the productivity/transmissivity becomes negative, the productivity percentage falls showing there are no net additions, rather there is a subtraction from the total flow passing this location. Below the point where the index becomes negative, the productivity percentage will fall.

Using rainstorm 02/03/74 as an illustration, the predicted data in Table 6.13 show that the slope section elements 19 to 7 are the most productive, corresponding to the unit 4 slopes. The unit 3 slopes are the next productive, followed by unit 1 and unit 2. It is interesting to note that whereas the productivity percentage for unit 1 elements increases downslope, it decreases downslope for unit 2. This corresponds to the routing capability of the slope section rather than the infiltration characteristics since the unit 2 slopes are characterised by a convex slope profile, with a steep gradient at the top, and shallower gradient at the bottom. The flow routing capability of this slope is low, contributing to the fall in per unit area productivity downslope. Part of this reduction results from the re-infiltration of runoff generated upslope and part of it relates to the increase in area of the elements since the flow-line diverges gradually from top to bottom, and individual element lengths vary with their gradient.

The channels should ideally be placed within the most productive slope section, and designed to avoid the least productive. Whilst there are still additions being made to runoff generated from a highly productive section and the total percentage productivity is high, then this is obviously the prime location for a single channel. In the case of the current cascade, this would be at element 7. Additional channels could then be located simply be sub-dividing the productive section from 19 down to 7, for instance, the second channel at 14, the second and third channels at 11 and 15, and the second, third and fourth channels at 10, 14 and 17. This corresponds very well to the channel locations identified in the previous matrix scan and is of course far simpler and less demanding of computer time. Returning back to the matrix Table 6.10 it is possible to see the result of building channels that intersect the slope at these locations (Table 6.22). The increase is not uniform as with the matrix identified locations. By altering the configuration of contributing areas, individual knock-on effects are modified which may result in local productivity being inhibited, as with the case of the three channels where a fall in productivity is achieved by providing an extra channel. However, comparing the productivity from two channels and four channels, it would be unlikely that the extra channels would be deemed productive although again, this must be taken in the context of the complete hillslope and not just an individual profile.

Table 6.22 Productivity Using Configurations Determined From Single Cascade Simulations

Rainstorm	Productivity	Channels
02/03/74	29.90	7,1
	34.26	14,7,1
	33.77	15,11,7,1
	37.02	17,14,10,7,1

Obviously, when considering a complete catchment system then designing the positions of channels would not take place on the basis of a single rainstorm or on individual cascades. Instead, a range of rainstorms should be used and a complete hillslope selected to account for the layout of the channels relative to the point to where water must be delivered. The frequency of particular rainstorm types and magnitudes and their productivity *vis á vis* the requirements of the runoff farm supplied by the harvesting system is important. The minimum channel configuration capable of providing the largest consistent annual production with the minimum of channels, in excess of the farm requirements would obviously be the optimum. The current example has shown how the productivity from different flow lines can be assessed in general terms. The phase of simulations described in Section 6.4.2 shows how a similar practice can be carried out at the increased scale.

6.4.1.d Overall Conclusions on the Applied Use of Cascade Simulations

This analysis has shown how an optimum combinations of channel locations can be identified by repetitive simulations of runoff production for selected rainstorms, and how consistent the productivity is, related to the combined characteristics of infiltration and flow routing. Additionally, using a more simple simulation of the unaltered cascade and assessment of indices of productivity, an easy way of determining suitable locations for channels has been shown. The next step is clearly to apply the similar principles to an assessment of efficient design on a larger scale for a complete or partial hillslope.

One obvious conclusion from the hillslope cascade simulation is that the positioning of channels must be systematic, geared to a knowledge of the productive characteristics of different slope sections. Evenly spacing them down a whole profile or adding extra channels to an already productive configuration would be a mistake since the improvement per unit channel length is minimal. The percentage productivity and productivity/transmissivity indices for the full profile give a good idea of the spatial pattern on the hillside and how it might be best tapped by a number of channels.

It is useful prior to simulation of full sub-catchments, to assess briefly why multiple channels have been, or should be introduced to a hillside, even though the increase in production from a given profile is not high in volumetric or percentage terms. The answer to this lies in the overall catchment context in which the man-made routing system is introduced. The channels have been built to harvest from a complete hillside, stretching several hundred metres, and with distinct, horizontally banded slope types across their length. At the foot of the relatively steep slopes is a large area of shallow, loess covered surface which because of its poor routing characteristics (i.e. equivalent to the last six elements of the profile) should be circumvented if runoff produced across the hillslope is to be used on the runoff farm at the outflow point of the catchment. Because the most productive sections occur in bands further up the sides of the catchment (as described in Chapters One and Two), channels built up across

the slope from the runoff farm must dissect the productive slope section at an angle, which means that no single channel can be positioned so that it harvests from this slope along its entire length. A sequence of channels are required, even if on each individual flow-line, the extra channels contribute little to the amount of water harvested. They will, however, contribute by harvesting water further across the hillside, routing water down from the more remote locations which are productive, but below where the higher channels could harvest and still maintain their gradient towards the runoff farm. The aptness of this conclusion can be assessed from a consideration of the full Avdat sub-catchment simulations described in Section 6.4.2.

6.4.2 The Avdat Water Harvesting System - A Design Evaluation

6.4.2.a Channel Siting and Contiguous Area Contribution

The choropleth maps of runoff efficiency (percentage output of input) contained in Appendices 5.4 to 5.7 help illustrate the nature of Contiguous Area Contribution and the role of the man-made channel system in tapping productive areas and avoiding consumptive ones. They also illustrate the concept of hydraulic remoteness.

From discussions in Chapter One of the arid hillslope hydrological system, Contiguous Area Contribution was defined as a reaching-down of runoff production from highly productive areas within a slope system, providing the dominant contribution to total stormwater flow. The productive flow-lines clearly must intercept channels which must in turn transmit water effectively down through the catchment to the point of interest. In the case of a water harvesting system supplying a runoff farm, this is the point of inflow to the terraces. Where productive areas are isolated from channels by areas of shallow gradient or high infiltration which act as a consumption barrier between local production and stormwater contribution, the area can be considered hydraulically remote. It may be that the productive area is geographically only a short distance from the terrace fields. However, water may never contribute to their inflow whereas areas more geographically remote may become major contributors due to their proximity to the channel network.

For a clear illustration of these concepts, an assessment of the choropleth maps in Appendices 5.4 and 5.5 should be made in conjunction with the flow-net map Appendix 5.2.1 and the unit distribution map Appendix 5.3.1. The red shading shows those hillslope elements with percentage productivity over 50% and the green shading under 50%. The lowest percentage class of 0 to 20% shows those areas for which a minimum of the input is converted to output and hence which have lowest productivity and transmissivity efficiency. There is a distinct pattern of efficiency throughout the catchment. The west of the catchment shows very low productivity, apart from a band of hillslope corresponding to the unit 3e distribution. This is true for both rainstorms 02/03/74 and 10/02/74

although the width of the productive zone in the latter is narrower and the productivity from the unit 5w, 4w and 6w slopes poor. The eastern hillslopes show very high productive efficiency percentages for 02/03/74 corresponding to the bands of unit 1e, 2e, 3e and 4e slopes although the unit 1e and 2e slopes change to lower productivity for rainstorm 10/02/74 which has overall lower rainfall intensities. Also apparent for rainstorm 02/03/74, is the effect of cutting off flow from above on the productive efficiency of the lower unit 2e slopes at the southern end of the catchment where the channel of sub-catchment six cuts through the unit. A band of green is observed immediately below the channel showing the knock-on effect of run-on from above, raising the productivity levels of the lower slope. This band also corresponds with a gradual worsening of flow routing conditions since the unit 2e slopes represent a convex-concave profile across a bed of underlying chalk.

One simple conclusion from the comparison of the choropleth maps from rainstorm 02/03/74 and 10/02/74 is that the lowest depth rainstorm produces the highest overall levels of runoff efficiency and vice versa. This was observed previously in the sensitivity and cascade simulations. With higher intensities, a greater depth of rainfall excess is produced, surface flow stages are high and runoff rapid. A large proportion of water can be transmitted across the surface and into the channels before rainfall cessation and detention storage comprises a lower proportion of total input volumes. Consequently, subsequent transmission losses are less significant in proportional terms and so runoff efficiency remains high.

From the predictive performance for the two rainstorms, it is also clear that the large area of green shading predicted for sub-catchments 1, 2 and 7 (predominantly unit 5e, 5w and 6w slopes) is incorrect. These should not appear as so productively inefficient since it is clear that the infiltration and/or the transmissivity of these sections is insensitively reproduced by the model parameters. They are predominantly shallow slopes of long, unbroken lengths from their respective divides to the channels. Opportunity for transmission loss is great but would be significantly enhanced if the routing conditions on these sections were poorly handled. In particular this relates to the slope gradient, since in the earlier run-on/runoff plot simulations, the use of a single Mannings n coefficient apparently leads to an over-estimation of low-flow transmissivity. The gradients are generally low, and have been provided by a geometrical simplification technique that provides the overall slope gradients through a roughly 20 m by 20 m spot-height sampling. These spot-heights are then converted to a grid matrix by a computer mapping program, and then to a contour map (Appendix 3.1) from which the arrangement of flow-line cascades are derived as shown in Appendix 3.2 or Appendix 5.2.1. However, from qualitative field observations, both during rainstorms and from the local micro-morphology, the surface is obviously more complex with local depressions and hollows concentrating water and producing more defined flow patterns across surfaces. These are not channels but neither are they planes. However, by virtue of the need for spatial representation of the complex surface, they are

smoothed and averaged and hence the overall slope gradient used to describe the element is at too large a resolution to adequately reproduce observed conditions.

Having explained the limitations of the simulations in terms of showing a true picture of the catchment conditions for part of the catchment area, this does not prevent the choropleths from being used as an illustration of the concepts and importance of intra-hillslope variation and Contiguous Area Contribution. This is clear. By tapping the highly productive, but geographically remote mid-slope areas of the eastern sub-catchments 3, 4, 5 and 6, a much more efficient harvesting of water is achieved. How important this is volumetrically, of course, depends on both the size of the area harvested and its productive efficiency. This was explained briefly in the cascade simulations. The productive areas that are separated from the harvesting channels by long, shallow, consumptive slopes, for instance those in sub-catchment two or in sub-catchment seven, although they are geographically close to the terraces, remain hydraulically remote and do not contribute to stormwater flow. They remain dis-contiguous from the harvesting system and play no part. Accepting that the eastern hillslopes are relatively well modelled by the given parameters, and the efficiency portrayed in the choropleth maps is a true one (although over-estimated somewhat in rainstorm 10/02/74), the ancient harvesters were correct to build a sequence of channels across the eastern side, harvesting as much as possible off its mid-slopes. This maximises efficiency, increases productivity, and avoids the consumption that would occur if flow was allowed to continue down into the wadi area, as it is on the west side. However, in volumetric terms, to harvest as much water as possible, they were also right to build channels at the foot of sub-catchment seven, and around sub-catchment one. These comprise large surface areas, and allowing for the under-predictions by the model for these slope areas, the actual volume of water collected is high. This is shown in the observed data for the two rainstorms, in which sub-catchments 1, 2 and 7 contribute 61% of the total discharge for 02/03/74 and 72% for 10/02/74. Although their efficiency may not be high, their overall volumetric production is. In an environment which requires as much of the available resources as possible to be utilised to ensure that even in the poor years the runoff farm is supplied with sufficient water for all or some of the terraces to raise an effective crop, then both efficiency and total productivity must be maximised. The runoff farm at Avdat would seem to be designed to do this sensibly.

6.4.2.b Improvements of the Ancient System

To assess the effectiveness of the water harvesting system designed for the Avdat catchment, two controlled simulations have been made of the catchment for the two selected rainstorms. As described above, the current reconstructed system has been simulated. Additionally, a second, hypothetical flow-net has been produced for the catchment (Appendix 3.3 or 5.2.2) from which an idea can be gauged as to the relative sizes of stormwater input to the farm area from the man-made and natural system and the important characteristics of the change.

To do this, the assumption must be made that the errors encountered in the predictions of the man-made system discharge are of a similar order of magnitude to those made for the unaltered system. The poor predictions of runoff from the western sub-catchments and the sub-catchment seven flow-lines, are assumed identical for the unaltered catchment, as are the over-productions of runoff from the eastern sub-catchments for rainstorm 10/02/74. In this way, the relative values of the two predicted discharge totals show the magnitude of the improvement in volumetric production by manipulating the drainage network.

Table 6.23 Comparative Characteristics of the Current and Unaltered Catchments

	Area (m^2)	Channel Length (m)	Drainage Density (m^2m^{-1})
Unaltered	180202.4	1126.8	159.9
Current	295234.9	4999.6	59.1

The first conclusion from a comparison of statistics on the current and unaltered catchment systems listed in Table 6.23 shows how without the man-made system, the upper terraces of the runoff farm would potentially receive water from a catchment area only 61% the size of the current one. The added 3870 m of channels have expanded the contributing area by 115032 m^2 whilst increasing the drainage density from 160 to 59 m^2m^{-1}. Individual flow-lines are therefore much shorter.

Table 6.24 Comparative Productivity of the Current and Unaltered Catchments

02/03/74

	Input Volume (m^3)	Output Volume (m^3)	Productivity (%)
Unaltered	1338.8	185.4	13.8
Current	2193.3	382.3	17.4

10/02/74

	Input Volume (m^3)	Output Volume (m^3)	Productivity (%)
Unaltered	1975.8	147.8	7.5
Current	3236.9	354.6	11.0

The second conclusion is that more significantly, the increase in discharge for both rainfall events are far in excess of the increase in area. This means it is not just the expansion of the catchment that accounts for the improved water harvest but the change in the character of the routing and its effect on patterns of hydraulic remoteness and contiguous area contribution. The predicted runoff volume (with errors) for the unaltered catchment is 185.4 m^3 and 147.8 m^3 for rainstorms 02/03/74 and

10/02/74 respectively (as shown in Table 6.24). The predicted volume from the current man-made configuration is 382.3 m^3 and 354.6 m^3 respectively. Thus the current production averages at 2.2 times that of the unaltered production for the events selected and the given parameters. Even allowing for the errors in predictions, this suggests that the manipulation of the routing pattern, rather than the expansion of contributing area is the most important factor for the improved performance. The hydraulic remoteness of different areas within the system before and after management is important as illustrated in comparisons of the choropleth maps for each rainstorm, Appendix 5.4 and 5.6, and 5.5 and 5.7.

It is easy to see the role played by Contiguous Area Contribution. The interplay between the channels and the different slope types is paramount in determining the system productivity. By reaching-out across the flow-lines, the man-made channels tap into the runoff producing areas that might otherwise not reach down far enough to contribute. Where runoff efficiency is high, with large productivity percentages, but there is no channel to tap it, flow is dissipated on its long journey downslope. Looking at the areas of high productivity percentages on the eastern hillslopes this is clear. Without the channels, the red shaded area extends down flow-lines past where the man-made channels are located and into the footslopes of the wadi depression, raising the relative productivity of these areas vis á vis the productivity predicted for the man-made channel configuration. The knock-on effect of run-on reduces time to run-off for the lower slopes and enhances the flow routing, building up higher flow levels and increasing transmissivity. However, the knock-on effect is gradually overtaken by the consumptive effect as the slope gradients decrease towards the dendritic natural channel network. The red shading is gradually replaced by green shading showing the dissipation of the stormwater runoff from the more productive areas. Thus the hydraulic remoteness is maintained.

Another interesting observation, is that the knock-on effect is not experienced equally laterally across the hillslope profile, a feature that is an important illustration of a hillslope hydrological process. Those flow-lines that converge, i.e. where a concavity exists, produce a more extended knock-on effect as volumes of runoff are routed onto increasingly smaller areas from larger areas. Where the flow-lines diverge, for instance at the northern end of the catchment, then the knock-on effect is limited as water is routed onto increasingly larger surface areas in its passage downslope. The choropleth maps show this very well. By placing a channel to intercept the flow-lines, the productivity is tapped more effectively, limiting the chances for flow-dissipation, preventing the knock-on effect onto consumptive areas.

The water harvesting system introduced to Avdat is therefore successful on both the accounts listed at the end of the previous section. By expanding the catchment area, a larger total volume of runoff will be produced as a function of this expansion. This is true even if the percentage productivity of the surface is low because each length of channel has a positive marginal return. By increasing the

drainage density into the highly productive slope areas, the volume of the harvest is also increased since the internal losses from transmission are reduced as hydraulic remoteness is decreased and contiguous area contribution increased.

6.4.3 The Model and Water Harvesting System Design

It is clear from these two simple uses of the WATERH model, at the cascade and the multiple sub-catchment level, that its capability for use as a tool in the design and analysis of water harvesting systems is considerable. Through theoretical manipulation of a basic geometric and channel network data-set, a complete range of hillslope and channel configurations could be simulated for a given catchment area. Given sufficiently sensitive parameters of infiltration, flow resistance and hillslope gradient, the performance of each configuration could be assessed for an individual, or sequence of rainstorms. This would be true for existing drainage systems in need of enhancement, for instance to examine the effect of introducing an additional channel length to a hillslope sequence, or for virgin catchments for which an appropriate and efficient design is required.

The engineering considerations are clear, that channels are required to maintain negative gradients towards the outflow point for their whole length. Given this consideration, the actual route they take should depend on where they can best tap into productive flow-lines for the longest proportion of their length. On slopes where production is from selective bands (as with the Avdat simulations) then channels should be built in sequence so that the whole length of the band is tapped. In catchments where the problem is one of insufficient contributing area and hence insufficient volume of water for a potential runoff farm, channels can be built to exploit all topographic subtleties and route additional water from wherever it is possible to augment the existing supply. The effects of building either type of drainage configuration for a given catchment could be analysed by the model and clearly illustrated through the graphical and numerical indices produced during the simulations. Modelling the Avdat catchment system and its individual sub-components of hillslope cascades and sub-catchments has been invaluable in providing a clear illustration of these concepts.

CHAPTER SEVEN SUMMARY AND CONCLUSIONS

This chapter presents a summary of the areas covered in this thesis and the conclusions derived from a structured approach in which a review of current understanding of arid lands hydrology has been coupled with extensive fieldwork in the arid Negev and a systematic modelling programme of plot, hillslope and catchment simulations. The initial summaries and conclusions focus on the specific results of the model simulations and an examination of the sensitivity of the hydrological response of idealised hillslope systems to a range of parameters and parameter combinations. Following this, the lessons learned in using the model as a design tool with the purpose of answering specific questions about arid lands hydrology and water harvesting system efficiency are discussed. The outcome of applying the model to assess the operational characteristics of the Avdat design is briefly evaluated along with the potential for its wider use. The success of any wider application of models like WATERH appears to be limited by how well future studies can overcome some of the problems of hydrological research and analysis in the arid environments. Limitations currently relate to fieldwork, the provision of critical data, and the development of modelling mechanisms appropriate to the highly variable process conditions through both time and space. The direction to be taken by further applied studies can be broadly assessed from a summary of the conclusions drawn from the sensitivity analysis viewed in the context of the literature review. The critical processes and scales that need concentrating on can be identified. The weaknesses in current abilities to measure and model these process dynamics are important because they show the paths future research must take.

7.1 SIMULATION RESULTS AND SENSITIVITY

7.1.1 Sensitivity to Process Parameters

The sensitivity analysis undertaken using the model WATERH analysed the affects of different parameters on hillslope runoff response to rainfall, focused on the factors significant for controlling water harvesting system productivity namely the scale of and distribution of flow parameters along a flow-line, and tested the effects of certain routing assumptions related to the use of sheetflow or complex flow, particularly on the interaction of the infiltration and routing components. A small set of parameters representing the range of conditions on the Negev hillslopes and within the Avdat water harvesting system were used and included; slope gradient, slope resistance coefficient (Mannings n), flow boundary shape, infiltration regime, rainfall intensity and distribution, spatial arrangement and hillslope scale.

One of the most important conclusions resulting from simple, single plot simulations was how the effect of the assumption that the surface of the plot was either micro-smooth or micro-rough influenced the predictions to a greater degree than variations in slope gradient and resistance values. For

the same slope and roughness parameter combinations, the complex, micro-rough flow assumption produced a much reduced time to steady-state discharge and a considerable increase in steady-state velocity and decrease in steady-state flow-area compared to the sheetflow, micro-smooth case. Coupling a micro-rough surface with a high slope gradient and a low resistance resulted in the most favourable runoff transmission characteristics. Once rainfall ceases, then the more rapid the throughflow, the less opportunity for subsequent infiltration of surface water and so parameter combinations that produce high peak velocities and steep falling limbs produce proportionally more runoff under a given infiltration regime. Additionally, the effect of infiltration is dampened by assuming complex flow conditions. For worsening infiltration regimes, the decrease in runoff productivity for a given combination of slope gradient and roughness is less for a macro-rough than for a micro-rough slope. This shows some of the practical implications for using a sheetflow approach to routing surface flow, a fact which deserves greater attention by hydrologists.

Added to the complex inter-relationships between infiltration and flow routing parameters and assumptions, the intensity distribution of the rainfall is clearly an important factor in determining the runoff productivity from a hillslope surface. There is a complex relationship between infiltration and the rainfall intensity and temporal distribution. This to some extent depends on the infiltration model and the method of procedurisation as explained in Chapter Three in the discussion of Hortonian and storage approaches.

7.1.2 The Importance of the Hillslope Hydrological Context

The characteristics so far described become of critical importance when they are put into the context of a hillslope cascade in which conditions vary along flow-lines so that sub-sections with different parameter combinations juxtapose. The change of contributing slope length in the sensitivity tests coupled with the change of slope conditions along a flow-line aided understanding of the Contiguous Area Contribution concept of arid hillslope hydrology. Slope length becomes more important in controlling total productivity as flow routing and infiltration conditions worsen. Water generated on the slope moves more slowly and the potential for post-rainfall infiltration remains high relative to the volumes of water on the surface. In the circumstances when routing is more effective then for a given infiltration, productivity increases and the effect of slope length is suppressed. If a particular length of slope is also spatially variable, the arrangement and relative conditions of different slope types becomes critical. If a good producer is situated above a poor producer, then depending on their relative characteristics and the amount and timing of rainfall, the poor producer can act as a consumer, totally dissipating the high discharge running on from above, or the good producer can reach-down over the poor producer and help it to reach ponding more quickly and both generate and transmit runoff out of the slope and into a channel assumed to be located at its base. If the consuming effect is high, by locating a channel immediately below the good producer, the consumptive effects of the poor

producer could be avoided and the total productivity of the slope enhanced. If there is little spatial variability and slopes are uniformly good producers and transmitters, the introduction of additional channels would not appreciably increase the amount of water harvested from this kind of slope section. This has obvious relevance to the design and functioning of water harvesting systems. Since the effect of allowing water to flow un-obstructed over long consumptive sections of hillslopes is to dissipate potential productivity, then where water volumes supplied to a runoff farm are insufficient, channels must be introduced at selected points within the flow-line to increase productivity.

7.1.3 Lessons for Parameter Specification

The sensitivity analysis in particular has shown the importance of the routing parameters in determining the response from hillslopes in terms of the amount and timing of runoff production and transmission. To provide accurate assessments of hillslope hydrological characteristics models must take into account each of the three factors of slope gradient, flow resistance and flow boundary shape to an adequate level. Simplifying assumptions such as constant velocity (for example the model of Yair and Lavee described in Chapter One) could significantly modify the predicted response of a hillslope configuration and ignore key differences that changes in the flow velocity will cause. The stage-discharge relationship may be equally as important as infiltration in the determination of whether surface water generated at one location becomes runoff output to another, given the often short duration of rain events in arid environments.

7.2 THE MODEL AS A DESIGN TOOL

By applying the runoff model WATERH (and a modified version RORO for the run-on/runoff plots) to a variety of scales, its potential for illustrating the key controls on arid lands runoff productivity and the applied use of such a model for the assessment of water harvesting systems has been well illustrated. Knowing the characteristics of the parameters and their obvious effect on runoff production and transmission and using the model as an evaluation tool provides a clear insight into the critical nature of hydraulic remoteness and Contiguous Area Contribution and assesses the performance of a particular water harvesting catchment system design. Through theoretical manipulation of a basic geometric and channel network data-set, the model could be used to simulate a complete range of hillslope and channel configurations for a given catchment area. Given sufficiently sensitive parameters of infiltration, flow resistance and hillslope gradient, the performance of each configuration could be assessed for an individual, or sequence of rainstorms. This would be true for existing drainage systems in need of enhancement, for instance to examine the effect of introducing an additional channel length to a hillslope sequence, or for virgin catchments for which an appropriate and efficient design is required. The exacting requirements of parameter specification for the arid lands environment is discussed below.

7.2.1 The Successful Techniques of Routing Modification

Some general conclusions from applications of the model to the study of the Avdat water harvesting system are that the success of the type of system, with its additional channel network stretching out to hydraulically and geographically remote areas, relies on an increase in both channel density and the suitability of channel locations to harvest specific productive areas and avoid other consumptive ones. The two indices of productivity successfully focus on the characteristics controlling the successful functioning of water harvesting systems in spatially variable catchments. By determining the balance between total volumetric inputs and total volumetric outputs, the percentage runoff efficiency of each hillslope and channel element provides a measure of its relative ability to produce runoff water, identifying clearly the most important net producers and net consumers. The sensitivity, cascade and sub-catchment simulations show that channels should wherever possible be placed above locations where the runoff productivity falls considerably, and especially where it drops to zero or even negative values. Once the productivity/transmissivity becomes negative, the productivity percentage falls and there is a subtraction from the total flow passing this location. Below the point where the index becomes negative, the productivity percentage will fall. The positioning of channels must be systematic, geared to a knowledge of the productive characteristics of different slope sections. Evenly spacing them down a whole profile or adding extra channels to an already productive configuration would be a mistake since the improvement per unit channel length is minimal. For water harvesting to be effective in such an arid environment as the Negev requires as much of the available water resources as possible to be utilised to ensure that even in the poor years the runoff farm is supplied with sufficient water for all or some of the terraces to raise an effective crop, then both efficiency and total productivity must be maximised. By expanding the catchment area, a larger total volume of runoff will be produced as a function of this expansion. By increasing the drainage density into the highly productive slope areas, the volume of the harvest is also increased since the internal losses from transmission are reduced as hydraulic remoteness is decreased and Contiguous Area Contribution increased.

7.2.2 Evaluating the Ancient Hydro-Engineering Skills

It is clear that the designers possessed working knowledge of the major critical hydrological concepts determining the nature of runoff response from the small Negev catchments, and the effects the introduction of their channels would have. The principle of productive zones and unproductive zones was clearly understood. Observations made whilst walking over the catchment during two seasons of rainstorms indicated how clear the patterns of runoff production are, how the productive zones can be seen by watching the speed and depth of surface flow, the presence of un-ponded sections across the hillslopes, and the flow of water in channels dissipating on entry to the wadi (as illustrated in Plates F.1 to F.8). In their work on the Negev runoff farming systems, Shanan and Evenari (Shanan, 1975.

Evenari *et al*, 1980) stressed mostly the density aspects, stating that channels were introduced to create smaller catchment area sizes for a given field area. The productivity of a catchment in terms of the output-input ratio is held to be related directly to its size. However, the sensitivity analysis, the cascade simulations and the sub-catchment simulations have shown that reducing catchment size and increasing channel density alone is an incomplete strategy for maximising harvesting potential. It is clear that both a knowledge of the density effects and the role of Contiguous Area Contribution are required for effective harvesting of runoff. Taking account of inherent productive potential in siting channels is an equally important consideration and requires some knowledge of the hydraulic remoteness of any location.

7.3 PROBLEMS OF ARID ENVIRONMENT ANALYSIS

There are a number of problems in the study of arid environments, and hence water harvesting systems that provide effective limitations on the abilities of models to reproduce observed conditions and analyse catchment areas for their true water harvesting potential. These problems relate mainly to the provision of data of sufficiently high quality and quantity to parameterise model routing and infiltration procedures and provide a geometric simplification of the catchment space but also to the formulation of procedures sensitive at an appropriate resolution for the significant scale of application. The problems identified can be considered in their logical process order of rainfall, infiltration and routing.

7.3.1 Rainfall Intensity Variations and their Implications for Infiltration Models

The runoff generation process is highly sensitive to rainfall intensity. Large quantities of water can be produced from very short bursts of high intensity, which will move proportionally more quickly through the system and with lower proportional losses than for the smaller, slower flows. The smoothing of the intensities into longer, lower intensity blocks could significantly reduce sensitivity of the model vis á vis the observed response. Many rainstorms are also characterised by periods of intermittent low intensity, sufficient to classify the rainstorm as a single event, but effectively representing gaps between separate showers during which runoff may actually cease as intensities fall below conductivities. This requires the infiltration model to be sensitive to these variations in supply, a feature not common of most empirical models which are parameterised under constant input conditions. An improvement in the ability to model more complex rainstorms is required in the arid environment. The use of the Green and Ampt storage model for WATERH showed up several deficiencies in this respect. Infiltration is a complex function of time and time is assumed continuous. Where rainfall is limiting and intermittent the assumption of continuity is lost. A more appropriate model is required in which Equation 7.1 applies.

$$i(t) = A(t) + B(t)/t \qquad \text{Equation 7.1}$$

The tendency of many models, usually when used in Hortonian equations designed to determine a simple time-dependent rainfall excess, to predict 'negative' runoff is clearly a conceptual limitation which can become an important factor. The effect of choosing Hortonian or storage assumptions in predicting time to runoff for variable intensities was shown in theoretical terms in Chapter Three, illustrating the varying performance of each under conditions of varying intensity, but identical magnitude rainstorms.

7.3.2 Infiltration Parameter Errors and Bias

These problems are not so acute when models are used to simulate the response from short-duration rainfall events. However, even with these simple rainstorms, problems can arise due to the relative accuracy of infiltration parameters at forecasting correct infiltration rates in the initial or later time-periods. Most models of infiltration, due to the methods of parameter provision and the difficulties of measurement of infiltration rates during early phases, are most accurate in representing the steady state conditions. In the humid environments, when the majority of the stormwater runoff may be generated in conditions when infiltration is at or approaching steady-state, this is acceptable since the preliminary conditions will not have proportionally the same influence on actual or predicted response. In arid environments, with short rainfall durations and low rainfall magnitudes, the initial infiltration rates and the change towards the steady-state conditions take on enormous significance and play a major role in determining the quantity and timing of runoff generation. Many infiltration experiments include additions to detention storage in their initial infiltration calculations unless some explicit attempt is made to account for these time-lag effects in subsequent calculations. These additions reduce towards steady state. Added to this, the selection of plotting times for calculated infiltration rates helps determine the predictive ability of the infiltration models. Depending on the coarseness of the sampling resolution vis á vis the important time-scale for the process, plotting infiltration in a given time increment at the end of the time increment shifts the infiltration curve to the right resulting in an overestimate of actual infiltration. With short, high intensity rainstorms, this may well prove very significant in determining forecast times to runoff and the volume of runoff. This is compounded by the need for most high-resolution models to operate at a temporal resolution in excess of that from which the infiltration parameters were produced. The coarseness of observation times is important, relying on extrapolation of the infiltration curve fixed by only a small number of points prior to the steady-state.

7.3.3 Problems of Measuring Infiltration and Runoff in the Field

The method of experimentation for infiltration rate determination is therefore very important, each field technique having its own considerations. There are many sources of errors that can creep in to infiltration measurements, calculation and model fitting. There are considerable problems of measuring infiltration and runoff in the field. Conducting infiltration tests on steep, micro-rough plots is technically difficult especially considering the measurements must be most sensitive in the flux phase where water is input to a dry surface. Accurate accounting for detention storage and time-lags and measurements of shallow flows are required. The run-on/runoff plot method used at Avdat, for instance, over-estimates initial infiltration rates through areally and temporally averaging input, assuming that the infiltration process starts at time t=0 for all points on the surface and including the additions to surface detention storage in the volumes of water attributed to infiltration. The B parameter was seriously over-estimated and a specific and largely successful attempt was made to redress this characteristics, and in the process some important lessons were learned. It is clear that to use the storage model effectively, an accurate measure of time to runoff must be gained that excludes the influences of detention and time-lags.

7.3.4 Weak Links in the Data-Modelling Procedure Chain

Many studies in arid environments have concentrated on infiltration as discussed in Chapter One. Attention has been focussed on the characteristics of rainfall simulators, their intensity distributions, drop impacts and drop size variations. However, as shown from theoretical and more practical use of routing parameters in simulations, the accurate specification of the routing characteristics is as important as the specification of the infiltration rates. The combination of poor initial infiltration forecasts and poor routing of steady-state or peak flow can effectively combine to limit the success of model predictions due to the importance of both of these phases in the hydrological cycle. Where key areas of a catchment are characterised by low slope gradients, any errors in specifying the gradient become extremely important as the result can be a relatively large change in the value of the sine used in Mannings flow formula to calculate velocity. Again this comes back to the problems of measurement at the appropriate scale for the process. Flow across shallow slopes is difficult to reproduce with accuracy due partly to the specification of slope gradient and partly to the difficulties of measuring shallow flow depths and velocities. The current approach calculated depth as an areal average and velocity by modifying maximum measured rates. Insensitivity resulting from these measurements manifests itself in the Mannings n estimates produced from the plot data. In full sub-catchment simulations, the character of the hydrograph depends on the relative timing of the productivity from locations up and down-stream and the routing of flow along the channel length to the farm inlet. If the routing characteristics off all or part of the slope sections and through the channels are not closely

reproduced, then the hydrograph shape is unlikely to be similar to the observed regardless of how well the infiltration parameters might perform.

7.3.5 Strengthening the Routing Link

Many arid environments such as the Negev, are characterised by considerable variations in surface conditions such as elevation, slope gradient, surface materials and surface micro-topography. The mechanisms currently available to include these characteristics in model process procedures are limited. Although the current work has identified the significant role played by micro-rivulets in routing water, and developed a procedure by which the nature of micro-topography might be incorporated into the flow equation, procedurising this for actual application to real situations has not yet been achieved. Integration of this routing procedure with infiltration and flow resistance specification is an obvious next step. Since the development of a field methodology for infiltration and runoff appropriate to arid conditions and which is also also technically feasible has remained difficult and elusive, this next step may take a while. However, quantifying the surface texture of catchment hillslopes proved to be a valuable technique. Not only did it provide a means for quantifying and distinguishing between the physical character of particular areas, through its surface material size distribution and its micro-topographic variation from a downslope and cross-slope straight line, it also provided the means to take an alternative approach to flow dimensions than the traditional sheetflow assumption. By attempting to consider the complex shape of the overland flow surface and derive a relationship between cross-sectional area and boundary contact length for a number of flow stages, the changing nature of flow is accounted for. The assumption of a uniform sheet with an average depth is inappropriate for steep, rough arid hillslopes as shown by the work of Emmett (1970), Roels (1984b) and now the current study. The effects of this assumption in terms of runoff productivity and flow routing characteristics has been clearly shown in the sensitivity modelling using WATERH.

7.4 ARID LANDS HYDROLOGY AND THE NEGEV DEBATE

By considering the literature and piecing together the various scales of research on arid lands hydrological processes, from the catchment analysis of Lane *et al* (1977, 1978), to the hillside analyses of Yair and Lavee (*et seq*) and the intra-hillslope analyses of Hodges and Bryan (1982), a re-appraisal of arid lands hydrology at the individual catchment scale has been made. The different results have been synthesized into the concept of Contiguous Area Contribution which is a particular form of partial area contribution more specific to arid environments.

7.4.1 Hortonian Runoff Conditions as a Special Case

One clear conclusion from the range of simulations undertaken using Negev parameters and from a re-consideration of arid slope hydrology is that the classic Hortonian flow-state would clearly seem to be the extreme of the Arid Lands hydrological cycle. The whole hillslope will produce and transmit runoff along complete flow-lines only when rainfall durations and magnitudes are sufficiently high to exceed infiltration capacities throughout the surface area. Flow will only increase in direct proportion to downslope distance on uniform slopes, the variations in slope gradient, transmission losses and flow resistance all being sufficient to locally control conditions. Slope gradient is particularly important for most arid flow cases since its effect on flow velocity and detention storage may be sufficient to render the complete productivity further up the flow-lines irrelevant for stormflow production. This represents a complete contrast to stormwater flow in the humid environments. Whereas in the humid environments, water transmitted downslope via soil throughflow is required to raise footslope soil water levels to saturation and cause saturated overland flow, in the case of the arid zone, the lower slopes exert the opposite effect. If the infiltration rates and routing conditions of the lower slopes are not sufficiently productive, then all the flow from upslope will be lost.

7.4.2 Resolving the Debate on Key Runoff Producers in the Negev

The debate presented in the Negev literature concerning relative merits of different slope environments as effective runoff producers has been largely reconciled. As explained in Chapter One, the works of Shanan argued that only those areas adjacent to channels that are gentle, continuous loessial crusted slopes will contribute during the majority of rainfall events experienced in the Central Negev Highlands. These tend to be the floodplains adjacent to natural channels subject to alluvial deposition of loessial material, or isolated sections of palaeo-fluvial terraces mantled with aeolian deposits (Shanan, 1975). Yair and Lavee argued that these slopes are in fact barriers to storm-flow contribution having higher infiltration rates and less effective flow transmissivity than the steeper rocky slopes below which they tend to occur (Yair and Lavee, 1985, Yair, 1984). There are a range of controlling factors on runoff productivity such that different components of the erosional-depositional spectrum across hillslope profiles play different roles. Yair's studies have shown that the rock slopes are undoubtably the most productive units both in terms of the rapidity and the quantity of runoff. This has been supported somewhat by the field experiments at Avdat which show relatively low infiltration rates and rapid times to run-out for plots with a relatively high proportion of bedrock and stone cover and steeper slopes (the unit 3 plots). However, their total surface area is only a small part of most catchment's surface area, and their position is often hydraulically remote from natural channel systems. The relatively larger but less responsive and productive loess-covered slopes are therefore the major contributors to basin discharge under normal circumstances, runoff from elsewhere consumed on its passage downslope in all but the smallest catchments and most extreme rainfall events.

7.4.3 A Storage Model of Infiltration

In the analysis of infiltration the simplified Green and Ampt developed by Scoging and Thornes (1980), provided the best-fit to Avdat field data and corresponds to storage concepts of infiltration, with the condition that irrespective of applied intensity, there is always a fixed storage that must be filled before ponding can occur. This notion has been held to apply to the humid area environment, with well-developed, free-draining soil profiles. The storage model has only recently been presented as a possible mechanism for arid soils and has not yet received any wide-scale evaluation. The current study, whilst representing only a small assessment of the range of infiltration environments within an arid catchment, nevertheless supports the observations of Scoging (1988) for S.E. Spain that the storage model is in fact an appropriate one for arid field conditions and produces the best-fit of all models when applied to the data. The storage volumes are very small, in the order of only a few millimetres, explaining the rapid runoff experienced in a large number of infrequent, small rainfall events. In the Negev, it was noticed that even in the rainfall events of only a couple of mm, some slope areas produced surface ponding and embryonic overland flow every time, although insufficient to cause channel stormflow. Short high intensity storms will produce almost instant runoff, whereas long duration low intensity storms may produce no runoff at all, regardless of the total depth unless there are infrequent periods of slightly higher intensity throughout the duration. The short, high intensity rainfalls will be responsible for larger floods than will the long duration low intensity rainfalls, even though the total rainfall of the latter may be considerably higher. This was witnessed at all stages of the simulations and is a characteristic noted for many arid environments.

7.5 PROCESS DYNAMICS AND MODELLING PROCEDURES

A successful rainfall-runoff modelling exercise depends upon the accurate simulation of the amount, temporal and spatial distribution of lateral inflow to a sequence of physical elements used to describe the system, which to a large degree is determined by the infiltration parameters (Woolhiser, 1981). This has been clearly demonstrated in the phases of simulation carried out during this thesis. However, infiltration is but one factor controlling lateral inflow. Routing is of key importance because it can significantly determine the volume if not the rate of infiltration due to its affects on flow time-lag, the knock-on effect down flow-lines, the rise in detention storage and the length of time a given volume of water is available for infiltration.

7.5.1 Considering the Complex Nature of Overland Flow Routing at the Intra-Hillslope Scale

The more efficient character of the rilled flow-shape on a micro-rough surface, with relatively large hydraulic radius, transmits water more efficiently than a more shallow, sheet-like flow section

where total length in contact with the water area is large, and depth small relative to individual surface materials. Water moving over the varied surface has greater velocities, with more rapid throughflow, promoting lower detention storage and higher total infiltration volumes. Observations that flow was not sufficiently concentrated or the micro-rills sufficiently large to qualify as individual channels led to the development of the current approach termed here the complex geometry approach. This is in answer to a direct call by Huggins and Monke in 1968 that a means of quantitatively describing the overall flow conditions of a hillslope element without analysing the rigorous hydrodynamic conditions governing the flow in tiny channels was required. The method developed of defining a relationship between flow area and boundary length with a rising stage using micro-topographic profiles can be considered a useful advancement of modelling techniques that deserves wider consideration and further research into effective field measurement, integration with other process parameters, and practical application. In field tests in which all the routing parameters are measured and from which Manning's n can be calculated by substitution, the assumption of sheetflow and complex flow leads to considerably different parameter values due to the difference between average depth and hydraulic radius. By developing a relationship between flow area and boundary length for a micro-topographically rough surface the effect of the sheetflow assumption was assessed to a limited degree, both through calculations of n for each case and through sensitivity simulations using the two flow assumptions for the same sets of Manning's n values. In this case, assuming sheetflow produces a lower estimate of n for a given discharge and for a given n, the sheetflow assumption predicts a lower discharge for the same input conditions on both the rising and falling limb of the hydrograph.

7.5.2 Orders of Magnitude of Manning's n Coefficient

It is clear from an analysis of the literature that the orders of magnitude of Manning's n for hillslope overland flow, particularly on arid hillslopes where shallow flows over rough surfaces dominate, are relatively higher than for channels. The Avdat field Manning's n values fall in line well with those in the literature both in terms of the order of magnitude and the range of values observed within the catchment area on different types of hillslope. The values of Manning's n developed for channel flow situations, even for the gravel-bedded rivers usually assumed most relevant to overland flow on stony un-vegetated hillslopes, are inappropriate for use in this environment. They actually have n values that are an order of magnitude lower as shown in the literature review and field tests carried out at Avdat. From a review of the hydraulic literature, a case was made for a methodology by which a dynamic roughness coefficient can be provided for use in a flow equation. It is clear that resistance should vary directly with discharge, since the ratio of water body dimensions to boundary dimensions increases, and therefore the per-unit effect of boundary resistance decreases. A roughness coefficient that is considered as a constant value for all flow states may misrepresent the true nature of the roughness phenomenon. Future research work in arid hillslope hydrological modelling should

concentrate on these twin components of the routing equations, flow dimensions and flow resistance, if an accurate picture of rapid, spatially variable stormwater generation processes is to be achieved.

REFERENCES

Abbott M.B., 1979. Computational hydraulics: Elements of the theory of free-surface flows. Pitman, 324 p.

Agassi M., Benyamini Y., Morin J., Morish S. and Henkin E., 1986. The Israeli concept for runoff and erosion control in semi-arid and arid zones in Mediterranean Basin. PAP. Regional Activity Centre. UNEP. Split Project No. DA-8/me 5102-83-05.

Agassi M., Shainberg I. and Morin J., 1981. Effect of electrolyte concentration and soil sodicity on infiltration rate and crust formation. Soil Science Society of America Journal 45(5), pp. 848-851.

Agassi M., Morin J. and Shainberg I, 1982. Laboratory studies of infiltration and runoff control in semi-arid soils in Israel. Geoderma 28, pp. 345-356.

Agassi M., Shainberg I. and Morin J., 1985a. Effect of raindrop impact energy and soil water salinity on infiltration rates in sodic soils. Soil Science Society of America Journal 49, pp. 186-190.

Agassi M., Shainberg I. and Morin J., 1985b. Infiltration and runoff in wheat fields in the semi-arid region of Israel. Geomderma 36, pp. 263-276.

Anderson M.G. and Kneale P.E., 1980. Topography and hillslope soil water relationships in a catchment of low relief. Journal of Hydrology 47, pp. 115-128.

Anderson M.G. and Burt T.P., 1978. The role of topography in controlling throughflow generation. Earth Surface Processes 3, pp. 331-334.

Arkin. Y., Bartov Y., Druckman Y., Lewy Z., Mimran Y., Steinitz G., Weissbrod T. and Zilberman E., 1984. Outlines of the geology of the northwestern Negev. Geological Survey of Israel Report GSI/19/84, pp. 107.

Arteaga F.E. and Rantz S.E., 1971. Application of the surface area concept of storm runoff to a small Arizona watershed. Journal of Research. United States Geological Survey 1, 4, pp. 493-498.

Bathurst J.C., 1982a. Theoretical aspects of flow resistance. Chapter 5 in Hey R.D, Bathurst J.C. and Thorne C.R., Eds., Gravel Bed Rivers. John Wiley and Sons Ltd.

Bathurst J.C., 1982b. Flow resistance in boulder-bed streams. Chapter 16 in Hey R.D, Bathurst J.C. and Thorne C.R., Eds., Gravel Bed Rivers. John Wiley and Sons Ltd.

Bathurst J.C., 1986a. Physically-based distributed modelling of an upland catchment using the Systeme Hydrologique Europeen. Journal of Hydrology 87, pp. 79-102.

Bathurst J.C., 1986b. Sensitivity analysis of the Systeme Hydrologique Europeen for an upland catchment. Journal of Hydrology 87, pp. 103-123.

Bell F.C. and Vorst P.C., 1980. Geomorphic parameters of representative basins and their hydrologic significance. Australian Water Resources Council Technical Paper No. 58.

Ben-Hur M., Shainberg I, Keren R. amd Gal M., 1985. The effect of water quality and drying on soil and crust properties. Soil Science Society of America Journal 49, pp. 191-196.

Betson R.P., 1964. What is watershed runoff? Journal of Geophysical Research 69, pp. 1541-1552.

Beven K.J. and O'Connell P.E., 1982. On the role of physically-based distributed modelling in hydrology. Institute of Hydrology Report No.81. Wallingford, Oxfordshire, U.K. p. 35.

Beven K.J. and Clarke R.T., 1986. On the variation of infiltration into a homogeneous soil matrix containing a population of macropores. Water Resources Research 22(3), pp. 383-388.

Beven K.J. and Kirkby M.J., 1978. A physically based variable-contributing area model of basin hydrology. Hydrological Sciences Bulletin 24, pp. 27-53.

Beven K.J. and Germann P., 1982. Macropores and waterflow in soils. Water Resources Research 18, 5, pp. 1311-1325.

Bloomfield P.H., Pilgrim D.H. and Watson K.K., 1981. The infiltration-soil water storage relationship at a point in watershed modelling. Water Resources Research 17, 2, pp. 370-376.

Bork H.R. and Rohdenburg H., 1981. Rainfall simulation in southeast Spain: analysis of overland flow and infiltration in Soil Conservation Problems and Prospects ed. Morgan R.P.C. Wiley Press.

Brackensiek D.L., 1966. Hydrodynamics of overland flow and non-prismatic channels. Transactions of the American Society of Agricultural Engineers, 9, 1, pp. 119-122.

Brackensiek D.L., 1967. Kinematic flood routing. Transactions of the American Society of Agricultural Engineers. 10, 3, pp. 340-343.

Braun M. 1967. Type sections of Avedat group, Eocene formations in the Negev (southern Israel). Geological Survey of Israel Stratigraphic Sections No.4, p. 14.

Bray D.I., 1979. Estimating average velocity in gravel-bed rivers. Proceedings of the Amercican Association of Civil Engineers HY9, pp. 1103-1121.

Bray D.I., 1982. Flow resistance in gravel-bed rivers. Chapter 6 in Hey R.D, Bathurst J.C. and Thorne C.R., Eds., Gravel Bed Rivers, John Wiley and Sons Ltd.

Bryan R.B., Yair A. and Hodges W.K., 1978. Factors controlling the initiation of runoff and piping in Dinosaur provincial Park badlands, Alberta, Canada. Zeitschrift fur Geomorphologie Suppl. Bd. 29, pp. 151-168.

Burwell R.E., Allmaras R.R, and Amemiya., 1963. A field measurement of total porosity and surface microrelief of soils. Soil Science Society Proceedings, pp. 697-700.

Button B.J. and Ben-Asher J., 1983. Intensity-duration relationships of desert precipitation at Avdat, Israel. Journal of Arid Environments 6, pp. 1-12.

Chow V.T., 1959. Open-Channel Hydraulics. McGraw-Hill, 680 p.

Chow V.T., 1981. Open-Channel Hydraulics. McGraw-Hill, 680 p.

Christian C.S., 1957. The concept of land units and land systems. Proceedings of the Ninth Pacific Science Congress 20, pp. 74-81.

Clarke R.T., 1973. A review of some mathematical models used in hydrology, with observations on their calibration and use. Journal of Hydrology 19, pp. 1-20.

Collis-George N., 1977. Infiltration equations for simple soil systems. Water Resources Research 13(2), pp. 395-403.

Cowan W.L., 1956. Estimating hydraulic roughness coefficients. Agricultural Engineering, 37, 7, pp. 473-475.

Crawford N.H. and Linsley R.K., 1966. Digital simulation in hydrology - Stanford Watershed Model IV. Stanford University Department of Civil Engineering Technical Report 39.

Cundy T.W. and Tento S.W., 1985. Solution to the kinematic wave approach to overland flow routing with rainfall excess given by Philip's equation. Water Resources Research 21(8), pp. 1132-1140.

Dingman S.L., 1971. Hydrology of the Glenn Creek watershed, Tanana River Drainage, Central Alaska. US Army Cold Regions Research and Engineering Lab. Research Report 297.

Dingman S.L., 1984. Fluvial Hydrology. W.H. Freeman and Co., New York, 383 p.

Dixon R.M., 1975. Infiltration control through soil surface management. Proceedings of the Irrigation and Drainage Division Symposium on Watershed Management, Logan, Utah, American Society of Civil Engineers, pp. 543-567.

Dixon R.M., 1977. Infiltration effects of soil surface conditions. Proceedings of the Agricultural Research Service Infiltration Research Planning Workshop Instrumentation Panel, St. Luis, Missouri, 6 p.

Dixon R.M., Simanton J.R. and Lane L.J., 1978. Simple time-power functions for rainwater infiltration and runoff. Hydrology and Water Resources in Arizona and the Southwest 8, pp. 79-89.

Dunne T., 1983. Relation of field studies and modelling in the prediction of storm runoff. Journal of Hydrology 65, pp. 25-48.

Dunne T. and Black R.D., 1970. Partial area contributions to storm runoff in a small New England watershed. Water Resources Research 6(5), pp. 1296-1311.

Dunne T. and Leopold L.B., 1978. Water in environmental planning. Freeman, San Francisco.

Dunne T., Moore T.R. and Taylor C.H., 1975. Recognition and prediction of runoff-producing zones in humid regions. Hydrological Sciences Bulletin 20(3), pp. 305-327.

Ebdon D., 1983. Statistics in geography. Blackwell, 195 p.

Ellison W.D., 1944. Studies of raindrop erosion. Agricultural Engineering, pp. 131-136.

Emmett W.W., 1970. The hydraulics of overland flow on hillslopes. Geology Survey Professional Paper 662-A, 68 p.

Emmett W.W., 1978. Overland flow; Chapter 5, Hillslope Hydrology, ed. M.J. Kirkby, Wiley, pp. 145-176.

Engman E.T. and Rogowski A.S., 1974. A partial area model for storm flow synthesis. Water Resources Research 10(3), pp. 464-472.

Evenari M., Yaalon D.H. and Gutterman Y., 1974. Note on soils with vesicular structure in deserts. Zeitschrift fur Geomorphologie 18(2), pp. 162-172.

Evenari M., Tadmor N. and Shanan L., 1982. The Negev : Challenge of the Desert. Harvard University Press.

Farres P., 1978. The role of time and aggregate size in the crusting process. Earth Surface Processes 3, pp. 243-254.

Fogel M.M., 1969. Effect of rainfall variability on runoff from small semiarid wartersheds. Transactions of the American Society of Agricultural Engineers, pp. 808-811.

Freeze R.A., 1972. Role of subsurface flow in generating surface runoff. 2. Upstream source areas. Water Resources Research 8(5), pp. 1272-1283.

Freeze R.A., 1978. Mathematical models of hillslope hydrology, in Kirkby M.J. (Ed.), Hillslope Hydrology, John Wiley.

Freeze R.A., 1980. A stochastic conceptual analysis of rainfall-runoff processes on a hillslope. Water Resources Resarch 16, pp. 391-408.

Gardiner V. and Dackombe R.V., 1983. Geomorphological Field Manual. Allen and Unwin, London.

Garfunkel Z. and Horowitz A., 1966. The upper tertiary and quaternary morphology of the Negev, Israel. Israel Journal of Earth-sciences 15, pp. 101-117.

Gregory K.J., and Walling D.E., 1973. Drainage basin form and process. John Wiley, New York.

Haque M.I. and Mahmood K., 1983. Analytical determination of form friction factor. American Society of Civil Engineers Journal of Hydraulic Engineering, 109, 4, pp. 590-610.

Hendrikson B.H., 1934. The choking of pore-space in the soil and its relation to runoff and erosion. Transactions of the American Geophysical Union pp. 500-505.

Henderson F.M., 1963. Flood waves in prismatic channels. Journal of the Hydraulics Division of the American Society of Civil Engineers, 89, HY4, pp. 39-67.

Henderson F.M., 1966. Open-channel flow. McMillan, New York, 522 p.

Henderson F.M. and Wooding R.A., 1964. Overland flow and groundwater flow from a steady rainfall of finite duration. Journal of Geophysical Research, 69, 8, pp. 1531-1540.

Hewlett J.D., 1961. Soil moisture as a source of base flow from steep mountain watersheds. Forest Service Research Paper No. 132, United States Department of Agriculture, N. Carolina Station, 11 p.

Hewlett J.D. and Hibbert A.R., 1967. Factors affecting the response of small watersheds to precipitation in humid areas. in Sapper W.E. and Lull H.W. (Eds), Forest Hydrology, Pergamon Press, Oxford, pp. 275-290.

Hewlett J.D. and Nutter W.L., 1970. The varying source area of streamflow from upland basins. Symposium on Interdisciplinary Aspects of Watershed Mangement, Montana State University, pp. 65-83.

Hickok R.B. and Osborn H.B., 1969. Some limitations on estimates of infiltration as a basis for predicting watershed runoff. Transactions of the American Society of Agricultural Engineers 12(6).

Hillel D., 1960. Crust formation in loessial soils. Proceedings of the 7th International Congress of Soil Science, pp. 330-339.

Hillel D. and Gardner, 1969. Steady infiltration into crust-topped profiles. Soil Science 108, pp. 137-142.

Hills R.C., 1970. The determination of the infiltration capacity of field soils using the cylinder infiltrometer. British Geomorphological Research Group Technical Bulletin No. 3, 24 p.

Hodges W.K. and Bryan R.B., 1982. The influence of material behaviour on runoff initiation in the Dinosaur Badlands, Canada. in Bryan R.B. and Yair A. (Eds.) Badland Geomorphology and Piping pp. 13-46 Geobooks, Norwich.

Horton R.E., 1933. The role of infiltration in the hydrologic cycle. American Geophysical Union 14, pp. 446-460.

Horton R.E., 1938. The interpretation and application of runoff plot experiments with reference to soil erosion problems. Proceedings of the Soil Science Society of America, 3, pp. 340-349.

Huggins L.F. and Monke E.J., 1968. A mathematical model for simulating the hydrologic response of a watershed. Water Resources Research 3, pp. 529-539.

Issar A., Karnieli A., Bruins H.J. and Giliead I., 1984. The quaternary geology and hydrology of Sede Zin, Negev, Israel. Israel Journal of Earth-sciences 33, pp. 34-42.

Iwagaki Y., 1955. Fundamental studies on the runoff analysis by characteristics. Bulletin 10 of the Disaster Prevention Research Institute, Kyoto Univeristy, Japan.

Jaywardena A.W. and White J.K., 1977. A finite-element distributed catchment model, I. Analytical basis. Journal of Hydrology 34, pp. 269-286.

Jaywardena A.W. and White J.K., 1979. A finite-element distributed catchment model, II. Application to real catchments. Journal of Hydrology 42, pp. 231-249.

Johnson M., 1964. Channel roughness in steep mountain streams. Paper presented at the Annual Meeting of the American Geophysics Union.

Karnieli A., Ben-Asher J., Dodi A., Issar A. and Oron G., 1985. An empirical approach for predicting runoff under desert conditions. Unpublished, Institute for Desert Research, Sede Boqer, Israel, 16 p.

Kibler D.F. and Woolhiser D.A., 1970. The kinematic cascade as a hydrological model. Colorado State University Hydrology Paper 39, 27p.

Kibler D.F. and Woolhiser D.A., 1972. Mathematical properties of the kinematic cascade. Journal of Hydrology 15, pp. 131-147.

Kirkby M.J., Callan J., Weyman D. and Wood J., 1976. Measurement and modelling of dynamic contributing areas in very small catchments. School of Geography Working Paper No. 167, University of Leeds, U.K. 38 p.

Kirkby M.J., 1978. Implications for sediment transport. in Kirkby M.J. (Ed.), Hillslope Hydrology, pp. 325-363.

Kirkby M.J., 1980. Modelling water erosion processes. in Kirkby M.J. and Morgan R.P.C., Eds. Soil Erosion John wiley and Sons, pp. 183-216.

Knapp B.J., 1978. Infiltration and storage of soil water. in Kirkby M.J. (Ed.), Hillslope Hydrology pp. 43-72.

Kohler M., 1963. Rainfall-runoff models. International Association of Scientific Hydrology Publication No. 63, 479 p.

Lane L.J. and Renard K.G., 1972. Evaluation of a basin-wide stochastic model for ephemeral runoff from semiarid watersheds. Transactions of the American Society of Agricultural Engineers, pp. 280-283.

Lane L.J., Woolhiser D.A. and Yevjevich V., 1975. Influence of simplifications in watershed geometry in simulation of surface runoff. Colorado State University Hydrology Papers No.81, Fort Collins, USA, 50 p.

Lane L.J. and Wallace D.E., 1976. Simulation of partial area response from a small semiarid watershed. Hydrology and Water Resources in Arizona and the Southwest 6, pp. 137-147.

Lane L.J., Morton H.L., Wallace D.E., Wilson R.E. and Martin R.D., 1977. Nonpoint-source pollutants to determine runoff source areas. Hydrology and Water Resources in Arizona and the Southwest 7, pp. 89-102.

Lane L.J. and Woolhiser D.A., 1977. Simplifications of watershed geometry affecting simulation of surface runoff. Journal of Hydrology 35, pp. 173-190.

Lane L.J., Diskin M.H., Wallace D.E, and Dixon R.M., 1978. Partial area response on small semiarid watersheds. Water Resources Bulletin 14(5), pp. 1143-1158.

Lane L.J. and Renard K.G., 1979. Optimal representation of topography for simulation of surface runoff. Draft Paper 79-2038, American Society of Agricultural Engineers and Canadian Society of Agricultural Engineering, Unpublished , 22 p.

Lane L.J., 1982. Distributed model for small semiarid watersheds. Journal of the Hydraulics Division, American Society of Civil Engineers 108(HY10), pp. 1114-1131.

Lane L.J., 1985. Estimating transmission losses. Proceedings of the Speciality Conference 'Development and Management Aspects of Irrigation and Drainage systems', Irrigation Division of the American society of Civil Engineers, San Antonio, Texas, pp. 106-113.

Lavee H. 1985. A deterministic simulation model for rainfall-runoff relationship on arid hillslopes. Unpublished Paper, Department of Geography, Bar Ilan University, Israel, 20 p.

Leopold L.B. and Maddock T., 1953. The hydraulic geometry of stream channels and some physiographic implications. United States Geological Survey Professional Paper, 252, 57 p.

Leopold L.B. and Wolman M.G., 1957. River channel patterns; braided, meandering and straight. United States Geological Survey Professional Paper, 282-B, 85 p.

Leopold L.B., Wolman M.G. and Miller J.F., 1964. Fluvial processes in geomorphology. W.H. Freeman and Co., San Francisco, 522 p.

Li R-M. and Simons D.B., 1982. Geomorphological and hydraulic analysis of mountain streams. Chapter 15 in Hey R.D, Bathurst J.C. and Thorne C.R., Eds., Gravel Bed Rivers John Wiley and Sons Ltd.

Li R.M., Simons D.B. and Stevens M.A., 1975. Non-linear kinematic wave approximation for water routing. Water Resources Research, 11, 2, pp. 245-252.

Liggett J.A. and Cunge J.A., 1975. Numerical methods of solution of the unsteady flow equations, in Mahmood K. and Yevjevivh V. (Eds.) Unsteady flow in open channels, Water Resources Publications.

Liggett J.A., 1975. Basic equations of unsteady flow, in Mahmood K. and Yevjevivh V. (Eds.) Unsteady flow in open channels, Water Resources Publications.

Liggett J.A. and Woolhiser D.A., 1967. The use of the shallow water equations in runoff computation. Proceedings of the Third Annual American Water Resources Conference, American Water Resources Association, San Francisco, pp. 117-126.

Lighthill M.J. and Whitham G.B., 1955. On kinematic waves: I. Flood movement in long rivers. Proceedings of the Royal Society, Series A, 229, pp. 281-316.

Limerinos J.T., 1970. Determination of the Manning coefficient from measured bed roughness in natural channels. United States Geological Survey Water Supply Paper, 1898-B, 47 p.

Loague K.M. and Freeze R.A., 1985. A comparison of rainfall-runoff modeling techniques on small upland catchments. Water Resources Research 21(2), pp. 229-248.

Mabbutt J.A. and Stewart G.A., 1963. The application of geomorphology in resource surveys in Australia and New Guinea. Revue Géomporphologie Dynamique 14, pp. 97-109.

McIntyre, 1958a. Permeability Measurements on surface crusts formed by raindrop impact. Soil Science 85, pp. 185-189.

McIntyre, 1958b. Soil splash and the formation of surface crusts by raindrop impacts. Soil Science 85, pp. 262-266.

Mein R.G. and Larson C.L., 1973. Modeling infiltration during a steady rain. Water Resources Research 9(2), pp. 384-394.

Miller J.E., 1984. Basic concepts of kinematic wave models. U.S. Geological Survey Professional Paper 1302, 30 p.

Miller W.A. and Cunge J.A., 1975. Simplified equations of unsteady flow, in Mahmood K. and Yevjevivh V. (Eds.) Unsteady flow in open channels, Water Resources Publications.

Morgali J.R. and Linsley R.K., 1965. Computer analysis of overland flow. Journal of the Hydraulics Division, Proceedings of the American Society of Civil Engineers 91(HY3), pp. 81-100.

Morgan R.P.C., 1980. Field studies of sediment transport by overland flow. Earth Surface Processes, 5, pp. 307-316.

Morin J. and Benyamini Y., 1977. Rainfall infiltration into bare soils. Water Resources Research, 13, 5, pp. 813-817.

Morin J., Benyamini Y. and Michaeli A., 1981. The effect of raindrop impact on the dynamics of soil surface crusting and water movement in the profile. Journal of Hydrology 52, pp. 321-335.

Morin J. and Cluff C.B., 1980. Runoff calculations on semi-arid watersheds using a rotadisk rainulator. Water Resources Research 16, 6, pp. 1085-1093.

Morin J. and Jarosh H.S., 1977. Rainfall runoff analysis for bare soils. Pamphlet No. 164, Bet Dagan Israel: Volcani Centre, Division of Scientific Publications, 22 p.

Morris E.M. and Woolhiser D.A., 1980. Unsteady one-dimensional flow over a plane: partial equilibrium and recession hydrographs. Water Resources Research 16(2), pp. 355-360.

Overton D.E. and Meadows M.E., 1977. Stormwater modelling. Academic Press.

Pearce A.J., 1976. Magnitude and frequency of erosion by Hortonian overland flow. Journal of Geology, 84, pp. 65-80.

Philip J.R., 1957. Theory of infiltration 1. the infiltration equation and its solution. Soil Science 83, pp. 345-357.

Philip, J.R., 1969. Theory of infiltration. in Advances in Hydroscience, (Ed) Chow V.T., Academic Press, New York.

Pilgrim D.H. and Huff D.D., 1978. A field evaluation of subsurface and surface runoff. Journal of Hydrology 38, pp. 299-318.

Poesen J., 1984. The influence of slope angle on infiltration and Hortonian overland flow volume. Zeitschrift fur Geomorphologie Suppl-Bd. 49, pp. 117-131.

Poesen J., 1986. Surface sealing as influenced by slope angle and position of simulated stones in the top layer of loose sediments. Earth Surface Processes and Landforms 11, pp. 1-10.

Richards K.S., 1982. Rivers: Form and process in alluvial channels. Methuen, 358 p.

Roels J.M., 1984a. Surface runoff and sediment yield in the Ardeche rangelands. Earth Surface Processes and Landforms 9, pp. 371-381.

Roels J.M., 1984b. Flow resistance in concentrated overland flow on rough slope surfaces. Earth Surface Processes and Landforms 9, pp. 541-551.

Rogers C.C.M., Beven K.J., Morris E.M. and Anderson M.G., 1985. Sensitivity analysis, calibration and predictive uncertainty of the Institute of Hydrolgy distributed model. Journal of Hydrology 81, pp. 179-191.

Sampson R. J., 1978. Surface II Graphics System. Series on Spatial Analysis, University of Manchester Regional Computer Centre, 245 p.

Schaake J.C., 1965. Modelling urban runoff as a deterministic process. Treatise on Urban Water Systems. Proceedings. Institute of Urban Water Systems. Fort Collins, Colorado Chapter VI-A, pp. 343-383.

Schafer R.L. and Lovely W.G., 1967. Recording soil surface profile meter. Agricultural Engineering, 48, 5, pp. 280-282.

Schick A.P., 1978. Field experiments in arid fluvial environments: considerations for research design. Zeitschrift fur Geomorphologie Suppl. Bd.29, pp. 22-28.

Scoging H.M., 1976. A stochastic model of daily rainfall simulation in a semi-arid environment. London School of Economics. Department of Geography Discussion Paper No.59. Houghton Street. London WC2A 2AE. U.K., 28 p.

Scoging H., 1979. The relevance of time and space in modelling potential sheet erosion from semi-arid fields. Proceedings of the Workshop on Soil Erosion in Europe and the USA. Ghent. Belgium. pp. 349-360.

Scoging H.M. and Thornes J.B., 1980. Infiltration characteristics in a semiarid environment. Proceedings of the Canberra Symposium on the Hydrology of Areas of Low Precipitation. IAHS-AISH Publication No.128. pp. 159-168.

Scoging H.M., 1988. A theoretical and empirical investigation of soil erosion in a semi-arid environment. Ph.D. Thesis. University of London, England.

Shanan L., 1975. Rainfall and runoff relationships in small watersheds in the Avdat region of the Negev Desert Highlands. Hebrew University of Jerusalem, Israel.

Shanan L. and Schick A.P., 1979. A hydrological model for the Negev Desert highlands: effects of infiltration, runoff and ancient agriculture. Proceedings of the Canberra Symposium on the Hydrology of Areas of Low Precipitation. IAHS-AISH Publication No.128. pp. 269-282.

Sharma M.L., Gander G.A. and Hunt C.G., 1980. Spatial variability of infiltration in a watershed. Journal of Hydrology 45, pp. 101-122.

Sharon D., 1974. On the modelling of correlation functions for raionfall studies. Journal of Hydrology 22, pp. 219-224.

Sharon D., 1980. The distribution of hydrologically effective rainfall incident on sloping ground. Journal of Hydrology 46, pp. 165-188.

Shen H.W., 1976. Modelling of rivers. Wiley International.

Simanton J.R., Dixon R.M. and McGowan I., 1978. A microroughness meter for evaluating rainwater infiltration. Hydrology and Water Resources in Arizona and the Southwest 8, pp. 171-174.

Simanton J.R. and Renard K.G., 1982. Seasonal change in infiltration and erosion from USLE plots in southeastern Arizona. Hydrology and Water Resources in Arizona and the Southwest 12, pp. 37-46.

Smith R.E. and Woolhiser D.A., 1971. Overland flow on and infiltrating surface. Water Resources Research 7(4), pp. 899-913.

Smith R.E. and Chery D.L., 1973. Rainfall excess modelfrom soil water flow theory. Journal of the Hydraulics Division. American Society of Civil Engineers 99(HY9), pp. 1337-1350.

Swartzendruber D. and Hillel D., 1975. Infiltration and runoff for small field plots under constant intensity rainfall. Water Resources Research 11(3), pp. 445-451.

Tackett J.L. and Pearson R.W., 1965. Some characteristics of soil crusts formed by simulated rainfall. Soil Science, 99, pp. 407-413.

Thornes J.B. and Gilman A., 1983. Potential and actual erosion around archaeological sites in south east Spain. Catena Supplement 4, pp. 91-113.

Van Liew M.W. and Saxton K.E., 1984. Dynamic flow resistance for hydrlogic simulations. Journal of Hydraulic Engineering 110(12), pp. 1719-1731.

Wooding R.A., 1965. A hydraulic model for the catchment stream problem: I. Kinematic wave theory. Journal of Hydrology, 3, pp. 268-282.

Woolhiser D.A. and Saxton K.E., 1965. Computer program for the reduction and preliminary analyses of runoff data. United States Department of Agriculture, Agriculture Research Service Publication No.ARS41-109, 33 p.

Woolhiser D.A., 1967. General report. Symposium on New Ideas and Scientific Methods In Deterministic Hydrology, Fort Collins, Colorado, USA, 12 p.

Woolhiser D.A., 1969. Overland flow on a converging surface. Transactions of the American Society of Agricultural Engineers, pp. 460-462.

Woolhiser D.A., Hanson C.L. and Kuhlman A.R., 1970. Overland flow on range,and watersheds. Journal of Hydrology 9(2), pp. 336-356.

Woolhiser D.A., Holland M.E., Smith G.L. and Smith R.E., 1971. Experimental investigation of converging overland flow. Transactions of the American Society of Agricultural Engineers 14(4), pp. 684-687.

Woolhiser D.A., 1975. The watershed approach to understanding our environment. Journal of Environmental Quality 4(1), pp. 17-21.

Woolhiser D.A., 1981. Physically based models of watershed runoff. Proceedings of the International Symposium on Rainfall-Runoff Modeling, Mississippi State University, USA, pp. 189-202.

Woolhiser D.A., 1985. KINEROS 85 documentation. (personal communication).

Wu Y-H, Woolhiser D.A. and Yevjevich V., 1982. Effects of spatial variability of hydraulic resistance of runoff hydrographs. Journal of Hydrology 59, pp. 231-248.

Wu J., 1985. Hydrodynamically smooth flows over surface material in alluvial channels. Journal of Hydraulic Engineering 111(11), pp. 1423-1427.

Yaalon D.H. and Dan J., 1974. Accumulation and distribution of loess-derived deposits in the semi-desert fringe areas of Israel. Zeitschrift fur Geomorphologie Suppl. Bd.20, pp. 91-105.

Yair A., 1973. Theoretical considerations on the evolution of convex hillslopes. Zeitschrift fur Geomorphologie Suppl. Bd.18, pp. 1-9.

Yair A. and Klein M., 1973. The influence of surface properties on flow and erosion processes on debris covered slopes in an arid area. Catena 1, pp. 1-18.

Yair A. and Lavee H., 1974. Areal contribution to runoff on scree slopes in an extreme arid environment-a simulated rainstorm experiment. Zeitschrift fur Geomorphologie Suppl. Bd.21, pp. 106-121.

Yair A. and Lavee H., 1976. Runoff generative process and runoff from arid talus mantled slopes. Earth Surface Processes 1, pp. 235-247.

Yair A. and Lavee H., 1977. Trends of sediment removal from arid scree slopes under simulated rainstorm experiments. Hydrological Sciences Bulletin 22(3), pp. 379-391.

Yair A. and De Ploey J., 1979. Field observations and laboratory experiments concerning the creep process of rock blocks in an arid environment. Catena 6, pp. 245-258.

Yair A. and Danin A., 1980. Spatial variations in vegetation as related to the soil moisture regime over an arid limestone hillside, northern Negev, Israel. Oecologia 47, pp. 83-88.

Yair A., Lavee H., Bryan R.B. and Adar E., 1980a. Runoff and erosion processe and rates in the Zin Valley Badlands, northern Negev, Israel. Earth Surface Processes 5, pp. 205-225.

Yair A., Lavee H., Goldberg P. and Bryan R.B., 1980b. Present and past geomorphic evidence in the development of a badlands landscape: Zin Valley, northern Negev, Israel. Palaeoecology of Africa and the Surrounding Islands 12, pp. 125-135.

Yair A., Sharon D. and Lavee H., 1980c. Trends in runoff and erosion processes over an arid limestone hillside, northern Negev, Israel. Hydrological Sciences Bulletin 25(3), pp. 243-255.

Yair A. and Lavee H., 1981. An investigation of source areas of sediment and sediment transport by overland flow along arid hillslopes. Proceedings of the Florence Symposium on Erosion and Sediment Transport Measurement. IAHS Publication No.133. pp. 433-445.

Yair A. and Rutin J., 1981. Some aspects of the regional variation in the amount of available sediment produced by isopods and porcupines, northern Negev, Israel. Earth Surface Processes and Landforms 6, pp. 221-234.

Yair A. and Lavee H., 1982. Application of the concept of partial area contribution to small semi arid watersheds. Rainfall-Runoff Relationship. Water resources Publications. Colorado. pp. 335-350.

Yair A. and Shachak M., 1982. A case study of energy, water and soil flow chains in an arid ecosystem. Oecologia 54, pp. 389-397.

Yair A., 1983. Hillslope hydrology water harvesting and areal distribution of some ancient agricultural systems in the northern Negev desert. Journal of Arid Environments 6, pp. 283-301.

Yair A. and Lavee H., 1985. Runoff generation in arid and semi-arid zones. in Anderson M.G. and Burt T.P., Eds., Hydrological Forcasting. John Wiley and sons. pp. 183-220.

Yevjevich V. and Barnes A.H., 1970. Flood routing through storm drains. Part IV Numerical computer methods of solution. Hydrology Paper No. 46 Colorado State University, Fort Collins, 46p.

Zarmi Y., Ben-Asher J. and Greengard T., 1983. Constant velocity kinematic analysis of an infiltrating microcatchment hydrograph. Water Resources Research 19(1), pp. 277-283.

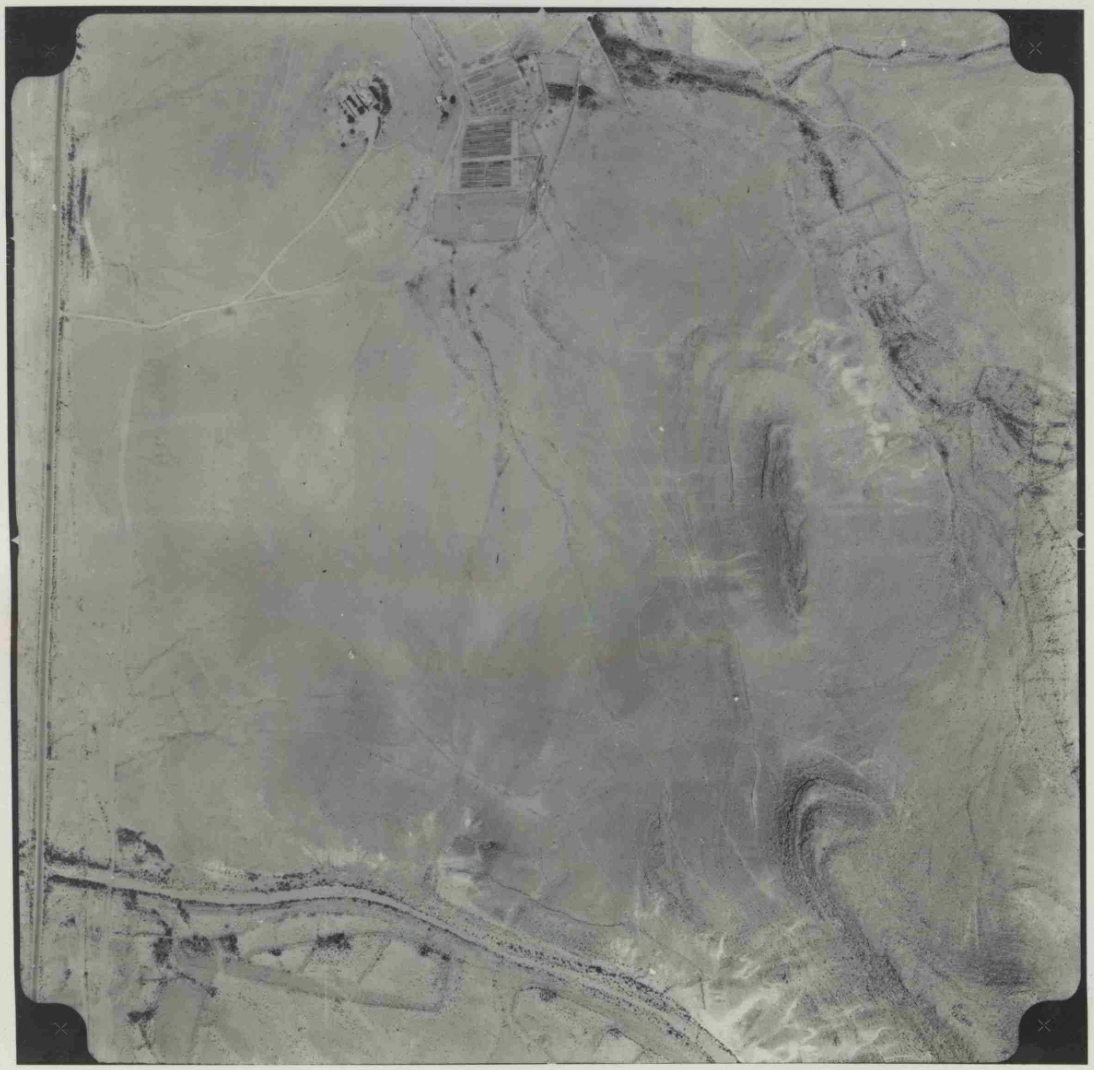

Plate C.1 Aerial photograph of the Avdat Runoff Farm and catchment system.
Note terraced fields and man-made drainage channels (see Appendix 3.1).

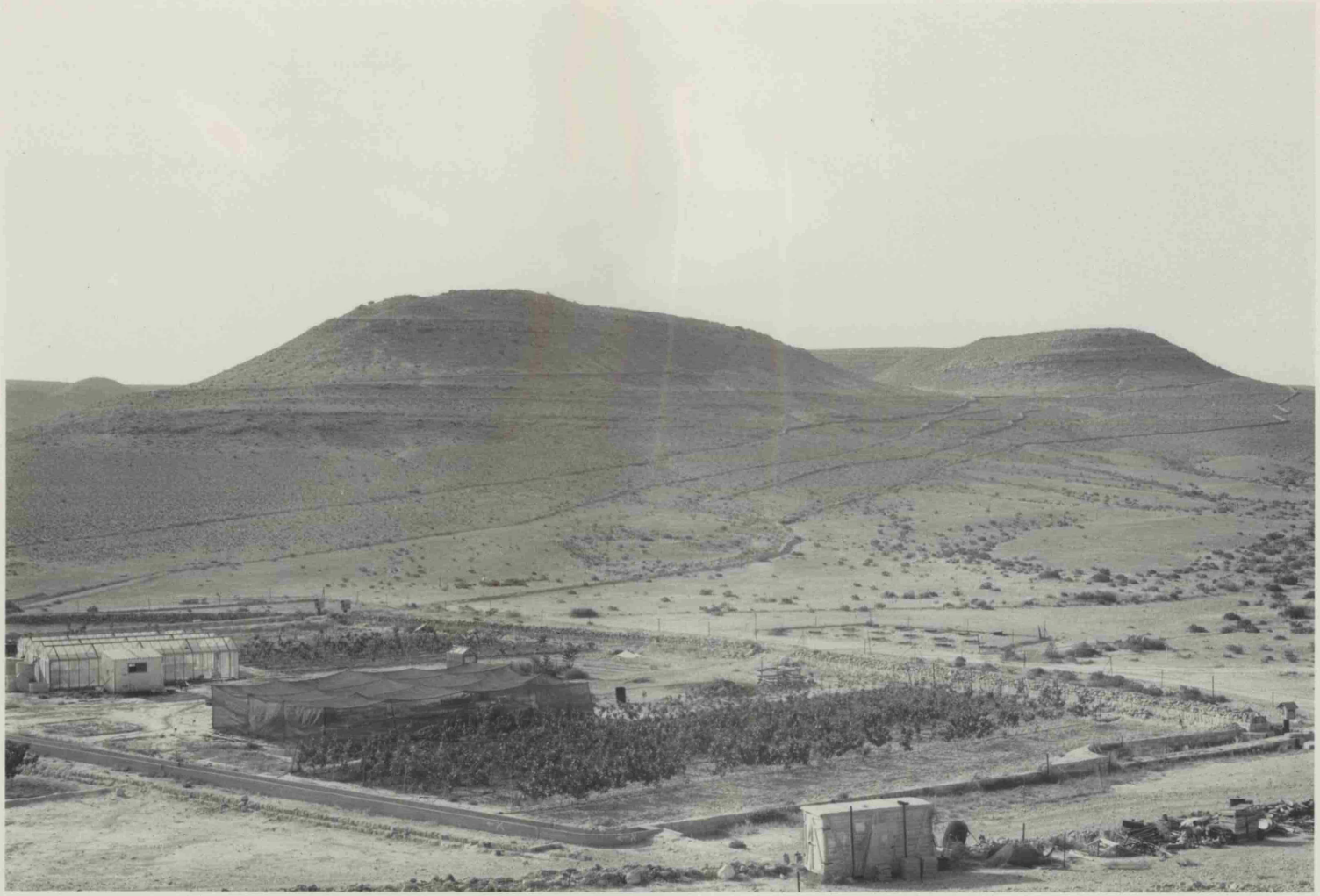

Plate C.2 Oblique view of the northern and southern knolls that form the eastern slope sections of the study catchment. Note the four man-made ditches routing water away from the midslopes and avoiding passage across the footslopes and into the natural wadi channel network. Note the stage recorders at the inlet to the farm upper terrace.

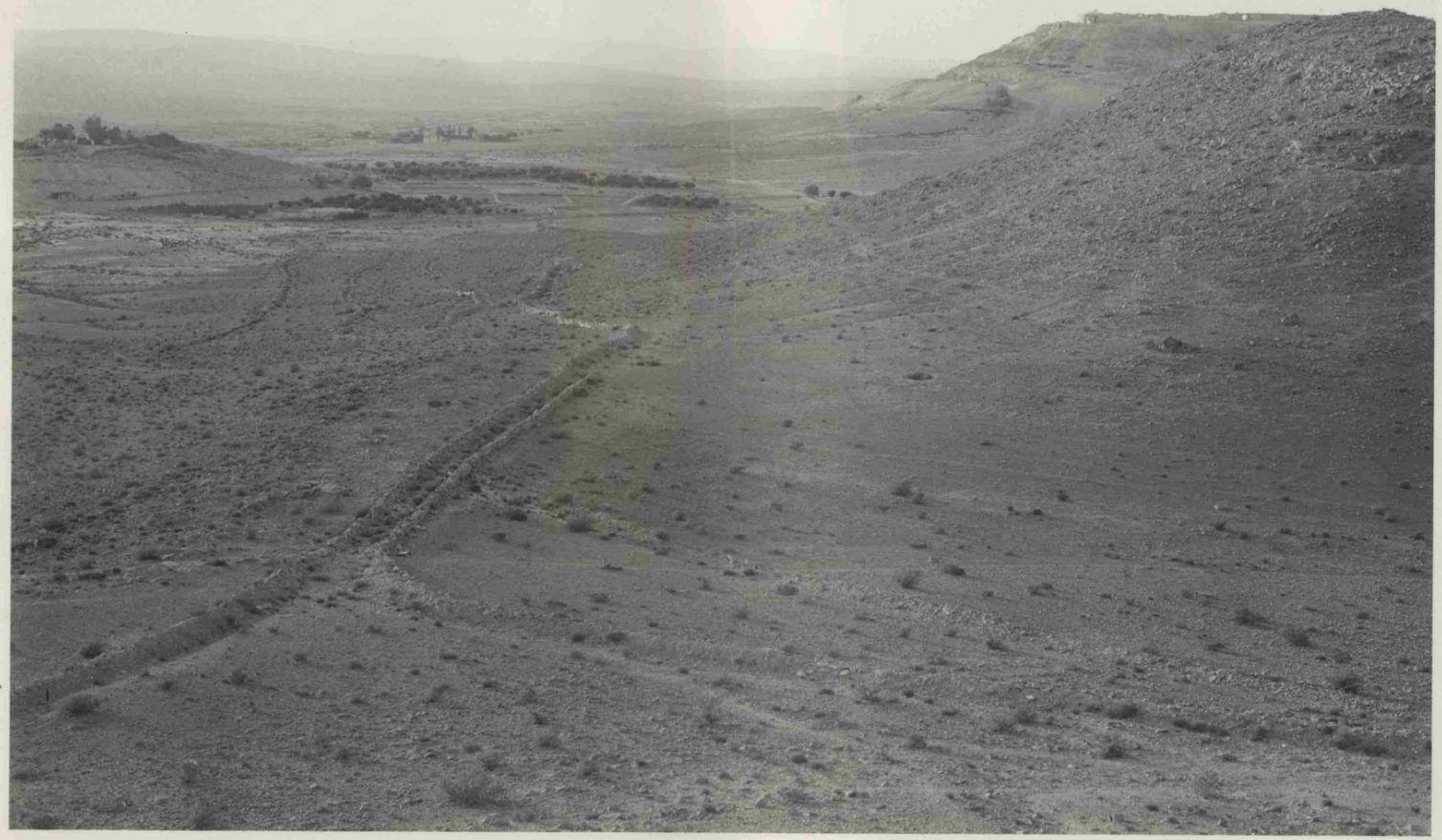

Plate C.3 Oblique view from the southern knoll northwards along the line of the man-made ditches collecting from the eastern slope sections.



Plate A.1 Stage recorder and weir apparatus at one of the seven inlets from the sub-catchments into the farm upper level terraces. Note stilling inlet at base of stand and recording arm marking revolving chart.



Plate A.2 Large-orifice recording raingauge (B on terrace). Note the revolving chart on which the rising level in the gauge reservoir is marked calibrated to mm rainfall equivalent.

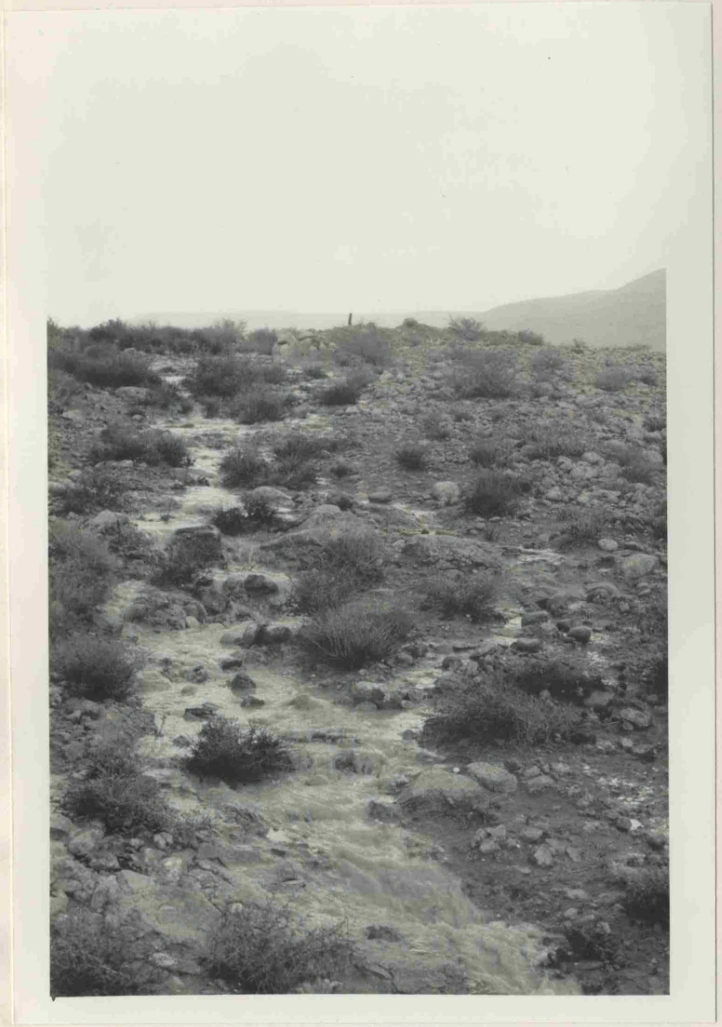

Plate F.1 An upstream view of concentrated rivulet flow discharging from the eastern hillslope unit 3 section into the lower ditch of sub-catchment four.



Plate F.2 An upsteam view of the man-made channel of sub-catchment 6 experiencing rapid flow across the steeply graded bedrock bed.



Plate F.3 The mid-section of ditch 6 collecting from the unit 4 sections of the eastern hillslope. Note rapid flow past Stage Recorder 11. Note marker in foreground indicating 5 metre distance.

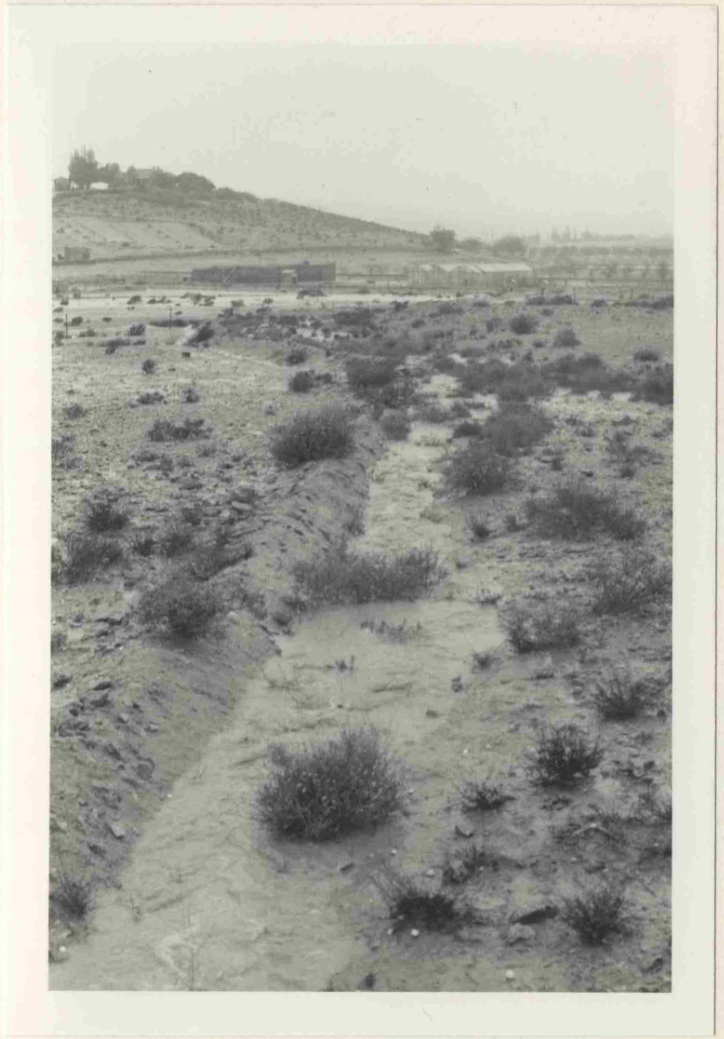

Plate F.4 The bottom section of the lower ditch of sub-catchment 4 looking downstream to the farm terraces. Contrast the nature of flow with the conditions in the wadi channels at a similar distance upstream.

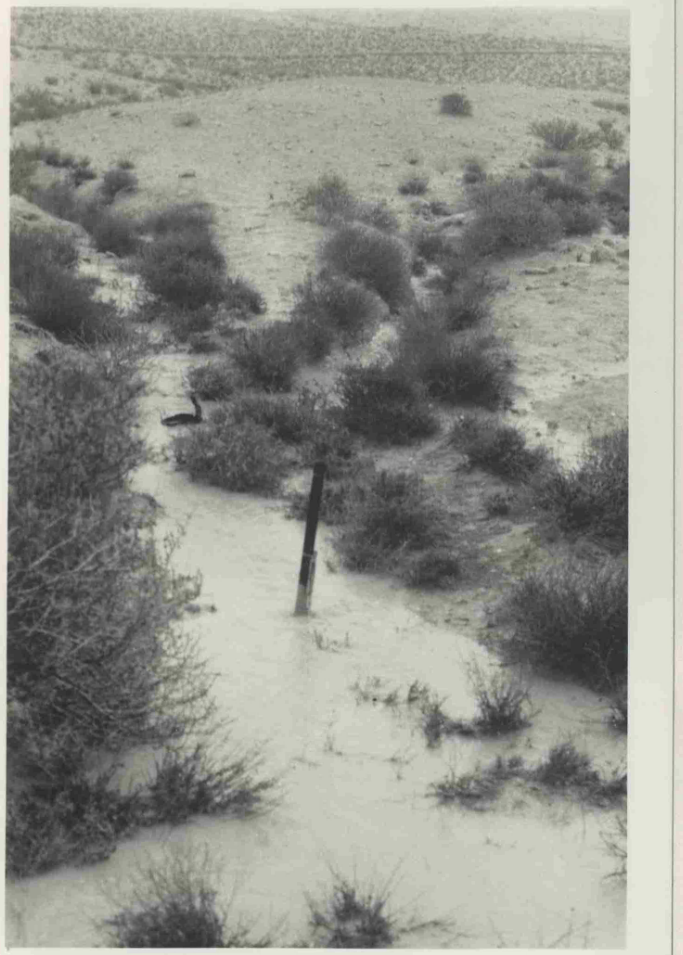

Plate F.5 Flow at the confluence of two branches upstream of Stage Recorder 14. Bankfull discharge is derived from remote rather than adjacent slopes.

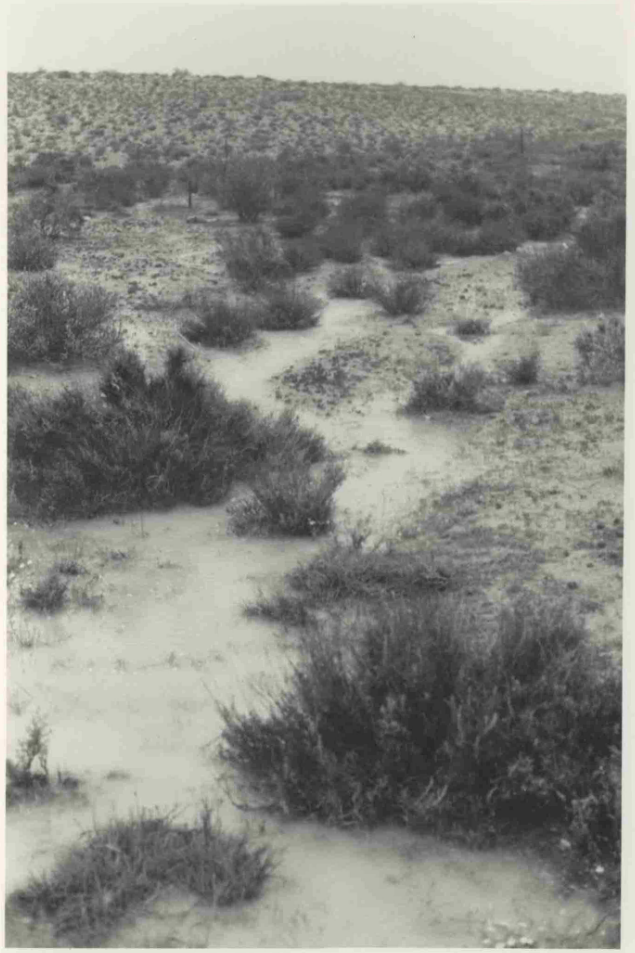

Plate F.6 Bankfull discharge flowing across the break in slope from the palaeo-terrace into the wadi-bed drainage system. Note extensive channel vegetation and consequent flow dissipation.

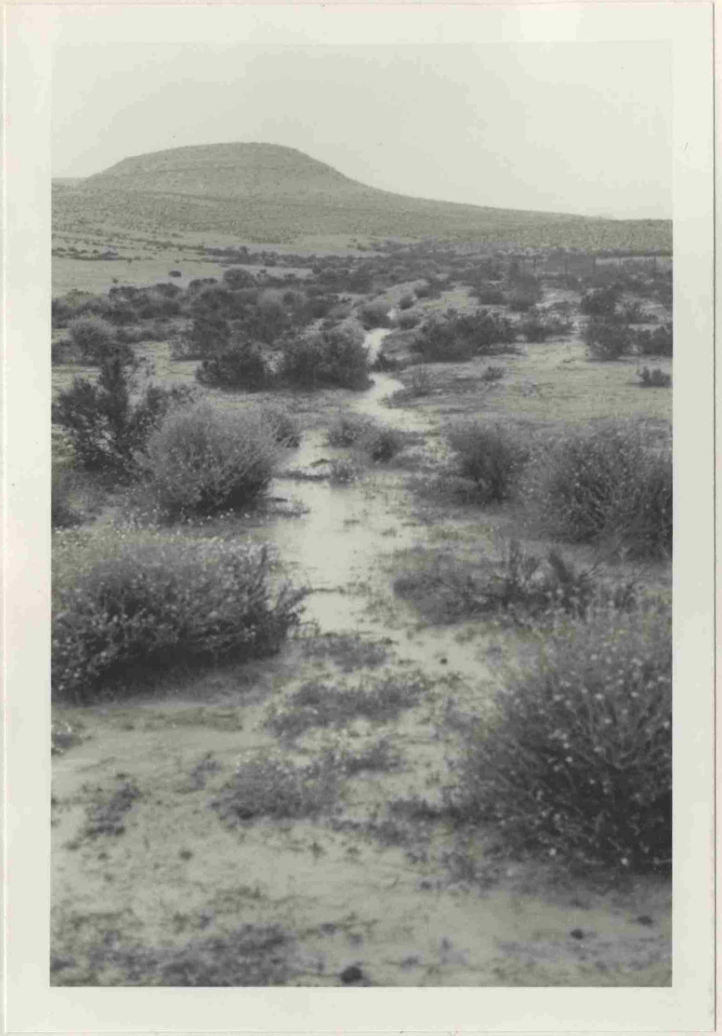

Plate F.7 Discharge along the man-made ditch collecting water from the natural channel flowing down from the terrace area of sub-catchment 2. See Plate F.8 to see its dissipation onto the wadi-bed above the farm.



Plate F.8 An upstream view back to the previous location showing the ponding and infiltration of outflow onto the wadi before the inlet to the upper terrace. Note vegetation density at exit of man-made ditch.

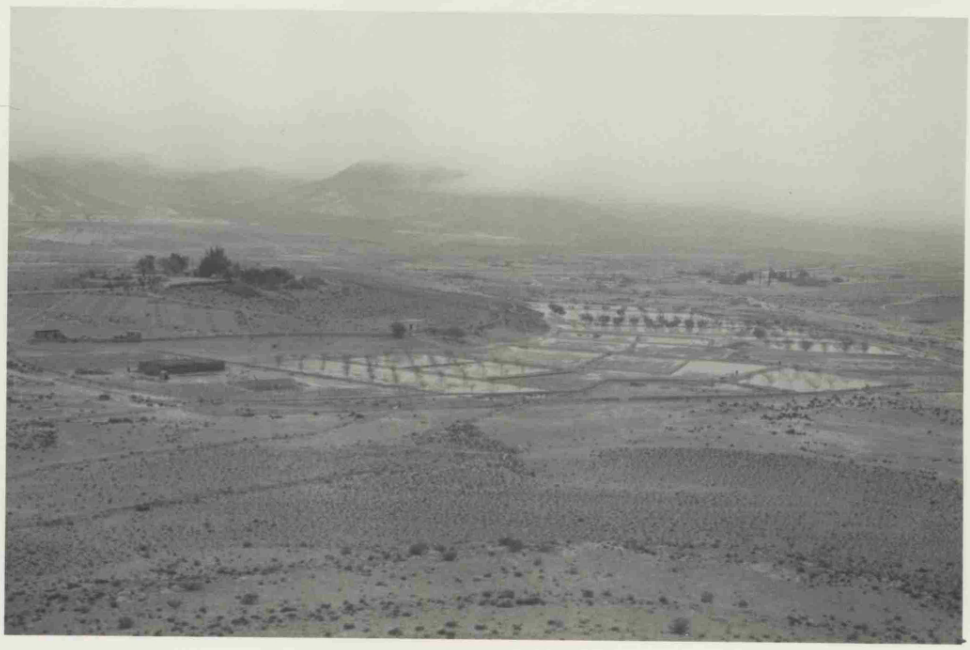

Plate F.9 View from the peak of the northern knoll looking north-west to the farm.



Plate F.10 The flooded terrace supplied by sub-catchment 7.
The ancient city of Avdat overlooks from the plateau.

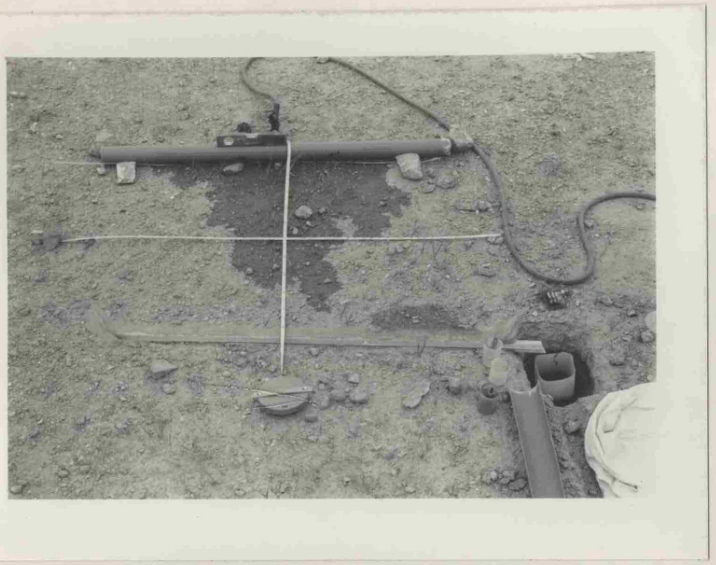

Plate I.1 View of infiltration plot - note spreader tube and catching trough.

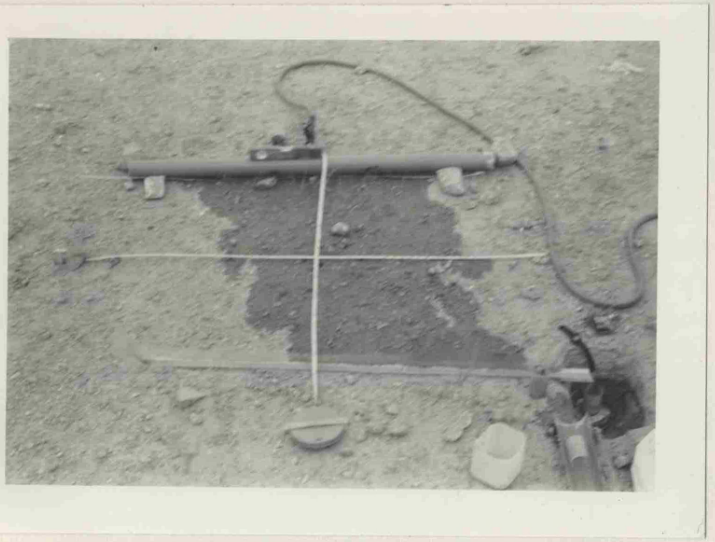

Plate I.2 View of wetted area spreading across the slope towards the trough.



Plate I.3 Close-up view of wetted plot - note water flowing out tube.

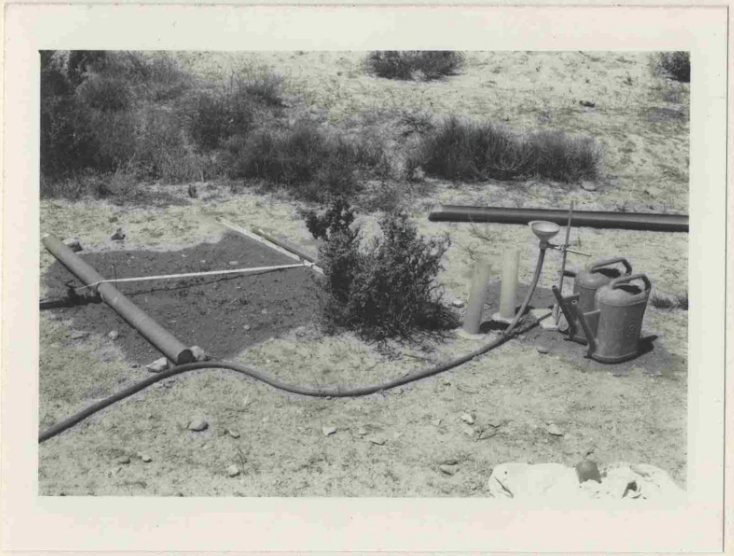

Plate I.4 View of complete experimental set-up of run-on/runoff infiltration plot. Note constant head device.



Plate P.17 Profile 2 Sample 1 Unit 1e



Plate P.18 Profile 2 Sample 2 Unit 1e (Run-on/Runoff Plot 18/1e)



Plate P.19 Profile 2 Sample 3 Unit 2e



Plate P.20 Profile 2 Sample 4 Unit 2e (Run-on/Runoff Plot 20/2e)



Plate P.21 Profile 2 Sample 5 Unit 2e



Plate P.22 Profile 2 Sample 6 Unit 3e



Plate P.23 Profile 2 Sample 7 Unit 3e (Run-on/Runoff Plot 23/3e)



Plate P.24 Profile 2 Sample 8 Unit 4e



Plate P.25 Profile 2 Sample 9 Unit 4e (Run-on/Runoff Plot 25/4e upper)



Plate P.26 Profile 2 Sample 10 Unit 4e



Plate P.27 Profile 2 Sample 11 Unit 4e



Plate P.28 Profile 2 Sample 12 Unit 4e (Run-on/Runoff Plot 28/4e lower)

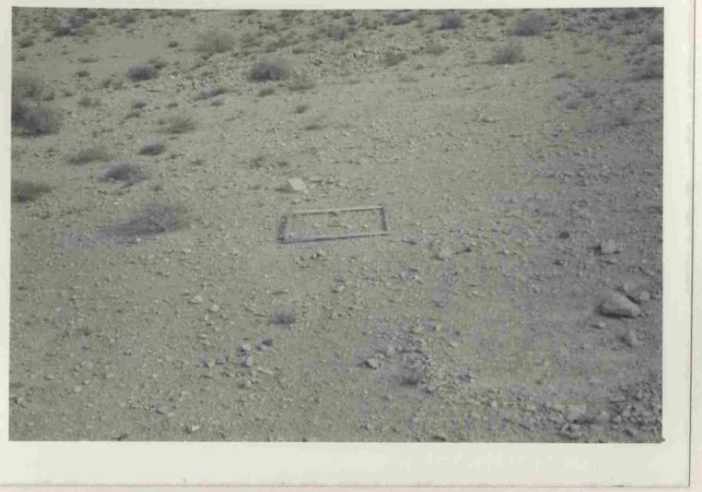

Plate P.29 Profile 2 Sample 13 Unit 4e



Plate P.30 Profile 2 Sample 14 Unit 5e



Plate P.31 Profile 2 Sample 15 Unit 5e



Plate P.32 Profile 2 Sample 16 Unit 5e (Run-on/Runoff Plot 32/5e)

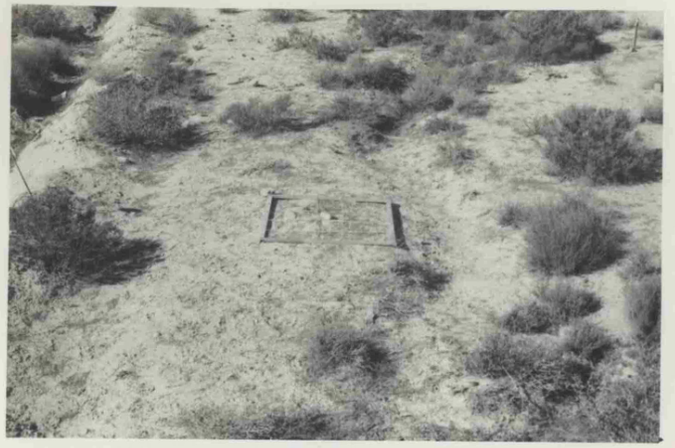

Plate P.33 Profile 2 Sample 17 Unit 5w



Plate P.34 Profile 2 Sample 18 Unit 5w (Run-on/Runoff Plot 34/5w lower)

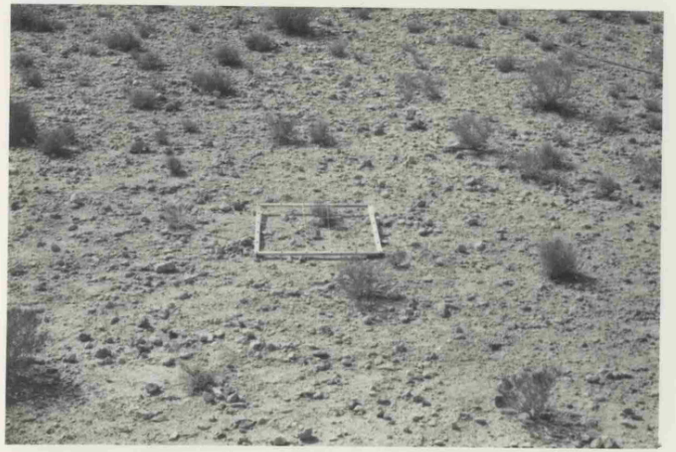

Plate P.35 Profile 2 Sample 19 Unit 4w



Plate P.36 Profile 2 Sample 20 Unit 4w (Run-on/Runoff Plot 36/4w)



Plate P.37 Profile 2 Sample 21 Unit 3w



Plate P.38 Profile 2 Sample 22 Unit 3w (Run-on/Runoff Plot 38/3w)

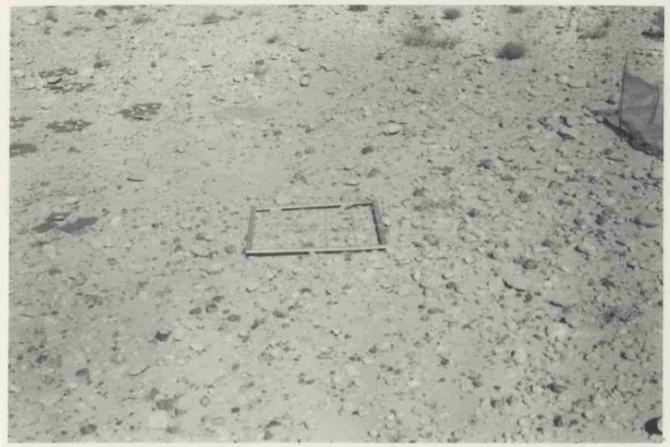

Plate P.39 Profile 2 Sample 23 Unit 6w



Plate P.40 Profile 2 Sample 24 Unit 6w



Plate P.41 Profile 2 Sample 25 Unit 6w

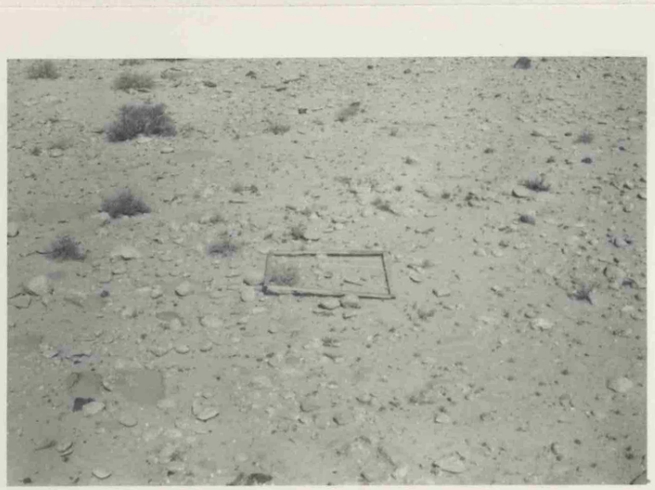

Plate P.42 Profile 2 Sample 26 Unit 6w (Run-on/Runoff Plot 42/6w)

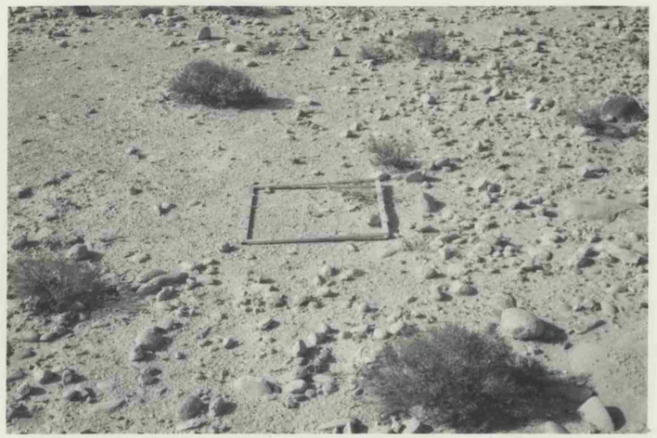

Plate P.43 Profile 2 Sample 27 Unit 6w



Plate P.44 Profile 2 Sample 28 Unit 6w



Plate P.45 Profile 2 Sample 29 Unit 4w

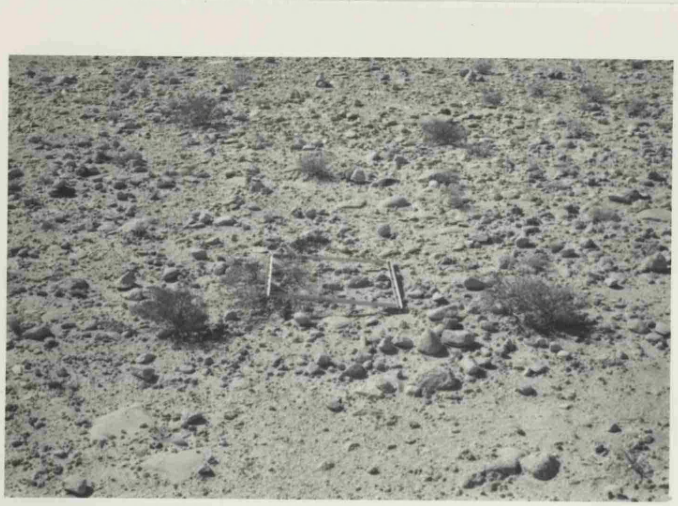

Plate P.46 Profile 2 Sample 30 Unit 4w



Plate P.47 Profile 2 Sample 31 Unit 5w (Run-on/Runoff Plot 47/5w upper)

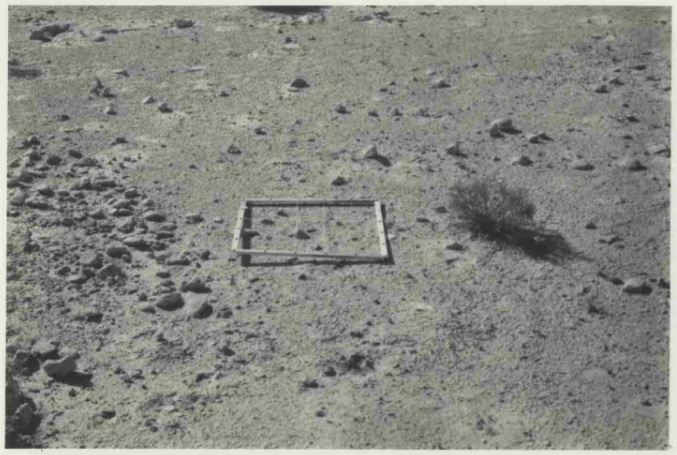

Plate P.48 Profile 2 Sample 32 Unit 5w

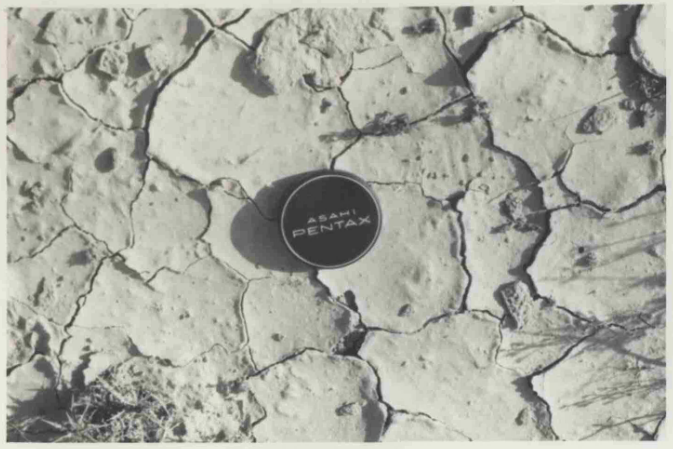

Plate L.1 Loessial crust surface on western terrace



Plate L.2 Loessial crust surface on wadi alluvium at foot of eastern hillslope profile



Plate L.3 Loessial crust following disturbance by grazing herd.



Plate L.4 Loessial crust following disturbance by porcupines. Note aggregate formation and depression storage excavation.

Appendix 1.1 An Annotated Aerial Photograph Showing the Location of Sample Flow-Line Profiles and Sample Locations

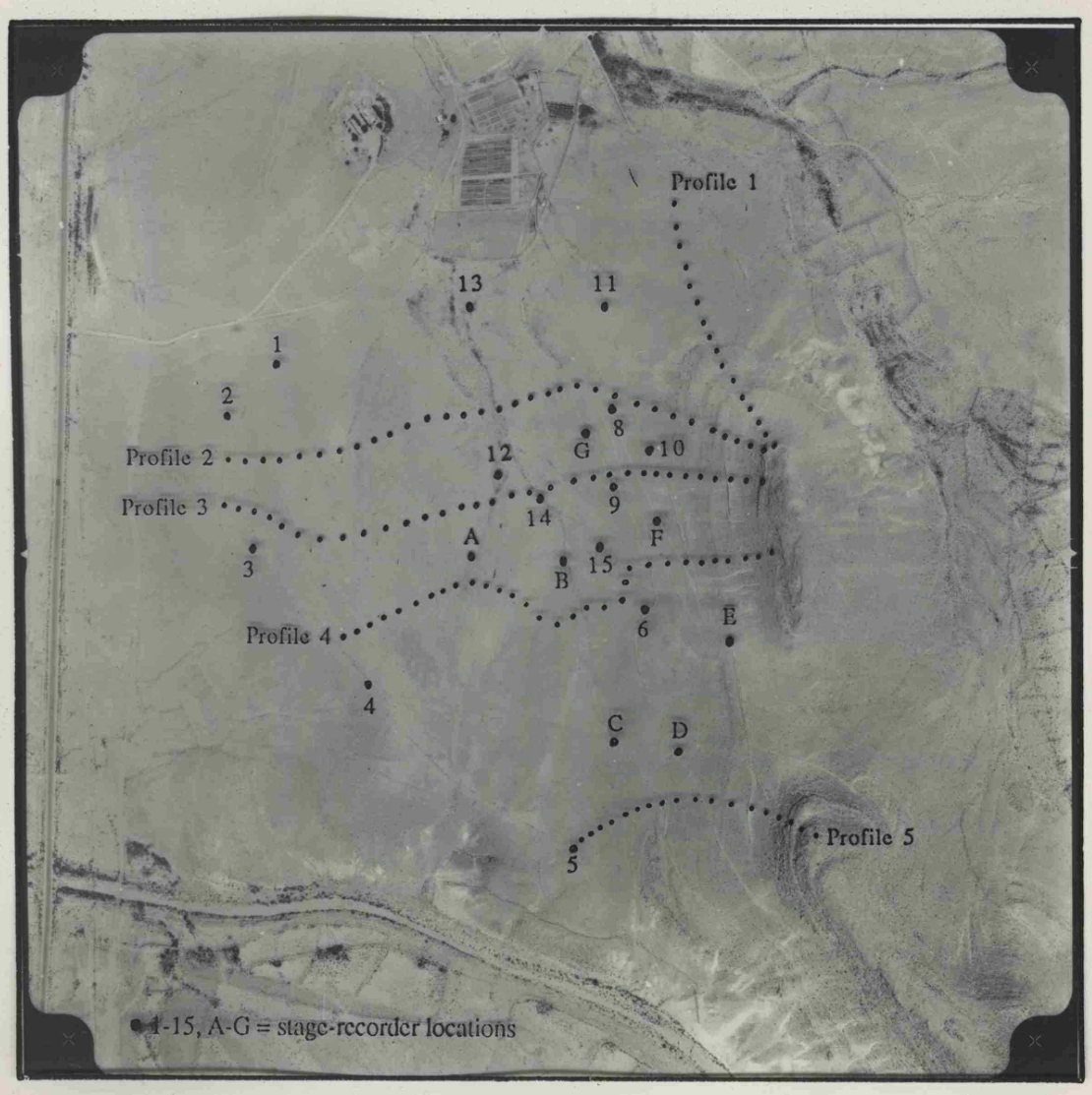

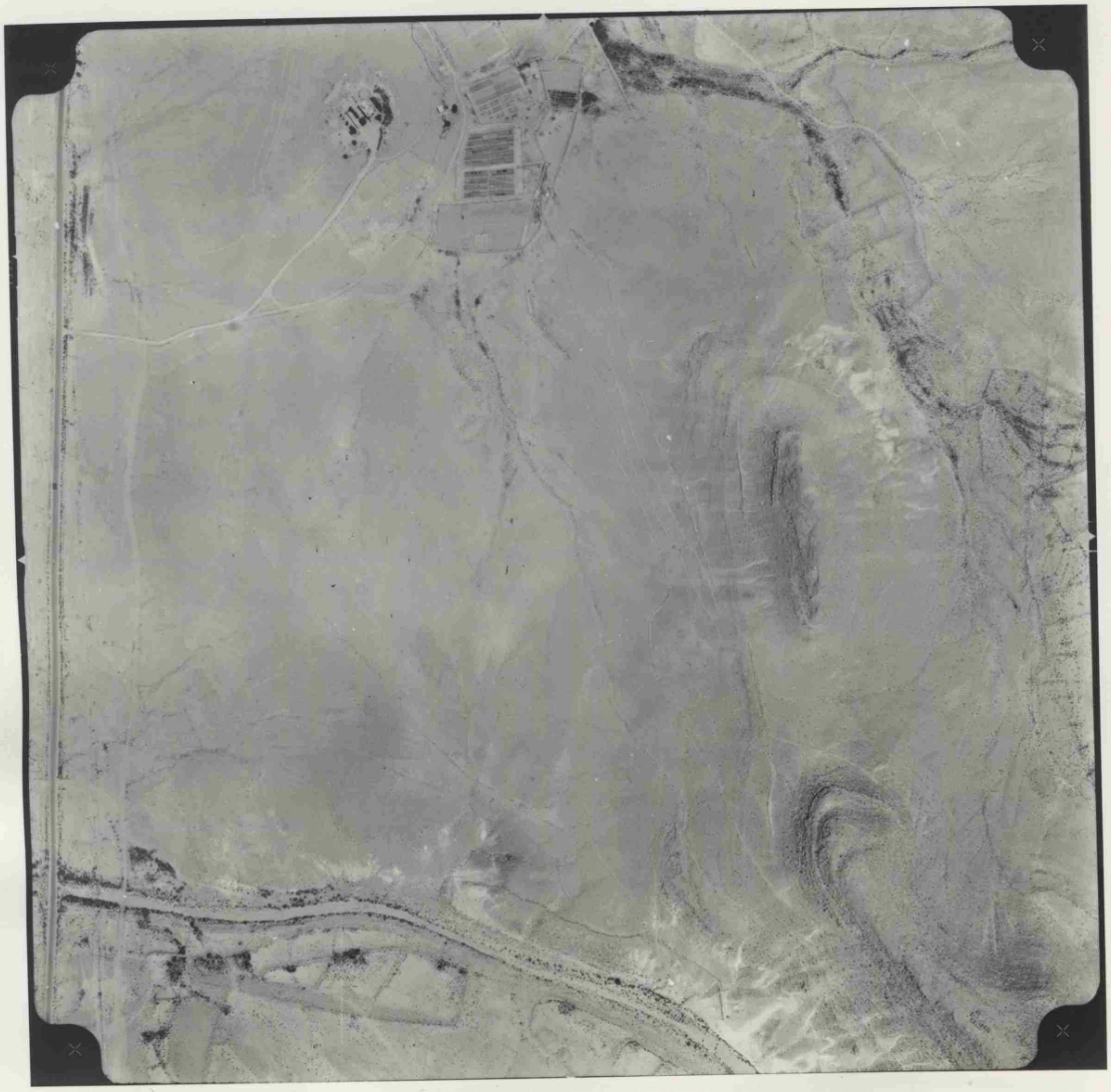

Appendix 1.2 The Sample Flow-Line Profiles in Cross-Section

The following diagrams show graphically the morphological character of each of the five flow-line profiles selected for the placement of sample plots, and the distribution of the unit types across them as identified by field estimation. This should be viewed in conjunction with the preceding aerial photograph and overlay Appendix 1.2 which shows the profile positions on the catchment surface, along with the placement of samples. In addition, Plates P.17 to P.48 provide a photo-transect across Profile 2, with a plate for each of the 32 plot sample environments.

Profile 1 Unit Arrangement

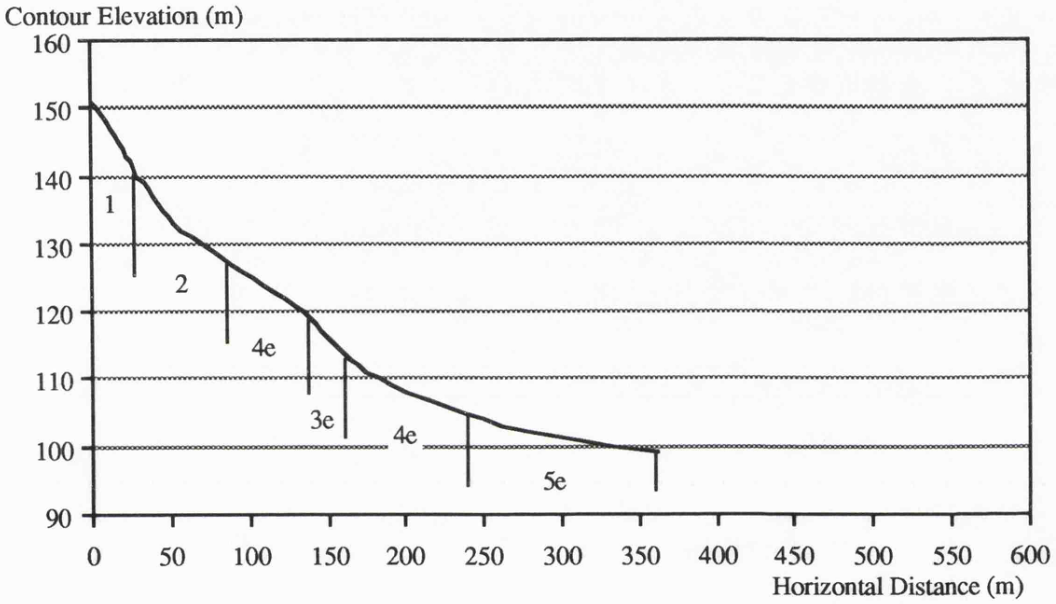

Profile 2 Unit Arrangement

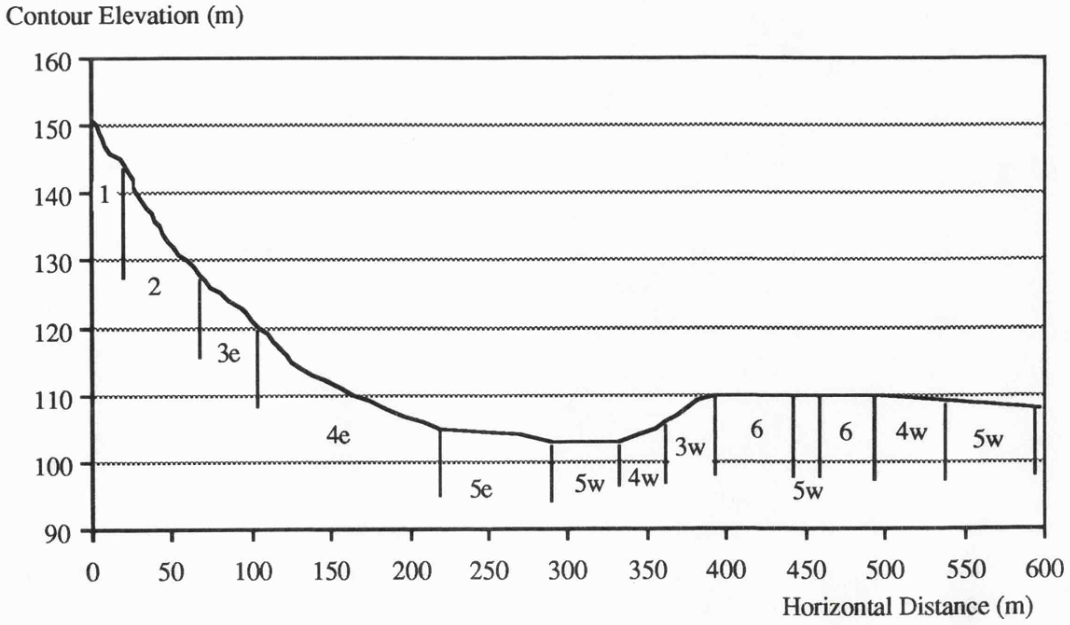

Profile 3 Unit Arrangement

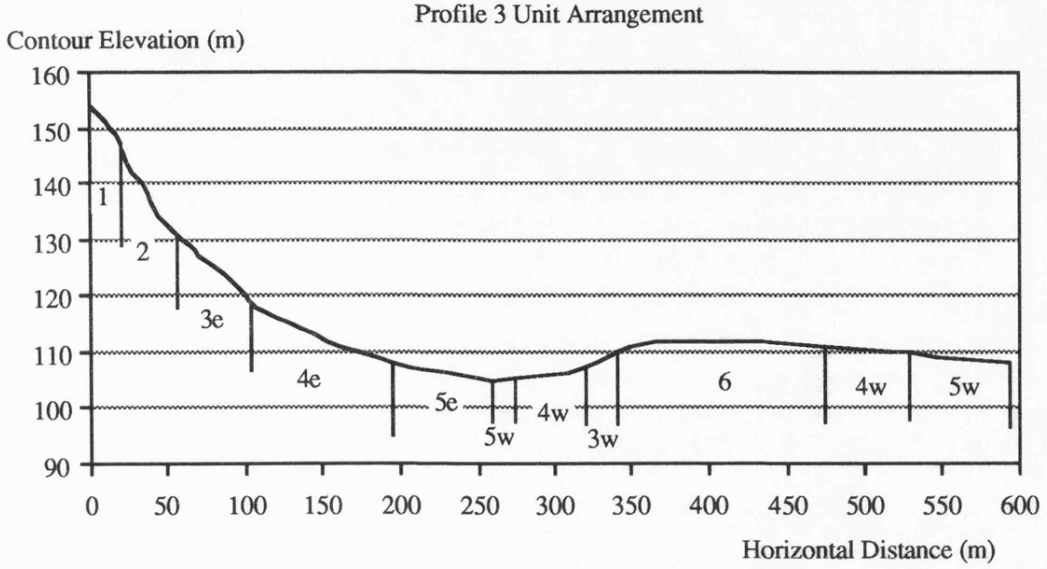

Profile 4 Unit Arrangement

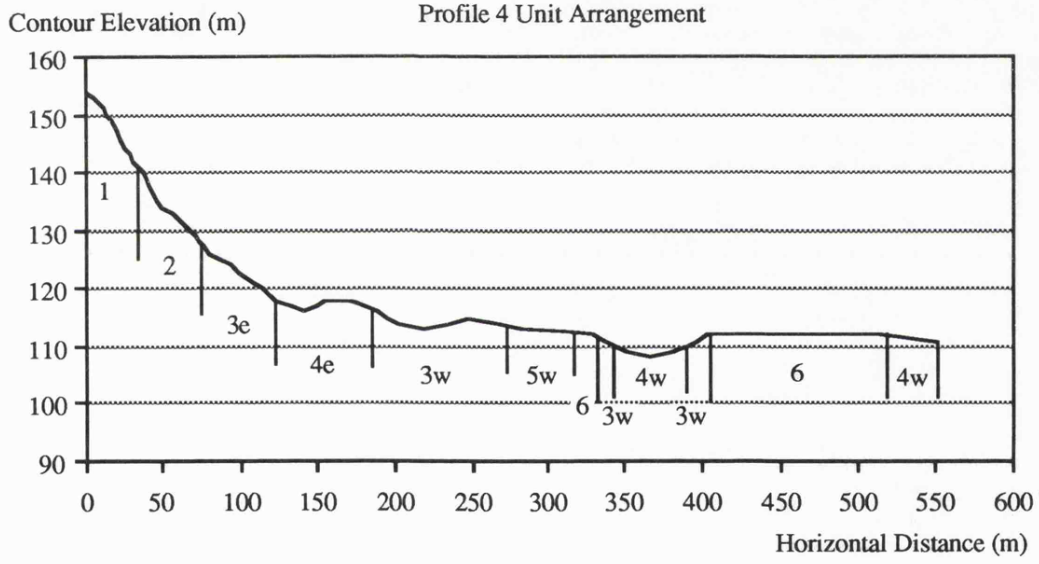

Profile 5 Unit Arrangement

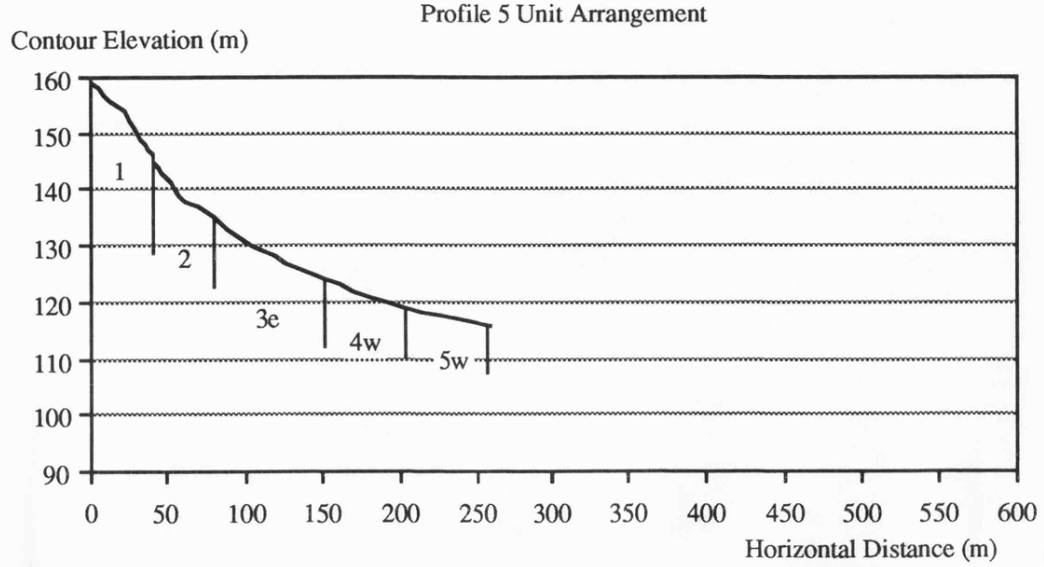

Appendix 1.3 Plot Sample Groupings by Overall Catchment Unit, and by Sub-Divided Unit

The field samples were positioned along the profiles in sequence from east to west.

Samples	Profile
1 to 16	One
17 to 48	Two
49 to 80	Three
81 to 111	Four
112 to 127	Five

1. The Unit Groups 1 to 6

	Profile 1	Profile 2	Profile 3	Profile 4	Profile5
Unit 1	1,2	17,18	49,50	81,82	112,113
Unit 2	3,4,5	19,20,21	51,52	83,84,85	114,115,116
Unit 3	8	22,23,24,37 38	53,54,55,68,	86,87,92,93, 94,95,96,101, 104	117,118,119, 120
Unit 4	6,7,9,10,11, 12,13,14,15	25,26,27,28, 29,35,36,45, 45,46	56,57,58,59, 60,61,66,67, 76,77,78	88,89,90,91, 102,103,110, 111	121,122,123
Unit 5	16	30,31,32,33, 34,41,47,48	62,63,64,65, 79,80	97,98,99	124,125,126, 127
Unit 6		39,40,42,43, 44	69,70,71,72, 73,74,75	100,105,106, 107,108,109	

2. The Sub-Divided Unit Groups 1e to 6w

	Profile 1	Profile 2	Profile 3	Profile 4	Profile5
Unit 1e (1)	1,2	17,18	49,50	81,82	112,113
Unit 2e (2)	3,4,5	19,20,21	51,52	83,84,85	114,115,116
Unit 3e (3)	8	22,23	53,54,55	86,87,92,93	117,118,119, 120
Unit 4e (4)	6,7,9,10,11 12,13,14,15	24,25,26,27, 28,29	56,57,58,59, 60,61	88,89,90,91	
Unit 5e (5)	16	30,31,32	62,63,64		
Unit 5w (6)		33,34,41,47, 48	65,79,80	97,98,99	124,125,126, 127
Unit 4w (7)		35,36,45,46	66,67,76,77, 78	102,103,110, 111	121,122,123
Unit 3w (8)		37,38	68	94,95,96,101, 104	
Unit 6w (9)		39,40,42,43 44,	69,79,71,72, 73,74,75	100,105,106, 107,108,109	

APPENDIX 1.4 A Simplified Example of the Methodology of Flow-Line Construction and Catchment Discretisation

Figure 1.4.1 is a simple imaginary contour map illustrating the position of the channels within the catchment and the location of nodes surveyed as spot-heights.

For the Avdat catchment, the nodes from which the flow-lines are constructed represent every 20m spacing (the survey spot-height channel nodes) from the outflow of a given network branch, with each point of confluence warranting a new flow-line, followed by a flow-line at the next 20m node (unless the next point of confluence is reached first) and so on. The flow-lines are drawn up both contributing slopes in the case of natural channels (where possible since the requirement for constructing a flow-line is that there is at least one metre, i.e. one contour, between the channel node and the divide) or up the single contributing slope in the case of the raised downslope bank artificial channel as shown in Figure 1.4.2.

The flow-nets provide the base for catchment discretisation through computerised digitisation of the sequences of flow-net nodes marked by each orthogonal and channel or contour intersection. The digitisation is performed based on the following procedure. Firstly on an overlay of the discretised flow-net, the channel network of the natural drainage, and the mostly linear artificial ditches are drawn along with the divides (which maybe the next ditch upslope) appropriate to each single branch. Secondly the branches are ordered according to a Strahler topological bifurcation network performed in reverse using a symmetrical individual numbering format. This is illustrated in Figure 1.4.3.

Taking the highest order channel branch as branch number 1 and working back upstream (hence a confluence becomes a division), the two branches into which it could divide are numbered 2 and 3, or more correctly n+n and n+(n+1). Taking branch 2 the two branches into which it could divide are numbers 4 and 5, and taking branch 3, it divides into the two branches numbered 6 and 7. This n+n and n+(n+1) numbering allows the computer algorithm for channel routing to know which channel branch number in a straightforward numerical loop discharges into which other channel in that loop, and can therefore preserve topological and gravitational sequences of the original (a requirement for an acceptable routing procedure). This numbering procedure illustrated in Figure 1.4.3 for a perfectly symmetrical five-order Strahler network allows the consideration of any shape of branching structure using the proviso that for an asymmetrical network, like that of the Avdat natural channels (see Appendix 3.1), the missing branches are filled with dummy branches with the real branches numbered according to the symmetrical n+n and n+(n+1) procedure. This is shown using the branching network of the hypothetical natural network in Figure 1.4.4.

The dummy branch is recognised during the simulation because the number of individual segments (the channel interval between two intersecting flow-line nodes) is set to zero in the parameterisation and the model ignores this branch for the simulation calculations. For the first-order channels, the routing algorithm that determines the loop structure automatically assumes the correct boundary conditions (i.e. no channel inflow for the uppermost segment) for the branch, as it does with the first branch downstream of the dummy sequence also.

Once the branches are numbered, the sequence (cascade) of trapezoids bounded by two adjacent flow-lines and the sequence of contours are counted in ascending order from the channel segment to the divide, taking each segment in turn from the lowest segment of each channel branch to its uppermost, numbering each segment in ascending order. For example if branch 3 has four segments the first will be segment 1 and the last segment 4. If the segment has two cascades contributing, the eastern cascade is numbered cascade 1 and the western number 2 (since all the channels have a general south-north alignment). If it has only one cascade due to being an artificial ditch or because of the difficulties in flow-line construction, it is numbered cascade 1. This is illustrated in Figure 1.4.5.

Each location in the catchment can be identified by its string of four numbers (i.e. four-dimensional array). Hillslope elements have the sequence (IC,IS,NC,I) where IC refers to channel branch, IS channel segment, NC hillslope cascade, and I element position in cascade, and channel segments have the notation (IC,IS).

Following this procedure for each element in each cascade into every segment in every channel branch, digitisation can be undertaken. Taking the highest numbered non-dummy branch, the segments are considered in turn from the highest number (uppermost) to the lowest number. For each segment the cascades are considered in turn, first cascade 1 and then, if present, cascade 2. Starting at the flow divide of the cascade (the top boundary of the uppermost, highest numbered element) the node on the upstream flow line is digitised followed by the node of the downstream flow-line, for the divide, then for each contour line, and finally for the channel segment itself giving n+1 pairs of digitised nodes for n cascade elements. This is repeated for the second cascade, and then for each successive segment down to segment 1 when the next highest numbered channel branch is selected for a repetition of the same process. This ensures that both the topological and the gravitational sequence of flow routing will be retained by the flow model on reading in the digitised data. This procedure is graphically illustrated in Figure 1.4.6 by the simple two-order catchment network illustrated below, the numbering sequence 1 to 72 illustrating the order in which the nodes are digitised for the second first-order branch number 3.

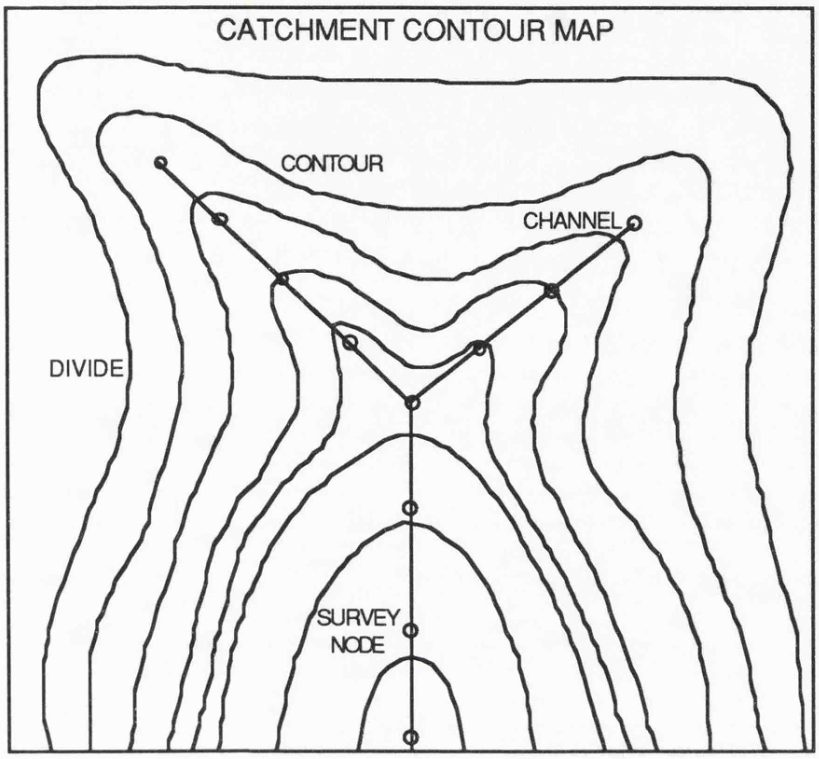

Figure 1.4.1 A Generalised Example Catchment Contour map

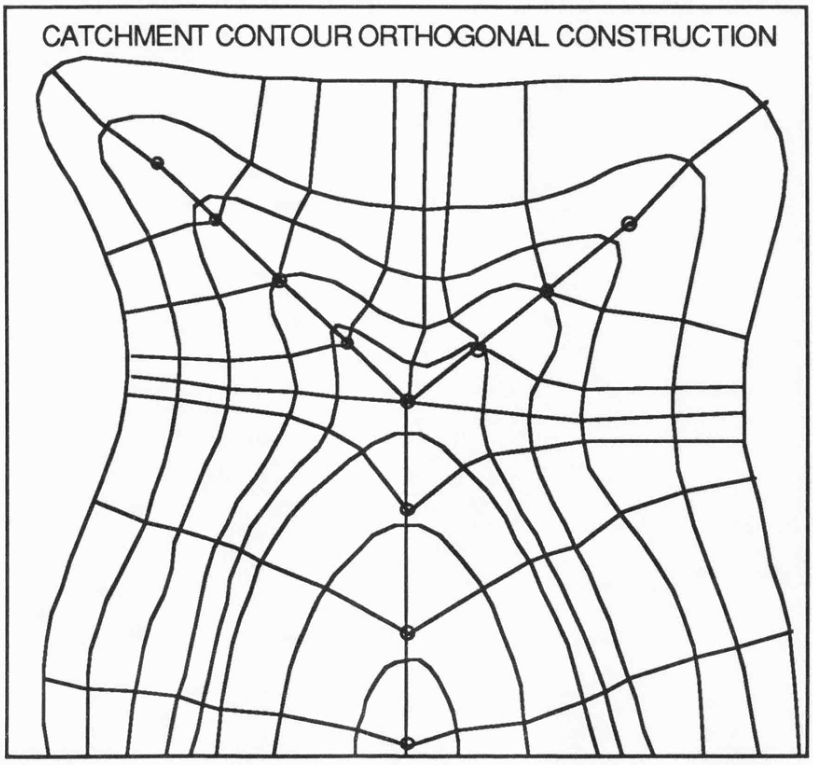

Figure 1.4.2 The Construction of Catchment Contour Orthogonal Flow Lines

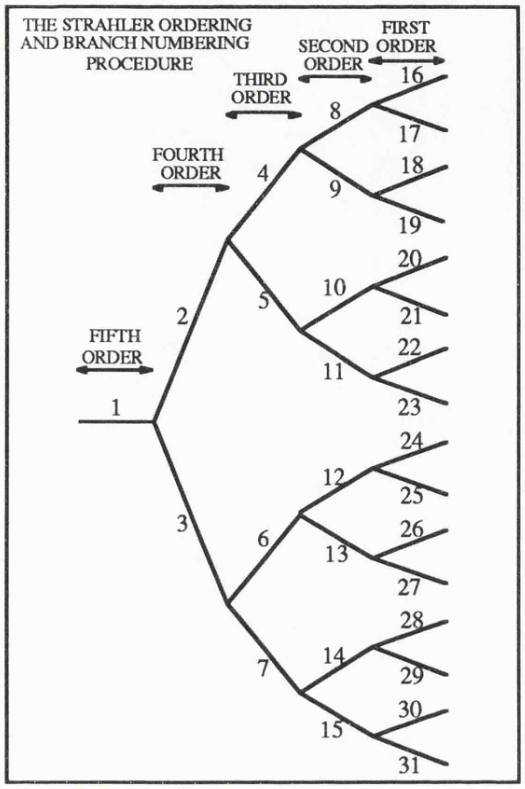

Figure 1.4.3 Channel Branch Ordering Notation

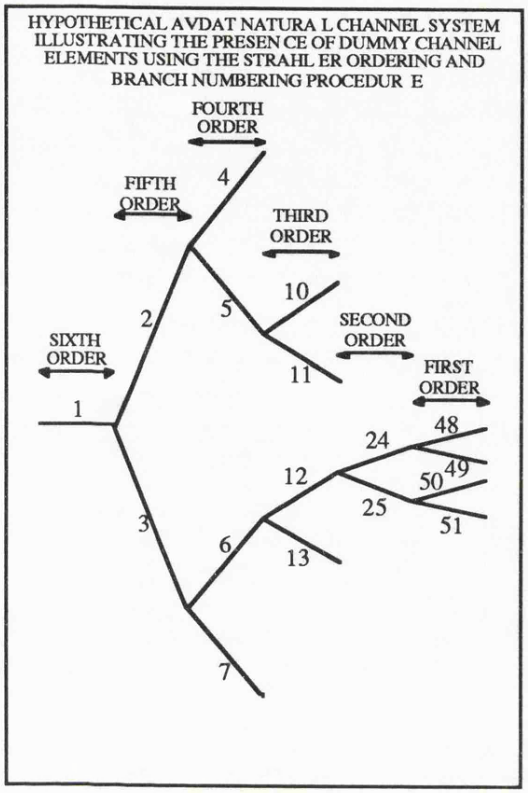

Figure 1.4.4 Illustration of Dummy Branches in the Channel Order

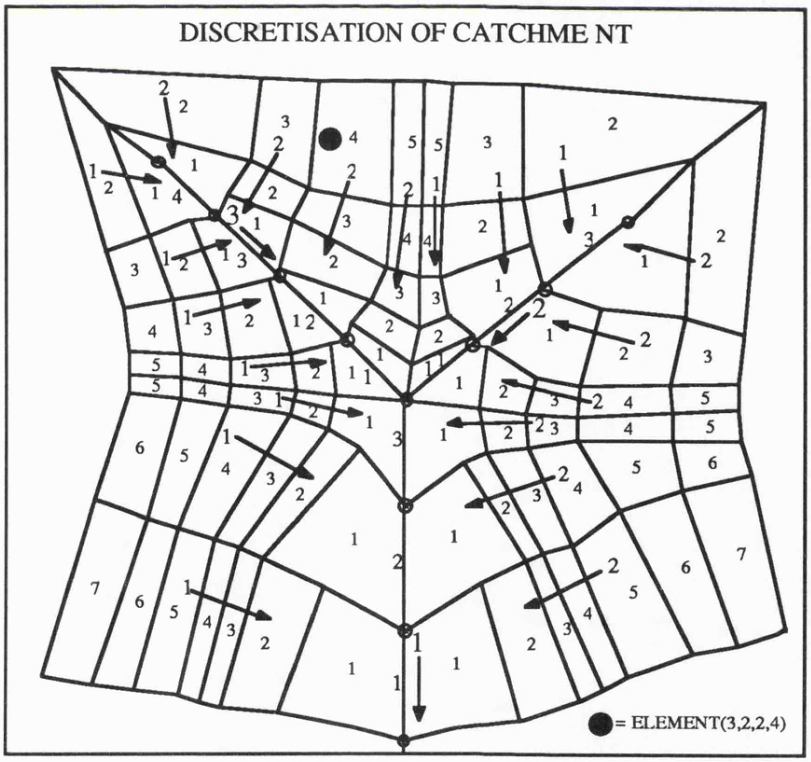

Figure 1.4.5 The Discretisation of the Example Catchment Flow Net

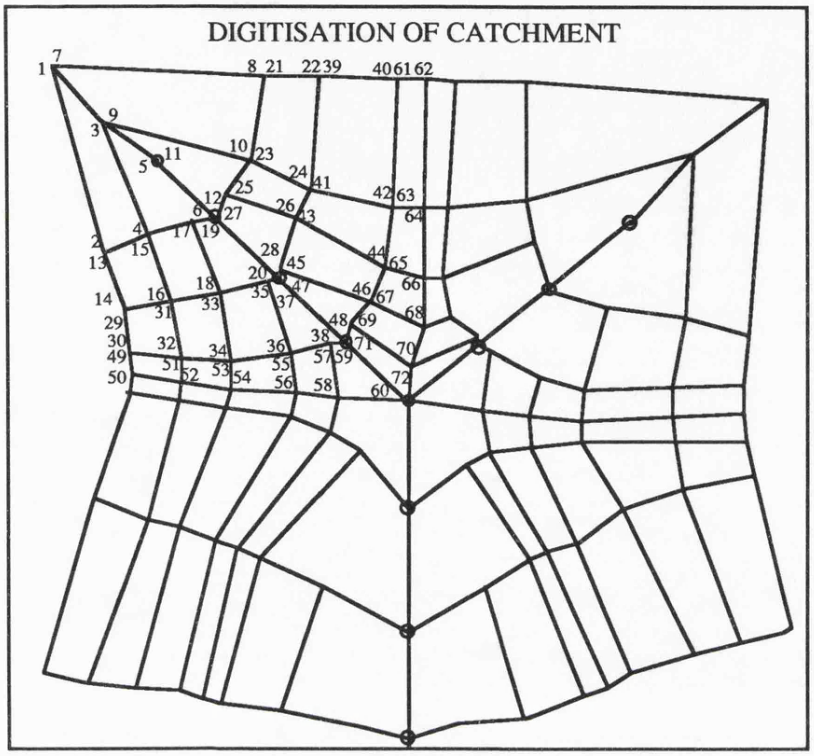

Figure 1.4.6 The Digitisation of the Imaginary Catchment Flow Net

Appendix 2.1.1 Selected Surface Material Characteristics for Each Sample Plot																
Profile	1	1	1	1	1	1	1	1	1	1	1	1	1	1	1	1
Plot	1	2	3	4	5	6	7	8	9	10	11	12	13	14	15	16
Unit	1e	1e	2e	2e	2e	4e	4e	3e	4e	4e	4e	4e	4e	4e	4e	5e
% bedrock	7.00	35.75	25.75	5.75	0.00	0.00	0.00	44.00	1.00	4.50	3.75	0.00	0.50	0.00	3.25	0.00
% stones	75.25	49.00	42.00	35.50	12.00	46.50	38.50	26.75	63.75	55.00	48.75	38.75	41.75	39.50	37.75	27.25
% fines	17.75	15.25	32.25	58.75	77.00	53.50	61.50	29.25	35.25	40.50	47.50	61.25	57.75	60.50	59.00	72.75
mean Ba mm	40.00	30.37	60.19	30.94	46.10	29.88	31.77	40.81	31.40	28.89	41.51	30.41	25.44	19.30	28.77	16.27
Profile	2	2	2	2	2	2	2	2	2	2	2	2	2	2	2	2
Plot	17	18	19	20	21	22	23	24	25	26	27	28	29	30	31	32
Unit	1e	1e	2e	2e	2e	3e	3e	4e	4e	4e	4e	4e	4e	5e	5e	5e
% bedrock	14.50	16.50	3.00	0.25	0.75	23.50	20.25	1.25	3.50	9.50	1.00	0.25	0.00	0.00	0.00	0.00
% stones	72.25	68.00	80.25	71.50	42.75	56.00	56.25	62.25	70.00	63.50	53.50	50.75	69.00	42.50	22.00	62.50
% fines	13.25	15.50	16.75	28.25	56.50	20.50	23.50	36.50	26.50	27.00	45.50	49.00	31.00	57.50	78.00	37.50
mean Ba mm	51.83	56.97	72.59	49.70	36.57	43.10	38.74	41.59	35.63	33.04	33.76	35.53	19.26	14.52	12.48	11.36
Profile	2	2	2	2	2	2	2	2	2	2	2	2	2	2	2	2
Plot	33	34	35	36	37	38	39	40	41	42	43	44	45	46	47	48
Unit	5w	5w	4w	4w	3w	3w	6w	6w	5w	6w	6w	6w	4w	4w	5w	5w
% bedrock	0.00	0.00	0.00	0.00	1.75	26.50	0.25	0.00	0.00	3.00	2.75	3.75	2.25	2.00	0.00	0.50
% stones	1.00	2.25	30.25	39.00	48.75	35.25	40.25	34.25	4.25	25.50	17.50	28.25	45.50	34.75	6.25	10.50
% fines	99.00	97.75	69.75	61.00	49.50	38.25	59.50	65.75	95.75	71.50	49.75	68.00	52.25	63.25	93.75	89.00
mean Ba mm	40.00	17.78	28.35	34.64	36.13	39.72	47.08	43.70	97.88	76.11	71.71	61.23	51.81	55.51	19.52	47.12
Profile	3	3	3	3	3	3	3	3	3	3	3	3	3	3	3	3
Plot	49	50	51	52	53	54	55	56	57	58	59	60	61	62	63	64
Unit	1e	1e	2e	2e	3e	3e	3e	4e	4e	4e	4e	4e	4e	5e	5e	5e
% bedrock	16.00	14.50	3.25	1.00	8.00	13.00	5.50	6.50	2.25	35.50	3.25	1.00	0.25	0.00	0.00	0.00
% stones	55.00	58.25	68.50	65.25	62.00	46.75	27.00	65.25	65.25	0.50	56.00	49.75	55.75	28.50	66.25	67.25
% fines	29.00	27.25	28.25	33.75	30.00	40.25	67.50	28.25	32.50	64.00	40.75	49.25	44.00	71.50	33.75	32.75
mean Ba mm	46.46	59.91	47.26	36.49	49.87	39.98	42.82	52.21	39.98	32.65	37.04	38.86	25.33	23.46	12.09	10.20
Profile	3	3	3	3	3	3	3	3	3	3	3	3	3	3	3	3
Plot	65	66	67	68	69	70	71	72	73	74	75	76	77	78	79	80
Unit	5w	4w	4w	3w	6w	6w	6w	6w	6w	6w	6w	4w	4w	4w	5w	5w
% bedrock	0.00	2.75	1.00	10.25	2.50	0.50	1.00	2.00	3.75	0.25	0.25	2.50	3.25	5.50	0.00	0.25
% stones	7.00	41.50	37.00	39.00	16.75	15.25	14.75	19.00	31.00	17.00	4.25	35.50	34.25	35.00	5.00	3.00
% fines	93.00	55.75	62.00	50.75	80.75	84.25	84.25	79.00	65.25	82.75	95.25	62.00	62.50	59.50	95.00	96.75
mean Ba mm	28.93	31.73	35.07	40.11	65.27	75.43	74.14	72.29	52.52	22.56	31.59	50.14	53.44	42.16	0.00	83.50
Profile	4	4	4	4	4	4	4	4	4	4	4	4	4	4	4	4
Plot	81	82	83	84	85	86	87	88	89	90	91	92	93	94	95	96
Unit	1e	1e	2e	2e	2e	3e	3e	4e	4e	4e	4e	3e	3e	3w	3w	3w
% bedrock	35.25	6.50	2.50	0.75	1.75	8.75	31.50	1.25	0.25	0.50	0.50	23.25	8.25	6.25	32.50	3.25
% stones	48.50	56.00	85.00	57.75	52.00	55.00	39.25	61.75	42.25	49.50	67.00	44.50	48.25	38.25	15.87	45.00
% fines	16.25	37.50	12.50	41.50	46.25	36.25	29.25	37.00	57.50	50.00	32.50	32.25	43.50	55.50	35.75	51.75
mean Ba mm	76.42	110.26	62.19	40.13	31.59	40.57	46.81	40.35	43.99	41.10	25.28	37.92	48.05	49.41	37.14	39.42
Profile	4	4	4	4	4	4	4	4	4	4	4	4	4	4	4	
Plot	97	98	99	100	101	102	103	104	105	106	107	108	109	110	111	
Unit	5w	5w	5w	6w	3w	4w	4w	3w	6w	6w	6w	6w	6w	4w	4w	
% bedrock	0.00	0.00	0.25	18.75	0.50	0.00	9.00	7.00	3.00	0.25	1.25	2.75	3.50	8.00	5.75	
% stones	20.50	24.25	10.50	32.00	43.50	29.00	39.75	21.25	13.50	18.75	17.25	22.00	20.75	34.25	41.50	
% fines	79.50	75.75	89.25	49.25	56.00	71.00	51.25	71.75	83.50	81.00	81.50	75.25	75.75	57.75	52.75	
mean Ba mm	19.07	19.11	18.55	34.37	46.24	47.42	40.13	57.05	56.85	73.48	36.07	63.70	71.60	81.70	80.70	
Profile	5	5	5	5	5	5	5	5	5	5	5	5	5	5	5	5
Plot	112	113	114	115	116	117	118	119	120	121	122	123	124	125	126	127
Unit	1e	1e	2e	2e	2e	3e	3e	3e	3e	4w	4w	4w	5w	5w	5w	5w
% bedrock	55.50	15.75	2.00	0.25	2.00	13.75	6.25	11.00	12.75	1.25	14.00	5.00	0.00	0.00	0.00	0.00
% stones	38.25	40.50	57.25	50.50	55.75	54.75	59.50	41.00	47.50	53.75	52.00	45.50	49.25	49.25	45.50	43.00
% fines	6.25	43.75	40.75	49.25	42.25	34.00	34.25	48.00	39.75	45.00	34.00	59.50	50.75	50.75	54.50	57.00
mean Ba mm	39.06	118.80	68.38	31.85	21.73	28.61	26.26	32.17	25.47	33.15	26.49	35.72	17.27	16.46	14.43	11.86

Appendix 2.1.2			Micro-Topographic Profile Standard Deviations from the Best-Fit Line											
			for Each Sample Plot (Cross-slope and Downslope)											
Profile	Sample	Unit	S.D.	plot	p1	p2	p3	p4	p5	p6	p7	p8	p9	p10
1	1	1e	Down	5.25	5.38	2.30	2.52	2.42	3.28	3.27	1.22	1.39	1.41	0.70
			Cross	4.93	6.56	3.47	3.91	2.00	2.02	3.00	4.31	5.18	9.52	5.56
1	2	1e	Down	16.88	2.56	2.78	4.38	0.82	5.69	1.68	26.06	4.08	15.06	13.70
			Cross	7.61	13.70	14.00	3.69	5.46	3.83	9.40	2.40	7.44	1.58	3.65
1	3	2e	Down	7.74	2.11	2.89	1.47	1.59	6.82	1.71	6.56	4.87	7.01	2.25
			Cross	4.94	6.21	3.14	5.85	9.61	2.77	2.17	4.68	1.65	3.87	6.81
1	4	2e	Down	2.68	0.92	2.04	1.92	1.27	1.23	1.31	0.64	1.34	1.40	2.76
			Cross	4.08	1.24	6.12	2.42	4.95	2.07	5.24	2.19	4.51	1.02	7.00
1	5	2e	Down	2.11	1.84	2.50	2.58	2.00	1.19	1.26	1.23	1.68	1.44	1.69
			Cross	2.72	2.24	3.12	3.02	2.51	2.68	1.79	2.00	1.11	2.34	5.10
1	6	4e	Down	1.60	1.33	0.66	0.89	1.70	1.01	0.47	1.77	1.25	1.72	0.93
			Cross	1.35	1.81	2.14	1.04	1.51	1.07	1.75	1.18	1.10	0.63	0.80
1	7	4e	Down	1.87	1.76	2.36	2.02	1.13	2.16	0.73	1.46	1.15	0.83	0.85
			Cross	1.91	1.52	1.32	3.41	2.46	2.23	0.74	1.23	1.52	0.95	2.50
1	8	3e	Down	12.00	9.15	2.01	10.33	2.70	9.10	2.26	9.03	2.71	10.22	2.35
			Cross	7.14	2.71	4.37	12.40	12.90	2.43	10.50	1.56	4.94	1.91	6.60
1	9	4e	Down	1.39	0.77	1.43	1.55	1.06	0.73	1.26	1.41	1.50	1.10	0.95
			Cross	1.47	1.65	1.24	1.49	1.64	1.15	0.61	2.82	1.39	1.01	0.87
1	10	4e	Down	1.45	1.81	0.94	1.53	0.85	1.25	0.85	1.33	0.88	1.18	1.31
			Cross	1.54	2.12	1.43	1.67	2.71	1.76	0.95	0.86	1.21	0.85	1.15
1	11	4e	Down	1.63	1.51	1.43	1.05	1.10	0.74	1.17	2.11	1.53	0.96	1.28
			Cross	6.70	5.59	3.04	1.01	2.52	1.62	1.96	2.61	1.46	1.84	2.14
1	12	4e	Down	1.02	0.91	1.01	1.10	0.91	1.19	0.82	0.74	1.23	1.15	1.03
			Cross	0.98	0.79	1.21	0.63	1.57	0.73	0.97	0.93	0.92	1.18	0.67
1	13	4e	Down	1.21	0.86	1.35	1.18	1.00	0.97	1.00	0.79	0.84	0.64	0.92
			Cross	0.97	1.20	1.01	0.81	1.06	0.59	0.98	0.57	1.28	1.08	1.12
1	14	4e	Down	1.01	1.32	0.52	0.42	0.39	0.68	0.84	0.64	1.23	0.74	0.40
			Cross	0.66	0.87	0.60	0.04	0.67	0.85	0.43	0.52	0.83	0.20	0.98
1	15	4e	Down	1.06	0.86	1.25	0.92	1.18	0.52	1.41	0.93	0.59	1.45	1.19
			Cross	1.09	0.88	1.48	0.96	1.14	1.65	0.78	0.83	1.17	0.67	1.23
1	16	5e	Down	0.49	0.39	0.66	0.59	0.62	0.57	0.42	0.36	0.40	0.32	0.34
			Cross	0.54	0.29	0.57	0.54	0.69	0.74	0.22	0.41	0.84	0.51	0.42

Appendix 2.1.2			Micro-Topographic Profile Standard Deviations from the Best-Fit Line for Each Sample Plot (Cross-slope and Downslope)											
Profile	Sample	Unit	S.D.	plot	p1	p2	p3	p4	p5	p6	p7	p8	p9	p10
2	17	1e	Down	5.13	1.25	3.24	1.34	1.71	7.42	4.02	1.67	3.01	7.31	3.17
			Cross	4.88	3.20	7.96	4.46	4.73	2.85	3.30	4.04	6.61	3.00	6.96
2	18	1e	Down	7.88	2.06	4.67	2.24	3.40	6.95	3.60	5.06	3.42	7.96	7.06
			Cross	6.18	2.83	10.50	3.51	6.68	9.57	5.37	6.90	5.49	4.02	3.33
2	19	2e	Down	6.84	2.19	5.77	5.30	9.00	5.77	4.76	3.55	6.92	5.60	6.27
			Cross	7.01	5.08	6.58	5.96	4.87	5.88	10.50	5.30	12.10	3.79	7.24
2	20	2e	Down	3.35	3.60	3.41	2.67	4.60	2.59	2.28	2.09	3.34	1.92	2.10
			Cross	3.32	2.29	4.04	4.08	4.60	3.03	5.20	1.31	1.66	3.55	1.73
2	21	2e	Down	2.21	1.32	1.43	2.03	0.97	1.41	1.07	1.83	0.77	1.65	1.24
			Cross	2.19	2.07	1.90	3.24	3.24	1.38	1.79	1.02	1.41	2.93	2.17
2	22	3e	Down	3.74	4.63	2.89	2.45	2.23	3.49	2.88	1.59	2.38	4.51	2.41
			Cross	3.93	4.60	4.16	3.95	2.18	2.80	6.80	2.75	4.47	3.46	3.05
2	23	3e	Down	3.09	1.56	2.99	2.28	1.38	4.98	2.14	1.75	1.52	1.00	2.97
			Cross	3.68	3.41	5.36	2.09	4.95	4.51	1.09	2.59	2.75	2.21	5.65
2	24	4e	Down	2.28	1.88	1.61	1.95	0.80	1.69	1.28	2.85	1.03	2.52	1.11
			Cross	3.52	3.50	3.04	2.26	2.10	2.01	7.64	1.72	3.68	2.83	3.44
2	25	4e	Down	1.70	0.98	0.92	1.25	1.29	1.20	1.13	2.22	2.15	1.80	2.17
			Cross	4.43	5.29	3.81	5.40	2.45	6.12	2.32	5.33	4.34	5.53	2.24
2	26	4e	Down	1.18	1.68	1.31	1.60	1.30	1.00	1.28	0.70	0.72	0.57	0.84
			Cross	2.65	2.45	3.62	2.96	3.00	1.78	2.75	2.23	2.63	2.94	2.33
2	27	4e	Down	1.71	1.89	1.76	1.08	1.20	1.23	0.92	1.71	1.16	1.55	0.89
			Cross	4.20	4.98	2.73	6.49	3.57	6.25	2.47	4.43	1.99	5.29	1.15
2	28	4e	Down	1.67	0.68	0.96	0.94	1.04	1.09	1.12	0.86	1.41	0.78	0.84
			Cross	3.47	6.03	4.37	3.39	4.07	1.45	3.23	2.41	2.44	3.81	1.99
2	29	4e	Down	0.87	0.52	0.63	0.92	0.38	1.31	0.87	0.50	0.51	0.50	0.67
			Cross	1.44	3.47	0.98	1.32	0.50	1.37	0.46	1.27	0.92	1.19	0.78
2	30	5e	Down	0.48	0.49	0.36	0.40	0.34	0.23	0.30	0.30	0.57	0.41	0.47
			Cross	2.97	3.28	3.29	3.12	2.84	3.50	2.50	3.54	2.35	2.13	2.55
2	31	5e	Down	0.62	0.65	0.38	0.52	0.40	0.57	0.53	0.67	0.13	0.33	0.30
			Cross	2.00	2.67	1.89	3.47	1.77	2.45	1.25	2.13	0.97	1.68	0.41
2	32	5e	Down	0.71	0.32	0.33	0.43	0.24	0.24	0.80	0.26	0.42	0.52	0.40
			Cross	1.16	1.20	0.85	0.90	1.09	1.16	1.27	0.72	1.39	1.43	1.55
2	33	5w	Down	2.58	1.10	0.84	2.34	2.52	1.41	0.38	0.63	0.76	1.15	0.69
			Cross	4.54	3.29	2.29	7.13	3.24	6.65	3.48	6.61	3.00	4.49	2.65
2	34	5w	Down	0.90	0.51	0.55	0.80	0.37	0.61	0.41	0.32	0.56	0.56	0.43
			Cross	1.32	1.04	1.12	2.24	0.87	1.44	0.88	1.51	1.00	0.84	1.78
2	35	4w	Down	1.30	0.57	1.08	1.50	0.70	0.95	0.62	0.69	1.19	0.66	0.83
			Cross	2.09	2.00	2.27	2.10	2.55	2.11	1.16	2.41	1.90	2.50	2.16
2	36	4w	Down	1.64	0.90	1.29	1.58	0.95	1.04	1.18	1.44	1.08	1.24	1.58
			Cross	1.66	1.70	2.56	1.48	1.14	1.31	1.26	3.17	1.07	0.81	0.96
2	37	3w	Down	1.47	1.74	1.21	1.27	0.84	0.87	1.46	1.08	1.57	1.20	1.45
			Cross	2.30	2.35	3.00	2.61	2.86	2.58	2.30	1.71	2.37	2.14	1.68
2	38	3w	Down	2.00	0.73	2.00	2.31	1.65	1.10	2.90	1.47	2.18	3.08	0.58
			Cross	3.51	3.53	2.81	2.58	3.14	3.78	4.41	3.40	4.29	3.98	3.56
2	39	6w	Down	2.00	0.73	2.00	2.31	1.65	1.10	2.90	1.47	2.18	3.08	0.58
			Cross	3.51	3.53	2.81	2.58	3.14	3.78	4.41	3.40	4.29	3.98	3.56
2	40	6w	Down	1.27	1.11	1.65	1.14	1.43	1.38	0.68	1.41	1.06	1.40	0.43
			Cross	2.97	3.40	2.69	3.23	2.46	3.61	2.97	3.51	2.79	3.08	2.40
2	41	5w	Down	0.92	0.81	0.85	0.89	0.81	0.68	1.13	0.88	0.92	0.99	0.80
			Cross	1.49	2.00	1.05	1.47	1.06	2.13	1.31	1.50	1.15	2.05	0.84
2	42	6w	Down	1.97	1.01	3.07	0.69	0.62	1.43	1.70	0.91	1.50	2.78	3.00
			Cross	1.64	0.98	0.91	1.12	2.51	2.37	1.59	1.96	0.98	1.25	2.05
2	43	6w	Down	1.50	2.29	1.57	0.81	1.78	1.04	0.93	2.00	0.49	1.14	0.62
			Cross	2.18	2.00	3.14	1.59	2.34	2.49	2.46	1.88	1.84	2.07	2.00
2	44	6w	Down	1.30	1.33	1.95	1.64	1.22	1.18	0.90	1.31	0.48	0.41	0.53
			Cross	1.93	1.49	2.15	1.30	1.70	2.22	1.80	1.54	2.04	2.67	2.41
2	45	4w	Down	1.72	1.49	1.08	2.10	0.66	1.47	1.03	2.45	1.22	1.21	1.33
			Cross	2.15	2.93	1.90	1.74	3.70	1.90	0.90	1.51	1.68	2.30	2.16
2	46	4w	Down	1.65	0.85	1.88	1.77	0.94	0.97	1.57	2.27	1.59	0.50	1.28
			Cross	2.09	0.91	0.62	1.76	2.09	1.12	2.55	2.78	2.90	2.35	2.77
2	47	5w	Down	0.83	0.56	0.27	0.89	0.84	0.39	0.34	0.25	0.93	0.28	0.42
			Cross	0.89	0.27	1.40	0.41	1.31	0.83	0.91	1.33	0.85	0.39	1.02
2	48	5w	Down	0.90	0.84	0.29	0.44	0.48	0.50	0.26	1.28	0.79	1.06	0.78
			Cross	1.15	0.87	1.18	1.16	0.78	2.09	0.74	0.68	1.45	1.13	1.02

Appendix 2.1.2			Micro-Topographic Profile Standard Deviations from the Best-Fit Line for Each Sample Plot (Cross-slope and Downslope)											
Profile	Sample	Unit	S.D.	plot	p1	p2	p3	p4	p5	p6	p7	p8	p9	p10
3	49	1e	Down	7.98	5.94	6.78	10.88	4.90	7.57	0.93	3.10	4.97	7.54	1.13
			Cross	6.72	1.14	8.23	8.16	7.26	4.78	4.50	11.10	5.38	6.43	7.01
3	50	1e	Down	9.20	5.38	3.13	11.85	7.92	6.82	2.11	5.37	2.98	7.35	3.16
			Cross	6.47	8.54	6.17	6.33	7.68	6.73	8.50	2.36	3.36	8.12	4.66
3	51	2e	Down	7.77	4.26	5.63	5.17	4.59	4.28	3.57	2.42	3.80	4.93	4.56
			Cross	4.77	10.20	4.53	3.76	4.03	3.38	4.03	1.48	3.08	2.90	4.69
3	52	2e	Down	3.72	2.80	1.91	1.48	2.24	2.75	1.40	2.74	1.81	3.58	2.20
			Cross	5.81	2.90	2.23	2.20	2.48	2.10	3.50	3.80	12.60	3.73	11.20
3	53	3e	Down	3.60	1.99	3.04	3.48	2.66	2.62	2.47	2.95	6.21	2.12	3.15
			Cross	3.35	6.10	2.20	1.98	1.40	2.75	3.10	2.14	2.50	3.87	5.13
3	54	3e	Down	3.71	1.20	2.36	2.22	2.17	4.75	1.52	1.96	2.77	1.63	4.20
			Cross	2.16	2.21	2.43	2.49	2.40	1.39	1.34	2.60	2.16	1.93	2.71
3	55	3e	Down	2.12	1.29	1.88	2.28	1.76	3.02	1.82	1.40	1.16	2.60	1.98
			Cross	2.44	3.25	2.36	2.20	2.00	2.08	2.92	2.86	1.90	1.52	3.39
3	56	4e	Down	3.71	2.00	4.62	1.47	1.99	1.75	1.23	2.28	1.73	2.20	2.19
			Cross	3.03	2.91	1.12	2.68	2.33	1.02	4.27	3.75	2.73	3.72	3.96
3	57	4e	Down	1.96	1.16	0.81	2.53	2.35	0.99	1.77	1.47	1.24	1.11	1.20
			Cross	1.91	2.81	1.00	1.14	0.75	2.51	2.78	2.28	1.76	1.05	1.75
3	58	4e	Down	2.32	1.18	0.79	1.46	1.53	1.14	1.53	0.78	1.51	1.24	1.40
			Cross	2.55	2.41	1.85	2.92	1.65	1.52	2.30	2.11	3.74	2.39	4.02
3	59	4e	Down	1.55	0.90	0.85	1.31	0.96	1.54	1.60	2.18	1.81	1.16	0.79
			Cross	2.47	3.23	2.19	2.24	2.98	1.83	1.97	2.45	2.11	3.96	1.21
3	60	4e	Down	1.46	1.36	0.95	1.15	1.38	1.05	1.71	1.02	0.85	1.75	0.97
			Cross	2.44	2.72	1.69	1.62	2.55	1.61	3.41	1.68	3.21	2.86	2.75
3	61	4e	Down	1.33	0.68	2.34	1.61	0.41	0.93	1.18	0.72	1.17	0.85	0.85
			Cross	1.77	2.06	1.90	1.91	1.86	1.86	1.94	1.99	1.48	1.05	1.82
3	62	5e	Down	1.58	0.64	0.92	1.96	0.45	0.61	1.32	0.84	1.42	0.39	1.00
			Cross	2.40	2.40	4.10	2.60	1.40	1.83	1.98	2.36	2.67	2.48	1.74
3	63	5e	Down	1.12	0.48	0.42	0.45	0.35	0.43	0.24	1.08	0.30	0.67	0.41
			Cross	2.24	1.41	5.30	1.23	2.93	1.28	1.18	1.39	2.00	1.52	1.63
3	64	5e	Down	0.79	0.43	0.44	0.47	0.70	0.60	0.57	0.25	0.59	0.50	0.37
			Cross	0.63	1.09	0.43	0.47	0.29	0.27	0.47	0.79	1.01	0.60	0.45
3	65	5w	Down	2.31	0.91	0.84	1.28	1.43	0.77	1.19	1.47	1.64	0.98	1.14
			Cross	2.68	1.79	0.50	2.39	1.85	2.51	2.00	3.68	2.08	3.95	4.34
3	66	4w	Down	1.59	1.24	1.47	1.20	1.17	1.28	1.63	1.84	1.42	1.17	0.77
			Cross	1.94	1.81	1.68	1.36	2.30	2.18	1.46	1.84	1.48	2.24	2.95
3	67	4w	Down	1.97	0.84	1.22	1.05	2.36	0.83	1.53	1.39	0.97	0.81	4.13
			Cross	2.22	2.48	2.57	2.44	1.74	2.63	1.56	1.76	3.54	2.07	0.88
3	68	3w	Down	1.52	1.01	1.45	1.12	2.39	1.15	1.72	1.51	1.57	0.84	1.14
			Cross	2.44	2.78	2.20	2.15	1.98	1.74	2.30	3.89	1.48	1.89	3.45
3	69	6w	Down	1.36	0.88	0.46	0.62	0.51	2.14	1.14	1.11	1.02	2.72	0.82
			Cross	1.34	1.38	1.67	1.73	1.17	1.36	1.82	1.13	1.01	0.96	1.20
3	70	6w	Down	2.38	0.76	1.71	0.33	2.47	0.52	0.72	2.00	3.93	4.28	2.22
			Cross	1.73	1.97	2.22	1.44	1.21	1.29	1.30	2.86	1.86	1.52	1.28
3	71	6w	Down	1.58	0.51	0.42	0.69	1.42	1.16	2.29	1.22	3.32	0.85	0.33
			Cross	1.76	1.43	1.32	1.46	1.86	1.27	1.99	2.70	2.14	0.69	2.27
3	72	6w	Down	2.25	1.28	2.80	2.74	1.45	1.79	1.85	2.13	0.92	2.00	3.33
			Cross	2.05	2.13	2.25	2.27	1.96	1.51	2.13	1.56	2.20	1.77	2.85
3	73	6w	Down	1.51	0.88	0.93	1.29	1.03	1.12	1.26	2.71	0.72	0.91	1.33
			Cross	2.13	3.25	2.13	2.42	1.87	1.90	2.56	2.21	1.36	1.80	1.67
3	74	6w	Down	0.90	1.14	0.44	0.80	0.64	0.89	0.33	0.76	0.45	0.59	0.47
			Cross	1.64	0.98	0.91	1.12	2.51	2.37	1.59	1.96	0.98	1.25	2.05
3	75	6w	Down	0.76	0.32	2.72	0.70	0.44	0.27	0.32	0.23	0.76	0.42	0.39
			Cross	1.05	1.01	10.00	1.13	0.66	0.91	0.38	1.12	0.95	0.80	2.04
3	76	4w	Down	1.73	0.57	0.69	0.98	0.80	1.48	0.47	2.20	2.70	1.25	3.05
			Cross	2.21	2.00	1.74	1.90	3.08	2.43	1.64	2.09	1.53	1.55	3.62
3	77	4w	Down	1.88	1.27	1.33	1.25	0.76	1.45	2.52	1.58	1.81	1.08	2.89
			Cross	2.16	0.51	2.89	1.29	1.45	1.68	1.96	2.43	3.20	3.32	1.57
3	78	4w	Down	1.87	0.98	3.15	1.74	0.66	0.72	2.22	1.92	1.04	1.57	1.97
			Cross	2.12	1.89	4.06	1.86	2.56	1.49	1.78	1.60	1.65	1.58	1.92
3	79	5w	Down	0.81	0.60	0.26	0.24	0.50	0.39	0.26	0.91	0.76	1.01	0.54
			Cross	1.39	1.03	0.47	0.98	2.37	2.05	1.34	1.68	1.36	0.93	0.94
3	80	5w	Down	0.73	0.23	1.52	0.49	0.66	0.49	0.32	0.80	0.25	0.63	0.21
			Cross	1.22	0.77	1.35	1.00	1.21	1.30	0.97	1.05	1.82	8.00	1.78

Appendix 2.1.2			Micro-Topographic Profile Standard Deviations from the Best-Fit Line for Each Sample Plot (Cross-slope and Downslope)											
Profile	Sample	Unit	S.D.	plot	p1	p2	p3	p4	p5	p6	p7	p8	p9	p10
4	81	1e	Down	7.65	3.91	4.71	6.36	9.26	7.24	6.77	5.47	3.98	8.28	5.44
			Cross	7.51	8.15	14.70	7.13	6.61	10.40	3.01	5.55	5.41	3.78	4.44
4	82	1e	Down	6.48	5.65	2.50	1.90	3.96	4.22	6.54	8.71	5.13	5.51	8.14
			Cross	8.21	9.01	8.45	3.54	4.61	4.79	11.18	15.30	7.59	6.91	4.14
4	83	2e	Down	5.22	2.34	2.44	2.39	3.19	1.89	2.32	5.37	2.52	7.60	2.21
			Cross	4.05	2.87	2.70	2.53	3.14	2.12	3.46	3.52	4.14	8.82	4.06
4	84	2e	Down	3.63	1.32	2.81	2.23	2.35	1.20	2.55	2.42	1.19	3.78	1.48
			Cross	4.19	2.44	7.29	4.36	1.41	4.99	2.49	3.33	1.71	5.05	5.73
4	85	2e	Down	3.41	0.80	0.86	2.63	1.61	4.04	4.02	2.46	2.17	2.05	1.53
			Cross	11.33	19.70	7.33	12.70	4.76	12.60	6.81	16.30	6.00	13.50	5.84
4	86	3e	Down	4.57	4.87	3.75	2.85	1.64	3.72	1.90	1.71	1.47	1.05	1.02
			Cross	11.73	15.50	7.50	23.10	8.27	15.20	6.64	9.32	5.49	11.70	4.10
4	87	3e	Down	4.43	1.12	3.76	3.45	5.96	2.35	3.28	2.47	2.34	2.00	1.89
			Cross	6.04	2.10	1.83	4.16	5.21	3.91	2.29	7.00	3.55	13.30	8.77
4	88	4e	Down	2.08	1.41	1.84	0.34	2.49	2.23	2.32	1.75	1.09	1.95	1.61
			Cross	2.83	4.69	3.33	3.59	1.66	1.74	1.70	2.40	2.79	3.48	1.90
4	89	4e	Down	3.54	1.47	1.25	1.60	2.06	1.84	1.62	1.24	2.73	2.09	1.17
			Cross	3.48	4.90	2.09	1.26	3.09	2.52	3.52	1.85	2.53	3.51	6.79
4	90	4e	Down	1.72	0.94	1.27	2.50	2.09	1.29	1.60	1.63	1.21	1.45	1.23
			Cross	1.88	1.22	1.71	2.34	1.77	1.44	1.91	2.19	1.42	2.88	1.75
4	91	4e	Down	1.46	1.13	0.70	0.80	0.79	0.66	1.36	1.21	0.85	0.58	0.75
			Cross	1.54	1.20	1.45	0.95	1.55	2.00	1.36	1.47	2.19	1.86	1.59
4	92	3e	Down	3.51	1.63	2.25	1.46	1.71	2.16	3.38	11.39	4.61	2.23	3.60
			Cross	2.97	0.65	3.87	1.84	1.26	4.73	5.52	2.01	1.08	3.09	2.14
4	93	3e	Down	1.59	1.20	1.44	2.64	0.67	2.07	1.05	0.66	0.82	1.23	1.13
			Cross	1.76	1.31	1.04	2.58	1.80	2.21	1.73	1.83	2.21	0.93	1.61
4	94	3w	Down	2.99	2.69	1.50	3.56	1.06	2.99	1.07	2.68	1.49	3.53	1.80
			Cross	2.99	4.72	3.29	4.02	3.65	2.59	1.84	2.82	3.11	1.31	1.36
4	95	3w	Down	1.85	1.58	1.26	3.26	0.90	0.93	1.57	0.92	1.12	1.08	1.30
			Cross	3.21	3.21	4.63	2.81	4.11	1.83	4.24	1.46	3.31	1.89	3.63
4	96	3w	Down	1.36	1.88	1.26	2.30	0.82	1.12	0.87	1.16	0.74	1.39	1.16
			Cross	1.48	1.83	1.69	1.57	1.46	0.87	1.49	1.00	1.04	2.13	1.25
4	97	5w	Down	0.66	0.29	0.85	0.45	0.32	0.38	0.47	0.36	0.57	0.80	0.52
			Cross	1.36	1.27	1.67	1.23	1.44	2.15	1.08	1.74	0.49	1.44	0.60
4	98	5w	Down	0.85	0.85	1.26	0.46	1.09	0.46	0.61	0.78	0.51	0.63	0.63
			Cross	1.54	2.41	0.63	1.95	0.64	1.50	1.04	1.92	1.18	1.97	1.51
4	99	5w	Down	1.48	0.25	0.27	0.34	0.28	0.44	0.32	0.21	0.47	0.22	0.32
			Cross	1.23	0.97	1.27	0.76	1.63	1.00	1.29	1.39	1.89	0.41	1.59
4	100	6w	Down	2.52	3.86	1.86	1.24	1.72	1.81	1.46	1.30	0.84	2.54	1.95
			Cross	1.69	1.40	1.62	2.56	1.15	1.24	1.09	1.27	2.86	1.60	1.51
4	101	3w	Down	2.11	1.71	2.42	1.49	2.51	3.35	1.27	1.62	1.68	0.85	1.29
			Cross	1.83	1.38	0.83	1.33	2.15	1.38	2.24	2.66	1.25	2.43	2.14
4	102	4w	Down	1.98	1.20	0.81	1.86	1.53	1.66	1.68	1.22	2.11	3.01	1.08
			Cross	1.94	1.03	1.72	1.99	1.66	1.51	3.05	2.26	1.51	1.92	2.50
4	103	4w	Down	2.21	1.31	0.85	2.02	1.53	2.52	2.32	2.95	1.64	1.07	2.47
			Cross	2.29	1.30	1.69	2.87	1.83	2.37	1.60	1.53	3.55	3.21	2.29
4	104	3w	Down	1.69	0.95	1.84	1.78	0.92	0.69	0.52	0.86	1.13	1.76	1.75
			Cross	1.69	1.47	0.30	0.65	1.24	1.75	1.22	2.57	0.67	3.66	0.86
4	105	6w	Down	0.69	0.80	0.39	0.49	0.55	0.88	0.51	0.27	0.68	1.05	0.74
			Cross	1.30	1.05	1.03	2.34	1.76	0.92	1.03	1.15	1.10	0.71	1.00
4	106	6w	Down	3.01	0.47	0.48	4.05	0.49	1.47	0.51	3.90	0.61	1.13	0.37
			Cross	2.36	1.90	1.87	5.28	1.98	2.04	1.40	1.57	2.44	1.75	1.35
4	107	6w	Down	0.65	0.96	0.30	0.61	0.41	0.93	0.25	0.43	0.64	1.24	0.75
			Cross	2.18	1.79	1.53	4.12	2.03	1.42	1.60	1.63	1.90	2.30	2.60
4	108	6w	Down	2.96	2.28	0.60	0.88	1.95	2.43	0.56	2.61	6.02	1.95	1.70
			Cross	1.82	1.00	3.47	1.29	1.17	2.80	0.85	2.00	0.96	2.12	1.10
4	109	6w	Down	1.48	1.45	1.26	0.49	1.82	0.80	0.65	0.54	1.29	1.31	2.18
			Cross	1.68	0.95	0.59	1.66	2.34	1.29	1.65	0.54	2.12	1.72	2.81
4	110	4w	Down	2.90	0.81	2.01	2.27	2.57	3.51	2.27	2.28	2.28	2.52	2.43
			Cross	4.08	1.86	1.56	12.10	2.24	1.47	1.42	2.50	2.02	1.58	0.88
4	111	4w	Down	1.20	1.11	1.26	0.81	0.88	1.55	1.43	1.28	1.12	1.17	1.06
			Cross	1.20	2.26	0.93	0.92	0.86	1.00	1.33	0.66	0.99	1.34	1.30

Appendix 2.1.2			Micro-Topographic Profile Standard Deviations from the Best-Fit Line for Each Sample Plot (Cross-slope and Downslope)											
Profile	Sample	Unit	S.D.	plot	p1	p2	p3	p4	p5	p6	p7	p8	p9	p10
5	112	1e	Down	9.78	1.68	11.07	1.44	5.74	2.90	8.44	2.39	13.15	5.00	10.55
			Cross	8.30	1.03	2.95	2.23	6.69	3.32	2.69	14.60	4.81	11.60	16.50
5	113	1e	Down	8.01	4.97	4.00	4.41	5.58	6.33	10.57	2.55	4.96	10.61	6.20
			Cross	10.67	23.10	13.90	3.84	14.10	12.70	6.65	4.93	3.06	2.29	2.74
5	114	2e	Down	4.18	2.01	1.55	2.46	2.83	3.24	4.25	3.05	3.15	2.51	5.29
			Cross	4.89	8.14	8.72	2.81	4.86	2.06	5.20	4.99	2.68	2.79	2.47
5	115	2e	Down	2.93	1.47	1.18	1.99	1.36	3.71	1.01	1.25	2.67	1.12	2.20
			Cross	2.68	2.48	1.61	1.68	1.03	2.87	2.33	2.58	5.38	1.88	3.16
5	116	2e	Down	1.46	0.46	0.77	1.18	0.83	0.99	1.30	1.24	2.26	0.86	1.59
			Cross	1.33	1.75	1.14	1.19	1.00	1.01	1.24	0.83	1.68	1.03	2.26
5	117	3e	Down	1.68	1.53	0.85	1.39	1.13	2.44	1.98	1.00	1.56	0.70	0.83
			Cross	1.57	1.20	1.42	2.04	1.00	0.38	1.91	1.77	2.60	1.81	0.60
5	118	3e	Down	1.64	1.26	0.79	1.34	1.48	1.54	1.01	1.88	1.04	0.91	1.35
			Cross	1.08	1.11	0.85	1.44	1.20	1.22	1.60	0.89	0.79	0.76	0.89
5	119	3e	Down	2.20	1.24	0.81	1.59	1.23	2.76	2.10	2.37	1.44	1.43	1.86
			Cross	2.28	2.50	2.69	3.71	1.08	1.52	2.88	1.00	1.69	1.54	2.93
5	120	3e	Down	1.99	3.03	0.91	1.09	0.99	3.01	1.46	1.16	0.61	1.14	1.25
			Cross	2.38	3.73	0.80	4.66	1.53	1.82	1.84	2.21	0.80	2.81	0.60
5	121	4w	Down	1.49	1.01	2.17	1.23	1.59	1.04	1.72	0.93	1.05	1.02	0.95
			Cross	1.58	1.70	1.73	1.52	0.64	1.28	1.94	2.34	0.93	2.16	1.06
5	122	4w	Down	2.07	0.71	2.86	1.81	2.42	1.00	1.80	0.55	0.59	2.62	1.22
			Cross	4.21	1.54	1.85	1.37	1.33	9.89	3.85	5.84	2.25	4.29	2.45
5	123	4w	Down	1.82	1.28	1.56	2.42	2.00	2.38	0.91	1.28	1.00	0.57	1.50
			Cross	1.86	1.21	1.81	2.57	2.09	1.86	1.51	2.30	1.23	2.30	1.63
5	124	5w	Down	0.61	0.66	0.69	0.52	0.66	0.73	0.63	0.68	0.42	0.46	0.31
			Cross	1.25	1.40	1.36	1.04	0.84	0.67	1.32	0.84	1.09	1.11	1.70
5	125	5w	Down	1.18	1.01	0.36	0.72	0.67	0.65	2.16	0.52	1.13	0.81	1.28
			Cross	1.29	1.02	1.79	0.93	0.74	1.14	1.14	1.14	1.71	2.00	0.93
5	126	5w	Down	0.94	1.18	0.78	0.83	0.45	0.53	0.62	0.41	0.64	0.28	0.32
			Cross	3.35	6.24	3.21	4.46	3.21	3.53	2.18	3.43	1.59	1.58	0.84
5	127	5w	Down	0.85	0.29	0.53	0.65	0.44	0.52	0.29	0.75	0.63	1.07	0.97
			Cross	3.00	1.43	2.71	1.60	2.80	1.41	4.42	1.12	5.28	1.37	3.00

Appendix 2.1.3 Complex Flow Geometry Regression Results for Each Sample Plot

Profile 1

Plot	Unit	A	B	corr	R.sq.	F	d.f.
1	1e	1.35	0.37	0.97	94.4	749	1/43
2	1e	1.34	0.37	0.98	94.9	840	1/44
3	2e	1.39	0.34	0.95	90.5	546	1/56
4	2e	1.28	0.46	0.99	96.8	597	1/19
5	2e	1.30	0.49	0.99	97.6	595	1/13
6	4e	1.45	0.45	0.95	94.3	134	1/7
7	4e	1.40	0.43	0.95	90.4	152	1/15
8	3e	1.56	0.24	0.93	86.1	670	1/108
9	4e	1.32	0.57	1.00	99.4	1030	1/5
10	4e	1.43	0.44	0.97	92.8	156	1/11
11	4e	1.67	0.26	0.90	79.3	104	1/26
12	4e	1.91	0.31	0.95	89.9	134	1/14
13	4e	1.55	0.34	0.96	92.1	188	1/15
14	4e	1.41	0.52	0.99	97.0	131	1/3
15	4e	1.46	0.41	0.95	88.4	92	1/11
16	5e	1.35	0.61	1.00	99.8	1048	1/1

Profile 2

Plot	Unit	A	B	corr	R.sq.	F	d.f.
17	1e	1.32	0.43	0.99	97.0	913	1/27
18	1e	1.31	0.41	0.98	95.5	799	1/36
19	2e	1.41	0.35	0.92	93.7	659	1/43
20	2e	1.36	0.41	0.98	95.6	503	1/22
21	2e	1.28	0.48	0.98	95.8	368	1/15
22	3e	1.33	0.42	0.97	94.7	473	1/25
23	3e	1.37	0.38	1.00	90.9	359	1/35
24	4e	1.28	0.47	0.98	95.0	389	1/19
25	4e	1.37	0.38	0.98	95.7	640	1/28
26	4e	1.36	0.46	0.98	96.2	361	1/13
27	4e	1.35	0.45	0.97	94.7	335	1/18
28	4e	1.39	0.36	0.93	85.5	249	1/42
29	4e	1.33	0.49	0.96	91.4	118	1/10
30	5e	1.19	0.55	0.99	98.4	666	1/10
31	5e	1.32	0.47	0.97	92.6	164	1/12
32	5e	1.30	0.58	0.99	98.3	233	1/3
33	5w	1.37	0.42	0.98	95.6	434	1/19
34	5w	1.35	0.52	0.99	97.6	241	1/5
35	4w	1.44	0.38	0.94	87.5	162	1/22
36	4w	1.34	0.46	0.98	95.4	313	1/14
37	3w	1.52	0.35	0.96	91.0	193	1/18
38	3w	1.42	0.34	0.95	89.3	355	1/41
39	6w	1.25	0.49	0.99	97.2	626	1/17
40	6w	1.32	0.54	0.97	93.8	107	1/6
41	5w	1.27	0.53	0.99	97.4	380	1/9
42	6w	1.48	0.34	0.93	86.7	191	1/28
43	6w	1.27	0.50	0.98	96.4	375	1/13
44	6w	1.34	0.43	0.97	94.1	320	1/19
45	4w	1.42	0.38	0.98	94.8	520	1/21
46	4w	1.48	0.34	0.96	92.7	354	1/27
47	5w	1.54	0.35	0.91	81.2	53	1/11
48	5w	1.39	0.41	0.94	87.6	129	1/17

Profile 3

Plot	Unit	A	B	corr	R.sq.	F	d.f.
49	1e	1.4	0.35	0.97	94.4	1213.9	1/70
50	1e	1.2	0.49	0.99	97.5	1124.4	1/28
51	2e	1.3	0.43	0.96	92.6	397.7	1/31
52	2e	1.4	0.36	0.95	90.5	325.5	1/33
53	3e	1.4	0.35	0.97	93.4	461.5	1/31
54	3e	1.4	0.49	0.99	98.7	859.6	1/10
55	3e	1.3	0.5	1	99	973.5	1/9
56	4e	1.4	0.4	0.98	95.1	473.3	1/23
57	4e	1.4	0.47	0.98	95.1	194	1/9
58	4e	1.5	0.38	0.96	91.3	222.4	1/20
59	4e	1.6	0.29	0.94	87.4	139.96	1/19
60	4e	1.4	0.41	0.98	95	268.4	1/13
61	4e	1.3	0.55	0.99	98.7	672.9	1/8
62	5e	1.1	0.56	0.99	96.9	533.6	1/16
63	5e	1.4	0.38	0.95	89.8	169.3	1/18
64	5e	1.4	0.58	0.99	96.7	59.2	1/1
65	5w	1.5	0.32	0.96	90.5	380	1/30
66	4w	1.4	0.36	0.97	92.9	436.7	1/32
67	4w	1.5	0.38	0.96	92.4	267.7	1/21
68	3w	1.4	0.48	0.98	95.4	275.2	1/12
69	6w	1.6	0.25	0.91	81.9	272.52	1/59
70	6w	1.3	0.49	0.99	97.6	405	1/9
71	6w	1.4	0.44	0.98	96	263	1/10
72	6w	1.5	0.36	0.97	92.7	242.6	1/18
73	6w	1.3	0.45	0.99	97	442.4	1/13
74	6w	1.3	0.46	0.98	95.4	394.6	1/18
75	6w	1.4	0.44	0.97	92.7	178.6	1/13
76	4w	1.6	0.28	0.9	80.3	102.6	1/24
77	4w	1.3	0.46	0.99	97.7	598.1	1/13
78	4w	1.7	0.21	0.89	78.7	178.6	1/47
79	5w	1.3	0.48	0.98	96.2	379.1	1/14
80	5w	1.3	0.6	0.99	97.6	204.61	1/4

Profile 4

Plot	Unit	A	B	corr	R.sq.	F	d.f.
81	1e	1.31	0.36	0.95	90.7	714	1/72
82	1e	1.29	0.40	0.99	97.0	1498	1/46
83	2e	1.43	0.38	0.96	92.6	338	1/26
84	2e	1.26	0.43	0.97	93.3	475	1/33
85	2e	1.14	0.44	0.97	92.9	861	1/64
86	3e	1.34	0.33	0.93	86.9	637	1/95
87	3e	1.60	0.23	0.90	81.4	429	1/97
88	4e	1.30	0.45	0.98	94.9	411	1/21
89	4e	1.39	0.40	0.96	92.7	289	1/22
90	4e	1.38	0.50	0.99	98.0	395	1/7
91	4e	1.39	0.48	0.98	95.5	190	1/8
92	3e	1.39	0.41	0.98	95.0	346	1/17
93	3e	1.40	0.49	1.00	99.3	1082	1/7
94	3w	1.42	0.39	0.97	94.5	351	1/19
95	3w	1.46	0.34	0.94	87.9	240	1/32
96	3w	1.31	0.56	0.98	96.4	186	1/6
97	5w	1.40	0.47	0.98	96.3	185	1/6
98	5w	1.41	0.43	0.99	96.7	326	1/10
99	5w	1.40	0.42	0.97	93.4	172	1/11
100	6w	1.48	0.36	0.96	91.6	220	1/19
101	3w	1.53	0.33	0.94	87.0	155	1/22
102	4w	1.40	0.41	0.94	87.1	136	1/19
103	4w	1.37	0.40	0.96	91.8	279	1/24
104	3w	1.57	0.30	0.94	86.8	146	1/21
105	6w	1.44	0.40	0.94	88.3	122	1/15
106	6w	1.32	0.44	0.96	91.5	194	1/17
107	6w	1.41	0.41	0.96	91.5	151	1/13
108	6w	1.41	0.43	0.98	95.4	207	1/9
109	6w	1.61	0.26	0.93	85.3	227	1/38
110	4w	1.65	0.25	0.88	77.0	128	1/37
111	4w	1.52	0.42	0.96	91.3	85	1/7

Profile 5

Plot	Unit	A	B	corr	R.sq.	F	d.f.
112	1e	1.51	0.29	0.95	90.0	451	1/49
113	1e	1.45	0.30	0.96	92.0	874	1/76
114	2e	1.38	0.40	0.98	95.5	505	1/23
115	2e	1.29	0.49	1.00	99.0	1264	1/12
116	2e	1.29	0.60	0.99	98.2	338	1/5
117	3e	1.45	0.37	0.96	92.1	247	1/20
118	3e	1.59	0.32	0.93	85.3	88	1/14
119	3e	1.45	0.34	0.94	88.0	256	1/34
120	3e	1.37	0.42	0.98	94.9	339	1/17
121	4w	1.49	0.35	0.97	92.9	275	1/20
122	4w	1.40	0.37	0.95	89.2	291	1/34
123	4w	1.54	0.30	0.92	83.7	192	1/36
124	5w	1.30	0.57	0.99	98.1	257	1/4
125	5w	1.27	0.61	0.99	96.9	185	1/5
126	5w	1.33	0.41	0.96	92.0	290	1/24
127	5w	1.37	0.42	0.95	90.1	156	1/16

Appendix 2.2 The Results Matrices from the ANOVA of Micro-Topographic and Surface Material Characteristics for the Different Unit Groupings of Sample Plots

1. Analysis of Variance of Stone Particle-Size Distributions (upper value = Aa, middle = Ba, lower = Ca)

Overall Unit Classification ANOVA

	Unit1	Unit2	Unit3	Unit4	Unit5	Unit6
Unit1		73.1	323.6	663.2	960.6	19.9
		64.9	281.0	581.1	881.6	6.5
		41.7	194.5	398.2	598.6	**0.1**
Unit2			58.9	165.0	605.1	13.8
			53.5	153.1	604.4	29.5
			34.7	97.1	406.1	43.4
Unit3				16.8	941.9	182.4
				16.7	920.8	237.2
				12.0	956.9	323.5
Unit4					920.7	357.9
					893.3	446.3
					856.4	535.4
Unit5						1265.1
						1344.7
						1470.1
obs	2244	3148	3931	7952	2391	1637

Eastern Slopes Units ANOVA

	Unit1	Unit2	Unit3	Unit4	Unit5
Unit1		124.8	303.5	838.7	876.5
		120.7	309.2	829.5	902.3
		78.9	260.6	672.6	654.4
Unit2			64.3	288.9	731.1
			79.0	311.7	793.4
			74.6	263.9	541.1
Unit3				38.1	603.7
				28.7	524.7
				24.4	517.3
Unit4					634.9
					595.9
					530.1
Unit5					
obs	2244	3148	2449	5423	1269

Western Slopes Units ANOVA

	Unit1	Unit2	Unit3	Unit4	Unit5	Unit6
Unit1						
Unit2						
Unit3				**0.1**	301.4	200.4
				0.1	372.0	203.5
				0.2	421.8	194.9
Unit4					294.4	203.6
					320.5	223.7
					385.5	192.3
Unit5						1819.0
						1816.8
						1726.1
obs			1482	2797	1080	1637

East versus West Units ANOVA

	Unit3e	Unit4e	Unit5e	Unit3w	Unit4w	Unit5w
Unit3e		14.7	127.3	**0.0**	1.2	71.8
		11.8	116.6	**1.9**	8.6	60.9
		6.8	81.1	8.1	31.2	33.8
Unit4e			236.5	11.6	57.1	118.9
			229.9	30.2	105.0	106.4
			167.2	53.9	189.6	58.3
Unit5e				118.6	392.1	5.1
				133.1	414.8	5.7
				155.9	548.7	7.7
Unit3w					**1.8**	68.8
					0.7	76.8
					2.6	79.6
Unit4w						251.6
						260.4
						293.1
obs	2449	5423	1269	1482	2529	1122

Appendix 2.2 The Results Matrices from the ANOVA of Micro-Topographic and Surface Material Characteristics for the Different Unit Groupings of Sample Plots

2. Analysis of Variance of Downslope Profile Standard Deviations (Profile Best-Fit)

Overall Unit Classification ANOVA

	Unit1	Unit2	Unit3	Unit4	Unit5	Unit6
Unit1		55.7	103.4	420.2	340.6	202.0
Unit2			6.6	185.2	307.3	96.3
Unit3				82.1	180.1	45.7
Unit4					254.3	1.8
Unit5						89.6
mean	5.3	2.6	2.2	1.3	0.6	1.3
st.d	3.7	1.6	1.7	0.6	0.4	0.9
obs	100	140	210	410	220	190

Eastern Slopes Units ANOVA

	Unit1	Unit2	Unit3	Unit4	Unit5
Unit1		55.7	52.7	280.6	126.4
Unit2			**0.5**	148.9	119.6
Unit3				93.6	80.9
Unit4					101.1
Unit5					
mean	5.3	2.6	2.5	1.3	0.6
st.d	3.7	1.6	1.8	0.5	0.4
obs	100	140	120	250	80

Western Slopes Units ANOVA

	Unit1	Unit2	Unit3	Unit4	Unit5	Unit6
Unit1						
Unit2						
Unit3				5.8	93.9	14.6
Unit4					168.7	5.8
Unit5						58.3
mean			1.8	1.5	0.7	1.3
st.d			1.3	0.7	0.3	0.9
obs			90	160	140	190

East versus West Units ANOVA

	Unit3e	Unit4e	Unit5e	Unit3w	Unit4w	Unit5w
Unit3e		93.6	80.9	9.9	41.4	134.0
Unit4e			101.1	25.7	11.5	149.3
Unit5e				58.8	109.9	**0.9**
Unit3w					5.8	93.9
Unit4w						168.7
mean	2.5	1.3	0.6	1.8	1.5	0.7
st.d	1.8	0.5	0.4	1.3	0.7	0.3
obs	120	250	80	90	160	140

3. Analysis of Variance of Crosslope Profile Standard Deviations (Profile Best-Fit)

Overall Unit Classification ANOVA

	Unit1	Unit2	Unit3	Unit4	Unit5	Unit6
Unit1		24.0	71.5	347.2	259.7	246.7
Unit2			10.3	117.2	104.1	95.8
Unit3				40.0	46.1	39.1
Unit4					11.8	7.1
Unit5						**0.9**
mean	6.4	4.2	3.1	2.1	1.7	1.8
st.d	3.9	3.2	2.8	1.3	1.3	0.8
obs	100	140	210	410	220	190

Eastern Slopes Units ANOVA

	Unit1	Unit2	Unit3	Unit4	Unit5
Unit1		24.0	30.9	234.8	94.2
Unit2			**1.7**	77.9	34.6
Unit3				35.3	16.6
Unit4					**1.2**
Unit5					
mean	6.4	4.2	3.6	2.2	2.0
st.d	3.9	3.2	3.5	1.3	1.5
obs	100	140	120	250	80

Western Slopes Units ANOVA

	Unit1	Unit2	Unit3	Unit4	Unit5	Unit6
Unit1						
Unit2						
Unit3				7.8	39.5	33.4
Unit4					11.4	**3.2**
Unit5						6.9
mean			2.5	2.0	1.6	1.8
st.d			1.1	1.3	1.1	0.8
obs			90	160	140	190

East versus West Units ANOVA

	Unit3e	Unit4e	Unit5e	Unit3w	Unit4w	Unit5w
Unit3e		35.3	16.6	9.4	28.8	44.3
Unit4e			**1.2**	4.5	**0.8**	19.9
Unit5e				7.0	**0.2**	5.1
Unit3w					7.8	39.5
Unit4w						11.4
mean		2.2	2.0	2.5	2.0	1.6
st.d		1.3	1.5	1.1	1.3	1.1
obs		250	80	90	160	140

Appendix 2.2 The Results Matrices from the ANOVA of Micro-Topographic and Surface Material Characteristics for the Different Unit Groupings of Sample Plots

4. Analysis of Variance of Downslope Profile Standard Deviations (Sample Best-Fit)

Overall Unit Classification ANOVA

	Unit1	Unit2	Unit3	Unit4	Unit5	Unit6
Unit1		14.2	26.2	140.9	98.5	68.1
Unit2			**2.1**	44.2	46.5	23.7
Unit3				10.9	16.2	6.2
Unit4					26.7	**0.5**
Unit5						11.2
mean	8.3	4.1	3.0	1.7	1.0	1.6
st.d	3.5	2.1	2.3	0.6	0.5	0.7
obs	10	14	21	41	22	19

Eastern Slopes Units ANOVA

	Unit1	Unit2	Unit3	Unit4	Unit5
Unit1		14.2	11.9	87.0	34.0
Unit2			**0.1**	28.4	16.1
Unit3				11.8	6.9
Unit4					5.5
Unit5					
mean	8.3	4.1	3.7	1.7	1.0
st.d	3.5	2.1	2.8	0.7	0.7
obs	10	14	12	25	8

Western Slopes Units ANOVA

	Unit1	Unit2	Unit3	Unit4	Unit5	Unit6
Unit1						
Unit2						
Unit3				**0.9**	21.9	**1.8**
Unit4					34.7	**0.8**
Unit5						10.5
mean			2.0	1.8	0.9	1.6
st.d			0.7	0.4	0.4	0.7
obs			9	16	14	19

East versus West Units ANOVA

	Unit3e	Unit4e	Unit5e	Unit3w	Unit4w	Unit5w
Unit3e		11.8	6.9	3.2	7.4	13.7
Unit4e			5.5	**1.3**	**0.3**	14.8
Unit5e				8.0	11.5	**0.2**
Unit3w					**0.9**	21.9
Unit4w						34.7
mean	3.7	1.7	1.0	2.0	1.8	0.9
st.d	2.8	0.7	0.7	0.7	0.4	0.4
obs	12	25	8	9	16	14

5. Analysis of Variance of Crosslope Profile Standard Deviations (Sample Best-Fit)

Overall Unit Classification ANOVA

	Unit1	Unit2	Unit3	Unit4	Unit5	Unit6
Unit1		8.4	19.9	112.3	124.0	161.3
Unit2			**1.9**	19.9	21.6	21.0
Unit3				5.3	8.0	7.0
Unit4					**3.3**	2.5
Unit5						**0.1**
mean	7.1	4.5	3.4	2.3	1.8	1.9
st.d	1.7	2.5	2.4	1.2	1.0	0.4
obs	10	14	21	41	22	19

Eastern Slopes Units ANOVA

	Unit1	Unit2	Unit3	Unit4	Unit5
Unit1		8.4	8.6	74.2	47.0
Unit2			**0.3**	12.0	6.8
Unit3				4.8	**2.8**
Unit4					**0.4**
Unit5					
mean	7.1	4.5	4.0	2.4	2.1
st.d	1.7	2.5	3.1	1.4	1.3
obs	10	14	12	25	8

Western Slopes Units ANOVA

	Unit1	Unit2	Unit3	Unit4	Unit5	Unit6
Unit1						
Unit2						
Unit3				**1.2**	8.3	9.7
Unit4					**3.7**	2.2
Unit5						**1.3**
mean			2.6	2.2	1.7	1.9
st.d			0.7	0.8	0.8	0.4
obs			9	16	14	19

East versus West Units ANOVA

	Unit3e	Unit4e	Unit5e	Unit3w	Unit4w	Unit5w
Unit3e		4.8	**2.8**	**1.9**	5.1	7.8
Unit4e			**0.4**	**0.1**	**0.3**	**3.7**
Unit5e				**1.0**	**0.1**	**0.8**
Unit3w					**1.2**	8.3
Unit4w						**3.7**
mean	4.0	2.4	2.1	2.6	2.2	1.7
st.d	3.0	1.4	1.3	0.7	0.8	0.8
obs	12	25	8	9	16	14

Appendix 2.3 Run-on/Runoff Plot Infiltration Data Sets

1. Infiltration Data for Plot 18 (unit 1)

WA (cm^2)	Σt (s)	Δt (s)	run-on (cm^3)	runoff (cm^3)	i (cm^3)	plotting t (mins)	raw i (mm hr^{-1})	pred i (B1)	pred i (B2)
7500	85	85	1273	0	.....	.....	.....	.....	.....
7500	267	182	2727	1190	1537	2.93	40.5	41.3	20.5
7500	534	267	4000	2610	1390	6.68	25.0	26.5	17.4
8100	793	259	4000	2640	1360	11.06	23.3	21.9	16.4
8100	1051	258	4000	2730	1270	15.37	21.9	19.9	16.0
8100	1307	256	4000	2564	1436	19.65	24.9	18.8	15.7
8100	1564	257	4000	2690	1310	23.93	22.7	18.1	15.6
10300	1828	264	4000	2756	1244	28.27	16.5	17.6	15.5
10300	2092	264	4000	2732	1268	32.67	16.8	17.3	15.4
10300	2358	266	4000	2834	1166	37.08	15.3	17.0	15.3
10300	2626	268	4000	2774	1226	41.53	16.0	16.8	15.3
10300	2902	276	4000	2892	1108	46.07	14.0	16.6	15.3
10300	3173	271	4000	2726	1274	50.63	16.4	16.4	15.2
10300	3443	270	4000	2760	1240	55.13	16.1	16.3	15.2
10300	3717	274	4000	2752	1248	59.67	15.9	16.2	15.2
10300	3990	273	4000	2780	1220	64.23	15.6	16.1	15.2
10300	4275	285	4000	2878	1122	68.88	13.8	16.0	15.1
10300	4557	282	4000	2856	1144	73.60	14.2	16.0	15.1
10300	4827	270	4000	2764	1236	78.20	16.0	15.9	15.1

Best-fit curve to raw data $i = 0.000414 + 0.1290/t$

2. Infiltration Data for Plot 20 (unit 2)

WA (cm^2)	Σt (s)	Δt (s)	run-on (cm^3)	runoff (cm^3)	i (cm^3)	plotting t (mins)	raw i (mm hr^{-1})	pred i (B1)	pred i (B2)
12000	215	215	2245	0	.....	.....	.....	.....	.....
12000	383	168	1755	248	1507	4.98	26.9	28.7	16.6
12500	606	223	4000	1760	2240	8.24	28.9	23.5	16.1
12500	827	221	4000	2592	1408	11.94	18.3	20.9	15.9
12500	1038	211	4000	2616	1384	15.54	18.9	19.7	15.8
12500	1243	205	4000	2632	1368	19.01	19.2	18.9	15.7
12500	1444	201	4000	2710	1290	22.39	18.5	18.3	15.7
12500	1652	208	4000	2700	1300	25.80	18.0	18.0	15.6
12500	1858	206	4000	2702	1298	29.25	18.1	17.6	15.6
12800	2066	208	4000	2752	1248	32.70	16.9	17.4	15.6
12800	2270	204	4000	2844	1156	36.13	15.9	17.2	15.5
12800	2476	206	4000	2782	1218	39.55	16.6	17.1	15.5
12800	2685	209	4000	2756	1244	43.01	16.7	16.9	15.5
12800	2885	200	4000	2808	1192	46.42	16.8	16.8	15.5
12800	3096	211	4000	2730	1270	49.84	16.9	16.7	15.5
12800	3317	221	4000	2792	1208	53.44	15.4	16.6	15.5
12800	3531	214	4000	2816	1184	57.07	15.6	16.5	15.5
12800	3746	215	4000	2820	1180	60.64	15.4	16.5	15.5
12800	3954	208	4000	2750	1250	64.17	16.9	16.4	15.5
12800	4171	217	4000	2610	1390	67.71	18.0	16.4	15.5
12800	4386	215	4000	2760	1240	71.31	16.2	16.3	15.5
12800	4605	219	4000	2720	1280	74.93	16.4	16.3	15.5
12800	4819	214	4000	2672	1328	78.53	17.5	16.2	15.5
12800	5029	210	4000	2724	1276	82.07	17.1	16.2	15.4

Best-fit curve to raw data $i = 0.000427 + 0.1110/t$

3. Infiltration Data for Plot 23 (unit 3e)

WA (cm^2)	Σt (s)	Δt (s)	run-on (cm^3)	runoff (cm^3)	i (cm^3)	plotting t (mins)	raw i (mm hr^{-1})	pred i (B1)	pred i (B2)
9560	37	37	492	0	.....	.....	.....	.....	.....
9560	301	264	3508	2032	1476	2.82	21.1	21.1	9.3
9560	606	305	4000	3168	832	7.56	10.3	11.9	7.5
9560	905	299	4000	3222	778	12.59	9.8	9.7	7.1
9560	1210	305	4000	3316	684	17.63	8.4	8.8	6.9
9560	1525	315	4000	3222	778	22.79	9.3	8.2	6.8
9560	1826	301	4000	3102	898	27.93	11.2	7.9	6.7
9560	2123	297	4000	3170	830	32.91	10.5	7.7	6.7
9560	2412	289	4000	3288	712	37.79	9.3	7.5	6.7
9560	2697	285	4000	3258	742	42.58	9.8	7.4	6.6
9560	3009	312	4000	3636	364	47.55	4.4	7.3	6.6
9560	3301	292	4000	3398	602	52.58	7.8	7.2	6.6
9560	3575	274	4000	3234	766	57.30	10.5	7.2	6.6
9560	3886	311	4000	3774	226	62.18	2.7	7.1	6.6
9560	4190	304	4000	3510	490	67.30	6.1	7.1	6.6
9560	4485	295	4000	3716	284	72.29	3.6	7.0	6.6
9560	4774	289	4000	3590	410	77.16	5.3	7.0	6.5

Best-fit curve to raw data $i = 0.000179 + 0.0686/t$

4. Infiltration Data for Plot 25 (unit 4e upper)

WA (cm^2)	Σt (s)	Δt (s)	run-on (cm^3)	runoff (cm^3)	i (cm^3)	plotting t (mins)	raw i (mm hr^{-1})	pred i (B1)	pred i (B2)
11800	37	37	804	0	.....	.....	.....	.....	.....
11800	184	147	3196	1262	1934	1.84	40.1	37.2	7.8
11800	382	198	4000	3270	730	4.72	11.2	15.6	4.1
11800	582	200	4000	3578	412	8.03	6.3	9.8	3.1
11800	779	197	4000	3556	444	11.34	6.9	7.5	2.7
11800	968	189	4000	3706	294	14.56	4.7	6.2	2.5
11800	1189	221	4000	3649	351	17.98	4.8	5.3	2.3
11800	1405	216	4000	3768	232	21.62	3.3	4.7	2.2
11800	1616	211	4000	3673	327	25.18	4.7	4.3	2.1
11800	1839	223	4000	3647	353	28.79	4.8	4.0	2.1
11800	2061	222	4000	3749	251	32.50	3.4	3.7	2.0
11800	2286	225	4000	3792	208	36.23	2.8	3.5	2.0
11800	2506	220	4000	3827	173	39.93	2.4	3.3	2.0
11800	2724	218	4000	3786	214	43.58	3.0	3.2	2.0
11800	2940	216	4000	3767	233	47.20	3.3	3.1	1.9
11800	3148	208	4000	3685	315	50.73	4.6	3.0	1.9
11800	3363	215	4000	3517	483	54.26	6.9	2.9	1.9
11800	3585	222	4000	3835	165	57.90	2.3	2.8	1.9
11800	3802	217	4000	3905	95	61.56	1.3	2.8	1.9
11800	4016	214	4000	3773	227	65.15	3.2	2.7	1.9
11800	4230	214	4000	3656	344	68.72	4.9	2.6	1.9
11800	4446	216	4000	3745	255	72.30	3.6	2.6	1.8
11800	4659	213	4000	3741	259	75.88	3.7	2.6	1.8
11800	4870	211	4000	3800	200	79.41	2.9	2.5	1.8
11800	5089	219	4000	3842	158	82.99	2.2	2.5	1.8
11800	5306	217	4000	3624	376	86.63	5.3	2.4	1.8
11800	5534	228	4000	3933	77	90.33	1.0	2.4	1.8

Best-fit curve to raw data $i = 0.000047 + 0.1090/t$

5. Infiltration Data for Plot 28 (unit 4e lower)

WA (cm^2)	Σt (s)	Δt (s)	run-on (cm^3)	runoff (cm^3)	i (cm^3)	plotting t (mins)	raw i (mm hr^{-1})	pred i (B1)	pred i (B2)
5500	48	48	662	0	.....	.....	.....	.....	.....
5500	290	242	3338	1669	1669	2.82	45.14	44.7	22.3
7500	569	279	4000	2592	1408	7.16	24.2	25.4	16.6
7500	825	256	4000	2617	1383	11.62	25.9	20.6	15.2
11300	1096	271	4000	2896	1104	16.01	13.0	18.5	14.6
11300	1369	273	4000	2719	1281	20.54	14.9	17.3	14.2
10870	1654	285	4000	2773	1227	25.19	14.3	16.5	14.0
10870	1928	274	4000	2815	1185	29.85	14.3	15.9	13.8
10870	2210	282	4000	2707	1293	34.48	15.2	15.5	13.7
10870	2482	272	4000	2622	1378	39.10	16.8	15.2	13.6
10870	2776	294	4000	2749	1251	43.82	14.1	15.0	13.5
10870	3072	296	4000	2623	1377	48.73	15.4	14.8	13.5
10870	3367	295	4000	2715	1285	53.66	14.4	14.6	13.4
10870	3674	307	4000	2688	1312	58.68	14.2	14.4	13.4
10870	3967	293	4000	2636	1364	63.68	15.4	14.3	13.3
10870	4274	307	4000	2697	1303	68.68	14.1	14.2	13.3
10870	4577	303	4000	2553	1447	73.76	15.8	14.1	13.3
10870	4876	299	4000	2612	1388	78.78	15.4	14.1	13.3
10870	5167	291	4000	2666	1334	83.69	15.2	14.0	13.2
10870	5471	304	4000	2614	1386	88.65	15.1	13.9	13.2

Best-fit curve to raw data $i = 0.000359 + 0.1490/t$

6. Infiltration Data for Plot 32 (unit 5e)

WA (cm^2)	Σt (s)	Δt (s)	run-on (cm^3)	runoff (cm^3)	i (cm^3)	plotting t (mins)	raw i (mm hr^{-1})	pred i (B1)	pred i (B2)
8300	120	120	1928	0	.....	.....	.....	.....	.....
8300	249	129	2072	244	1828	3.08	61.5	58.0	27.7
10200	510	261	4000	1528	2472	6.33	33.4	39.1	24.4
10800	770	260	4000	1694	2306	10.67	29.6	31.9	23.2
11400	1031	261	4000	1750	2250	15.01	27.2	28.8	22.6
11400	1290	259	4000	1808	2192	19.34	26.7	27.1	22.3
11400	1554	264	4000	1840	2160	23.70	25.8	26.1	22.1
11400	1818	264	4000	1808	2192	28.10	26.2	25.3	22.0
11700	2089	271	4000	1854	2146	32.56	24.4	24.8	21.9
11700	2358	269	4000	1858	2142	37.06	24.5	24.4	21.8
11700	2624	266	4000	1854	2146	41.52	24.8	24.0	21.8
11700	2893	269	4000	1854	2146	45.98	24.5	23.8	21.7
11700	3159	266	4000	1878	2122	50.43	24.5	23.5	21.7
11700	3436	277	4000	1916	2084	54.96	23.1	23.4	21.7
11700	3774	338	4000	1526	2474	60.08	22.5	23.2	21.6
11700	4126	352	4000	1402	2598	65.83	22.7	23.0	21.6
11700	4419	293	4000	1634	2366	71.21	24.8	22.9	21.6
11700	4710	291	4000	1774	2226	76.08	23.5	22.8	21.6
11700	4971	261	4000	1876	2124	80.68	25.0	22.7	21.6
11700	5242	271	4000	2034	1966	85.11	22.3	22.6	21.5
11700	5507	265	4000	2012	1988	89.58	23.1	22.6	21.5

Best-fit curve to raw data $i = 0.000592 + 0.1880/t$

7. Infiltration Data for Plot 34 (unit 5w lower)

WA (cm^2)	Σt (s)	Δt (s)	run-on (cm^3)	runoff (cm^3)	i (cm^3)	plotting t (mins)	raw i (mm hr^{-1})	pred i (B1)	pred i (B2)
5000	222	222	2784	0	.....	.....	.....	.....	.....
5000	319	97	1216	68	1148	4.51	85.2	80.4	63.9
5400	674	355	4000	732	3268	8.28	61.4	71.5	62.5
5600	987	313	4000	924	3076	13.84	63.2	67.2	61.8
5500	1280	293	4000	978	3022	18.89	67.5	65.5	61.6
5400	1582	302	4000	910	3090	23.85	68.2	64.5	61.4
5400	1887	305	4000	900	3100	28.91	67.8	63.9	61.3
5400	2198	311	4000	952	3048	34.04	65.3	63.4	61.2
5400	2518	320	4000	1002	2998	39.30	62.5	63.1	61.2
5400	2825	307	4000	998	3002	44.53	65.2	62.8	61.1
5400	3142	317	4000	1058	2942	49.73	61.9	62.6	61.1
5400	3459	317	4000	1056	2944	55.01	61.9	62.4	61.1
5400	3769	310	4000	1026	2974	60.23	64.0	62.3	61.1
5400	4081	312	4000	1032	2968	65.42	63.4	62.2	61.0
5400	4398	317	4000	1046	2954	70.66	62.1	62.1	61.0
5400	4734	336	4000	1084	2916	76.10	57.9	62.0	61.0
5400	5058	324	4000	1054	2946	81.60	60.6	61.9	61.0
5400	5378	320	4000	1038	2962	86.97	61.7	61.9	61.0

Best-fit curve to raw data $i = 0.001690 + 0.1470/t$

8. Infiltration Data for Plot 36 (unit 4w)

WA (cm^2)	Σt (s)	Δt (s)	run-on (cm^3)	runoff (cm^3)	i (cm^3)	plotting t (mins)	raw i (mm hr^{-1})	pred i (B1)	pred i (B2)
8000	107	107	1451	0	.....	.....	.....	.....	.....
8000	295	188	2549	286	2263	3.35	54.2	56.3	32.1
8100	592	297	4000	1038	2962	7.39	44.3	40.8	29.9
8400	878	286	4000	1558	2442	12.25	36.6	35.7	29.1
8400	1170	292	4000	1630	2370	17.07	34.8	33.5	28.8
8400	1449	279	4000	1660	2340	21.83	35.9	32.3	28.6
9100	1739	290	4000	1810	2190	26.57	29.9	31.5	28.5
8800	2031	292	4000	1820	2180	31.42	30.5	31.0	28.4
8800	2323	292	4000	1906	2094	36.28	29.3	30.6	28.4
8800	2620	297	4000	1890	2110	41.19	29.1	30.3	28.3
8800	2910	290	4000	1884	2116	46.08	29.8	30.0	28.3
8800	3198	288	4000	1876	2124	50.90	30.2	29.8	28.2
8800	3482	284	4000	1948	2052	55.67	29.6	29.7	28.2
8800	3774	292	4000	1850	2150	60.47	30.1	29.5	28.2
8800	4068	294	4000	1864	2136	65.35	29.7	29.4	28.2
8800	4368	300	4000	1878	2122	70.30	28.9	29.3	28.2
8800	4671	303	4000	1918	2082	75.33	28.1	29.2	28.2
8800	4977	306	4000	1960	2040	80.40	27.3	29.2	28.1

Best-fit curve to raw data $i = 0.000777 + 0.1580/t$

9. Infiltration Data for Plot 38 (unit 3w)

WA (cm^2)	Σt (s)	Δt (s)	run-on (cm^3)	runoff (cm^3)	i (cm^3)	plotting t (mins)	raw i (mm hr^{-1})	pred i (B1)	pred i (B2)
16950	115	115	2473	0	.....	.....	.....	.....	.....
16950	186	71	1527	905	622	2.51	18.6	18.5	7.7
16950	366	180	4000	3010	990	4.60	11.7	12.9	7.0
16950	546	180	4000	2950	1050	7.60	12.4	10.2	6.7
16950	780	234	4000	3100	900	11.05	8.2	9.0	6.5
16950	1014	234	4000	3000	1000	14.95	9.1	8.2	6.4
16950	1250	236	4000	3030	970	18.87	8.7	7.8	6.4
16950	1493	243	4000	3300	700	22.86	6.1	7.5	6.3
16950	1737	244	4000	3240	760	26.92	6.6	7.3	6.3
16950	1978	241	4000	3140	860	30.96	7.6	7.2	6.3
16950	2208	230	4000	3320	680	34.88	6.3	7.0	6.3
16950	2423	215	4000	3280	720	38.59	7.1	7.0	6.3
16950	2665	242	4000	3410	590	42.40	5.2	6.9	6.2
16950	2918	253	4000	3100	900	46.53	7.6	6.8	6.2
16950	3160	242	4000	3330	670	50.65	5.9	6.8	6.2
16950	3393	233	4000	3230	770	54.61	7.0	6.7	6.2
16950	3628	235	4000	3400	600	58.51	5.4	6.7	6.2
16950	3863	235	4000	3330	670	62.43	6.1	6.7	6.2
16950	4102	239	4000	3300	700	66.38	6.2	6.6	6.2
16950	4352	250	4000	3120	880	70.45	7.5	6.6	6.2
16950	4579	227	4000	3070	930	74.43	8.7	6.6	6.2
16950	4814	235	4000	3180	820	78.28	7.4	6.6	6.2
16950	5052	238	4000	3250	750	82.22	6.7	6.5	6.2
16950	5300	248	4000	3220	780	86.27	6.7	6.5	6.2
16950	5531	231	4000	3340	660	90.26	6.1	6.5	6.2

Best-fit curve to raw data $i = 0.000171 + 0.0516/t$

10. Infiltration Data for Plot 42 (unit 6)

WA (cm^2)	Σt (s)	Δt (s)	run-on (cm^3)	runoff (cm^3)	i (cm^3)	plotting t (mins)	raw i (mm hr^{-1})	pred i (B1)	pred i (B2)
9590	66	66	1158	0	.....	.....	.....	.....	.....
9590	228	162	2842	1600	1242	2.45	28.8	27.0	10.8
9590	477	249	4000	3200	800	5.88	12.1	15.3	8.5
9590	742	265	4000	3360	640	10.16	9.1	11.8	7.9
9590	1007	265	4000	3350	650	14.58	9.2	10.3	7.6
9590	1269	262	4000	3220	780	18.97	11.2	9.5	7.4
9590	1543	274	4000	3400	600	23.43	8.2	9.0	7.3
9590	1825	282	4000	3340	660	28.07	8.8	8.7	7.3
9590	2113	288	4000	3220	780	32.82	10.2	8.4	7.2
9590	2403	290	4000	3290	710	37.63	9.2	8.3	7.2
9590	2708	305	4000	3260	740	42.59	9.1	8.1	7.2
9590	3017	309	4000	3250	750	47.71	9.1	8.0	7.1
9590	3327	310	4000	3470	530	52.87	6.4	7.9	7.1
9590	3638	311	4000	3250	750	58.04	9.1	7.8	7.1
9590	3950	312	4000	3380	620	63.23	7.5	7.7	7.1

Best-fit curve to raw data $i = 0.000193 + 0.0820/t$

11. Infiltration Data for Plot 47 (unit 5w upper)

WA (cm^2)	Σt (s)	Δt (s)	run-on (cm^3)	runoff (cm^3)	i (cm^3)	plotting t (mins)	raw i (mm hr^{-1})	pred i (B1)	pred i (B2)
7200	68	68	1545	0	.....	.....	.....	.....	.....
7200	176	108	2455	870	1585	2.03	73.4	70.1	27.2
10100	354	178	4000	2330	1670	4.42	33.4	39.7	19.9
10100	532	178	4000	2730	1270	7.38	25.4	29.2	17.4
10100	709	177	4000	2780	1220	10.34	24.6	24.8	16.4
10100	887	178	4000	2820	1180	13.30	23.6	22.3	15.8
10100	1067	180	4000	2930	1070	16.28	21.2	20.8	15.4
10100	1250	183	4000	2770	1230	19.31	24.0	19.7	15.1
10100	1433	183	4000	2970	1030	22.36	20.1	18.8	14.9
10100	1616	183	4000	3030	970	25.41	18.9	18.2	14.8
10100	1798	182	4000	3300	700	28.45	13.7	17.7	14.7
11400	1982	184	4000	2970	1030	31.50	17.7	17.4	14.6
11400	2160	178	4000	2900	1100	34.52	19.5	17.0	14.5
11400	2382	222	4000	3020	980	37.85	13.9	16.7	14.4
11400	2600	218	4000	2760	1240	41.52	18.0	16.5	14.4
11400	2822	222	4000	3020	980	45.18	13.9	16.3	14.3
11400	3047	225	4000	2840	1160	48.91	16.3	16.1	14.3
11400	3274	227	4000	2760	1240	52.68	17.3	15.9	14.2
11400	3502	228	4000	2850	1150	56.47	15.9	15.7	14.2
11400	3736	234	4000	2880	1120	60.32	15.1	15.6	14.2
11400	3968	232	4000	2800	1200	64.20	16.3	15.5	14.1
11400	4198	230	4000	2820	1180	68.05	16.2	15.4	14.1
11400	4421	223	4000	2860	1140	71.83	16.1	15.3	14.1
11400	4658	237	4000	2860	1140	75.66	15.2	15.2	14.1

Best-fit curve to raw data $i = 0.000381 + 0.191/t$

Appendix 2.4 Rainfall Recurrence Interval Data Set

Year	Rainfall mm	Rank	R.I.	Prob % >
1960/61	73.5	13	2.00	50.0
1961/62	65.0	19	1.37	73.1
1962/63	30.0	25	1.04	96.2
1963/64	163.0	1	26.00	3.8
1964/65	157.5	2	13.00	7.7
1965/66	90.5	9	2.89	34.6
1966/67	85.0	12	2.17	46.2
1967/68	86.5	11	2.36	42.3
1968/69	71.0	14	1.86	53.8
1969/70	58.0	21	1.24	80.8
1970/71	96.0	8	3.25	30.8
1971/72	111.5	5	5.20	19.2
1972/73	53.5	23	1.13	88.5
1973/74	135.0	3	8.67	11.5
1974/75	87.0	10	2.60	38.5
1975/76	67.5	17.5	1.49	67.3
1976/77	63.5	20	1.30	76.9
1977/78	67.5	17.5	1.49	67.3
1978/79	56.0	22	1.18	84.6
1979/80	103.5	6	4.33	23.1
1980/81	101.0	7	3.71	26.9
1981/82	69.5	15	1.73	57.7
1982/83	125.0	4	6.50	15.4
1983/84	31.0	24	1.08	92.3
1984/85	68.0	16	1.63	61.5
			Eq 1	Eq 2
Eq 1	R.I. = (NY+1)/R			
Eq 2	Prob % = (R/(NY+1))*100			
R = rank	NY = number years (25)			

p mm	Freq	Rank	R.I.	Prob % >
49.5	1	1	24.00	4.17
34.0	1	2	12.00	8.33
29.5	1	3	8.00	12.50
25.5	1	4	6.00	16.66
24.0	2	5.5	4.36	22.91
21.5	1	7	3.43	29.16
20.5	1	8	3.00	33.33
19.0	1	9	2.67	37.50
18.5	2	10.5	2.29	43.75
18.0	2	12.5	1.92	52.08
17.0	2	14.5	1.66	60.41
16.5	1	16	1.50	66.66
15.5	1	17	1.41	70.83
15.0	1	18	1.33	74.99
14.5	3	20	1.20	83.32
14.0	3	23	1.04	95.82
13.5	4	26.5	0.91	110.40
13.0	6	31.5	0.76	131.24
12.5	3	36	0.67	149.98
12.0	3	39	0.62	162.48
10.5	2	41.5	0.58	172.90
10.0	3	44	0.55	183.31
9.5	6	48.5	0.49	202.06
9.0	1	52	0.46	216.64
8.5	6	55.5	0.43	231.22
8.0	9	63	0.38	262.47
7.5	8	71.5	0.34	297.88
7.0	8	79.5	0.30	331.21
6.5	10	88.5	0.27	368.71
6.0	14	100.5	0.24	418.70
5.5	18	117.5	0.20	489.53
5.0	15	133	0.18	554.10
4.5	13	147	0.16	612.43
4.0	25	166	0.14	691.59
3.5	21	189	0.13	787.41
3.0	23	211	0.11	879.07
2.5	25	235.5	0.10	981.14
2.0	40	267.5	0.09	1114.46
1.5	62	318.5	0.08	1326.93
1.0	71	385	0.06	1603.98
0.5	81	461	0.05	1920.61
<0.25	4	503.5	0.05	2097.68
Total=	505		Eq 1	Eq 2
Eq 1	R.I. =((365 *NY)+1)/(R*365)			
Eq 2	Prob % = ((R*365)/((365*NY)+1))*100			
R = rank	NR = number raindays (505)			
NY = number years (24)				

Appendix 3.1 Base-map Avdat Catchment Contour Map

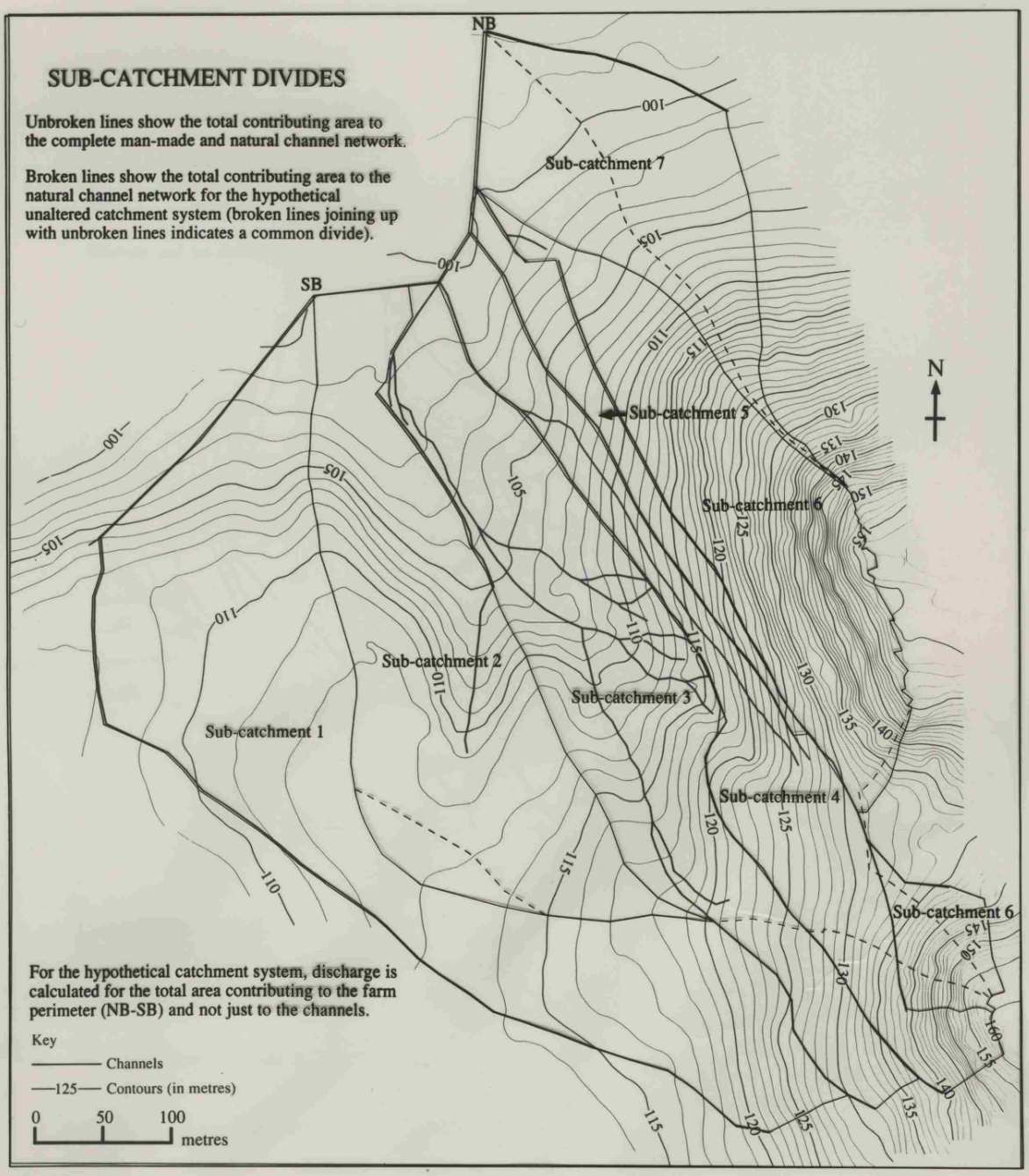

Appendix 3.1 Base-map Avdat Catchment Contour Map

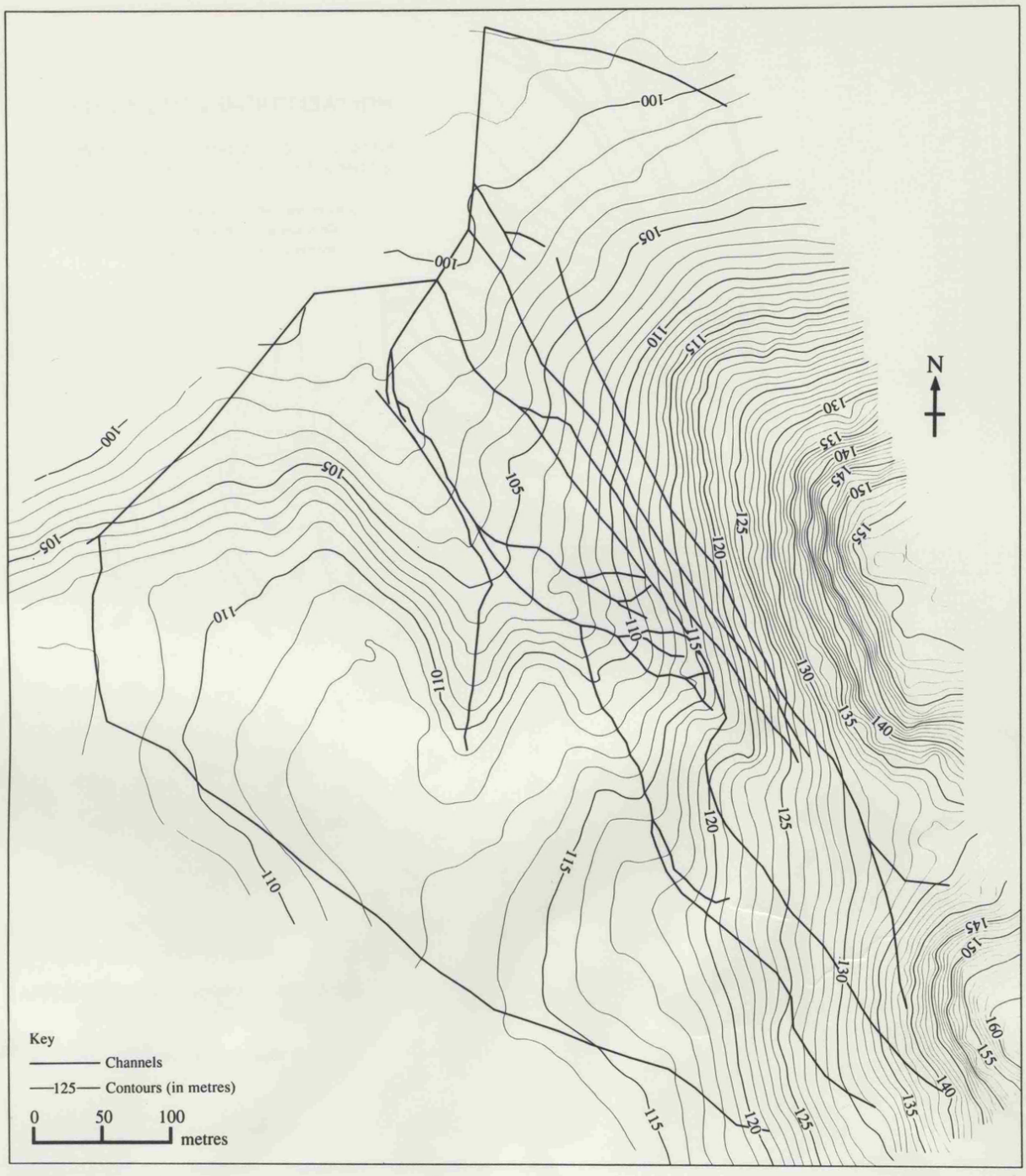

Appendix 3.2

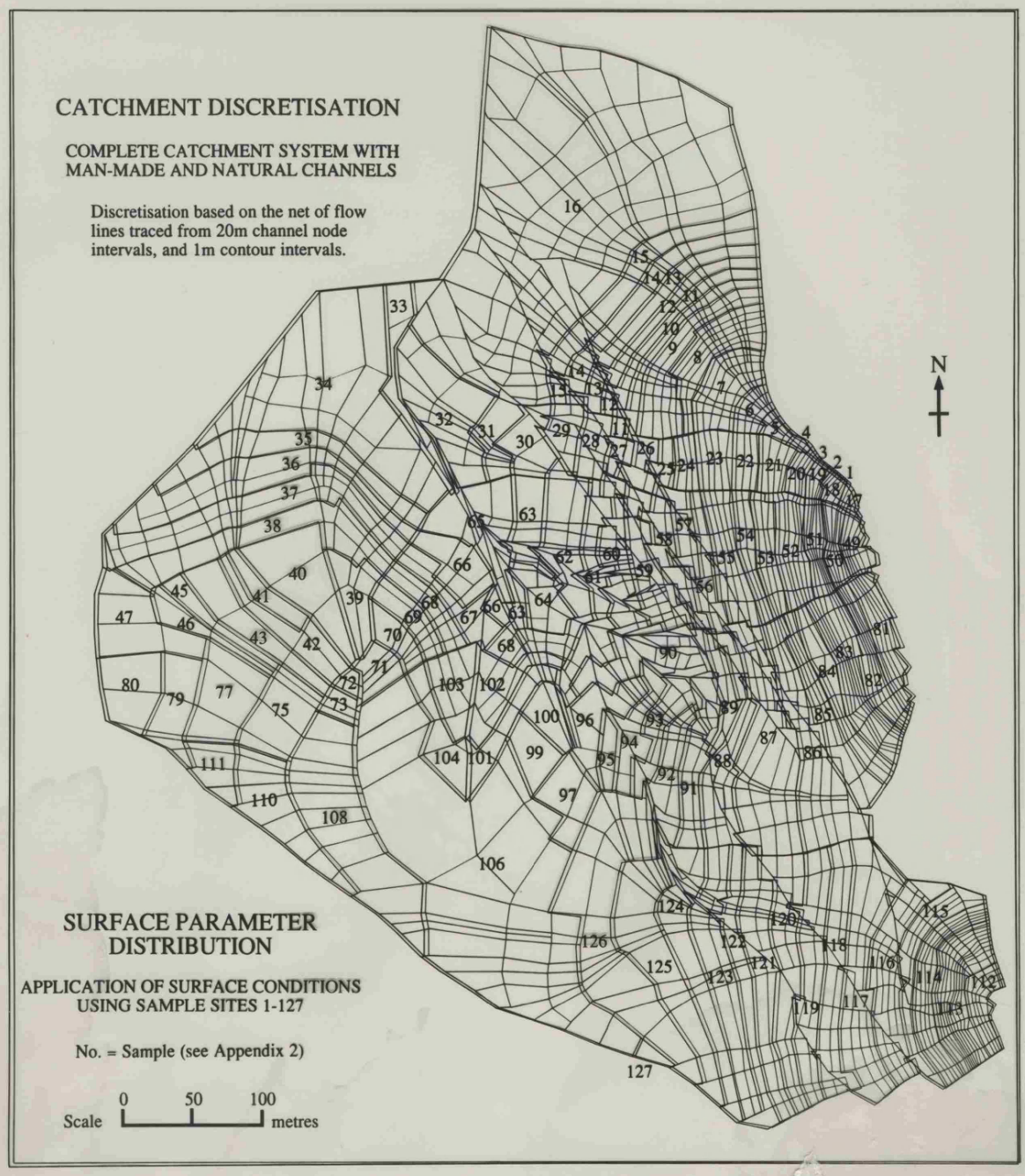
CATCHMENT DISCRETISATION
COMPLETE CATCHMENT SYSTEM WITH MAN-MADE AND NATURAL CHANNELS
Discretisation based on the net of flow lines traced from 20m channel node intervals, and 1m contour intervals.
SURFACE PARAMETER DISTRIBUTION
APPLICATION OF SURFACE CONDITIONS USING SAMPLE SITES 1-127
No. = Sample (see Appendix 2)
Scale 0 50 100 metres
N

Appendix 3.2

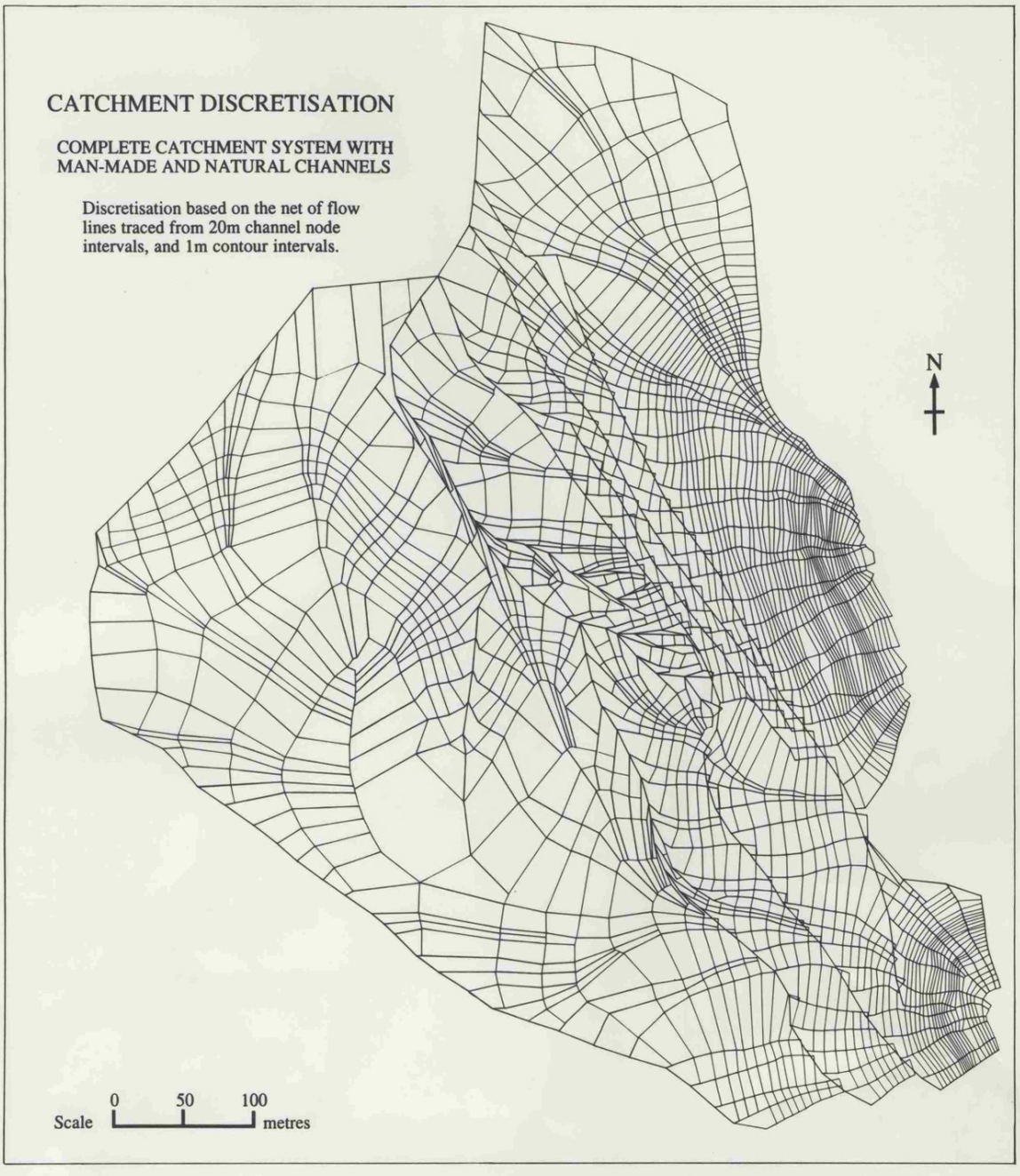
CATCHMENT DISCRETISATION
COMPLETE CATCHMENT SYSTEM WITH MAN-MADE AND NATURAL CHANNELS
Discretisation based on the net of flow lines traced from 20m channel node intervals, and 1m contour intervals.
N
Scale
0
50
100
metres

Appendix 3.3

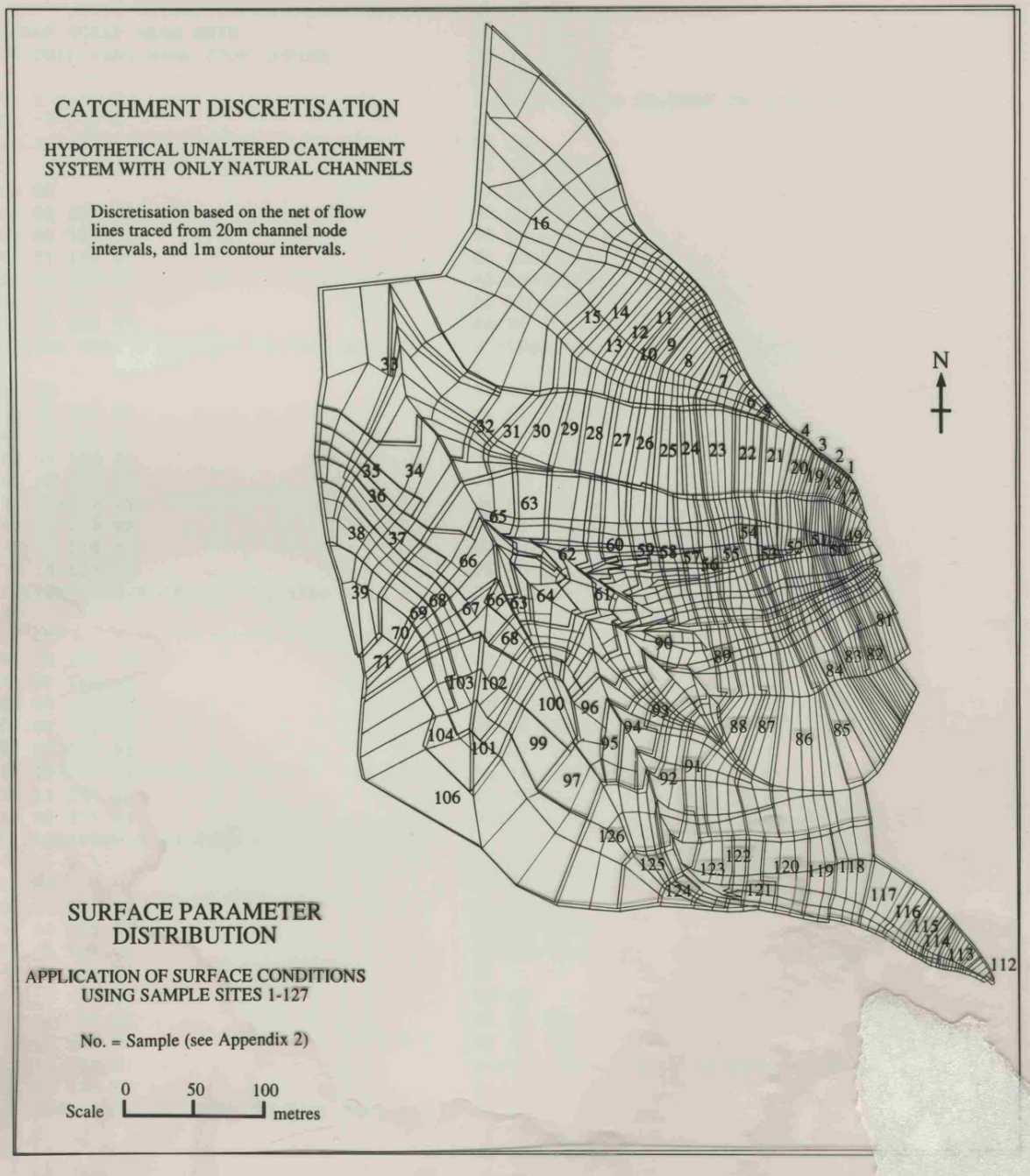
CATCHMENT DISCRETISATION
HYPOTHETICAL UNALTERED CATCHMENT SYSTEM WITH ONLY NATURAL CHANNELS
Discretisation based on the net of flow lines traced from 20m channel node intervals, and 1m contour intervals.
N
SURFACE PARAMETER DISTRIBUTION
APPLICATION OF SURFACE CONDITIONS USING SAMPLE SITES 1-127
No. = Sample (see Appendix 2)
Scale 0 50 100 metres

Appendix 3.3

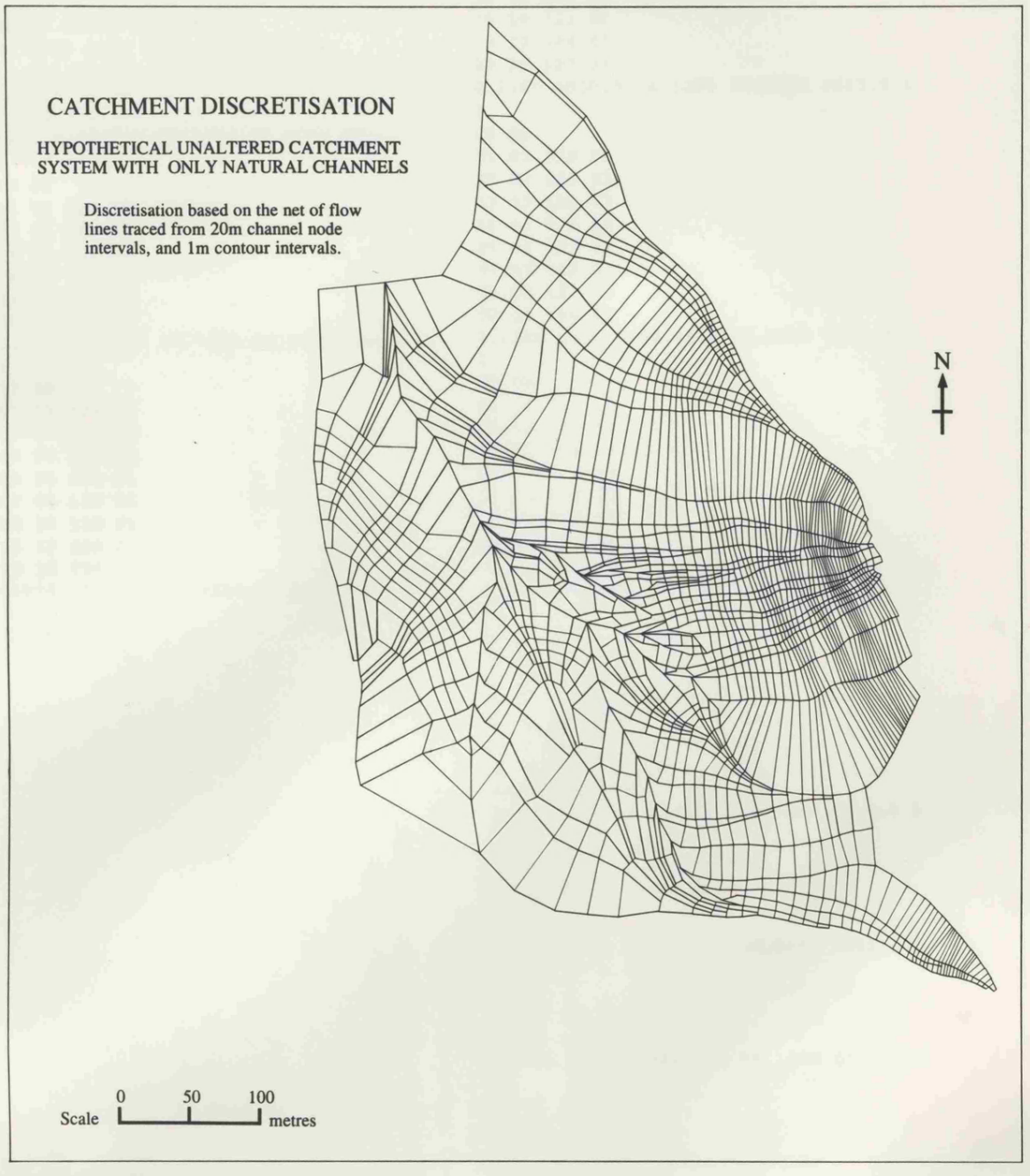
CATCHMENT DISCRETISATION
HYPOTHETICAL UNALTERED CATCHMENT SYSTEM WITH ONLY NATURAL CHANNELS
Discretisation based on the net of flow lines traced from 20m channel node intervals, and 1m contour intervals.
N
Scale
0
50
100
metres

APPENDIX 3.4.1 Sub-Catchment One Discretised Flow-Net Structure and Channel Data

```
Template
(See Appendix 4.1)
NSUB K33 K44
NCHA
NSEG
NCAS
NELM
MCELF MCELT MSAM MHYE
.... ..... .... ....
MCELF MCELT MSAM MHYE
EC CWID EANG WANG CTOP IOFLOW

01 1 1
01
46
1
09 06
01 01 122 01
02 03 121 01
04 05 120 01
06 07 119 01
08 09 118 01
10 10 122 01
0.1100 0000.0 03.7302 03.7302 0023.5 1
1
12 08
01 01 124 01
02 03 123 01
04 04 122 01
05 06 121 01
07 08 120 01
09 10 119 01
11 12 118 01
13 13 124 01
0.1100 0000.0 03.3250 03.3250 0020.0 1
1
11 08
01 01 125 01
02 02 124 01
03 04 123 01
05 05 122 01
06 07 121 01
08 09 120 01
10 11 119 01
12 12 125 01
0.1100 0000.0 03.4845 03.4845 0019.5 1
1
11 09
01 01 126 01
02 02 125 01
03 03 124 01
04 05 123 01
06 06 122 01
07 08 121 01
09 10 120 01
11 11 119 01
12 12 126 01
0.1100 0000.0 06.9648 06.9648 0016.0 1
1
22 09
01 02 127 01
03 04 126 01
05 06 125 01
07 08 124 01
09 12 123 01
13 14 122 01
15 18 121 01
19 22 120 01
23 23 127 01
0.1100 0000.0 16.1020 16.1020 0015.0 1
1
22 09
01 02 127 01
03 04 126 01
05 06 125 01
07 08 124 01
09 12 123 01
13 14 122 01
15 18 121 01
19 22 120 01
23 23 127 01
0.1100 0000.0 16.1020 16.1020 0015.0 1
1
08 08
01 01 106 01
02 02 126 01
03 03 125 01
04 04 124 01
05 06 123 01
07 07 122 01
08 08 121 01
09 09 106 01
0.1100 0000.0 08.4688 08.4688 0015.5 1
1
08 08
01 01 106 01
02 02 126 01
03 03 125 01
04 04 124 01
05 06 123 01
07 07 122 01
08 08 121 01
09 09 106 01
0.1100 0000.0 04.4026 04.4026 0023.0 1
1
08 07
01 02 127 01
03 03 126 01
04 04 125 01
05 05 124 01
06 07 123 01
08 08 122 01
09 09 106 01
0.1100 0000.0 05.8359 05.8359 0014.5 1
1
03 03
01 02 106 01
03 03 126 01
04 04 106 01
0.1100 0000.0 06.8480 06.8480 0012.5 1
1
03 02
01 03 106 01
04 04 106 01
0.1100 0000.0 06.1070 06.1070 0013.5 1
1
05 04
01 03 106 01
04 04 126 01
05 05 125 01
06 06 106 01
0.1100 0000.0 05.7648 05.7648 0018.5 1
1
04 03
01 03 106 01
04 04 126 01
05 05 106 01
0.1100 0000.0 08.0960 08.0960 0012.5 1
```

```
1
09 06
01 04 106 01
05 05 126 01
06 06 125 01
07 07 124 01
08 09 123 01
10 10 106 01
0.1100 0000.0 08.0102 08.0102 0014.0 1
1
04 03
01 01 108 01
02 04 106 01
05 05 108 01
0.1100 0000.0 06.0802 06.0802 0018.0 1
1
03 03
01 01 108 01
02 03 106 01
04 04 108 01
0.1100 0000.0 06.3841 06.3841 0017.0 1
1
09 07
01 01 108 01
02 04 106 01
05 05 126 01
06 06 125 01
07 07 124 01
08 09 123 01
10 10 108 01
0.1100 0000.0 06.6523 06.6523 0016.0 1
1
02 03
01 01 110 01
02 02 108 01
03 03 110 01
0.1100 0000.0 05.9917 05.9917 0019.0 1
1
02 03
01 01 110 01
02 02 108 01
03 03 110 01
0.1100 0000.0 04.4423 04.4423 0023.0 1
1
02 03
01 01 110 01
02 02 108 01
03 03 110 01
0.0490 0000.0 04.0671 04.0671 0021.5 1
1
02 03
01 01 110 01
02 02 108 01
03 03 110 01
0.0490 0000.0 06.9632 06.9632 0012.5 1
1
02 03
01 01 110 01
02 02 108 01
03 03 110 01
0.0490 0000.0 05.0227 05.0227 0021.0 1
1
03 04
01 01 111 01
02 02 110 01
03 03 108 01
04 04 111 01
0.0490 0000.0 05.1012 05.1012 0021.0 1
1
03 04
01 01 111 01
02 02 110 01
03 03 108 01
04 04 111 01
0.0490 0000.0 07.7366 07.7366 0013.5 1
1
03 04
01 01 079 01
02 02 111 01
03 03 110 01
04 04 079 01
0.0490 0000.0 07.0507 07.0507 0013.5 1
1
04 05
01 01 079 01
02 02 111 01
03 03 110 01
04 04 108 01
05 05 079 01
0.0490 0000.0 05.7958 05.7958 0017.0 1
1
03 04
01 01 080 01
02 02 079 01
03 03 077 01
04 04 080 01
0.0490 0000.0 09.5833 09.5833 0012.0 1
1
04 05
01 01 080 01
02 02 079 01
03 03 077 01
04 04 075 01
05 05 080 01
0.0490 0000.0 12.4980 12.4980 0018.5 1
1
05 06
01 01 080 01
02 02 079 01
03 03 077 01
04 04 075 01
05 05 108 01
06 06 080 01
0.0480 0000.0 08.7360 08.7360 0012.5 1
1
05 05
01 02 047 01
03 03 077 01
04 04 075 01
05 05 108 01
06 06 047 01
0.0480 0000.0 09.3622 09.3622 0014.0 1
1
05 05
01 01 047 01
02 03 046 01
04 04 075 01
05 05 073 01
06 06 047 01
0.0480 0000.0 12.3860 12.3860 0011.5 1
1
01 02
01 01 047 01
02 02 047 01
0.0480 0000.0 15.5930 15.5930 0019.0 1
1
02 03
01 01 037 01
```

```
02 02 047 01
03 03 037 01
0.0480 0000.0 09.1124 09.1124 0013.0 1
1
03 03
01 02 037 01
03 03 038 01
04 04 037 01
0.0480 0000.0 05.9369 05.9369 0020.5 1
1
05 05
01 01 036 01
02 03 037 01
04 04 038 01
05 05 046 01
06 06 036 01
0.0480 0000.0 06.2304 06.2304 0016.0 1
1
09 07
01 02 036 01
03 04 037 01
05 05 038 01
06 07 045 01
08 08 075 01
09 09 073 01
10 10 036 01
0.0980 0000.0 03.9928 03.9928 0029.0 1
1
10 07
01 01 035 01
02 03 036 01
04 05 037 01
06 06 038 01
07 09 043 01
10 10 072 01
11 11 035 01
0.0980 0000.0 12.1320 12.1320 0009.5 1
1
10 07
01 01 035 01
02 03 036 01
04 05 037 01
06 06 038 01
07 09 042 01
10 10 072 01
11 11 035 01
0.0980 0000.0 06.1250 06.1250 0020.0 1
1
11 09
01 01 034 01
02 02 035 01
03 04 036 01
05 06 037 01
07 07 038 01
08 09 041 01
10 10 042 01
11 11 072 01
12 12 034 01
0.0980 0000.0 04.6397 04.6397 0024.5 1
1
07 06
01 01 034 01
02 02 035 01
03 04 036 01
05 06 037 01
07 07 038 01
08 08 034 01
0.0980 0000.0 05.3462 05.3462 0019.0 1
1
03 04
01 01 034 01
02 02 035 01
03 03 036 01
04 04 034 01
0.0980 0000.0 07.9667 07.9667 0014.5 1
1
05 04
01 02 034 01
03 03 035 01
04 05 036 01
06 06 034 01
0.0980 0000.0 03.3118 03.3118 0028.5 1
1
09 06
01 03 034 01
04 04 035 01
05 06 036 01
07 08 037 01
09 09 038 01
10 10 034 01
0.0980 0000.0 02.4507 02.4507 0037.0 1
1
24 07
01 06 034 01
07 08 035 01
09 12 036 01
13 16 037 01
17 18 038 01
19 24 040 01
25 25 034 01
0.0980 0000.0 02.7179 02.7179 0027.5 1
1
24 07
01 06 034 01
07 08 035 01
09 12 036 01
13 16 037 01
17 18 038 01
19 24 040 01
25 25 034 01
0.0980 0000.0 02.7179 02.7179 0027.5 1
1
08 05
01 03 034 01
04 04 035 01
05 06 036 01
07 08 037 01
09 09 034 01
0.0980 0000.0 03.9907 03.9907 0027.5 1
```

APPENDIX 3.4.2 Sub-Catchment One Digitised Coordinate Pairs for Flow Net Elements and Segments

Template
(See Appendix 4.1)
First line
XO YO
Other paired lines
X(1) Y(1) Z(1)
X(2) Y(2) Z(2)

270.77 631.48

639.90	57.53	130.00
638.78	61.55	130.00
631.15	54.13	129.00
629.53	59.60	129.00
623.47	52.03	128.00
621.90	58.08	128.00
617.63	49.53	127.00
614.97	56.83	127.00
612.75	46.55	126.00
609.17	55.13	126.00
607.85	44.03	125.00
603.67	53.78	125.00
603.40	41.95	124.00
599.00	51.80	124.00
597.88	39.17	123.00
593.25	49.58	123.00
592.35	36.05	122.00
587.47	47.35	122.00
584.50	32.50	120.90
563.90	36.13	118.60
638.50	61.78	130.00
637.17	66.83	130.00
629.78	59.22	129.00
628.13	65.15	129.00
621.42	58.20	128.00
619.80	63.72	128.00
614.85	56.88	127.00
612.67	62.83	127.00
608.92	55.33	126.00
606.70	61.65	126.00
603.63	53.88	125.00
600.53	61.22	125.00
598.78	52.10	124.00
595.65	59.88	124.00
593.10	49.72	123.00
589.38	58.58	123.00
587.35	47.08	122.00
583.25	57.10	122.00
580.10	43.92	121.00
576.47	55.38	121.00
571.97	40.28	120.00
569.17	53.40	120.00
565.20	37.63	119.00
562.08	50.97	119.00
561.20	35.95	118.60
548.75	47.90	117.60
620.03	63.70	128.00
619.10	83.25	128.00
613.05	62.63	127.00
611.40	83.35	127.00
606.67	61.70	126.00
603.10	83.83	126.00
600.67	61.10	125.00
597.15	82.85	125.00
595.70	59.72	124.00
592.05	80.28	124.00
589.38	58.13	123.00
586.75	78.30	123.00
583.17	57.05	122.00
578.95	76.17	122.00
576.40	55.22	121.00
571.72	73.92	121.00
569.05	53.47	120.00
565.25	71.92	120.00
561.85	51.22	119.00
558.03	70.03	119.00
553.15	48.95	118.00
549.15	67.72	118.00
548.50	47.50	117.60
531.00	63.25	116.50
611.45	83.35	127.00
610.22	94.83	127.00
602.75	83.40	126.00
601.05	94.50	126.00
596.97	83.00	125.00
594.47	93.75	125.00
592.17	80.20	124.00
587.92	92.33	124.00
586.63	78.65	123.00
583.40	91.00	123.00
578.60	76.13	122.00
576.20	89.00	122.00
571.88	74.17	121.00
569.25	87.72	121.00
565.33	72.17	120.00
564.30	87.70	120.00
558.30	70.28	119.00
555.38	87.30	119.00
549.28	67.78	118.00
545.88	85.63	118.00
538.00	65.17	117.00
533.40	82.80	117.00
530.35	63.05	116.50
513.95	75.38	115.50
601.08	94.40	126.00
605.17	109.53	126.00
597.69	94.17	125.50
601.63	109.75	125.50
594.30	93.95	125.00
597.65	109.97	125.00
591.21	93.33	124.50
593.63	113.80	124.50
588.13	92.72	124.00
590.01	117.52	124.00
585.81	91.86	123.50
586.58	116.92	123.50
583.50	91.10	123.00
583.15	116.40	123.00
579.87	90.17	122.50
579.14	115.29	122.50
576.25	89.25	122.00
575.15	114.23	122.00
572.83	88.40	121.50
570.69	113.20	121.50
569.42	87.55	121.00
566.64	112.09	121.00
566.76	87.61	120.50
562.66	111.37	120.50
564.10	87.67	120.00
559.10	110.66	120.00
559.84	87.29	119.50
554.59	109.73	119.50
555.58	86.90	119.00
550.00	108.88	119.00
550.90	86.24	118.50
544.37	107.31	118.50
546.22	85.58	118.00
538.67	106.19	118.00
539.80	84.33	117.50
530.98	102.45	117.50
533.38	83.08	117.00
524.66	099.00	117.00
525.83	80.30	116.50
514.80	093.27	116.50
518.28	77.53	116.00
506.31	087.47	116.00
516.04	076.61	115.75
503.48	083.58	115.75
513.80	75.70	115.50
500.65	079.70	115.45
605.17	109.53	126.00
609.35	124.58	126.00
601.63	109.75	125.50
605.57	125.33	125.50
597.65	109.97	125.00
601.80	126.08	125.00
593.63	113.80	124.50
596.85	134.20	124.50
590.01	117.52	124.00
591.90	142.33	124.00
586.58	116.92	123.50
587.35	141.98	123.50
583.15	116.40	123.00
582.80	141.63	123.00
579.14	115.29	122.50
578.42	140.42	122.50
575.15	114.23	122.00
574.05	139.22	122.00
570.69	113.20	121.50
568.55	137.92	121.50
566.64	112.09	121.00
563.05	136.63	121.00
562.66	111.37	120.50
558.57	135.14	120.50
559.10	110.66	120.00
554.10	133.65	120.00
554.59	109.73	119.50
549.34	132.17	119.50
550.00	108.88	119.00
544.58	130.70	119.00
544.37	107.31	118.50
537.85	128.39	118.50
538.67	106.19	118.00
531.13	126.08	118.00
530.98	102.45	117.50
522.16	120.50	117.50
524.66	099.00	117.00
513.20	114.92	117.00
514.80	093.27	116.50
503.77	106.17	116.50
506.31	087.47	116.00
494.35	97.42	116.00
503.48	083.58	115.75
490.92	090.52	115.75
500.65	079.70	115.45
487.50	83.63	115.40
582.65	141.58	123.00
580.25	150.55	123.00
574.05	139.10	122.00
570.80	148.75	122.00
563.10	136.30	121.00
560.33	145.63	121.00
554.47	133.50	120.00
550.70	142.78	120.00
544.28	130.92	119.00
541.17	137.85	119.00
530.50	126.15	118.00
528.38	130.83	118.00

513.20	115.00	117.00	352.45	145.65	113.10	340.70	209.10	112.50
507.55	123.85	117.00	477.77	159.13	117.00	313.23	231.42	112.50
493.92	97.38	116.00	477.02	160.67	117.00	293.42	203.88	112.00
473.15	114.83	116.00	449.40	143.78	116.00	280.00	220.33	112.00
487.17	83.80	115.40	449.00	151.22	116.00	288.08	200.92	111.60
461.63	92.47	114.90	425.38	143.33	115.00	272.13	212.17	111.30
580.17	150.47	123.00	426.15	149.92	115.00	313.35	231.60	112.50
579.80	153.03	123.00	393.05	144.65	114.00	305.95	245.42	112.50
570.70	148.65	122.00	394.42	154.85	114.00	279.98	220.50	112.00
569.67	152.65	122.00	353.33	145.20	113.10	266.67	236.20	112.00
560.15	145.45	121.00	337.70	156.70	112.90	272.27	212.13	111.30
559.03	149.13	121.00	552.00	172.90	121.00	254.00	226.30	111.10
550.85	142.47	120.00	551.72	174.83	121.00	306.15	245.47	112.50
549.72	146.17	120.00	541.33	173.45	120.00	301.50	255.35	112.50
541.20	137.53	119.00	541.03	177.00	120.00	266.70	236.10	112.00
539.28	141.90	119.00	529.30	173.15	119.00	257.10	248.83	112.00
528.55	130.55	118.00	528.58	178.38	119.00	254.25	225.97	111.10
525.90	137.97	118.00	511.02	170.50	118.00	240.30	238.35	111.00
507.58	124.00	117.00	507.98	177.33	118.00	301.52	255.15	112.50
504.23	134.58	117.00	476.95	160.67	117.00	298.45	264.03	112.50
473.48	114.83	116.00	474.17	167.90	117.00	257.55	248.75	112.00
457.30	122.85	116.00	449.33	151.42	116.00	250.80	263.08	112.00
462.00	92.17	114.90	450.30	168.15	116.00	240.45	238.53	111.00
437.13	102.85	114.60	425.95	149.78	115.00	223.32	251.53	110.70
569.70	151.85	122.00	428.45	164.75	115.00	298.13	264.47	112.50
564.22	172.95	122.00	394.80	154.60	114.00	295.55	273.60	112.50
558.95	149.45	121.00	396.35	167.75	114.00	250.85	262.75	112.00
551.75	172.58	121.00	341.35	157.05	113.00	245.35	274.38	112.00
549.65	146.35	120.00	341.88	176.22	113.00	223.60	251.70	110.70
541.45	173.40	120.00	337.90	157.13	112.90	203.90	266.33	110.40
539.58	142.33	119.00	322.70	172.85	112.40	295.90	273.47	112.50
529.25	174.00	119.00	449.13	163.38	116.00	294.38	278.38	112.50
525.83	137.92	118.00	450.83	168.60	116.00	245.60	274.45	112.00
511.35	170.05	118.00	428.38	164.63	115.00	243.88	281.72	112.00
504.33	134.67	117.00	428.85	169.00	115.00	210.18	267.78	111.00
484.45	157.03	117.00	396.38	167.72	114.00	207.60	280.28	111.00
457.98	123.00	116.00	396.98	172.28	114.00	203.45	266.17	110.40
452.38	130.38	116.00	341.75	176.13	113.00	184.25	279.35	110.10
442.02	107.90	115.00	340.38	181.92	113.00	294.52	278.28	112.50
428.88	118.13	115.00	323.33	172.75	112.40	292.58	286.55	112.50
436.83	102.63	114.60	315.13	179.78	112.30	243.93	281.65	112.00
415.80	109.97	114.30	428.80	168.65	115.00	243.85	290.33	112.00
483.75	157.05	117.00	429.13	172.13	115.00	207.32	280.10	111.00
480.92	158.08	117.00	396.67	172.38	114.00	206.73	291.55	111.00
452.23	130.67	116.00	397.13	175.95	114.00	184.63	278.95	110.10
450.42	134.80	116.00	340.45	181.88	113.00	173.43	292.90	109.80
428.48	117.97	115.00	339.50	187.90	113.00	243.60	286.95	112.00
426.27	124.90	115.00	315.80	179.83	112.30	243.85	290.50	112.00
416.02	110.00	114.30	307.23	187.17	112.10	206.93	291.08	111.00
391.38	118.70	113.70	551.85	174.97	121.00	208.70	301.72	111.00
450.48	134.65	116.00	552.58	180.65	121.00	177.65	293.70	110.00
450.40	136.28	116.00	541.15	177.13	120.00	173.00	307.13	110.00
426.55	125.25	115.00	541.72	181.55	120.00	173.38	292.70	109.80
425.55	133.55	115.00	528.85	178.45	119.00	160.35	306.17	109.40
399.15	119.58	114.00	528.38	183.65	119.00	292.70	286.25	112.50
394.65	135.90	114.00	507.83	177.30	118.00	292.02	291.40	112.50
391.27	119.15	113.70	505.02	186.08	118.00	243.95	290.55	112.00
374.20	131.47	113.40	474.05	168.20	117.00	246.38	299.45	112.00
511.27	170.33	118.00	473.65	182.38	117.00	208.52	302.17	111.00
509.75	173.30	118.00	450.25	168.47	116.00	207.73	309.70	111.00
484.17	156.97	117.00	453.77	184.40	116.00	172.93	307.15	110.00
477.20	160.55	117.00	428.70	172.08	115.00	170.57	312.28	110.00
450.10	136.25	116.00	429.10	186.60	115.00	160.18	306.30	109.40
449.38	143.67	116.00	396.95	175.63	114.00	139.23	316.95	108.80
425.40	133.50	115.00	399.58	192.92	114.00	207.90	309.67	111.00
425.30	143.38	115.00	339.30	187.42	113.00	208.52	312.08	111.00
394.83	135.97	114.00	340.48	208.92	113.00	170.45	312.60	110.00
393.30	145.05	114.00	307.33	187.22	112.10	170.25	315.75	110.00
374.20	131.17	113.40	288.25	200.58	111.60	142.00	316.72	109.00

143.23	320.15	109.00	149.57	418.13	109.00	193.82	492.83	105.00
138.98	317.15	108.80	154.73	423.85	109.00	173.85	496.65	104.00
116.75	327.60	108.20	130.23	439.63	108.00	190.38	505.73	104.00
245.25	296.53	112.00	146.02	444.75	108.00	166.77	509.15	103.10
246.05	299.33	112.00	125.38	449.92	107.00	181.32	523.48	102.70
208.05	309.92	111.00	144.10	454.95	107.00	296.92	348.75	112.50
210.77	320.47	111.00	124.15	460.53	106.00	296.88	359.58	112.50
170.65	315.92	110.00	142.00	461.97	106.00	282.10	355.63	112.00
179.15	336.92	110.00	123.32	467.88	105.30	291.33	362.50	112.00
143.15	320.22	109.00	137.43	481.35	103.90	255.35	389.15	111.00
155.85	346.72	109.00	294.15	325.25	112.50	261.50	401.10	111.00
117.07	327.42	108.20	295.15	331.05	112.50	220.00	412.88	110.00
112.45	349.65	108.15	268.63	336.55	112.00	231.60	422.13	110.00
292.17	291.42	112.50	272.10	341.65	112.00	202.23	446.20	109.00
292.23	307.72	112.50	236.55	360.92	111.00	209.57	449.47	109.00
246.05	299.50	112.00	240.50	366.75	111.00	198.70	462.00	108.00
254.60	313.70	112.00	190.73	392.78	110.00	205.68	464.47	108.00
210.48	320.17	111.00	194.80	398.72	110.00	196.82	472.42	107.00
224.80	340.15	111.00	154.95	424.08	109.00	204.40	475.20	107.00
179.00	337.15	110.00	170.02	432.45	109.00	195.70	482.17	106.00
186.73	370.00	110.00	146.05	444.67	108.00	202.68	484.42	106.00
156.00	346.15	109.00	166.95	450.17	108.00	193.77	492.77	105.00
156.32	376.70	109.00	144.05	454.78	107.00	200.93	496.13	105.00
112.70	349.67	108.15	164.40	459.53	107.00	190.35	505.70	104.00
110.20	372.67	108.10	141.65	461.53	106.00	200.35	511.38	104.00
292.05	307.38	112.50	161.98	467.50	106.00	182.95	519.80	103.00
293.30	321.08	112.50	139.18	470.50	105.00	197.35	528.33	103.00
254.73	313.33	112.00	158.95	476.28	105.00	181.60	523.38	102.70
265.85	332.67	112.00	137.18	481.30	103.90	194.57	538.15	102.20
224.75	339.83	111.00	151.65	495.23	103.50	206.85	449.08	109.00
233.65	356.42	111.00	294.85	331.08	112.50	208.43	449.35	109.00
186.45	369.70	110.00	296.38	340.05	112.50	205.73	464.65	108.00
188.85	386.05	110.00	272.15	341.78	112.00	209.05	464.30	108.00
156.43	376.53	109.00	277.08	350.28	112.00	204.57	474.92	107.00
153.75	396.85	109.00	240.27	366.75	111.00	209.20	475.88	107.00
110.03	372.65	108.10	247.43	376.78	111.00	202.35	484.40	106.00
109.32	396.50	108.05	194.60	398.70	110.00	208.90	485.65	106.00
293.52	320.75	112.50	212.93	407.92	110.00	200.93	496.27	105.00
293.85	325.58	112.50	170.02	432.75	109.00	205.38	497.60	105.00
265.92	332.38	112.00	196.88	442.42	109.00	200.70	511.10	104.00
268.60	336.58	112.00	166.85	450.00	108.00	205.68	513.15	104.00
233.57	356.20	111.00	191.77	458.38	108.00	197.35	528.23	103.00
236.75	360.97	111.00	164.10	459.83	107.00	206.80	533.17	103.00
188.70	386.05	110.00	187.63	467.92	107.00	194.45	538.05	102.20
190.80	392.53	110.00	162.13	467.50	106.00	206.77	553.08	101.80
153.82	396.70	109.00	183.55	476.38	106.00	205.40	497.45	105.00
149.68	418.45	109.00	158.88	476.45	105.00	207.02	497.63	105.00
109.43	396.13	108.05	179.43	485.58	105.00	205.63	512.83	104.00
110.30	418.22	108.00	155.20	486.58	104.00	208.90	514.17	104.00
149.13	415.40	109.00	173.85	496.75	104.00	206.93	533.03	103.00
149.43	416.47	109.00	151.30	494.80	103.50	211.20	533.98	103.00
110.28	418.08	108.00	166.95	509.13	103.10	206.82	553.05	101.80
116.43	436.90	107.80	296.60	339.88	112.50	219.82	569.83	101.30
149.20	416.60	109.00	297.25	348.72	112.50	206.05	485.20	106.00
149.98	418.65	109.00	277.05	350.25	112.00	208.90	485.33	106.00
120.63	434.42	108.00	282.58	355.65	112.00	205.57	497.55	105.00
122.80	436.88	108.00	247.32	377.17	111.00	208.95	497.67	105.00
116.85	437.08	107.80	255.70	389.22	111.00	208.80	514.23	104.00
114.93	459.72	106.00	213.20	408.08	110.00	211.02	514.33	104.00
150.05	418.63	109.00	220.52	413.03	110.00	211.02	534.08	103.00
151.25	421.95	109.00	196.85	442.45	109.00	216.07	533.73	103.00
122.57	436.67	108.00	202.73	446.63	109.00	216.00	557.25	102.00
130.48	439.42	108.00	191.65	458.15	108.00	221.68	555.92	102.00
118.85	448.70	107.00	198.88	462.13	108.00	220.25	569.70	101.30
125.53	450.10	107.00	187.63	468.05	107.00	232.20	584.58	100.90
115.45	459.80	106.00	197.13	472.80	107.00	208.27	449.55	109.00
123.40	468.03	105.30	183.40	476.65	106.00	209.82	449.42	109.00
189.80	390.72	110.00	195.70	482.25	106.00	208.80	464.15	108.00
190.93	392.40	110.00	179.20	485.67	105.00	211.90	464.38	108.00

209.10	475.95	107.00	288.26	393.51	111.50
212.07	476.15	107.00	271.61	410.28	111.00
208.82	485.53	106.00	281.20	419.28	111.00
213.13	485.88	106.00	261.75	422.69	110.50
208.95	497.55	105.00	276.72	433.64	110.50
214.38	497.20	105.00	251.91	435.10	110.00
210.82	514.42	104.00	272.25	448.00	110.00
218.50	513.03	104.00	245.98	446.91	109.50
215.80	533.73	103.00	271.29	458.04	109.50
225.40	531.83	103.00	240.05	458.73	109.00
221.77	555.90	102.00	270.33	468.08	109.00
231.95	551.90	102.00	240.00	465.99	108.50
228.05	573.67	101.00	269.28	475.18	108.50
240.00	570.33	101.00	239.96	473.26	108.00
232.27	584.65	100.90	268.23	482.28	108.00
244.75	599.75	100.60	239.17	478.47	107.50
291.10	362.53	112.00	266.36	486.88	107.50
293.21	365.14	112.00	238.38	483.69	107.00
276.56	381.90	111.50	264.50	491.48	107.00
282.41	387.70	111.50	237.82	488.43	106.50
262.02	401.28	111.00	263.01	495.84	106.50
271.61	410.28	111.00	237.26	493.17	106.00
246.79	411.74	110.50	261.52	500.20	106.00
261.75	422.69	110.50	237.50	498.31	105.50
231.57	422.20	110.00	261.26	504.96	105.50
251.91	435.10	110.00	237.75	503.46	105.00
220.67	435.79	109.50	261.00	509.73	105.00
245.98	446.91	109.50	238.89	509.96	104.50
209.77	449.38	109.00	261.21	514.96	104.50
240.05	458.73	109.00	240.03	516.46	104.00
210.73	456.81	108.50	261.42	520.20	104.00
240.00	465.99	108.50	241.07	524.23	103.50
211.70	464.25	108.00	260.00	526.26	103.50
239.96	473.26	108.00	242.11	532.00	103.00
211.98	470.07	107.50	258.58	532.33	103.00
239.17	478.47	107.50	242.95	541.08	102.50
212.27	475.90	107.00	257.20	540.39	102.50
238.38	483.69	107.00	243.79	550.16	102.00
212.63	481.02	106.50	255.82	548.45	102.00
237.82	488.43	106.50	246.93	560.56	101.50
213.00	486.15	106.00	257.95	560.00	101.50
237.26	493.17	106.00	250.06	570.96	101.00
213.75	491.67	105.50	260.08	571.55	101.00
237.50	498.31	105.50	250.67	589.32	100.80
214.50	497.20	105.00	258.74	593.55	100.80
237.75	503.46	105.00	251.27	607.67	100.45
216.57	504.96	104.50	257.40	615.55	100.30
238.89	509.96	104.50	266.23	482.47	108.00
218.65	512.73	104.00	268.50	482.55	108.00
240.03	516.46	104.00	264.17	491.48	107.00
222.15	522.20	103.50	267.27	492.15	107.00
241.07	524.23	103.50	261.13	500.48	106.00
225.65	531.67	103.00	265.02	500.33	106.00
242.11	532.00	103.00	261.05	509.50	105.00
228.71	541.77	102.50	265.25	509.38	105.00
242.95	541.08	102.50	261.25	520.15	104.00
231.77	551.88	102.00	266.40	520.88	104.00
243.79	550.16	102.00	258.77	532.13	103.00
235.91	561.13	101.50	266.88	532.58	103.00
246.93	560.56	101.50	255.65	548.48	102.00
240.05	570.38	101.00	267.75	546.98	102.00
250.06	570.96	101.00	260.05	571.67	101.00
242.60	585.09	100.80	272.00	566.83	101.00
250.67	589.32	100.80	257.23	615.13	100.30
245.15	599.80	100.60	270.42	631.73	100.00
251.27	607.67	100.45			
293.21	365.14	112.00			
295.33	367.75	112.00			
282.41	387.70	111.50			

APPENDIX 3.4.3 Sub-Catchment Two Discretised Flow-Net Structure and Channel Data

```
Template
(See Appendix 4.1)
NSUB K33 K44
NCHA
NSEG
NCAS
NELM
MCELF MCELT MSAM MHYE
....  ..... .... ....
MCELF MCELT MSAM MHYE
EC CWID EANG WANG CTOP IOFLOW

01 1 1
02
14
2
10 07
01 02 101 01
03 05 106 01
06 07 126 01
08 08 125 01
09 09 124 01
10 10 123 01
11 11 101 01
04 03
01 02 104 01
03 03 106 01
05 05 101 01
0.1580 0000.0 07.9287 07.9287 0013.5 3
2
08 07
01 01 102 01
02 02 101 01
03 04 106 01
05 05 097 01
06 07 126 01
08 08 125 01
09 09 102 01
03 04
01 01 103 01
02 02 104 01
03 03 106 01
04 04 102 01
0.1580 0000.0 07.9287 07.9287 0013.5 3
2
09 06
01 03 102 01
04 04 101 01
05 05 099 01
06 07 097 01
08 09 126 01
10 10 102 01
05 04
01 03 103 01
04 04 104 01
05 05 106 01
06 06 102 01
0.1580 0000.0 07.9287 07.9287 0013.5 3
2
06 04
01 04 102 01
05 05 101 01
06 06 100 01
07 07 102 01
06 04
01 04 103 01
05 05 104 01
06 06 105 01
07 07 102 01
0.1580 0000.0 11.5085 11.5085 0011.5 3
2
06 05
01 01 067 01
02 04 068 01
05 05 102 01
06 06 101 01
07 07 067 01
07 06
01 01 067 01
02 03 068 01
04 05 069 01
06 06 070 01
07 07 071 01
08 08 067 01
0.1580 0000.0 07.5013 07.5013 0019.5 3
2
05 04
01 01 066 01
02 05 068 01
05 05 102 01
06 06 066 01
06 05
01 01 067 01
02 03 068 01
04 05 069 01
06 06 070 01
07 07 066 01
0.1580 0000.0 44.6910 44.6910 0014.5 3
1
07 06
01 01 066 01
02 02 067 01
03 04 068 01
05 06 069 01
07 07 070 01
08 08 066 01
0.0850 0000.0 03.6010 03.6010 0022.5 1
1
09 07
01 02 066 01
03 03 067 01
04 05 068 01
06 07 069 01
08 08 070 01
09 09 071 01
10 10 067 01
0.0850 0000.0 05.0020 05.0020 0019.5 1
1
10 08
01 01 065 01
02 03 066 01
04 04 067 01
05 06 068 01
07 08 069 01
09 09 070 01
10 10 071 01
11 11 065 01
0.0850 0000.0 05.2082 05.2082 0017.5 1
1
10 08
01 01 065 01
02 02 066 01
03 04 067 01
05 06 068 01
07 08 069 01
09 09 070 01
10 10 071 01
11 11 065 01
```

```
0.0850 0000.0 01.4969 01.4969 0041.5 1
1
10 07
01 01 034 01
02 02 035 01
03 03 036 01
04 05 037 01
06 08 038 01
09 10 039 01
11 11 034 01
0.0850 0000.0 02.0752 02.0752 0034.5 1
1
09 07
01 01 034 01
02 02 035 01
03 03 036 01
04 05 037 01
06 08 038 01
09 09 039 01
10 10 034 01
0.0850 0000.0 02.0949 02.0949 0036.0 1
1
26 07
01 08 034 01
09 12 035 01
13 19 036 01
20 21 037 01
22 24 038 01
25 26 039 01
27 27 034 01
0.0850 0000.0 03.9658 03.9658 0019.5 1
1
09 06
01 02 034 01
03 03 035 01
04 04 036 01
05 07 037 01
08 09 038 01
10 10 034 01
0.0850 0000.0 04.2578 04.2578 0015.0 1
03
1
01 02
01 01 033 01
02 02 033 01
0.0850 0000.0 04.0000 04.0000 0020.0 1
1
08 05
01 03 034 01
04 04 035 01
05 05 036 01
06 08 037 01
09 09 034 01
0.0850 0000.0 04.0000 04.0000 0020.0 1
1
07 05
01 03 034 01
04 04 035 01
05 05 036 01
06 07 037 01
08 08 034 01
0.0850 0000.0 04.0000 04.0000 0020.0 1
```

APPENDIX 3.4.4 Sub-Catchment Two Digitised Coordinate Pairs for Flow Net Elements and Segments

Template
(See Appendix 4.1)
First line
XO YO
Other paired lines
X(1) Y(1) Z(1)
X(2) Y(2) Z(2)

270.77 631.48
541.72 181.35 120.00
542.17 183.60 120.00
528.20 183.55 119.00
529.15 188.45 119.00
505.17 186.05 118.00
508.88 198.55 118.00
473.58 182.25 117.00
479.73 214.67 117.00
453.67 184.33 116.00
461.20 224.97 116.00
428.83 186.40 115.00
447.65 230.40 115.00
399.88 193.22 114.00
429.88 239.85 114.00
376.85 228.60 113.00
410.52 264.85 113.00
372.25 266.90 112.00
392.45 294.38 112.00
374.00 299.63 111.00
379.95 303.45 111.00
373.85 303.53 110.70
372.42 313.25 110.00
402.83 200.00 114.00
399.85 193.10 114.00
376.90 228.50 113.00
340.77 209.58 113.00
372.02 266.42 112.00
339.23 300.28 112.00
374.10 299.70 111.00
362.38 307.17 111.00
373.95 303.53 110.70
372.27 313.47 110.00
505.80 193.10 118.00
509.10 198.75 118.00
479.80 214.45 117.00
485.20 223.42 117.00
461.15 225.30 116.00
467.85 242.53 116.00
447.67 230.42 115.00
455.63 249.13 115.00
430.08 239.80 114.00
441.42 255.42 114.00
410.92 264.72 113.00
418.00 269.17 113.00
392.83 294.83 112.00
401.27 311.60 112.00
379.65 303.45 111.00
391.42 317.13 111.00
372.13 313.28 110.00
376.08 336.42 108.70
295.15 276.10 112.50
292.10 296.25 112.50
339.30 300.47 112.00
347.63 324.67 112.00
363.27 307.97 111.00
355.20 325.83 111.00
371.95 313.40 110.00
376.10 336.53 108.70
482.67 222.50 117.00
484.98 223.50 117.00
467.98 242.80 116.00
475.80 252.03 116.00
455.60 249.28 115.00
466.05 272.75 115.00
441.45 255.17 114.00
455.35 287.92 114.00
417.92 269.00 113.00
445.67 301.85 113.00
401.42 311.13 112.00
410.77 329.50 112.00
391.40 316.83 111.00
402.38 335.05 111.00
383.15 322.42 110.00
398.75 339.28 110.00
378.42 331.88 109.00
391.55 344.67 109.00
376.35 336.40 108.70
380.02 358.13 107.60
291.92 296.20 112.50
292.75 312.60 112.50
347.40 324.35 112.00
338.52 337.80 112.00
354.95 325.75 111.00
347.35 347.47 111.00
362.83 327.78 110.00
355.55 349.55 110.00
373.70 333.03 109.00
362.90 350.47 109.00
376.38 336.60 108.70
379.98 358.20 107.60
442.02 298.75 113.00
445.67 302.10 113.00
410.67 329.22 112.00
425.65 349.88 112.00
402.55 335.15 111.00
413.90 356.58 111.00
398.63 338.90 110.00
407.42 360.22 110.00
391.55 344.55 109.00
402.38 364.33 109.00
383.27 349.97 108.00
394.75 367.97 108.00
380.05 357.78 107.60
382.10 381.30 106.50
292.75 312.55 112.50
295.70 335.00 112.50
338.50 338.05 112.00
329.00 357.40 112.00
347.23 347.42 111.00
342.88 366.38 111.00
355.70 349.45 110.00
350.80 368.92 110.00
363.15 350.80 109.00
357.35 371.83 109.00
372.98 353.75 108.00
364.85 374.78 108.00
380.10 357.88 107.60
381.77 381.13 106.50
422.55 347.47 112.00
425.42 350.28 112.00
413.70 356.75 111.00
420.80 362.47 111.00
407.10 360.75 110.00
414.48 369.90 110.00
402.48 364.28 109.00
410.52 376.45 109.00
394.65 368.05 108.00
405.30 384.38 108.00
384.88 373.75 107.00
400.15 390.20 107.00
381.92 380.97 106.50
384.55 403.67 105.60
295.60 334.85 112.50
296.88 344.05 112.50
328.88 357.47 112.00
324.92 369.15 112.00
342.80 366.63 111.00
340.63 373.85 111.00
350.70 369.10 110.00
348.05 378.03 110.00
357.45 371.92 109.00
355.10 380.60 109.00
365.00 374.78 108.00
362.15 383.20 108.00
374.33 378.40 107.00
369.63 387.08 107.00
382.17 381.33 106.50
384.27 403.80 105.60
417.85 362.03 111.00
420.83 362.55 111.00
414.45 370.15 110.00
417.35 372.05 110.00
410.75 376.50 109.00
413.98 379.42 109.00
405.30 384.92 108.00
408.98 388.92 108.00
400.20 390.28 107.00
405.58 395.15 107.00
384.45 403.97 105.60
394.15 421.63 105.10
327.00 364.13 112.00
326.08 367.42 112.00
340.63 373.72 111.00
338.00 380.13 111.00
348.35 378.08 110.00
344.80 385.75 110.00
355.13 380.42 109.00
350.98 390.40 109.00
362.33 383.05 108.00
357.15 394.67 108.00
369.27 386.88 107.00
363.35 398.28 107.00
384.15 404.05 105.40
394.00 421.90 105.10
326.30 367.15 112.00
324.75 369.38 112.00
337.67 380.10 111.00
334.95 384.60 111.00
344.88 385.83 110.00
342.33 391.35 110.00
350.83 390.63 109.00
347.95 396.25 109.00
356.92 394.60 108.00
354.30 400.90 108.00
363.05 398.53 107.00
359.88 404.85 107.00
371.83 404.10 106.00
367.38 411.28 106.00
394.05 421.67 105.10
390.27 431.65 104.70
296.73 344.08 112.50
296.75 351.35 112.50
325.20 369.33 112.00
321.50 373.25 112.00
335.35 384.60 111.00
329.98 391.30 111.00
342.42 391.40 110.00
337.52 398.45 110.00
347.90 396.63 109.00
342.80 404.20 109.00
354.05 400.92 108.00

347.75 409.85 108.00
359.77 404.90 107.00
352.38 415.58 107.00
367.15 411.30 106.00
357.58 421.03 106.00
376.80 420.50 105.00
365.05 429.45 105.00
390.38 431.78 104.70
379.00 450.72 103.90
297.20 351.35 112.50
296.80 355.92 112.50
321.67 373.28 112.00
318.10 376.13 112.00
330.45 391.45 111.00
326.30 396.58 111.00
337.60 398.67 110.00
333.17 403.67 110.00
342.88 404.60 109.00
337.73 409.70 109.00
347.85 410.42 108.00
342.23 415.78 108.00
352.15 415.78 107.00
346.70 422.20 107.00
357.55 421.08 106.00
350.55 427.30 106.00
364.85 429.58 105.00
358.00 436.03 105.00
376.90 448.53 104.00
368.90 454.42 104.00
379.05 451.05 103.90
373.65 470.17 103.40
297.02 355.90 112.50
291.42 361.95 112.50
317.73 376.20 112.00
306.70 383.00 112.00
326.48 396.38 111.00
304.48 413.03 111.00
332.95 403.85 110.00
309.85 422.42 110.00
337.20 409.97 109.00
314.40 428.80 109.00
341.83 415.72 108.00
318.83 434.70 108.00
346.60 422.35 107.00
322.98 439.15 107.00
350.27 427.45 106.00
327.20 444.65 106.00
357.98 436.05 105.00
333.42 451.72 105.00
368.92 454.58 104.00
340.48 460.90 104.00
373.70 470.28 103.40
362.70 489.63 102.70
306.75 382.38 112.00
298.02 368.88 112.00
304.52 412.85 111.00
291.75 419.42 111.00
309.50 423.28 110.00
296.85 435.15 110.00
314.33 428.78 109.00
302.17 441.35 109.00
318.92 434.50 108.00
307.63 447.10 108.00
322.50 439.20 107.00
311.83 451.65 107.00
326.80 444.97 106.00
316.95 455.72 106.00
333.27 451.17 105.00
322.30 462.25 105.00
340.08 460.92 104.00
327.88 468.70 104.00
346.05 473.28 103.00
336.13 480.30 103.00
362.80 489.92 102.70
351.33 508.80 102.30
292.00 419.63 111.00
287.98 422.20 111.00
297.05 434.65 110.00
290.60 441.45 110.00
302.08 441.33 109.00
295.45 449.88 109.00
307.50 446.97 108.00
300.35 456.05 108.00
312.02 451.97 107.00
304.38 460.97 107.00
316.90 455.90 106.00
308.77 464.88 106.00
322.20 462.47 105.00
313.95 469.75 105.00
327.42 468.70 104.00
319.25 476.50 104.00
335.73 480.25 103.00
326.35 485.85 103.00
351.40 508.40 102.30
339.52 526.25 101.80
297.98 368.70 112.00
294.70 367.60 112.00
291.88 419.03 111.00
280.92 418.90 111.00
290.77 441.15 110.00
272.52 447.42 110.00
295.05 449.67 109.00
277.88 466.42 109.00
300.05 456.05 108.00
281.23 477.67 108.00
304.50 460.92 107.00
284.65 484.83 107.00
308.70 465.17 106.00
288.08 492.10 106.00
309.96 466.37 105.75
288.88 493.39 105.75
311.23 467.57 105.50
289.67 494.67 105.50
312.50 468.77 105.25
290.47 495.96 105.25
313.77 469.97 105.00
291.27 497.25 105.00
315.17 471.48 104.75
292.20 498.58 104.75
316.57 473.00 104.50
293.12 499.92 104.50
317.98 474.51 104.25
294.00 501.26 104.25
319.38 476.03 104.00
294.98 502.60 104.00
321.11 478.51 103.75
296.31 504.33 103.75
322.84 481.00 103.50
297.64 506.07 103.50
324.57 483.48 103.25
298.97 507.81 103.25
326.30 485.97 103.00
300.30 509.55 103.00
327.96 490.00 102.75
303.42 523.75 102.75
329.62 496.01 102.50
306.82 517.95 102.50
331.29 501.03 102.25
310.21 522.16 102.25
332.95 506.05 102.00
313.61 526.36 102.00
334.61 511.07 101.95
318.63 530.56 101.95
336.27 516.09 101.90
323.65 534.76 101.90
337.93 521.11 101.85
328.67 538.97 101.85
339.60 526.13 101.80
326.92 543.17 101.50
277.63 447.90 110.00
272.50 447.63 110.00
278.55 466.50 109.00
270.70 467.53 109.00
281.55 477.85 108.00
268.33 482.65 108.00
284.67 485.35 107.00
275.85 491.42 107.00
288.60 492.65 106.00
277.75 498.95 106.00
291.50 497.80 105.00
279.35 506.63 105.00
295.00 502.92 104.00
281.40 513.23 104.00
300.02 509.65 103.00
286.92 523.55 103.00
308.40 519.58 102.00
293.30 533.08 102.00
327.05 543.25 101.50
313.38 560.73 101.10
339.48 614.55 100.50
319.17 604.10 100.50
337.48 637.30 100.30
317.73 635.33 100.20
273.23 481.67 108.00
268.42 482.38 108.00
275.40 491.60 107.00
267.10 492.25 107.00
277.13 499.13 106.00
270.77 500.00 106.00
279.08 506.73 105.00
271.55 508.13 105.00
281.48 514.00 104.00
273.15 518.80 104.00
286.73 523.28 103.00
276.48 529.28 103.00
292.70 533.33 102.00
280.92 542.60 102.00
320.45 569.70 101.00
302.20 578.23 101.00
317.80 635.40 100.20
297.23 633.60 100.10
270.95 492.55 107.00
267.48 492.10 107.00
271.08 500.17 106.00
265.15 500.42 106.00
271.52 508.50 105.00
265.20 509.35 105.00
273.27 519.15 104.00
266.52 520.53 104.00
276.67 528.95 103.00
267.10 532.63 103.00
281.00 542.90 102.00
267.83 546.75 102.00
302.20 578.35 101.00
272.25 566.60 101.00
297.50 633.65 100.10
270.17 631.05 100.00

APPENDIX 3.4.5 Sub-Catchment Three Discretised Flow-Net Structure and Channel Data

```
Template
(See Appendix 4.1)
NSUB K33 K44
NCHA
NSEG
NCAS
NELM
MCELF MCELT MSAM MHYE
.... ..... .... ....
MCELF MCELT MSAM MHYE
EC CWID EANG WANG CTOP IOFLOW

01 1 1
27
02
2
01 02
01 01 090 01
02 02 090 01
02 02
01 02 090 01
03 03 090 01
0.0700 0000.0 09.6640 09.6640 0012.5 3
2
01 02
01 01 090 01
02 02 090 01
03 03
01 01 093 01
02 03 090 01
04 04 090 01
0.0700 0000.0 10.1701 10.1701 0011.5 3
01
1
01 02
01 01 090 01
02 02 090 01
0.0700 0000.0 07.3964 07.3964 0013.5 3
02
1
01 02
01 01 090 01
02 02 090 01
0.0700 0000.0 13.5950 13.5950 0011.0 3
1
03 02
01 03 090 01
04 04 090 01
0.0700 0000.0 11.5432 11.5432 0009.0 3
02
1
01 02
01 01 090 01
02 02 090 01
0.0700 0000.0 07.8189 07.8189 0013.5 3
1
03 03
01 01 060 01
02 03 059 01
04 04 060 01
0.0700 0000.0 06.1891 06.1891 0016.5 3
00
00
00
00
00
00
00
00
00
13
1
07 03
01 03 117 01
04 07 116 01
08 08 117 01
0.2210 0000.0 06.6286 06.6286 0017.5 1
1
07 04
01 01 118 01
02 04 117 01
05 07 116 01
08 08 118 01
0.2210 0000.0 05.0283 05.0283 0023.0 1
1
09 04
01 02 118 01
03 06 117 01
07 09 116 01
10 10 118 01
0.2210 0000.0 06.3608 06.3608 0018.5 1
1
08 05
01 01 119 01
02 03 118 01
04 07 117 01
08 08 116 01
09 09 119 01
0.2201 0000.0 04.6548 04.6548 0019.5 1
1
09 04
01 02 119 01
03 04 118 01
05 09 117 01
10 10 119 01
0.2201 0000.0 05.5956 05.5956 0019.0 1
1
06 05
01 01 120 01
02 03 119 01
04 05 118 01
06 06 117 01
07 07 120 01
0.2201 0000.0 07.2633 07.2633 0015.5 1
1
05 04
01 01 121 01
02 03 120 01
04 05 119 01
06 06 121 01
0.1330 0000.0 02.1142 02.1142 0036.0 1
1
06 04
01 02 121 01
03 04 120 01
05 06 119 01
07 07 121 01
0.1330 0000.0 04.8457 04.8457 0018.0 1
1
06 05
01 01 122 01
02 03 121 01
04 05 120 01
06 06 119 01
07 07 122 01
```

```
0.1330 0000.0 05.2853 05.2853 0019.0 1
1
08 06
01 02 123 01
03 03 122 01
04 05 121 01
06 07 120 01
08 08 119 01
09 09 123 01
0.1330 0000.0 06.1157 06.1157 0011.0 1
2
09 07
01 01 124 01
02 03 123 01
04 04 122 01
05 06 121 01
07 08 120 01
09 09 119 01
10 10 124 01
01 02
01 01 124 01
02 02 124 01
0.0700 0000.0 22.6000 22.6000 0005.5 3
2
02 02
01 02 124 01
03 03 124 01
01 02
01 01 124 01
02 02 124 01
0.0700 0000.0 07.9219 07.9219 0008.0 3
2
02 02
01 02 125 01
03 03 124 01
02 02
01 02 126 01
03 03 126 01
0.0700 0000.0 21.3827 21.3827 0004.5 3
05
1
05 04
01 01 122 01
02 03 121 01
04 05 120 01
06 06 122 01
0.1460 0000.0 05.9758 05.9758 0017.0 3
1
05 05
01 01 123 01
02 02 122 01
03 04 121 01
05 05 120 01
06 06 123 01
0.1460 0000.0 21.7500 21.7500 0004.0 3
1
06 05
01 01 124 01
02 03 123 01
04 04 122 01
05 06 121 01
07 07 124 01
0.1460 0000.0 05.4306 05.4306 0019.5 3
1
06 05
01 02 124 01
03 04 123 01
05 05 122 01
06 06 121 01
07 07 124 01
0.1460 0000.0 07.3800 07.3800 0011.5 3
1
05 04
01 01 092 01
02 03 091 01
04 05 088 01
06 06 092 01
0.1460 0000.0 11.1719 11.1719 0018.0 3
03
2
01 02
01 01 090 01
02 02 090 01
05 04
01 02 093 01
03 04 092 01
05 05 090 01
06 06 090 01
0.0700 0000.0 07.1883 07.1883 0015.5 3
2
01 02
01 01 090 01
02 02 090 01
06 05
01 01 094 01
02 03 093 01
04 05 092 01
06 06 090 01
07 07 090 01
0.0700 0000.0 13.0796 13.0796 0008.5 3
2
05 02
01 05 090 01
06 06 090 01
07 06
01 01 090 01
02 02 096 01
03 03 094 01
04 05 093 01
06 07 092 01
08 08 090 01
0.0700 0000.0 05.4697 05.4697 0014.5 3
01
2
03 03
01 01 060 01
02 03 059 01
04 04 060 01
01 02
01 01 090 01
02 02 060 01
0.0700 0000.0 13.5185 13.5185 0019.0 3
02
1
02 02
01 02 059 01
03 03 059 01
0.0700 0000.0 07.5740 07.5740 0013.0 3
1
03 03
01 01 060 01
02 03 059 01
04 04 060 01
0.0700 0000.0 15.1111 15.1111 0007.5 3
01
1
02 02
01 02 060 01
```

03 03 059 01
0.0700 0000.0 12.7751 12.7751 008.5 3
00
00
08
2
05 04
01 01 092 01
02 03 091 01
04 05 088 01
06 06 092 01
01 02
01 01 126 01
02 02 126 01
0.0700 0000.0 11.1719 11.1719 0008.0 3
2
06 04
01 02 092 01
03 04 091 01
05 06 088 01
07 07 092 01
04 04
01 02 126 01
03 03 125 01
04 04 124 01
05 05 092 01
0.0700 0000.0 11.1326 11.1326 0004.0 3
2
06 05
01 01 093 01
02 03 092 01
04 05 091 01
06 06 088 01
07 07 093 01
05 05
01 01 093 01
02 03 126 01
04 04 125 01
05 05 124 01
06 06 093 01
0.0700 0000.0 14.5312 14.5312 0008.0 3
2
06 04
01 02 094 01
03 04 092 01
05 06 091 01
07 07 094 01
05 04
01 02 094 01
03 04 126 01
05 05 125 01
06 06 094 01
0.1460 0000.0 19.3651 19.3651 0020.5 3
2
07 05
01 01 094 01
02 03 093 01
04 05 092 01
06 07 091 01
08 08 094 01
05 04
01 02 094 01
03 04 126 01
05 05 125 01
06 06 094 01
0.1460 0000.0 04.9330 04.9330 0016.5 3
2
07 06
01 01 096 01
02 02 094 01
03 04 093 01
05 06 092 01
07 07 091 01
08 08 096 01
04 02
01 04 096 01
05 05 096 01
0.1460 0000.0 06.1592 06.1592 0018.5 3
2
05 05
01 01 090 01
02 02 096 01
03 03 094 01
04 05 093 01
06 06 090 01
02 03
01 01 061 01
02 02 090 01
03 03 090 01
0.1460 0000.0 04.3424 04.3424 0021.0 3
2
03 04
01 01 061 01
02 02 090 01
03 04 096 01
05 05 061 01
04 03
01 03 061 01
04 04 096 01
05 05 061 01
0.1460 0000.0 02.8661 02.8661 0028.5 3
02
2
04 03
01 02 060 01
03 04 059 01
05 05 060 01
05 05
01 02 090 01
03 03 096 01
04 04 094 01
05 05 093 01
06 06 090 01
0.0700 0000.0 05.4697 05.4697 0014.5 3
2
02 03
01 01 061 01
02 02 061 01
03 03 060 01
08 07
01 02 061 01
03 03 090 01
04 04 096 01
05 05 094 01
06 07 093 01
08 08 092 01
09 09 061 01
0.0700 0000.0 02.5633 02.5633 0035.0 3
02
2
03 03
01 02 060 01
03 03 059 01
04 04 060 01
01 02
01 01 060 01
02 02 060 01
0.0700 0000.0 07.5740 07.5740 0013.0 3

```
2
04 04
01 01 061 01
02 03 060 01
04 04 059 01
05 05 061 01
01 02
01 01 061 01
02 02 061 01
0.0700 0000.0 15.1111 15.1111 0007.5 3
02
1
01 02
01 01 061 01
02 02 061 01
0.0700 0000.0 10.8642 10.8642 0009.0 3
1
02 03
01 01 061 01
02 02 060 01
03 03 061 01
0.0700 0000.0 11.5625 11.5625 0008.0 3
06
2
02 03
01 01 062 01
02 02 061 01
03 03 062 01
04 03
01 03 062 01
04 04 102 01
05 05 062 01
0.1680 0000.0 05.1022 05.1022 0022.5 3
2
02 03
01 01 064 01
02 02 061 01
03 03 064 01
06 06
01 01 064 01
02 03 062 01
04 04 102 01
05 05 101 01
06 06 100 01
07 07 064 01
0.1680 0000.0 06.1498 06.1498 0014.5 3
2
02 02
01 02 064 01
03 03 064 01
07 06
01 02 064 01
03 04 062 01
05 05 102 01
06 06 101 01
07 07 100 01
08 08 064 01
0.1680 0000.0 05.6749 05.6749 0016.5 3
2
02 02
01 02 064 01
03 03 064 01
07 05
01 03 063 01
04 05 062 01
06 06 102 01
07 07 101 01
08 08 064 01
0.1680 0000.0 04.1430 04.1430 0023.5 3
2
03 03
01 01 065 01
02 03 064 01
04 04 065 01
04 04
01 01 065 01
02 03 063 01
04 04 062 01
05 05 065 01
0.1680 0000.0 02.5922 02.5922 0032.5 3
2
03 03
01 01 065 01
02 03 063 01
04 04 065 01
03 03
01 02 065 01
03 03 063 01
04 04 065 01
0.1680 0000.0 03.0018 03.0018 0026.5 3
05
1
04 03
01 02 061 01
03 04 060 01
05 05 061 01
0.1680 0000.0 14.4889 14.4889 0007.5 3
2
04 04
01 01 062 01
02 02 061 01
03 04 060 01
05 05 062 01
01 02
01 01 062 01
02 02 062 01
0.1680 0000.0 13.0667 13.0667 0007.5 3
2
05 04
01 02 062 01
03 03 061 01
04 05 060 01
06 06 062 01
02 02
01 02 062 01
03 03 062 01
0.1680 0000.0 05.1200 05.1200 0012.5 3
2
05 05
01 01 063 01
02 03 062 01
04 04 061 01
05 05 060 01
06 06 063 01
02 02
01 02 063 01
03 03 063 01
0.1680 0000.0 22.8642 22.8642 0014.5 3
2
07 06
01 01 065 01
02 02 063 01
03 04 062 01
05 05 061 01
06 07 060 01
08 08 065 01
01 02
01 01 065 01
```

02 02 065 01
0.1680 0000.0 03.0018 03.0018 0026.5 3
11
2
07 06
01 02 065 01
03 03 063 01
04 05 062 01
06 06 061 01
07 07 060 01
08 08 065 01
01 02
01 01 065 01
02 02 065 01
0.0850 0000.0 03.3230 03.3230 0024.0 3
2
05 04
01 02 065 01
03 03 063 01
04 05 062 01
06 06 065 01
01 02
01 01 065 01
02 02 065 01
0.0850 0000.0 02.0734 02.0734 0027.5 3
1
04 05
01 01 032 01
02 02 031 01
03 03 030 01
04 04 062 01
05 05 032 01
0.0850 0000.0 05.4486 05.4486 0013.5 3
2
04 04
01 02 032 01
03 03 031 01
04 04 030 10
05 05 032 01
01 02
01 01 033 01
02 02 032 01
0.0850 0000.0 02.3923 02.3923 0035.5 3
2
03 03
01 02 032 01
03 03 031 01
04 04 032 01
01 02
01 01 033 01
02 02 032 01
0.0850 0000.0 21.1358 21.1358 0024.5 3
2
04 03
01 03 032 01
04 04 031 01
05 05 032 01
01 02
01 01 033 01
02 02 032 01
0.0850 0000.0 11.1644 11.1644 0007.5 3
1
03 03
01 02 032 01
03 03 031 01
04 04 032 01
0.0850 0000.0 04.0039 04.0039 0016.0 1
1
04 03
01 02 032 01
03 04 031 01
05 05 032 01
0.0850 0000.0 03.6010 03.6010 0016.0 1
1
06 04
01 03 032 01
04 04 031 01
05 06 030 01
07 07 032 01
0.0850 0000.0 12.5896 12.5896 0010.5 1
1
03 02
01 03 016 01
04 04 016 01
0.0850 0000.0 02.5872 02.5872 0024.5 1
1
03 02
01 03 016 01
04 04 016 01
0.0850 0000.0 06.9136 06.9136 0013.5 1

APPENDIX 3.4.6 Sub-Catchment Three Digitised Coordinate Pairs for Flow Net Elements and Segments

Template
(See Appendix 4.1)
First line
XO YO
Other paired lines
X(1) Y(1) Z(1)
X(2) Y(2) Z(2)

270.77	631.48	
550.55	324.15	117.00
557.00	329.88	117.00
548.60	329.78	115.60
542.00	336.47	114.60
549.70	317.13	118.00
545.83	316.33	118.00
550.33	324.15	117.00
542.50	324.00	117.00
548.50	329.78	115.60
541.88	336.75	114.60
549.65	333.90	116.00
550.25	351.78	116.00
541.75	336.83	114.60
530.10	352.78	113.10
545.85	316.35	118.00
543.83	314.65	118.00
542.85	323.88	117.00
537.72	324.08	117.00
541.50	330.55	116.00
536.30	329.80	116.00
541.83	336.72	114.60
529.92	352.60	113.10
551.22	355.38	116.00
550.35	351.55	116.00
545.45	356.25	115.40
529.95	352.65	113.60
537.90	369.63	115.00
536.20	374.67	115.00
528.85	368.58	113.60
510.67	374.58	111.50
530.78	375.15	114.00
529.83	381.65	114.00
523.35	375.10	113.00
522.67	382.13	113.00
514.47	374.53	112.00
514.45	382.83	112.00
510.30	374.65	111.50
494.48	383.35	109.90
535.45	382.85	115.00
533.20	391.85	115.00
529.70	382.10	114.20
513.42	385.63	111.60
529.08	391.00	114.00
528.17	394.44	114.00
522.05	388.55	113.00
528.17	392.14	113.00
514.90	386.30	112.00
513.55	389.78	112.00
512.65	385.67	111.60
494.52	383.35	109.90
690.70	69.28	138.00
687.05	79.85	138.00
687.05	67.55	137.00
681.83	77.03	137.00
683.15	65.35	136.00
677.65	74.40	136.00
678.88	63.00	135.00
673.50	72.17	135.00
675.25	60.45	134.00
669.20	69.47	134.00
670.67	56.92	133.00
664.13	66.20	133.00
666.15	52.90	132.00
657.70	63.35	132.00
659.28	47.65	131.00
640.67	57.67	129.90
681.78	77.03	137.00
677.95	85.63	137.00
677.63	74.55	136.00
673.05	83.85	136.00
673.53	72.03	135.00
668.33	81.53	135.00
669.08	69.30	134.00
663.95	79.83	134.00
664.10	66.10	133.00
658.35	77.60	133.00
657.90	62.90	132.00
652.22	74.92	132.00
650.20	60.40	131.00
644.25	72.40	131.00
640.72	57.75	129.90
624.40	70.55	128.50
677.83	85.72	137.00
675.67	91.20	137.00
672.92	83.85	136.00
670.80	90.33	136.00
668.30	81.80	135.00
665.90	89.97	135.00
663.85	79.85	134.00
660.40	88.97	134.00
658.42	77.58	133.00
654.97	88.13	133.00
652.13	74.75	132.00
648.47	87.15	132.00
644.35	72.00	131.00
642.00	86.70	131.00
636.38	70.63	130.00
634.70	86.38	130.00
627.60	70.97	129.00
626.53	85.90	129.00
624.20	70.80	128.50
613.90	86.67	127.30
665.97	90.15	135.00
663.55	101.30	135.00
660.47	88.97	134.00
658.60	101.58	134.00
654.88	88.03	133.00
653.20	101.33	133.00
648.45	87.08	132.00
647.45	101.63	132.00
642.08	86.67	131.00
641.17	101.55	131.00
634.50	86.22	130.00
634.20	101.28	130.00
626.47	85.75	129.00
626.50	101.08	129.00
618.72	86.15	128.00
619.13	101.08	128.00
613.67	86.50	127.30
603.05	104.45	126.10
658.53	101.65	135.00
657.75	113.42	135.00
652.92	101.60	134.00
652.58	113.85	134.00
647.30	101.47	133.00
647.55	113.95	133.00
641.33	101.67	132.00
643.00	114.70	132.00
634.28	101.10	131.00
636.05	115.30	131.00
626.92	101.05	130.00
628.83	116.88	130.00
619.13	101.05	129.00
621.67	118.03	129.00
611.15	102.15	128.00
614.55	120.40	128.00
607.01	103.65	127.00
608.29	123.10	127.00
602.88	104.88	126.10
602.03	125.80	125.10
642.95	114.55	131.00
644.97	140.95	131.00
636.08	114.90	130.00
639.38	143.22	130.00
628.65	116.80	129.00
632.45	145.70	129.00
621.75	118.10	128.00
625.47	147.05	128.00
614.55	120.53	127.00
617.40	147.53	127.00
608.63	122.13	126.00
609.00	146.83	126.00
601.90	125.20	125.10
592.20	143.17	123.90
625.22	147.33	128.00
625.10	163.67	128.00
617.13	147.88	127.00
615.90	163.95	127.00
609.00	146.85	126.00
606.08	162.95	126.00
601.88	145.55	125.00
596.30	161.90	125.00
594.25	143.90	124.00
588.65	160.00	124.00
591.90	143.38	123.90
575.95	157.40	122.60
625.22	163.65	128.00
625.42	167.33	128.00
616.17	163.55	127.00
616.28	167.92	127.00
606.00	163.05	126.00
606.13	170.15	126.00
596.47	161.88	125.00
595.88	171.67	125.00
588.67	159.78	124.00
586.45	172.60	124.00
579.50	157.65	123.00
575.72	171.85	123.00
575.78	157.25	122.60
559.92	171.20	121.60
616.22	167.72	127.00
616.33	171.60	127.00
605.88	169.92	126.00
606.67	173.75	126.00
595.50	171.75	125.00
596.40	176.70	125.00
586.45	172.33	124.00
586.72	180.22	124.00
575.60	171.85	123.00
574.85	182.20	123.00
564.67	170.22	122.00
563.58	183.00	122.00
560.15	170.72	121.60
540.97	188.13	119.70

616.58	171.72	127.00	589.60	192.28	124.00	534.53	334.10	115.00
616.58	174.20	127.00	575.40	188.35	123.00	529.70	330.67	115.00
606.83	173.72	126.00	577.03	195.72	123.00	530.92	344.13	114.00
607.70	176.65	126.00	564.40	189.28	122.00	524.60	340.88	114.00
596.28	176.58	125.00	566.70	196.63	122.00	529.95	352.92	113.10
597.42	179.85	125.00	563.92	189.17	121.30	510.40	354.47	111.50
586.63	180.25	124.00	549.95	194.08	120.40	519.28	356.05	113.00
587.58	182.70	124.00	599.35	188.78	125.00	519.65	359.15	113.00
574.97	181.95	123.00	600.72	197.92	125.00	510.27	354.60	111.50
575.15	185.10	123.00	589.72	192.38	124.00	496.13	367.33	110.20
563.42	183.03	122.00	590.72	200.20	124.00	542.67	311.78	118.00
564.08	186.65	122.00	577.03	195.83	123.00	541.90	310.97	118.00
553.05	184.60	121.00	578.20	201.22	123.00	534.72	322.95	117.00
553.78	188.53	121.00	566.45	196.47	122.00	530.58	315.75	117.00
543.53	187.20	120.00	567.22	200.92	122.00	532.28	327.45	116.00
544.63	190.65	120.00	558.55	196.42	121.00	525.35	320.80	116.00
540.35	187.83	119.70	557.42	200.92	121.00	529.67	330.75	115.00
524.97	200.85	118.40	549.53	193.92	120.40	520.90	324.35	115.00
612.83	174.92	127.00	534.75	202.90	118.60	524.55	340.65	114.00
613.13	178.88	127.00	590.72	200.13	124.00	514.95	330.75	114.00
607.50	176.55	126.00	590.83	208.08	124.00	517.20	347.65	113.00
608.08	179.40	126.00	577.95	201.50	123.00	509.60	336.20	113.00
597.38	180.00	125.00	579.17	209.22	123.00	510.25	354.45	111.50
598.05	182.17	125.00	567.25	200.75	122.00	496.00	366.90	110.20
587.25	182.65	124.00	567.20	208.22	122.00	541.13	361.65	115.00
588.13	184.92	124.00	557.33	200.72	121.00	537.70	369.58	115.00
574.92	185.08	123.00	557.28	208.28	121.00	526.53	358.63	114.00
575.53	188.10	123.00	547.47	200.80	120.00	530.83	368.53	114.00
563.80	186.45	122.00	549.78	209.03	120.00	519.60	358.67	113.00
564.47	189.08	122.00	539.08	202.13	119.00	523.33	370.30	113.00
553.78	188.53	121.00	541.70	209.60	119.00	512.60	360.40	112.00
554.80	192.35	121.00	533.95	203.22	118.60	515.08	372.95	112.00
544.53	190.67	120.00	519.95	217.88	117.50	505.25	363.20	111.00
546.10	195.90	120.00	579.05	208.85	123.00	506.73	374.63	111.00
534.90	195.47	119.00	579.92	232.55	123.00	496.00	367.10	110.20
536.20	198.58	119.00	567.17	208.22	122.00	482.58	382.85	109.20
524.88	200.60	118.40	568.97	233.78	122.00	531.40	318.38	117.00
514.78	215.78	117.40	557.30	208.20	121.00	530.88	315.88	117.00
531.95	192.42	119.00	559.15	233.83	121.00	525.38	320.90	116.00
530.35	191.22	119.00	550.10	208.70	120.00	523.28	317.22	116.00
525.13	200.65	118.40	549.38	232.70	120.00	520.80	324.72	115.00
514.90	215.65	117.40	541.47	209.72	119.00	518.58	322.00	115.00
545.15	193.50	120.00	541.42	231.60	119.00	514.92	330.95	114.00
546.08	195.78	120.00	527.92	212.75	118.00	512.40	327.50	114.00
536.20	198.63	119.00	534.70	231.72	118.00	510.02	336.17	113.00
537.42	201.20	119.00	519.72	217.65	117.50	506.92	332.80	113.00
514.50	215.85	117.40	513.88	235.03	116.60	504.08	343.60	112.00
507.25	235.10	116.80	559.20	233.90	121.00	500.15	340.42	112.00
519.08	205.45	118.00	555.47	248.25	121.00	497.50	354.20	111.00
515.85	204.22	118.00	549.30	232.80	120.00	492.00	352.53	111.00
514.53	215.85	117.40	547.70	246.90	120.00	496.20	366.72	110.20
507.13	234.72	116.80	541.38	231.80	119.00	482.33	382.97	109.20
522.90	209.35	118.00	539.85	245.60	119.00	528.17	394.44	114.00
526.78	210.75	118.00	534.53	231.45	118.00	527.30	397.85	114.00
513.42	226.47	117.00	532.00	244.67	118.00	520.94	392.14	113.00
516.20	228.00	117.00	519.53	232.00	117.00	519.92	395.80	113.00
507.13	235.05	116.80	523.97	245.47	117.00	513.55	389.78	112.00
505.17	252.42	115.90	514.05	234.92	116.60	512.35	393.22	112.00
516.13	204.25	118.00	505.40	252.15	115.90	494.52	383.35	109.90
514.22	203.67	118.00	542.88	356.78	115.00	482.17	383.05	109.20
509.00	224.80	117.00	541.22	361.90	115.00	508.80	375.65	111.00
505.05	224.38	117.00	529.90	352.92	113.10	506.77	374.25	111.00
507.15	234.60	116.80	510.42	354.58	111.50	494.60	383.17	109.90
505.20	252.58	115.90	544.08	314.80	118.00	482.52	382.90	109.20
607.97	179.38	126.00	542.55	311.35	118.00	518.15	400.33	113.00
609.40	186.38	126.00	537.67	324.28	117.00	516.35	407.90	113.00
597.78	182.10	125.00	534.75	322.85	117.00	510.70	398.05	112.00
599.60	188.80	125.00	535.95	329.92	116.00	507.92	405.70	112.00
588.03	185.10	124.00	532.35	327.22	116.00	503.48	396.08	110.90

493.90	401.05	110.20	529.72	189.70	119.00	530.90	316.15	117.00
516.33	407.72	113.00	528.63	188.33	119.00	522.10	312.72	116.00
514.58	415.03	113.00	512.53	202.38	118.00	523.03	317.25	116.00
508.08	405.50	112.00	508.60	198.63	118.00	514.47	314.08	115.00
505.75	411.45	112.00	501.67	223.80	117.00	514.88	318.10	115.00
499.27	402.38	111.00	495.33	222.72	117.00	507.77	315.97	114.00
497.17	408.05	111.00	498.10	252.15	116.00	508.83	320.85	114.00
493.92	401.05	110.20	490.60	253.03	116.00	497.77	318.75	113.00
482.75	408.42	109.30	497.67	267.45	115.00	499.92	325.33	113.00
513.75	418.00	113.00	489.45	268.65	115.00	485.67	323.55	112.00
514.58	415.00	113.00	497.88	281.83	114.40	489.85	331.42	112.00
504.25	415.08	112.00	489.83	297.95	112.90	470.42	332.13	110.90
506.00	411.13	112.00	539.22	284.90	119.00	464.10	350.17	109.70
500.35	414.53	111.20	546.30	297.42	119.00	468.15	273.53	115.00
482.83	408.33	109.30	530.92	285.85	118.00	465.83	272.78	115.00
555.42	248.22	121.00	537.40	302.47	118.00	465.02	290.65	114.00
554.58	253.72	121.00	524.03	285.90	117.00	455.23	288.05	114.00
547.92	246.90	120.00	529.10	306.63	117.00	466.52	300.83	113.00
547.10	253.03	120.00	517.20	287.45	116.00	445.45	301.80	113.00
539.60	245.33	119.00	521.15	307.97	116.00	467.92	312.58	112.00
539.42	251.30	119.00	509.25	289.20	115.00	444.83	331.95	112.00
532.10	244.97	118.00	513.58	309.05	115.00	470.70	332.20	110.90
531.60	251.33	118.00	500.80	292.08	114.00	463.95	350.00	109.70
523.95	245.38	117.00	506.60	310.20	114.00	514.88	318.00	115.00
524.70	251.63	117.00	489.98	297.58	112.90	516.42	320.05	115.00
505.15	252.58	115.90	481.17	315.78	112.00	508.92	320.63	114.00
503.77	262.45	115.40	509.60	200.03	118.00	510.17	323.50	114.00
506.05	224.63	117.00	508.35	198.83	118.00	500.13	325.30	113.00
504.83	224.55	117.00	495.35	222.97	117.00	501.95	329.25	113.00
505.38	252.33	115.90	484.92	223.30	117.00	490.15	331.15	112.00
503.48	262.20	115.40	490.60	252.95	116.00	495.13	335.30	112.00
554.53	253.65	121.00	479.02	253.20	116.00	477.75	341.25	111.00
553.38	273.67	121.00	489.38	268.65	115.00	480.23	349.28	111.00
546.88	252.80	120.00	476.20	273.30	115.00	464.00	350.30	109.70
545.95	275.03	120.00	489.60	283.28	114.00	460.15	369.60	108.70
539.22	251.30	119.00	478.02	285.60	114.00	444.83	332.25	112.00
538.10	276.05	119.00	489.88	297.92	112.90	441.13	341.60	112.00
531.42	251.28	118.00	480.83	315.75	112.00	452.85	339.70	111.00
530.95	276.65	118.00	546.17	297.13	119.00	446.67	348.63	111.00
524.50	251.42	117.00	548.83	300.72	119.00	463.98	350.17	109.70
523.30	276.78	117.00	537.50	302.08	118.00	460.00	369.38	108.70
511.13	256.08	116.00	540.78	308.42	118.00	492.63	333.88	112.00
515.78	276.50	116.00	528.90	306.45	117.00	495.27	335.50	112.00
503.85	262.42	115.40	530.13	311.17	117.00	480.05	349.20	111.00
498.00	282.05	114.40	521.35	307.85	116.00	481.67	350.15	111.00
530.53	191.25	119.00	522.15	312.92	116.00	469.50	361.13	110.00
529.28	189.45	119.00	513.55	308.78	115.00	472.25	363.97	110.00
518.80	205.38	118.00	514.25	314.20	115.00	459.77	369.63	108.70
512.30	202.00	118.00	506.58	310.20	114.00	456.00	391.50	107.30
504.77	224.40	117.00	507.98	316.17	114.00	451.85	303.75	113.00
501.58	223.83	117.00	497.17	312.95	113.00	449.27	304.20	113.00
501.58	251.75	116.00	497.77	318.58	113.00	441.33	341.70	112.00
497.63	252.28	116.00	480.98	315.80	112.00	437.13	347.50	112.00
503.90	262.67	115.40	470.55	332.35	110.90	446.50	348.40	111.00
497.85	281.63	114.40	488.30	223.72	117.00	438.67	360.30	111.00
545.90	274.97	120.00	485.00	223.35	117.00	453.38	359.45	110.00
547.35	282.67	120.00	479.20	253.33	116.00	445.30	365.30	110.00
538.08	276.00	119.00	475.75	252.03	116.00	460.00	369.97	108.70
538.90	285.10	119.00	476.25	273.25	115.00	456.08	391.45	107.30
530.88	276.72	118.00	466.02	272.95	115.00	519.80	395.60	113.00
531.05	285.53	118.00	477.88	285.63	114.00	518.28	400.30	113.00
523.45	276.65	117.00	464.80	290.58	114.00	512.53	392.80	112.00
524.10	286.00	117.00	478.98	296.65	113.00	510.67	397.92	112.00
515.80	276.30	116.00	466.10	300.55	113.00	503.92	390.00	111.00
517.42	287.35	116.00	481.17	315.83	112.00	502.15	396.22	111.00
503.58	278.15	115.00	470.67	332.08	110.90	494.60	387.70	110.00
509.38	289.40	115.00	540.60	308.47	118.00	492.92	392.60	110.00
497.90	282.13	114.40	542.50	311.40	118.00	482.15	383.22	109.20
489.58	298.22	112.90	529.97	311.03	117.00	474.33	387.25	108.50

512.55	327.28	114.00	480.42	434.20	110.00	424.52	363.38	111.00
510.75	326.00	114.00	472.67	428.65	109.10	420.80	362.50	111.00
506.83	333.00	113.00	455.30	426.10	107.50	421.98	372.25	110.00
504.35	330.88	113.00	474.33	396.70	109.00	417.42	372.13	110.00
500.33	340.13	112.00	474.52	399.50	109.00	420.25	379.95	109.00
497.48	337.42	112.00	465.42	394.70	108.00	414.25	379.33	109.00
492.25	352.65	111.00	463.40	400.05	108.00	418.30	389.30	108.00
486.42	351.65	111.00	456.08	391.83	107.30	412.77	388.95	108.00
485.88	367.20	110.00	446.77	395.75	106.90	417.90	396.45	107.00
480.67	366.92	110.00	441.48	358.30	111.00	411.67	398.00	107.00
482.52	382.55	109.20	438.80	360.78	111.00	416.05	407.33	106.00
474.45	387.42	108.50	445.30	365.50	110.00	409.85	407.67	106.00
492.67	392.42	110.00	440.23	367.92	110.00	414.67	418.35	105.30
490.55	400.88	110.00	448.45	372.65	109.00	402.00	433.60	104.80
480.73	388.75	109.00	441.70	377.10	109.00	434.52	423.03	107.00
474.25	399.50	109.00	452.17	381.53	108.00	435.77	425.15	107.00
474.75	387.22	108.50	444.08	384.17	108.00	421.95	430.53	106.00
456.08	391.80	107.30	456.13	391.65	107.30	422.85	435.40	106.00
523.45	318.65	116.00	446.35	395.55	106.90	404.83	432.10	105.00
522.80	317.28	116.00	463.38	399.85	108.00	406.40	438.08	105.00
518.65	322.13	115.00	462.42	414.92	108.00	401.98	433.90	104.80
516.50	319.90	115.00	451.67	396.92	107.00	391.70	448.40	104.40
512.70	327.33	114.00	438.52	415.42	107.00	415.52	380.55	109.00
510.15	323.33	114.00	446.73	395.75	106.90	414.13	379.28	109.00
504.58	330.80	113.00	430.23	405.22	106.30	413.02	388.80	108.00
501.83	329.13	113.00	449.55	303.92	113.00	408.70	388.60	108.00
497.55	337.78	112.00	447.58	303.80	113.00	411.50	397.85	107.00
495.20	334.95	112.00	437.67	347.65	112.00	405.58	395.20	107.00
487.02	351.63	111.00	433.13	350.40	112.00	410.05	407.67	106.00
481.67	350.15	111.00	438.75	360.42	111.00	403.92	408.30	106.00
480.50	367.33	110.00	428.95	363.63	111.00	402.25	433.65	104.80
472.40	363.55	110.00	440.25	367.95	110.00	391.38	448.35	104.40
476.60	379.33	109.00	427.90	372.53	110.00	435.65	424.97	107.00
466.40	373.75	109.00	441.83	377.35	109.00	436.77	426.33	107.00
474.27	387.67	108.50	428.20	379.33	109.00	423.08	435.30	106.00
456.23	391.85	107.30	444.42	384.70	108.00	423.42	438.70	106.00
503.02	418.25	112.00	428.45	386.45	108.00	406.65	438.05	105.00
502.60	422.42	112.00	446.38	395.83	106.90	407.77	443.85	105.00
495.30	414.42	111.00	430.10	405.17	106.30	391.55	448.22	104.40
493.70	423.72	111.00	445.50	421.22	108.00	382.80	465.72	103.70
488.23	410.67	110.00	442.02	422.55	108.00	406.98	397.60	107.00
484.25	422.42	110.00	439.27	415.78	107.00	405.35	395.28	107.00
482.83	408.50	109.30	434.95	419.45	107.00	403.85	408.25	106.00
468.58	417.38	108.30	431.75	405.95	106.30	399.05	408.08	106.00
487.60	403.08	110.00	416.33	418.72	105.30	397.92	427.05	105.00
477.33	408.28	110.00	447.85	303.80	113.00	393.30	424.85	105.00
482.60	408.67	109.30	445.50	302.33	113.00	391.50	448.25	104.40
468.42	417.03	108.30	433.30	350.20	112.00	382.63	465.47	103.70
502.55	422.33	112.00	425.45	350.17	112.00	491.20	435.40	111.00
502.35	425.30	112.00	428.80	363.83	111.00	490.80	438.08	111.00
493.55	423.65	111.00	424.35	363.40	111.00	480.33	434.20	110.00
493.17	427.15	111.00	428.00	372.83	110.00	479.98	437.15	110.00
484.10	422.33	110.00	422.08	372.22	110.00	469.98	432.10	109.00
482.30	426.90	110.00	427.83	379.55	109.00	468.73	434.92	109.00
475.25	418.85	109.00	420.27	379.40	109.00	460.27	427.53	108.00
473.35	425.60	109.00	428.60	386.65	108.00	459.17	430.72	108.00
468.50	417.38	108.30	418.27	389.17	108.00	454.75	425.70	107.50
455.00	426.15	107.50	429.58	395.92	107.00	449.70	427.88	107.30
476.63	406.10	109.00	417.30	396.53	107.00	490.58	438.15	111.00
462.02	414.65	109.00	430.15	405.22	106.30	489.85	441.28	111.00
468.65	417.25	108.30	414.58	418.17	105.30	479.75	437.00	110.00
455.23	425.70	107.50	434.85	419.35	107.00	479.13	441.17	110.00
502.38	425.15	112.00	435.33	423.40	107.00	468.83	434.92	109.00
501.65	432.80	112.00	423.88	418.65	106.00	466.88	440.97	109.00
492.85	426.25	111.00	424.20	430.50	106.00	458.88	430.45	108.00
473.00	428.65	109.10	416.10	418.53	105.30	456.10	441.63	108.00
491.88	431.30	111.00	404.95	432.90	104.80	449.85	427.78	107.30
491.23	435.60	111.00	428.05	351.30	112.00	434.50	441.55	106.30
481.27	430.25	110.00	425.45	350.42	112.00	462.20	414.75	108.00

444.33	420.38	108.00	407.58	460.17	105.00	347.83	544.67	102.00
449.70	427.88	107.30	408.58	465.72	105.00	339.65	538.30	101.90
434.23	441.78	106.30	387.77	463.50	104.00	328.52	553.55	101.30
489.92	441.13	111.00	390.60	469.08	104.00	348.02	524.55	102.00
489.05	444.97	111.00	382.80	465.47	103.70	344.92	518.90	102.00
479.00	440.95	110.00	378.42	473.10	103.40	339.88	538.30	101.90
478.85	445.45	110.00	384.52	458.20	104.00	328.55	553.73	101.30
467.10	440.88	109.00	383.55	458.08	104.00	389.05	516.60	104.00
467.17	444.28	109.00	382.67	465.72	103.70	390.83	518.55	104.00
456.08	441.75	108.00	378.23	473.25	103.40	376.42	529.35	103.00
456.17	445.47	108.00	458.58	463.45	108.00	378.17	532.17	103.00
443.88	441.63	107.00	462.63	492.65	108.00	347.77	545.17	102.00
443.65	445.55	107.00	445.30	464.22	107.00	350.70	550.90	102.00
434.45	441.70	106.30	451.33	494.73	107.00	328.25	553.88	101.30
417.67	447.63	105.40	429.40	465.72	106.00	325.83	570.70	101.00
444.25	420.55	108.00	431.63	496.10	106.00	407.75	509.88	105.00
440.27	421.83	108.00	408.58	465.78	105.00	408.77	512.28	105.00
441.17	429.08	107.00	407.48	499.13	105.00	390.75	518.30	104.00
436.90	426.05	107.00	390.63	468.90	104.00	393.65	520.90	104.00
434.27	441.83	106.30	389.88	494.02	104.00	378.05	531.85	103.00
417.35	447.70	105.40	378.20	473.08	103.40	381.67	534.58	103.00
478.70	443.60	110.00	368.85	489.50	103.00	350.38	550.58	102.00
478.88	445.53	110.00	383.83	457.95	104.00	353.15	554.00	102.00
467.05	444.13	109.00	381.73	453.80	104.00	325.40	570.67	101.00
467.30	447.00	109.00	378.13	472.97	103.40	325.00	590.08	100.70
455.92	445.33	108.00	368.88	489.48	103.00	432.77	501.75	106.00
456.13	446.92	108.00	451.13	494.50	107.00	440.92	511.60	106.00
443.45	445.40	107.00	451.92	500.40	107.00	409.00	512.25	105.00
444.13	448.20	107.00	431.45	495.95	106.00	430.05	526.55	105.00
427.02	447.47	106.00	432.73	501.70	106.00	393.58	521.00	104.00
428.10	450.75	106.00	407.35	499.33	105.00	418.45	542.33	104.00
417.23	447.72	105.40	406.70	503.75	105.00	381.65	534.30	103.00
397.20	452.60	104.60	389.88	494.20	104.00	398.38	560.23	103.00
438.77	427.65	107.00	387.00	505.60	104.00	352.77	554.23	102.00
436.77	425.95	107.00	368.75	489.75	103.00	369.30	569.13	102.00
424.58	441.90	106.00	360.15	508.38	102.50	331.27	582.45	101.00
423.23	438.80	106.00	432.08	499.77	106.00	344.27	593.45	101.00
417.00	447.95	105.40	432.55	501.90	106.00	324.90	590.17	100.70
396.90	452.78	104.60	406.83	503.75	105.00	335.42	606.98	100.50
489.10	444.83	111.00	408.77	512.48	105.00	396.67	554.88	103.00
488.90	451.92	111.00	386.90	505.60	104.00	396.95	557.73	103.00
478.77	445.55	110.00	386.27	511.58	104.00	369.42	568.85	102.00
479.08	452.30	110.00	370.80	506.13	103.00	372.38	571.78	102.00
467.17	446.72	109.00	372.70	518.05	103.00	344.23	593.45	101.00
468.23	453.33	109.00	360.38	507.98	102.50	355.58	598.78	101.00
455.80	446.83	108.00	351.60	525.48	102.00	335.15	607.00	100.50
457.20	455.38	108.00	367.33	487.40	103.00	346.05	623.08	100.40
443.67	448.28	107.00	365.30	485.40	103.00	396.77	557.75	103.00
444.75	458.47	107.00	360.20	507.95	102.50	398.35	560.70	103.00
427.85	450.88	106.00	351.35	525.35	102.00	372.15	571.67	102.00
428.83	460.85	106.00	407.05	507.15	105.00	384.52	575.25	102.00
404.73	451.70	105.00	407.23	508.67	105.00	355.73	598.63	101.00
407.33	460.40	105.00	386.50	511.40	104.00	373.95	596.53	101.00
396.80	452.53	104.60	387.77	514.50	104.00	346.05	623.08	100.40
382.85	465.60	103.70	372.95	517.92	103.00	358.68	639.40	100.30
404.48	448.30	105.00	373.95	523.42	103.00			
404.98	444.50	105.00	351.15	525.67	102.00			
396.92	452.45	104.60	339.92	538.38	101.90			
383.02	465.38	103.70	363.92	490.42	103.00			
479.20	452.38	110.00	362.60	489.83	103.00			
478.98	461.72	110.00	351.70	525.53	102.00			
467.95	453.42	109.00	339.13	538.58	101.90			
469.50	462.40	109.00	407.05	508.48	105.00			
457.48	455.45	108.00	407.67	510.17	105.00			
458.83	463.80	108.00	387.60	514.33	104.00			
444.98	458.25	107.00	390.77	518.25	104.00			
445.42	464.05	107.00	374.15	523.10	103.00			
429.02	460.60	106.00	376.63	529.50	103.00			
429.33	465.85	106.00	346.08	537.03	102.00			

APPENDIX 3.4.7 Sub-Catchment Four Discretised Flow-Net Structure and Channel Data

```
Template
(See Appendix 4.1)
NSUB K33 K44
NCHA
NSEG
NCAS
NELM
MCELF MCELT MSAM MHYE
.... ..... .... ....
MCELF MCELT MSAM MHYE
EC CWID EANG WANG CTOP IOFLOW

01 1 1
03
30
1
21 05
01 01 115 01
02 06 114 01
07 16 113 01
17 21 112 01
22 22 115 01
0.2210 0000.0 06.4128 06.4128 0020.5 1
1
22 05
01 02 115 01
03 07 114 01
08 17 113 01
18 22 112 01
23 23 115 01
0.2210 0000.0 04.7919 04.7917 0024.0 1
1
23 06
01 01 116 01
02 03 115 01
04 08 114 01
09 18 113 01
19 23 112 01
24 24 116 01
0.2210 0000.0 05.0011 05.0011 0026.5 1
1
25 06
01 03 116 01
04 05 115 01
06 10 114 01
11 20 113 01
21 25 112 01
26 26 116 01
0.2210 0000.0 04.6160 04.6160 0025.0 1
1
20 06
01 01 117 01
02 05 116 01
06 07 115 01
08 12 114 01
13 20 113 01
21 21 117 01
0.2210 0000.0 01.7634 01.7634 0046.5 1
1
07 03
01 02 117 01
03 07 116 01
08 08 117 01
0.2210 0000.0 01.5745 01.5745 0055.5 1
1
08 04
01 01 118 01
02 04 117 01
05 08 116 01
09 09 118 01
0.2210 0000.0 02.0812 02.0812 0040.0 1
1
10 05
01 01 119 01
02 03 118 01
04 06 117 01
07 10 116 01
11 11 119 01
0.2210 0000.0 02.5182 02.5182 0031.0 1
1
10 05
01 02 119 01
03 04 118 01
05 07 117 01
08 10 116 01
11 11 119 01
0.2210 0000.0 05.5859 05.5859 0016.0 1
1
09 05
01 02 120 01
03 04 119 01
05 06 118 01
07 09 117 01
10 10 120 01
0.2210 0000.0 04.9573 04.9573 0019.5 1
1
08 05
01 03 120 01
04 05 119 01
06 07 118 01
08 08 117 01
09 09 120 01
0.2210 0000.0 02.9604 02.9604 0025.5 1
1
09 03
01 04 087 01
05 09 086 01
10 10 087 01
0.2210 0000.0 02.9107 02.9107 0029.5 1
1
09 04
01 01 088 01
02 05 087 01
06 09 086 01
10 10 088 01
0.2210 0000.0 03.1648 03.1648 0032.5 1
1
10 04
01 02 088 01
03 06 087 01
07 10 086 01
11 11 088 01
0.1130 0000.0 04.1645 04.1645 0028.0 1
1
08 04
01 03 088 01
04 07 087 01
08 08 086 01
09 09 088 01
0.1130 0000.0 02.3307 02.3307 0039.0 1
1
06 04
01 01 089 01
02 04 088 01
05 06 087 01
07 07 089 01
```

0.1130 0000.0 02.1942 02.1942 0044.5 1
1
25 05
01 06 089 01
07 16 088 01
17 21 087 01
22 25 086 01
26 26 089 01
0.1130 0000.0 03.5533 03.5533 0030.0 1
1
04 03
01 02 089 01
03 04 088 01
05 05 089 01
0.1130 0000.0 06.0194 06.0194 0019.0 1
1
03 03
01 01 090 01
02 03 089 01
04 04 090 01
0.0970 0000.0 02.2784 02.2784 0041.0 1
1
02 03
01 01 090 01
02 02 089 01
03 03 090 01
0.0970 0000.0 02.6939 02 6939 0035.0 1
1
01 02
01 01 059 01
02 02 059 01
0.0970 0000.0 04.8202 04.8202 0022.0 1
1
01 02
01 01 059 01
02 02 059 01
0.0970 0000.0 02.6514 02.6514 0032.0 1
1
01 02
01 01 059 01
02 02 059 01
0.1930 0000.0 05.4596 05.4596 0019.5 1
1
01 02
01 01 059 01
02 02 059 01
0.1930 0000.0 03.3106 03.3106 0026.0 1
1
02 03
01 01 060 01
02 02 059 01
03 03 060 01
0.1930 0000.0 02.5600 02.5600 0033.5 1
1
02 03
01 01 061 01
02 02 060 01
03 03 061 01
0.1930 0000.0 01.6934 01.6934 0044.0 1
1
03 04
01 01 062 01
02 02 061 01
03 03 060 01
04 04 062 01
0.1930 0000.0 05.0463 05.0463 0018.0 1
1
03 03
01 01 029 01
02 03 028 01
04 04 029 01
0.1930 0000.0 04.0000 04.0000 0020.0 1
1
02 02
01 02 029 01
03 03 029 01
0.1930 0000.0 06.2012 06.2012 0013.0 1
1
03 03
01 01 029 01
02 03 030 01
04 04 020 01
0.1930 0000.0 06.2012 06.2012 0018.0 1
18
1
04 03
01 01 087 01
02 04 086 01
05 05 087 01
0.0970 0000.0 01.4653 01.4653 0026.5 1
1
03 03
01 01 087 01
02 03 086 01
04 04 087 01
0.0970 0000.0 03.3138 03.3138 0028.0 1
1
02 02
01 02 087
03 03 087 01
0.0970 0000.0 03.0778 03.0778 0030.0 1
1
03 02
01 03 087 01
04 04 087 01
0.0970 0000.0 03.0967 03.0967 0034.0 1
1
03 02
01 03 087 01
04 04 087 01
0.0970 0000.0 02.4643 02.4643 0039.5 1
1
03 03
01 01 088 01
02 03 087 01
04 04 088 01
0.1710 0000.0 02.0359 02.0359 0037.5 1
1
02 02
01 02 088 01
03 03 088 01
0.1710 0000.0 03.8393 03.8393 0028.0 1
1
02 03
01 01 058 01
02 02 056 01
03 03 058 01
0.1710 0000.0 04.2973 04.2973 0026.0 1
1
03 03
01 02 058 01
03 03 056 01
04 04 058 01
0.1940 0000.0 02.4518 02.4518 0033.0 1
1
02 02
01 02 058 01
03 03 058 01

0.1940 0000.0 04.6397 04.6397 0024.5 1
1
01 02
01 01 058 01
02 02 058 01
0.1940 0000.0 05.0730 05.0730 0021.5 1
1
01 02
01 01 059 01
02 02 059 01
0.1940 0000.0 05.5662 05.5662 0021.5 1
1
01 02
01 01 059 01
02 02 059 01
0.1940 0000.0 04.5758 04.5758 0023.5 1
1
01 02
01 01 060 01
02 20 060 01
0.1940 0000.0 03.9571 03.9571 0026.0 1
1
02 03
01 01 028 01
02 02 027 01
03 03 028 01
0.1930 0000.0 04.7070 04.7070 0023.0 1
1
02 02
01 02 028 01
03 03 028 01
0.1930 0000.0 09.3384 09.3384 0021.5 1
1
02 03
01 01 029 01
02 02 028 01
03 03 029 01
0.1930 0000.0 09.3384 09.3384 0011.5 2
1
03 03
01 01 030 01
02 03 029 01
04 04 030 01
0.1930 0000.0 09.3384 09.3384 0011.5 2
06
1
04 04
01 02 016 01
03 03 015 01
04 04 014 01
05 05 016 01
0.3530 0000.0 17.0000 17.0000 0005.0 1
1
03 03
01 02 016 01
03 03 015 01
04 04 016 01
0.3530 0000.0 15.5556 15.5556 0006.0 1
1
04 03
01 03 016 01
04 04 015 01
05 05 016 01
0.3530 0000.0 13.3884 13.3884 0005.5 1
1
04 02
01 04 016 01
05 05 016 01
0.3530 0000.0 03.4870 03.4870 0031.5 1
1
05 02
01 05 016 01
06 06 016 01
0.3530 0000.0 02.0880 02.0880 0018.5 1
1
04 02
01 04 016 01
05 05 016 01
0.3530 0000.0 06.4291 06.4291 0017.0 1

APPENDIX 3.4.8 Sub-Catchment Four Digitised Coordinate Pairs for Flow Net Elements and Segments

Template
(See Appendix 4.1)
First line
XO YO
Other paired lines
X(1) Y(1) Z(1)
X(2) Y(2) Z(2)

270.58	632.15	
750.92	85.85	160.00
747.80	94.70	160.00
749.53	85.17	159.00
746.05	93.75	159.00
748.00	84.10	158.00
743.90	92.42	158.00
746.13	83.05	157.00
742.03	91.25	157.00
744.33	81.90	156.00
739.92	90.00	156.00
741.47	80.35	155.00
736.95	87.55	155.00
737.55	77.80	154.00
733.60	85.95	154.00
734.10	75.58	153.00
731.47	85.17	153.00
732.30	73.95	152.00
729.40	84.10	152.00
731.53	73.67	151.00
727.60	82.83	151.00
730.40	72.80	150.00
726.35	81.65	150.00
729.25	72.20	149.00
725.13	80.97	149.00
728.22	71.35	148.00
723.95	80.17	148.00
727.03	70.70	147.00
722.95	79.35	147.00
725.53	69.40	146.00
721.83	78.45	146.00
723.45	68.17	145.00
719.10	76.72	145.00
720.88	66.45	144.00
715.50	74.53	144.00
718.40	64.90	143.00
712.95	73.15	143.00
716.17	63.30	142.00
710.65	72.00	142.00
713.65	61.55	141.00
708.10	70.67	141.00
710.72	59.65	140.00
704.90	69.50	140.00
708.70	58.13	139.50
695.40	66.50	138.90
747.72	94.85	160.00
742.55	106.30	160.00
746.03	93.72	159.00
740.45	105.72	159.00
744.03	92.47	158.00
738.03	104.90	158.00
741.80	91.20	157.00
735.72	103.78	157.00
740.03	90.00	156.00
733.40	103.00	156.00
736.95	87.58	155.00
730.72	101.45	155.00
733.55	85.78	154.00
724.85	99.80	154.00
731.53	85.13	153.00
722.80	99.53	153.00
729.42	84.15	152.00
720.65	99.17	152.00
727.50	82.90	151.00
718.65	99.08	151.00
726.28	81.85	150.00
716.67	98.55	150.00
725.05	80.90	149.00
715.10	97.58	149.00
724.00	80.17	148.00
713.78	97.03	148.00
722.78	79.28	147.00
711.47	95.67	147.00
721.90	78.67	146.00
709.33	94.38	146.00
719.08	76.63	145.00
707.38	93.03	145.00
715.80	74.55	144.00
704.67	91.28	144.00
712.95	73.22	143.00
701.30	89.15	143.00
710.97	72.13	142.00
699.10	87.92	142.00
708.13	70.75	141.00
696.05	86.10	141.00
704.92	69.53	140.00
693.58	84.95	140.00
700.65	68.42	139.00
689.47	83.25	139.00
695.53	66.40	138.90
680.60	80.45	137.20
742.65	106.28	160.00
741.67	109.83	160.00
740.63	105.65	159.00
739.75	109.85	159.00
737.97	104.90	158.00
736.35	109.38	158.00
735.75	103.85	157.00
733.80	108.97	157.00
733.45	102.97	156.00
731.22	108.72	156.00
730.58	101.53	155.00
728.08	108.38	155.00
724.88	99.83	154.00
726.03	107.88	154.00
722.70	99.40	153.00
722.65	106.88	153.00
720.45	99.30	152.00
719.92	105.97	152.00
718.72	99.15	151.00
717.35	104.97	151.00
716.72	98.45	150.00
715.10	103.78	150.00
715.05	97.60	149.00
713.10	102.97	149.00
713.78	97.13	148.00
711.67	102.53	148.00
711.38	95.83	147.00
709.58	101.95	147.00
709.28	94.22	146.00
707.40	101.70	146.00
707.38	92.83	145.00
705.38	101.65	145.00
704.80	91.22	144.00
702.03	101.70	144.00
701.35	89.25	143.00
698.33	100.83	143.00
699.03	87.83	142.00
695.15	99.67	142.00
695.97	86.35	141.00
692.20	98.88	141.00
693.53	85.17	140.00
689.13	98.05	140.00
689.33	83.25	139.00
686.25	97.15	139.00
685.78	81.78	138.00
682.13	96.53	138.00
680.63	80.33	137.20
668.25	95.70	123.60
741.75	109.80	160.00
743.78	114.53	160.00
739.60	109.75	159.00
739.00	117.67	159.00
736.45	109.28	158.00
733.75	118.88	158.00
733.67	108.90	157.00
731.08	118.97	157.00
731.03	108.72	156.00
728.83	118.70	156.00
728.10	108.35	155.00
726.30	117.83	155.00
725.90	107.72	154.00
724.20	117.20	154.00
722.67	106.97	153.00
720.17	115.90	153.00
720.03	105.92	152.00
716.92	113.72	152.00
717.05	104.88	151.00
713.90	113.00	151.00
715.05	103.67	150.00
712.15	112.55	150.00
713.05	102.92	149.00
710.60	112.22	149.00
711.58	102.42	148.00
709.00	112.00	148.00
709.58	101.72	147.00
707.13	111.38	147.00
707.20	101.63	146.00
705.53	110.97	146.00
705.30	101.67	145.00
703.60	110.58	145.00
702.15	101.70	144.00
700.97	110.15	144.00
698.25	100.72	143.00
697.53	110.47	143.00
695.25	99.97	142.00
694.58	111.65	142.00
692.13	98.72	141.00
691.42	112.85	141.00
688.97	97.85	140.00
687.78	113.65	140.00
686.22	97.20	139.00
684.22	114.63	139.00
681.90	96.50	138.00
678.70	115.75	138.00
675.33	96.33	137.00
673.35	114.78	137.00
670.40	96.00	136.00
668.35	113.30	136.00
667.88	95.63	135.60
656.33	110.42	135.50
720.40	114.55	153.00
720.22	116.15	153.00
716.88	113.92	152.00
716.65	117.35	152.00

714.03	113.10	151.00	640.85	160.97	130.00	647.20	217.78	130.00
714.60	118.08	151.00	635.13	146.13	129.40	644.17	236.83	130.00
712.25	112.47	150.00	623.90	162.88	127.80	638.38	216.95	129.00
713.08	118.63	150.00	676.33	147.58	137.00	634.97	234.22	129.00
710.63	112.13	149.00	679.50	151.20	137.00	631.38	215.97	128.00
710.83	119.33	149.00	672.88	150.25	136.00	629.13	231.78	128.00
709.03	111.78	148.00	675.33	154.13	136.00	622.53	213.80	127.00
708.78	119.25	148.00	667.95	153.47	135.00	621.15	230.00	127.00
707.15	111.38	147.00	670.03	158.35	135.00	612.92	210.83	126.00
706.30	118.97	147.00	662.28	157.03	134.00	612.65	227.22	126.00
705.53	111.10	146.00	664.20	161.80	134.00	601.70	210.03	125.00
704.60	118.80	146.00	657.90	158.55	133.00	601.70	226.08	125.00
703.75	110.47	145.00	659.28	164.42	133.00	590.80	210.08	124.00
702.63	118.58	145.00	652.60	159.67	132.00	590.70	225.88	124.00
700.88	110.15	144.00	653.13	168.05	132.00	587.55	210.33	123.80
699.83	118.05	144.00	646.72	160.33	131.00	575.35	226.22	122.60
697.38	110.58	143.00	648.15	169.72	131.00	659.60	238.17	131.00
697.35	117.72	143.00	640.78	160.90	130.00	659.33	253.78	131.00
694.63	111.75	142.00	641.92	170.85	130.00	644.35	236.70	130.00
695.10	117.30	142.00	633.40	161.97	129.00	642.78	256.15	130.00
691.47	112.78	141.00	634.67	172.72	129.00	634.90	234.17	129.00
691.92	116.85	141.00	625.20	162.83	128.00	630.72	255.35	129.00
687.67	113.70	140.00	626.13	174.25	128.00	629.05	231.90	128.00
688.17	117.17	140.00	623.88	162.83	127.80	623.70	253.88	128.00
684.03	114.65	139.00	611.08	177.38	126.20	621.10	230.03	127.00
684.70	117.92	139.00	675.13	154.08	136.00	616.72	251.95	127.00
678.88	115.65	138.00	678.20	161.25	136.00	612.65	227.35	126.00
679.00	127.80	138.00	669.85	158.38	135.00	608.80	250.50	126.00
673.17	114.65	137.00	673.03	164.88	135.00	601.65	226.17	125.00
673.17	131.63	137.00	664.25	161.70	134.00	598.92	249.53	125.00
668.28	113.35	136.00	668.33	168.28	134.00	590.95	225.63	124.00
669.53	132.22	136.00	659.30	164.53	133.00	590.00	247.65	124.00
663.67	111.50	135.00	663.28	172.13	133.00	580.47	226.03	123.00
665.28	131.85	135.00	653.28	167.90	132.00	578.80	245.13	123.00
658.53	110.95	134.00	657.25	176.58	132.00	575.70	226.15	122.60
661.00	130.53	134.00	647.88	169.72	131.00	562.33	241.63	121.50
656.22	110.50	133.50	650.35	181.92	131.00	642.70	256.13	130.00
646.15	128.25	131.20	641.92	170.83	130.00	641.97	265.00	130.00
678.92	128.00	138.00	643.38	183.58	130.00	630.80	255.17	129.00
684.80	136.10	138.00	634.70	172.58	129.00	629.88	264.80	129.00
673.38	131.83	137.00	636.13	185.13	129.00	623.67	254.03	128.00
674.20	140.60	137.00	626.03	174.55	128.00	622.35	264.67	128.00
669.38	132.08	136.00	627.70	186.35	128.00	616.78	252.10	127.00
669.97	141.78	136.00	617.50	176.13	127.00	615.45	264.42	127.00
665.45	131.67	135.00	619.55	188.15	127.00	608.60	250.42	126.00
664.72	143.78	135.00	610.85	177.78	126.20	607.47	264.97	126.00
661.03	130.33	134.00	598.22	191.88	124.70	599.15	249.30	125.00
660.88	144.63	134.00	663.20	172.25	133.00	597.55	264.70	125.00
655.40	129.38	133.00	681.15	202.28	133.00	589.90	247.60	124.00
656.47	144.92	133.00	657.15	176.38	132.00	586.75	264.40	124.00
650.30	128.58	132.00	671.95	209.33	132.00	578.78	245.33	123.00
651.30	145.00	132.00	650.35	181.90	131.00	574.08	262.30	123.00
646.20	128.33	131.20	658.38	217.22	131.00	567.83	242.80	122.00
635.25	146.08	129.40	643.42	183.63	130.00	563.17	260.70	122.00
674.17	140.72	137.00	647.25	218.13	130.00	562.22	241.42	121.50
676.17	147.58	137.00	636.03	184.83	129.00	551.70	259.28	120.60
670.05	141.88	136.00	638.38	217.10	129.00	641.92	264.92	130.00
672.70	150.22	136.00	627.78	186.40	128.00	641.85	268.10	130.00
664.70	143.63	135.00	631.40	216.20	128.00	629.92	264.83	129.00
667.92	153.60	135.00	619.47	188.13	127.00	629.90	267.70	129.00
660.53	144.60	134.00	622.58	213.78	127.00	622.17	264.67	128.00
662.15	157.13	134.00	611.40	190.13	126.00	622.22	268.13	128.00
656.53	145.10	133.00	612.95	210.80	126.00	615.50	264.50	127.00
658.08	158.60	133.00	601.88	191.55	125.00	615.83	268.92	127.00
651.22	144.85	132.00	601.75	209.85	125.00	607.25	264.65	126.00
652.65	159.85	132.00	598.13	192.03	124.70	607.35	268.05	126.00
645.90	145.38	131.00	587.75	209.97	123.80	597.33	264.55	125.00
646.85	160.30	131.00	658.58	217.35	131.00	596.88	268.75	125.00
640.13	145.78	130.00	659.72	238.45	131.00	586.83	264.38	124.00

586.45	269.83	124.00	559.13	295.92	120.00	471.58	467.92	109.10
573.92	262.08	123.00	574.67	337.47	120.00	487.77	468.03	111.00
571.97	272.97	123.00	558.63	297.79	119.80	487.58	481.70	111.00
563.03	260.67	122.00	573.85	337.34	119.80	479.60	467.70	110.00
561.78	273.97	122.00	558.14	299.66	119.60	478.02	482.75	110.00
554.72	259.60	121.00	573.02	337.20	119.60	471.67	467.70	109.10
553.45	276.40	121.00	557.64	301.54	119.40	460.73	483.40	107.60
551.85	259.10	120.60	572.20	337.07	119.40	478.00	482.70	110.00
545.45	279.05	119.70	557.15	303.41	119.20	479.23	493.02	110.00
615.50	267.03	127.00	571.37	336.93	119.20	470.55	482.65	109.00
615.58	269.15	127.00	556.65	305.28	119.00	471.20	494.40	109.00
607.20	268.03	126.00	570.55	336.80	119.00	462.35	483.55	108.00
607.75	271.45	126.00	556.07	307.15	118.80	462.95	496.20	108.00
596.75	268.75	125.00	569.04	336.54	118.80	459.98	483.75	107.60
597.22	272.22	125.00	555.49	309.02	118.60	448.55	499.05	106.70
586.05	269.75	124.00	567.53	336.27	118.60	471.23	494.42	109.00
587.17	273.33	124.00	554.91	310.89	118.40	473.52	506.27	109.00
571.85	272.95	123.00	566.03	336.01	118.40	462.85	496.15	108.00
571.00	277.53	123.00	554.33	312.76	118.20	464.48	509.35	108.00
561.95	274.15	122.00	564.52	335.75	118.20	452.00	497.85	107.00
563.95	281.22	122.00	553.75	314.63	118.00	454.05	512.28	107.00
553.58	276.28	121.00	563.01	335.48	118.00	448.60	499.08	106.70
557.70	285.83	121.00	553.17	316.50	117.80	438.63	515.80	105.60
546.80	278.42	120.00	555.47	334.17	116.90	454.02	512.33	107.00
550.75	290.83	120.00	574.45	337.38	120.00	455.73	524.73	107.00
545.30	278.95	119.70	572.03	355.20	120.00	442.80	514.65	106.00
543.60	298.92	118.40	570.58	336.70	119.00	445.65	527.42	106.00
586.25	271.50	124.00	567.30	355.08	119.00	438.42	515.88	105.60
586.97	273.45	124.00	566.22	335.92	118.00	425.88	533.80	104.60
570.92	277.47	123.00	561.58	355.03	118.00	455.73	524.73	107.00
572.83	280.65	123.00	558.17	334.22	117.00	458.13	531.48	107.00
563.65	281.30	122.00	556.42	354.22	117.00	445.58	527.28	106.00
567.13	285.60	122.00	555.67	334.10	116.90	446.65	535.78	106.00
557.88	285.95	121.00	549.00	352.58	115.90	432.15	530.80	105.00
562.55	290.63	121.00	561.65	355.08	118.00	435.15	539.23	105.00
550.92	290.97	120.00	557.40	375.47	118.00	425.25	534.20	104.60
559.03	295.83	120.00	556.20	354.05	117.00	414.13	547.98	103.60
546.42	295.55	119.00	551.50	373.13	117.00	630.80	295.03	129.00
556.53	305.47	119.00	550.58	352.85	116.00	629.33	302.60	129.00
543.83	298.85	118.40	545.38	371.65	116.00	623.90	294.95	128.00
553.10	316.65	117.80	548.92	352.58	115.90	623.00	302.35	128.00
641.85	268.13	130.00	541.10	371.10	115.70	617.60	294.30	127.00
637.05	294.45	130.00	551.33	373.08	117.00	616.90	302.08	127.00
629.75	267.75	129.00	549.58	387.22	117.00	611.42	293.38	126.00
630.95	295.08	129.00	545.20	371.70	116.00	610.55	301.40	126.00
622.25	268.03	128.00	542.40	387.63	116.00	608.42	292.88	125.80
623.85	295.15	128.00	541.28	371.08	115.70	604.45	301.50	125.00
615.63	268.83	127.00	530.47	387.15	114.20	623.15	302.30	128.00
617.67	294.38	127.00	535.80	388.03	115.00	621.70	313.38	128.00
607.80	271.42	126.00	531.13	407.28	115.00	616.78	302.20	127.00
611.40	293.38	126.00	530.47	387.20	114.20	615.00	313.97	127.00
597.03	272.17	125.00	519.03	403.30	113.20	610.30	301.58	126.00
605.10	300.55	125.00	524.47	405.17	114.00	608.33	315.70	126.00
587.00	273.50	124.00	522.28	420.35	114.00	604.20	301.38	125.00
598.33	309.60	124.00	518.88	403.28	113.20	592.75	316.35	123.00
572.97	280.38	123.00	508.58	419.45	112.10	602.25	315.88	125.00
592.33	316.80	123.00	513.28	419.63	113.00	600.63	328.20	125.00
567.40	285.50	122.00	509.13	438.88	113.00	596.58	316.30	124.00
586.45	325.30	122.00	508.33	419.47	112.10	595.60	328.22	124.00
562.53	290.15	121.00	495.98	436.08	111.40	592.63	316.22	123.00
580.70	332.72	121.00	501.70	436.90	112.00	584.20	328.83	121.70
561.85	291.30	120.80	497.23	453.10	112.00	595.63	328.47	124.00
579.50	333.70	120.80	496.10	435.90	111.40	596.33	334.88	124.00
561.17	292.46	120.60	483.83	451.92	110.30	590.53	328.70	123.00
578.30	334.60	120.60	497.23	453.15	112.00	590.75	335.67	123.00
560.49	293.61	120.40	496.20	469.22	112.00	586.03	328.92	122.00
577.10	335.60	120.40	489.15	452.22	111.00	585.50	335.60	122.00
559.81	294.77	120.20	487.65	468.15	111.00	584.03	328.88	121.70
575.90	336.50	120.20	483.90	451.80	110.30	578.40	335.88	120.50

590.70	335.55	123.00	451.55	533.60	106.30	399.33	596.58	102.00
588.22	351.83	123.00	468.02	526.75	108.00	406.13	619.65	102.00
585.40	335.58	122.00	471.15	534.60	108.00	388.92	600.30	101.00
582.83	351.95	122.00	458.00	531.15	107.00	393.45	625.45	101.00
580.55	335.85	121.00	460.27	539.20	107.00	366.38	620.42	100.70
577.53	352.03	121.00	451.40	534.17	106.30	358.73	639.67	100.30
578.33	335.70	120.50	429.90	541.05	104.60			
568.30	352.08	119.10	460.13	539.17	107.00			
582.63	352.10	122.00	460.38	548.42	107.00			
578.53	372.33	122.00	448.10	541.78	106.00			
577.33	352.17	121.00	448.17	548.95	106.00			
573.97	371.30	121.00	435.83	540.98	105.00			
572.83	351.92	120.00	436.95	549.45	105.00			
569.10	370.13	120.00	430.08	540.92	104.60			
568.10	352.00	119.10	414.20	548.17	103.60			
558.67	368.25	117.90	460.45	548.38	107.00			
569.05	369.95	120.00	460.33	553.92	107.00			
564.10	385.13	120.00	447.88	549.15	106.00			
564.00	369.33	119.00	447.70	555.92	106.00			
560.35	385.35	119.00	437.10	549.33	105.00			
558.55	368.17	117.90	436.10	555.40	105.00			
545.45	383.92	116.30	422.67	548.08	104.00			
555.63	384.83	118.00	423.85	552.75	104.00			
550.45	399.35	118.00	413.63	548.45	103.60			
549.75	383.80	117.00	406.38	554.58	103.20			
545.47	399.25	117.00	447.55	555.83	106.00			
545.50	384.05	116.30	447.35	562.35	106.00			
532.38	400.00	114.90	435.98	555.30	105.00			
545.22	399.42	117.00	433.70	564.23	105.00			
543.10	417.03	117.00	423.73	552.50	104.00			
539.75	399.78	116.00	423.55	562.40	104.00			
536.15	417.10	116.00	406.08	554.55	103.20			
534.25	399.85	115.00	391.17	567.35	102.40			
528.88	416.63	115.00	447.38	562.17	106.00			
532.67	400.08	114.90	446.95	566.60	106.00			
522.20	416.17	114.00	433.92	564.35	105.00			
536.03	417.17	116.00	433.33	570.03	105.00			
534.13	432.65	116.00	423.63	562.40	104.00			
528.75	416.78	115.00	421.05	571.60	104.00			
526.75	432.85	115.00	399.85	562.80	103.00			
522.08	415.92	114.00	405.25	571.40	103.00			
511.17	432.15	113.00	390.92	567.58	102.40			
520.30	432.28	114.00	378.85	583.17	101.40			
515.63	447.88	114.00	433.50	569.85	105.00			
511.00	432.08	113.00	433.58	572.73	105.00			
500.95	449.78	112.20	421.05	571.48	104.00			
507.20	448.50	113.00	419.45	579.88	104.00			
506.17	463.95	113.00	405.42	571.45	103.00			
500.73	449.97	112.20	407.17	583.58	103.00			
492.15	467.78	111.40	386.63	577.48	102.00			
497.25	466.83	112.00	393.85	586.08	102.00			
498.75	478.65	112.00	378.60	583.25	101.40			
492.05	468.08	111.40	372.48	602.08	100.75			
481.75	485.17	110.30	433.75	572.75	105.00			
488.40	482.53	111.00	434.75	581.33	105.00			
489.77	492.95	111.00	419.20	579.95	104.00			
481.58	485.63	110.30	421.33	588.20	104.00			
471.63	500.33	108.70	407.10	583.33	103.00			
480.45	496.15	110.00	409.75	593.58	103.00			
484.35	507.77	110.00	393.73	585.88	102.00			
473.13	499.90	109.00	399.15	596.60	102.00			
474.85	511.55	109.00	377.42	595.15	101.00			
471.48	500.50	108.70	388.63	600.33	101.00			
459.85	517.65	107.50	372.27	602.45	100.75			
474.98	511.33	109.00	366.63	620.40	100.70			
478.02	521.67	109.00	421.20	588.17	104.00			
465.30	515.50	108.00	429.85	602.70	104.00			
468.27	526.83	108.00	409.88	593.40	103.00			
459.65	518.13	107.50	418.88	610.65	103.00			

APPENDIX 3.4.9 Sub-Catchment Five Discretised Flow-Net Structure and Channel Data

```
Template
(See Appendix 4.1)
NSUB K33 K44
NCHA
NSEG
NCAS
NELM
MCELF MCELT MSAM MHYE
....  ..... .... ....
MCELF MCELT MSAM MHYE
EC CWID EANG WANG CTOP IOFLOW


01 1 1
01
23
1
02 02
01 02 086 01
03 03 086 01
0.1760 0000.0 03.6111 03.6111 0027.0 1
1
01 02
01 01 086 01
02 02 086 01
0.1760 0000.0 03.6111 03.6111 0027.0 1
1
01 02
01 01 087 01
02 02 087 01
0.1760 0000.0 04.0820 04.0820 0024.5 1
1
01 02
01 01 087 01
02 02 087 01
0.1760 0000.0 03.1250 03.1250 0032.0 1
1
02 02
01 02 087 01
03 03 087 01
0.1760 0000.0 03.8460 03.8460 0026.0 1
1
02 02
01 02 087 01
03 03 087 01
0.1710 0000.0 04.4444 04.4444 0022.5 1
1
03 03
01 02 056 01
03 03 055 01
04 04 056 01
0.1710 0000.0 02.9460 02.9460 0028.0 1
1
03 03
01 02 056 01
03 03 055 01
04 04 056 01
0.1710 0000.0 04.2500 04.2500 0023.5 1
1
04 03
01 02 057 01
03 04 056 01
05 05 057 01
0.1710 0000.0 02.3720 02.3720 0039.0 1
1
03 03
01 01 058 01
02 03 057 01
04 04 058 01
0.1710 0000.0 03.6400 03.6400 0027.5 1
1
03 03
01 02 058 01
03 03 057 01
04 04 058 01
0.1940 0000.0 04.0800 04.0800 0024.5 1
1
03 03
01 01 059 01
02 03 058 01
04 04 059 01
0.1940 0000.0 06.2500 06.2500 0016.0 1
1
02 02
01 02 026 01
03 03 026 01
0.1940 0000.0 04.1670 04.1670 0024.0 1
1
03 03
01 02 027 01
03 03 026 01
04 04 027 01
0.3530 0000.0 04.5454 04.5454 0022.0 1
1
02 03
01 01 028 01
02 02 027 01
03 03 028 01
0.3530 0000.0 04.3480 04.3480 0023.0 1
1
02 03
01 01 013 01
02 02 012 01
03 03 013 01
0.3530 0000.0 05.5500 05.5500 0018.0 1
1
03 04
01 01 014 01
02 02 013 01
03 03 012 01
04 04 014 01
0.3530 0000.0 05.0000 05.0000 0020.0 1
1
03 04
01 01 015 01
02 02 014 01
03 03 013 01
04 04 015 01
0.3530 0000.0 04.3480 04.3480 0023.0 1
1
04 05
01 01 016 01
02 02 015 01
03 03 014 01
04 04 013 01
05 05 016 01
0.3530 0000.0 04.5454 04.5454 0022.0 1
1
05 05
01 02 016 01
03 03 015 01
04 04 014 01
05 05 013 01
06 06 016 01
0.3530 0000.0 05.0000 05.0000 0020.0 1
1
05 04
01 03 016 01
```

```
04 04 015 01
05 05 014 01
06 06 016 01
0.3530 0000.0 04.0820 04.0820 0024.5 1
1
05 03
01 04 016 01
05 05 015 01
06 06 015 01
0.3530 0000.0 02.8980 02.8980 0034.5 1
1
06 03
01 05 016 01
06 06 015 01
07 07 016 01
0.3530 0000.0 06.6667 06.6667 0015.0 1
```

APPENDIX 3.4.10 Sub-Catchment Five Digitised Coordinate Pairs for Flow Net Elements and Segments

Template
(See Appendix 4.1)
First line
XO YO
Other paired lines
X(1) Y(1) Z(1)
X(2) Y(2) Z(2)

270.77	631.48	
615.05	313.83	127.00
614.65	323.03	127.00
608.53	313.33	126.00
607.33	322.28	126.00
606.67	313.22	125.70
601.53	321.88	125.00
607.42	322.50	127.00
607.53	334.28	127.00
601.47	322.03	125.00
595.17	335.47	123.60
596.72	335.60	126.00
595.72	343.60	126.00
595.28	335.30	123.60
591.28	343.15	123.40
595.60	343.63	124.00
593.47	360.45	124.00
591.15	343.28	123.40
580.78	359.55	121.70
587.22	360.13	123.00
582.95	379.28	123.00
583.08	359.83	122.00
577.20	377.58	122.00
580.72	359.33	121.70
568.85	374.55	120.30
577.05	377.38	122.00
574.08	393.40	122.00
572.08	375.83	121.00
565.70	391.90	121.00
568.95	374.45	120.30
557.05	390.25	118.40
565.63	391.95	121.00
565.92	407.05	121.00
561.88	391.22	120.00
558.53	407.53	120.00
558.58	390.50	119.00
554.00	407.15	119.00
557.05	389.92	118.40
545.22	405.88	116.90
558.67	407.58	120.00
557.60	427.20	120.00
554.08	406.78	119.00
552.55	426.38	119.00
550.03	406.20	118.00
547.92	425.42	118.00
545.17	405.88	116.90
533.45	422.65	115.70
552.58	426.40	119.00
550.63	442.53	119.00
547.67	425.28	118.00
545.88	442.30	118.00
542.05	424.20	117.00
539.38	441.72	117.00
536.05	423.10	116.00
532.88	440.67	116.00
533.45	422.55	115.70
521.90	439.25	114.60
539.50	441.85	117.00
539.63	453.85	117.00
532.80	440.72	116.00
531.42	455.25	116.00
525.00	439.65	115.00
523.33	455.85	115.00
521.90	439.17	114.60
511.00	455.00	113.40
531.55	455.20	116.00
530.08	469.97	116.00
523.00	455.67	115.00
521.63	471.20	115.00
515.03	455.15	114.00
514.17	471.00	114.00
511.05	454.97	113.40
500.23	472.70	112.30
521.53	470.83	115.00
521.30	478.95	115.00
514.03	471.00	114.00
514.95	481.03	114.00
506.15	471.28	113.00
508.27	483.50	113.00
500.27	472.47	112.30
491.25	489.80	111.20
508.15	483.50	113.00
511.50	497.58	113.00
499.20	486.97	112.00
502.58	500.38	112.00
491.23	489.88	111.20
482.33	508.70	109.70
502.60	500.35	112.00
505.10	517.45	112.00
493.60	503.85	111.00
496.25	521.42	111.00
484.65	507.67	110.00
488.10	524.15	110.00
482.58	508.55	109.70
473.92	525.78	108.60
488.05	524.25	110.00
490.25	538.08	110.00
479.13	525.73	109.00
481.13	539.65	109.00
474.15	525.78	108.60
463.25	542.80	107.00
481.02	539.75	109.00
481.30	550.25	109.00
472.48	541.70	108.00
472.77	553.23	108.00
463.25	542.80	107.00
449.70	558.17	106.20
481.42	550.03	109.00
482.75	555.28	109.00
472.85	553.23	108.00
473.98	558.83	108.00
461.13	555.78	107.00
462.23	563.60	107.00
449.77	558.08	106.20
437.20	572.42	105.20
473.70	559.05	108.00
474.45	562.42	108.00
462.20	563.53	107.00
463.58	568.60	107.00
447.45	568.80	106.00
448.80	575.63	106.00
436.58	572.88	105.20
426.73	589.20	104.20
474.30	562.20	108.00
475.05	564.17	108.00
463.55	568.48	107.00
464.83	572.05	107.00
449.00	575.30	106.00
450.65	579.83	106.00
436.10	583.67	105.00
439.95	590.53	105.00
426.52	589.03	104.20
418.58	606.55	103.10
475.15	564.23	108.00
477.58	569.98	108.00
464.83	571.80	107.00
466.55	577.05	107.00
450.55	579.70	106.00
454.42	584.25	106.00
439.88	590.50	105.00
444.55	596.53	105.00
428.80	599.08	104.00
433.55	607.17	104.00
418.90	606.55	103.10
411.90	624.75	102.10
466.52	576.73	107.00
468.98	583.03	107.00
454.08	584.45	106.00
460.33	587.63	106.00
444.35	596.08	105.00
448.13	600.63	105.00
433.40	607.25	104.00
436.38	612.33	104.00
422.30	616.25	103.00
426.13	622.15	103.00
411.50	625.05	102.10
405.05	643.50	101.10
459.13	587.63	106.00
460.38	589.50	106.00
448.00	600.30	105.00
449.27	601.92	105.00
436.52	612.00	104.00
438.70	615.15	104.00
426.15	622.30	103.00
429.90	626.13	103.00
415.67	632.85	102.00
419.73	638.03	102.00
404.67	643.45	101.10
393.98	659.10	100.30
460.45	589.38	106.00
466.20	596.42	106.00
449.10	601.98	105.00
454.90	607.83	105.00
438.67	614.90	104.00
445.80	620.63	104.00
429.80	626.13	103.00
436.33	633.65	103.00
419.60	637.85	102.00
428.35	648.38	102.00
407.33	650.98	101.00
410.95	660.25	101.00
393.45	659.08	100.30
380.98	675.30	99.80

APPENDIX 3.4.11 Sub-Catchment Six Discretised Flow-Net Structure and Channel Data

```
Template
(See Appendix 4.1)
NSUB K33 K44
NCHA
NSEG
NCAS
NELM
MCELF MCELT MSAM MHYE
.... ..... .... ....
MCELF MCELT MSAM MHYE
EC CWID EANG WANG CTOP IOFLOW


01 1 1
03
05
1
22 05
01 02 113 01
03 07 114 01
08 17 113 01
18 22 112 01
23 23 113 01
0.1760 0000.0 05.0365 05.0365 0025.5 1
1
22 05
01 03 115 01
04 08 114 01
09 18 113 01
19 22 112 01
23 23 115 01
0.1760 0000.0 04.5568 04.5568 0020.5 1
1
20 05
01 01 116 01
02 05 115 01
06 10 114 01
11 20 113 01
21 21 116 01
0.1760 0000.0 03.1207 03.1207 0030.5 1
1
22 05
01 03 116 01
04 07 115 01
08 12 114 01
13 22 113 01
23 23 116 01
0.1760 0000.0 08.3330 08.3330 0015.5 1
1
27 07
01 01 117 01
02 04 116 01
05 08 115 01
09 13 114 01
14 23 113 01
24 27 112 01
28 28 117 01
0.1760 0000.0 04.7603 04.7603 0026.0 1
03
1
21 05
01 02 115 01
03 08 114 01
09 17 113 01
18 21 112 01
22 22 115 01
0.1760 0000.0 03.2322 03.2322 0026.0 1
1
24 06
01 01 116 01
02 05 115 01
06 10 114 01
11 20 113 01
21 24 112 01
25 25 116 01
0.1760 0000.0 11.1326 11.1326 0014.0 1
1
04 03
01 01 117 01
02 04 116 01
05 05 117 01
0.1760 0000.0 04.7828 04.7828 0025.5 1
26
1
20 06
01 02 085 01
03 05 084 01
06 13 083 01
14 18 082 01
19 20 081 01
21 21 085 01
0.1760 0000.0 05.6578 05.6578 0015.0 1
1
21 06
01 02 085 01
03 05 084 01
06 13 083 01
14 18 082 01
19 21 081 01
22 22 085 01
0.1760 0000.0 03.0881 03.0881 0033.0 1
1
24 07
01 01 086 01
02 04 085 01
05 07 084 01
08 14 083 01
15 20 082 01
21 24 081 01
25 25 086 01
0.1760 0000.0 03.4935 03.4935 0032.5 1
1
19 06
01 02 086 01
02 06 085 01
07 09 084 01
10 16 083 01
17 19 082 01
20 20 086 01
0.1760 0000.0 02.3665 02.3665 0043.5 1
1
28 07
01 03 086 01
04 07 085 01
08 10 084 01
11 17 083 01
18 23 082 01
24 28 081 01
29 29 086 01
0.1760 0000.0 03.4632 03.4632 0028.5 1
1
30 07
01 04 086 01
05 08 085 01
09 11 084 01
12 19 083 01
```

```
20 25 082 01
26 30 081 01
31 31 086 01
0.0970 0000.0 02.3004 02.3004 0034.5 1
1
32 08
01 01 087 01
02 05 086 01
06 09 085 01
10 12 084 01
13 22 083 01
23 26 082 01
27 32 081 01
33 33 087 01
0.0970 0000.0 02.8815 02.8815 0033.0 1
1
34 08
01 02 087 01
03 08 086 01
09 10 085 01
11 13 084 01
14 23 083 01
24 27 082 01
28 34 081 01
35 35 087 01
0.0970 0000.0 02.7049 02.7049 0037.0 1
1
35 08
01 03 055 01
04 06 054 01
07 10 053 01
11 17 052 01
18 24 051 01
25 30 050 01
31 35 049 01
36 36 055 01
0.0970 0000.0 04.9728 04.9728 0021.0 1
1
37 08
01 04 055 01
05 07 054 01
08 12 053 01
13 18 052 01
19 25 051 01
26 31 050 01
32 37 049 01
38 38 055 01
0.1710 0000.0 01.9254 01.9254 0049.0 1
1
38 08
01 05 055 01
06 08 054 01
09 12 053 01
13 19 052 01
20 26 051 01
27 32 050 01
33 38 049 01
39 39 055 01
0.1710 0000.0 02.4691 02.4691 0040.5 1
1
37 08
01 05 055 01
06 08 054 01
09 12 053 01
13 18 052 01
19 26 051 01
27 34 050 01
35 37 049 01
38 38 056 01
0.1710 0000.0 03.5140 03.5140 0028.0 1
1
40 10
01 01 057 01
02 03 056 01
04 08 055 01
09 11 054 01
12 15 053 01
16 22 052 01
23 29 051 01
30 35 050 01
36 40 049 01
41 41 057 01
0.1710 0000.0 01.7965 01.7965 0042.5 1
1
39 10
01 02 057 01
03 04 056 01
05 09 055 01
10 12 054 01
13 14 053 01
15 23 052 01
24 30 051 01
31 36 050 01
37 39 049 01
40 40 057 01
0.1710 0000.0 03.6889 03.6889 0031.0 1
1
40 10
01 02 025 01
03 06 024 01
07 11 023 01
12 15 022 01
16 20 021 01
21 25 020 01
26 31 019 01
32 35 018 01
36 40 017 01
41 41 025 01
0.1710 0000.0 01.3306 01.3306 0067.0 1
1
40 11
01 01 026 01
02 03 025 01
04 07 024 01
08 12 023 01
13 16 022 01
17 21 021 01
22 26 020 01
27 30 019 01
31 36 018 01
37 40 017 01
41 41 026 01
0.1940 0000.0 03.4114 03.4114 0031.5 1
1
24 08
01 01 010 01
02 07 009 01
08 09 008 01
10 14 007 01
15 18 006 01
19 21 005 01
22 24 004 01
25 25 010 01
0.1940 0000.0 02.4906 02.4906 0040.0 1
1
19 07
01 01 011 01
02 02 010 01
```

```
03 08 009 01
09 10 008 01
11 15 007 01
16 19 006 01
20 20 011 01
0.1940 0000.0 06.8320 06.8320 0016.5 1
1
20 08
01 01 012 01
02 02 011 01
03 03 010 01
04 08 009 01
09 11 008 01
12 16 007 01
17 20 006 01
21 21 012 01
0.3530 0000.0 02.8359 02.8359 0037.5 1
1
08 06
01 01 013 01
02 02 012 01
03 03 011 01
04 04 010 01
05 08 009 01
09 09 013 01
0.3530 0000.0 04.5333 04.5333 0022.5 1
1
25 12
01 01 015 01
02 02 014 01
03 03 013 01
04 04 012 01
05 05 011 01
06 06 010 01
07 11 009 01
12 14 008 01
15 19 007 01
20 22 006 01
23 25 005 01
26 26 015 01
0.3530 0000.0 04.0737 04.0737 0023.0 1
1
12 09
01 01 016 01
02 02 015 01
03 03 014 01
04 04 013 01
05 05 012 01
06 06 011 01
07 07 010 01
08 12 009 01
13 13 016 01
0.3530 0000.0 03.4793 03.4793 0019.5 1
1
23 12
01 02 016 01
03 03 015 01
04 04 014 01
05 05 013 01
06 06 012 01
07 07 011 01
08 08 010 01
09 11 009 01
12 16 008 01
17 21 007 01
22 23 006 01
24 24 016 01
0.3530 0000.0 06.4707 06.4707 0018.5 1
1
06 04
01 04 016 01
05 05 015 01
06 06 014 01
07 07 016 01
0.3530 0000.0 05.3214 05.3214 0014.0 1
1
22 11
01 05 016 01
06 06 015 01
07 07 014 01
08 08 013 01
09 09 012 01
10 10 011 01
11 11 010 01
12 13 009 01
14 19 008 01
20 22 007 01
23 23 016 01
0.3530 0000.0 16.0331 16.0331 0005.5 2
1
01 02
01 01 016 01
02 02 016 01
0.3530 0000.0 06.8318 06.8318 0031.5 2
```

APPENDIX 3.4.12 Sub-Catchment Six Digitised Coordinate Pairs for Flow Net Elements and Segments

Template
(See Appendix 4.1)
First line
XO YO
Other paired lines
X(1) Y(1) Z(1)
X(2) Y(2) Z(2)

270.52	631.30	
743.47	114.70	160.00
745.08	117.35	160.00
738.63	117.65	159.00
739.33	122.03	159.00
733.15	118.67	158.00
732.90	123.78	158.00
730.60	119.10	157.00
730.38	124.78	157.00
728.35	118.38	156.00
727.72	125.95	156.00
725.92	117.83	155.00
724.83	126.90	155.00
723.95	117.08	154.00
722.83	127.80	154.00
719.55	116.08	153.00
720.50	127.72	153.00
716.05	117.55	152.00
719.03	127.65	152.00
714.00	118.10	151.00
717.25	127.72	151.00
712.33	118.47	150.00
715.67	127.60	150.00
710.25	119.17	149.00
712.88	127.15	149.00
708.00	119.28	148.00
709.65	126.45	148.00
705.85	118.88	147.00
706.25	126.30	147.00
703.92	118.95	146.00
703.53	126.03	146.00
702.28	118.70	145.00
701.67	125.95	145.00
699.47	118.25	144.00
699.42	126.03	144.00
697.00	117.58	143.00
697.00	126.25	143.00
694.58	117.28	142.00
695.10	126.72	142.00
691.60	116.88	141.00
691.92	127.72	141.00
687.78	117.00	140.00
688.30	129.67	140.00
684.67	117.90	139.00
685.72	130.75	139.00
683.13	118.05	138.80
678.55	135.72	137.20
739.33	121.88	159.00
742.00	125.80	159.00
733.08	123.80	158.00
738.15	129.65	158.00
730.28	125.00	157.00
735.10	132.65	157.00
727.72	125.90	156.00
732.38	135.88	156.00
724.72	127.17	155.00
729.10	138.78	155.00
722.60	128.13	154.00
723.13	138.65	154.00
720.83	127.72	153.00
721.47	139.42	153.00
718.95	127.95	152.00
719.63	139.95	152.00
717.13	127.60	151.00
717.83	140.70	151.00
715.22	127.67	150.00
715.65	141.08	150.00
712.60	127.08	149.00
713.30	142.20	149.00
709.25	126.42	148.00
711.47	142.85	148.00
706.13	126.42	147.00
709.70	144.03	147.00
703.28	126.03	146.00
708.03	144.95	146.00
701.53	126.10	145.00
705.97	145.08	145.00
699.25	126.17	144.00
703.78	145.60	144.00
696.88	126.50	143.00
699.58	146.13	143.00
694.95	126.85	142.00
694.97	147.38	142.00
691.50	127.67	141.00
692.50	147.90	141.00
688.50	129.13	140.00
690.00	149.15	140.00
685.60	130.75	139.00
687.55	150.00	139.00
683.08	132.58	138.00
684.88	151.10	138.00
678.40	135.65	137.20
676.42	158.47	135.80
725.72	137.20	155.00
727.03	138.33	155.00
722.65	138.90	154.00
723.38	142.63	154.00
721.50	139.17	153.00
721.67	144.13	153.00
719.53	139.78	152.00
720.15	145.38	152.00
717.55	140.40	151.00
719.10	147.03	151.00
715.65	141.13	150.00
717.63	147.95	150.00
713.45	142.03	149.00
715.80	150.10	149.00
711.17	143.00	148.00
712.88	152.35	148.00
709.58	143.78	147.00
710.15	154.00	147.00
707.75	144.53	146.00
707.13	155.38	146.00
705.80	145.13	145.00
705.00	156.20	145.00
703.63	145.75	144.00
703.13	157.42	144.00
699.22	145.92	143.00
701.13	158.10	143.00
694.75	147.22	142.00
699.53	159.17	142.00
692.53	148.17	141.00
697.75	160.80	141.00
689.85	149.13	140.00
695.28	162.47	140.00
687.33	150.03	139.00
692.80	164.30	139.00
684.63	151.05	138.00
689.83	166.50	138.00
682.00	153.90	137.00
686.92	168.95	137.00
677.95	157.05	136.00
683.47	170.72	136.00
676.05	158.45	135.80
673.67	180.25	133.40
727.10	138.10	155.00
728.97	139.28	155.00
723.38	142.78	154.00
725.40	145.10	154.00
721.67	144.10	153.00
723.90	147.70	153.00
720.25	145.47	152.00
722.60	149.70	152.00
718.83	146.90	151.00
721.65	150.75	151.00
717.53	147.88	150.00
721.15	152.00	150.00
715.65	149.80	149.00
718.35	154.97	149.00
712.65	152.67	148.00
715.67	157.72	148.00
710.25	154.10	147.00
713.45	160.38	147.00
707.17	155.47	146.00
711.72	162.17	146.00
704.60	156.53	145.00
710.30	163.55	145.00
703.08	157.30	144.00
708.88	164.83	144.00
701.33	158.33	143.00
707.75	166.05	143.00
699.33	158.85	142.00
706.60	167.60	142.00
697.80	160.53	141.00
704.00	169.47	141.00
695.42	162.00	140.00
701.95	171.60	140.00
692.45	163.95	139.00
699.83	173.85	139.00
689.63	166.47	138.00
697.15	177.15	138.00
686.78	168.83	137.00
693.95	179.40	137.00
683.22	170.95	136.00
690.83	182.45	136.00
680.15	173.95	135.00
687.75	185.47	135.00
676.33	177.90	134.00
684.20	188.72	134.00
673.97	179.90	133.40
668.85	199.72	132.10
741.70	126.05	159.00
744.05	127.55	159.00
738.17	129.78	158.00
741.80	131.83	158.00
735.40	132.40	157.00
739.72	135.17	157.00
732.42	135.67	156.00
737.33	138.38	156.00
729.20	138.70	155.00
735.33	141.95	155.00
725.40	144.90	154.00
733.28	147.72	154.00
723.78	147.75	153.00
730.65	150.92	153.00

722.58	149.55	152.00	729.28	171.55	146.00	695.63	195.80	135.00
729.30	152.85	152.00	740.97	178.20	145.00	693.47	193.85	135.00
721.85	150.88	151.00	728.42	174.20	145.00	691.75	200.05	134.00
728.28	154.33	151.00	740.95	180.22	144.00	689.05	196.72	134.00
721.05	151.83	150.00	727.67	176.40	144.00	684.88	206.63	133.00
726.55	156.90	150.00	740.58	182.47	143.00	682.10	203.75	133.00
718.38	154.85	149.00	726.67	178.28	143.00	683.60	207.47	132.50
723.45	160.03	149.00	740.38	184.03	142.00	656.90	238.22	130.70
715.67	157.58	148.00	726.03	180.45	142.00	690.20	332.38	150.00
720.80	162.72	148.00	740.08	186.00	141.00	687.25	333.78	150.00
713.35	160.13	147.00	725.50	182.63	141.00	688.90	329.38	149.00
719.05	165.15	147.00	739.30	190.08	140.00	685.47	331.80	149.00
711.85	161.63	146.00	724.55	185.65	140.00	687.97	326.40	148.00
717.75	167.00	146.00	739.13	192.72	139.00	684.10	329.35	148.00
710.15	163.40	145.00	722.17	191.38	139.00	687.13	323.72	147.00
716.45	168.20	145.00	738.63	195.35	138.50	682.40	327.22	147.00
708.78	164.58	144.00	714.45	203.90	135.40	686.30	320.17	146.00
714.90	170.08	144.00	748.63	128.92	159.00	680.40	324.67	146.00
707.53	166.28	143.00	743.90	127.42	159.00	685.25	317.20	145.00
713.30	171.35	143.00	747.33	134.20	158.00	678.80	322.80	145.00
706.53	167.35	142.00	741.83	131.53	158.00	684.38	315.17	144.00
712.08	172.47	142.00	746.00	138.28	157.00	677.70	320.70	144.00
704.00	169.63	141.00	739.65	134.83	157.00	683.67	313.17	143.00
710.58	174.38	141.00	744.47	141.50	156.00	676.38	318.75	143.00
702.08	171.47	140.00	737.30	138.22	156.00	682.75	311.28	142.00
708.00	176.92	140.00	742.50	145.58	155.00	675.15	316.85	142.00
699.70	174.05	139.00	735.47	141.83	155.00	682.20	309.88	141.00
705.20	180.60	139.00	739.72	150.88	154.00	674.05	314.97	141.00
696.97	176.55	138.00	733.08	147.40	154.00	681.38	307.80	140.00
702.58	183.45	138.00	737.42	154.88	153.00	672.45	313.55	140.00
693.92	179.38	137.00	730.65	150.83	153.00	680.97	305.42	139.00
699.75	186.67	137.00	735.70	158.08	152.00	670.95	311.58	139.00
690.85	182.13	136.00	729.33	152.40	152.00	680.28	302.45	138.00
697.03	189.58	136.00	734.33	160.78	151.00	666.88	305.53	138.00
687.70	185.08	135.00	728.17	154.45	151.00	679.67	299.67	137.00
693.67	193.60	135.00	733.10	163.15	150.00	665.38	303.70	137.00
683.95	189.00	134.00	726.80	156.50	150.00	678.80	296.22	136.00
688.70	197.17	134.00	731.53	165.15	149.00	664.55	301.15	136.00
676.63	194.50	133.00	723.75	159.63	149.00	676.80	289.22	135.00
681.70	203.67	133.00	730.15	167.97	148.00	663.20	299.40	135.00
668.83	199.97	132.10	721.28	162.25	148.00	674.75	283.90	134.00
657.08	238.17	130.70	729.38	170.92	147.00	661.17	295.92	134.00
752.30	129.88	159.00	718.85	165.22	147.00	673.08	280.80	133.00
748.72	129.03	159.00	729.33	171.72	146.00	658.20	291.90	133.00
750.38	135.72	158.00	717.83	166.55	146.00	669.55	275.20	132.00
747.22	134.42	158.00	728.35	174.55	145.00	655.65	287.03	132.00
749.00	139.70	157.00	716.58	167.75	145.00	657.63	258.70	131.00
746.17	138.30	157.00	727.67	176.58	144.00	649.58	281.25	131.00
747.67	143.25	156.00	715.10	169.40	144.00	650.22	258.33	130.50
744.65	141.60	156.00	726.65	178.42	143.00	642.20	275.33	130.10
746.42	147.22	155.00	713.58	171.08	143.00	690.95	337.50	151.00
742.47	145.47	155.00	726.17	180.55	142.00	683.47	344.53	151.00
744.38	153.78	154.00	712.45	172.33	142.00	687.08	334.08	150.00
739.53	150.60	154.00	725.42	182.95	141.00	681.40	343.15	150.00
743.55	157.08	153.00	710.28	174.33	141.00	685.63	331.70	149.00
737.20	154.95	153.00	724.85	185.85	140.00	678.78	342.05	149.00
743.13	160.00	152.00	708.05	177.05	140.00	684.05	329.55	148.00
735.80	157.65	152.00	722.08	191.67	139.00	677.13	340.58	148.00
742.65	163.30	151.00	705.28	180.30	139.00	682.50	326.97	147.00
734.20	160.33	151.00	720.65	195.10	138.00	675.28	339.05	147.00
742.20	166.08	150.00	702.55	183.20	138.00	680.58	324.88	146.00
732.88	163.13	150.00	718.50	198.10	137.00	673.25	337.22	146.00
741.90	168.63	149.00	699.83	186.35	137.00	678.67	322.33	145.00
731.55	165.33	149.00	716.00	201.40	136.00	670.08	334.78	145.00
741.50	171.50	148.00	699.47	191.20	136.00	677.63	320.65	144.00
730.38	168.00	148.00	714.58	203.97	135.40	667.28	332.67	144.00
741.38	173.63	147.00	684.08	207.58	132.50	676.03	318.95	143.00
729.45	170.47	147.00	699.47	190.95	136.00	664.08	330.38	143.00
741.53	175.65	146.00	697.05	189.70	136.00	675.22	317.08	142.00

662.60	329.45	142.00	635.08	302.90	130.00	652.53	366.53	142.00
674.00	315.35	141.00	629.67	321.17	130.00	655.65	337.65	141.00
661.42	328.25	141.00	629.25	302.40	129.00	648.10	365.58	141.00
672.63	313.30	140.00	626.25	320.03	129.00	653.15	337.33	140.00
660.28	327.13	140.00	624.75	302.20	128.50	646.17	364.78	140.00
670.78	311.67	139.00	614.13	317.85	126.80	651.10	337.78	139.00
658.92	325.60	139.00	667.13	341.30	145.00	644.00	363.92	139.00
666.80	305.47	138.00	666.78	342.58	145.00	648.80	337.78	138.00
657.22	323.90	138.00	664.35	340.05	144.00	642.47	363.47	138.00
665.50	303.70	137.00	663.90	341.17	144.00	646.80	337.92	137.00
655.63	321.78	137.00	661.17	337.92	143.00	640.80	363.22	137.00
664.20	301.20	136.00	660.50	339.70	143.00	643.97	338.40	136.00
653.90	319.40	136.00	658.67	336.47	142.00	638.90	362.20	136.00
663.42	299.30	135.00	657.85	338.58	142.00	640.80	338.97	135.00
650.70	314.17	135.00	656.45	335.13	141.00	637.03	361.55	135.00
661.13	295.75	134.00	655.85	337.40	141.00	637.80	338.97	134.00
647.90	311.42	134.00	655.00	333.88	140.00	634.83	360.10	134.00
658.80	292.00	133.00	653.55	337.58	140.00	633.05	338.67	133.00
645.53	309.47	133.00	653.40	332.70	139.00	626.72	354.70	133.00
655.53	287.17	132.00	651.15	337.75	139.00	630.67	337.42	132.00
642.58	306.45	132.00	651.65	330.65	138.00	624.10	352.63	132.00
649.53	281.20	131.00	648.85	338.03	138.00	628.10	335.08	131.00
638.67	303.67	131.00	648.13	327.22	137.00	621.35	350.40	131.00
642.42	275.70	130.10	646.90	338.08	137.00	625.70	333.22	130.00
624.85	302.13	128.50	645.65	325.50	136.00	619.25	348.35	130.00
686.15	345.60	152.00	644.20	338.42	136.00	622.95	331.90	129.00
684.58	353.33	152.00	643.58	324.25	135.00	616.78	345.60	129.00
683.13	344.47	151.00	640.85	338.85	135.00	619.13	330.60	128.00
680.55	351.40	151.00	641.30	323.55	134.00	614.33	343.88	128.00
681.35	343.40	150.00	638.15	339.05	134.00	614.00	330.35	127.00
677.38	350.42	150.00	638.90	323.28	133.00	611.72	342.67	127.00
678.92	342.40	149.00	633.40	338.88	133.00	606.67	331.53	126.00
674.88	348.75	149.00	636.63	322.38	132.00	606.70	342.03	126.00
677.05	340.92	148.00	630.50	337.42	132.00	602.85	332.38	125.40
672.92	347.67	148.00	633.35	321.38	131.00	597.95	341.35	124.40
675.35	339.35	147.00	627.97	335.28	131.00	683.45	372.40	154.00
671.60	345.95	147.00	629.58	321.10	130.00	675.75	393.28	154.00
673.15	337.65	146.00	625.63	333.22	130.00	677.92	371.05	153.00
669.53	344.78	146.00	626.20	319.97	129.00	672.85	392.78	153.00
670.25	334.78	145.00	623.08	331.78	129.00	675.15	370.55	152.00
666.80	342.65	145.00	620.85	318.35	128.00	670.47	391.85	152.00
667.13	333.03	144.00	618.88	330.67	128.00	671.65	369.58	151.00
664.35	339.75	144.00	615.30	317.92	127.00	667.67	390.90	151.00
663.85	330.65	143.00	614.05	330.25	127.00	668.85	368.80	150.00
660.97	338.03	143.00	613.88	317.53	126.80	664.65	388.90	150.00
662.60	329.55	142.00	603.42	332.05	125.40	666.47	368.58	149.00
658.63	336.58	142.00	688.30	357.60	153.00	661.17	386.10	149.00
661.33	328.10	141.00	677.75	371.35	153.00	665.05	368.30	148.00
656.53	335.30	141.00	684.45	352.78	152.00	658.47	384.55	148.00
660.08	327.05	140.00	675.20	370.58	152.00	663.42	367.97	147.00
654.90	334.05	140.00	680.38	351.28	151.00	656.90	384.15	147.00
658.90	325.70	139.00	671.75	369.88	151.00	661.80	367.80	146.00
653.47	332.63	139.00	677.55	349.88	150.00	655.30	383.70	146.00
657.35	324.15	138.00	669.15	368.80	150.00	660.25	367.30	145.00
651.75	330.95	138.00	674.75	348.70	149.00	654.03	382.88	145.00
655.72	322.08	137.00	666.63	368.53	149.00	658.67	367.13	144.00
647.92	327.40	137.00	672.83	347.00	148.00	652.25	382.28	144.00
653.97	319.53	136.00	665.15	368.42	148.00	656.30	367.25	143.00
645.83	325.47	136.00	671.33	345.70	147.00	650.75	381.75	143.00
650.55	314.05	135.00	663.45	367.95	147.00	652.45	366.72	142.00
643.58	324.45	135.00	669.63	344.45	146.00	649.05	381.05	142.00
647.92	311.70	134.00	662.00	367.50	146.00	647.90	365.45	141.00
641.50	323.95	134.00	666.80	342.95	145.00	645.47	379.97	141.00
645.90	309.47	133.00	660.25	367.50	145.00	646.03	364.90	140.00
638.90	323.22	133.00	663.72	341.22	144.00	641.92	378.47	140.00
642.67	306.90	132.00	658.70	367.30	144.00	643.83	364.05	139.00
636.90	322.75	132.00	660.53	339.78	143.00	638.92	375.95	139.00
638.75	303.97	131.00	656.65	367.10	143.00	642.25	363.58	138.00
633.35	321.85	131.00	657.75	338.22	142.00	636.78	373.90	138.00

640.45	363.13	137.00	621.35	391.60	135.00	618.65	390.10	134.00
635.38	372.08	137.00	629.92	368.17	134.00	612.90	402.95	134.00
638.78	362.25	136.00	618.50	389.92	134.00	615.22	388.10	133.00
633.70	371.03	136.00	626.05	367.15	133.00	610.58	401.70	133.00
636.83	361.35	135.00	615.33	388.20	133.00	610.90	386.05	132.00
632.22	369.88	135.00	617.08	364.28	132.00	607.42	400.33	132.00
634.42	360.17	134.00	610.47	385.83	132.00	607.28	384.55	131.00
630.05	368.35	134.00	615.22	363.17	131.00	603.33	398.53	131.00
626.58	354.88	133.00	607.08	384.35	131.00	604.47	383.05	130.00
626.15	367.17	133.00	613.17	362.47	130.00	599.72	397.58	130.00
623.72	352.55	132.00	604.30	382.63	130.00	602.53	381.58	129.00
617.42	364.47	132.00	610.75	360.88	129.00	596.65	395.88	129.00
621.17	350.47	131.00	602.47	381.58	129.00	600.47	379.92	128.00
615.28	363.17	131.00	608.67	359.13	128.00	594.75	394.75	128.00
619.00	348.10	130.00	600.40	380.22	128.00	597.55	377.88	127.00
613.53	362.08	130.00	606.53	357.97	127.00	593.00	393.58	127.00
616.30	345.50	129.00	597.63	377.75	127.00	595.25	376.10	126.00
610.95	360.47	129.00	603.50	356.50	126.00	590.85	392.40	126.00
613.83	343.50	128.00	595.10	376.20	126.00	593.05	374.85	125.00
609.03	359.38	128.00	598.30	355.28	125.00	588.28	391.00	125.00
611.58	342.70	127.00	593.03	374.75	125.00	589.13	372.63	124.00
606.67	358.22	127.00	593.80	354.90	124.00	584.97	390.00	124.00
606.67	342.20	126.00	589.35	372.47	124.00	584.67	372.35	123.00
603.47	356.50	126.00	590.90	355.08	123.60	580.53	389.03	123.00
601.20	341.83	125.00	582.55	371.80	122.60	582.67	371.88	122.60
598.45	355.30	125.00	665.88	423.85	156.00	572.72	388.22	121.90
597.75	341.38	124.40	661.10	426.78	156.00	661.08	426.63	156.00
591.15	355.25	123.60	664.28	420.47	155.00	660.45	429.75	156.00
678.88	393.90	155.00	656.88	425.38	155.00	656.92	425.78	155.00
664.28	420.65	155.00	663.15	417.72	154.00	656.20	428.97	155.00
675.30	393.05	154.00	654.78	424.92	154.00	654.75	425.03	154.00
662.95	417.55	154.00	660.33	414.03	153.00	652.95	428.33	154.00
672.70	392.55	153.00	652.63	424.13	153.00	652.88	424.30	153.00
660.10	414.20	153.00	658.00	412.17	152.00	650.92	427.33	153.00
670.15	391.72	152.00	651.05	423.08	152.00	650.95	423.40	152.00
658.13	412.35	152.00	656.20	410.97	151.00	649.22	425.95	152.00
667.38	390.63	151.00	649.55	422.05	151.00	649.38	422.15	151.00
656.05	411.13	151.00	654.70	409.97	150.00	647.50	425.05	151.00
664.50	388.78	150.00	647.78	420.92	150.00	647.83	421.05	150.00
654.47	410.15	150.00	652.35	408.10	149.00	645.67	424.03	150.00
660.88	385.80	149.00	645.80	419.80	149.00	645.83	419.72	149.00
652.17	407.95	149.00	649.50	406.15	148.00	643.78	422.55	149.00
657.97	384.70	148.00	643.42	418.47	148.00	643.45	418.53	148.00
649.38	406.15	148.00	647.00	404.63	147.00	641.47	421.10	148.00
656.78	384.05	147.00	640.80	416.95	147.00	640.60	417.35	147.00
646.85	405.10	147.00	645.80	404.28	146.00	638.90	419.65	147.00
655.50	383.40	146.00	638.67	415.88	146.00	638.53	416.20	146.00
645.63	404.38	146.00	644.13	403.58	145.00	637.15	419.45	146.00
653.95	382.65	145.00	637.25	414.80	145.00	637.25	414.85	145.00
644.20	403.72	145.00	642.25	403.05	144.00	635.53	419.05	145.00
652.33	382.03	144.00	635.97	413.95	144.00	636.15	413.78	144.00
642.25	403.50	144.00	640.30	402.67	143.00	633.40	419.03	144.00
650.70	381.97	143.00	634.72	412.72	143.00	634.60	412.95	143.00
640.30	402.65	143.00	638.22	402.03	142.00	631.88	419.00	143.00
649.00	380.92	142.00	633.47	411.70	142.00	633.42	411.90	142.00
638.33	401.90	142.00	636.53	401.58	141.00	630.30	418.70	142.00
645.30	379.92	141.00	631.63	410.80	141.00	631.55	410.70	141.00
636.15	401.55	141.00	633.42	400.38	140.00	629.08	418.55	141.00
641.88	378.72	140.00	630.20	410.13	140.00	630.00	409.92	140.00
633.47	400.20	140.00	629.05	397.75	139.00	627.30	418.28	140.00
639.22	376.35	139.00	626.75	409.40	139.00	626.58	409.38	139.00
629.00	397.90	139.00	626.72	396.15	138.00	624.45	417.58	139.00
636.90	374.15	138.00	623.00	408.38	138.00	622.95	408.40	138.00
626.78	396.28	138.00	624.92	394.58	137.00	620.95	416.78	138.00
635.45	372.45	137.00	619.70	407.22	137.00	619.60	407.13	137.00
624.92	394.90	137.00	623.17	393.58	136.00	617.75	416.10	137.00
633.83	371.08	136.00	617.05	406.13	136.00	617.17	405.92	136.00
623.25	393.55	136.00	621.50	391.72	135.00	614.95	416.15	136.00
632.00	369.85	135.00	615.15	404.58	135.00	614.78	404.67	135.00

612.17	415.22	135.00	617.33	416.10	137.00	621.45	444.08	141.00
613.00	403.25	134.00	617.22	434.55	137.00	621.63	435.78	140.00
609.50	414.95	134.00	614.80	416.17	136.00	619.70	443.95	140.00
610.58	401.50	133.00	612.85	434.38	136.00	620.03	435.40	139.00
606.38	414.10	133.00	612.00	415.50	135.00	617.75	443.92	139.00
607.75	400.17	132.00	608.70	434.88	135.00	619.05	435.25	138.00
604.53	413.65	132.00	609.25	415.08	134.00	615.65	443.13	138.00
603.65	398.38	131.00	605.20	434.80	134.00	617.08	434.80	137.00
600.72	413.95	131.00	606.40	414.25	133.00	613.70	442.28	137.00
599.75	397.50	130.00	601.97	434.38	133.00	612.65	434.58	136.00
597.85	413.72	130.00	604.22	413.65	132.00	610.92	441.90	136.00
596.53	395.72	129.00	599.30	433.63	132.00	608.53	434.78	135.00
593.50	413.67	129.00	600.80	413.72	131.00	608.53	441.55	135.00
594.78	394.53	128.00	596.30	432.90	131.00	605.22	434.88	134.00
589.92	411.78	128.00	597.95	413.70	130.00	604.65	440.88	134.00
593.05	393.90	127.00	593.33	432.15	130.00	601.63	434.40	133.00
587.13	410.65	127.00	593.63	413.50	129.00	601.33	440.38	133.00
590.75	392.58	126.00	590.20	431.50	129.00	599.22	433.75	132.00
585.08	409.63	126.00	589.85	411.70	128.00	597.50	439.92	132.00
588.25	391.15	125.00	586.15	431.22	128.00	596.30	432.42	131.00
582.47	408.63	125.00	587.58	410.45	127.00	594.88	440.15	131.00
584.80	389.65	124.00	581.38	430.38	127.00	593.38	432.42	130.00
579.90	407.45	124.00	585.15	409.60	126.00	592.60	439.72	130.00
580.40	389.35	123.00	578.50	429.60	126.00	589.85	431.67	129.00
576.85	406.67	123.00	582.50	408.47	125.00	589.97	439.88	129.00
574.42	388.88	122.00	575.78	428.72	125.00	586.05	431.20	128.00
571.42	406.47	122.00	580.00	407.47	124.00	586.17	441.00	128.00
572.35	388.40	121.90	572.70	427.75	124.00	581.63	430.45	127.00
563.80	406.80	120.90	577.00	406.53	123.00	581.25	442.55	127.00
666.72	431.88	157.00	570.10	426.63	123.00	578.38	429.45	126.00
661.17	443.42	157.00	571.45	406.67	122.00	578.03	443.47	126.00
660.45	429.40	156.00	566.25	425.60	122.00	575.72	428.65	125.00
657.22	442.30	156.00	565.55	406.72	121.00	571.95	444.70	125.00
655.92	429.15	155.00	562.17	425.05	121.00	572.53	427.75	124.00
651.92	440.55	155.00	563.83	406.60	120.90	567.92	444.42	124.00
652.92	428.53	154.00	556.67	424.25	119.80	569.83	426.78	123.00
648.78	438.83	154.00	660.97	443.45	157.00	564.85	443.30	123.00
650.90	427.20	153.00	660.20	445.38	157.00	566.03	425.33	122.00
646.17	438.15	153.00	657.17	442.58	156.00	562.05	442.45	122.00
649.15	426.05	152.00	656.65	444.30	156.00	562.05	424.88	121.00
644.90	437.63	152.00	652.08	440.42	155.00	559.05	441.60	121.00
647.30	424.97	151.00	650.85	444.50	155.00	557.90	424.58	120.00
643.35	437.38	151.00	648.58	438.92	154.00	555.80	440.65	120.00
645.70	423.95	150.00	648.08	442.75	154.00	556.58	424.28	119.80
641.58	437.10	150.00	645.97	438.00	153.00	545.65	439.50	117.90
643.95	422.55	149.00	645.22	443.08	153.00	650.85	444.50	156.00
639.97	436.85	149.00	644.47	437.60	152.00	650.92	444.70	156.00
641.45	421.17	148.00	643.45	442.85	152.00	648.08	442.75	155.00
638.08	436.50	148.00	643.17	437.58	151.00	647.63	445.22	155.00
638.65	419.53	147.00	641.53	442.45	151.00	645.22	443.08	154.00
635.42	436.42	147.00	641.58	437.15	150.00	645.08	445.83	154.00
637.08	419.53	146.00	639.97	442.10	150.00	643.45	442.85	153.00
632.33	436.47	146.00	639.65	436.80	149.00	642.58	446.67	153.00
635.45	419.28	145.00	638.35	441.88	149.00	641.53	442.45	152.00
628.75	436.83	145.00	637.95	436.30	148.00	640.35	446.42	152.00
633.47	419.13	144.00	636.35	441.80	148.00	639.97	442.10	151.00
627.28	436.72	144.00	635.33	436.50	147.00	638.75	446.85	151.00
631.80	418.85	143.00	634.15	441.63	147.00	638.35	441.88	150.00
625.42	436.60	143.00	631.90	436.63	146.00	637.03	447.20	150.00
630.40	418.67	142.00	631.50	441.80	146.00	636.35	441.80	149.00
623.90	436.60	142.00	628.65	436.70	145.00	634.92	447.72	149.00
629.05	418.22	141.00	629.70	442.50	145.00	634.15	441.63	148.00
622.67	436.03	141.00	627.15	436.95	144.00	633.67	447.97	148.00
627.47	418.05	140.00	627.63	442.78	144.00	631.50	441.48	147.00
621.47	436.03	140.00	625.50	436.75	143.00	632.65	448.30	147.00
624.15	417.42	139.00	626.13	443.17	143.00	629.70	442.50	146.00
620.45	435.67	139.00	624.05	436.33	142.00	631.28	448.53	146.00
620.95	416.67	138.00	623.83	443.88	142.00	627.63	442.78	145.00
618.97	435.38	138.00	622.65	436.28	141.00	629.78	448.97	145.00

626.13	443.17	144.00	637.65	470.67	150.00	648.83	465.20	152.00
627.15	450.95	144.00	633.67	447.97	149.00	650.22	468.78	152.00
623.83	443.88	143.00	636.55	471.08	149.00	645.30	467.22	151.00
624.90	451.67	143.00	632.65	448.30	148.00	646.20	471.35	151.00
621.45	444.08	142.00	632.95	473.40	148.00	642.28	468.10	150.00
621.77	452.40	142.00	631.28	448.53	147.00	643.63	472.10	150.00
617.90	443.95	141.00	628.45	475.03	147.00	639.78	469.58	149.00
618.00	452.97	141.00	629.78	448.97	146.00	641.50	473.13	149.00
617.75	443.92	140.00	626.75	475.42	146.00	637.63	470.55	148.00
616.47	453.22	140.00	627.15	450.95	145.00	639.53	474.10	148.00
615.65	443.13	139.00	625.13	475.33	145.00	636.42	471.55	147.00
614.30	453.45	139.00	624.90	451.67	144.00	637.72	474.85	147.00
613.70	442.28	138.00	623.67	475.38	144.00	633.05	473.40	146.00
613.08	453.97	138.00	621.17	452.40	143.00	633.83	476.33	146.00
610.92	441.90	137.00	622.30	475.28	143.00	628.33	474.63	145.00
611.17	453.92	137.00	618.00	452.97	142.00	628.65	478.40	145.00
608.53	441.55	136.00	620.45	475.13	142.00	626.60	475.42	144.00
609.55	454.42	136.00	616.47	453.22	141.00	626.85	478.40	144.00
604.65	440.88	135.00	619.05	475.05	141.00	625.03	475.13	143.00
606.65	454.75	135.00	614.30	453.45	140.00	625.15	478.72	143.00
601.33	440.38	134.00	616.65	475.30	140.00	623.55	475.33	142.00
602.28	456.58	134.00	613.08	453.97	139.00	623.58	478.80	142.00
597.50	439.92	133.00	613.05	474.78	139.00	622.03	475.17	141.00
599.58	456.85	133.00	611.17	453.92	138.00	621.92	479.53	141.00
594.88	440.15	132.00	610.03	475.83	138.00	620.63	475.15	140.00
595.45	458.10	132.00	609.55	454.42	137.00	620.42	479.30	140.00
592.60	439.72	131.00	607.35	476.85	137.00	618.85	475.13	139.00
591.80	458.78	131.00	606.65	454.75	136.00	618.97	479.22	139.00
589.97	439.88	130.00	604.55	477.95	136.00	616.60	475.00	138.00
586.90	458.10	130.00	602.28	456.58	135.00	616.80	479.35	138.00
586.17	441.00	129.00	601.70	478.47	135.00	612.95	475.33	137.00
584.05	457.92	129.00	599.58	456.85	134.00	613.65	480.10	137.00
581.25	442.55	128.00	599.05	478.38	134.00	609.70	475.85	136.00
580.45	457.92	128.00	595.45	458.10	133.00	611.13	481.15	136.00
578.03	443.47	127.00	595.53	477.55	133.00	607.25	476.95	135.00
577.70	458.35	127.00	591.80	458.78	132.00	609.40	481.90	135.00
571.95	444.70	126.00	591.65	477.03	132.00	604.50	477.85	134.00
571.85	458.50	126.00	586.90	458.10	131.00	607.03	482.92	134.00
567.92	444.42	125.00	588.13	477.55	131.00	601.80	478.95	133.00
566.67	459.38	125.00	584.05	457.92	130.00	602.42	484.17	133.00
564.85	443.30	124.00	582.65	478.70	130.00	599.22	478.47	132.00
562.20	459.33	124.00	580.45	457.92	129.00	597.50	483.95	132.00
562.05	442.45	123.00	577.22	478.90	129.00	595.75	477.92	131.00
558.85	458.03	123.00	577.70	458.35	128.00	594.33	484.05	131.00
559.05	441.60	122.00	573.58	479.08	128.00	591.70	477.08	130.00
555.70	456.90	122.00	571.85	458.50	127.00	591.58	483.83	130.00
556.80	440.25	121.00	569.75	478.67	127.00	587.95	477.50	129.00
552.33	456.25	121.00	566.67	459.38	126.00	587.97	483.60	129.00
554.50	439.78	120.00	565.47	478.13	126.00	582.78	478.25	128.00
548.30	454.78	120.00	562.20	459.33	125.00	582.78	484.45	128.00
545.65	439.50	117.90	560.35	477.10	125.00	577.50	478.33	127.00
533.60	456.20	116.10	558.85	458.03	124.00	578.70	485.15	127.00
656.25	444.42	158.00	555.65	476.53	124.00	573.83	479.38	126.00
659.38	450.78	158.00	555.70	456.90	123.00	574.88	486.13	126.00
650.92	444.70	157.00	551.65	476.00	123.00	569.63	478.78	125.00
656.35	455.15	157.00	552.33	456.25	122.00	569.05	486.30	125.00
647.63	445.22	156.00	547.95	475.53	122.00	565.08	477.83	124.00
655.13	459.67	156.00	548.30	454.78	121.00	565.13	486.00	124.00
645.08	445.83	155.00	543.92	474.80	121.00	559.75	477.05	123.00
652.72	461.95	155.00	544.25	454.92	120.00	560.72	485.95	123.00
642.58	446.67	154.00	540.17	474.25	120.00	555.78	476.47	122.00
648.50	465.25	154.00	538.53	455.25	119.00	555.63	486.20	122.00
640.35	446.42	153.00	535.45	473.65	119.00	551.58	475.88	121.00
645.22	467.42	153.00	533.60	456.20	116.10	550.28	485.85	121.00
638.75	446.85	152.00	522.08	472.65	115.10	547.92	475.47	120.00
642.42	468.00	152.00	655.15	459.75	154.00	545.97	485.83	120.00
637.03	447.20	151.00	656.10	462.50	154.00	543.72	475.00	119.00
639.45	469.75	151.00	652.55	461.97	153.00	542.15	485.50	119.00
634.92	447.72	150.00	653.83	464.70	153.00	540.47	473.88	118.00

538.83	485.80	118.00	555.58	486.22	122.00	584.88	525.70	128.00
535.17	473.42	117.00	553.65	509.08	122.00	580.70	505.08	127.00
533.67	485.60	117.00	549.78	485.80	121.00	580.22	526.10	127.00
529.08	472.80	116.00	549.85	508.30	121.00	576.60	505.40	126.00
528.92	485.92	116.00	545.83	485.78	120.00	575.55	526.75	126.00
522.03	472.42	115.10	545.75	507.02	120.00	571.13	507.25	125.00
512.20	490.48	113.20	541.53	485.50	119.00	571.30	526.75	125.00
653.72	464.88	153.00	540.47	506.17	119.00	565.33	508.52	124.00
654.63	466.45	153.00	538.55	485.70	118.00	566.30	527.03	124.00
650.10	468.60	152.00	537.20	505.95	118.00	558.58	509.27	123.00
651.38	471.60	152.00	533.63	485.92	117.00	561.10	528.50	123.00
646.03	471.10	151.00	533.80	505.08	117.00	553.67	509.17	122.00
646.95	473.97	151.00	528.90	485.53	116.00	552.15	529.67	122.00
643.70	472.13	150.00	530.38	504.85	116.00	549.88	508.20	121.00
644.78	475.05	150.00	522.33	487.30	115.00	546.50	529.30	121.00
641.22	473.10	149.00	524.75	504.33	115.00	545.60	507.10	120.00
642.83	476.22	149.00	516.63	488.60	114.00	542.65	528.67	120.00
639.28	474.08	148.00	520.22	504.00	114.00	540.65	505.92	119.00
640.45	477.22	148.00	512.38	490.83	113.20	538.72	527.48	119.00
637.70	474.90	147.00	503.50	507.98	111.90	537.05	505.48	118.00
638.80	478.30	147.00	651.45	471.42	152.00	535.08	526.30	118.00
633.50	476.38	146.00	652.60	473.13	152.00	533.38	505.23	117.00
635.63	480.38	146.00	646.83	474.33	151.00	531.47	525.55	117.00
628.83	478.15	145.00	651.08	478.55	151.00	530.45	505.02	116.00
631.72	484.00	145.00	644.75	475.20	150.00	526.92	525.05	116.00
626.75	478.30	144.00	649.85	482.50	150.00	524.58	504.20	115.00
629.53	485.53	144.00	642.78	476.22	149.00	523.72	524.17	115.00
625.08	478.78	143.00	648.55	485.95	149.00	520.03	504.27	114.00
628.03	487.55	143.00	640.65	477.33	148.00	519.80	523.95	114.00
623.53	479.10	142.00	646.22	488.13	148.00	512.58	505.60	113.00
626.58	489.13	142.00	639.17	478.13	147.00	513.50	522.90	113.00
621.60	479.08	141.00	643.80	490.52	147.00	503.55	507.98	111.90
625.70	490.10	141.00	635.85	480.50	146.00	494.45	525.92	110.70
620.25	479.40	140.00	642.28	491.58	146.00	614.95	511.85	134.00
624.33	492.42	140.00	631.95	483.83	145.00	615.92	512.73	134.00
618.78	479.90	139.00	640.97	492.88	145.00	612.17	513.83	133.00
620.80	494.25	139.00	629.83	485.85	144.00	613.10	515.17	133.00
616.55	479.80	138.00	638.75	494.92	144.00	609.00	515.88	132.00
617.90	495.70	138.00	627.90	487.85	143.00	609.80	517.67	132.00
613.65	480.08	137.00	636.58	496.38	143.00	604.08	518.95	131.00
615.03	496.13	137.00	626.10	489.17	142.00	605.97	521.05	131.00
611.03	481.55	136.00	634.50	497.83	142.00	597.85	521.42	130.00
612.72	497.75	136.00	625.33	490.23	141.00	600.80	525.80	130.00
609.42	481.88	135.00	633.03	498.95	141.00	590.53	524.83	129.00
610.63	498.40	135.00	624.03	492.13	140.00	593.88	529.38	129.00
606.97	483.00	134.00	631.05	500.42	140.00	584.60	526.10	128.00
607.42	500.08	134.00	620.65	494.50	139.00	589.35	532.78	128.00
602.25	484.35	133.00	627.38	503.30	139.00	579.88	526.38	127.00
604.88	501.42	133.00	617.55	495.77	138.00	582.05	532.90	127.00
597.28	484.05	132.00	624.65	505.38	138.00	575.22	526.65	126.00
601.58	502.83	132.00	615.15	496.42	137.00	577.08	534.45	126.00
594.40	483.60	131.00	622.47	507.38	137.00	571.22	526.73	125.00
598.40	503.85	131.00	612.53	497.80	136.00	572.03	535.40	125.00
591.38	483.53	130.00	620.30	509.27	136.00	566.17	526.83	124.00
593.03	504.75	130.00	610.13	498.95	135.00	566.95	536.55	124.00
588.00	483.47	129.00	618.28	510.98	135.00	560.65	528.53	123.00
587.85	504.58	129.00	607.30	500.15	134.00	561.35	537.88	123.00
583.08	484.20	128.00	616.28	513.38	134.00	552.25	529.70	122.00
584.30	504.48	128.00	604.60	501.58	133.00	555.40	539.35	122.00
578.20	485.65	127.00	612.58	513.90	133.00	546.58	529.55	121.00
580.88	504.75	127.00	600.95	502.83	132.00	548.78	540.67	121.00
574.60	485.65	126.00	609.08	516.33	132.00	542.60	528.65	120.00
576.70	505.20	126.00	598.78	503.88	131.00	541.97	541.55	120.00
569.03	485.88	125.00	604.25	519.35	131.00	538.38	527.60	119.00
571.30	507.40	125.00	592.95	504.52	130.00	537.67	541.25	119.00
564.60	486.15	124.00	598.08	521.88	130.00	535.13	526.48	118.00
565.42	508.20	124.00	587.90	504.70	129.00	534.17	541.23	118.00
561.00	485.95	123.00	590.72	524.60	129.00	531.15	525.78	117.00
558.45	509.05	123.00	584.30	504.88	128.00	530.92	540.83	117.00

527.08	525.23	116.00	551.20	549.10	121.00	536.95	557.63	118.00
526.75	541.17	116.00	542.95	548.38	120.00	538.75	561.50	118.00
523.63	524.45	115.00	545.47	552.75	120.00	531.00	559.60	117.00
522.45	540.98	115.00	537.58	549.78	119.00	532.05	564.38	117.00
519.53	523.67	114.00	541.17	555.45	119.00	526.55	560.48	116.00
517.38	542.48	114.00	533.40	550.70	118.00	527.72	565.95	116.00
513.70	522.78	113.00	537.08	557.45	118.00	523.10	561.30	115.00
512.13	542.70	113.00	529.88	551.10	117.00	523.65	565.65	115.00
505.63	524.35	112.00	531.13	559.65	117.00	519.17	561.95	114.00
506.90	543.10	112.00	525.65	551.73	116.00	519.83	567.33	114.00
496.92	525.33	111.00	526.67	560.80	116.00	514.45	563.85	113.00
499.45	542.98	111.00	522.88	551.60	115.00	515.08	568.80	113.00
494.23	525.95	110.70	522.95	561.53	115.00	509.15	565.73	112.00
485.05	544.42	109.50	519.05	551.92	114.00	510.83	570.42	112.00
586.75	530.88	128.00	519.58	560.17	114.00	503.42	568.13	111.00
587.85	531.83	128.00	512.85	553.15	113.00	505.58	573.53	111.00
582.58	532.80	127.00	514.20	560.90	113.00	497.42	570.67	110.00
583.60	534.38	127.00	506.38	554.10	112.00	499.65	576.58	110.00
577.13	534.38	126.00	508.05	562.55	112.00	490.10	574.58	109.00
578.13	537.28	126.00	500.73	555.20	111.00	493.10	580.55	109.00
572.15	535.92	125.00	502.02	563.92	111.00	481.85	579.23	108.00
572.55	539.25	125.00	492.52	556.90	110.00	486.60	584.42	108.00
566.83	536.65	124.00	495.30	566.05	110.00	472.80	586.08	107.00
567.17	540.58	124.00	483.40	560.05	109.00	478.30	590.95	107.00
561.03	537.67	123.00	487.50	569.30	109.00	463.52	593.60	106.00
561.67	542.00	123.00	475.98	562.80	108.10	468.98	599.48	106.00
554.92	539.17	122.00	468.33	578.48	106.90	461.55	596.00	105.70
556.30	543.70	122.00	522.65	559.50	115.00	454.30	614.88	104.60
548.50	540.80	121.00	522.85	561.48	115.00	527.35	564.60	116.00
549.72	546.13	121.00	519.47	559.88	114.00	527.78	565.75	116.00
542.08	541.75	120.00	519.38	562.30	114.00	523.42	566.00	115.00
543.33	548.55	120.00	513.92	560.80	113.00	523.90	567.55	115.00
537.40	541.48	119.00	514.38	564.00	113.00	519.80	566.88	114.00
537.78	549.45	119.00	507.95	562.42	112.00	520.42	569.35	114.00
534.03	541.15	118.00	509.13	566.28	112.00	515.40	568.60	113.00
533.60	550.50	118.00	502.13	563.65	111.00	516.85	571.20	113.00
530.72	541.10	117.00	503.52	568.42	111.00	510.90	571.05	112.00
530.05	550.90	117.00	495.02	566.10	110.00	512.13	573.80	112.00
527.08	540.67	116.00	497.08	570.85	110.00	505.45	573.88	111.00
525.88	551.48	116.00	487.13	569.23	109.00	507.25	576.45	111.00
522.40	541.08	115.00	490.10	574.80	109.00	499.65	576.78	110.00
523.17	551.70	115.00	478.80	573.50	108.00	501.60	580.20	110.00
517.72	542.15	114.00	482.17	579.65	108.00	492.77	580.92	109.00
518.95	552.30	114.00	468.00	578.90	106.90	495.48	584.58	109.00
512.30	543.23	113.00	461.65	595.88	105.70	486.58	584.78	108.00
512.92	553.53	113.00	599.45	524.08	130.00	489.85	589.30	108.00
506.75	543.10	112.00	600.75	525.28	130.00	477.92	591.03	107.00
506.85	554.17	112.00	593.60	529.17	129.00	482.13	595.48	107.00
499.35	542.88	111.00	595.80	530.30	129.00	469.08	599.15	106.00
500.45	555.53	111.00	589.15	532.95	128.00	474.38	604.35	106.00
490.15	543.95	110.00	592.03	535.23	128.00	457.90	610.63	105.00
492.50	556.92	110.00	584.55	536.42	127.00	463.73	614.63	105.00
485.27	544.55	109.50	588.13	540.30	127.00	454.60	615.10	104.60
476.33	562.48	108.10	579.80	539.00	126.00	448.15	633.80	103.40
587.80	531.67	128.00	584.60	543.98	126.00	583.55	542.95	126.00
589.03	532.95	128.00	574.50	542.30	125.00	584.85	543.88	126.00
583.25	534.30	127.00	578.08	547.40	125.00	577.90	547.63	125.00
584.38	536.20	127.00	568.47	544.58	124.00	579.53	549.65	125.00
578.08	537.17	126.00	572.15	551.55	124.00	572.17	551.75	124.00
579.65	539.25	126.00	563.08	546.20	123.00	574.97	554.83	124.00
572.72	539.00	125.00	566.25	554.33	123.00	566.00	554.25	123.00
574.53	541.98	125.00	557.28	547.63	122.00	569.83	560.45	123.00
567.28	540.42	124.00	559.05	556.15	122.00	558.97	556.23	122.00
568.30	544.70	124.00	551.08	549.53	121.00	565.88	566.83	122.00
561.75	541.85	123.00	554.17	557.23	121.00	553.97	557.30	121.00
562.67	546.65	123.00	545.15	552.90	120.00	558.95	571.03	121.00
556.22	543.73	122.00	548.75	558.70	120.00	548.85	559.08	120.00
557.00	547.85	122.00	541.08	555.23	119.00	555.22	575.70	120.00
550.05	546.28	121.00	543.42	560.28	119.00	543.85	559.92	119.00

552.20	579.98	119.00	531.95	607.83	111.00
538.38	561.55	118.00	537.00	611.80	111.00
550.45	582.88	118.00	528.53	612.50	110.00
532.15	563.80	117.00	533.58	617.08	110.00
548.88	585.35	117.00	523.38	616.63	109.00
528.00	565.80	116.00	528.72	621.83	109.00
546.53	588.58	116.00	518.42	621.50	108.00
523.90	567.58	115.00	523.05	626.98	108.00
543.85	592.63	115.00	510.98	627.48	107.00
520.42	569.48	114.00	514.72	633.50	107.00
541.25	595.53	114.00	500.33	635.83	106.00
516.95	571.20	113.00	503.90	641.45	106.00
538.63	599.25	113.00	487.60	642.50	105.00
511.88	573.53	112.00	491.38	648.73	105.00
535.70	602.88	112.00	472.17	647.55	104.00
506.92	576.33	111.00	473.90	656.53	104.00
532.00	607.63	111.00	452.58	653.95	103.00
501.58	580.13	110.00	456.20	661.80	103.00
528.40	612.48	110.00	436.85	660.55	102.00
495.42	584.73	109.00	441.48	668.85	102.00
523.88	616.42	109.00	413.95	669.83	101.00
489.90	589.00	108.00	418.95	681.60	101.00
518.70	621.40	108.00	406.67	672.30	100.80
482.20	595.73	107.00	395.80	689.98	100.20
511.05	628.08	107.00	418.17	679.67	101.00
474.17	604.45	106.00	418.63	681.00	101.00
498.90	634.03	106.00	395.77	689.88	100.20
463.67	614.85	105.00	385.20	707.63	99.40
486.55	639.35	105.00			
455.10	627.83	104.00			
470.58	644.83	104.00			
448.55	633.92	103.40			
442.60	653.10	102.30			
509.83	626.78	107.00			
510.92	628.40	107.00			
499.15	633.53	106.00			
500.10	635.98	106.00			
486.33	638.98	105.00			
487.80	642.60	105.00			
470.60	644.83	104.00			
472.10	648.08	104.00			
451.98	651.85	103.00			
452.98	654.03	103.00			
432.95	653.03	102.00			
436.65	660.70	102.00			
420.63	652.33	101.60			
406.98	672.05	100.80			
564.75	565.90	122.00			
566.05	567.45	122.00			
558.90	570.92	121.00			
561.05	572.95	121.00			
554.85	575.58	120.00			
557.92	579.45	120.00			
551.97	580.17	119.00			
556.35	582.08	119.00			
550.40	583.03	118.00			
554.50	585.05	118.00			
548.65	585.35	117.00			
552.67	588.20	117.00			
546.25	588.73	116.00			
550.42	592.10	116.00			
543.72	592.53	115.00			
548.00	595.85	115.00			
541.35	595.92	114.00			
545.60	599.58	114.00			
538.33	599.17	113.00			
543.28	602.98	113.00			
535.83	602.78	112.00			
540.50	606.80	112.00			

APPENDIX 3.4.13 Sub-Catchment Seven Discretised Flow-Net Structure and Channel Data

```
Template
(See Appendix 4.1)
NSUB K33 K44
NCHA
NSEG
NCAS
NELM
MCELF MCELT MSAM MHYE
....  ..... .... ....
MCELF MCELT MSAM MHYE
EC CWID EANG WANG CTOP IOFLOW


02 1 1
01
05
1
23 11
01 06 016 01
07 07 015 01
08 08 014 01
09 09 013 01
10 10 012 01
11 11 011 01
12 12 010 01
13 14 009 01
15 20 008 01
21 23 007 01
24 24 016 01
0.0490 0000.0 03.5026 03.5026 0028.5 1
1
17 10
01 06 016 01
07 07 015 01
08 08 014 01
09 09 013 01
10 10 012 01
11 11 011 01
12 12 010 01
13 14 009 01
15 17 008 01
18 18 016 01
0.0490 0000.0 04.9682 04.9682 0021.0 1
1
50 17
01 06 016 01
07 07 015 01
08 08 014 01
09 09 013 01
10 10 012 01
11 11 011 01
12 12 010 01
13 14 009 01
15 20 007 01
21 25 007 01
26 29 006 01
30 33 005 01
34 37 004 01
38 43 003 01
44 48 002 01
49 50 001 01
51 51 016 01
0.0490 0000.0 04.3056 04.3056 0024.0 1
1
08 03
01 07 016 01
08 08 015 01
09 09 016 01
0.0490 0000.0 08.8403 08.8403 0012.0 1
1
03 02
01 03 016 01
04 04 016 01
0.0490 0000.0 10.5041 10.5041 0019.5 1
01
06
1
39 15
01 04 016 01
05 05 015 01
06 06 014 01
07 07 013 01
08 08 012 01
09 09 011 01
10 10 010 01
11 12 009 01
13 18 008 01
19 23 007 01
24 26 006 01
27 30 005 01
31 34 004 01
35 39 003 01
40 40 016 01
0.0490 0000.0 08.0000 08.0000 0015.0 1
1
26 12
01 06 016 01
07 07 015 01
08 08 014 01
09 09 013 01
10 10 012 01
11 11 011 01
12 12 010 01
13 14 009 01
15 20 008 01
21 25 007 01
26 26 006 01
27 27 016 01
0.0490 0000.0 08.0000 08.0000 0015.0 1
1
22 11
01 06 016 01
07 07 015 01
08 08 014 01
09 09 013 01
10 10 012 01
11 11 011 01
12 12 010 01
13 14 009 01
15 20 008 01
21 22 007 01
23 23 016 01
0.0490 0000.0 08.0000 08.0000 0015.0 1
1
27 12
01 07 016 01
08 08 015 01
09 09 014 01
10 10 013 01
11 11 012 01
12 12 011 01
13 13 010 01
14 15 009 01
16 21 008 01
22 26 007 01
27 27 006 01
```

```
28 28 016 01
0.0490 0000.0 08.0000 08.0000 0015.0 1
1
07 02
01 07 016 01
08 08 016 01
0.0490 0000.0 08.0000 08.0000 0015.0 1
1
02 02
01 02 016 01
03 03 016 01
0.0490 0000.0 08.0000 08.0000 0015.0 1
```

APPENDIX 3.4.14 Sub-Catchment Seven Digitised Coordinate Pairs for Flow Net Elements and Segments

Template
(See Appendix 4.1)
First line
XO YO
Other paired lines
X(1) Y(1) Z(1)
X(2) Y(2) Z(2)

270.50	632.00	
565.97	566.75	122.00
568.15	569.03	122.00
561.35	572.98	121.00
563.78	574.50	121.00
558.40	579.33	120.00
561.63	580.38	120.00
556.60	582.25	119.00
559.97	584.13	119.00
554.55	585.20	118.00
558.63	586.98	118.00
552.72	588.40	117.00
556.53	590.58	117.00
550.45	591.90	116.00
554.65	594.05	116.00
548.00	595.95	115.00
549.85	596.90	115.00
545.38	599.58	114.00
547.38	600.63	114.00
543.58	602.92	113.00
545.28	604.35	113.00
540.47	607.13	112.00
542.83	608.67	112.00
537.42	611.88	111.00
540.10	613.83	111.00
533.53	617.05	110.00
536.92	619.15	110.00
528.85	622.20	109.00
532.53	625.67	109.00
523.03	627.30	108.00
526.97	632.00	108.00
515.25	634.03	107.00
519.13	639.63	107.00
504.27	641.53	106.00
508.00	648.17	106.00
491.83	648.90	105.00
493.50	654.78	105.00
474.25	656.60	104.00
475.70	662.08	104.00
456.05	661.75	103.00
460.17	669.23	103.00
441.60	669.20	102.00
445.90	676.63	102.00
419.15	681.65	101.00
428.67	689.65	101.00
390.05	704.05	100.00
414.35	707.75	100.00
385.58	707.70	99.40
387.95	738.13	99.00
552.28	593.08	116.00
554.72	594.10	116.00
550.03	596.80	115.00
552.33	598.15	115.00
547.58	600.75	114.00
549.95	602.10	114.00
545.53	604.00	113.00
547.90	605.45	113.00
542.83	608.53	112.00
546.03	610.20	112.00
539.88	613.75	111.00
543.92	615.58	111.00
537.00	619.25	110.00
541.20	622.17	110.00
532.58	625.63	109.00
535.28	628.58	109.00
526.90	631.92	108.00
528.53	634.48	108.00
519.17	639.50	107.00
521.25	641.98	107.00
508.30	648.13	106.00
509.52	650.50	106.00
493.63	654.90	105.00
495.23	658.20	105.00
475.52	662.05	104.00
479.73	666.80	104.00
460.17	668.88	103.00
468.83	676.95	103.00
445.90	676.48	102.00
458.20	688.63	102.00
428.67	689.70	101.00
444.13	702.58	101.00
414.25	707.88	100.00
429.55	718.63	100.00
388.20	738.03	99.00
390.02	757.92	98.60
646.60	488.63	148.00
647.17	490.15	148.00
644.03	491.08	147.00
644.60	492.52	147.00
642.70	491.92	146.00
643.28	493.73	146.00
641.25	493.13	145.00
641.92	494.65	145.00
638.80	494.88	144.00
639.72	496.55	144.00
636.97	496.48	143.00
637.95	497.83	143.00
635.00	498.05	142.00
636.13	499.48	142.00
633.22	499.25	141.00
634.42	501.08	141.00
631.10	500.77	140.00
632.17	502.70	140.00
627.67	503.58	139.00
628.75	505.17	139.00
624.85	505.65	138.00
626.38	507.48	138.00
622.72	507.30	137.00
624.65	509.70	137.00
620.33	509.42	136.00
623.25	511.95	136.00
618.08	511.02	135.00
622.30	513.78	135.00
616.33	512.85	134.00
618.50	515.15	134.00
613.60	515.35	133.00
615.63	518.15	133.00
609.97	518.13	132.00
611.53	520.85	132.00
606.17	521.10	131.00
607.55	523.05	131.00
600.83	525.63	130.00
602.67	527.73	130.00
596.08	530.45	129.00
598.42	532.17	129.00
592.25	535.35	128.00
594.45	537.17	128.00
588.15	540.42	127.00
590.90	542.03	127.00
585.05	544.03	126.00
587.42	545.98	126.00
579.75	549.88	125.00
582.28	551.90	125.00
575.17	554.78	124.00
577.88	557.17	124.00
570.13	560.73	123.00
574.33	562.63	123.00
565.92	567.17	122.00
571.05	569.65	122.00
563.90	574.53	121.00
568.38	576.05	121.00
561.70	580.63	120.00
566.38	581.60	120.00
560.15	583.98	119.00
564.50	586.00	119.00
558.40	587.23	118.00
562.65	589.48	118.00
556.42	590.70	117.00
561.03	592.58	117.00
554.65	594.10	116.00
559.20	596.30	116.00
552.15	598.15	115.00
556.85	600.28	115.00
549.78	601.90	114.00
555.13	604.67	114.00
547.97	605.42	113.00
553.28	608.40	113.00
545.75	610.10	112.00
550.83	612.70	112.00
543.70	615.50	111.00
548.42	617.42	111.00
540.97	622.33	110.00
544.53	625.20	110.00
535.33	628.58	109.00
538.28	631.95	109.00
528.67	634.48	108.00
531.88	638.33	108.00
521.00	642.13	107.00
524.05	645.20	107.00
509.60	650.38	106.00
513.92	653.58	106.00
495.10	658.23	105.00
500.77	663.50	105.00
479.65	666.80	104.00
487.83	673.50	104.00
468.73	676.92	103.00
476.98	684.23	103.00
458.40	688.40	102.00
466.38	695.60	102.00
443.77	702.35	101.00
454.17	710.75	101.00
429.50	718.45	100.00
439.23	726.60	100.00
392.65	753.50	99.00
411.73	752.20	99.00
389.67	757.83	98.60
391.33	778.33	98.30
514.00	653.53	106.00
515.13	654.65	106.00
501.08	663.28	105.00
503.73	665.23	105.00
487.88	673.58	104.00
493.55	677.10	104.00
477.15	684.05	103.00
488.55	690.25	103.00

466.23	695.42	102.00	564.58	636.53	110.00	559.28	679.20	105.00
483.80	703.95	102.00	584.88	644.35	109.00	528.17	674.63	105.00
454.13	710.80	101.00	563.03	644.73	109.00	558.28	691.13	104.00
475.73	725.55	101.00	584.42	652.63	108.00	525.63	684.88	104.00
439.50	726.58	100.00	562.40	652.00	108.00	554.80	704.33	103.00
460.25	749.33	100.00	584.17	662.15	107.00	523.70	697.00	103.00
411.60	752.08	99.00	560.90	660.73	107.00	539.00	737.15	102.00
426.65	780.92	99.00	583.15	673.48	106.00	516.15	724.70	102.00
391.55	778.55	98.30	559.50	669.42	106.00	533.50	748.90	101.00
393.48	798.48	98.00	582.74	680.23	105.50	506.17	739.98	101.00
475.90	725.48	101.00	559.37	674.31	105.50	530.28	767.50	100.00
477.63	726.80	101.00	582.33	686.98	105.00	500.08	762.75	100.00
460.15	749.42	100.00	559.25	679.20	105.00	527.38	780.78	99.30
462.48	751.90	100.00	580.90	693.64	104.50	499.17	791.80	98.80
426.75	781.00	99.00	558.69	685.16	104.50	575.08	577.58	121.00
429.35	783.88	99.00	579.58	700.30	104.00	572.63	577.08	121.00
393.55	798.05	98.00	558.13	691.13	104.00	574.28	582.40	120.00
394.80	818.13	97.70	577.50	708.47	103.50	572.15	582.03	120.00
622.38	514.03	135.00	556.44	697.75	103.50	573.80	587.80	119.00
620.42	512.88	135.00	575.42	716.65	103.00	571.08	587.67	119.00
620.10	517.10	134.00	554.75	704.38	103.00	573.10	592.35	118.00
618.28	515.23	134.00	571.11	731.74	102.50	570.22	592.13	118.00
617.35	520.40	133.00	546.90	720.68	102.50	571.72	596.78	117.00
615.60	518.03	133.00	566.80	746.83	102.00	568.72	595.90	117.00
613.42	523.10	132.00	539.05	736.98	102.00	570.42	601.33	116.00
611.53	520.60	132.00	566.50	752.76	101.50	567.40	599.98	116.00
609.63	525.33	131.00	533.37	758.76	101.50	568.97	605.98	115.00
607.92	523.13	131.00	566.20	758.70	101.00	565.20	604.28	115.00
604.83	529.35	130.00	527.70	780.55	99.30	567.63	609.88	114.00
602.47	527.33	130.00	584.92	553.83	125.00	563.78	608.35	114.00
600.88	533.75	129.00	583.83	553.13	125.00	565.60	614.85	113.00
598.75	532.13	129.00	581.75	559.70	124.00	561.75	613.23	113.00
597.33	538.88	128.00	580.00	558.80	124.00	562.78	619.90	112.00
594.47	537.05	128.00	579.63	564.40	123.00	559.60	617.63	112.00
594.20	544.05	127.00	576.45	563.40	123.00	558.63	625.08	111.00
590.58	541.80	127.00	577.97	570.50	122.00	556.15	623.17	111.00
591.47	549.13	126.00	573.97	569.88	122.00	553.03	632.03	110.00
587.20	545.58	126.00	576.70	577.20	121.00	550.20	629.75	110.00
588.80	555.90	125.00	572.75	577.08	121.00	547.85	638.88	109.00
585.00	553.67	125.00	576.42	582.60	120.00	544.40	636.58	109.00
587.95	561.35	124.00	574.33	582.35	120.00	542.38	646.33	108.00
581.85	559.60	124.00	576.30	587.80	119.00	537.85	643.50	108.00
587.20	566.63	123.00	573.55	587.83	119.00	536.97	654.63	107.00
579.88	564.20	123.00	575.80	592.38	118.00	531.40	651.15	107.00
586.17	571.58	122.00	573.03	592.53	118.00	531.97	663.83	106.00
577.83	570.48	122.00	574.72	597.45	117.00	524.78	661.28	106.00
585.83	577.33	121.00	571.90	596.95	117.00	528.13	674.50	105.00
576.95	577.33	121.00	573.97	601.83	116.00	520.42	672.42	105.00
586.63	581.20	120.00	570.47	601.35	116.00	525.53	684.95	104.00
576.63	582.75	120.00	573.78	607.10	115.00	518.42	683.48	104.00
587.13	585.30	119.00	568.83	605.60	115.00	523.92	697.00	103.00
576.33	587.70	119.00	573.38	612.10	114.00	516.05	695.60	103.00
587.85	589.85	118.00	567.53	609.83	114.00	516.03	724.92	102.00
575.97	592.45	118.00	571.97	616.88	113.00	508.88	721.42	102.00
588.30	599.15	117.00	565.47	614.92	113.00	506.30	740.13	101.00
574.83	597.17	117.00	570.00	623.78	112.00	494.05	736.03	101.00
587.80	605.00	116.00	562.80	619.75	112.00	500.08	762.88	100.00
574.33	601.55	116.00	567.30	630.20	111.00	482.08	760.30	100.00
587.28	609.60	115.00	558.58	625.35	111.00	498.95	791.83	98.80
573.53	606.78	115.00	564.78	636.75	110.00	473.20	800.17	98.30
586.78	613.75	114.00	553.15	632.10	110.00	584.10	553.17	125.00
573.42	611.80	114.00	563.28	644.78	109.00	582.33	551.95	125.00
586.38	619.17	113.00	547.70	638.63	109.00	580.00	558.70	124.00
572.08	617.03	113.00	562.45	652.13	108.00	578.08	557.15	124.00
585.83	624.10	112.00	542.38	646.28	108.00	576.72	563.42	123.00
570.03	623.65	112.00	560.70	660.83	107.00	574.40	562.38	123.00
585.72	630.67	111.00	536.97	654.75	107.00	574.25	570.20	122.00
567.33	630.05	111.00	559.45	669.33	106.00	570.75	569.63	122.00
585.30	636.70	110.00	531.88	663.85	106.00	572.58	577.08	121.00

568.47	575.88	121.00
572.10	582.15	120.00
566.28	581.55	120.00
570.97	587.67	119.00
564.42	586.00	119.00
570.20	591.98	118.00
562.55	589.40	118.00
568.83	595.90	117.00
560.78	592.50	117.00
567.13	600.17	116.00
559.03	596.17	116.00
565.38	604.35	115.00
557.05	600.28	115.00
563.63	608.33	114.00
555.03	604.42	114.00
561.88	613.25	113.00
553.10	608.28	113.00
559.50	617.70	112.00
551.03	612.60	112.00
556.00	623.55	111.00
548.47	617.25	111.00
550.20	629.67	110.00
544.35	625.23	110.00
544.42	636.20	109.00
538.45	631.92	109.00
538.10	643.35	108.00
532.00	638.08	108.00
531.50	651.55	107.00
524.13	644.90	107.00
524.60	661.38	106.00
514.10	653.23	106.00
520.30	672.45	105.00
503.65	665.00	105.00
518.15	683.38	104.00
497.65	678.65	104.00
516.40	695.55	103.00
492.58	691.17	103.00
509.00	721.28	102.00
489.63	705.38	102.00
494.27	735.92	101.00
482.55	729.03	101.00
482.08	760.38	100.00
468.08	755.98	100.00
472.83	787.30	99.00
446.42	786.28	99.00
473.02	800.23	98.30
444.83	803.98	98.10
506.33	667.00	105.00
503.55	665.15	105.00
497.60	678.55	104.00
493.58	676.75	104.00
492.73	691.05	103.00
488.73	690.03	103.00
489.60	705.58	102.00
483.77	703.88	102.00
482.73	729.42	101.00
475.98	725.40	101.00
468.17	755.88	100.00
462.40	751.60	100.00
446.13	786.45	99.00
433.10	785.38	99.00
444.58	803.75	98.10
417.98	811.08	97.90
464.08	752.92	100.00
462.48	751.58	100.00
433.13	785.33	99.00
429.38	783.65	99.00
418.13	811.25	97.90
394.98	817.83	97.70

Appendix 4.1 Simulation Model WATERH Program Code

```
      PROGRAM WATERH
C the common statements show shared storage space and correct passover
C of variables from main to subprograms
      PARAMETER (IH=12,NF=16,I1=7,I2=46,I3=2,I4=54,I5=2)
C this parameter line needs to be changed for sub-catchment three and the
C unaltered catchment to I1=51 and I2=12.
      PARAMETER (NU=9,K9=2,MK=20,MJ=30,I4P=55,NSA=127,MT=100)
      PARAMETER (N1=11,N2=22,N3=33,N4=44,N5=55,N6=66,N7=77,N8=88,N9=90)
      COMMON/MAIN/NS,NSUB,IC,IS,NC,I,J,NTTOT,LAP,TINC,TIME,
     *LC,AREAM2(IH),CHANLENM(IH),IHV,WID(I1,I2,I3,I4),NCAS(I1,I2),
     *CHRAIN(I1,I2,I3,I4),CSUMI(I1,I2,I3,I4),HARM2(I1,I2,I3,I4),
     *CARM2(I1,I2),MAXU,AIN(NU),BIN(NU),UCM2(I1,I2,NU),SQ(I1,I2,I3,I4),
     *UHM2(I1,I2,I3,I4,NU),RAG(NSA),RBG(NSA),WWPRAT(NSA),
     *RAM(NU),RBM(NU),NSU(NSA),RIR(I1,I2,I3,I4),UIR(NU),
     *Q(I1,I2,I3,I4,I5),NITS,NR,NTMOD,NP,SLOPE(I1,I2,I3,I4)
      COMMON/RAINY/IHYE
      COMMON/CORD/Xa,Ya,Za,Xb,Yb,Zb,Xc,Yc,Zc,Xd,Yd,Zd,X(K9),Y(K9),Z(K9),
     *MNUN(MK),MHYE(MK),MI,JNUN(I4P),JHYE(I4P),MSAM(MK),JSAM(I4P),NCHIN
      COMMON/HILL/NELM(I1,I2,I3),IHY(I1,I2,I3,I4),A(I1,I2,I3,I4),
     *B(I1,I2,I3,I4),RLEN(I1,I2,I3,I4),HPOTI,
     *SUMI(I1,I2,I3,I4),HAREA(I1,I2,I3,I4,I5),HPOTI1,
     *TRAIN(I1,I2,I3,I4),K44,SRAIN(I4),
     *NUNIT(I1,I2,I3,I4),AP(I1,I2,I3,I4),RA(I1,I2,I3,I4),
     *RB(I1,I2,I3,I4),TPR(I1,I2,I3,I4),NUMA(I1,I2,I3,I4),
     *AM(I1,I2,I3,I4),BM(I1,I2,I3,I4),NUMB(I1,I2,I3,I4),TT(I1,I2,I3,I4),
     *SUMA(I1,I2,13,I4),VS(I1,I2,I3,I4),TO(I1,I2,I3,I4)
      COMMON/CHAN/NCHA,NSEG(I1),IHYC(I1,I2),EC(I1,I2),TTC(I1,I2),
     *CA(I1,I2),CB(I1,I2),CWID(I1,I2),EANG(I1,I2),WANG(I1,I2),
     *CTOP(I1,I2),CLEN(I1,I2),CGRA(I1,I2),CPER(I1,I2),COPEN(I1,I2),
     *CPOTI,SUMCI(I1,I2),CAREA(I1,I2,I5),CPOTI1,CQ(I1,I2,I5),
     *CSQ(I1,I2),CWP,DEPTH,CTRAIN(I1,I2),K33,CXSA(I1,I2),SCRAIN(I2),
     *CCRAIN(I1,I2),CSUMCI(I1,I2),NUNITC(I1,I2),APC(I1,I2),
     *CCLEN(I1,I2),IOFLOW(I1,I2),NUMAC(I1,I2),NUMBC(I1,I2)
      COMMON/COUR/CVEL(I1,I2,I3),VEL(I1,I2,I3,I4,I5),NSTIF,
     *INSTC(I1,I2),INSTH(I1,I2,I3,I4)
      COMMON/PRINT/NEX(IH),M1(IH,MJ),M2(IH,MJ),M3(IH,MJ),CATRAIN(MT),
     *M4(IH,MJ),M5(IH,MJ),M6(IH,MJ),NQOBS(IH),CATINF(MT),CATDISH(MT),
     *QT(IH,MT),QPCV(IH,MT),CATQT(MT),NCOBS,CATQS,QTS,NCQ,NQQ,TIMEQC
      COMMON/INF1/SUCK1,SUCK2
      COMMON/CINF1/CIN1,CIN2
      CHARACTER*11 PDAT,RDAT,OUTDAT,XYZ,HODAT,PREDH,PRODN,SAMPLE,FLOW
      REAL XO,YO,CATAREA,CATLEN,CATUNAR(NU),QR(IH,MT),QV(IH,MT),
     *QCV(IH,MT),QPR(IH,MT),QPV(IH,MT),TSTOR,CATR(MT),CATV(MT),
     *CATCV(MT),CATFLOW(MT),CATRATE(MT)
      INTEGER KK,MN,ML,MCELF(MK),MCELT(MK),IJ
      SAVE
      READ(NF,899) PDAT
      READ(NF,899) RDAT
      READ(NF,899) HODAT
      READ(NF,899) XYZ
      READ(NF,899) SAMPLE
      READ(NF,899) PREDH
      READ(NF,899) OUTDAT
      READ(NF,899) PRODN
      READ(NF,899) FLOW
C PDAT is the element and channel parameterisation file, RDAT is the
C rainfall file, XYZ is the flow-net coordinates, OUTDAT is the output
C file for times to runoff, cumulative rainfall, runoff and infiltration,
C PREDH is the predicted hydrograph file, HODAT is the observed
C hydrograph file, SAMPLE is the unit and plot parameters file, PRODN
C is the productivity percentage file, and FLOW is the predicted
C A, V, and Q file
c most calculations and variables are in units of cm and seconds although
c some input and output variables are in different units and must be
c converted
      OPEN(N1,FILE=PDAT,STATUS='OLD')
      OPEN(N2,FILE=RDAT,STATUS='OLD')
      OPEN(N5,FILE=XYZ,STATUS='OLD')
      OPEN(N4,FILE=OUTDAT,STATUS='NEW')
```

```
      OPEN(N6,FILE=PREDH,STATUS='NEW')
      OPEN(N7,FILE=HODAT,STATUS='OLD')
      OPEN(N8,FILE=SAMPLE,STATUS='OLD')
      OPEN(N9,FILE=PRODN,STATUS='NEW')
      OPEN(N3,FILE=FLOW,STATUS='NEW')
      write(*,*) 'WATERH1 VERSION 5.90 - 04.05.89 -
     *COPYRIGHT M.D.LEE - LSE GEOG'
c the structure of the model follows a procedure of subprograms
c designed to parameterise the elements geometrically representing the
c flow surface with dimensions and hydraulic characteristics (PARCHAN, PARHILL),
C control the input of rainfall into those elements (URAIN), handle
C the generation and routing of water across those hillslope elements (ROUT1
c and ROUT2 with their internal subroutines of INFIL1 and INFIL2 and DISC),
c and through the channel segments (CROUT1 and CROUT2 with their internal
c subroutines of CINFIL1, CINFIL2 and CDISC and CDQUAD).  It also handles
c the data stores to minimise the storage to a rolling time count of two
c time increments (RESET), and checks that the model obeys input-output
c continuity (CONTT).
C the reason why the routing subroutines only handle arrays with the
c time subscripts 1 and 2 is that in order to reduce storage space, only
c two time periods are considered in the finite difference calculations,
c the current (2) and the previous (1).  It is a backward
c differencing scheme and requires that store 2 is entered to store 1 when
c a new calculation loop is made for the IC channel segments, and I
c hillside elements
      READ(N2,999) IHYE,IHV
      READ(N2,1400) TINC,LAP
      TSTOR=TINC
      READ(N1,1510) NSUB,K33,K44
      READ(N8,1500) MAXU,MAXSAM,NCHIN
        DO 4 KK=1,MAXU
          READ(N8,1550) AIN(KK),BIN(KK),RAM(KK),RBM(KK),UIR(KK)
4       CONTINUE
        DO 6 KK=1,MAXSAM
          READ(N8,1575) RAG(KK),RBG(KK),WWPRAT(KK),NSU(KK)
6       CONTINUE
      WRITE(N4,1600) PDAT,RDAT,XYZ,SAMPLE,PREDH,PRODN,FLOW
c if IHV.GT.0 this means rain has been measured by a vertical
C raingauge and intensity should be adjusted by being multiplied by
C the COS(sin(SLOPE(IC,IS,NC,I))) or COS(SIN(CGRA(IC,IS)))
C
c   IHYE=1 rainfall is uniform variable or constant
c   IHYE>1 rainfall is non-uniform variable or constant
C
c  TINC is the initial time increment and LAP the frequency with which
c  data will be printed to a data file
c
C  NSUB are the number of subcatchments (usually 1 per simulation run)
c
      READ(N7,1150) NTTOT,NITS
c  NTTOT to total real time duration of the simulation, NITS is the
C  maximum number of iterations
      NR=1
      WRITE(N4,1700) TINC,NTTOT,LAP
      CALL URAIN
      NR=2
c  these are coordinates used in the scaling of the digitised points
      READ(N5,*) XO,YO
      IF (NSUB.GT.1) THEN
        READ(N7,5650) NCOBS
c  number of catchment cumulative discharge observations
      END IF
      DO 600 NS=1,NSUB
        IF ((NSUB.GT.1) .AND. (NS.EQ.1)) THEN
          DO 10 IJ=1,NCOBS
            READ(N7,*) CATQT(IJ),CATR(IJ),CATV(IJ),CATCV(IJ)
c  the time, discharge rate, ΔQ and ΣQ
10        CONTINUE
        END IF
```

```
c  this section reads in those locations in the catchment for which intermediate
c  predictions are required to illustrate spatial patterns, etc. M1 to
c  M6 identify the sub-catchment, channel, segment, cascade, element and
c  whether its a channel
       READ(N7,5700) NEX(NS),NQOBS(NS)
        DO 11 IJ=1,NEX(NS)
          READ(N7,5800) M1(NS,IJ),M2(NS,IJ),M3(NS,IJ),M4(NS,IJ),
     *M5(NS,IJ),M6(NS,IJ)
11      CONTINUE
        DO 12 IJ=1,NQOBS(NS)
          READ(N7,*) QT(NS,IJ),QR(NS,IJ),QV(NS,IJ),QCV(NS,IJ)
c  reads in the observed hydrograph for the sub-catchment NS - the time, discharge
c  rate, ΔQ and ΣQ
12      CONTINUE
        CATQS=CATQT(1)
        QTS=QT(NS,1)
        NQQ=1
        NCQ=1
c  loop for geometrical simplification and parameter provision using PARHILL and
c  PARCHAN subroutines
        READ(N1,1200) NCHA
c  number of channel branches in sub-catchment
        IF (NCHA.GT.0) THEN
          DO 19 IC=NCHA,1,-1
            READ(N1,1200) NSEG(IC)
c  number of segments in channel branch
            IF (NSEG(IC).GT.0) THEN
              DO 18 IS=NSEG(IC),1,-1
                READ(N1,1100) NCAS(IC,IS)
c  number of cascades into segment
                DO 17 NC=1,2
                    IF (NC.LE.NCAS(IC,IS)) THEN
                    READ(N1,1250) NELM(IC,IS,NC),MI
c  number of elements in cascade and number of sub-sections of different
c  unit class
                    IF (K44.EQ.1) THEN
                      READ(N5,*) X(1),Y(1),Z(1)
                      READ(N5,*) X(2),Y(2),Z(2)
                      Xc=X(1)
                      Yc=Y(1)
                      Zc=Z(1)
                      Xd=X(2)
                      Yd=Y(2)
                      Zd=Z(2)
                    END IF
c  reads in the highest element in a unit class sub-section, the lowest,
c  the sample plot used to provide parameters and the hyetograph used to
c  provide rainfall
                    DO 15 MN=1,MI
                      READ(N1,1300) MCELF(MN),MCELT(MN),MSAM(MN),
     *MHYE(MN)
                      IF (MN.LT.MI) THEN
c  provides the individual elements with their plot sample, hyetograph and unit
c  identification
                        DO 14 ML=MCELF(MN),MCELT(MN)
                          JSAM(ML)=MSAM(MN)
                          JHYE(ML)=MHYE(MN)
                          JNUN(ML)=NSU(MSAM(MN))
14                      CONTINUE
                      END IF
15                    CONTINUE
                      MNUN(MI)=NSU(MSAM(MI))
c  parameterises each hillslope element
                    DO 16 I=NELM(IC,IS,NC),1,-1
                      CALL PARHILL
16                    CONTINUE
                  END IF
17              CONTINUE
c  parameterises each channel segment
```

```
              CALL PARCHAN
18           CONTINUE
           END IF
19        CONTINUE
C
          TIME=0.0
          TIMEQC=0.0
          LC=LAP
          TINC=TSTOR
          AREAM2(NS)=0.0
          CHANLENM(NS)=0.0
c  this begins the flow simulation phase, setting initial and boundary conditions
c  and performing subsequent routing
          DO 500 J=1,NITS
            TIME=TIME+TINC
            DO 400 IC=NCHA,1,-1
              IF (NSEG(IC).GT.0) THEN
                DO 300 IS=NSEG(IC),1,-1
                  DO 200 NC=1,2
                    IF (NC.LE.NCAS(IC,IS)) THEN
c  calls all the subroutines to route water across the hillslope elements
                      DO 100 I=NELM(IC,IS,NC),1,-1
                        IF (J.EQ.1) THEN
                          INSTH(IC,IS,NC,I)=0
                          CALL ROUT1
                        ELSE IF (J.GT.1) THEN
                          CALL ROUT2
                        END IF
100                   CONTINUE
                    END IF
200                 CONTINUE
c  calls all the suboutines to route water through the channel segments
                  IF (J.EQ.1) THEN
                     INSTC(IC,IS)=0
                     CALL CROUT1
                   ELSE IF (J.GT.1) THEN
                     CALL CROUT2
                   END IF
300              CONTINUE
               END IF
400          CONTINUE
c  calls the subroutine to update finite difference stores (t) to (t-1)
             CALL FDRESET
500        CONTINUE
c  a second set of calls for when there are no channels and a cascade is simulated
         ELSE IF (NCHA.EQ.0) THEN
           IC=1
           IS=1
           NC=1
           READ(N1,1250) NELM(IC,IS,NC),MI
           IF (K44.EQ.1) THEN
             READ(N5,*) X(1),Y(1),Z(1)
             READ(N5,*) X(2),Y(2),Z(2)
             Xc=X(1)
             Yc=Y(1)
             Zc=Z(1)
             Xd=X(2)
             Yd=Y(2)
             Zd=Z(2)
           END IF
           DO 515 MN=1,MI
             READ(N1,1300) MCELF(MN),MCELT(MN),MSAM(MN),MHYE(MN)
             DO 514 ML=MCELF(MN),MCELT(MN)
               JSAM(ML)=MSAM(MN)
               JHYE(ML)=MHYE(MN)
               JNUN(ML)=NSU(MSAM(MN))
514          CONTINUE
515        CONTINUE
           DO 516 I=NELM(IC,IS,NC),1,-1
```

```
          CALL PARHILL
516       CONTINUE
          TIME=0.0
          TIMEQC=0.0
          LC=LAP
          TINC=TSTOR
          AREAM2(NS)=0.0
          CHANLENM(NS)=0.0
          DO 550 J=1,NITS
            TIME=TIME+TINC
            DO 530 I=NELM(IC,IS,NC),1,-1
              IF (J.EQ.1) THEN
                INSTH(IC,IS,NC,I)=0
                CALL ROUT1
              ELSE IF (J.GT.1) THEN
                CALL ROUT2
              END IF
530           CONTINUE
              CALL FDRESET
550         CONTINUE
        END IF
c  a call to the subroutine writing final data sets and checking on continuity
        CALL CONTT
c  calculating total catchment surface area, channel length and the surface
c  area of particular unit classes
        CATAREA=CATAREA+AREAM2(NS)
        CATLEN=CATLEN+CHANLENM(NS)
        DO 580 KK=1,MAXU
          IF (NCHA.GT.0) THEN
            CATUNAR(KK)=CATUNAR(KK)+UCM2(1,1,KK)
          ELSE IF (NCHA.EQ.0) THEN
            CATUNAR(KK)=CATUNAR(KK)+UHM2(1,1,1,1,KK)
          END IF
580     CONTINUE
c output of the predicted hydrograph for the sub-catchment
        DO 590 NQ=1,NQOBS(NS)
          QPCV(NS,NQ)=QPCV(NS,NQ)/1000000.0
          QT(NS,NQ)=QT(NS,NQ)/3600.0
          IF (NQ.GT.1) THEN
            QPV(NS,NQ)=QPCV(NS,NQ)-QPCV(NS,(NQ-1))
            QPR(NS,NQ)=QPV(NS,NQ)/(QT(NS,NQ)-QT(NS,(NQ-1)))
          ELSE IF (NQ.EQ.1) THEN
            QPV(NS,NQ)=QPCV(NS,NQ)
            QPR(NS,NQ)=QPV(NS,NQ)/QT(NS,NQ)
          END IF
c  time, discharge rate, volumetric ΔQ and ΣQ in cubic metres
          WRITE(N6,*) QT(NS,NQ),QPR(NS,NQ),QPV(NS,NQ),QPCV(NS,NQ)
590     CONTINUE
600   CONTINUE
c  if more than one sub-catchment is simulated in a given run then the hydrograph
c  also needs to be calculated and written out
      IF (NSUB.GT.1) THEN
        DO 610 NQ=1,NCOBS
          CATDISH(NQ)=CATDISH(NQ)/1000000.0
          CATQT(NQ)=CATQT(NQ)/3600.0
          IF (NQ.GT.1) THEN
            CATFLOW(NQ)=CATDISH(NQ)-CATDISH(NQ-1)
            CATRATE(NQ)=CATFLOW(NQ)/(CATQT(NQ)-CATQT(NQ-1))
          ELSE IF (NQ.EQ.1) THEN
            CATFLOW(NQ)=CATDISH(NQ)
            CATRATE(NQ)=CATFLOW(NQ)/CATQT(NQ)
          END IF
c  time, discharge rate, volumetric ΔQ and ΣQ in cubic metres
          WRITE(N6,*) CATQT(NQ),CATRATE(NQ),CATFLOW(NQ),CATDISH(NQ)
610     CONTINUE
      END IF
c  output of the total catchment area, unit area, and channel length
      WRITE(N4,4200) CATAREA,(CATUNAR(KK),KK=1,MAXU),CATLEN
      STOP
```

```
899   FORMAT(A11)
999   FORMAT(1X,I2,1X,I1)
1100  FORMAT(1X,I1)
1150  FORMAT(1X,I5,1X,I7)
1200  FORMAT(1X,I2)
1250  FORMAT(2(1X,I2))
1300  FORMAT(2(1X,I2),1X,I3,1X,I2)
1400  FORMAT(1X,F5.1,1X,I4)
1510  FORMAT(1X,I2,2(1X,I1))
1500  FORMAT(1X,I1,1X,I3,1X,I1)
1550  FORMAT(1X,F8.6,1X,F6.4,2(1X,F7.4),1X,F5.3)
1575  FORMAT(1X,F4.2,1X,F5.3,1X,F6.4,1X,I1)
1580  FORMAT(1X,F8.6,1X,F6.3,1X,F7.4)
1600  FORMAT(6(1X,A11))
1700  FORMAT(1X,F5.1,1X,I5,1X,I4)
4100  FORMAT(1X,F8.2,6(1X,F11.1))
4200  FORMAT(1X,F8.1,9(F6.1),1X,F6.1)
5650  FORMAT(1X,I2)
5700  FORMAT(1X,I3,1X,I2)
5800  FORMAT(3(1X,I2),1X,I1,1X,I2,1X,I1)
5900  FORMAT(1X,F8.2,3(1X,F7.2))
      END
C*********************************************************************
C
      SUBROUTINE PARHILL
C
      PARAMETER (IH=12,NF=16,I1=7,I2=46,I3=2,I4=54,I5=2)
      PARAMETER (NU=9,K9=2,MK=20,MJ=30,I4P=55,NSA=127,MT=100)
      PARAMETER (N1=11,N2=22,N3=33,N4=44,N5=55,N6=66,N7=77,N8=88,N9=90)
      COMMON/MAIN/NS,NSUB,IC,IS,NC,I,J,NTTOT,LAP,TINC,TIME,
     *LC,AREAM2(IH),CHANLENM(IH),IHV,WID(I1,I2,I3,I4),NCAS(I1,I2),
     *CHRAIN(I1,I2,I3,I4),CSUMI(I1,I2,I3,I4),HARM2(I1,I2,I3,I4),
     *CARM2(I1,I2),MAXU,AIN(NU),BIN(NU),UCM2(I1,I2,NU),SQ(I1,I2,I3,I4),
     *UHM2(I1,I2,I3,I4,NU),RAG(NSA),RBG(NSA),WWPRAT(NSA),
     *RAM(NU),RBM(NU),NSU(NSA),RIR(I1,I2,I3,I4),UIR(NU),
     *Q(I1,I2,I3,I4,I5),NITS,NR,NTMOD,NP,SLOPE(I1,I2,I3,I4)
      COMMON/HILL/NELM(I1,I2,I3),IHY(I1,I2,I3,I4),A(I1,I2,I3,I4),
     *B(I1,I2,I3,I4),RLEN(I1,I2,I3,I4),HPOTI,
     *SUMI(I1,I2,I3,I4),HAREA(I1,I2,I3,I4,I5),HPOTI1,
     *TRAIN(I1,I2,I3,I4),K44,SRAIN(I4),
     *NUNIT(I1,I2,I3,I4),AP(I1,I2,I3,I4),RA(I1,I2,I3,I4),
     *RB(I1,I2,I3,I4),TPR(I1,I2,I3,I4),NUMA(I1,I2,I3,I4),
     *AM(I1,I2,I3,I4),BM(I1,I2,I3,I4),NUMB(I1,I2,I3,I4),TT(I1,I2,I3,I4),
     *SUMA(I1,I2,13,I4),VS(I1,I2,I3,I4),TO(I1,I2,I3,I4)
      COMMON/CORD/Xa,Ya,Za,Xb,Yb,Zb,Xc,Yc,Zc,Xd,Yd,Zd,X(K9),Y(K9),Z(K9),
     *MNUN(MK),MHYE(MK),MI,JNUN(I4P),JHYE(I4P),MSAM(MK),JSAM(I4P),NCHIN
      REAL AB,BD,AD,DC,BC
      REAL CSD,DD,ABD,S1,CSB,BB,BCD,S2,ABCD,AVL,AVS,TAVS,AVW
      REAL A2B,A2C,B2D,ZT,ZL,ZZ,AREAH
      INTEGER KK
c (K44.EQ.1) digitised spot-height data is used, 4 points marking the
c intersection of two contours and two flow-lines which mark the boundary
c of the element in question.
c (K44.EQ.2) planimetric map derived data is used, namely five lengths
c measured off the map-the four lengths describing the outside of the
c polygon projected down onto the horizontal, and the diagonal bisector of
c points B and D.
c if (K44.EQ.3) pre-processed data is used
c
c SLOPE(IC,IS,NC,I) slope gradient in sines
c ROUGH slope roughness - Manning's n
c A(IC,IS,NC,I) and B(IC,IS,NC,I) Green and Ampt coefficients
c RLEN(IC,IS,NC,I) length of element
c WID(IC,IS,NC,I) width of cell whose variation downslope accounts for flow
C divergence or convergence
c TINC time increment for calculations in seconds
C IHY(IC,IS,NC,I) is the hyetograph applicable to the hillslope element
c location
C AREAM2(NS) is the total area of the subcatchment NS in square metres
```

```
      SAVE
      TT(IC,IS,NC,I)=0.0
      TO(IC,IS,NC,I)=0.0
      NUMA(IC,IS,NC,I)=0
      NUMB(IC,IS,NC,I)=0
      VS(IC,IS,NC,I)=0.0
      SUMA(IC,IS,NC,I)=0.0
      IHY(IC,IS,NC,I)=JHYE(I)
      RA(IC,IS,NC,I)=RAG(JSAM(I))
      RB(IC,IS,NC,I)=RBG(JSAM(I))
      TPR(IC,IS,NC,I)=WWPRAT(JSAM(I))
      AM(IC,IS,NC,I)=RAM(JNUN(I))
      BM(IC,IS,NC,I)=RBM(JNUN(I))
      A(IC,IS,NC,I)=AIN(JNUN(I))
      B(IC,IS,NC,I)=BIN(JNUN(I))
      RIR(IC,IS,NC,I)=UIR(JNUN(I))
      NUNIT(IC,IS,NC,I)=JNUN(I)
      IF (K44.EQ.1) THEN
        READ(N5,*) X(1),Y(1),Z(1)
        READ(N5,*) X(2),Y(2),Z(2)
        Xa=Xc
        Ya=Yc
        Za=Zc
        Xb=Xd
        Yb=Yd
        Zb=Zd
        Xc=X(1)
        Yc=Y(1)
        Zc=Z(1)
        Xd=X(2)
        Yd=Y(2)
        Zd=Z(2)
        IF (I.EQ.1) THEN
          Zc=(Zc+Zd)/2.0
          Zd=Zc
        END IF
c
c the above if accounts for the uneven lengths of the lower pair of
c nodes of element I which are channel nodes and do not lie on the same
c elevation
c
        AB=SQRT(((Xa-Xb)**2.0)+((Ya-Yb)**2.0))
        BC=SQRT(((Zb-Zc)**2.0)+(((Xb-Xc)**2.0)+((Yb-Yc)**2.0)))
        AC=SQRT(((Za-Zc)**2.0)+(((Xa-Xc)**2.0)+((Ya-Yc)**2.0)))
        DC=SQRT(((Xd-Xc)**2.0)+((Yd-Yc)**2.0))
        BD=SQRT(((Zb-Zd)**2.0)+(((Xb-Xd)**2.0)+((Yb-Yd)**2.0)))
        CSD=((AC**2.0)+(BC**2.0)-(AB**2.0))/(2.0*AC*BC)
        CC=ACOS(CSD)
        ABC=(BC*AC*SIN(CC))/2.0
        S1=ASIN((Za-Zc)/AC)
        CSB=((BC**2.0)+(BD**2.0)-(DC**2.0))/(2.0*BC*BD)
        BB=ACOS(CSB)
        BCD=(BD*BC*SIN(BB))/2.0
        S2=ASIN((Zb-Zd)/BD)
        ABCD=ABC+BCD
        AVL=(AC+BD)/2.0
        AVS=(S1+S2)/2.0
        TAVS=SIN(AVS)
        AVW=ABCD/AVL
        RLEN(IC,IS,NC,I)=AVL*100.0
        WID(IC,IS,NC,I)=AVW*100.0
        SLOPE(IC,IS,NC,I)=TAVS
      ELSE IF (K44.EQ.2) THEN
        READ(N1,1200) AB,DC,A2C,A2D,B2C,ZT,ZL
        ZZ=ZT-ZL
        AC=SQRT((ZZ**2.0)+(A2C**2.0))
        BD=SQRT((ZZ**2.0)+(B2D**2.0))
        BC=SQRT((ZZ**2.0)+(B2C**2.0))
        Za=ZT
```

```
        Zb=ZT
        Zc=ZL
        Zd=ZL
        CSD=((AC**2.0)+(BC**2.0)-(AB**2.0))/(2.0*AC*BC)
        CC=ACOS(CSD)
        ABC=(BC*AC*SIN(CC))/2.0
        S1=ASIN((Za-Zc)/AC)
        CSB=((BC**2.0)+(BD**2.0)-(DC**2.0))/(2.0*BC*BD)
        BB=ACOS(CSB)
        BCD=(BD*BC*SIN(BB))/2.0
        S2=ASIN((Zb-Zd)/BD)
        ABCD=ABC+BCD
        AVL=(AC+BD)/2.0
        AVS=(S1+S2)/2.0
        TAVS=SIN(AVS)
        AVW=ABCD/AVL
        RLEN(IC,IS,NC,I)=AVL*100.0
        WID(IC,IS,NC,I)=AVW*100.0
        SLOPE(IC,IS,NC,I)=TAVS
      ELSE IF (K44.EQ.3) THEN
        READ(N1,1300) RLEN(IC,IS,NC,I),WID(IC,IS,NC,I),
     *SLOPE(IC,IS,NC,I)
      END IF
      AREAH=((RLEN(IC,IS,NC,I)*WID(IC,IS,NC,I))/10000.0)
      AREAM2(NS)=AREAM2(NS)+AREAH
      IF (I.LT.NELM(IC,IS,NC)) THEN
        HARM2(IC,IS,NC,I)=AREAH+HARM2(IC,IS,NC,(I+1))
      ELSE IF (I.EQ.NELM(IC,IS,NC)) THEN
        HARM2(IC,IS,NC,I)=AREAH
      END IF
      DO 800 KK=1,MAXU
        IF (JNUN(I).EQ.KK) THEN
          IF (I.LT.NELM(IC,IS,NC)) THEN
            UHM2(IC,IS,NC,I,KK)=AREAH+UHM2(IC,IS,NC,(I+1),KK)
          ELSE IF (I.EQ.NELM(IC,IS,NC)) THEN
            UHM2(IC,IS,NC,I,KK)=AREAH
          END IF
        END IF
        IF (JNUN(I).NE.KK) THEN
          IF (I.LT.NELM(IC,IS,NC)) THEN
            UHM2(IC,IS,NC,I,KK)=UHM2(IC,IS,NC,(I+1),KK)
          ELSE IF (I.EQ.NELM(IC,IS,NC)) THEN
            UHM2(IC,IS,NC,I,KK)=0.0
          END IF
        END IF
800   CONTINUE
      RETURN
1200  FORMAT(7(1X,F6.1))
1300  FORMAT(1X,I2,2(1X,F6.1),1X,F6.4)
      END
C
C*************************************************************************
C
      SUBROUTINE PARCHAN
C
      PARAMETER (IH=12,NF=16,I1=7,I2=46,I3=2,I4=54,I5=2)
      PARAMETER (NU=9,K9=2,MK=20,MJ=30,I4P=55,NSA=127,MT=100)
      PARAMETER (N1=11,N2=22,N3=33,N4=44,N5=55,N6=66,N7=77,N8=88,N9=90)
      COMMON/MAIN/NS,NSUB,IC,IS,NC,I,J,NTTOT,LAP,TINC,TIME,
     *LC,AREAM2(IH),CHANLENM(IH),IHV,WID(I1,I2,I3,I4),NCAS(I1,I2),
     *CHRAIN(I1,I2,I3,I4),CSUMI(I1,I2,I3,I4),HARM2(I1,I2,I3,I4),
     *CARM2(I1,I2),MAXU,AIN(NU),BIN(NU),UCM2(I1,I2,NU),SQ(I1,I2,I3,I4),
     *UHM2(I1,I2,I3,I4,NU),RAG(NSA),RBG(NSA),WWPRAT(NSA),
     *RAM(NU),RBM(NU),NSU(NSA),RIR(I1,I2,I3,I4),UIR(NU),
     *Q(I1,I2,I3,I4,I5),NITS,NR,NTMOD,NP,SLOPE(I1,I2,I3,I4)
      COMMON/CHAN/NCHA,NSEG(I1),IHYC(I1,I2),EC(I1,I2),TTC(I1,I2),
     *CA(I1,I2),CB(I1,I2),CWID(I1,I2),EANG(I1,I2),WANG(I1,I2),
     *CTOP(I1,I2),CLEN(I1,I2),CGRA(I1,I2),CPER(I1,I2),COPEN(I1,I2),
     *CPOTI,SUMCI(I1,I2),CAREA(I1,I2,I5),CPOTI1,CQ(I1,I2,I5),
```

```
     *CSQ(I1,I2),CWP,DEPTH,CTRAIN(I1,I2),K33,CXSA(I1,I2),SCRAIN(I2),
     *CCRAIN(I1,I2),CSUMCI(I1,I2),NUNITC(I1,I2),APC(I1,I2),
     *CCLEN(I1,I2),IOFLOW(I1,I2),NUMAC(I1,I2),NUMBC(I1,I2)
      COMMON/CORD/Xa,Ya,Za,Xb,Yb,Zb,Xc,Yc,Zc,Xd,Yd,Zd,X(K9),Y(K9),Z(K9),
     *MNUN(MK),MHYE(MK),MI,JNUN(I4P),JHYE(I4P),MSAM(MK),JSAM(I4P),NCHIN
      REAL BC,AC,AREAC,RLATERAL
      INTEGER KK,NIC
c
c this subroutine is designed to calculate channel dimensions of length
c CLEN(IC,IS) and gradient CGRA(IC,IS)
c if (K33.EQ.1) spot-height data of the two nodes defining the upper and
c lower boundaries of the channel segment are used
c if (K33.EQ.2) planimetric map derived data is used, namely the length
c of the segment in the horizontal measured from the map, plus the
c elevation change from lower node to upper node
c if (K33.EQ.3) the actual pre-prepared data is used
c
C CROUGH is the channel roughness - Mannings N
c CA(IC,IS) and CB(IC,IS) are the channel Green and Ampt infiltration
c coefficients assumed equal to those of the adjacent slope elements
c IHYC(IC,IS) is the hyetograph applicable to the channel segment
c location and is established from the model base map
c CWID(IC,IS), EANG(IC,IS), WANG(IC,IS), and CTOP(IC,IS) define the
c dimensions of the channel cross-section.
c CWID(IC,IS) the width of the horizontal bed (0.0 for a triangle)
c EANG(IC,IS) and WANG(IC,IS) the tangents of the angles of the
c east and west banks to the vertical (0.0 for rectangle)
c CTOP(IC,IS) is the height of the channel bank shoulders above the bed
c these allow calculation of perimiter CPER(IC,IS), top width
c COPEN(IC,IS), and cross sectional area CXSA(IC,IS)
C AREAM2(NS) is the total area of the subcatchment NS in square metres
c CHANLENM(NS) is the total calculated channel length for catchment NS
C IOFLOW(IC,IS) indicates the kind of channel - a banked hill
c  channel (1), or a simple ditch or natural channel (2,3)
C
      READ(N1,1000) EC(IC,IS),
     *CWID(IC,IS),EANG(IC,IS),WANG(IC,IS),CTOP(IC,IS),IOFLOW(IC,IS)
      IHYC(IC,IS)=MHYE(MI)
      CA(IC,IS)=AIN(MNUN(MI))
      CB(IC,IS)=BIN(MNUN(MI))
      NUNITC(IC,IS)=MNUN(MI)
      IF (NCHIN.EQ.1) THEN
        CA(IC,IS)=0.0
        CB(IC,IS)=0.0
      END IF
      IF (K33.EQ.1) THEN
        Xa=X(1)
        Ya=Y(1)
        Za=Z(1)
        Xb=X(2)
        Yb=Y(2)
        Zb=Z(2)
        CLEN(IC,IS)=SQRT(((Za-Zb)**2.0)+((Xa-Xb)**2.0)+
     *((Ya-Yb)**2.0))*100.0
        CGRA(IC,IS)=(Za-Zb)/SQRT(((Xa-Xb)**2.0)+((Ya-Yb)**2.0))
      ELSE IF (K33.EQ.2) THEN
        READ(N1,1200) BC,AC
        CLEN(IC,IS)=SQRT((BC**2.0)+(AC**2.0))*100.0
        CGRA(IC,IS)=AC/BC
      ELSE IF (K33.EQ.3) THEN
        READ(N1,1300) CLEN(IC,IS),CGRA(IC,IS)
      END IF
      CPER(IC,IS)=CWID(IC,IS)+(CTOP(IC,IS)/COS(ATAN(EANG(IC,IS))))+
     *(CTOP(IC,IS)/COS(ATAN(WANG(IC,IS))))
      COPEN(IC,IS)=CWID(IC,IS)+(CTOP(IC,IS)*EANG(IC,IS))+
     *(CTOP(IC,IS)*WANG(IC,IS))
      CXSA(IC,IS)=((COPEN(IC,IS)+CWID(IC,IS))/2.0)*CTOP(IC,IS)
      AREAC=((CLEN(IC,IS)*COPEN(IC,IS))/10000.0)
      AREAM2(NS)=AREAM2(NS)+AREAC
```

```
      CHANLENM(NS)=CHANLENM(NS)+(CLEN(IC,IS)/100.0)
      NIC=NCHA-((NCHA+1)/2)
      IF (NCAS(IC,IS).EQ.1) THEN
        RLATERAL=HARM2(IC,IS,1,1)
      ELSE IF (NCAS(IC,IS).EQ.2) THEN
        RLATERAL=HARM2(IC,IS,1,1)+HARM2(IC,IS,2,1)
      END IF
      IF ((IC.GT.NIC) .AND. (IS.EQ.NSEG(IC))) THEN
        CARM2(IC,IS)=AREAC+RLATERAL
        CCLEN(IC,IS)=(CLEN(IC,IS)/100.0)
      ELSE IF ((IC.GT.NIC) .AND. (IS.LT.NSEG(IC))) THEN
        CARM2(IC,IS)=AREAC+RLATERAL+CARM2(IC,(IS+1))
        CCLEN(IC,IS)=(CLEN(IC,IS)/100.0)+CCLEN(IC,(IS+1))
      ELSE IF ((IC.LE.NIC) .AND. (IS.EQ.NSEG(IC))) THEN
        CARM2(IC,IS)=AREAC+RLATERAL+CARM2((IC+IC),1)+
     *CARM2((IC+IC+1),1)
        CCLEN(IC,IS)=(CLEN(IC,IS)/100.0)+CCLEN((IC+IC),1)+
     *CCLEN((IC+IC+1),1)
      ELSE IF ((IC.LE.NIC) .AND. (IS.LT.NSEG(IC))) THEN
        CARM2(IC,IS)=AREAC+RLATERAL+CARM2(IC,(IS+1))
        CCLEN(IC,IS)=(CLEN(IC,IS)/100.0)+CCLEN(IC,(IS+1))
      END IF
      DO 800 KK=1,MAXU
        IF (NCAS(IC,IS).EQ.1) THEN
          RLATERAL=UHM2(IC,IS,1,1,KK)
        ELSE IF (NCAS(IC,IS).EQ.2) THEN
          RLATERAL=UHM2(IC,IS,1,1,KK)+UHM2(IC,IS,2,1,KK)
        END IF
        IF (KK.EQ.MNUN(MI)) THEN
          IF ((IC.GT.NIC) .AND. (IS.EQ.NSEG(IC))) THEN
            UCM2(IC,IS,KK)=AREAC+RLATERAL
          ELSE IF ((IC.GT.NIC) .AND. (IS.LT.NSEG(IC))) THEN
            UCM2(IC,IS,KK)=AREAC+RLATERAL+UCM2(IC,(IS+1),KK)
          ELSE IF ((IC.LE.NIC) .AND. (IS.EQ.NSEG(IC))) THEN
            UCM2(IC,IS,KK)=AREAC+RLATERAL+UCM2((IC+IC),1,KK)+
     *UCM2((IC+IC+1),1,KK)
          ELSE IF ((IC.LE.NIC) .AND. (IS.LT.NSEG(IC))) THEN
            UCM2(IC,IS,KK)=AREAC+RLATERAL+UCM2(IC,(IS+1),KK)
          END IF
        ELSE IF (KK.NE.MNUN(MI)) THEN
          IF ((IC.GT.NIC) .AND. (IS.EQ.NSEG(IC))) THEN
            UCM2(IC,IS,KK)=RLATERAL
          ELSE IF ((IC.GT.NIC) .AND. (IS.LT.NSEG(IC))) THEN
            UCM2(IC,IS,KK)=RLATERAL+UCM2(IC,(IS+1),KK)
          ELSE IF ((IC.LE.NIC) .AND. (IS.EQ.NSEG(IC))) THEN
            UCM2(IC,IS,KK)=RLATERAL+UCM2((IC+IC),1,KK)+
     *UCM2((IC+IC+1),1,KK)
          ELSE IF ((IC.LE.NIC) .AND. (IS.LT.NSEG(IC))) THEN
            UCM2(IC,IS,KK)=RLATERAL+UCM2(IC,(IS+1),KK)
          END IF
        END IF
800   CONTINUE
    RETURN
1000  FORMAT(1X,F6.4,1X,F6.1,2(1X,F7.4),1X,F6.1,1X,I1)
1200  FORMAT(2(1X,F6.1))
1300  FORMAT(1X,I2,1X,F6.1,1X,F6.4)
      END
C
C *****************************************************************
C
      SUBROUTINE URAIN
C
      PARAMETER (IH=12,NF=16,I1=7,I2=46,I3=2,I4=54,I5=2)
      PARAMETER (NU=9,K9=2,MK=20,MJ=30,I4P=55,NSA=127,MT=100)
      PARAMETER (N1=11,N2=22,N3=33,N4=44,N5=55,N6=66,N7=77,N8=88,N9=90)
      PARAMETER (M=40,MM=40)
      COMMON/MAIN/NS,NSUB,IC,IS,NC,I,J,NTTOT,LAP,TINC,TIME,
     *LC,AREAM2(IH),CHANLENM(IH),IHV,WID(I1,I2,I3,I4),NCAS(I1,I2),
     *CHRAIN(I1,I2,I3,I4),CSUMI(I1,I2,I3,I4),HARM2(I1,I2,I3,I4),
```

```
     *CARM2(I1,I2),MAXU,AIN(NU),BIN(NU),UCM2(I1,I2,NU),SQ(I1,I2,I3,I4),
     *UHM2(I1,I2,I3,I4,NU),RAG(NSA),RBG(NSA),WWPRAT(NSA),
     *RAM(NU),RBM(NU),NSU(NSA),RIR(I1,I2,I3,I4),UIR(NU),
     *Q(I1,I2,I3,I4,I5),NITS,NR,NTMOD,NP,SLOPE(I1,I2,I3,I4)
      COMMON/RAINY/IHYE
      COMMON/HILL/NELM(I1,I2,I3),IHY(I1,I2,I3,I4),A(I1,I2,I3,I4),
     *B(I1,I2,I3,I4),RLEN(I1,I2,I3,I4),HPOTI,
     *SUMI(I1,I2,I3,I4),HAREA(I1,I2,I3,I4,I5),HPOTI1,
     *TRAIN(I1,I2,I3,I4),K44,SRAIN(I4),
     *NUNIT(I1,I2,I3,I4),AP(I1,I2,I3,I4),RA(I1,I2,I3,I4),
     *RB(I1,I2,I3,I4),TPR(I1,I2,I3,I4),NUMA(I1,I2,I3,I4),
     *AM(I1,I2,I3,I4),BM(I1,I2,I3,I4),NUMB(I1,I2,I3,I4),TT(I1,I2,I3,I4),
     *SUMA(I1,I2,13,I4),VS(I1,I2,I3,I4),TO(I1,I2,I3,I4)
      COMMON/CHAN/NCHA,NSEG(I1),IHYC(I1,I2),EC(I1,I2),TTC(I1,I2),
     *CA(I1,I2),CB(I1,I2),CWID(I1,I2),EANG(I1,I2),WANG(I1,I2),
     *CTOP(I1,I2),CLEN(I1,I2),CGRA(I1,I2),CPER(I1,I2),COPEN(I1,I2),
     *CPOTI,SUMCI(I1,I2),CAREA(I1,I2,I5),CPOTI1,CQ(I1,I2,I5),
     *CSQ(I1,I2),CWP,DEPTH,CTRAIN(I1,I2),K33,CXSA(I1,I2),SCRAIN(I2),
     *CCRAIN(I1,I2),CSUMCI(I1,I2),NUNITC(I1,I2),APC(I1,I2),
     *CCLEN(I1,I2),IOFLOW(I1,I2),NUMAC(I1,I2),NUMBC(I1,I2)
c
C URAIN fills the RAIN array with the relevant precipitation intensity
c in cm/sec
c some important variables include;
c NRAT(K1,K2), NCRAT(K1).time increment counters up to which specific
c intensities PREC(K1,K2),CPREC(K1).apply.(mm/hr converted to cm/sec)
c
      REAL PREC(IH,M),CPREC(M),COUNT,COUNTC,RNRAT(IH,M),RNCRAT(M),
     *STOR1,STOR2,STOR1C,STOR2C
      INTEGER NIBL(M),L,N,K,NIB,NRAT(IH,M),NCRAT(M),II
      SAVE
      L=0
C
C if (IHYE.EQ.1) then rainfall is variable through time but constant
c through space such that each channel segment and hillslope receive the
c same rainfall rates, but those intensities change through time according
c to a finite number (NIB) of intensity blocks
c
c if (IHYE.GT.1) rainfall is variable through time and space so
c different channel segments and hillslope elements can receive different
c rainfall rates at different times. each hyetograph II=1,IHYE has a store
c of rainfall intensities changing through time according to a finite
c number (NIBL(II)) of intensity blocks
c
      IF (NR.EQ.1) THEN
        IF (IHYE.GT.1) THEN
          DO 80 II=1,IHYE
            READ(N2,1200) NIBL(II)
            NIBL(II)=NIBL(II)+1
            DO 75 L=1,NIBL(II)
              IF (L.LT.NIBL(II)) THEN
                READ(N2,1250) NRAT(II,L), PREC(II,L)
                PREC(II,L)=PREC(II,L)/36000.0
              ELSE IF (L.EQ.NIBL(II)) THEN
                NRAT(II,L)=NTTOT
                PREC(II,L)=0.0
              END IF
75          CONTINUE
80        CONTINUE
        ELSE IF (IHYE.EQ.1) THEN
          READ(N2,1200) NIB
          NIB=NIB+1
          DO 175 L=1,NIB
            IF (L.LT.NIB) THEN
              READ(N2,1250) NCRAT(L), CPREC(L)
              CPREC(L)=CPREC(L)/36000.0
            ELSE IF (L.EQ.NIB) THEN
              NCRAT(L)=NTTOT
              CPREC(L)=0.0
```

```
          END IF
175       CONTINUE
        END IF
      ELSE IF (NR.EQ.2) THEN
        COUNT=TIME-TINC
        COUNTC=TIME-TINC
        IF (IHYE.GT.1) THEN
          IF (NP.EQ.1) THEN
            DO 180 L=1,NIBL(IHY(IC,IS,NC,I))
              RNRAT(IHY(IC,IS,NC,I),L)=REAL(NRAT(IHY(IC,IS,NC,I),L))
              IF (COUNT.LT.RNRAT(IHY(IC,IS,NC,I),L)) THEN
                STOR1=RNRAT(IHY(IC,IS,NC,I),L)-COUNT
                IF (STOR1.GT.TINC) THEN
                  SRAIN(I)=PREC(IHY(IC,IS,NC,I),L)*TINC
                  L=NIBL(IHY(IC,IS,NC,I))+1
                ELSE IF (STOR1.LT.TINC) THEN
                  STOR2=TINC-STOR1
                  IF (NRAT(IHY(IC,IS,NC,I),L).LT.NTTOT) THEN
                    SRAIN(I)=(PREC(IHY(IC,IS,NC,I),(L-1))*STOR2)+
     *(STOR1*PREC(IHY(IC,IS,NC,I),L))
                    L=NIBL(IHY(IC,IS,NC,I))+1
                  ELSE IF (NRAT(IHY(IC,IS,NC,I),L).EQ.NTTOT) THEN
                    SRAIN(I)=(STOR1*PREC(IHY(IC,IS,NC,I),L))
                  END IF
                END IF
              END IF
180         CONTINUE
          ELSE IF (NP.EQ.2) THEN
            DO 200 L=1,NIBL(IHYC(IC,IS))
              RNRAT(IHYC(IC,IS),L)=REAL(NRAT(IHYC(IC,IS),L))
              IF (COUNTC.LT.RNRAT(IHYC(IC,IS),L)) THEN
                STOR1C=RNRAT(IHYC(IC,IS),L)-COUNTC
                IF (STOR1C.GT.TINC) THEN
                  SCRAIN(IS)=PREC(IHYC(IC,IS),L)*TINC
                  L=NIBL(IHYC(IC,IS))+1
                ELSE IF (STOR1C.LT.TINC) THEN
                  STOR2C=TINC-STOR1C
                  IF (NRAT(IHY(IC,IS,NC,I),L).LT.NTTOT) THEN
                    SCRAIN(IS)=(PREC(IHYC(IC,IS),(L-1))*STOR2C)+
     *(STOR1C*PREC(IHYC(IC,IS),L))
                    L=NIBL(IHYC(IC,IS))+1
                  ELSE IF (NRAT(IHY(IC,IS,NC,I),L).EQ.NTTOT) THEN
                    SCRAIN(IS)=(STOR1C*PREC(IHYC(IC,IS),L))
                    L=NIBL(IHYC(IC,IS))+1
                  END IF
                END IF
              END IF
200         CONTINUE
          END IF
        ELSE IF (IHYE.EQ.1) THEN
          DO 275 L=1,NIB
            RNCRAT(L)=REAL(NCRAT(L))
            IF (NP.EQ.1) THEN
              IF (COUNT.LT.RNCRAT(L)) THEN
                STOR1=RNCRAT(L)-COUNT
                IF (STOR1.GE.TINC) THEN
                  IF (L.LT.NIB) THEN
                    SRAIN(I)=CPREC(L)*TINC
                    L=NIB
                  END IF
                ELSE IF (STOR1.LT.TINC) THEN
                  STOR2=TINC-STOR1
                  IF (L.LT.NIB) THEN
                    SRAIN(I)=(CPREC(L)*STOR1)+(CPREC(L+1)*STOR2)
                    L=NIB
                  END IF
                END IF
              END IF
            ELSE IF (NP.EQ.2) THEN
```

```
              IF (COUNTC.LT.RNCRAT(L)) THEN
                STOR1C=RNCRAT(L)-COUNTC
                IF (STOR1C.GE.TINC) THEN
                  IF (L.LT.NIB) THEN
                    SCRAIN(IS)=CPREC(L)*TINC
                     L=NIB
                  END IF
                ELSE IF (STOR1C.LT.TINC) THEN
                  STOR2C=TINC-STOR1C
                  IF (L.LT.NIB) THEN
                    SCRAIN(IS)=(CPREC(L)*STOR1C)+(STOR2C*CPREC(L+1))
                    L=NIB
                  END IF
                END IF
              END IF
            END IF
275       CONTINUE
        END IF
      END IF
      RETURN
1200  FORMAT(1X,I3)
1250  FORMAT(1X,I5,1X,F6.2)
      END
C
C*********************************************************************
C
      SUBROUTINE ROUT1
C
      PARAMETER (IH=12,NF=16,I1=7,I2=46,I3=2,I4=54,I5=2)
      PARAMETER (NU=9,K9=2,MK=20,MJ=30,I4P=55,NSA=127,MT=100)
      PARAMETER (N1=11,N2=22,N3=33,N4=44,N5=55,N6=66,N7=77,N8=88,N9=90)
      COMMON/MAIN/NS,NSUB,IC,IS,NC,I,J,NTTOT,LAP,TINC,TIME,
     *LC,AREAM2(IH),CHANLENM(IH),IHV,WID(I1,I2,I3,I4),NCAS(I1,I2),
     *CHRAIN(I1,I2,I3,I4),CSUMI(I1,I2,I3,I4),HARM2(I1,I2,I3,I4),
     *CARM2(I1,I2),MAXU,AIN(NU),BIN(NU),UCM2(I1,I2,NU),SQ(I1,I2,I3,I4),
     *UHM2(I1,I2,I3,I4,NU),RAG(NSA),RBG(NSA),WWPRAT(NSA),
     *RAM(NU),RBM(NU),NSU(NSA),RIR(I1,I2,I3,I4),UIR(NU),
     *Q(I1,I2,I3,I4,I5),NITS,NR,NTMOD,NP,SLOPE(I1,I2,I3,I4)
      COMMON/HILL/NELM(I1,I2,I3),IHY(I1,I2,I3,I4),A(I1,I2,I3,I4),
     *B(I1,I2,I3,I4),RLEN(I1,I2,I3,I4),HPOTI,
     *SUMI(I1,I2,I3,I4),HAREA(I1,I2,I3,I4,I5),HPOTI1,
     *TRAIN(I1,I2,I3,I4),K44,SRAIN(I4),
     *NUNIT(I1,I2,I3,I4),AP(I1,I2,I3,I4),RA(I1,I2,I3,I4),
     *RB(I1,I2,I3,I4),TPR(I1,I2,I3,I4),NUMA(I1,I2,I3,I4),
     *AM(I1,I2,I3,I4),BM(I1,I2,I3,I4),NUMB(I1,I2,I3,I4),TT(I1,I2,I3,I4),
     *SUMA(I1,I2,13,I4),VS(I1,I2,I3,I4),TO(I1,I2,I3,I4)
      COMMON/INF1/SUCK1,SUCK2
C
c they seek to deal with infiltration under conditions of rainfall
c pre-ponding, rainfall and overland flow, and overland flow post-rainfall
c whilst attempting to decide if a negative depth is occurring due to
c infiltration excess over rainfall and inflow (which
c results in the total infiltration in that time period being equal to the
c rainfall and the inflow..seperated into SUCK1 and
C SUCK2, and the area HAREA(IC,IS,NC,I,1/2) set to zero or due
C to routing instabilities which will eventually cause the program to crash
C and error messages to be printed out
c
c SUCK1..the infiltration from rainfall J=1
C HAREA(IC,IS,NC,I,1)..flow area in cell after the first time period
c SUMI(IC,IS,NC,I)..sum of infiltration in cell I in volumetric terms
C
      SAVE
C
      REAL AA
      SUCK1=0.0
      SRAIN(I)=0.0
      HPOTI=0.0
      HPOTI1=0.0
```

```
NP=1
CALL URAIN
IF (IHV.GT.0) THEN
  SRAIN(I)=SRAIN(I)*COS(ASIN(SLOPE(IC,IS,NC,I)))
END IF
IF (A(IC,IS,NC,I).GT.0.0) THEN
  IF (NUMA(IC,IS,NC,I).GT.0) THEN
    TT(IS,IC,NC,I)=TT(IC,IS,NC,I)+TINC
  ELSE IF (NUMA(IC,IS,NC,I).EQ.0) THEN
    AA=SRAIN(I)/(TINC*TPR(IC,IS,NC,I))
    IF (AA.GE.A(IC,IS,NC,I)) THEN
      NUMA(IC,IS,NC,I)=1
      TT(IC,IS,NC,I)=TINC
      AP(IC,IS,NC,I)=AP(IC,IS,NC,I)+(AA*TINC)
    END IF
  END IF
  IF (NUMB(IC,IS,NC,I).EQ.0) THEN
    IF (NUMA(IC,IS,NC,I).GT.0) THEN
      AA=SRAIN(I)*WID(IC,IS,NC,I)/TINC
      TO(IC,IS,NC,I)=B(IC,IS,NC,I)/((AA
*/(WID(IC,IS,NC,I)*TPR(IC,IS,NC,I)))-A(IC,IS,NC,I))
      SUMA(IC,IS,NC,I)=SUMA(IC,IS,NC,I)+AA
      IF ((TO(IC,IS,NC,I).GT.0.0) .AND. (TO(IC,IS,NC,I).LE.
*TT(IC,IS,NC,I))) THEN
        NUMB(IC,IS,NC,I)=1
        VS(IC,IS,NC,I)=((AA/(WID(IC,IS,NC,I)*
*TPR(IC,IS,NC,I)))*B(IC,IS,NC,I))/((AA/
*(WID(IC,IS,NC,I)*TPR(IC,IS,NC,I)))-A(IC,IS,NC,I))
        WRITE(N4,9000) IC,IS,NC,I,NUNIT(IC,IS,NC,I),
*TIME,TO(IC,IS,NC,I),VS(IC,IS,NC,I)
      END IF
    END IF
  END IF
  IF (NUMB(IC,IS,NC,I).GT.0) THEN
    HPOTI=(A(IC,IS,NC,I)+(B(IC,IS,NC,I)/TT(IC,IS,NC,I)))*
*TINC*TPR(IC,IS,NC,I)*WID(IC,IS,NC,I)
    HPOTI1=((SRAIN(I)*WID(IC,IS,NC,I))-HPOTI)
    IF (HPOTI1.LT.(0.0)) THEN
      HAREA(IC,IS,NC,I,1)=0.0
      SUCK1=SRAIN(I)*WID(IC,IS,NC,I)
    ELSE IF (HPOTI1.GE.(0.0)) THEN
      HAREA(IC,IS,NC,I,1)=HPOTI1
      SUCK1=(SRAIN(I)*WID(IC,IS,NC,I))-HPOTI1
    END IF
    SUMI(IC,IS,NC,I)=SUCK1*RLEN(IC,IS,NC,I)
  ELSE IF (NUMB(IC,IS,NC,I).EQ.0) THEN
    SUMI(IC,IS,NC,I)=SRAIN(I)*WID(IC,IS,NC,I)*RLEN(IC,IS,NC,I)
  END IF
ELSE IF (A(IC,IS,NC,I).EQ.0.0) THEN
  IF (NUMA(IC,IS,NC,I).GT.0) THEN
    TT(IS,IC,NC,I)=TT(IC,IS,NC,I)+TINC
    HAREA(IC,IS,NC,I,1)=SRAIN(I)*WID(IC,IS,NC,I)
  ELSE IF (NUMA(IC,IS,NC,I).EQ.0) THEN
    IF (SRAIN(I).GT.0.0) THEN
      NUMA(IC,IS,NC,I)=1
      TT(IC,IS,NC,I)=TINC
      HAREA(IC,IS,NC,I,1)=SRAIN(I)*WID(IC,IS,NC,I)
    END IF
  END IF
END IF
TRAIN(IC,IS,NC,I)=SRAIN(I)*RLEN(IC,IS,NC,I)*WID(IC,IS,NC,I)
IF (I.LT.NELM(IC,IS,NC)) THEN
  CHRAIN(IC,IS,NC,I)=TRAIN(IC,IS,NC,I)+CHRAIN(IC,IS,NC,(I+1))
  CSUMI(IC,IS,NC,I)=SUMI(IC,IS,NC,I)+CSUMI(IC,IS,NC,(I+1))
ELSE IF (I.EQ.NELM(IC,IS,NC)) THEN
  CHRAIN(IC,IS,NC,I)=TRAIN(IC,IS,NC,I)
  CSUMI(IC,IS,NC,I)=SUMI(IC,IS,NC,I)
END IF
IF (HAREA(IC,IS,NC,I,1).LT.(0.0)) THEN
```

```
        WRITE(*,1000) TIME,IC,IS,NC,I,HAREA(IC,IS,NC,I,1)
       END IF
       CALL DISC
       RETURN
1000   FORMAT(1X,'Error 1',1X,F8.2,1X,I2,1X,I2,1X,I1,1X,I2,1X,F9.3)
9000   FORMAT(1X,'Excess ',I2,1X,I2,1X,I1,1X,I2,1X,I2,' time ',
      *1X,F8.2,1X,' To and Vs ',F9.4,1X,F7.4)
       END
C
C*****************************************************************
C
       SUBROUTINE ROUT2
C
       PARAMETER (IH=12,NF=16,I1=7,I2=46,I3=2,I4=54,I5=2)
       PARAMETER (NU=9,K9=2,MK=20,MJ=30,I4P=55,NSA=127,MT=100)
       PARAMETER (N1=11,N2=22,N3=33,N4=44,N5=55,N6=66,N7=77,N8=88,N9=90)
       PARAMETER (CON=10.0)
       COMMON/MAIN/NS,NSUB,IC,IS,NC,I,J,NTTOT,LAP,TINC,TIME,
      *LC,AREAM2(IH),CHANLENM(IH),IHV,WID(I1,I2,I3,I4),NCAS(I1,I2),
      *CHRAIN(I1,I2,I3,I4),CSUMI(I1,I2,I3,I4),HARM2(I1,I2,I3,I4),
      *CARM2(I1,I2),MAXU,AIN(NU),BIN(NU),UCM2(I1,I2,NU),SQ(I1,I2,I3,I4),
      *UHM2(I1,I2,I3,I4,NU),RAG(NSA),RBG(NSA),WWPRAT(NSA),
      *RAM(NU),RBM(NU),NSU(NSA),RIR(I1,I2,I3,I4),UIR(NU),
      *Q(I1,I2,I3,I4,I5),NITS,NR,NTMOD,NP,SLOPE(I1,I2,I3,I4)
       COMMON/HILL/NELM(I1,I2,I3),IHY(I1,I2,I3,I4),A(I1,I2,I3,I4),
      *B(I1,I2,I3,I4),RLEN(I1,I2,I3,I4),HPOTI,
      *SUMI(I1,I2,I3,I4),HAREA(I1,I2,I3,I4,I5),HPOTI1,
      *TRAIN(I1,I2,I3,I4),K44,SRAIN(I4),
      *NUNIT(I1,I2,I3,I4),AP(I1,I2,I3,I4),RA(I1,I2,I3,I4),
      *RB(I1,I2,I3,I4),TPR(I1,I2,I3,I4),NUMA(I1,I2,I3,I4),
      *AM(I1,I2,I3,I4),BM(I1,I2,I3,I4),NUMB(I1,I2,I3,I4),TT(I1,I2,I3,I4),
      *SUMA(I1,I2,13,I4),VS(I1,I2,I3,I4),TO(I1,I2,I3,I4)
       COMMON/INF1/SUCK1,SUCK2
c subroutine ROUT2 handles the routing calculations of infiltration and
c discharge for times greater than J=1, i.e. where flows from an upper to
c a lower element can occur
c infiltration is calculated by using the average of two rates; the rate
c at the start of the time period plus the rate at the end of the time period in
c question multiplied by the time period and divided by 2
c
c  the subroutine infiltrates from rainfall and/or a ponded store
c  and accounts for the level of infiltration under all circumstances
c
c the subroutine ROUT2 works out HPOTI1 which is the
c difference between the rainfall and the potential infiltration in the time
c period TINC
c SUCK1 is the infiltration from rainfall
c if HPOTI1 is negative it means all rain infiltrates and total
c infiltration will depend on the size of HPOTI1 and the
c previous depth and discharges and SUCK2 will be > 0
C if HPOTI1 is positive it means rainfall is greater than
C infiltration potential and actual infiltration will thus be this potential
C rate with SUCK2 equal to zero
c
       INTEGER NUMC(I1,I2,I3,I4)
       REAL ASTOR,HWP,ASTOR2,AA,sarea
       SAVE
       SUCK1=0.0
       SUCK2=0.0
       HWP=0.0
C
       SRAIN(I)=0.0
       HPOTI=0.0
       HPOTI1=0.0
       NP=1
       CALL URAIN
       IF (IHV.GT.0) THEN
         SRAIN(I)=SRAIN(I)*COS(ASIN(SLOPE(IC,IS,NC,I)))
       END IF
```

```
 IF (A(IC,IS,NC,I).GT.0.0) THEN
   IF (I.LT.NELM(IC,IS,NC)) THEN
     AA=((SRAIN(I)*WID(IC,IS,NC,I))+(Q(IC,IS,NC,I+1,1)/
*RLEN(IC,IS,NC,I)))/(TINC*WID(IC,IS,NC,I)*TPR(IC,IS,NC,I))
   ELSE IF (I.EQ.NELM(IC,IS,NC)) THEN
     AA=SRAIN(I)/(TPR(IC,IS,NC,I)*TINC)
   END IF
   IF (NUMA(IC,IS,NC,I).GT.0) THEN
     TT(IC,IS,NC,I)=TT(IC,IS,NC,I)+TINC
     AP(IC,IS,NC,I)=AP(IC,IS,NC,I)+(AA*TINC)
   ELSE IF (NUMA(IC,IS,NC,I).EQ.0) THEN
     IF (AA.GE.A(IC,IS,NC,I)) THEN
       NUMA(IC,IS,NC,I)=1
       TT(IC,IS,NC,I)=TINC
       AP(IC,IS,NC,I)=AP(IC,IS,NC,I)+(AA*TINC)
     END IF
   END IF
   IF (NUMB(IC,IS,NC,I).EQ.0) THEN
     IF (NUMA(IC,IS,NC,I).GT.0) THEN
       TO(IC,IS,NC,I)=B(IC,IS,NC,I)/((AP(IC,IS,NC,I)/
*TT(IC,IS,NC,I))-A(IC,IS,NC,I))
       IF ((TO(IC,IS,NC,I).GT.0.0) .AND. (TO(IC,IS,NC,I)
*.LE.TT(IC,IS,NC,I))) THEN
         NUMB(IC,IS,NC,I)=1
         VS(IC,IS,NC,I)=(AP(IC,IS,NC,I)/TT(IC,IS,NC,I)*
*B(IC,IS,NC,I))/((AP(IC,IS,NC,I)/TT(IC,IS,NC,I))-A(IC,IS,NC,I))
         WRITE(N4,9000) IC,IS,NC,I,NUNIT(IC,IS,NC,I),time,
*TO(IC,IS,NC,I),VS(IC,IS,NC,I)
       END IF
     END IF
   END IF
   IF (NUMB(IC,IS,NC,I).GT.0) THEN
     HPOTI=(A(IC,IS,NC,I)+(B(IC,IS,NC,I)/TT(IC,IS,NC,I)))*TINC*
*TPR(IC,IS,NC,I)*WID(IC,IS,NC,I)
     HPOTI1=((SRAIN(I)*WID(IC,IS,NC,I))-HPOTI)
     TRAIN(IC,IS,NC,I)=TRAIN(IC,IS,NC,I)+(SRAIN(I)*
*RLEN(IC,IS,NC,I)*WID(IC,IS,NC,I))
     IF (I.LT.NELM(IC,IS,NC)) THEN
       CHRAIN(IC,IS,NC,I)=TRAIN(IC,IS,NC,I)+CHRAIN(IC,IS,NC,(I+1))
       HAREA(IC,IS,NC,I,2)=HAREA(IC,IS,NC,I,1)+
*((Q(IC,IS,NC,(I+1),1)-Q(IC,IS,NC,I,1))/RLEN(IC,IS,NC,I))
     ELSE IF (I.EQ.NELM(IC,IS,NC)) THEN
       CHRAIN(IC,IS,NC,I)=TRAIN(IC,IS,NC,I)
       HAREA(IC,IS,NC,I,2)=HAREA(IC,IS,NC,I,1)-(Q(IC,IS,NC,I,1)/
*RLEN(IC,IS,NC,I))
     END IF
     ASTOR=HAREA(IC,IS,NC,I,2)
     IF (HPOTI1.LT.(0.0)) THEN
       SUCK1=SRAIN(I)*WID(IC,IS,NC,I)
     ELSE IF (HPOTI1.GE.(0.0)) THEN
       SUCK1=(SRAIN(I)*WID(IC,IS,NC,I))-HPOTI1
     END IF
     IF ((HPOTI1.LT.(0.0)) .AND. (ASTOR.GE.(0.0))) THEN
       HPOTI1=HPOTI1/RIR(IC,IS,NC,I)
       IF (ASTOR.GT.0.0) THEN
         ASTOR2=ASTOR/(WID(IC,IS,NC,I)/190.0)
         HWP=CON**(RA(IC,IS,NC,I)+(RB(IC,IS,NC,I)*LOG10(ASTOR2)))
         IF (HWP.GT.(190.0*TPR(IC,IS,NC,I))) THEN
           HWP=TPR(IC,IS,NC,I)*190.0
         END IF
         HWP=HWP*(WID(IC,IS,NC,I)/190.0)
       END IF
       HAREA(IC,IS,NC,I,2)=ASTOR+(HPOTI1*(HWP/(WID(IC,IS,NC,I)*
*TPR(IC,IS,NC,I))))
       IF (HAREA(IC,IS,NC,I,2).LE.(0.0)) THEN
         SUCK2=ASTOR
         HAREA(IC,IS,NC,I,2)=0.0
       ELSE IF (HAREA(IC,IS,NC,I,2).GT.(0.0)) THEN
         SUCK2=ABS(HPOTI1*(HWP/(WID(IC,IS,NC,I)*TPR(IC,IS,NC,I))))
```

```
          END IF
        END IF
        IF ((HPOTI1.GE.(0.0)) .AND. (ASTOR.GE.(0.0))) THEN
          HAREA(IC,IS,NC,I,2)=ASTOR+HPOTI1
          SUCK2=0.0
        END IF
        SUMI(IC,IS,NC,I)=SUMI(IC,IS,NC,I)+((SUCK1+
     *SUCK2)*RLEN(IC,IS,NC,I))
        IF ((HAREA(IC,IS,NC,I,2).EQ.0.0) .AND.
     *(NUMC(IC,IS,NC,I).EQ.0)) THEN
          WRITE(N4,9100) IC,IS,NC,I,NUNIT(IC,IS,NC,I),TIME
          NUMC(IC,IS,NC,I)=1
        END IF
      ELSE IF (NUMB(IC,IS,NC,I).EQ.0) THEN
        TRAIN(IC,IS,NC,I)=TRAIN(IC,IS,NC,I)+(SRAIN(I)*
     *RLEN(IC,IS,NC,I)*WID(IC,IS,NC,I))
        IF (I.LT.NELM(IC,IS,NC)) THEN
          CHRAIN(IC,IS,NC,I)=TRAIN(IC,IS,NC,I)+CHRAIN(IC,IS,NC,(I+1))
          SUMI(IC,IS,NC,I)=TRAIN(IC,IS,NC,I)+SQ(IC,IS,NC,(I+1))
        ELSE IF (I.EQ.NELM(IC,IS,NC)) THEN
          CHRAIN(IC,IS,NC,I)=TRAIN(IC,IS,NC,I)
          SUMI(IC,IS,NC,I)=TRAIN(IC,IS,NC,I)
        END IF
      END IF
     ELSE IF (A(IC,IS,NC,I).EQ.0.0) THEN
       IF (NUMA(IC,IS,NC,I).GT.0) THEN
         TT(IC,IS,NC,I)=TT(IC,IS,NC,I)+TINC
       ELSE IF (NUMA(IC,IS,NC,I).EQ.0) THEN
         IF ((SRAIN(I).GT.0.0) .OR. (SQ(IC,IS,NC,(I+1)).GT.0.0)) THEN
           NUMA(IC,IS,NC,I)=1
           TT(IC,IS,NC,I)=TINC
         END IF
       END IF
       TRAIN(IC,IS,NC,I)=TRAIN(IC,IS,NC,I)+(SRAIN(I)*
     *RLEN(IC,IS,NC,I)*WID(IC,IS,NC,I))
       IF (I.LT.NELM(IC,IS,NC)) THEN
         CHRAIN(IC,IS,NC,I)=TRAIN(IC,IS,NC,I)+CHRAIN(IC,IS,NC,(I+1))
         HAREA(IC,IS,NC,I,2)=HAREA(IC,IS,NC,I,1)+(SRAIN(I)*
     *WID(IC,IS,NC,I))+
     *((Q(IC,IS,NC,(I+1),1)-Q(IC,IS,NC,I,1))/RLEN(IC,IS,NC,I))
       ELSE IF (I.EQ.NELM(IC,IS,NC)) THEN
         CHRAIN(IC,IS,NC,I)=TRAIN(IC,IS,NC,I)
         HAREA(IC,IS,NC,I,2)=HAREA(IC,IS,NC,I,1)-(Q(IC,IS,NC,I,1)/
     *RLEN(IC,IS,NC,I))+(SRAIN(I)*WID(IC,IS,NC,I))
       END IF
     END IF
     IF (I.LT.NELM(IC,IS,NC)) THEN
       CSUMI(IC,IS,NC,I)=SUMI(IC,IS,NC,I)+CSUMI(IC,IS,NC,(I+1))
     ELSE IF (I.EQ.NELM(IC,IS,NC)) THEN
       CSUMI(IC,IS,NC,I)=SUMI(IC,IS,NC,I)
     END IF
     IF (HAREA(IC,IS,NC,I,2).LT.(0.0)) THEN
       WRITE(*,1000) TIME,IC,IS,NC,I,HAREA(IC,IS,NC,I,2)
     END IF
     CALL DISC
     RETURN
1000 FORMAT(1X,'Error 2',1X,F8.2,1X,I2,1X,I2,1X,I1,1X,I2,1X,F9.3)
9000 FORMAT(1X,'Excess ',I2,1X,I2,1X,I1,1X,I2,1X,I2,' time ',
    *1X,F8.2,1X,' To and Vs ',F9.4,1X,F7.4)
9100 FORMAT(1X,'Dried up ',I2,1X,I2,1X,I1,1X,I2,1X,I2,' time ',
    *1x,f8.2)
     END
C
C*****************************************************************
C
     SUBROUTINE DISC
C
     PARAMETER (IH=12,NF=16,I1=7,I2=46,I3=2,I4=54,I5=2)
     PARAMETER (NU=9,K9=2,MK=20,MJ=30,I4P=55,NSA=127,MT=100)
```

```
      PARAMETER (N1=11,N2=22,N3=33,N4=44,N5=55,N6=66,N7=77,N8=88,N9=90)
      PARAMETER (CON=10.0)
      COMMON/MAIN/NS,NSUB,IC,IS,NC,I,J,NTTOT,LAP,TINC,TIME,
     *LC,AREAM2(IH),CHANLENM(IH),IHV,WID(I1,I2,I3,I4),NCAS(I1,I2),
     *CHRAIN(I1,I2,I3,I4),CSUMI(I1,I2,I3,I4),HARM2(I1,I2,I3,I4),
     *CARM2(I1,I2),MAXU,AIN(NU),BIN(NU),UCM2(I1,I2,NU),SQ(I1,I2,I3,I4),
     *UHM2(I1,I2,I3,I4,NU),RAG(NSA),RBG(NSA),WWPRAT(NSA),
     *RAM(NU),RBM(NU),NSU(NSA),RIR(I1,I2,I3,I4),UIR(NU),
     *Q(I1,I2,I3,I4,I5),NITS,NR,NTMOD,NP,SLOPE(I1,I2,I3,I4)
      COMMON/HILL/NELM(I1,I2,I3),IHY(I1,I2,I3,I4),A(I1,I2,I3,I4),
     *B(I1,I2,I3,I4),RLEN(I1,I2,I3,I4),HPOTI,
     *SUMI(I1,I2,I3,I4),HAREA(I1,I2,I3,I4,I5),HPOTI1,
     *TRAIN(I1,I2,I3,I4),K44,SRAIN(I4),
     *NUNIT(I1,I2,I3,I4),AP(I1,I2,I3,I4),RA(I1,I2,I3,I4),
     *RB(I1,I2,I3,I4),TPR(I1,I2,I3,I4),NUMA(I1,I2,I3,I4),
     *AM(I1,I2,I3,I4),BM(I1,I2,I3,I4),NUMB(I1,I2,I3,I4),TT(I1,I2,I3,I4),
     *SUMA(I1,I2,13,I4),VS(I1,I2,I3,I4),TO(I1,I2,I3,I4)
      COMMON/COUR/CVEL(I1,I2,I3),VEL(I1,I2,I3,I4,I5),NSTIF,
     *INSTC(I1,I2),INSTH(I1,I2,I3,I4)
C
c subroutine DISC calculates the velocity and discharge
c VEL(IC,IS,NC,I,1/2)..the velocity of flow as calculated by Manning's
c uniform flow equation and adjusted to cm/sec from the original
C formula by a multiplication by the constant 4.64
C Q(IC,IS,NC,I,1/2)..the volumetric discharge
C SQ(IC,IS,NC,I)..the sum of Q over time 1-NTTOT
c
      COMMON/INF1/SUCK1,SUCK2
      SAVE
      REAL HWP,ASTOR2
      HWP=0.0
      ROUGH=0.0
      IF (J.EQ.1) THEN
        IF (HAREA(IC,IS,NC,I,1).GT.0.0) THEN
          ASTOR2=HAREA(IC,IS,NC,I,1)/(WID(IC,IS,NC,I)/190.0)
          HWP=CON**(RA(IC,IS,NC,I)+(RB(IC,IS,NC,I)*LOG10(ASTOR2)))
          IF (HWP.GT.(190.0*TPR(IC,IS,NC,I))) THEN
            HWP=TPR(IC,IS,NC,I)*190.0
          END IF
          HWP=HWP*(WID(IC,IS,NC,I)/190.0)
          ROUGH=AM(IC,IS,NC,I)+(BM(IC,IS,NC,I)*SLOPE(IC,IS,NC,I))
          VEL(IC,IS,NC,I,1)=((SQRT(SLOPE(IC,IS,NC,I))/
     *ROUGH)*((HAREA(IC,IS,NC,I,1)/HWP)**
     *(2.0/3.0))*4.64)
          NSTIF=1
          CALL COURANT
        END IF
        Q(IC,IS,NC,I,1)=VEL(IC,IS,NC,I,1)*HAREA(IC,IS,NC,I,1)*TINC
        SQ(IC,IS,NC,I)=0.0
      ELSE IF (J.GT.1) THEN
        IF (HAREA(IC,IS,NC,I,2).GT.0.0) THEN
          ASTOR2=HAREA(IC,IS,NC,I,2)/(WID(IC,IS,NC,I)/190.0)
          HWP=CON**(RA(IC,IS,NC,I)+(RB(IC,IS,NC,I)*LOG10(ASTOR2)))
          IF (HWP.GT.(190.0*TPR(IC,IS,NC,I))) THEN
            HWP=TPR(IC,IS,NC,I)*190.0
          END IF
          HWP=HWP*(WID(IC,IS,NC,I)/190.0)
          ROUGH=AM(IC,IS,NC,I)+(BM(IC,IS,NC,I)*SLOPE(IC,IS,NC,I))
          VEL(IC,IS,NC,I,2)=((SQRT(SLOPE(IC,IS,NC,I))/
     *ROUGH)*((HAREA(IC,IS,NC,I,2)/HWP)**(2.0/3.0))*4.64)
          NSTIF=1
          CALL COURANT
        END IF
        Q(IC,IS,NC,I,2)=VEL(IC,IS,NC,I,2)*HAREA(IC,IS,NC,I,2)*TINC
        SQ(IC,IS,NC,I)=SQ(IC,IS,NC,I)+Q(IC,IS,NC,I,2)
      END IF
      RETURN
      END
C
```

```
C**********************************************************************
C
      SUBROUTINE CROUT1
C
      PARAMETER (IH=12,NF=16,I1=7,I2=46,I3=2,I4=54,I5=2)
      PARAMETER (NU=9,K9=2,MK=20,MJ=30,I4P=55,NSA=127,MT=100)
      PARAMETER (N1=11,N2=22,N3=33,N4=44,N5=55,N6=66,N7=77,N8=88,N9=90)
      COMMON/MAIN/NS,NSUB,IC,IS,NC,I,J,NTTOT,LAP,TINC,TIME,
     *LC,AREAM2(IH),CHANLENM(IH),IHV,WID(I1,I2,I3,I4),NCAS(I1,I2),
     *CHRAIN(I1,I2,I3,I4),CSUMI(I1,I2,I3,I4),HARM2(I1,I2,I3,I4),
     *CARM2(I1,I2),MAXU,AIN(NU),BIN(NU),UCM2(I1,I2,NU),SQ(I1,I2,I3,I4),
     *UHM2(I1,I2,I3,I4,NU),RAG(NSA),RBG(NSA),WWPRAT(NSA),
     *RAM(NU),RBM(NU),NSU(NSA),RIR(I1,I2,I3,I4),UIR(NU),
     *Q(I1,I2,I3,I4,I5),NITS,NR,NTMOD,NP,SLOPE(I1,I2,I3,I4)
      COMMON/CHAN/NCHA,NSEG(I1),IHYC(I1,I2),EC(I1,I2),TTC(I1,I2),
     *CA(I1,I2),CB(I1,I2),CWID(I1,I2),EANG(I1,I2),WANG(I1,I2),
     *CTOP(I1,I2),CLEN(I1,I2),CGRA(I1,I2),CPER(I1,I2),COPEN(I1,I2),
     *CPOTI,SUMCI(I1,I2),CAREA(I1,I2,I5),CPOTI1,CQ(I1,I2,I5),
     *CSQ(I1,I2),CWP,DEPTH,CTRAIN(I1,I2),K33,CXSA(I1,I2),SCRAIN(I2),
     *CCRAIN(I1,I2),CSUMCI(I1,I2),NUNITC(I1,I2),APC(I1,I2),
     *CCLEN(I1,I2),IOFLOW(I1,I2),NUMAC(I1,I2),NUMBC(I1,I2)
      COMMON/CINF1/CIN1,CIN2
      INTEGER NIC
      REAL ASTOR,WETR,RLATERAL,RLATIN,AA,TOC(I1,I2),VSC(I1,I2)
C
C this subroutine first works out the potential infiltration rate
c CPOTI into the total channel perimeter CPER(IC,IS) in the first
c time period for the channel segment (IC,IS).
      SAVE
c CIN1..the infiltration from rainfall
C CIN2..the infiltration from inflow and throughflow if
c infiltration is more than rainfall
C CAREA(IC,IS,1)..depth in segment after the first time period
c SUMI(IC,IS)..sum of infiltration in segment IS in volumetric terms
c
      CIN1=0.0
      CIN2=0.0
      CWP=0.0
      WETR=0.0
      RLATIN=0.0
      RLATERAL=0.0
      SCRAIN(IS)=0.0
      CPOTI=0.0
      CPOTI1=0.0
      NP=2
      CALL URAIN
      IF (IHV.GT.0) THEN
        SCRAIN(IS)=SCRAIN(IS)*COS(ASIN(CGRA(IC,IS)))
      END IF
      IF (CA(IC,IS).GT.0.0) THEN
        IF (NUMAC(IC,IS).GT.0) THEN
          TTC(IC,IS)=TTC(IC,IS)+TINC
        ELSE IF (NUMAC(IC,IS).EQ.0) THEN
          AA=SCRAIN(IS)/TINC
          IF (AA.GE.CA(IC,IS)) THEN
            NUMAC(IC,IS)=1
            TTC(IC,IS)=TINC
            APC(IC,IS)=APC(IC,IS)+(AA*TINC)
          END IF
        END IF
        IF (NUMBC(IC,IS).EQ.0) THEN
          IF (NUMAC(IC,IS).GT.0) THEN
            AA=SCRAIN(IS)*COPEN(IC,IS)/TINC
            TOC(IC,IS)=CB(IC,IS)/((AA/CPER(IC,IS))-CA(IC,IS))
            IF ((TOC(IC,IS).GT.0.0) .AND. (TOC(IC,IS).LE.
     *TTC(IC,IS))) THEN
              NUMBC(IC,IS)=1
              VSC(IC,IS)=((AA/CPER(IC,IS))*CB(IC,IS))/((AA/CPER(IC,IS))
     *-CA(IC,IS))
```

```
        write(n4,9000) ic,is,NUNITC(IC,IS),time,
*toc(ic,is),vsc(ic,is)
       END IF
     END IF
   END IF
   IF (NUMBC(IC,IS).GT.0) THEN
     CPOTI=((CA(IC,IS)+(CB(IC,IS)/TTC(IC,IS)))*TINC)*CPER(IC,IS)
     CPOTI1=(SCRAIN(IS)*COPEN(IC,IS))-CPOTI
     CTRAIN(IC,IS)=SCRAIN(IS)*COPEN(IC,IS)*CLEN(IC,IS)
     IF (NCAS(IC,IS).EQ.1) THEN
       RLATERAL=Q(IC,IS,1,1,1)
     ELSE IF (NCAS(IC,IS).EQ.2) THEN
       RLATERAL=Q(IC,IS,1,1,1)+Q(IC,IS,2,1,1)
     END IF
     CAREA(IC,IS,1)=(RLATERAL/CLEN(IC,IS))
     ASTOR=CAREA(IC,IS,1)
     IF (CPOTI1.LT.(0.0)) THEN
       CIN1=SCRAIN(IS)*COPEN(IC,IS)
     ELSE IF (CPOTI1.GE.(0.0)) THEN
       CIN1=(SCRAIN(IS)*COPEN(IC,IS))-CPOTI1
     END IF
     IF ((CPOTI1.LT.(0.0)) .AND. (ASTOR.GE.(0.0))) THEN
       IF (ASTOR.GT.0.0) THEN
         CALL CDQUAD
       END IF
       IF (CWP.LE.CPER(IC,IS)) THEN
         WETR=(CWP/CPER(IC,IS))
       ELSE IF (CWP.GT.CPER(IC,IS)) THEN
         WETR=1.0
       END IF
       CAREA(IC,IS,1)=ASTOR+(CPOTI1*WETR)
       IF (CAREA(IC,IS,1).LE.(0.0)) THEN
         CIN2=ASTOR
         CAREA(IC,IS,1)=0.0
       ELSE IF (CAREA(IC,IS,1).GT.(0.0)) THEN
         CIN2=ABS(CPOTI1*WETR)
       END IF
     END IF
     IF ((CPOTI1.GE.(0.0)) .AND. (ASTOR.GE.(0.0))) THEN
       CAREA(IC,IS,1)=ASTOR+CPOTI1
       CIN2=0.0
     END IF
     SUMCI(IC,IS)=(CIN1+CIN2)*CLEN(IC,IS)
   ELSE IF (NUMBC(IC,IS).EQ.0) THEN
     CTRAIN(IC,IS)=SCRAIN(IS)*COPEN(IC,IS)*CLEN(IC,IS)
     IF (NCAS(IC,IS).EQ.1) THEN
       RLATERAL=Q(IC,IS,1,1,1)
     ELSE IF (NCAS(IC,IS).EQ.2) THEN
       RLATERAL=Q(IC,IS,1,1,1)+Q(IC,IS,2,1,1)
     END IF
     SUMCI(IC,IS)=(SCRAIN(IS)*COPEN(IC,IS)*CLEN(IC,IS))+RLATERAL
   END IF
 ELSE IF (CA(IC,IS).EQ.0.0) THEN
   IF (NUMAC(IC,IS).GT.0) THEN
     TTC(IC,IS)=TTC(IC,IS)+TINC
   ELSE IF (NUMAC(IC,IS).EQ.0) THEN
     IF ((SCRAIN(IS).GT.0.0) .OR. (Q(IC,IS,2,1,1).GT.0.0)
* .OR. (Q(IC,IS,1,1,1).GT.0.0)) THEN
       NUMAC(IC,IS)=1
       TTC(IC,IS)=TINC
     END IF
   END IF
   IF (NCAS(IC,IS).EQ.1) THEN
     RLATERAL=Q(IC,IS,1,1,1)
   ELSE IF (NCAS(IC,IS).EQ.2) THEN
     RLATERAL=Q(IC,IS,1,1,1)+Q(IC,IS,2,1,1)
   END IF
   CAREA(IC,IS,1)=(RLATERAL/CLEN(IC,IS))+(SCRAIN(IS)*
*COPEN(IC,IS))
```

```
        CTRAIN(IC,IS)=SCRAIN(IS)*COPEN(IC,IS)*CLEN(IC,IS)
       END IF
       IF (NCAS(IC,IS).EQ.1) THEN
         RLATERAL=CHRAIN(IC,IS,1,1)
       ELSE IF (NCAS(IC,IS).EQ.2) THEN
         RLATERAL=CHRAIN(IC,IS,1,1)+CHRAIN(IC,IS,2,1)
       END IF
       NIC=NCHA-((NCHA+1)/2)
       IF ((IC.GT.NIC) .AND. (IS.EQ.NSEG(IC))) THEN
         CCRAIN(IC,IS)=CTRAIN(IC,IS)+RLATERAL
       ELSE IF ((IC.GT.NIC) .AND. (IS.LT.NSEG(IC))) THEN
         CCRAIN(IC,IS)=CTRAIN(IC,IS)+CCRAIN(IC,(IS+1))+RLATERAL
       ELSE IF ((IC.LE.NIC) .AND. (IS.EQ.NSEG(IC))) THEN
         CCRAIN(IC,IS)=CTRAIN(IC,IS)+CCRAIN((IC+IC),1)+
      *CCRAIN((IC+IC+1),1)+RLATERAL
       ELSE IF ((IC.LE.NIC) .AND. (IS.LT.NSEG(IC))) THEN
         CCRAIN(IC,IS)=CTRAIN(IC,IS)+CCRAIN(IC,(IS+1))+RLATERAL
       END IF
       IF (NCAS(IC,IS).EQ.1) THEN
         RLATERAL=CSUMI(IC,IS,1,1)
       ELSE IF (NCAS(IC,IS).EQ.2) THEN
         RLATERAL=CSUMI(IC,IS,1,1)+CSUMI(IC,IS,2,1)
       END IF
       IF ((IC.GT.NIC) .AND. (IS.EQ.NSEG(IC))) THEN
         CSUMCI(IC,IS)=SUMCI(IC,IS)+RLATERAL
       ELSE IF ((IC.GT.NIC) .AND. (IS.LT.NSEG(IC))) THEN
         CSUMCI(IC,IS)=SUMCI(IC,IS)+CSUMCI(IC,(IS+1))+RLATERAL
       ELSE IF ((IC.LE.NIC) .AND. (IS.EQ.NSEG(IC))) THEN
         CSUMCI(IC,IS)=SUMCI(IC,IS)+CSUMCI((IC+IC),1)+
      *CSUMCI((IC+IC+1),1)+RLATERAL
       ELSE IF ((IC.LE.NIC) .AND. (IS.LT.NSEG(IC))) THEN
         CSUMCI(IC,IS)=SUMCI(IC,IS)+CSUMCI(IC,(IS+1))+RLATERAL
       END IF
       IF (CAREA(IC,IS,1).LT.(0.0)) THEN
         WRITE(*,1000) TIME,IC,IS,CAREA(IC,IS,1)
       END IF
1000   FORMAT(1X,'Error 3',1X,F8.2,1X,I2,1X,I2,5X,1X,F9.3)
9000   FORMAT(1X,'Excess channel',I2,1X,I2,1X,I2,1X,
      *' time = ',F8.2,1X,' To and Vs ',F9.4,1X,F7.4)
C
       CALL CDISC
       RETURN
       END
C
C*****************************************************************
C
       SUBROUTINE CROUT2
C
       PARAMETER (IH=12,NF=16,I1=7,I2=46,I3=2,I4=54,I5=2)
       PARAMETER (NU=9,K9=2,MK=20,MJ=30,I4P=55,NSA=127,MT=100)
       PARAMETER (N1=11,N2=22,N3=33,N4=44,N5=55,N6=66,N7=77,N8=88,N9=90)
       COMMON/MAIN/NS,NSUB,IC,IS,NC,I,J,NTTOT,LAP,TINC,TIME,
      *LC,AREAM2(IH),CHANLENM(IH),IHV,WID(I1,I2,I3,I4),NCAS(I1,I2),
      *CHRAIN(I1,I2,I3,I4),CSUMI(I1,I2,I3,I4),HARM2(I1,I2,I3,I4),
      *CARM2(I1,I2),MAXU,AIN(NU),BIN(NU),UCM2(I1,I2,NU),SQ(I1,I2,I3,I4),
      *UHM2(I1,I2,I3,I4,NU),RAG(NSA),RBG(NSA),WWPRAT(NSA),
      *RAM(NU),RBM(NU),NSU(NSA),RIR(I1,I2,I3,I4),UIR(NU),
      *Q(I1,I2,I3,I4,I5),NITS,NR,NTMOD,NP,SLOPE(I1,I2,I3,I4)
       COMMON/CHAN/NCHA,NSEG(I1),IHYC(I1,I2),EC(I1,I2),TTC(I1,I2),
      *CA(I1,I2),CB(I1,I2),CWID(I1,I2),EANG(I1,I2),WANG(I1,I2),
      *CTOP(I1,I2),CLEN(I1,I2),CGRA(I1,I2),CPER(I1,I2),COPEN(I1,I2),
      *CPOTI,SUMCI(I1,I2),CAREA(I1,I2,I5),CPOTI1,CQ(I1,I2,I5),
      *CSQ(I1,I2),CWP,DEPTH,CTRAIN(I1,I2),K33,CXSA(I1,I2),SCRAIN(I2),
      *CCRAIN(I1,I2),CSUMCI(I1,I2),NUNITC(I1,I2),APC(I1,I2),
      *CCLEN(I1,I2),IOFLOW(I1,I2),NUMAC(I1,I2),NUMBC(I1,I2)
       COMMON/CINF1/CIN1,CIN2
       REAL ASTOR,WETR,RLATERAL,RLATIN,AA,TOC(I1,I2),VSC(I1,I2)
       INTEGER NIC,NUMCC(I1,I2)
C
```

```
c the infiltration not satisfied by rainfall is calculated as the
c difference between the two - CPOTI1
c the subroutine also works out the amount of throughflow in the channel
c for the time increment by calculating a net balance between the flow
c area at the end of the last time period 1; CAREA(IC,IS,1), the lateral
c inflow (in area dimensions) into the particular channel segment;
c Q(IC,IS,1,1,2) and Q(IC,IS,2,1,2), and the difference between the
c discharge in from the previous segment in the previous time and
c the discharge out the proceeding segment in the previous time.
C if CPOTI1 is negative then infiltration is equal to CIN1 plus CIN2 where
c CIN1 is the infiltration satisfied by rainfall CIN2 is the infiltration
c satisfied by throughflow.
c if the net flow area CAREA(IC,IS,2) is positive and CPOTI1 is
c negative then infiltration will occur.  it is assumed that this will be
c in direct proportion to the wetted perimiter and thus the actual
c infiltration from the flow area is CPOTI1 multiplied by the
c ratio of the wetted perimiter and the total channel perimiter (with
c which the maximum potential infiltration was calculated).
c to establish the wetted perimiter, the flow depth must be calculated
c which is done in the subroutine CDQUAD.  this calculates the depth for
c the cross-section at segment (IC,IS) corresponding to flow area
c CAREA(IC,IS,2).
c if the new CAREA(IC,IS,2) is negative after subtracting this potential
c infiltration, it means that there is infiltration excess and no water
c will be available for routing.
      SAVE
      CWP=0.0
      WETR=0.0
      CIN1=0.0
      CIN2=0.0
      RLATIN=0.0
      RLATERAL=0.0
      SCRAIN(IS)=0.0
      CPOTI=0.0
      CPOTI1=0.0
      NP=2
      CALL URAIN
      IF (IHV.GT.0) THEN
        SCRAIN(IS)=SCRAIN(IS)*COS(ASIN(CGRA(IC,IS)))
      END IF
      IF (CA(IC,IS).GT.0.0) THEN
        IF (NUMAC(IC,IS).GT.0) THEN
          TTC(IC,IS)=TTC(IC,IS)+TINC
          IF (TIME.GE.REAL(NTTOT)) THEN
            RLATIN=0.0
          ELSE IF (TIME.LT.REAL(NTTOT)) THEN
            IF (NCAS(IC,IS).EQ.1) THEN
              RLATIN=Q(IC,IS,1,1,2)/CLEN(IC,IS)
            ELSE IF (NCAS(IC,IS).EQ.2) THEN
              RLATIN=(Q(IC,IS,1,1,2)+Q(IC,IS,2,1,2))/CLEN(IC,IS)
            END IF
          END IF
          NIC=NCHA-((NCHA+1)/2)
          IF ((IC.GT.NIC) .AND. (IS.EQ.NSEG(IC))) THEN
            AA=((SCRAIN(IS)*COPEN(IC,IS))+RLATIN)/(TINC*CPER(IC,IS))
          ELSE IF ((IC.GT.NIC) .AND. (IS.LT.NSEG(IC))) THEN
            AA=((SCRAIN(IS)*COPEN(IC,IS))+RLATIN+(CQ(IC,(IS+1),1)
     */CLEN(IC,IS)))/(TINC*CPER(IC,IS))
          ELSE IF ((IC.LE.NIC) .AND. (IS.EQ.NSEG(IC))) THEN
            AA=((SCRAIN(IS)*COPEN(IC,IS))+RLATIN+((CQ((IC+IC),1,1)
     *+CQ((IC+IC+1),1,1))/CLEN(IC,IS)))/(TINC*CPER(IC,IS))
          ELSE IF ((IC.LE.NIC) .AND. (IS.LT.NSEG(IC))) THEN
            AA=((SCRAIN(IS)*COPEN(IC,IS))+RLATIN+(CQ(IC,(IS+1),1)/
     *CLEN(IC,IS)))/(TINC*CPER(IC,IS))
          END IF
          IF (NUMAC(IC,IS).GT.0) THEN
            TTC(IC,IS)=TTC(IC,IS)+TINC
            APC(IC,IS)=APC(IC,IS)+(AA*TINC)
          ELSE IF (NUMAC(IC,IS).EQ.0) THEN
```

```
       IF (AA.GE.CA(IC,IS)) THEN
         NUMAC(IC,IS)=1
         TTC(IC,IS)=TINC
         APC(IC,IS)=APC(IC,IS)+(AA*TINC)
       END IF
     END IF
   END IF
   IF (NUMBC(IC,IS).EQ.0) THEN
     IF (NUMAC(IC,IS).GT.0) THEN
       TOC(IC,IS)=CB(IC,IS)/((APC(IC,IS)/TTC(IC,IS))-CA(IC,IS))
       IF ((TOC(IC,IS).GT.0.0) .AND. (TOC(IC,IS).LE.
*TTC(IC,IS))) THEN
         NUMBC(IC,IS)=1
         VSC(IC,IS)=((APC(IC,IS)/TTC(IC,IS))*CB(IC,IS))/
*((APC(IC,IS)/TTC(IC,IS))-CA(IC,IS))
       write(n4,9000) ic,is,NUNITC(IC,IS),time,
*toc(ic,is),vsc(ic,is)
       END IF
     END IF
   END IF
   IF (NUMBC(IC,IS).GT.0) THEN
     CPOTI=CA(IC,IS)+(CB(IC,IS)/TTC(IC,IS))*TINC*CPER(IC,IS)
     CPOTI1=(SCRAIN(IS)*COPEN(IC,IS))-CPOTI
     CTRAIN(IC,IS)=CTRAIN(IC,IS)+(SCRAIN(IS)*
*CLEN(IC,IS)*COPEN(IC,IS))
     IF (TIME.GE.REAL(NTTOT)) THEN
       RLATIN=0.0
     ELSE IF (TIME.LT.REAL(NTTOT)) THEN
       IF (NCAS(IC,IS).EQ.1) THEN
         RLATIN=Q(IC,IS,1,1,2)/CLEN(IC,IS)
       ELSE IF (NCAS(IC,IS).EQ.2) THEN
         RLATIN=(Q(IC,IS,1,1,2)+Q(IC,IS,2,1,2))/CLEN(IC,IS)
       END IF
     END IF
     NIC=NCHA-((NCHA+1)/2)
     IF ((IC.GT.NIC) .AND. (IS.EQ.NSEG(IC))) THEN
       CAREA(IC,IS,2)=CAREA(IC,IS,1)+RLATIN-(CQ(IC,IS,1)/
*CLEN(IC,IS))
     ELSE IF ((IC.GT.NIC) .AND. (IS.LT.NSEG(IC))) THEN
       CAREA(IC,IS,2)=CAREA(IC,IS,1)+RLATIN+((CQ(IC,(IS+1),1)
*-CQ(IC,IS,1))/CLEN(IC,IS))
     ELSE IF ((IC.LE.NIC) .AND. (IS.EQ.NSEG(IC))) THEN
       CAREA(IC,IS,2)=CAREA(IC,IS,1)+RLATIN+((CQ((IC+IC),1,1)
*+CQ((IC+IC+1),1,1)-CQ(IC,IS,1))/CLEN(IC,IS))
     ELSE IF ((IC.LE.NIC) .AND. (IS.LT.NSEG(IC))) THEN
       CAREA(IC,IS,2)=CAREA(IC,IS,1)+RLATIN+((CQ(IC,(IS+1),1)
*-CQ(IC,IS,1))/CLEN(IC,IS))
     END IF
     ASTOR=CAREA(IC,IS,2)
     IF (CPOTI1.LT.(0.0)) THEN
       CIN1=SCRAIN(IS)*COPEN(IC,IS)
     ELSE IF (CPOTI1.GE.(0.0)) THEN
       CIN1=(SCRAIN(IS)*COPEN(IC,IS))-CPOTI1
     END IF
     IF ((CPOTI1.LT.(0.0)) .AND. (ASTOR.GE.(0.0))) THEN
       IF (ASTOR.GT.0.0) THEN
         CALL CDQUAD
       END IF
       IF (CWP.LE.CPER(IC,IS)) THEN
         WETR=(CWP/CPER(IC,IS))
       ELSE IF (CWP.GT.CPER(IC,IS)) THEN
         WETR=1.0
       END IF
       CAREA(IC,IS,2)=ASTOR+(CPOTI1*WETR)
       IF (CAREA(IC,IS,2).LE.(0.0)) THEN
         CIN2=ASTOR
         CAREA(IC,IS,2)=0.0
       ELSE IF (CAREA(IC,IS,2).GT.(0.0)) THEN
         CIN2=ABS(CPOTI1*WETR)
```

```
        END IF
      END IF
      IF ((CPOTI1.GE.(0.0)) .AND. (ASTOR.GE.(0.0))) THEN
        CAREA(IC,IS,2)=ASTOR+CPOTI1
        CIN2=0.0
      END IF
      SUMCI(IC,IS)=SUMCI(IC,IS)+((CIN1+CIN2)*CLEN(IC,IS))
       IF ((CAREA(IC,IS,2).EQ.0.0) .AND. (NUMCC(IC,IS).EQ.0)) THEN
         WRITE(N4,9100) IC,IS,NUNITC(IC,IS),TIME
         NUMCC(IC,IS)=1
       END IF
    ELSE IF (NUMBC(IC,IS).EQ.0) THEN
      CTRAIN(IC,IS)=CTRAIN(IC,IS)+(SCRAIN(IS)*
*CLEN(IC,IS)*COPEN(IC,IS))
        IF (NCAS(IC,IS).EQ.1) THEN
          RLATIN=Q(IC,IS,1,1,2)
        ELSE IF (NCAS(IC,IS).EQ.2) THEN
          RLATIN=(Q(IC,IS,1,1,2)+Q(IC,IS,2,1,2))
        END IF
      NIC=NCHA-((NCHA+1)/2)
      IF ((IC.GT.NIC) .AND. (IS.EQ.NSEG(IC))) THEN
        SUMCI(IC,IS)=SUMCI(IC,IS)+RLATIN
*+(SCRAIN(IS)*COPEN(IC,IS)*CLEN(IC,IS))
      ELSE IF ((IC.GT.NIC) .AND. (IS.LT.NSEG(IC))) THEN
        SUMCI(IC,IS)=SUMCI(IC,IS)+RLATIN+CQ(IC,(IS+1),1)
*+(SCRAIN(IS)*COPEN(IC,IS)*CLEN(IC,IS))
      ELSE IF ((IC.LE.NIC) .AND. (IS.EQ.NSEG(IC))) THEN
        SUMCI(IC,IS)=SUMCI(IC,IS)+RLATIN+CQ((IC+IC),1,1)
*+CQ((IC+IC+1),1,1)+(SCRAIN(IS)*COPEN(IC,IS)*CLEN(IC,IS))
      ELSE IF ((IC.LE.NIC) .AND. (IS.LT.NSEG(IC))) THEN
        SUMCI(IC,IS)=SUMCI(IC,IS)+RLATIN+CQ(IC,(IS+1),1)
*+(SCRAIN(IS)*COPEN(IC,IS)*CLEN(IC,IS))
      END IF
    END IF
  ELSE IF (CA(IC,IS).EQ.0.0) THEN
    IF (NUMAC(IC,IS).GT.0) THEN
      TTC(IC,IS)=TTC(IC,IS)+TINC
    ELSE IF (NUMAC(IC,IS).EQ.0) THEN
      IF ((SCRAIN(IS).GT.0.0) .OR. (SQ(IC,IS,2,1).GT.0.0) .OR.
*(SQ(IC,IS,1,1).GT.0.0) .OR. ((IS.LT.NSEG(IC)) .AND.
*(CSQ(IC,(IS+1)).GT.0.0)) .OR. ((IS.EQ.NSEG(IC)) .AND.
*((CSQ((IC+IC),1).GT.0.0) .OR. (CSQ((IC+IC+1),1).GT.0.0)))) THEN
        NUMAC(IC,IS)=1
        TTC(IC,IS)=TINC
      END IF
    END IF
    CTRAIN(IC,IS)=CTRAIN(IC,IS)+(SCRAIN(IS)*
*CLEN(IC,IS)*COPEN(IC,IS))
      IF (NCAS(IC,IS).EQ.1) THEN
        RLATIN=Q(IC,IS,1,1,2)/CLEN(IC,IS)
      ELSE IF (NCAS(IC,IS).EQ.2) THEN
        RLATIN=(Q(IC,IS,1,1,2)+Q(IC,IS,2,1,2))/CLEN(IC,IS)
      END IF
    NIC=NCHA-((NCHA+1)/2)
    IF ((IC.GT.NIC) .AND. (IS.EQ.NSEG(IC))) THEN
      CAREA(IC,IS,2)=CAREA(IC,IS,1)+RLATIN-(CQ(IC,IS,1)/
*CLEN(IC,IS))+(SCRAIN(IS)*COPEN(IC,IS))
    ELSE IF ((IC.GT.NIC) .AND. (IS.LT.NSEG(IC))) THEN
      CAREA(IC,IS,2)=CAREA(IC,IS,1)+RLATIN+((CQ(IC,(IS+1),1)
*-CQ(IC,IS,1))/CLEN(IC,IS))+(SCRAIN(IS)*COPEN(IC,IS))
    ELSE IF ((IC.LE.NIC) .AND. (IS.EQ.NSEG(IC))) THEN
      CAREA(IC,IS,2)=CAREA(IC,IS,1)+RLATIN+((CQ((IC+IC),1,1)
*+CQ((IC+IC+1),1,1)-CQ(IC,IS,1))/CLEN(IC,IS))+(SCRAIN(IS)*
*COPEN(IC,IS))
    ELSE IF ((IC.LE.NIC) .AND. (IS.LT.NSEG(IC))) THEN
      CAREA(IC,IS,2)=CAREA(IC,IS,1)+RLATIN+((CQ(IC,(IS+1),1)
*-CQ(IC,IS,1))/CLEN(IC,IS))+(SCRAIN(IS)*COPEN(IC,IS))
    END IF
  END IF
```

```
      IF (NCAS(IC,IS).EQ.1) THEN
        RLATERAL=CSUMI(IC,IS,1,1)
      ELSE IF (NCAS(IC,IS).EQ.2) THEN
        RLATERAL=CSUMI(IC,IS,1,1)+CSUMI(IC,IS,2,1)
      END IF
      NIC=NCHA-((NCHA+1)/2)
      IF ((IC.GT.NIC) .AND. (IS.EQ.NSEG(IC))) THEN
        CSUMCI(IC,IS)=SUMCI(IC,IS)+RLATERAL
      ELSE IF ((IC.GT.NIC) .AND. (IS.LT.NSEG(IC))) THEN
        CSUMCI(IC,IS)=SUMCI(IC,IS)+CSUMCI(IC,(IS+1))+RLATERAL
      ELSE IF ((IC.LE.NIC) .AND. (IS.EQ.NSEG(IC))) THEN
        CSUMCI(IC,IS)=SUMCI(IC,IS)+CSUMCI((IC+IC),1)+
     *CSUMCI((IC+IC+1),1)+RLATERAL
      ELSE IF ((IC.LE.NIC) .AND. (IS.LT.NSEG(IC))) THEN
        CSUMCI(IC,IS)=SUMCI(IC,IS)+CSUMCI(IC,(IS+1))+RLATERAL
      END IF
      IF (CAREA(IC,IS,2).LT.(0.0)) THEN
        WRITE(*,1000) TIME,IC,IS,CAREA(IC,IS,2)
      END IF
      IF (NCAS(IC,IS).EQ.1) THEN
        RLATERAL=CHRAIN(IC,IS,1,1)
      ELSE IF (NCAS(IC,IS).EQ.2) THEN
        RLATERAL=CHRAIN(IC,IS,1,1)+CHRAIN(IC,IS,2,1)
      END IF
      NIC=NCHA-((NCHA+1)/2)
      IF ((IC.GT.NIC) .AND. (IS.EQ.NSEG(IC))) THEN
        CCRAIN(IC,IS)=CTRAIN(IC,IS)+RLATERAL
      ELSE IF ((IC.GT.NIC) .AND. (IS.LT.NSEG(IC))) THEN
        CCRAIN(IC,IS)=CTRAIN(IC,IS)+CCRAIN(IC,(IS+1))+RLATERAL
      ELSE IF ((IC.LE.NIC) .AND. (IS.EQ.NSEG(IC))) THEN
        CCRAIN(IC,IS)=CTRAIN(IC,IS)+CCRAIN((IC+IC),1)+
     *CCRAIN((IC+IC+1),1)+RLATERAL
      ELSE IF ((IC.LE.NIC) .AND. (IS.LT.NSEG(IC))) THEN
        CCRAIN(IC,IS)=CTRAIN(IC,IS)+CCRAIN(IC,(IS+1))+RLATERAL
      END IF
      CALL CDISC
      RETURN
1000  FORMAT(1X,'Error 4',1X,F8.2,1X,I2,1X,I2,5X,1X,F9.3)
9000  FORMAT(1X,'Excess channel',I2,1X,I2,1X,I2,1X,
     *' time = ',F8.2,1X,' To and Vs ',F9.4,1X,F7.4)
9100  Format(1x,'Dried up ',i2,1x,i2,1x,i2,1x,' time = ',f8.2)
      END
C*********************************************************************
C
      SUBROUTINE CDISC
C
      PARAMETER (IH=12,NF=16,I1=7,I2=46,I3=2,I4=54,I5=2)
      PARAMETER (NU=9,K9=2,MK=20,MJ=30,I4P=55,NSA=127,MT=100)
      PARAMETER (N1=11,N2=22,N3=33,N4=44,N5=55,N6=66,N7=77,N8=88,N9=90)
      PARAMETER (CON=10.0)
      COMMON/MAIN/NS,NSUB,IC,IS,NC,I,J,NTTOT,LAP,TINC,TIME,
     *LC,AREAM2(IH),CHANLENM(IH),IHV,WID(I1,I2,I3,I4),NCAS(I1,I2),
     *CHRAIN(I1,I2,I3,I4),CSUMI(I1,I2,I3,I4),HARM2(I1,I2,I3,I4),
     *CARM2(I1,I2),MAXU,AIN(NU),BIN(NU),UCM2(I1,I2,NU),SQ(I1,I2,I3,I4),
     *UHM2(I1,I2,I3,I4,NU),RAG(NSA),RBG(NSA),WWPRAT(NSA),
     *RAM(NU),RBM(NU),NSU(NSA),RIR(I1,I2,I3,I4),UIR(NU),
     *Q(I1,I2,I3,I4,I5),NITS,NR,NTMOD,NP,SLOPE(I1,I2,I3,I4)
      COMMON/CHAN/NCHA,NSEG(I1),IHYC(I1,I2),EC(I1,I2),TTC(I1,I2),
     *CA(I1,I2),CB(I1,I2),CWID(I1,I2),EANG(I1,I2),WANG(I1,I2),
     *CTOP(I1,I2),CLEN(I1,I2),CGRA(I1,I2),CPER(I1,I2),COPEN(I1,I2),
     *CPOTI,SUMCI(I1,I2),CAREA(I1,I2,I5),CPOTI1,CQ(I1,I2,I5),
     *CSQ(I1,I2),CWP,DEPTH,CTRAIN(I1,I2),K33,CXSA(I1,I2),SCRAIN(I2),
     *CCRAIN(I1,I2),CSUMCI(I1,I2),NUNITC(I1,I2),APC(I1,I2),
     *CCLEN(I1,I2),IOFLOW(I1,I2),NUMAC(I1,I2),NUMBC(I1,I2)
      COMMON/COUR/CVEL(I1,I2,I3),VEL(I1,I2,I3,I4,I5),NSTIF,
     *INSTC(I1,I2),INSTH(I1,I2,I3,I4)
C
      REAL CROUGH
C
```

```
c subroutine CDISC calculates the velocity and discharge
c CVEL(IC,IS,2)..the velocity of flow as calculated by Manning's uniform flow
c equation and adjusted to cm/sec from the original formula by a
C multiplication by the constant 4.64
C CQ(IC,IS,2)..the channel discharge
C CSQ(IC,IS)..the sum of CQ over time 1-NTTOT
c
      SAVE
c
c in order to calculate the velocity using Mannings equation for uniform
c channel flow, it is necessary to calculate the hydraulic radius of the
c flow cross-section which involves knowing the depth of flow from the
c water surface to the channel bed (for rectangular and trapezoidal
c channels) or to the channel apex (for triangular channels).  since depth
c calculations involve a quadratic equation this is handled in a
c seperate subroutine CDQUAD
c CDQUAD handles overbank flow by calculating the dimensions of
c the boundary as the channel up to ctop, and then the overbank depth
c according to whether the channel is a ditch or natural channel, or an
c artificially banked channel.
c It is accepted that the presence
c of overbank sections will change the nature of the velocity and the
c contact zone for infiltration.  However, the current assumption is that
c for the increase in area, the consequent increase in wetted perimiter
c will lead to lower velocity values and account somewhat for the slow
c moving parts of the cross-section.
      CROUGH=0.0
      CWP=0.0
      IF (J.EQ.1) THEN
        IF (CAREA(IC,IS,1).GT.0.0) THEN
          CALL CDQUAD
          CROUGH=EC(IC,IS)
          CVEL(IC,IS,1)=(SQRT(CGRA(IC,IS))/CROUGH)*
     *((CAREA(IC,IS,1)/CWP)**(2.0/3.0))*4.64
          NSTIF=2
          CALL COURANT
        END IF
        CQ(IC,IS,1)=CAREA(IC,IS,1)*CVEL(IC,IS,1)*TINC
        CSQ(IC,IS)=0.0
      ELSE IF (J.GT.1) THEN
        IF (CAREA(IC,IS,2).GT.0.0) THEN
          CALL CDQUAD
          CROUGH=EC(IC,IS)
          CVEL(IC,IS,2)=(SQRT(CGRA(IC,IS))/CROUGH)*
     *((CAREA(IC,IS,2)/CWP)**(2.0/3.0))*4.64
          NSTIF=2
          CALL COURANT
        END IF
        CQ(IC,IS,2)=CAREA(IC,IS,2)*CVEL(IC,IS,2)*TINC
        CSQ(IC,IS)=CSQ(IC,IS)+CQ(IC,IS,2)
      END IF
      RETURN
      END
C
C*********************************************************************
C
      SUBROUTINE CDQUAD
C
      PARAMETER (IH=12,NF=16,I1=7,I2=46,I3=2,I4=54,I5=2)
      PARAMETER (NU=9,K9=2,MK=20,MJ=30,I4P=55,NSA=127,MT=100)
      PARAMETER (N1=11,N2=22,N3=33,N4=44,N5=55,N6=66,N7=77,N8=88,N9=90)
      COMMON/MAIN/NS,NSUB,IC,IS,NC,I,J,NTTOT,LAP,TINC,TIME,
     *LC,AREAM2(IH),CHANLENM(IH),IHV,WID(I1,I2,I3,I4),NCAS(I1,I2),
     *CHRAIN(I1,I2,I3,I4),CSUMI(I1,I2,I3,I4),HARM2(I1,I2,I3,I4),
     *CARM2(I1,I2),MAXU,AIN(NU),BIN(NU),UCM2(I1,I2,NU),SQ(I1,I2,I3,I4),
     *UHM2(I1,I2,I3,I4,NU),RAG(NSA),RBG(NSA),WWPRAT(NSA),
     *RAM(NU),RBM(NU),NSU(NSA),RIR(I1,I2,I3,I4),UIR(NU),
     *Q(I1,I2,I3,I4,I5),NITS,NR,NTMOD,NP,SLOPE(I1,I2,I3,I4)
      COMMON/CHAN/NCHA,NSEG(I1),IHYC(I1,I2),EC(I1,I2),TTC(I1,I2),
```

```
     *CA(I1,I2),CB(I1,I2),CWID(I1,I2),EANG(I1,I2),WANG(I1,I2),
     *CTOP(I1,I2),CLEN(I1,I2),CGRA(I1,I2),CPER(I1,I2),COPEN(I1,I2),
     *CPOTI,SUMCI(I1,I2),CAREA(I1,I2,I5),CPOTI1,CQ(I1,I2,I5),
     *CSQ(I1,I2),CWP,DEPTH,CTRAIN(I1,I2),K33,CXSA(I1,I2),SCRAIN(I2),
     *CCRAIN(I1,I2),CSUMCI(I1,I2),NUNITC(I1,I2),APC(I1,I2),
     *CCLEN(I1,I2),IOFLOW(I1,I2),NUMAC(I1,I2),NUMBC(I1,I2)
      REAL DEPTH1,DEPTH2,OFAREA
C
c DEPTH1, DEPTH2 are two possible roots to the equation establishing
c depth for a given flow area
c CWP is the wetted perimeter corresponding to this depth and flow area
C the following procedures calculate the depth of flow in the channel section
c for a given flow area predicted by the model.
      DEPTH=0.0
      DEPTH1=0.0
      DEPTH2=0.0
      OFAREA=0.0
      CWP=0.0
      IF (J.EQ.1) THEN
        IF ((EANG(IC,IS).EQ.0.0) .AND. (WANG(IC,IS).EQ.0.0)) THEN
          DEPTH=CAREA(IC,IS,1)/CWID(IC,IS)
        ELSE IF ((EANG(IC,IS).GT.0.0) .OR. (WANG(IC,IS).GT.0.0))
     *THEN
          DEPTH1=((-CWID(IC,IS))+SQRT((CWID(IC,IS)**2.0)+
     *(2.0*EANG(IC,IS)*CAREA(IC,IS,1))+(2.0*WANG(IC,IS)*
     *CAREA(IC,IS,1))))/(EANG(IC,IS)+WANG(IC,IS))
          DEPTH2=((-CWID(IC,IS))-SQRT((CWID(IC,IS)**2.0)+
     *(2.0*EANG(IC,IS)*CAREA(IC,IS,1))+(2.0*WANG(IC,IS)*
     *CAREA(IC,IS,1))))/(EANG(IC,IS)+WANG(IC,IS))
          IF ((DEPTH2.LT.0.0) .AND. (DEPTH1.GE.0.0)) THEN
            DEPTH=DEPTH1
          ELSE IF ((DEPTH1.LT.0.0) .AND. (DEPTH2.GE.0.0)) THEN
            DEPTH=DEPTH2
          ELSE IF (((DEPTH1.LT.0.0) .AND. (DEPTH2.LT.
     *0.0)) .OR. ((DEPTH2.GT.0.0) .AND. (DEPTH1.GT.0.0))) THEN
            WRITE(*,*) 'BOTH SOLUTIONS TO QUADRATIC UNTENABLE'
            DEPTH=-1000000.0
          END IF
        END IF
        IF (DEPTH.LE.CTOP(IC,IS)) THEN
          CWP=CWID(IC,IS)+(DEPTH/COS(ATAN
     *(EANG(IC,IS))))+(DEPTH/COS(ATAN(WANG(IC,IS))))
        ELSE IF (DEPTH.GT.CTOP(IC,IS)) THEN
          OFAREA=CAREA(IC,IS,1)-CXSA(IC,IS)
          IF (IOFLOW(IC,IS).EQ.1) THEN
            DEPTH1=((-COPEN(IC,IS))+SQRT((COPEN(IC,IS)**2.0)+
     *(2.0*OFAREA/TAN(ASIN(SLOPE(IC,IS,1,1))))+(2.0*OFAREA*
     *WANG(IC,IS))))/((1.0/TAN(ASIN(SLOPE(IC,IS,1,1))))+
     *WANG(IC,IS))
            DEPTH2=((-COPEN(IC,IS))-SQRT((COPEN(IC,IS)**2.0)+
     *(2.0*OFAREA/TAN(ASIN(SLOPE(IC,IS,1,1))))+(2.0*OFAREA*
     *WANG(IC,IS))))/((1.0/TAN(ASIN(SLOPE(IC,IS,1,1))))+
     *WANG(IC,IS))
          ELSE IF ((IOFLOW(IC,IS).GT.1) .AND. (NCAS(IC,IS).GT.1)) THEN
            DEPTH1=((-COPEN(IC,IS))+SQRT((COPEN(IC,IS)**2.0)+
     *(2.0*OFAREA/TAN(ASIN(SLOPE(IC,IS,1,1))))+(2.0*OFAREA/
     *TAN(ASIN(SLOPE(IC,IS,2,1))))))/((1.0/
     *TAN(ASIN(SLOPE(IC,IS,1,1))))+(1.0/TAN(ASIN(SLOPE(IC,IS,2,1)))))
            DEPTH2=((-COPEN(IC,IS))-SQRT((COPEN(IC,IS)**2.0)+
     *(2.0*OFAREA/TAN(ASIN(SLOPE(IC,IS,1,1))))+(2.0*OFAREA/
     *TAN(ASIN(SLOPE(IC,IS,2,1))))))/((1.0/
     *TAN(ASIN(SLOPE(IC,IS,1,1))))+(1.0/TAN(ASIN(SLOPE(IC,IS,2,1)))))
          ELSE IF ((IOFLOW(IC,IS).GT.1) .AND. (NCAS(IC,IS).EQ.1)) THEN
            DEPTH1=((-COPEN(IC,IS))+SQRT((COPEN(IC,IS)**2.0)+
     *(2.0*OFAREA/TAN(ASIN(SLOPE(IC,IS,1,1))))+(2.0*OFAREA/
     *TAN(ASIN(SLOPE(IC,IS,1,1))))))/((1.0/
     *TAN(ASIN(SLOPE(IC,IS,1,1))))+(1.0/TAN(ASIN(SLOPE(IC,IS,1,1)))))
            DEPTH2=((-COPEN(IC,IS))-SQRT((COPEN(IC,IS)**2.0)+
     *(2.0*OFAREA/TAN(ASIN(SLOPE(IC,IS,1,1))))+(2.0*OFAREA/
```

```
*TAN(ASIN(SLOPE(IC,IS,1,1))))))/((1.0/
*TAN(ASIN(SLOPE(IC,IS,1,1))))+(1.0/TAN(ASIN(SLOPE(IC,IS,1,1)))))
      END IF
      IF ((DEPTH2.LT.0.0) .AND. (DEPTH1.GE.0.0)) THEN
        DEPTH=DEPTH1
      ELSE IF ((DEPTH1.LT.0.0) .AND. (DEPTH2.GE.0.0)) THEN
        DEPTH=DEPTH2
      ELSE IF (((DEPTH1.LT.0.0) .AND. (DEPTH2.LT.
*0.0)) .OR. ((DEPTH2.GT.0.0) .AND. (DEPTH1.GT.0.0))) THEN
        WRITE(*,*) 'BOTH SOLUTIONS TO QUADRATIC UNTENABLE'
        DEPTH=-1000000.0
      END IF
      IF (IOFLOW(IC,IS).EQ.1) THEN
        CWP=CPER(IC,IS)+(DEPTH/COS(ATAN(WANG(IC,IS))))+
*(DEPTH/SLOPE(IC,IS,1,1))
      ELSE IF ((IOFLOW(IC,IS).GT.1) .AND. (NCAS(IC,IS).GT.1)) THEN
        CWP=CPER(IC,IS)+(DEPTH/(SLOPE(IC,IS,2,1)))+
*(DEPTH/SLOPE(IC,IS,1,1))
      ELSE IF ((IOFLOW(IC,IS).GT.1) .AND. (NCAS(IC,IS).EQ.1)) THEN
        CWP=CPER(IC,IS)+(DEPTH/(SLOPE(IC,IS,1,1)))+
*(DEPTH/SLOPE(IC,IS,1,1))
      END IF
    END IF
  ELSE IF (J.GT.1) THEN
    IF ((EANG(IC,IS).EQ.0.0) .AND. (WANG(IC,IS).EQ.0.0)) THEN
      DEPTH=CAREA(IC,IS,2)/CWID(IC,IS)
    ELSE IF ((EANG(IC,IS).GT.0.0) .OR. (WANG(IC,IS).GT.0.0))
*THEN
      DEPTH1=((-CWID(IC,IS))+SQRT((CWID(IC,IS)**2.0)+
*(2.0*EANG(IC,IS)*CAREA(IC,IS,2))+(2.0*WANG(IC,IS)*
*CAREA(IC,IS,2))))/(EANG(IC,IS)+WANG(IC,IS))
      DEPTH2=((-CWID(IC,IS))-SQRT((CWID(IC,IS)**2.0)+
*(2.0*EANG(IC,IS)*CAREA(IC,IS,2))+(2.0*WANG(IC,IS)*
*CAREA(IC,IS,2))))/(EANG(IC,IS)+WANG(IC,IS))
      IF ((DEPTH2.LT.0.0) .AND. (DEPTH1.GE.0.0)) THEN
        DEPTH=DEPTH1
      ELSE IF ((DEPTH1.LT.0.0) .AND. (DEPTH2.GE.0.0)) THEN
        DEPTH=DEPTH2
      ELSE IF (((DEPTH1.LT.0.0) .AND. (DEPTH2.LT.
*0.0)) .OR. ((DEPTH2.GT.0.0) .AND. (DEPTH1.GT.0.0))) THEN
        WRITE(*,*) 'BOTH SOLUTIONS TO QUADRATIC UNTENABLE'
        DEPTH=-1000000.0
      END IF
    END IF
    IF (DEPTH.LE.CTOP(IC,IS)) THEN
      CWP=CWID(IC,IS)+(DEPTH/COS(ATAN
*(EANG(IC,IS))))+(DEPTH/COS(ATAN(WANG(IC,IS))))
    ELSE IF (DEPTH.GT.CTOP(IC,IS)) THEN
      OFAREA=CAREA(IC,IS,2)-CXSA(IC,IS)
      IF (IOFLOW(IC,IS).EQ.1) THEN
        DEPTH1=((-COPEN(IC,IS))+SQRT((COPEN(IC,IS)**2.0)+
*(2.0*OFAREA/TAN(ASIN(SLOPE(IC,IS,1,1))))+(2.0*OFAREA*
*WANG(IC,IS))))/((1.0/TAN(ASIN(SLOPE(IC,IS,1,1))))+
*WANG(IC,IS))
        DEPTH2=((-COPEN(IC,IS))-SQRT((COPEN(IC,IS)**2.0)+
*(2.0*OFAREA/TAN(ASIN(SLOPE(IC,IS,1,1))))+(2.0*OFAREA*
*WANG(IC,IS))))/((1.0/TAN(ASIN(SLOPE(IC,IS,1,1))))+
*WANG(IC,IS))
      ELSE IF ((IOFLOW(IC,IS).GT.1) .AND. (NCAS(IC,IS).GT.1)) THEN
        DEPTH1=((-COPEN(IC,IS))+SQRT((COPEN(IC,IS)**2.0)+
*(2.0*OFAREA/TAN(ASIN(SLOPE(IC,IS,1,1))))+(2.0*OFAREA/
*TAN(ASIN(SLOPE(IC,IS,2,1))))))/((1.0/
*TAN(ASIN(SLOPE(IC,IS,1,1))))+(1.0/TAN(ASIN(SLOPE(IC,IS,2,1)))))
        DEPTH2=((-COPEN(IC,IS))-SQRT((COPEN(IC,IS)**2.0)+
*(2.0*OFAREA/TAN(ASIN(SLOPE(IC,IS,1,1))))+(2.0*OFAREA/
*TAN(ASIN(SLOPE(IC,IS,2,1))))))/((1.0/
*TAN(ASIN(SLOPE(IC,IS,1,1))))+(1.0/TAN(ASIN(SLOPE(IC,IS,2,1)))))
      ELSE IF ((IOFLOW(IC,IS).GT.1) .AND. (NCAS(IC,IS).EQ.1)) THEN
        DEPTH1=((-COPEN(IC,IS))+SQRT((COPEN(IC,IS)**2.0)+
```

```
     *(2.0*OFAREA/TAN(ASIN(SLOPE(IC,IS,1,1))))+(2.0*OFAREA/
     *TAN(ASIN(SLOPE(IC,IS,1,1))))))/((1.0/
     *TAN(ASIN(SLOPE(IC,IS,1,1))))+(1.0/TAN(ASIN(SLOPE(IC,IS,1,1)))))
            DEPTH2=((-COPEN(IC,IS))-SQRT((COPEN(IC,IS)**2.0)+
     *(2.0*OFAREA/TAN(ASIN(SLOPE(IC,IS,1,1))))+(2.0*OFAREA/
     *TAN(ASIN(SLOPE(IC,IS,1,1))))))/((1.0/
     *TAN(ASIN(SLOPE(IC,IS,1,1))))+(1.0/TAN(ASIN(SLOPE(IC,IS,1,1)))))
           END IF
           IF ((DEPTH2.LT.0.0) .AND. (DEPTH1.GE.0.0)) THEN
             DEPTH=DEPTH1
           ELSE IF ((DEPTH1.LT.0.0) .AND. (DEPTH2.GE.0.0)) THEN
             DEPTH=DEPTH2
           ELSE IF (((DEPTH1.LT.0.0) .AND. (DEPTH2.LT.
     *0.0)) .OR. ((DEPTH2.GT.0.0) .AND. (DEPTH1.GT.0.0))) THEN
             WRITE(*,*) 'BOTH SOLUTIONS TO QUADRATIC UNTENABLE'
             DEPTH=-1000000.0
           END IF
           IF (IOFLOW(IC,IS).EQ.1) THEN
             CWP=CPER(IC,IS)+(DEPTH/COS(ATAN(WANG(IC,IS))))+
     *(DEPTH/SLOPE(IC,IS,1,1))
           ELSE IF ((IOFLOW(IC,IS).GT.1) .AND. (NCAS(IC,IS).GT.1)) THEN
             CWP=CPER(IC,IS)+(DEPTH/(SLOPE(IC,IS,2,1)))+
     *(DEPTH/SLOPE(IC,IS,1,1))
           ELSE IF ((IOFLOW(IC,IS).GT.1) .AND. (NCAS(IC,IS).EQ.1)) THEN
             CWP=CPER(IC,IS)+(DEPTH/(SLOPE(IC,IS,1,1)))+
     *(DEPTH/SLOPE(IC,IS,1,1))
           END IF
         END IF
       END IF
       IF (CWP.LE.0.0) THEN
         WRITE(*,1100) TIME,IC,IS,CAREA(IC,IS,2),CTOP(IC,IS),
     *DEPTH1,DEPTH2,DEPTH
       END IF
       RETURN
1100   FORMAT(1X,'Error 5',1X,F8.2,1X,I2,1X,I2,5X,5(1X,F9.3))
       END
C
C*****************************************************************
C
       SUBROUTINE FDRESET
C
       PARAMETER (IH=12,NF=16,I1=7,I2=46,I3=2,I4=54,I5=2)
       PARAMETER (NU=9,K9=2,MK=20,MJ=30,I4P=55,NSA=127,MT=100)
       PARAMETER (N1=11,N2=22,N3=33,N4=44,N5=55,N6=66,N7=77,N8=88,N9=90)
       COMMON/MAIN/NS,NSUB,IC,IS,NC,I,J,NTTOT,LAP,TINC,TIME,
      *LC,AREAM2(IH),CHANLENM(IH),IHV,WID(I1,I2,I3,I4),NCAS(I1,I2),
      *CHRAIN(I1,I2,I3,I4),CSUMI(I1,I2,I3,I4),HARM2(I1,I2,I3,I4),
      *CARM2(I1,I2),MAXU,AIN(NU),BIN(NU),UCM2(I1,I2,NU),SQ(I1,I2,I3,I4),
      *UHM2(I1,I2,I3,I4,NU),RAG(NSA),RBG(NSA),WWPRAT(NSA),
      *RAM(NU),RBM(NU),NSU(NSA),RIR(I1,I2,I3,I4),UIR(NU),
      *Q(I1,I2,I3,I4,I5),NITS,NR,NTMOD,NP,SLOPE(I1,I2,I3,I4)
       COMMON/HILL/NELM(I1,I2,I3),IHY(I1,I2,I3,I4),A(I1,I2,I3,I4),
      *B(I1,I2,I3,I4),RLEN(I1,I2,I3,I4),HPOTI,
      *SUMI(I1,I2,I3,I4),HAREA(I1,I2,I3,I4,I5),HPOTI1,
      *TRAIN(I1,I2,I3,I4),K44,SRAIN(I4),
      *NUNIT(I1,I2,I3,I4),AP(I1,I2,I3,I4),RA(I1,I2,I3,I4),
      *RB(I1,I2,I3,I4),TPR(I1,I2,I3,I4),NUMA(I1,I2,I3,I4),
      *AM(I1,I2,I3,I4),BM(I1,I2,I3,I4),NUMB(I1,I2,I3,I4),TT(I1,I2,I3,I4),
      *SUMA(I1,I2,13,I4),VS(I1,I2,I3,I4),TO(I1,I2,I3,I4)
       COMMON/CHAN/NCHA,NSEG(I1),IHYC(I1,I2),EC(I1,I2),TTC(I1,I2),
      *CA(I1,I2),CB(I1,I2),CWID(I1,I2),EANG(I1,I2),WANG(I1,I2),
      *CTOP(I1,I2),CLEN(I1,I2),CGRA(I1,I2),CPER(I1,I2),COPEN(I1,I2),
      *CPOTI,SUMCI(I1,I2),CAREA(I1,I2,I5),CPOTI1,CQ(I1,I2,I5),
      *CSQ(I1,I2),CWP,DEPTH,CTRAIN(I1,I2),K33,CXSA(I1,I2),SCRAIN(I2),
      *CCRAIN(I1,I2),CSUMCI(I1,I2),NUNITC(I1,I2),APC(I1,I2),
      *CCLEN(I1,I2),IOFLOW(I1,I2),NUMAC(I1,I2),NUMBC(I1,I2)
       COMMON/PRINT/NEX(IH),M1(IH,MJ),M2(IH,MJ),M3(IH,MJ),CATRAIN(MT),
      *M4(IH,MJ),M5(IH,MJ),M6(IH,MJ),NQOBS(IH),CATINF(MT),CATDISH(MT),
      *QT(IH,MT),QPCV(IH,MT),CATQT(MT),NCOBS,CATQS,QTS,NCQ,NQQ,TIMEQC
```

```
      COMMON/COUR/CVEL(I1,I2,I3),VEL(I1,I2,I3,I4,I5),NSTIF,
     *INSTC(I1,I2),INSTH(I1,I2,I3,I4)
      INTEGER L1,L2,L3,L4,IJ
C subroutine FDRESET is the finite difference reset function which
c allows a two-time increment store to be used
c all the hydrograph information is calculated and where relevant for the
c individual channel and hillslope locations, data is written to output
c files.
      SAVE
      IF (NCHA.GT.0) THEN
        DO 40 L1=NCHA,1,-1
          IF (NSEG(L1).GT.0) THEN
            DO 30 L2=NSEG(L1),1,-1
              DO 20 L3=1,2
                IF (L3.LE.NCAS(L1,L2)) THEN
                  DO 10 L4=NELM(L1,L2,L3),1,-1
                    IF (J.GT.1) THEN
                      HAREA(L1,L2,L3,L4,1)=HAREA(L1,L2,L3,L4,2)
                      Q(L1,L2,L3,L4,1)=Q(L1,L2,L3,L4,2)
                      IF (HAREA(L1,L2,L3,L4,2).EQ.0.0)
     *VEL(L1,L2,L3,L4,2)=0.0
                      Q(L1,L2,L3,L4,2)=Q(L1,L2,L3,L4,2)/TINC
                    END IF
                    IF ((TIME.GE.REAL(LC)) .OR. (TIME.GE.REAL(NTTOT)))
     *THEN
                      DO 5 IJ=1,NEX(NS)
                        IF ((M1(NS,IJ).EQ.NS) .AND. (M2(NS,IJ).EQ.L1)
     *.AND. (M3(NS,IJ).EQ.L2) .AND. (M4(NS,IJ).EQ.L3) .AND.
     *(M5(NS,IJ).EQ.L4)) THEN
                          WRITE(N4,100) TIME,NS,L1,L2,L3,L4,
     *CHRAIN(L1,L2,L3,L4),CSUMI(L1,L2,L3,L4),SQ(L1,L2,L3,L4)
                          WRITE(N3,300) TIME,NS,L1,L2,L3,L4,
     *HAREA(L1,L2,L3,L4,2),VEL(L1,L2,L3,L4,2),Q(L1,L2,L3,L4,2)
                          IF (TIME.GE.REAL(NTTOT)) THEN
                          WRITE(N4,150) HARM2(L1,L2,L3,L4),
     *(UHM2(L1,L2,L3,L4,KK),KK=1,MAXU)
                          END IF
                        END IF
5                     CONTINUE
                    END IF
10                CONTINUE
                  END IF
20              CONTINUE
                IF (J.GT.1) THEN
                  CAREA(L1,L2,1)=CAREA(L1,L2,2)
                  CQ(L1,L2,1)=CQ(L1,L2,2)
                  IF (CAREA(L1,L2,2).EQ.0.0) CVEL(L1,L2,2)=0.0
                  CQ(L1,L2,2)=CQ(L1,L2,2)/TINC
                END IF
                IF ((L1.EQ.1) .AND. (L2.EQ.1)) THEN
                  IF (CSQ(1,1).GT.0.0) THEN
                    IF (NSUB.GT.1) THEN
                      IF (NCQ.LE.NCOBS) THEN
                        IF (TIME.GE.CATQT(NCQ)) THEN
                          CATRAIN(NCQ)=CATRAIN(NCQ)+CCRAIN(1,1)
                          CATINF(NCQ)=CATINF(NCQ)+SUMCI(1,1)
                          CATDISH(NCQ)=CATDISH(NCQ)+CSQ(1,1)
                          NCQ=NCQ+1
                        END IF
                      END IF
                    END IF
                    IF (NQQ.LE.NQOBS(NS)) THEN
                      IF (TIME.GE.QT(NS,NQQ)) THEN
                        QPCV(NS,NQQ)=CSQ(1,1)
                        NQQ=NQQ+1
                      END IF
                    END IF
                  END IF
                END IF
```

```
          IF ((TIME.GE.REAL(LC)) .OR. (TIME.GE.REAL(NTTOT)))
     *THEN
            DO 25 IJ=1,NEX(NS)
              IF ((M1(NS,IJ).EQ.NS) .AND. (M2(NS,IJ).EQ.L1) .AND.
     *(M3(NS,IJ).EQ.L2) .AND. (M6(NS,IJ).EQ.1)) THEN
                WRITE(N4,200) TIME,NS,L1,L2,CCRAIN(L1,L2),
     *CSUMCI(L1,L2),CSQ(L1,L2)
                WRITE(N3,350) TIME,NS,L1,L2,
     *CAREA(L1,L2,2),CVEL(L1,L2,2),CQ(L1,L2,2)
                IF (TIME.GE.REAL(NTTOT)) THEN
                  WRITE(N4,250) CARM2(L1,L2),(UCM2(L1,L2,KK),
     *KK=1,MAXU),CCLEN(L1,L2)
                END IF
              END IF
25          CONTINUE
          END IF
30      CONTINUE
        END IF
40    CONTINUE
      ELSE IF (NCHA.EQ.0) THEN
        L1=1
        L2=1
        L3=1
        DO 60 L4=NELM(L1,L2,L3),1,-1
          IF (J.GT.1) THEN
            HAREA(L1,L2,L3,L4,1)=HAREA(L1,L2,L3,L4,2)
            Q(L1,L2,L3,L4,1)=Q(L1,L2,L3,L4,2)
            IF (HAREA(L1,L2,L3,L4,2).EQ.0.0) VEL(L1,L2,L3,L4,2)=0.0
            Q(L1,L2,L3,L4,2)=Q(L1,L2,L3,L4,2)/TINC
          END IF
          IF (L4.EQ.1) THEN
            IF (SQ(1,1,1,1).GT.0.0) THEN
              IF (NSUB.GT.1) THEN
                IF (NCQ.LE.NCOBS) THEN
                  IF (TIME.GE.CATQT(NCQ)) THEN
                    CATRAIN(NCQ)=CATRAIN(NCQ)+CHRAIN(1,1,1,1)
                    CATINF(NCQ)=CATINF(NCQ)+CSUMI(1,1,1,1)
                    CATDISH(NCQ)=CATDISH(NCQ)+SQ(1,1,1,1)
                    NCQ=NCQ+1
                  END IF
                END IF
              END IF
              IF (NQQ.LE.NQOBS(NS)) THEN
                IF (TIME.GE.QT(NS,NQQ)) THEN
                  QPCV(NS,NQQ)=SQ(1,1,1,1)
                  NQQ=NQQ+1
                END IF
              END IF
            END IF
          END IF
          IF ((TIME.GE.REAL(LC)) .OR. (TIME.GE.REAL(NTTOT)))
     *THEN
            DO 55 IJ=1,NEX(NS)
              IF ((M1(NS,IJ).EQ.NS) .AND. (M2(NS,IJ).EQ.L1)
     *.AND. (M3(NS,IJ).EQ.L2) .AND. (M4(NS,IJ).EQ.L3) .AND.
     *(M5(NS,IJ).EQ.L4)) THEN
                WRITE(N4,100) TIME,NS,L1,L2,L3,L4,
     *CHRAIN(L1,L2,L3,L4),CSUMI(L1,L2,L3,L4),SQ(L1,L2,L3,L4)
                WRITE(N3,300) TIME,NS,L1,L2,L3,L4,
     *HAREA(L1,L2,L3,L4,2),VEL(L1,L2,L3,L4,2),Q(L1,L2,L3,L4,2)
                IF (TIME.GE.REAL(NTTOT)) THEN
                  WRITE(N4,150) HARM2(L1,L2,L3,L4),
     *(UHM2(L1,L2,L3,L4,KK),KK=1,MAXU)
                END IF
              END IF
55          CONTINUE
          END IF
60      CONTINUE
      END IF
```

```
      IF (TIME.GE.REAL(LC)) LC=LC+LAP
      IF (TIME.GE.REAL(NTTOT)) THEN
        WRITE(*,*) 'J SET TO NITS AT J=',J,' WITH TIME = ',time
        J=NITS+1
      END IF
      IF (NTMOD.EQ.1) THEN
        TINC=TINC/10.0
        IF (TINC.LT.1.0) TINC=1.0
      ELSE IF (NTMOD.EQ.2) THEN
        TINC=TINC
      ELSE IF (NTMOD.EQ.3) THEN
        TINC=TINC*10.0
      END IF
      NTMOD=0
      RETURN
100   FORMAT(1X,F8.2,3(1X,I2),1X,I1,1X,I2,1X,3(F13.2,1X))
150   FORMAT(1X,F8.1,9(F7.1))
250   FORMAT(1X,F9.1,9(F7.1),1X,F6.1)
200   FORMAT(1X,F8.2,3(1X,I2),6X,3(F13.2,1X))
300   FORMAT(1X,F8.2,3(1X,I2),1X,I1,1X,I2,3(1X,F13.6))
350   FORMAT(1X,F8.2,3(1X,I2),1X,'0',1X,'00',3(1X,F13.6))
      END
C
C*********************************************************************
      SUBROUTINE CONTT
C
      PARAMETER (IH=12,NF=16,I1=7,I2=46,I3=2,I4=54,I5=2)
      PARAMETER (NU=9,K9=2,MK=20,MJ=30,I4P=55,NSA=127,MT=100)
      PARAMETER (N1=11,N2=22,N3=33,N4=44,N5=55,N6=66,N7=77,N8=88,N9=90)
      COMMON/MAIN/NS,NSUB,IC,IS,NC,I,J,NTTOT,LAP,TINC,TIME,
     *LC,AREAM2(IH),CHANLENM(IH),IHV,WID(I1,I2,I3,I4),NCAS(I1,I2),
     *CHRAIN(I1,I2,I3,I4),CSUMI(I1,I2,I3,I4),HARM2(I1,I2,I3,I4),
     *CARM2(I1,I2),MAXU,AIN(NU),BIN(NU),UCM2(I1,I2,NU),SQ(I1,I2,I3,I4),
     *UHM2(I1,I2,I3,I4,NU),RAG(NSA),RBG(NSA),WWPRAT(NSA),
     *RAM(NU),RBM(NU),NSU(NSA),RIR(I1,I2,I3,I4),UIR(NU),
     *Q(I1,I2,I3,I4,I5),NITS,NR,NTMOD,NP,SLOPE(I1,I2,I3,I4)
      COMMON/HILL/NELM(I1,I2,I3),IHY(I1,I2,I3,I4),A(I1,I2,I3,I4),
     *B(I1,I2,I3,I4),RLEN(I1,I2,I3,I4),HPOTI,
     *SUMI(I1,I2,I3,I4),HAREA(I1,I2,I3,I4,I5),HPOTI1,
     *TRAIN(I1,I2,I3,I4),K44,SRAIN(I4),
     *NUNIT(I1,I2,I3,I4),AP(I1,I2,I3,I4),RA(I1,I2,I3,I4),
     *RB(I1,I2,I3,I4),TPR(I1,I2,I3,I4),NUMA(I1,I2,I3,I4),
     *AM(I1,I2,I3,I4),BM(I1,I2,I3,I4),NUMB(I1,I2,I3,I4),TT(I1,I2,I3,I4),
     *SUMA(I1,I2,13,I4),VS(I1,I2,I3,I4),TO(I1,I2,I3,I4)
      COMMON/CHAN/NCHA,NSEG(I1),IHYC(I1,I2),EC(I1,I2),TTC(I1,I2),
     *CA(I1,I2),CB(I1,I2),CWID(I1,I2),EANG(I1,I2),WANG(I1,I2),
     *CTOP(I1,I2),CLEN(I1,I2),CGRA(I1,I2),CPER(I1,I2),COPEN(I1,I2),
     *CPOTI,SUMCI(I1,I2),CAREA(I1,I2,I5),CPOTI1,CQ(I1,I2,I5),
     *CSQ(I1,I2),CWP,DEPTH,CTRAIN(I1,I2),K33,CXSA(I1,I2),SCRAIN(I2),
     *CCRAIN(I1,I2),CSUMCI(I1,I2),NUNITC(I1,I2),APC(I1,I2),
     *CCLEN(I1,I2),IOFLOW(I1,I2),NUMAC(I1,I2),NUMBC(I1,I2)
      REAL TIN(IH),TLOSS(IH),TSTOR(IH),CONT(IH),SUMQ(IH),PERC(IH),
     *SUMV(IH),SUMCV(IH),SUMCQ(IH),VH,VC,REFF,PROD,RLATEQ,RLATEA,
     *RLATER
C
c in order to check that the computation obeys continuity of mass and
C all the stores operate properly, this subroutine CONTT calculates for
c each subcatchment; the input, storage and outputs to see if they match....
c SUMCQ(NS) = total sum of volumetric discharges out of the last segment
c of the highest order channel section CSQ(1,1) minus the
c calculation of CQ(1,1,1) for the time J=NTTOT, which because
c of the backward difference scheme, does not leave the catchment.
C CONT(NS) = the difference between the calculated inputs TIN(NS) and
C the storages and outputs from the system TLOSS(NS), TSTOR(NS) and
C SUMCQ(NS)
C PERC(NS) = the ratio between CONT(NS) and the volume of input
c TIN(NS) multiplied by 100 this should be zero, but
c may be an acceptably small number due to rounding of real number
c stores by the computer
```

```
c
c  REFF is the water harvesting productivity percentage index
C  PROD is the per unit area productivity index
C  Both are calculated from the sum of input stores and output stores giving
c  the mass balance
      SAVE
      SUMV(NS)=0.0
      SUMCV(NS)=0.0
      IF (NCHA.GT.0) THEN
        DO 400 IC=NCHA,1,-1
          IF (NSEG(IC).GT.0) THEN
            DO 300 IS=NSEG(IC),1,-1
              DO 200 NC=1,2
                IF (NC.LE.NCAS(IC,IS)) THEN
                  DO 100 I=NELM(IC,IS,NC),1,-1
                    VH=0.0
                    VH=HAREA(IC,IS,NC,I,1)*RLEN(IC,IS,NC,I)
                    SUMV(NS)=SUMV(NS)+VH
                    IF (I.LT.NELM(IC,IS,NC)) THEN
                      REFF=((SQ(IC,IS,NC,I)-Q(IC,IS,NC,I,1)+VH)/
     *(SQ(IC,IS,NC,(I+1))-Q(IC,IS,NC,(I+1),1)+CHRAIN(IC,IS,NC,I)-
     *CHRAIN(IC,IS,NC,(I+1))))*100.0
                      PROD=(SQ(IC,IS,NC,I)-Q(IC,IS,NC,I,1)+VH-
     *(SQ(IC,IS,NC,(I+1))-Q(IC,IS,NC,(I+1),1)))/
     *(HARM2(IC,IS,NC,I)-HARM2(IC,IS,NC,(I+1)))
                    ELSE IF (I.EQ.NELM(IC,IS,NC)) THEN
                      REFF=((SQ(IC,IS,NC,I)-Q(IC,IS,NC,I,1)+VH)/
     *CHRAIN(IC,IS,NC,I))*100.0
                      PROD=(SQ(IC,IS,NC,I)-Q(IC,IS,NC,I,1)+VH)/
     *HARM2(IC,IS,NC,I)
                    END IF
                    WRITE(N9,7500) NS,IC,IS,NC,I,NUNIT(IC,IS,NC,I),
     *REFF,PROD,HARM2(IC,IS,NC,I)
100                 CONTINUE
                  END IF
200             CONTINUE
                VC=0.0
                VC=CAREA(IC,IS,1)*CLEN(IC,IS)
                SUMCV(NS)=SUMCV(NS)+VC
                NIC=NCHA-((NCHA+1)/2)
                IF (NCAS(IC,IS).EQ.1) THEN
                  RLATER=CHRAIN(IC,IS,1,1)
                  RLATEQ=SQ(IC,IS,1,1)
                  RLATEA=HARM2(IC,IS,1,1)
                ELSE IF (NCAS(IC,IS).EQ.2) THEN
                  RLATER=CHRAIN(IC,IS,1,1)+CHRAIN(IC,IS,2,1)
                  RLATEQ=SQ(IC,IS,1,1)+SQ(IC,IS,2,1)
                  RLATEA=HARM2(IC,IS,1,1)+HARM2(IC,IS,2,1)
                END IF
                IF ((IC.GT.NIC) .AND. (IS.EQ.NSEG(IC))) THEN
                  REFF=((CSQ(IC,IS)-CQ(IC,IS,1)+VC)/(CCRAIN(IC,IS)+
     *RLATEQ-RLATER))*100.0
                  PROD=(CSQ(IC,IS)-CQ(IC,IS,1)+VC-RLATEQ)/
     *(CARM2(IC,IS)-RLATEA)
                ELSE IF ((IC.GT.NIC) .AND. (IS.LT.NSEG(IC))) THEN
                  REFF=((CSQ(IC,IS)-CQ(IC,IS,1)+VC)/(CCRAIN(IC,IS)+
     *CSQ(IC,(IS+1))-CQ(IC,(IS+1),1)+
     *RLATEQ-CCRAIN(IC,(IS+1))-RLATER))*100.0
                  PROD=(CSQ(IC,IS)-CQ(IC,IS,1)+VC-(CSQ(IC,(IS+1))-
     *CQ(IC,(IS+1),1))-RLATEQ)/(CARM2(IC,IS)-CARM2(IC,(IS+1))-RLATEA)
                ELSE IF ((IC.LE.NIC) .AND. (IS.EQ.NSEG(IC))) THEN
                  REFF=((CSQ(IC,IS)-CQ(IC,IS,1)+VC)/(CCRAIN(IC,IS)+
     *CSQ((IC+IC),1)-CQ((IC+IC),1,1)+CSQ((IC+IC+1),1)-
     *CQ((IC+IC+1),1,1)+RLATEQ-CCRAIN((IC+IC),1)-
     *CCRAIN((IC+IC+1),1)-RLATER))*100.0
                  PROD=(CSQ(IC,IS)-CQ(IC,IS,1)+VC-(CSQ((IC+IC),1)-
     *-CQ((IC+IC),1,1))-(CSQ((IC+IC+1),1)-CQ((IC+IC+1),1,1))-
     *RLATEQ)/(CARM2(IC,IS)-CARM2((IC+IC),1)-
     *CARM2((IC+IC+1),1)-RLATEA)
```

```
            ELSE IF ((IC.LE.NIC) .AND. (IS.LT.NSEG(IC))) THEN
              REFF=((CSQ(IC,IS)-CQ(IC,IS,1)+VC)/(CCRAIN(IC,IS)+
     *CSQ(IC,(IS+1))-CQ(IC,(IS+1),1)+
     *RLATEQ-CCRAIN(IC,(IS+1))-RLATER))*100.0
              PROD=(CSQ(IC,IS)-CQ(IC,IS,1)+VC-(CSQ(IC,(IS+1))-
     *-CQ(IC,(IS+1),1))-RLATEQ)/
     *(CARM2(IC,IS)-CARM2(IC,(IS+1))-RLATEA)
            END IF
            WRITE(N9,7600) NS,IC,IS,NUNITC(IC,IS),
     *REFF,PROD,CARM2(IC,IS),CCLEN(IC,IS)
300       CONTINUE
        END IF
400     CONTINUE
      ELSE IF (NCHA.EQ.0) THEN
        IC=1
        IS=1
        NC=1
        DO 450 I=NELM(IC,IS,NC),1,-1
          VH=0.0
          VH=HAREA(IC,IS,NC,I,1)*RLEN(IC,IS,NC,I)
          SUMV(NS)=SUMV(NS)+VH
          IF (I.LT.NELM(IC,IS,NC)) THEN
            REFF=((SQ(IC,IS,NC,I)-Q(IC,IS,NC,I,1)+VH)/
     *(SQ(IC,IS,NC,(I+1))-Q(IC,IS,NC,(I+1),1)+
     *CHRAIN(IC,IS,NC,I)-CHRAIN(IC,IS,NC,(I+1))))*100.0
            PROD=(SQ(IC,IS,NC,I)-Q(IC,IS,NC,I,1)+VH-
     *(SQ(IC,IS,NC,(I+1))-Q(IC,IS,NC,(I+1),1)))/
     *(HARM2(IC,IS,NC,I)-HARM2(IC,IS,NC,(I+1)))
          ELSE IF (I.EQ.NELM(IC,IS,NC)) THEN
            REFF=((SQ(IC,IS,NC,I)-Q(IC,IS,NC,I,1)+VH)/
     *CHRAIN(IC,IS,NC,I))*100.0
            PROD=(SQ(IC,IS,NC,I)-Q(IC,IS,NC,I,1)+VH)/
     *HARM2(IC,IS,NC,I)
          END IF
          WRITE(N9,7500) NS,IC,IS,NC,I,NUNIT(IC,IS,NC,I),
     *REFF,PROD,HARM2(IC,IS,NC,I)
450     CONTINUE
      END IF
      IF (NCHA.GT.0) THEN
        SUMCQ(NS)=CSQ(1,1)-CQ(1,1,1)
        TIN(NS)=CCRAIN(1,1)
        TLOSS(NS)=CSUMCI(1,1)
        TSTOR(NS)=SUMV(NS)+SUMCV(NS)
      ELSE IF (NCHA.EQ.0) THEN
        SUMCQ(NS)=SQ(1,1,1,1)-Q(1,1,1,1,1)
        TIN(NS)=CHRAIN(1,1,1,1)
        TLOSS(NS)=CSUMI(1,1,1,1)
        TSTOR(NS)=SUMV(NS)
      END IF
      CONT(NS)=TIN(NS)-TLOSS(NS)-TSTOR(NS)-SUMCQ(NS)
      PERC(NS)=(CONT(NS)/TIN(NS))*100.0
      IF (PERC(NS).GT.0.01) THEN
        WRITE(*,7250) NS,CONT(NS),PERC(NS),TIN(NS),TLOSS(NS),
     *TSTOR(NS),SUMCQ(NS)
      END IF
      IF (PERC(NS).LT.(-0.01)) THEN
        WRITE(*,7250) NS,CONT(NS),PERC(NS),TIN(NS),TLOSS(NS),
     *TSTOR(NS),SUMCQ(NS)
      END IF
         WRITE(*,7250) NS,CONT(NS),PERC(NS),TIN(NS),TLOSS(NS),
     *TSTOR(NS),SUMCQ(NS)
      RETURN
7250  FORMAT(1X,I2,1X,F12.2,1X,F7.3,4(1X,F12.2))
7500  FORMAT(3(1X,I2),1X,I1,1X,I2,1X,I2,1X,F7.3,1X,F10.2,
     *1X,F9.2)
7600  FORMAT(3(1X,I2),6X,I2,1X,F7.3,1X,F10.2,1X,F9.2,1X,F7.2)
      END
C
*********************************************************************
```

```
      SUBROUTINE COURANT
C
      PARAMETER (IH=12,NF=16,I1=7,I2=46,I3=2,I4=54,I5=2)
      PARAMETER (NU=9,K9=2,MK=20,MJ=30,I4P=55,NSA=127,MT=100)
      PARAMETER (N1=11,N2=22,N3=33,N4=44,N5=55,N6=66,N7=77,N8=88,N9=90)
      PARAMETER (CON=10.0)
      COMMON/MAIN/NS,NSUB,IC,IS,NC,I,J,NTTOT,LAP,TINC,TIME,
     *LC,AREAM2(IH),CHANLENM(IH),IHV,WID(I1,I2,I3,I4),NCAS(I1,I2),
     *CHRAIN(I1,I2,I3,I4),CSUMI(I1,I2,I3,I4),HARM2(I1,I2,I3,I4),
     *CARM2(I1,I2),MAXU,AIN(NU),BIN(NU),UCM2(I1,I2,NU),SQ(I1,I2,I3,I4),
     *UHM2(I1,I2,I3,I4,NU),RAG(NSA),RBG(NSA),WWPRAT(NSA),
     *RAM(NU),RBM(NU),NSU(NSA),RIR(I1,I2,I3,I4),UIR(NU),
     *Q(I1,I2,I3,I4,I5),NITS,NR,NTMOD,NP,SLOPE(I1,I2,I3,I4)
      COMMON/HILL/NELM(I1,I2,I3),IHY(I1,I2,I3,I4),A(I1,I2,I3,I4),
     *B(I1,I2,I3,I4),RLEN(I1,I2,I3,I4),HPOTI,
     *SUMI(I1,I2,I3,I4),HAREA(I1,I2,I3,I4,I5),HPOTI1,
     *TRAIN(I1,I2,I3,I4),K44,SRAIN(I4),
     *NUNIT(I1,I2,I3,I4),AP(I1,I2,I3,I4),RA(I1,I2,I3,I4),
     *RB(I1,I2,I3,I4),TPR(I1,I2,I3,I4),NUMA(I1,I2,I3,I4),
     *AM(I1,I2,I3,I4),BM(I1,I2,I3,I4),NUMB(I1,I2,I3,I4),TT(I1,I2,I3,I4),
     *SUMA(I1,I2,13,I4),VS(I1,I2,I3,I4),TO(I1,I2,I3,I4)
      COMMON/CHAN/NCHA,NSEG(I1),IHYC(I1,I2),EC(I1,I2),TTC(I1,I2),
     *CA(I1,I2),CB(I1,I2),CWID(I1,I2),EANG(I1,I2),WANG(I1,I2),
     *CTOP(I1,I2),CLEN(I1,I2),CGRA(I1,I2),CPER(I1,I2),COPEN(I1,I2),
     *CPOTI,SUMCI(I1,I2),CAREA(I1,I2,I5),CPOTI1,CQ(I1,I2,I5),
     *CSQ(I1,I2),CWP,DEPTH,CTRAIN(I1,I2),K33,CXSA(I1,I2),SCRAIN(I2),
     *CCRAIN(I1,I2),CSUMCI(I1,I2),NUNITC(I1,I2),APC(I1,I2),
     *CCLEN(I1,I2),IOFLOW(I1,I2),NUMAC(I1,I2),NUMBC(I1,I2)
      COMMON/COUR/CVEL(I1,I2,I3),VEL(I1,I2,I3,I4,I5),NSTIF,
     *INSTC(I1,I2),INSTH(I1,I2,I3,I4)
      REAL STABC1,STABC2,STABH1,STABH2,CONDC,CONDH,ASTOR2,HWP
      INTEGER IC1,IS1,NIC
C for channels.....
      STABC1=0.0
      STABC2=0.0
      STABH1=0.0
      STABH2=0.0
      HWP=0.0
      ASTOR2=0.0
      IF (NSTIF.EQ.2) THEN
C
        IF (J.EQ.1) THEN
          STABC1=ABS(1.0/(CVEL(IC,IS,1)+SQRT(981*
     *DEPTH)))
          IF ((CVEL(IC,IS,1)-SQRT(981*DEPTH)).NE.0.0) THEN
            STABC2=ABS(1.0/(CVEL(IC,IS,1)-SQRT(981*
     *DEPTH)))
          ELSE IF ((CVEL(IC,IS,1)-SQRT(981*DEPTH)).EQ.0.0) THEN
            STABC2=100.0
          END IF
        ELSE IF (J.GT.1) THEN
          STABC1=ABS(1.0/(CVEL(IC,IS,2)+SQRT(981*
     *DEPTH)))
          IF ((CVEL(IC,IS,2)-SQRT(981*DEPTH)).NE.0.0) THEN
            STABC2=ABS(1.0/(CVEL(IC,IS,2)-SQRT(981*
     *DEPTH)))
          ELSE IF ((CVEL(IC,IS,2)-SQRT(981*DEPTH)).EQ.0.0) THEN
            STABC2=100.0
          END IF
        END IF
C
        CONDC=TINC/CLEN(IC,IS)
C
        IF ((STABC1.LT.(CONDC*10.0)) .AND. (STABC2.LT.
     *(CONDC*10.0))) THEN
          NTMOD=1
          INSTC(IC,IS)=1
        ELSE IF (((STABC1.GE.(CONDC*10.0)) .AND. (STABC1.LE.
     *(CONDC*20.0))) .AND. ((STABC2.GE.(CONDC*10.0)) .AND.
```

```
     *(STABC2.LE.(CONDC*20.0)))) THEN
          IF (NTMOD.NE.1) THEN
            NTMOD=2
          END IF
        ELSE IF ((STABC1.GT.(CONDC*20.0)) .AND. (STABC2.GT.
     *(CONDC*20.0))) THEN
          IF ((NTMOD.LT.1) .OR. (NTMOD.GT.2)) THEN
            NTMOD=3
          END IF
        END IF
       ELSE IF (NSTIF.EQ.1) THEN
C for hillslope........
        IF (J.EQ.1) THEN
          ASTOR2=HAREA(IC,IS,NC,I,1)/(WID(IC,IS,NC,I)/190.0)
          HWP=(CON**(RA(IC,IS,NC,I)+(RB(IC,IS,NC,I)*LOG10(ASTOR2))))
          IF (HWP.GT.(190.0*TPR(IC,IS,NC,I))) THEN
            HWP=TPR(IC,IS,NC,I)*190.0
          END IF
          DEPTHH=ASTOR2/HWP
        STABH1=ABS(1.0/(VEL(IC,IS,NC,I,1)+SQRT(981*DEPTHH)))
        IF ((VEL(IC,IS,NC,I,1)-SQRT(981*DEPTHH)).NE.0.0) THEN
          STABH2=ABS(1.0/(VEL(IC,IS,NC,I,1)-SQRT(981*
     *DEPTHH)))
        ELSE IF ((VEL(IC,IS,NC,I,1)-SQRT(981*DEPTHH)).EQ.0.0) THEN
          STABH2=100.0
        END IF
        ELSE IF (J.GT.1) THEN
          ASTOR2=HAREA(IC,IS,NC,I,2)/(WID(IC,IS,NC,I)/190.0)
          HWP=(CON**(RA(IC,IS,NC,I)+(RB(IC,IS,NC,I)*LOG10(ASTOR2))))
          IF (HWP.GT.(190.0*TPR(IC,IS,NC,I))) THEN
            HWP=TPR(IC,IS,NC,I)*190.0
          END IF
          DEPTHH=ASTOR2/HWP
          STABH1=ABS(1.0/(VEL(IC,IS,NC,I,2)+SQRT(981*DEPTHH)))
          IF ((VEL(IC,IS,NC,I,2)-SQRT(981*DEPTHH)).NE.0.0) THEN
            STABH2=ABS(1.0/(VEL(IC,IS,NC,I,2)-SQRT(981*
     *DEPTHH)))
          ELSE IF ((VEL(IC,IS,NC,I,2)-SQRT(981*DEPTHH)).EQ.0.0) THEN
            STABH2=100.0
          END IF
        END IF
        CONDH=TINC/RLEN(IC,IS,NC,I)
        IF ((STABH1.LT.(CONDH*10.0)) .AND. (STABH2.LT.
     *(CONDH*10.0))) THEN
          NTMOD=1
          INSTH(IC,IS,NC,I)=1
        ELSE IF (((STABH1.GE.(CONDH*10.0)) .AND. (STABH1.LE.
     *(CONDH*20.0))) .AND. ((STABH2.GE.(CONDH*10.0)) .AND.
     *(STABH2.LE.(CONDH*20.0)))) THEN
          IF (NTMOD.NE.1) THEN
            NTMOD=2
          END IF
        ELSE IF ((STABH1.GT.(CONDH*20.0)) .AND. (STABH2.GT.
     *(CONDH*20.0))) THEN
          IF ((NTMOD.LT.1) .OR. (NTMOD.GT.2)) THEN
            NTMOD=3
          END IF
        END IF
       END IF
       RETURN
 1000  FORMAT(1X,F7.1,1X,F7.2,1X,I2,1X,I2,1X,F6.2,1X,F6.1,1X,F6.1,1X,
     *F8.2,3(1X,F8.5))
 1100  FORMAT(1X,F7.1,1X,F7.2,1X,I2,1X,I2,1X,I1,1X,I2,1X,F6.2,1X,F6.1,
     *1X,F8.2,3(1X,F8.5))
 1200  FORMAT(2(1X,F7.2),1X,F6.3,2(1X,F6.3),1X,F6.4,2(1X,F7.4))
 1300  FORMAT(2(1X,F6.1),1X,F6.3,3(1X,F5.1),1X,F7.1,2(1X,F7.4),
     *1X,F6.4,1X,F8.5)
       END
```

Appendix 4.2 Modified Run-on/Runoff Plot Simulation Model RORO Program Code

```
      PROGRAM RORO
      PARAMETER (CON=10.0,I1=30,I2=10,I3=10,I4=11,I5=2)
      CHARACTER*11 PLOT,OBSE,FLOW,PRED,DELT
      INTEGER NWC,NOB,NTT,NTOB(I1),NITS,K,J,I,NOP,NTWC(I2),
     *NTO(2),NUMR,NUMA1(I3),NUMA2(I3),NUMB1(I3),NUMB2(I3)
      REAL A1,B1,SLOPE,LEN,RS,DQ1,ST1,
     *TWC(I2),WID(I4,I2),T4L(I1),LOF(I1),TOB(I1),Q2(I1),Q1(I1),QOBS,
     *TOBS,TINC,TIME,TIME1,COUNT,STOR,QQ1(I4,I5),QQ2(I4,I5),
     *STOR2,PI1(I3),DUW1(I3,2),INF1,ISUM1(I3),
     *VEL1(I3,2),SQ1(I3),ASTOR,HWP,ROUGH,SUMA(I3),A,AA,WP,
     *VQQ1(I3,2),QIN,SUMI1,RESV1,VS,PP(I4),QNA(I4),
     *CONT1,PERC1,OBS,T1(I3),T2(I3),TO1(I3)
      DATA (NUMA1(I),NUMA2(I),NUMB1(I),NUMB2(I),I=1,I3)/40*0/
      DATA (T1(I),T2(I),TO1(I),SUMA(I),I=1,I3)/40*0.0/
      READ(10,999) PLOT
      READ(10,999) OBSE
      READ(10,999) FLOW
      READ(10,999) PRED
      READ(10,999) DELT
      OPEN(11,FILE=PLOT,STATUS='OLD')
      OPEN(12,FILE=OBSE,STATUS='OLD')
      OPEN(13,FILE=FLOW,STATUS='NEW')
      OPEN(14,FILE=PRED,STATUS='NEW')
      OPEN(15,FILE=DELT,STATUS='NEW')
C
c  this version of the program is written to handle 5 elements in a flow
c  sequence only

      READ(11,1000) A1,B1,RS,SLOPE,LEN
      READ(11,1100) NWC
c  A1 and B1 are infiltration parameters, RS is roughness
c  WPA and WPB are the regression coefficients in the WP-A equation
c  TPR is the ratio of top width to maximum WP, SLOPE is the gradient sine
c  and LEN is Δx
C  loop to read in when the widths change
      DO 25 K=1,NWC
        READ(11,1200) NTWC(K)
        TWC(K)=REAL(NTWC(K))
        READ(11,1300) (WID(I,K),I=5,1,-1)
25    CONTINUE
      WID(6,1)=100.0
      READ(12,1100) NOB
      NTT=0
      NOP=1
c  loop to read in number of input and output data observations and calculate the
c  input discharge in cm/s
      DO 50 K=1,NOB
        READ(12,1400) NTOB(K),T4L(K),LOF(K)
        NTT=NTT+NTOB(K)
        TOB(K)=REAL(NTT)
        Q2(K)=4000.0/(T4L(K)*60.0)
        Q1(K)=Q2(K)/100.0
50    CONTINUE
      TOBS=TOB(1)
      READ(11,1500) NITS,TINC
      QIN=0.0
      TIME=0.0
      TIME1=0.0
      NTO(1)=0
      NTO(2)=0
C start of time loop from 1 to the number of iterations (truncated when
c end of the plot test is reached)
      DO 500 J=1,NITS
        TIME=TIME+TINC
        TIME1=TIME-TINC
        COUNT=TIME
        T1(5)=TIME
        T2(5)=TIME
c loop to assign constant rate discharges for a given time period into
```

```
c the upper cell
        DO 75 K=1,NOB
          IF (COUNT.LT.TOB(K)) THEN
            STOR=TOB(K)-COUNT
            IF (STOR.GE.TINC) THEN
              QQ1(6,1)=Q1(K)*TINC
              QQ2(6,1)=Q2(K)*TINC
              K=NOB+1
            ELSE IF (STOR.LT.TINC) THEN
              STOR2=TINC-STOR
              QQ1(6,1)=(Q1(K-1)*STOR2)+(Q1(K)*STOR)
              QQ2(6,1)=(Q2(K-1)*STOR2)+(Q2(K)*STOR)
              K=NOB+1
            END IF
            QIN=QIN+QQ2(6,1)
          END IF
75      CONTINUE
c  cell loop from top=5 to bottom = 1
        DO 400 I=5,1,-1
c  sections to calculate the average p for cells other than the upper one since
c  the rate of discharge out of each cell increases with time past the time to
c  ponding.  only depth equivalent in excess of p is assumed to add to storage
          IF (I.LT.5) THEN
            IF (NUMA1(I).GT.0) THEN
              T1(I)=T1(I)+TINC
              IF (NUMA2(I).EQ.0) THEN
                PP(I)=SQ1(I+1)/(WID(I,1)*T1(I)*LEN)
                QNA(I)=SQ1(I+1)
              END IF
              IF (PP(I).GE.A1) THEN
                T2(I)=T2(I)+TINC
                NUMA2(I)=1
              END IF
            ELSE IF (NUMA1(I).EQ.0) THEN
              IF (SQ1(I+1).GT.0.0) THEN
                NUMA1(I)=1
                T1(I)=TINC
              END IF
            END IF
          END IF
c  sections for first time period only to calculate when time to ponding occurs
c  when the average input
          IF (J.EQ.1) THEN
            IF (I.EQ.5) THEN
              IF (NUMB1(I).EQ.0) THEN
                TO1(I)=B1/((QIN/(WID(I,1)*T1(I)*LEN))-A1)
                IF ((TO1(I).GT.0.0) .AND. (TO1(I).LE.T1(I))) THEN
                  NUMB1(I)=1
                  VS=((QIN/WID(I,1)*T1(I)*LEN)*B1)/((QIN/(WID(I,1)*
     *T1(I)*LEN))-A1)
                  WRITE(14,*) 'A Cell=',I,' Time=',TIME,' To=',
     *TO1(I),' Vs=',VS
                END IF
              END IF
c  section to calculate routing using Manning's and the finite difference equations
C  to calculate the depth of flow DUW1 and velocity VEL1
c  Green and Ampt equation provides infiltration PI1
              IF (NUMB1(I).GT.0) THEN
                PI1(I)=(A1+(B1/T1(I)))*TINC
                DUW1(I,1)=((QQ1(I+1,1)/TINC)*(WID(6,1)/
     *WID(I,1)))
                XS=DUW1(I,1)-PI1(I)
                IF (XS.LT.0.0) THEN
                  INF1=DUW1(I,1)*WID(I,1)
                  DUW1(I,1)=0.0
                ELSE IF (XS.GE.0.0) THEN
                  DUW1(I,1)=XS
                  INF1=PI1(I)*WID(I,1)
                END IF
```

```
                ISUM1(I)=INF1*LEN
                COUR=TINC/LEN
                IF (DUW1(I,1).GT.0.0) THEN
                  ROUGH=RS
                  VEL1(I,1)=(SQRT(SLOPE)/ROUGH)*(DUW1(I,1)**
     *(2.0/3.0))*4.64
                END IF
                QQ1(I,1)=VEL1(I,1)*DUW1(I,1)*TINC
                SQ1(I)=0
              ELSE IF (NUMB1(I).EQ.0) THEN
                ISUM1(I)=QIN
              END IF
            END IF
c  sections for all subsequent time periods
          ELSE IF (J.GT.1) THEN
            DO 90 K=1,NWC
              IF (TIME.LE.TWC(K)) THEN
                WID(I,1)=WID(I,K)
                K=NWC+1
              END IF
90          CONTINUE
c  procedures to calculate when ponding occurs (to and Vs)
           IF (NUMB1(I).EQ.0) THEN
c  for the top element I=5
              IF (I.EQ.5) THEN
                TO1(I)=B1/((QIN/(WID(I,1)*T1(I)*LEN))-A1)
                IF ((TO1(I).GT.0.0) .AND. (TO1(I).LE.T1(I))) THEN
                  NUMB1(I)=1
                  VS=((QIN/(WID(I,1)*T1(I)*LEN))*B1)/((QIN/(WID(I,1)*
     *T1(I)*LEN))-A1)
                  WRITE(14,*) 'A Cell=',I,' Time=',TIME,' To=',
     *TO1(I),' Vs=',VS
                END IF
c  for the lower elements
              ELSE IF (I.LT.5) THEN
                IF (NUMA2(I).GT.0) THEN
                  TO1(I)=B1/(((SQ1(I+1)-QNA(I))/(WID(I,1)*T2(I)*LEN))
     *-A1)
                  IF ((TO1(I).GT.0.0) .AND. (TO1(I).LE.T2(I))) THEN
                    NUMB1(I)=1
                    VS=(((SQ1(I+1)-QNA(I))/(WID(I,1)*T2(I)*LEN))*B1)/
     *(((SQ1(I+1)-QNA(I))/(WID(I,1)*T2(I)*LEN))-A1)
                    WRITE(14,*) 'A Cell=',I,' Time=',TIME,' To=',
     *TO1(I),' Vs=',VS
                  END IF
                END IF
              END IF
            END IF
c  section to calculate routing using Manning's and the finite difference equations
C  to calculate the depth of flow DUW1 and velocity VEL1
c  Green and Ampt equation provides infiltration PI1
            IF (NUMB1(I).GT.0) THEN
              PI1(I)=(A1+(B1/T2(I)))*TINC
              DUW1(I,2)=DUW1(I,1)+(((QQ1(I+1,1)*(WID(I+1,1)/
     *WID(I,1)))-QQ1(I,1))/LEN)
              IF (DUW1(I,2).LT.0.0) THEN
                WRITE(*,*) 'ERROR IN ROUTING EQUATION DUW1(I,2)
     *NEG',J,I
              ELSE IF (DUW1(I,2).GE.0.0) THEN
                XS=DUW1(I,2)-PI1(I)
                IF (XS.LT.0.0) THEN
                  INF1=DUW1(I,2)*WID(I,1)
                  DUW1(I,2)=0.0
                ELSE IF (XS.GE.0.0) THEN
                  DUW1(I,2)=XS
                  INF1=PI1(I)*WID(I,1)
                END IF
              END IF
              ISUM1(I)=ISUM1(I)+(INF1*LEN)
```

```
            IF (DUW1(I,2).GT.0.0) THEN
              ROUGH=RS
              VEL1(I,2)=(SQRT(SLOPE)/ROUGH)*(DUW1(I,2)**
     *(2.0/3.0))*4.64
            END IF
            QQ1(I,2)=VEL1(I,2)*DUW1(I,2)*TINC
            IF (NTO(1).EQ.0) THEN
              IF (QQ1(1,2).GT.0.0) NTO(1)=1
              IF (NTO(1).EQ.1) THEN
                WRITE(14,*) 'TIME TO RUN-OUT METH A = ',TIME,J
                NTO(1)=2
              END IF
            END IF
            SQ1(I)=SQ1(I)+(QQ1(I,2)*WID(I,1))
          ELSE IF (NUMB1(I).EQ.0) THEN
            ISUM1(I)=SQ1(I+1)
          END IF
        END IF
400     CONTINUE
c  routines to write predictions to data files for comparison with observed
        DO 425 K=NOP,NOB
          IF (TIME.GE.TOBS) THEN
c  these provide a set of observations of velocity, depth, volumetric discharge
c  rate, the sum of infiltration and the cumulative volumetric discharge
            WRITE(13,*) TIME,J
            WRITE(13,1600) (VEL1(I,2),I=1,5)
            WRITE(13,1700) (DUW1(I,2),I=1,5)
            do 410 i=1,5
              VQQ1(I,2)=QQ1(I,2)*WID(I,1)
410         continue
            WRITE(13,1800) (VQQ1(I,2),I=1,5)
            WRITE(13,1900) (ISUM1(I),I=1,5)
            WRITE(13,1900) (SQ1(I),I=1,5)
c  these write the observed and predicted ΔQ and ΣQ values to a data file at
c  predetermined times
            OBS=OBS+(LOF(K)*1000.0)
            QOBS=LOF(K)*1000.0
            DQ1=SQ1(1)-ST1
            WRITE(15,2000) TIME,QOBS,DQ1,OBS,SQ1(1)
            ST1=SQ1(1)
c  this resets the observed time counter to the next counter following writing out
            IF (K.LT.NOB) THEN
              NOP=NOP+1
              TOBS=TOB(K+1)
            ELSE IF (K.EQ.NOB) THEN
              TOBS=REAL(NTT)*10.0
            END IF
          END IF
425     CONTINUE
c  this resets data-stores for use in the finite difference equation (t-1)
        DO 450 I=1,5
          VEL1(I,1)=VEL1(I,2)
          DUW1(I,1)=DUW1(I,2)
          VQQ1(I,1)=VQQ1(I,2)
          QQ1(I,1)=QQ1(I,2)
450     CONTINUE
        IF (TIME.GE.REAL(NTT)) THEN
          WRITE(14,*) 'J SET TO NITS AT J=',J
          J=NITS+1
        END IF
500   CONTINUE
c  this checks to see the model has obeyed laws of continuity and all inputs equal
c  outputs plus storages
      DO 600 I=1,5
        SUMI1=SUMI1+ISUM1(I)
        RESV1=RESV1+(DUW1(I,1)*WID(I,1)*LEN)
600   CONTINUE
      CONT1=QIN-(SQ1(1)-VQQ1(1,1)+SUMI1+RESV1)
      PERC1=(CONT1/QIN)*100.0
```

```
      WRITE(13,2100) PERC1,QIN,SQ1(1),VQQ1(1,1),SUMI1,RESV1,CONT1
      STOP
999   FORMAT(1X,A11)
1000  FORMAT(1X,F8.6,1X,F6.4,1X,F5.3,1X,F6.4,1X,F5.1)
1025  FORMAT(5(1X,F5.3))
1100  FORMAT(1X,I3)
1200  FORMAT(1X,I4)
1300  FORMAT(5(1X,F6.1))
1400  FORMAT(1X,I4,2(1X,F5.3))
1500  FORMAT(1X,I5,1X,F5.1)
1600  FORMAT(5(1X,F7.4))
1700  FORMAT(5(1X,F7.3))
1800  FORMAT(5(1X,F7.4))
1900  FORMAT(5(1X,F7.1))
2000  FORMAT(1X,F6.1,5(1X,F10.3))
2100  FORMAT(1X,F7.1,1X,F8.1,1X,F8.1,1X,F7.1,1X,F8.1,1X,F8.2,1X,F8.2)
      END
```

APPENDIX 4.3 Unit and Sample Data Set Used for Parameter Provision

```
Template (See Appendix 4.1)
MAXU MAXSAM NCHIN
AIN BIN RAM RBM UIR
... ... ..... ...
RAG RBG WWPRAT NSU
9 127 1
0.000414 0.0274 00.4600  0.0000 1.000
0.000427 0.0106 00.4200  0.0000 1.000
0.000179 0.0133 00.3800  0.0000 1.000
0.000047 0.0188 00.4800  0.0000 1.000
0.000087 0.1710 00.4100  0.0000 1.000
0.000087 0.1710 00.2800  0.0000 1.000
0.000777 0.0233 00.3500  0.0000 1.000
0.000171 0.0065 00.2600  0.0000 1.000
0.000193 0.0156 00.2600  0.0000 1.000
2.28 0.000 1.0000 1
2.28 0.000 1.0000 1
2.28 0.000 1.0000 2
2.28 0.000 1.0000 2
2.28 0.000 1.0000 2
2.28 0.000 1.0000 4
2.28 0.000 1.0000 4
2.28 0.000 1.0000 3
2.28 0.000 1.0000 4
2.28 0.000 1.0000 4
2.28 0.000 1.0000 4
2.28 0.000 1.0000 4
2.28 0.000 1.0000 4
2.28 0.000 1.0000 5
2.28 0.000 1.0000 1
2.28 0.000 1.0000 1
2.28 0.000 1.0000 2
2.28 0.000 1.0000 2
2.28 0.000 1.0000 2
2.28 0.000 1.0000 3
2.28 0.000 1.0000 3
2.28 0.000 1.0000 3
2.28 0.000 1.0000 4
2.28 0.000 1.0000 4
2.28 0.000 1.0000 4
2.28 0.000 1.0000 4
2.28 0.000 1.0000 4
2.28 0.000 1.0000 5
2.28 0.000 1.0000 5
2.28 0.000 1.0000 5
2.28 0.000 1.0000 6
2.28 0.000 1.0000 6
2.28 0.000 1.0000 7
2.28 0.000 1.0000 7
2.28 0.000 1.0000 8
2.28 0.000 1.0000 9
2.28 0.000 1.0000 9
2.28 0.000 1.0000 9
2.28 0.000 1.0000 9
2.28 0.000 1.0000 9
2.28 0.000 1.0000 9
2.28 0.000 1.0000 9
2.28 0.000 1.0000 7
2.28 0.000 1.0000 7
2.28 0.000 1.0000 6
2.28 0.000 1.0000 7
2.28 0.000 1.0000 7
2.28 0.000 1.0000 6
2.28 0.000 1.0000 6
2.28 0.000 1.0000 1
2.28 0.000 1.0000 1
2.28 0.000 1.0000 2
2.28 0.000 1.0000 2
2.28 0.000 1.0000 2
2.28 0.000 1.0000 3
2.28 0.000 1.0000 3
2.28 0.000 1.0000 3
2.28 0.000 1.0000 3
2.28 0.000 1.0000 7
2.28 0.000 1.0000 7
2.28 0.000 1.0000 7
2.28 0.000 1.0000 6
2.28 0.000 1.0000 6
2.28 0.000 1.0000 6
2.28 0.000 1.0000 6
```

Appendix 5.1.1 Results from Plot 18 Unit 1e

A	B1	n	S	Δt	Δx
0.000414	0.129	0.300	0.1461	1.0	20.0

t	5	4	3	2	1
721	95.2	83.0	72.8	65.4	58.6
1801	97.0	88.0	80.2	73.6	66.2
4828	100.5	102.5	103.0	104.0	105.0

Σt	Obs ΔQ	B1 ΔQ	Obs ΣQ	B1 ΣQ
85.0	0.000	0.000	0.000	0.000
267.0	1190.000	164.664	1190.000	164.664
534.0	2610.000	2234.456	3800.000	2399.120
793.0	2640.000	2743.562	6440.000	5142.682
1051.0	2730.000	2804.534	9170.000	7947.216
1307.0	2564.000	2890.123	11734.000	10837.339
1564.0	2690.000	2939.576	14424.000	13776.915
1828.0	2756.000	3034.618	17180.000	16811.533
2092.0	2732.000	2703.371	19912.000	19514.904
2358.0	2834.000	2703.014	22746.000	22217.918
2626.0	2774.000	2711.535	25520.000	24929.453
2902.0	2892.000	2699.750	28412.000	27629.203
3173.0	2726.000	2712.289	31138.000	30341.492
3443.0	2760.000	2734.809	33898.000	33076.301
3717.0	2752.000	2733.875	36650.000	35810.176
3990.0	2780.000	2737.285	39430.000	38547.461
4275.0	2878.000	2711.742	42308.000	41259.203
4557.0	2856.000	2705.461	45164.000	43964.664
4827.0	2764.000	2749.078	47928.000	46713.742

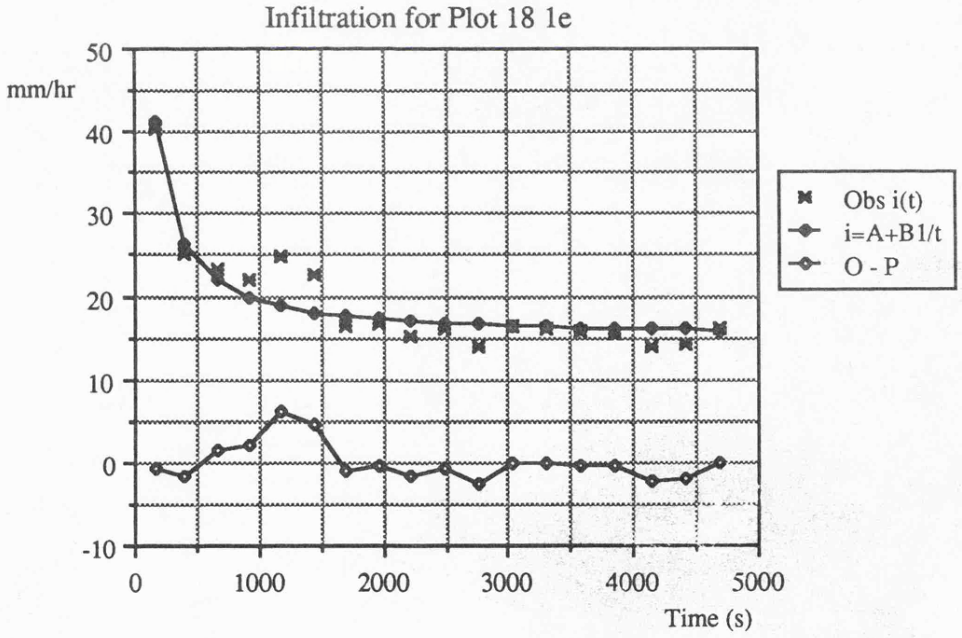

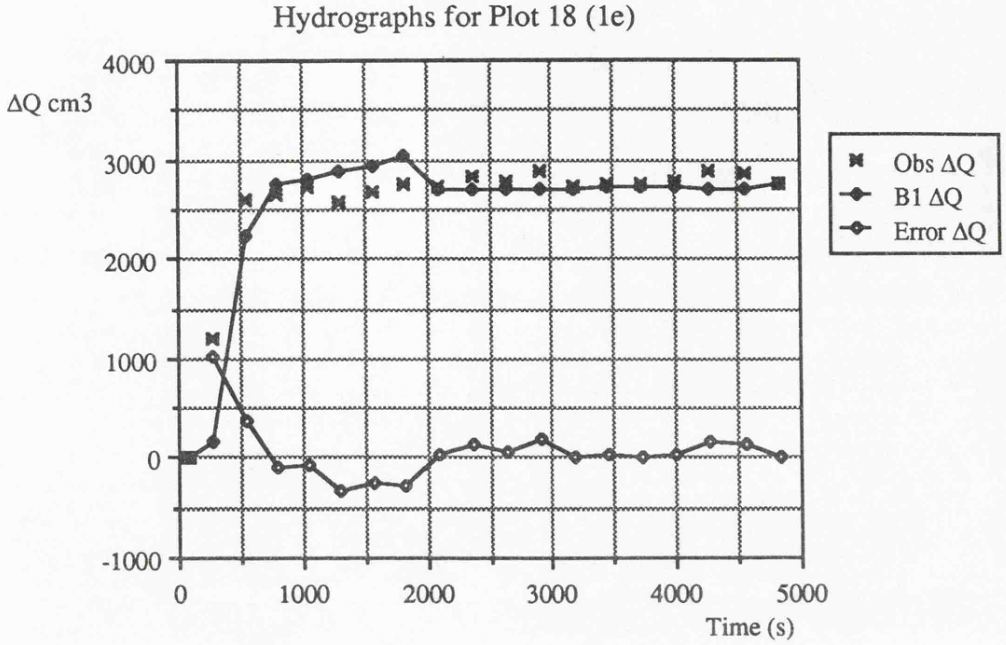

to5	Qin	WA	p	A	B2
17.3	14.9813	7500	0.0019975	0.000414	0.0274

Σt	Obs ΔQ	B1 ΔQ	Obs ΣQ	B1 ΣQ
85.0	0.000	6.481	0.000	6.481
267.0	1190.000	1747.193	1190.000	1753.674
534.0	2610.000	3008.815	3800.000	4762.490
793.0	2640.000	3111.538	6440.000	7874.028
1051.0	2730.000	3067.305	9170.000	10941.333
1307.0	2564.000	3087.440	11734.000	14028.773
1564.0	2690.000	3099.045	14424.000	17127.818
1828.0	2756.000	3175.484	17180.000	20303.303
2092.0	2732.000	2852.803	19912.000	23156.105
2358.0	2834.000	2835.209	22746.000	25991.314
2626.0	2774.000	2829.697	25520.000	28821.012
2902.0	2892.000	2808.811	28412.000	31629.822
3173.0	2726.000	2809.482	31138.000	34439.305
3443.0	2760.000	2823.418	33898.000	37262.723
3717.0	2752.000	2816.703	36650.000	40079.426
3990.0	2780.000	2813.801	39430.000	42893.227
4275.0	2878.000	2786.043	42308.000	45679.270
4557.0	2856.000	2774.055	45164.000	48453.324
4827.0	2764.000	2811.016	47928.000	51264.340

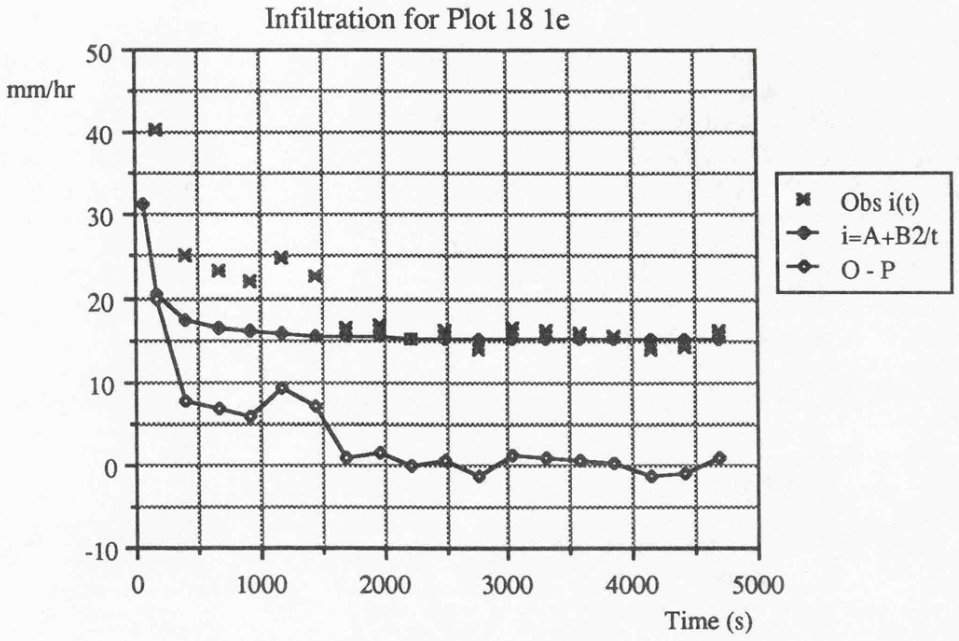
Infiltration for Plot 18 1e
mm/hr
50
40
30
20
10
0
-10
0
1000
2000
3000
4000
5000
Time (s)
Obs i(t)
i=A+B2/t
O - P

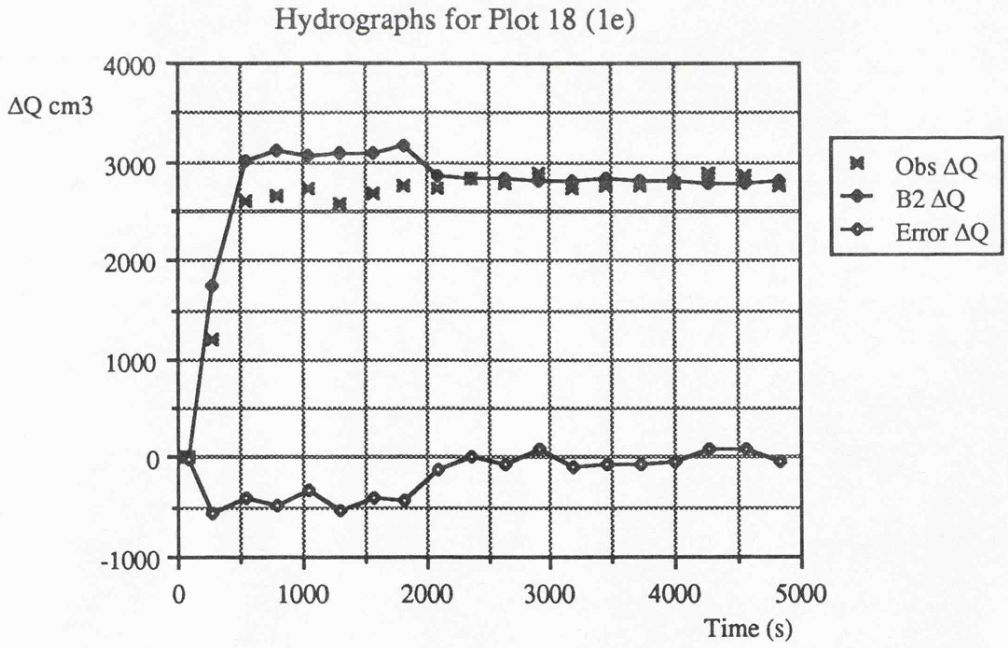
Hydrographs for Plot 18 (1e)
ΔQ cm3
4000
3000
2000
1000
0
-1000
0
1000
2000
3000
4000
5000
Time (s)
Obs ΔQ
B2 ΔQ
Error ΔQ

B1 and B2 Infiltration Curves for Plot 18 (1e)

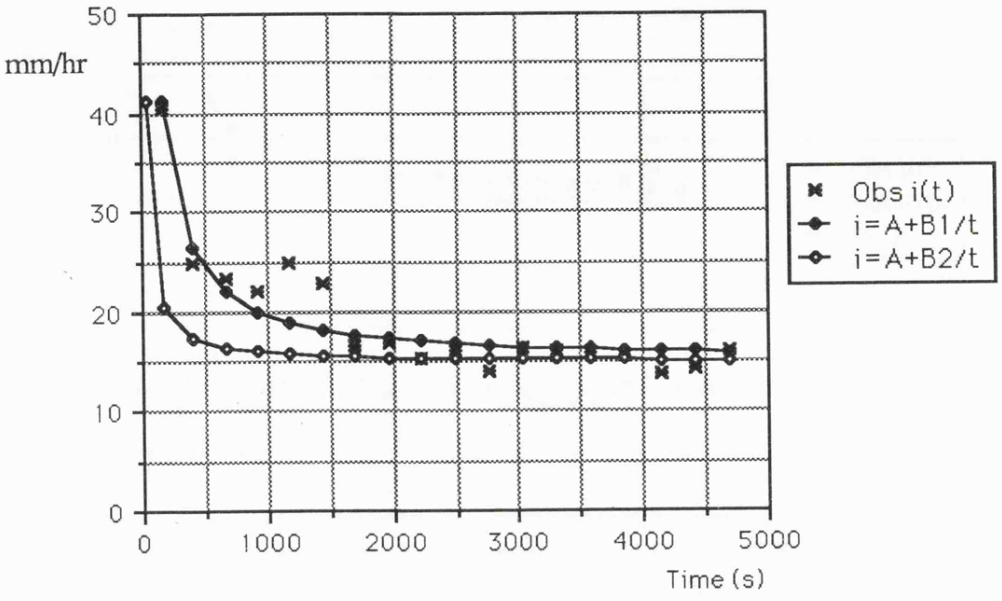

Hydrographs for Plot 18 (1e)

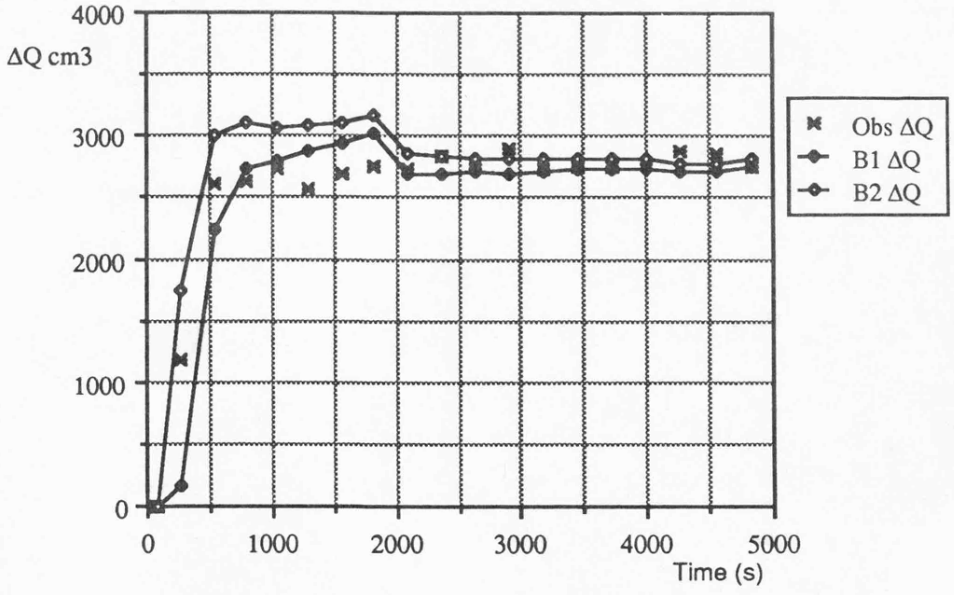

Appendix 5.1.2 Results from Plot 20 Unit 2e

A	B1	n	S	Δt	Δx
0.000427	0.111	0.37	0.3123	1.0	20.0

t	5	4	3	2	1
1801	103.0	113.0	120.0	128.0	136.0
3601	103.2	115.0	125.0	135.0	146.3
5030	118.5	124.5	132.0	130.0	135.0

Σt	Obs ΔQ	B1 ΔQ	Obs ΣQ	B1 ΣQ
215.0	0.000	0.000	0.000	0.000
383.0	248.000	0.000	248.000	0.000
606.0	1760.000	836.176	2008.000	836.176
827.0	2592.000	2185.542	4600.000	3021.719
1038.0	2616.000	2465.337	7216.000	5487.055
1243.0	2632.000	2628.684	9848.000	8115.739
1444.0	2710.000	2714.336	12558.000	10830.075
1652.0	2700.000	2747.144	15258.000	13577.219
1858.0	2702.000	2773.291	17960.000	16350.510
2066.0	2752.000	2729.896	20712.000	19080.406
2270.0	2844.000	2749.971	23556.000	21830.377
2476.0	2782.000	2778.941	26338.000	24609.318
2685.0	2756.000	2768.113	29094.000	27377.432
2885.0	2808.000	2791.920	31902.000	30169.352
3096.0	2730.000	2808.695	34632.000	32978.047
3317.0	2792.000	2756.254	37424.000	35734.301
3531.0	2816.000	2738.977	40240.000	38473.277
3746.0	2820.000	2786.172	43060.000	41259.449
3954.0	2750.000	2753.477	45810.000	44012.926
4171.0	2610.000	2772.320	48420.000	46785.246
4386.0	2760.000	2737.996	51180.000	49523.242
4605.0	2720.000	2743.238	53900.000	52266.480
4819.0	2672.000	2741.828	56572.000	55008.309
5029.0	2724.000	2773.324	59296.000	57781.633

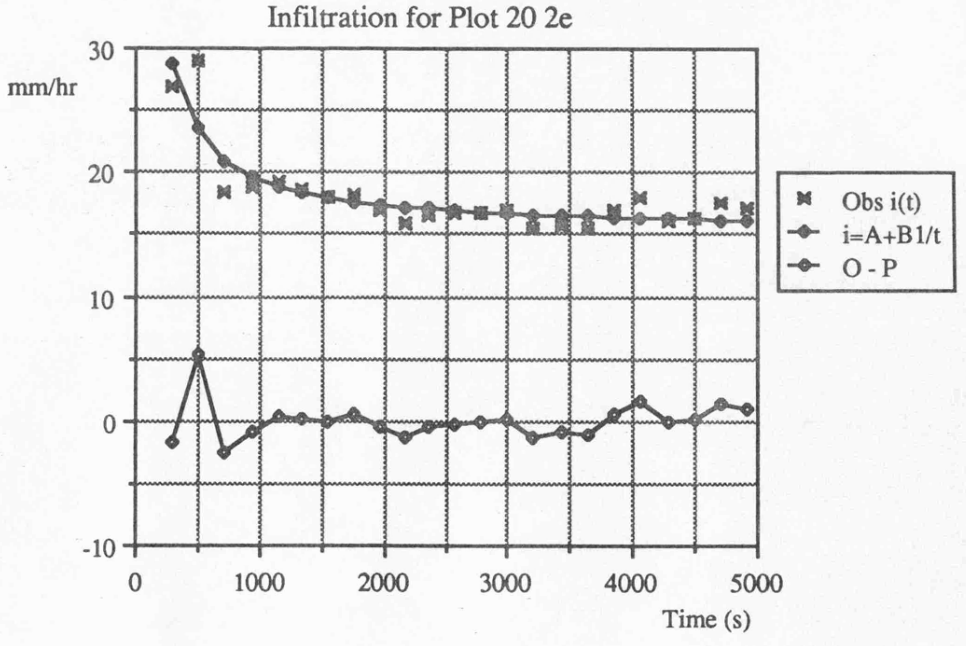

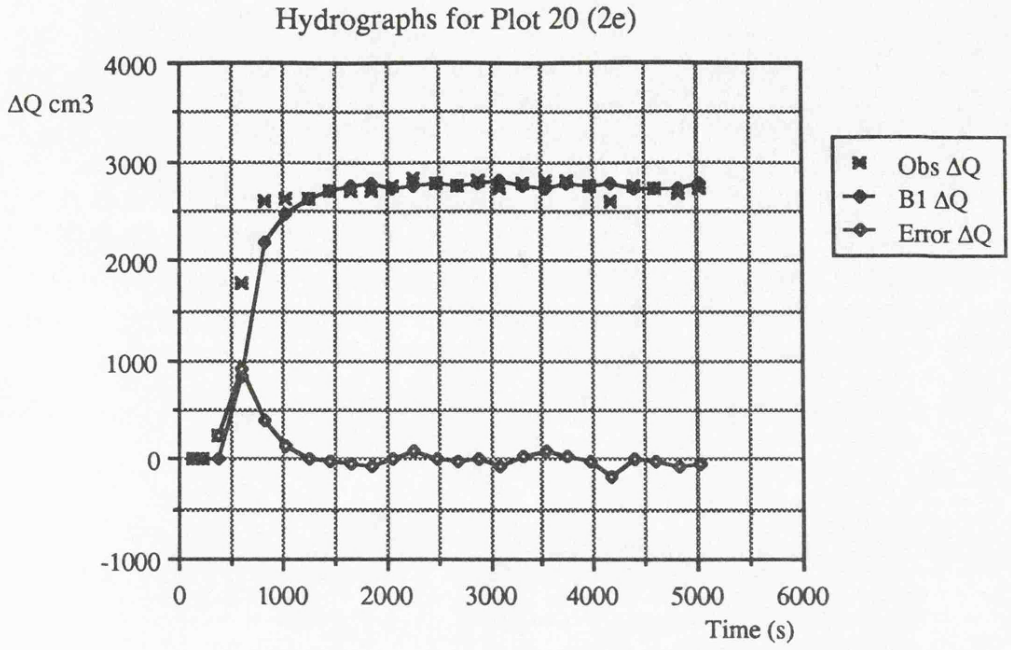

to5	Qin	WA	p	A	B2
23.93	10.444	12000	0.00087	0.000427	0.0106

Σt	Obs ΔQ	B2 ΔQ	Obs ΣQ	B2 ΣQ
215.0	0.000	182.885	0.000	182.885
383.0	248.000	777.285	248.000	960.170
606.0	1760.000	2427.325	2008.000	3387.495
827.0	2592.000	2809.679	4600.000	6197.174
1038.0	2616.000	2848.090	7216.000	9045.265
1243.0	2632.000	2908.532	9848.000	11953.797
1444.0	2710.000	2936.115	12558.000	14889.912
1652.0	2700.000	2939.385	15258.000	17829.297
1858.0	2702.000	2939.564	17960.000	20768.861
2066.0	2752.000	2881.816	20712.000	23650.678
2270.0	2844.000	2883.170	23556.000	26533.848
2476.0	2782.000	2900.230	26338.000	29434.078
2685.0	2756.000	2880.102	29094.000	32314.180
2885.0	2808.000	2890.871	31902.000	35205.051
3096.0	2730.000	2904.727	34632.000	38109.777
3317.0	2792.000	2849.594	37424.000	40959.371
3531.0	2816.000	2823.328	40240.000	43782.699
3746.0	2820.000	2865.992	43060.000	46648.691
3954.0	2750.000	2827.422	45810.000	49476.113
4171.0	2610.000	2844.883	48420.000	52320.996
4386.0	2760.000	2806.313	51180.000	55127.309
4605.0	2720.000	2809.156	53900.000	57936.465
4819.0	2672.000	2803.254	56572.000	60739.719
5029.0	2724.000	2830.934	59296.000	63570.652

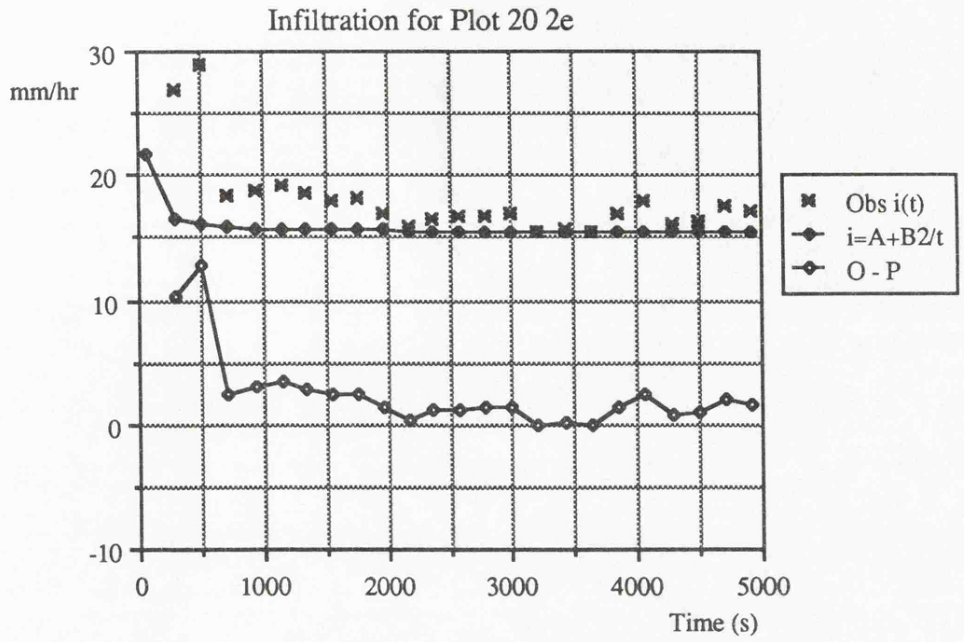
Infiltration for Plot 20 2e
mm/hr
30
20
10
0
-10
0
1000
2000
3000
4000
5000
Time (s)
Obs i(t)
i=A+B2/t
O - P

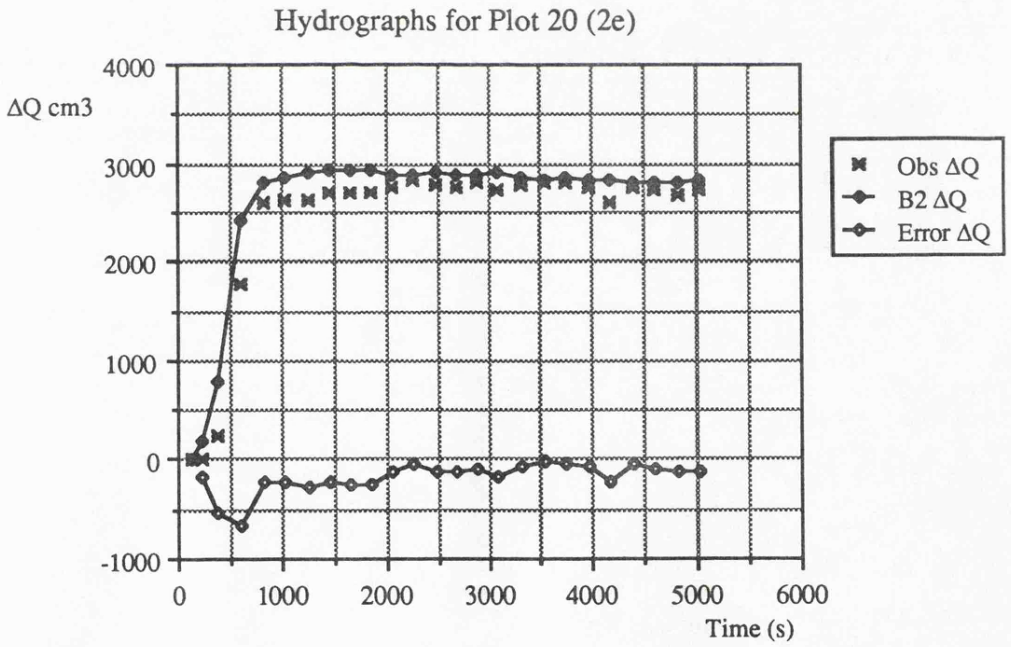
Hydrographs for Plot 20 (2e)
ΔQ cm3
4000
3000
2000
1000
0
-1000
0
1000
2000
3000
4000
5000
6000
Time (s)
Obs ΔQ
B2 ΔQ
Error ΔQ

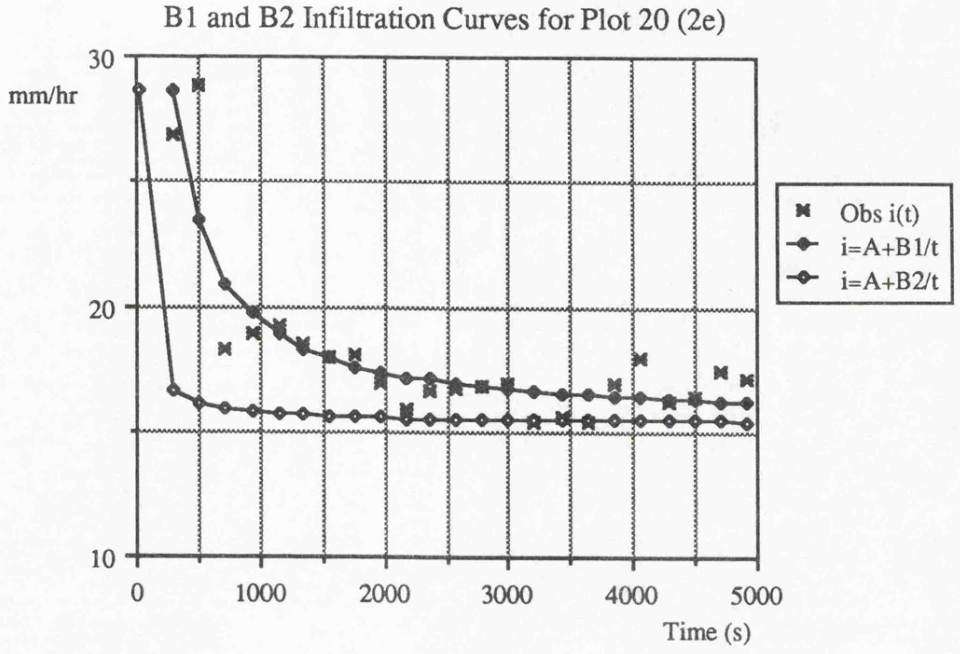
B1 and B2 Infiltration Curves for Plot 20 (2e)
mm/hr
30
20
10
0
1000
2000
3000
4000
5000
Time (s)
Obs i(t)
i=A+B1/t
i=A+B2/t

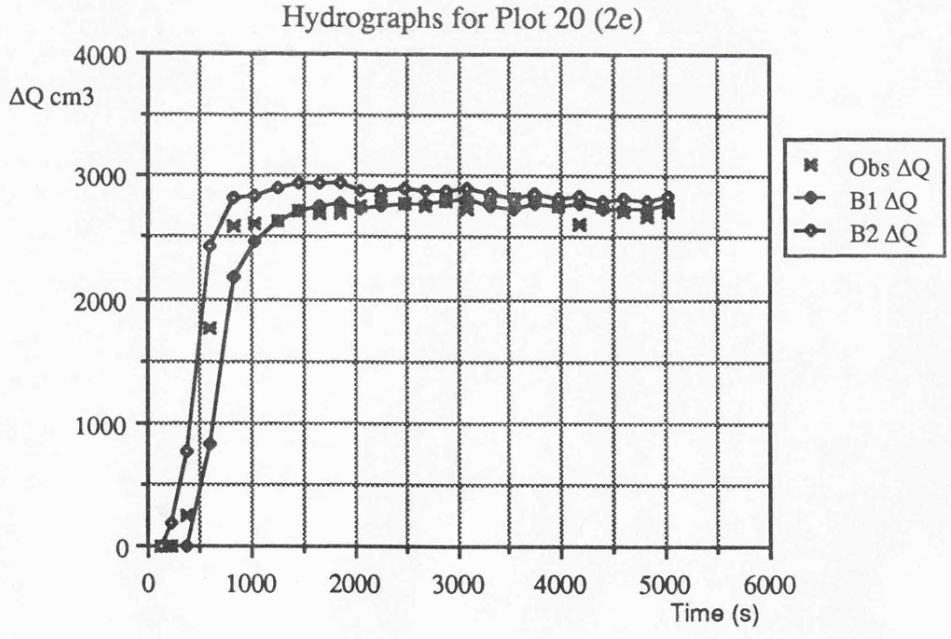
Hydrographs for Plot 20 (2e)
ΔQ cm3
4000
3000
2000
1000
0
0
1000
2000
3000
4000
5000
6000
Time (s)
Obs ΔQ
B1 ΔQ
B2 ΔQ

Appendix 5.1.3 **Results from Plot 23 Unit 3e**

A	B1	n	S	Δt	Δx
0.000179	0.0686	0.34	0.2554	1.0	20.0

t	5	4	3	2	1
4775	103.5	94.0	76.5	92.5	111.5

Σt	Obs ΔQ	B1 ΔQ	Obs ΣQ	B1 ΣQ
37.0	0.000	0.000	0.000	0.000
301.0	2032.000	716.194	2032.000	716.194
606.0	3168.000	2894.656	5200.000	3610.850
905.0	3222.000	3180.560	8422.000	6791.411
1210.0	3316.000	3276.722	11738.000	10068.133
1525.0	3222.000	3315.354	14960.000	13383.486
1826.0	3102.000	3340.285	18062.000	16723.771
2123.0	3170.000	3381.762	21232.000	20105.533
2412.0	3288.000	3400.936	24520.000	23506.469
2697.0	3258.000	3428.314	27778.000	26934.783
3009.0	3638.000	3441.572	31416.000	30376.355
3301.0	3398.000	3399.516	34814.000	33775.871
3575.0	3234.000	3431.332	38048.000	37207.203
3886.0	3774.000	3482.387	41822.000	40689.590
4190.0	3510.000	3415.133	45332.000	44104.723
4485.0	3716.000	3430.566	49048.000	47535.289
4774.0	3590.000	3456.785	52638.000	50992.074

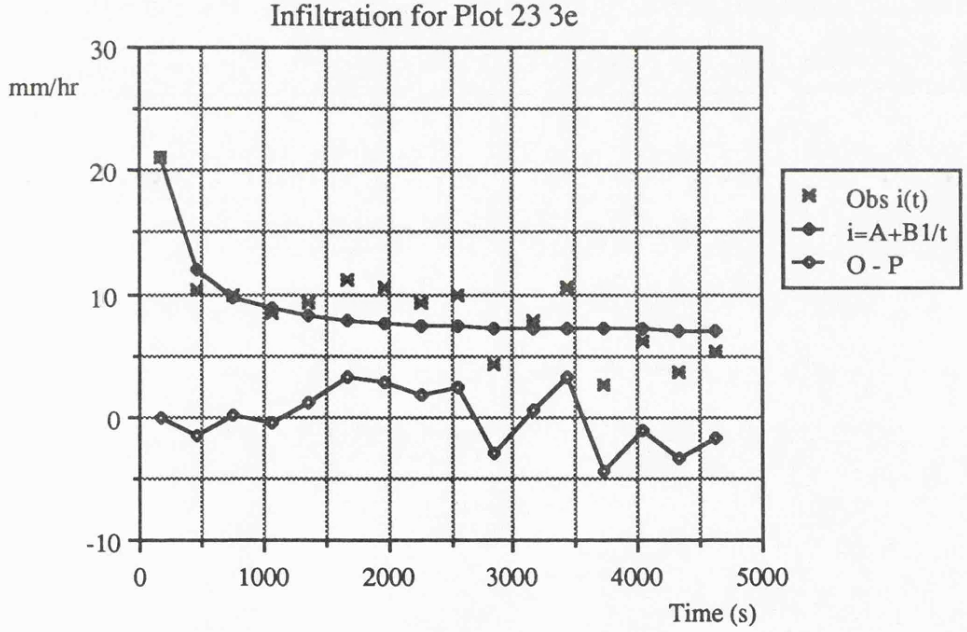

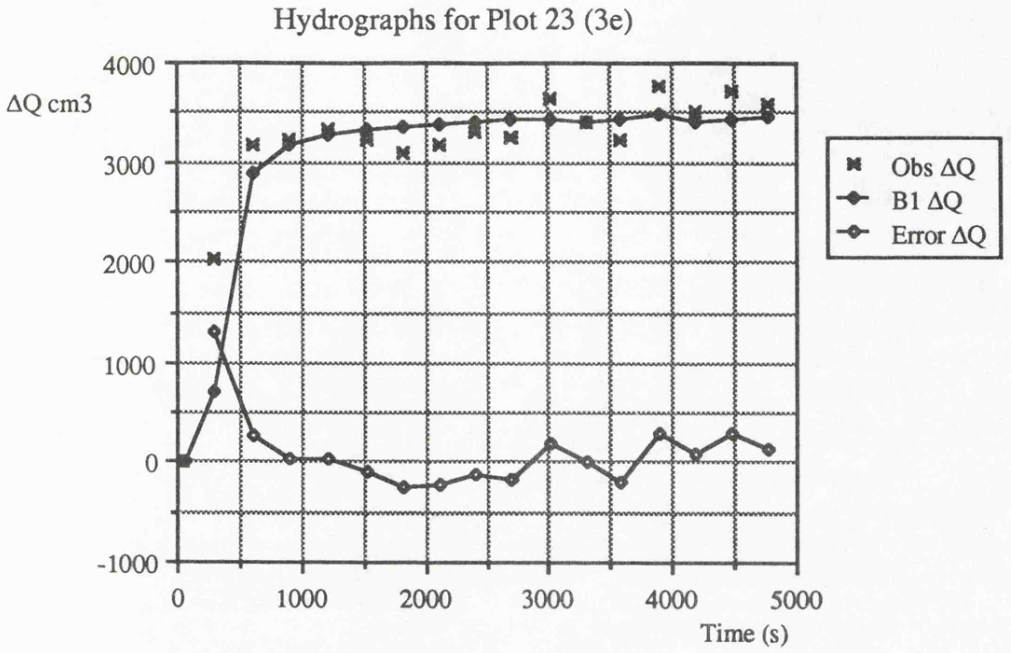

to5	Qin	WA	p	A	B2
11.0	13.289	9560	0.00139	0.000179	0.0133

Σt	Obs ΔQ	B2 ΔQ	Obs ΣQ	B2 ΣQ
37.0	0.000	0.000	0.000	0.000
301.0	2032.000	2116.142	2032.000	2116.142
606.0	3168.000	3385.147	5200.000	5501.290
905.0	3222.000	3425.308	8422.000	8926.598
1210.0	3316.000	3445.798	11738.000	12372.396
1525.0	3222.000	3446.883	14960.000	15819.278
1826.0	3102.000	3441.509	18062.000	19260.787
2123.0	3170.000	3465.508	21232.000	22726.295
2412.0	3288.000	3471.445	24520.000	26197.740
2697.0	3258.000	3489.680	27778.000	29687.420
3009.0	3638.000	3501.264	31416.000	33188.684
3301.0	3398.000	3450.082	34814.000	36638.766
3575.0	3234.000	3474.863	38048.000	40113.629
3886.0	3774.000	3527.457	41822.000	43641.086
4190.0	3510.000	3455.906	45332.000	47096.992
4485.0	3716.000	3467.219	49048.000	50564.211
4774.0	3590.000	3490.469	52638.000	54054.680

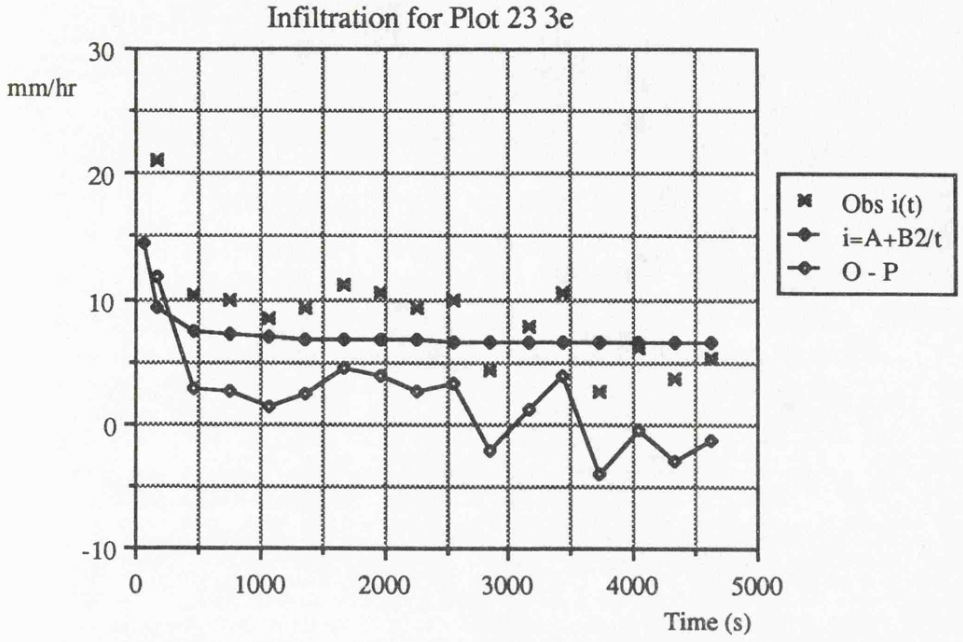
Infiltration for Plot 23 3e
mm/hr
30
20
10
0
-10
0
1000
2000
3000
4000
5000
Time (s)
Obs i(t)
i=A+B2/t
O - P

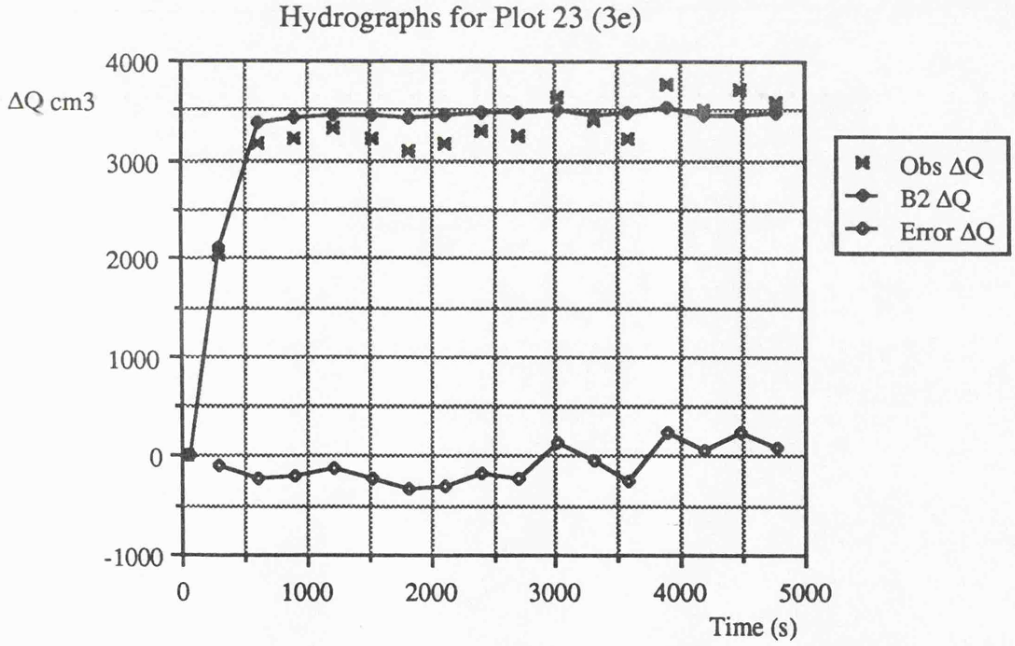
Hydrographs for Plot 23 (3e)
ΔQ cm3
4000
3000
2000
1000
0
-1000
0
1000
2000
3000
4000
5000
Time (s)
Obs ΔQ
B2 ΔQ
Error ΔQ

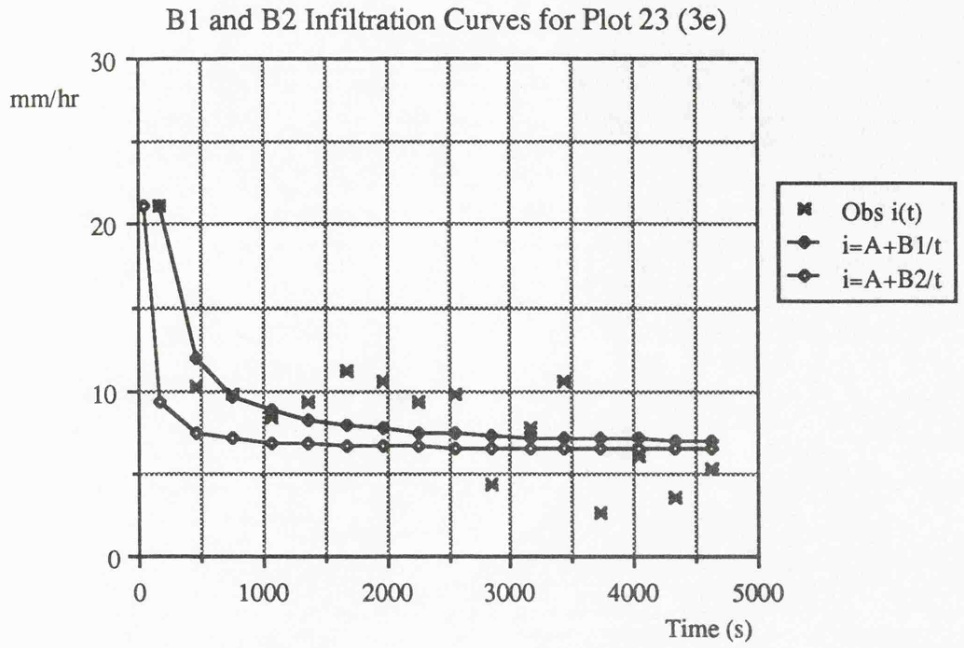
B1 and B2 Infiltration Curves for Plot 23 (3e)
mm/hr
30
20
10
0
0
1000
2000
3000
4000
5000
Time (s)
Obs i(t)
i=A+B1/t
i=A+B2/t

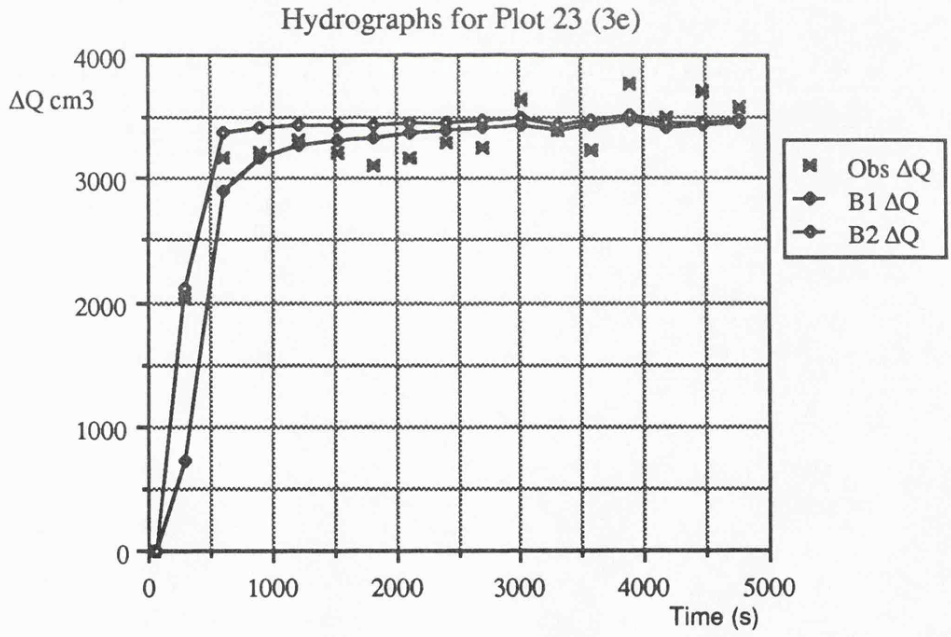
Hydrographs for Plot 23 (3e)
ΔQ cm3
4000
3000
2000
1000
0
0
1000
2000
3000
4000
5000
Time (s)
Obs ΔQ
B1 ΔQ
B2 ΔQ

Appendix 5.1.4 Results from Plot 25 Unit 4e lower

A	B1	n	S	Δt	Δx
0.000047	0.109	0.48	0.2010	1.0	20.0

t	5	4	3	2	1
5535	104.0	103.5	113.5	128.5	140.5

Σt	Obs ΔQ	B1 ΔQ	Obs ΣQ	B1 ΣQ
37.0	0.000	0.000	0.000	0.000
184.0	1262.000	0.000	1262.000	0.000
382.0	3270.000	2154.112	4532.000	2154.112
582.0	3578.000	3216.298	8110.000	5370.410
779.0	3556.000	3442.042	11666.000	8812.452
968.0	3706.000	3540.452	15372.000	12352.904
1189.0	3649.000	3735.440	19021.000	16088.345
1405.0	3768.000	3625.204	22789.000	19713.549
1616.0	3673.000	3665.797	26462.000	23379.346
1839.0	3647.000	3757.197	30109.000	27136.543
2061.0	3749.000	3720.301	33858.000	30856.844
2286.0	3792.000	3748.309	37650.000	34605.152
2506.0	3827.000	3731.363	41477.000	38336.516
2724.0	3786.000	3761.254	45263.000	42097.770
2940.0	3767.000	3770.926	49030.000	45868.695
3148.0	3685.000	3755.141	52715.000	49623.836
3363.0	3517.000	3826.707	56232.000	53450.543
3585.0	3835.000	3823.156	60067.000	57273.699
3802.0	3905.000	3778.059	63972.000	61051.758
4016.0	3773.000	3792.344	67745.000	64844.102
4230.0	3656.000	3809.180	71401.000	68653.281
4446.0	3745.000	3822.578	75146.000	72475.859
4659.0	3741.000	3807.250	78887.000	76283.109
4870.0	3800.000	3813.063	82687.000	80096.172
5089.0	3842.000	3855.211	86529.000	83951.383
5306.0	3624.000	3822.086	90153.000	87773.469
5534.0	3933.000	3865.680	94086.000	91639.148

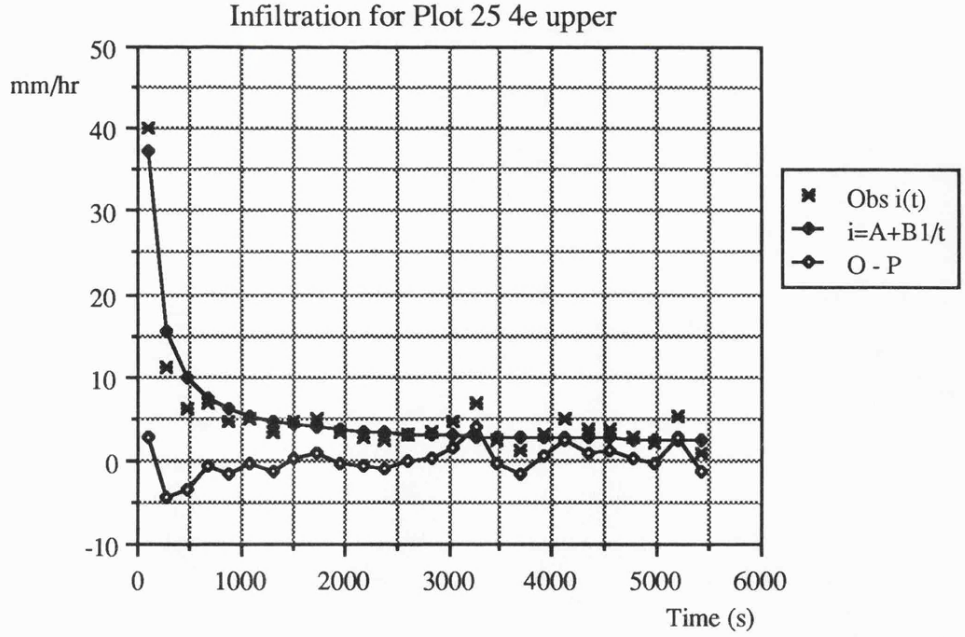

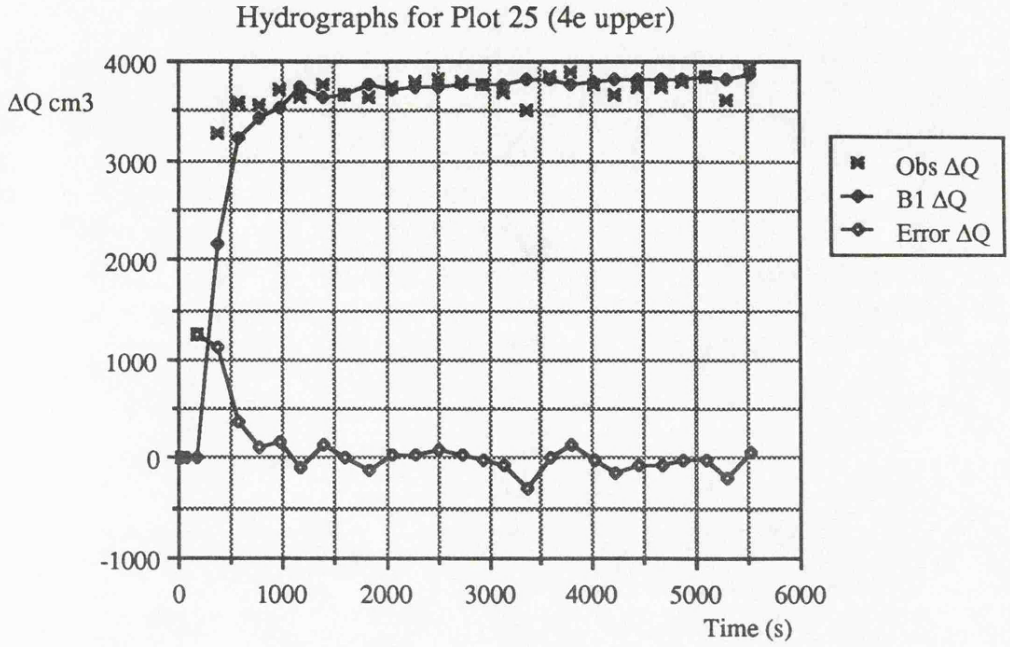

to5	Qin	WA	p	A	B2
10.49	21.739	11800	0.00184	0.000047	0.0188

Σt	Obs ΔQ	B2 ΔQ	Obs ΣQ	B2 ΣQ
37.0	0.000	0.000	0.000	0.000
184.0	1262.000	1452.148	1262.000	1452.148
382.0	3270.000	3756.199	4532.000	5208.347
582.0	3578.000	3796.137	8110.000	9004.484
779.0	3556.000	3809.472	11666.000	12813.956
968.0	3706.000	3803.294	15372.000	16617.250
1189.0	3649.000	3975.256	19021.000	20592.506
1405.0	3768.000	3818.535	22789.000	24411.041
1616.0	3673.000	3825.785	26462.000	28236.826
1839.0	3647.000	3903.035	30109.000	32139.861
2061.0	3749.000	3848.377	33858.000	35988.238
2286.0	3792.000	3863.938	37650.000	39852.176
2506.0	3827.000	3833.680	41477.000	43685.855
2724.0	3786.000	3853.668	45263.000	47539.523
2940.0	3767.000	3855.223	49030.000	51394.746
3148.0	3685.000	3830.586	52715.000	55225.332
3363.0	3517.000	3899.148	56232.000	59124.480
3585.0	3835.000	3893.051	60067.000	63017.531
3802.0	3905.000	3842.688	63972.000	66860.219
4016.0	3773.000	3852.250	67745.000	70712.469
4230.0	3656.000	3865.375	71401.000	74577.844
4446.0	3745.000	3876.938	75146.000	78454.781
4659.0	3741.000	3858.336	78887.000	82313.117
4870.0	3800.000	3861.078	82687.000	86174.195
5089.0	3842.000	3902.492	86529.000	90076.688
5306.0	3624.000	3867.125	90153.000	93943.813
5534.0	3933.000	3911.086	94086.000	97854.898

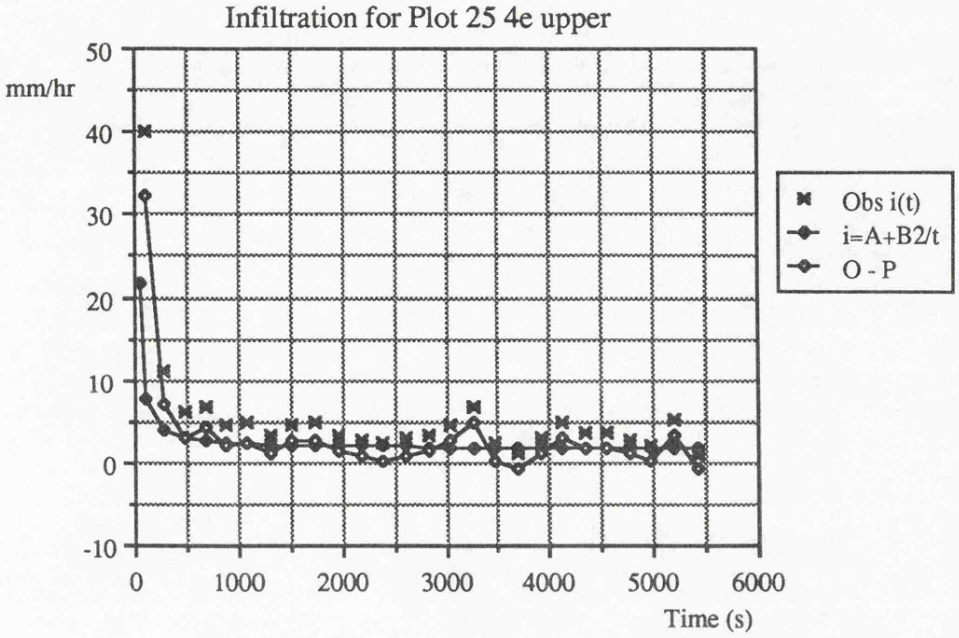
Infiltration for Plot 25 4e upper
mm/hr
50
40
30
20
10
0
-10
0
1000
2000
3000
4000
5000
6000
Time (s)
Obs i(t)
i=A+B2/t
O - P

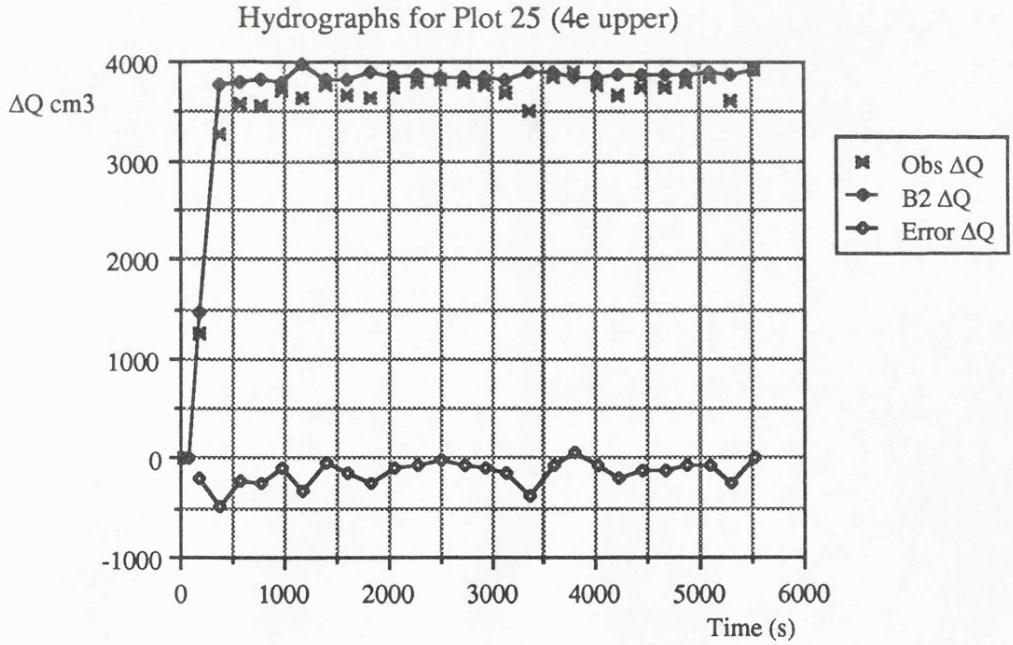
Hydrographs for Plot 25 (4e upper)
ΔQ cm3
4000
3000
2000
1000
0
-1000
0
1000
2000
3000
4000
5000
6000
Time (s)
Obs ΔQ
B2 ΔQ
Error ΔQ

B1 and B2 Infiltration Curves for Plot 25 (4e upper)

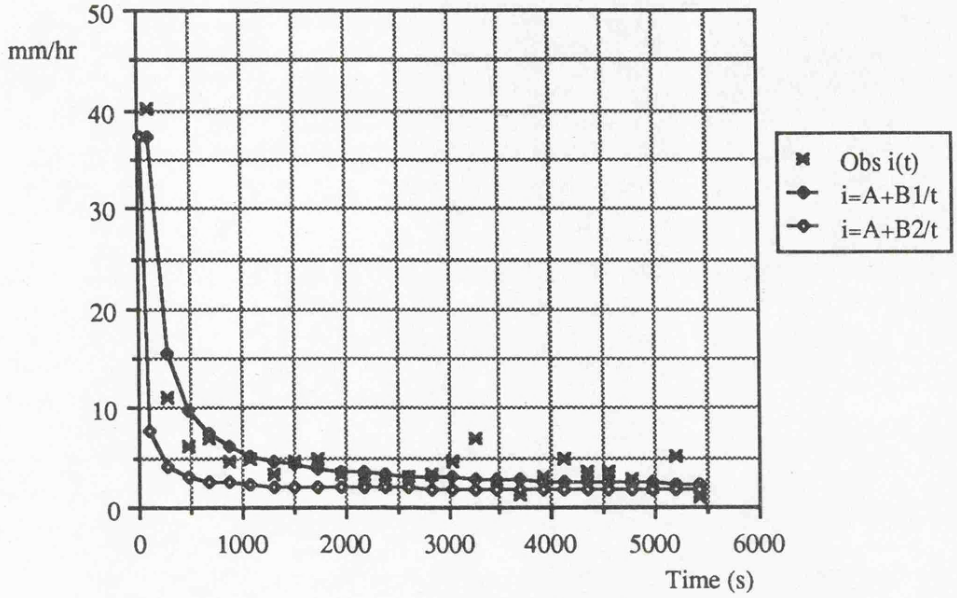

Hydrographs for Plot 25 (4e upper)

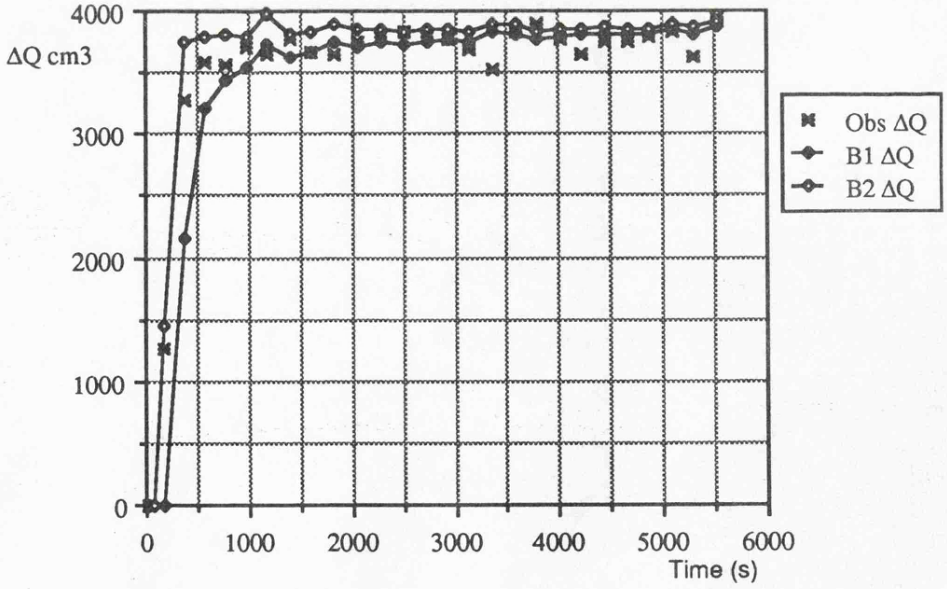

Appendix 5.1.5 Results from Plot 28 Unit 4e lower

A	B1	n	S	Δt	Δx
0.000359	0.149	0.20	0.0593	1.0	20.0

t	5	4	3	2	1
421	90.0	65.5	49.5	38.5	31.5
721	95.2	83.0	73.3	65.4	58.0
1501	111.0	122.5	113.5	104.5	113.5
5472	112.0	130.5	117.5	102.0	81.5

Σt	Obs ΔQ	B1 ΔQ	Obs ΣQ	B1 ΣQ
48.0	0.000	0.000	0.000	0.000
290.0	1669.000	437.519	1669.000	437.519
569.0	2592.000	2693.047	4261.000	3130.566
825.0	2617.000	2889.378	6878.000	6019.944
1096.0	2896.000	2398.026	9774.000	8417.970
1369.0	2719.000	2483.881	12493.000	10901.851
1654.0	2773.000	2549.880	15266.000	13451.730
1928.0	2815.000	2642.644	18081.000	16094.374
2210.0	2707.000	2688.042	20788.000	18782.416
2482.0	2622.000	2710.553	23410.000	21492.969
2776.0	2749.000	2718.070	26159.000	24211.039
3072.0	2623.000	2681.420	28782.000	26892.459
3367.0	2715.000	2690.975	31497.000	29583.434
3674.0	2688.000	2687.525	34185.000	32270.959
3967.0	2656.000	2692.838	36841.000	34963.797
4274.0	2697.000	2713.633	39538.000	37677.430
4577.0	2553.000	2695.770	42091.000	40373.199
4876.0	2612.000	2714.730	44703.000	43087.930
5167.0	2666.000	2748.691	47369.000	45836.621
5471.0	2614.000	2753.750	49983.000	48590.371

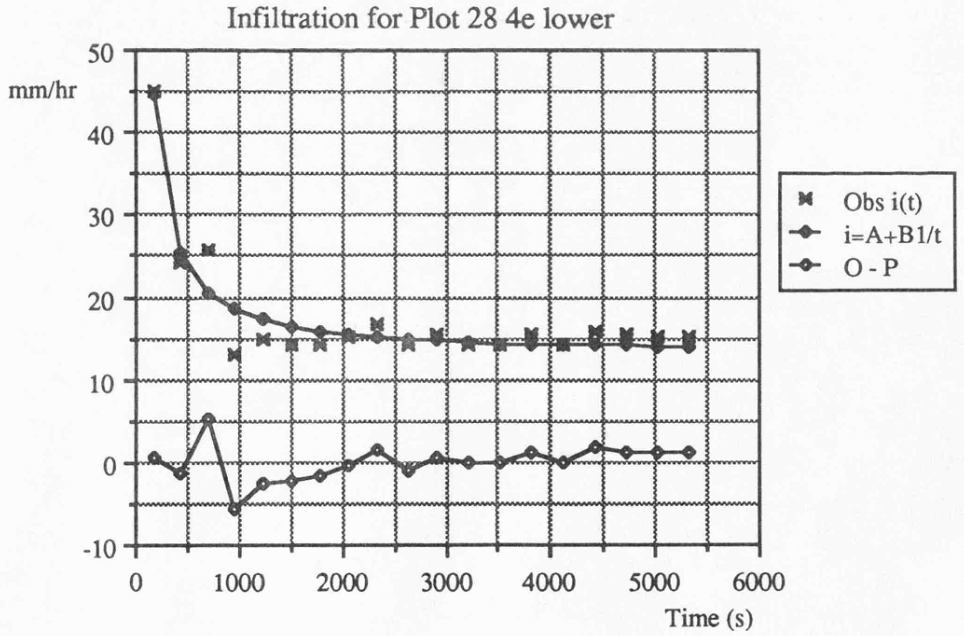

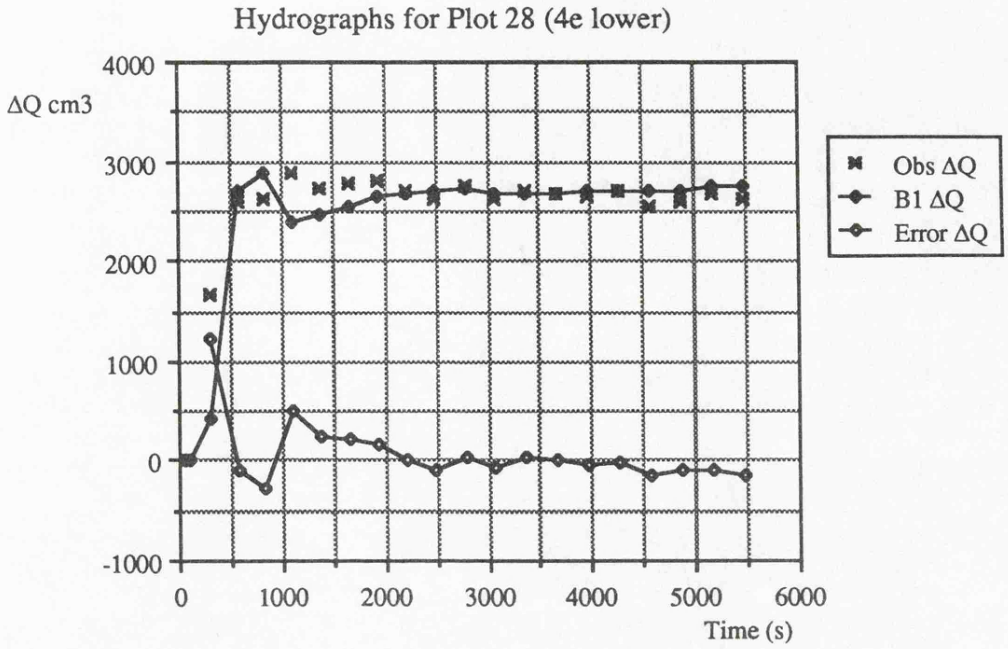

to5	Qin	WA	p	A	B2
20.38	13.7931	5500	0.002508	0.000359	0.0438

Σt	Obs ΔQ	B2 ΔQ	Obs ΣQ	B2 ΣQ
48.0	0.000	0.000	0.000	0.000
290.0	1669.000	1755.227	1669.000	1755.227
569.0	2592.000	3329.696	4261.000	5084.923
825.0	2617.000	3309.353	6878.000	8394.275
1096.0	2896.000	2789.820	9774.000	11184.096
1369.0	2719.000	2780.723	12493.000	13964.818
1654.0	2773.000	2789.232	15266.000	16754.051
1928.0	2815.000	2831.723	18081.000	19585.773
2210.0	2707.000	2853.975	20788.000	22439.748
2482.0	2622.000	2851.092	23410.000	25290.840
2776.0	2749.000	2851.920	26159.000	28142.760
3072.0	2623.000	2802.455	28782.000	30945.215
3367.0	2715.000	2800.125	31497.000	33745.340
3674.0	2688.000	2790.844	34185.000	36536.184
3967.0	2656.000	2783.816	36841.000	39320.000
4274.0	2697.000	2801.297	39538.000	42121.297
4577.0	2553.000	2776.418	42091.000	44897.715
4876.0	2612.000	2789.141	44703.000	47686.855
5167.0	2666.000	2816.844	47369.000	50503.699
5471.0	2614.000	2820.559	49983.000	53324.258

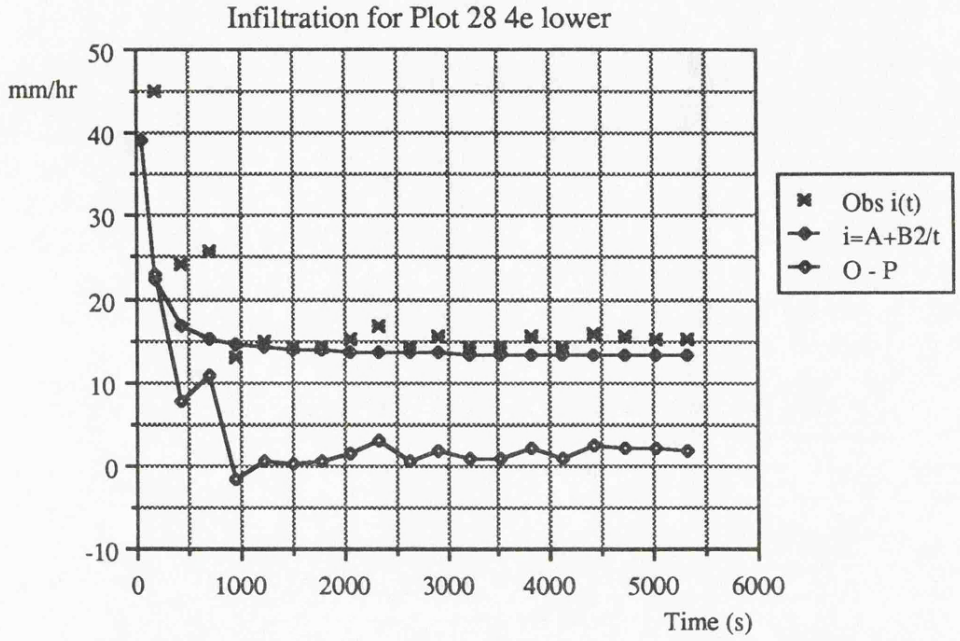
Infiltration for Plot 28 4e lower
mm/hr
50
40
30
20
10
0
-10
0
1000
2000
3000
4000
5000
6000
Time (s)
Obs i(t)
i=A+B2/t
O - P

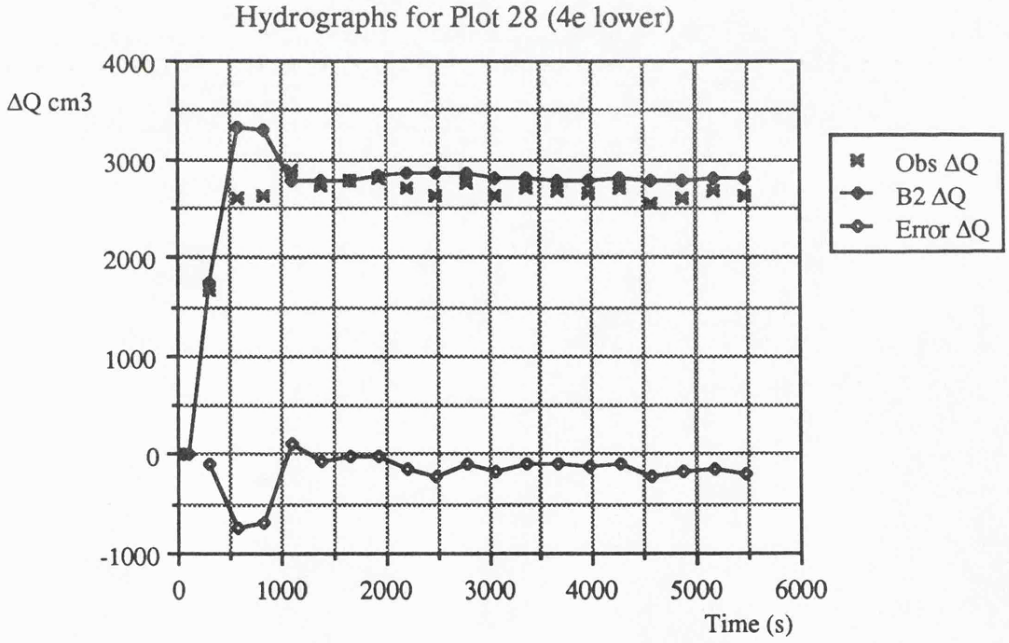
Hydrographs for Plot 28 (4e lower)
ΔQ cm3
4000
3000
2000
1000
0
-1000
0
1000
2000
3000
4000
5000
6000
Time (s)
Obs ΔQ
B2 ΔQ
Error ΔQ

B1 and B2 Infiltration Curves for Plot 28 (4e lower)

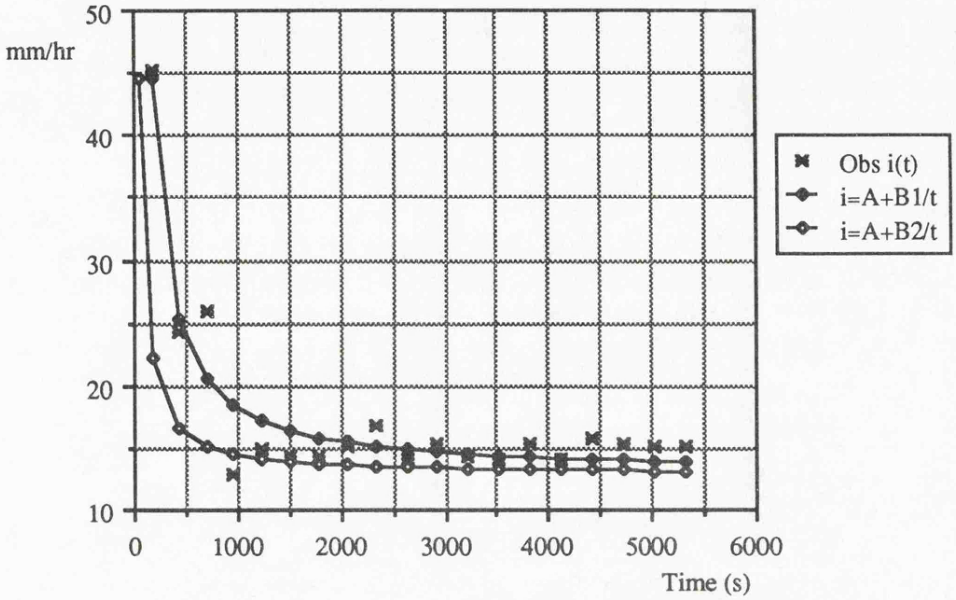

Hydrographs for Plot 28 (4e lower)

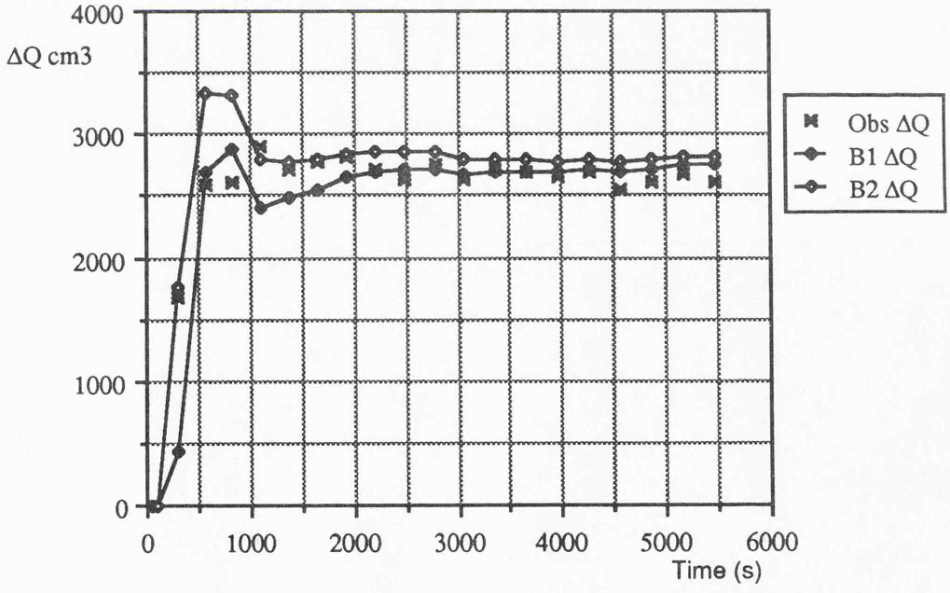

Appendix 5.1.6 Results from Plot 32 Unit 5e

A	B1	n	S	Δt	Δx
0.000592	0.188	0.30	0.0940	1.0	20.0

t	5	4	3	2	1
241	97.0	88.8	82.0	76.4	70.8
421	100.0	101.5	102.0	102.5	104.0
661	101.0	105.0	109.0	111.0	114.0
1501	102.0	110.0	114.0	118.0	126.0
1861	102.5	112.0	117.0	122.0	131.5
3781	102.5	112.0	117.0	122.0	131.5
4381	102.0	109.5	113.0	116.5	123.0
5508	102.5	112.0	117.0	122.0	131.5

Σt	Obs ΔQ	B1 ΔQ	Obs ΣQ	B1 ΣQ
120.0	0.000	0.000	0.000	0.000
249.0	244.000	0.000	244.000	0.000
510.0	1528.000	4.150	1772.000	4.150
770.0	1694.000	929.502	3466.000	933.651
1031.0	1750.000	1415.595	5216.000	2349.247
1290.0	1808.000	1655.852	7024.000	4005.099
1554.0	1840.000	1774.991	8864.000	5780.090
1818.0	1808.000	1782.099	10672.000	7562.188
2089.0	1854.000	1803.682	12526.000	9365.870
2358.0	1858.000	1838.592	14384.000	11204.462
2624.0	1854.000	1894.638	16238.000	13099.100
2893.0	1854.000	1911.688	18092.000	15010.787
3159.0	1878.000	1941.252	19970.000	16952.039
3436.0	1916.000	1919.658	21886.000	18871.697
3774.0	1526.000	1613.805	23412.000	20485.502
4126.0	1402.000	1455.273	24814.000	21940.775
4419.0	1634.000	1749.463	26448.000	23690.238
4710.0	1774.000	1840.629	28222.000	25530.867
4971.0	1876.000	1971.512	30098.000	27502.379
5242.0	2034.000	2033.176	32132.000	29535.555
5507.0	2012.000	2035.787	34144.000	31571.342

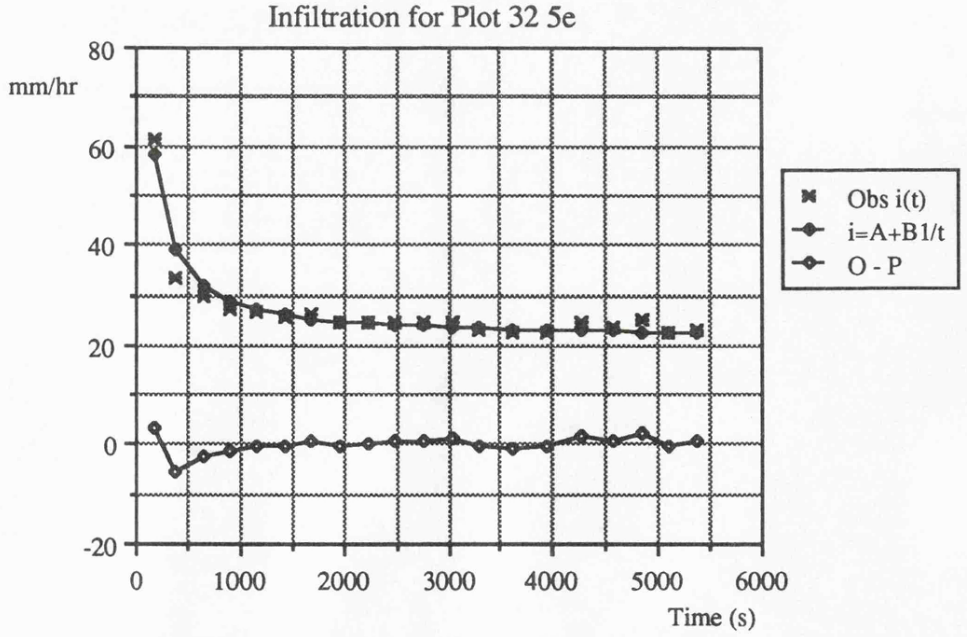

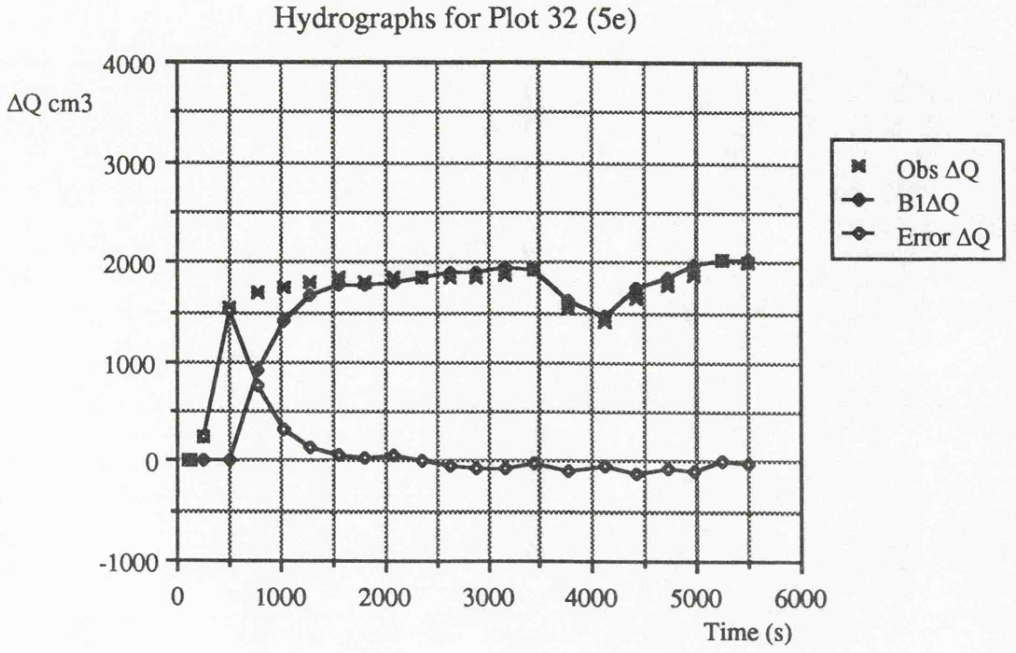

to5	Qin	WA	p	A	B2
24.45	16.064	8300	0.001935	0.000592	0.0328

Σt	Obs ΔQ	B2 ΔQ	Obs ΣQ	B2 ΣQ
120.0	0.000	0.004	0.000	0.004
249.0	244.000	910.315	244.000	910.319
510.0	1528.000	2290.794	1772.000	3201.113
770.0	1694.000	2169.611	3466.000	5370.724
1031.0	1750.000	2122.007	5216.000	7492.731
1290.0	1808.000	2152.169	7024.000	9644.900
1554.0	1840.000	2168.619	8864.000	11813.520
1818.0	1808.000	2111.012	10672.000	13924.531
2089.0	1854.000	2088.234	12526.000	16012.766
2358.0	1858.000	2083.457	14384.000	18096.223
2624.0	1854.000	2108.039	16238.000	20204.262
2893.0	1854.000	2104.176	18092.000	22308.438
3159.0	1878.000	2113.816	19970.000	24422.254
3436.0	1916.000	2082.658	21886.000	26504.912
3774.0	1526.000	1792.289	23412.000	28297.201
4126.0	1402.000	1620.486	24814.000	29917.688
4419.0	1634.000	1879.295	26448.000	31796.982
4710.0	1774.000	1962.084	28222.000	33759.066
4971.0	1876.000	2075.215	30098.000	35834.281
5242.0	2034.000	2133.469	32132.000	37967.750
5507.0	2012.000	2129.379	34144.000	40097.129

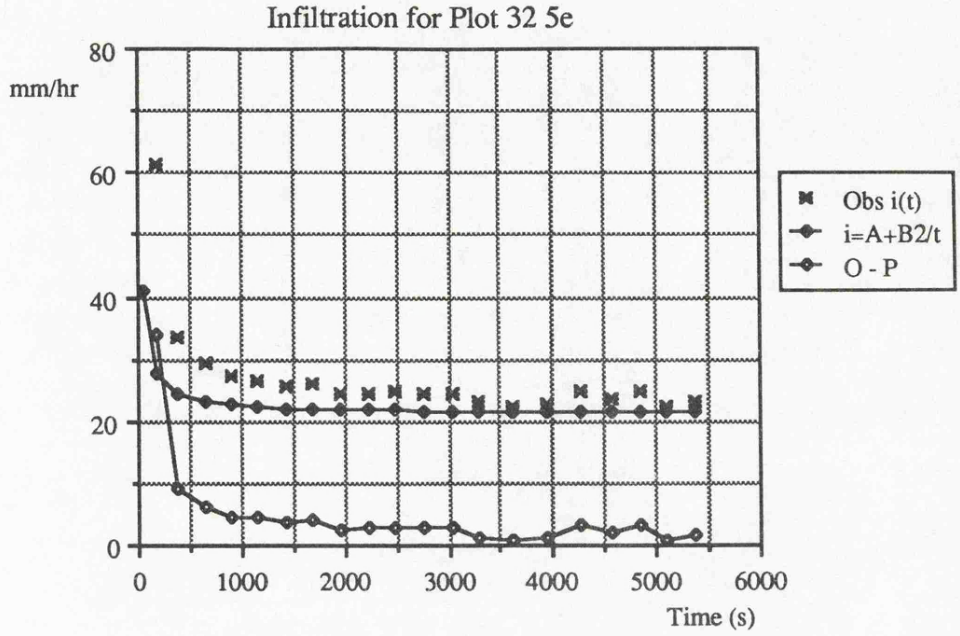
Infiltration for Plot 32 5e
mm/hr
80
60
40
20
0
0
1000
2000
3000
4000
5000
6000
Time (s)
Obs i(t)
i=A+B2/t
O - P

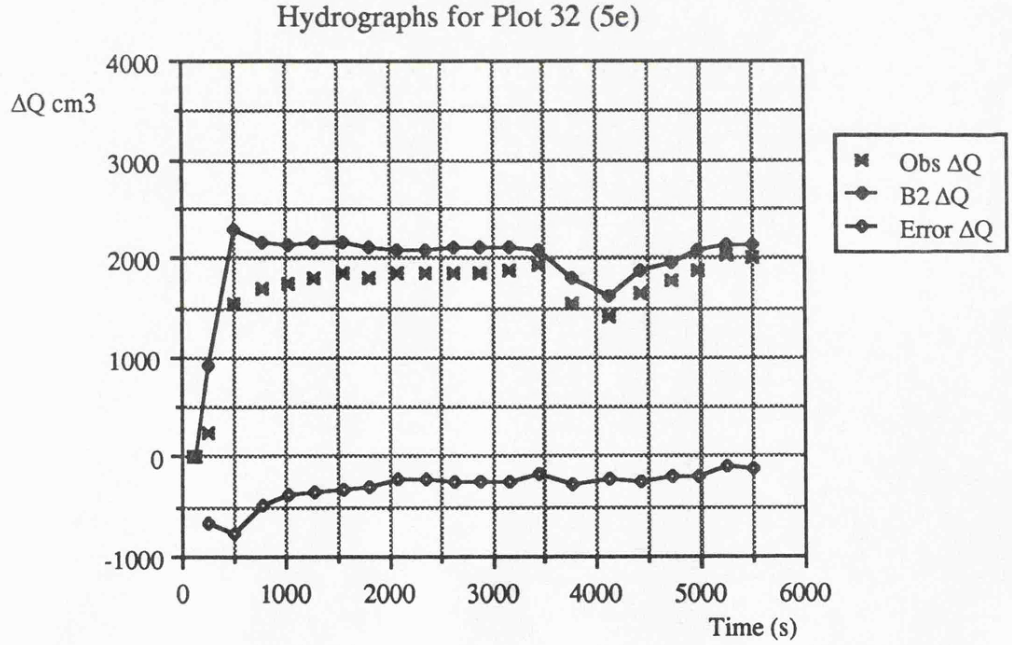
Hydrographs for Plot 32 (5e)
ΔQ cm3
4000
3000
2000
1000
0
-1000
0
1000
2000
3000
4000
5000
6000
Time (s)
Obs ΔQ
B2 ΔQ
Error ΔQ

B1 and B2 Infiltration Curves for Plot 32 (5e)

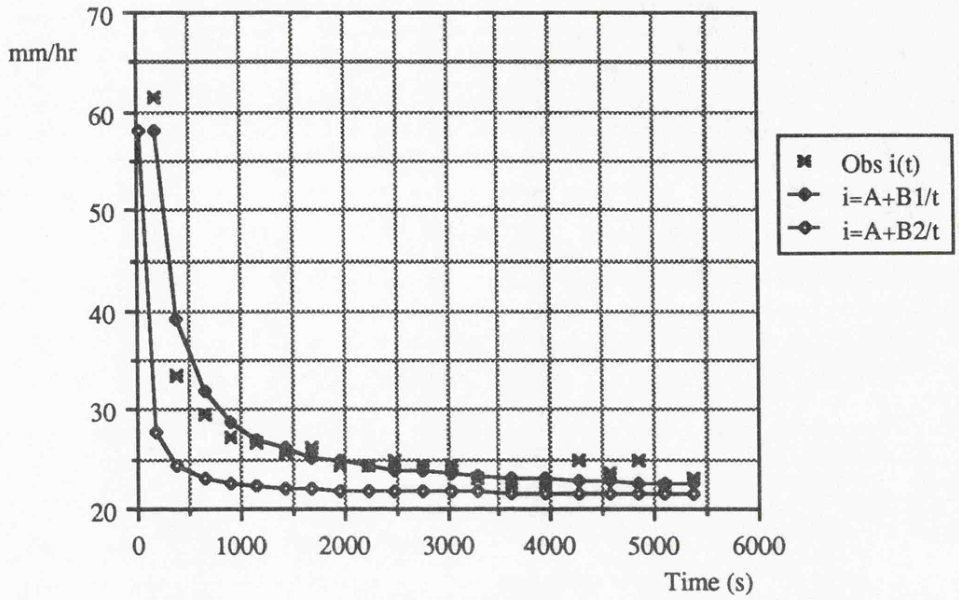

Hydrographs for Plot 32 (5e)

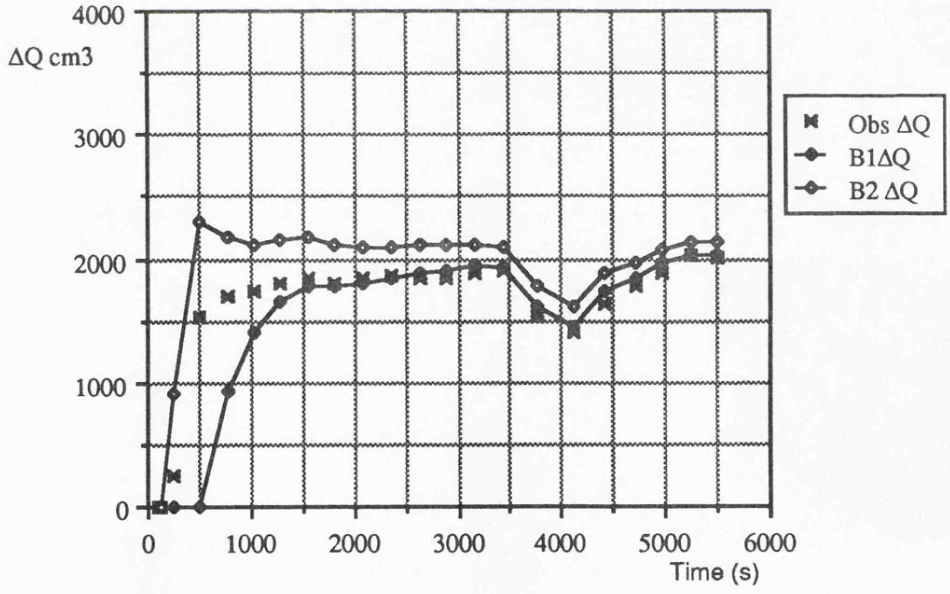

Appendix 5.1.7 Results from Plot 34 Unit 5w lower

A	B1	n	S	Δt	Δx
0.0001690	0.147	0.40	0.044	1.0	20.0

t	5	4	3	2	1
301	90.0	58.0	40.0	32.5	29.5
601	90.0	60.5	40.0	40.0	39.5
901	92.5	61.5	41.0	42.0	43.0
1381	92.5	61.5	41.5	40.5	40.0
1981	91.5	58.0	41.5	40.0	39.0
3181	91.5	58.0	41.5	40.0	39.0
4921	91.5	58.0	41.5	40.0	39.0
5379	91.5	58.0	41.5	40.0	39.0

Σt	Obs ΔQ	B1 ΔQ	Obs ΣQ	B1 ΣQ
222.0	0.000	0.000	0.000	0.000
319.0	68.000	0.000	68.000	0.000
674.0	732.000	0.000	800.000	0.000
987.0	924.000	147.958	1724.000	147.958
1280.0	978.000	869.625	2702.000	1017.583
1582.0	910.000	1007.230	3612.000	2024.812
1887.0	900.000	1056.154	4512.000	3080.966
2198.0	952.000	1042.425	5464.000	4123.391
2518.0	1002.000	982.961	6466.000	5106.352
2825.0	998.000	1054.830	7464.000	6161.182
3142.0	1058.000	1044.631	8522.000	7205.813
3459.0	1056.000	1024.008	9578.000	8229.820
3769.0	1026.000	1072.484	10604.000	9302.305
4081.0	1032.000	1090.670	11636.000	10392.975
4398.0	1046.000	1061.813	12682.000	11454.787
4734.0	1084.000	932.375	13766.000	12387.162
5058.0	1054.000	949.711	14820.000	13336.873
5378.0	1038.000	1017.212	15858.000	14354.085

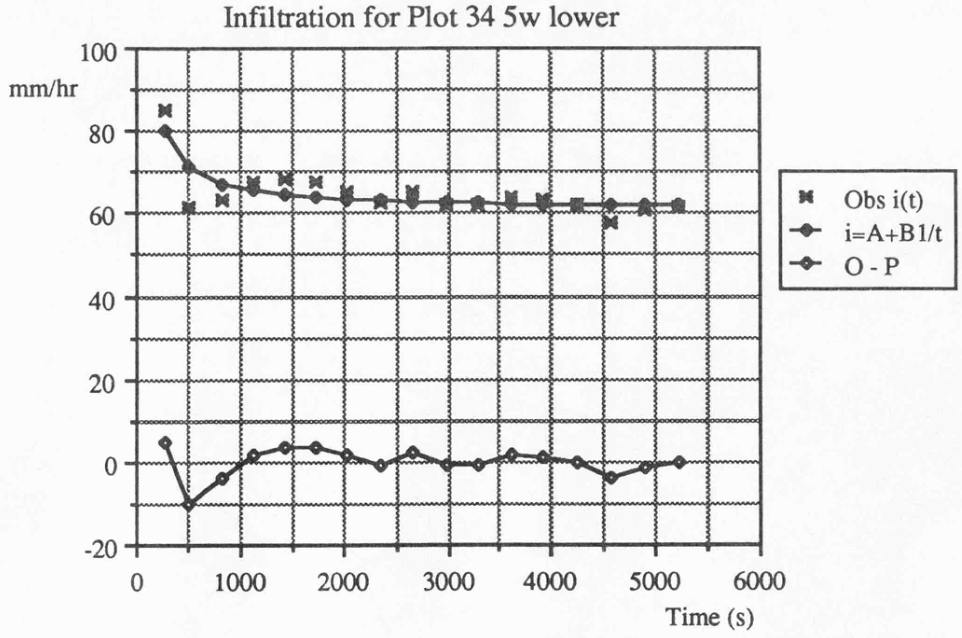

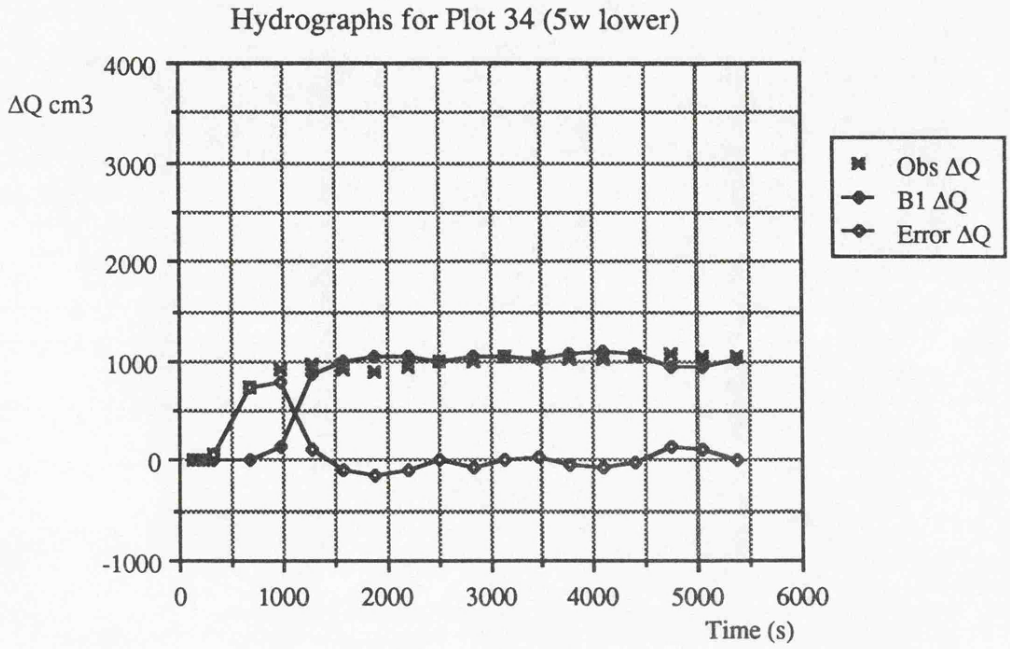

to5	Qin	WA	p	A	B2
27.88	12.539	5000	0.002508	0.000169	0.0228

Σt	Obs ΔQ	B2 ΔQ	Obs ΣQ	B2 ΣQ
222.0	0.000	12.256	0.000	12.256
319.0	68.000	285.710	68.000	297.966
674.0	732.000	772.272	800.000	1070.238
987.0	924.000	858.251	1724.000	1928.490
1280.0	978.000	1163.237	2702.000	3091.727
1582.0	910.000	1200.493	3612.000	4292.220
1887.0	900.000	1203.964	4512.000	5496.184
2198.0	952.000	1164.505	5464.000	6660.689
2518.0	1002.000	1088.323	6466.000	7749.012
2825.0	998.000	1143.358	7464.000	8892.370
3142.0	1058.000	1123.997	8522.000	10016.367
3459.0	1056.000	1095.331	9578.000	11111.698
3769.0	1026.000	1135.764	10604.000	12247.462
4081.0	1032.000	1148.537	11636.000	13395.999
4398.0	1046.000	1115.787	12682.000	14511.786
4734.0	1084.000	984.748	13766.000	15496.534
5058.0	1054.000	997.501	14820.000	16494.035
5378.0	1038.000	1061.004	15858.000	17555.039

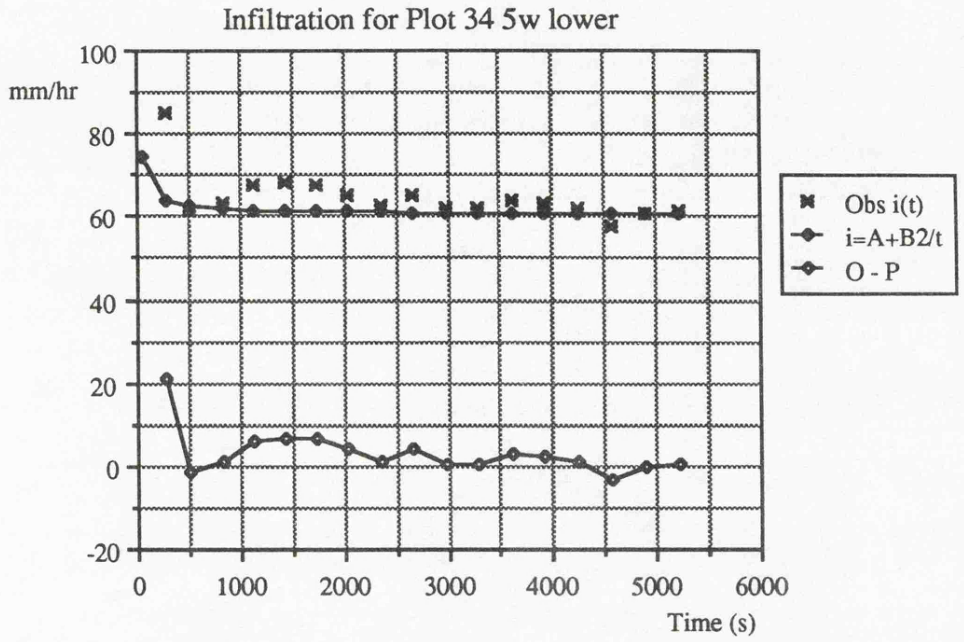
Infiltration for Plot 34 5w lower
mm/hr
100
80
60
40
20
0
-20
0
1000
2000
3000
4000
5000
6000
Time (s)
Obs i(t)
i=A+B2/t
O - P

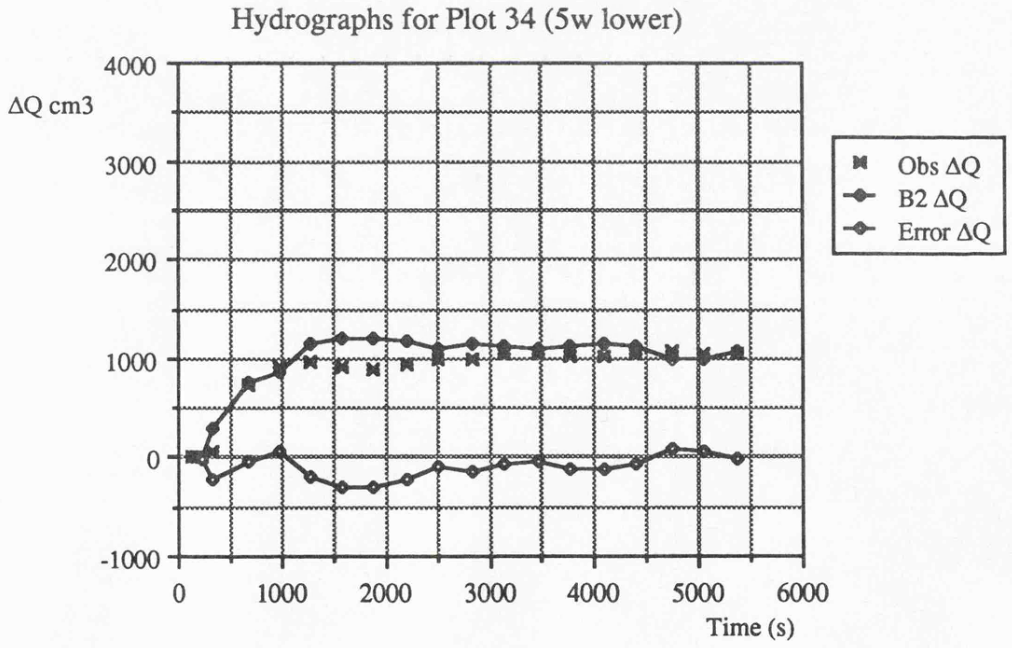
Hydrographs for Plot 34 (5w lower)
ΔQ cm3
4000
3000
2000
1000
0
-1000
0
1000
2000
3000
4000
5000
6000
Time (s)
Obs ΔQ
B2 ΔQ
Error ΔQ

B1 and B2 Infiltration Curves for Plot 34 (5w lower)

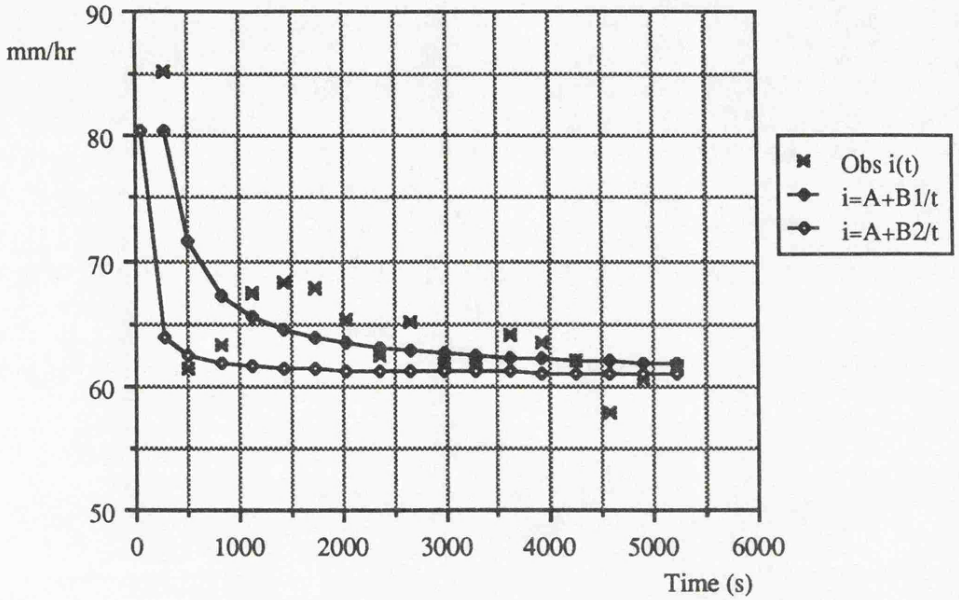

Hydrographs for Plot 34 (5w lower)

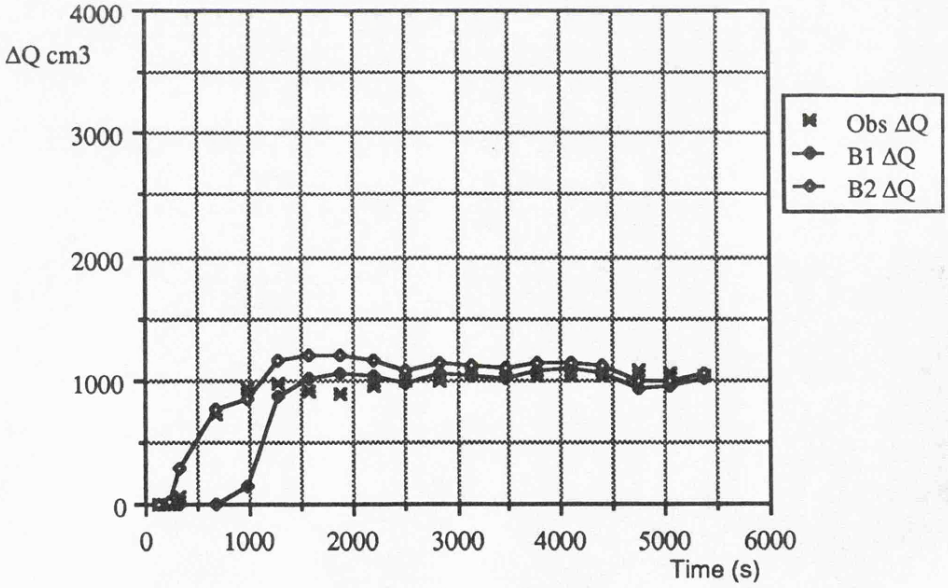

Appendix 5.1.8 Results from Plot 36 Unit 4w

A	B1	n	S	Δt	Δx
0.000777	0.158	0.34	0.1461	1.0	20.0

t	5	4	3	2	1
481	96.7	89.6	82.5	71.6	59.7
751	96.5	90.9	84.4	71.6	61.5
1501	97.8	92.1	86.2	77.0	68.7
1861	102.9	103.1	96.7	82.4	69.9
4978	100.0	100.0	98.1	88.6	69.6

Σt	Obs ΔQ	B1 ΔQ	Obs ΣQ	B1 ΣQ
107.0	0.000	0.000	0.000	0.000
295.0	286.000	0.000	286.000	0.000
592.0	1038.000	344.254	1324.000	344.254
878.0	1558.000	1444.183	2882.000	1788.436
1170.0	1630.000	1623.463	4512.000	3411.899
1449.0	1660.000	1802.146	6172.000	5214.045
1739.0	1810.000	1775.961	7982.000	6990.006
2031.0	1820.000	1692.119	9802.000	8682.125
2323.0	1906.000	1722.710	11708.000	10404.835
2620.0	1890.000	1719.997	13598.000	12124.832
2910.0	1884.000	1765.453	15482.000	13890.285
3198.0	1876.000	1808.145	17358.000	15698.430
3482.0	1948.000	1847.941	19306.000	17546.371
3774.0	1850.000	1833.039	21156.000	19379.410
4068.0	1864.000	1807.852	23020.000	21187.262
4368.0	1878.000	1780.461	24898.000	22967.723
4671.0	1918.000	1757.979	26816.000	24725.701
4977.0	1960.000	1742.291	28776.000	26467.992

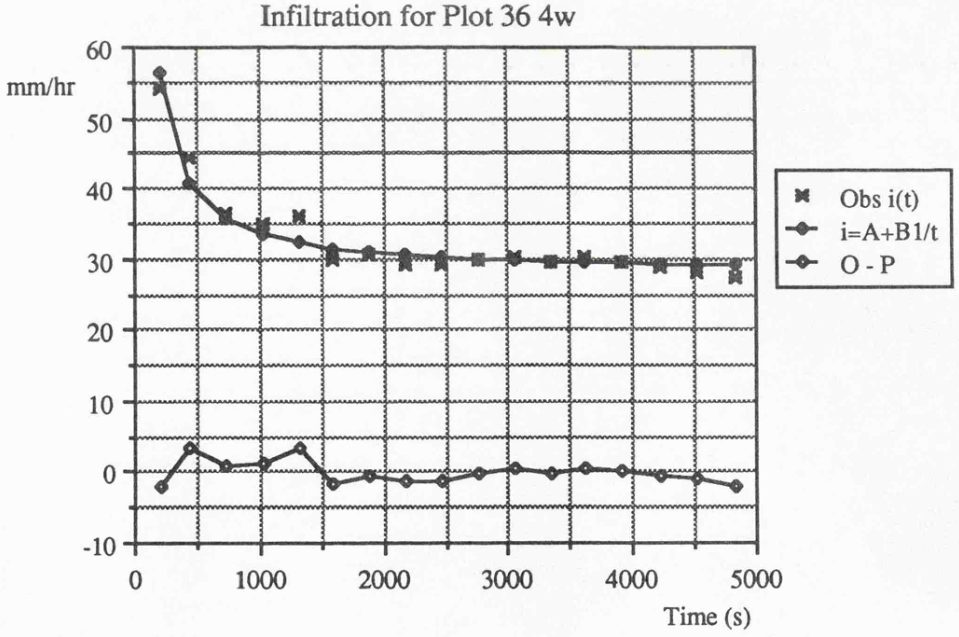

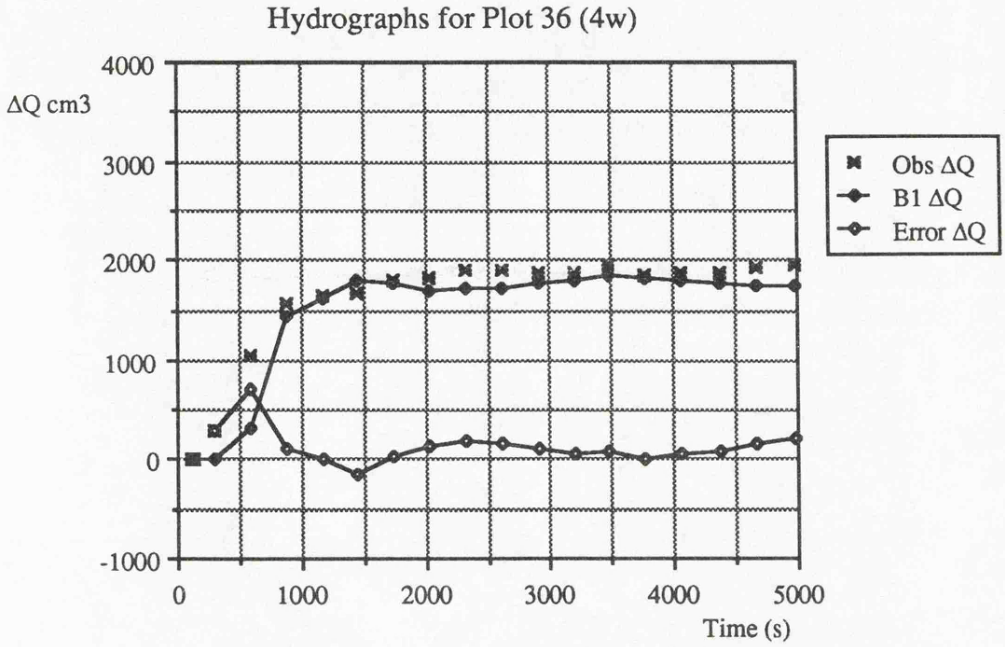

to5	Qin	WA	p	A	B2
25.36	13.559	8000	0.001695	0.000777	0.0233

Σt	Obs ΔQ	B2 ΔQ	Obs ΣQ	B2 ΣQ
107.0	0.000	0.000	0.000	0.000
295.0	286.000	791.049	286.000	791.049
592.0	1038.000	1992.395	1324.000	2783.445
878.0	1558.000	2086.359	2882.000	4869.804
1170.0	1630.000	2038.073	4512.000	6907.876
1449.0	1660.000	2093.279	6172.000	9001.155
1739.0	1810.000	2026.630	7982.000	11027.785
2031.0	1820.000	1906.562	9802.000	12934.347
2323.0	1906.000	1905.222	11708.000	14839.568
2620.0	1890.000	1881.121	13598.000	16720.689
2910.0	1884.000	1905.158	15482.000	18625.848
3198.0	1876.000	1932.533	17358.000	20558.381
3482.0	1948.000	1959.461	19306.000	22517.842
3774.0	1850.000	1937.639	21156.000	24455.480
4068.0	1864.000	1905.021	23020.000	26360.502
4368.0	1878.000	1872.182	24898.000	28232.684
4671.0	1918.000	1844.217	26816.000	30076.900
4977.0	1960.000	1823.686	28776.000	31900.586

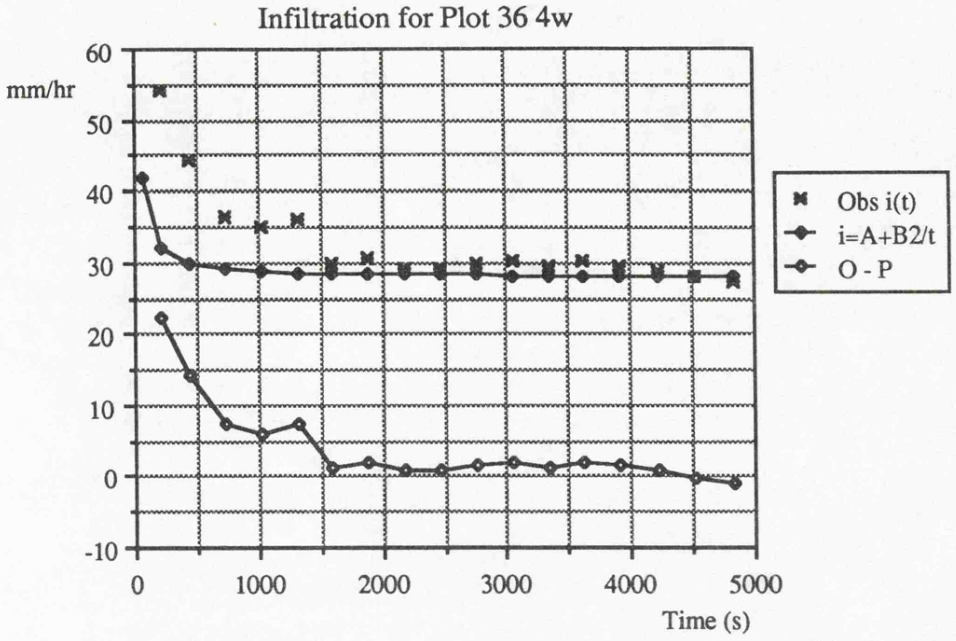
Infiltration for Plot 36 4w
mm/hr
60
50
40
30
20
10
0
-10
0
1000
2000
3000
4000
5000
Time (s)
Obs i(t)
i=A+B2/t
O - P

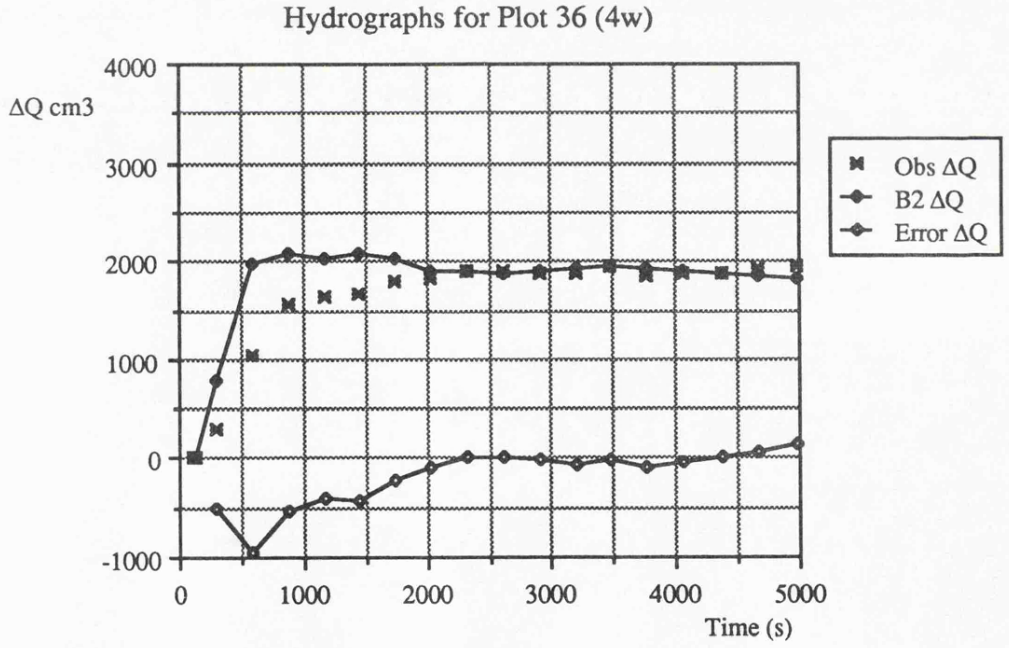
Hydrographs for Plot 36 (4w)
ΔQ cm3
4000
3000
2000
1000
0
-1000
0
1000
2000
3000
4000
5000
Time (s)
Obs ΔQ
B2 ΔQ
Error ΔQ

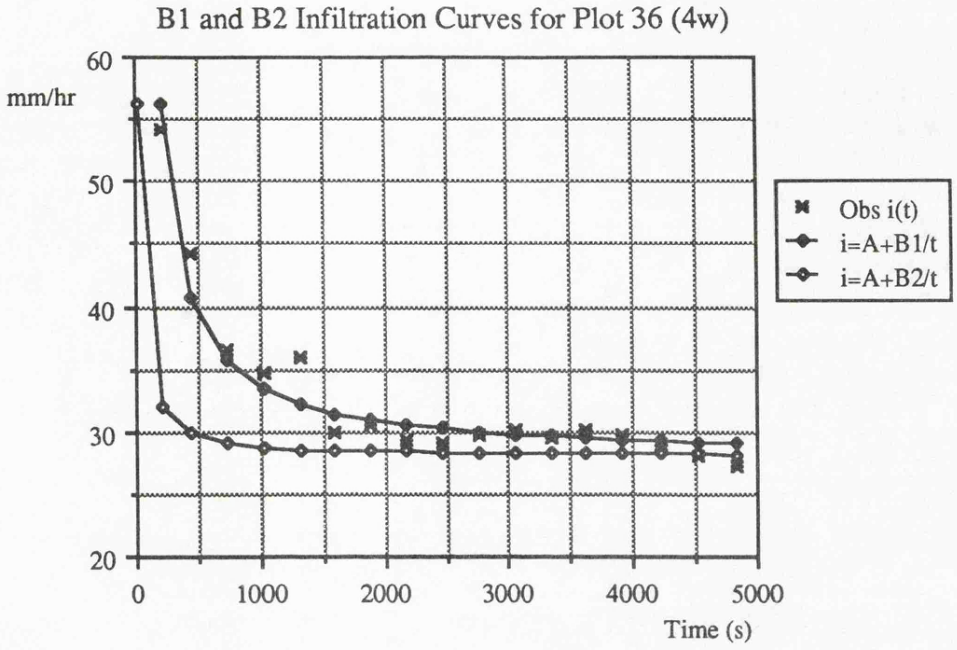
B1 and B2 Infiltration Curves for Plot 36 (4w)
mm/hr
60
50
40
30
20
0
1000
2000
3000
4000
5000
Time (s)
Obs i(t)
i=A+B1/t
i=A+B2/t

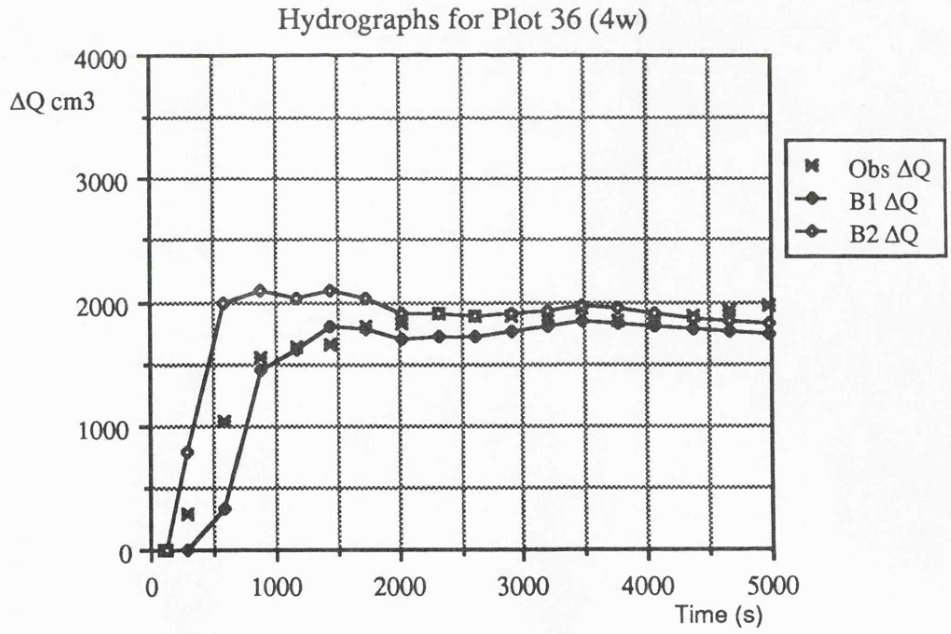
Hydrographs for Plot 36 (4w)
ΔQ cm3
4000
3000
2000
1000
0
0
1000
2000
3000
4000
5000
Time (s)
Obs ΔQ
B1 ΔQ
B2 ΔQ

Appendix 5.1.9 Results from Plot 38 Unit 3w

A	B1	n	S	Δt	Δx
0.000171	0.0516	0.25	0.1426	1.0	20.0

t	5	4	3	2	1
5532	120.8	165.1	178.1	186.6	196.8

Σt	Obs ΔQ	B1 ΔQ	Obs ΣQ	B1 ΣQ
115.0	0.000	0.000	0.000	0.000
186.0	905.000	105.523	905.000	105.523
366.0	3010.000	2492.114	3915.000	2597.637
546.0	2950.000	3047.051	6865.000	5644.688
780.0	3100.000	3193.107	9965.000	8837.795
1014.0	3000.000	3068.227	12965.000	11906.021
1250.0	3030.000	3127.836	15995.000	15033.857
1493.0	3300.000	3154.141	19295.000	18187.998
1737.0	3240.000	3153.783	22535.000	21341.781
1978.0	3140.000	3169.492	25675.000	24511.273
2208.0	3320.000	3198.045	28995.000	27709.318
2423.0	3280.000	3240.797	32275.000	30950.115
2665.0	3410.000	3312.014	35685.000	34262.129
2918.0	3100.000	3225.285	38785.000	37487.414
3160.0	3330.000	3196.371	42115.000	40683.785
3393.0	3230.000	3234.258	45345.000	43918.043
3628.0	3400.000	3263.766	48745.000	47181.809
3863.0	3330.000	3259.410	52075.000	50441.219
4102.0	3300.000	3269.086	55375.000	53710.305
4352.0	3120.000	3255.852	58495.000	56966.156
4579.0	3070.000	3222.691	61565.000	60188.848
4814.0	3180.000	3300.215	64745.000	63489.063
5052.0	3250.000	3282.000	67995.000	66771.063
5300.0	3220.000	3267.023	71215.000	70038.086
5531.0	3340.000	3235.586	74555.000	73273.672

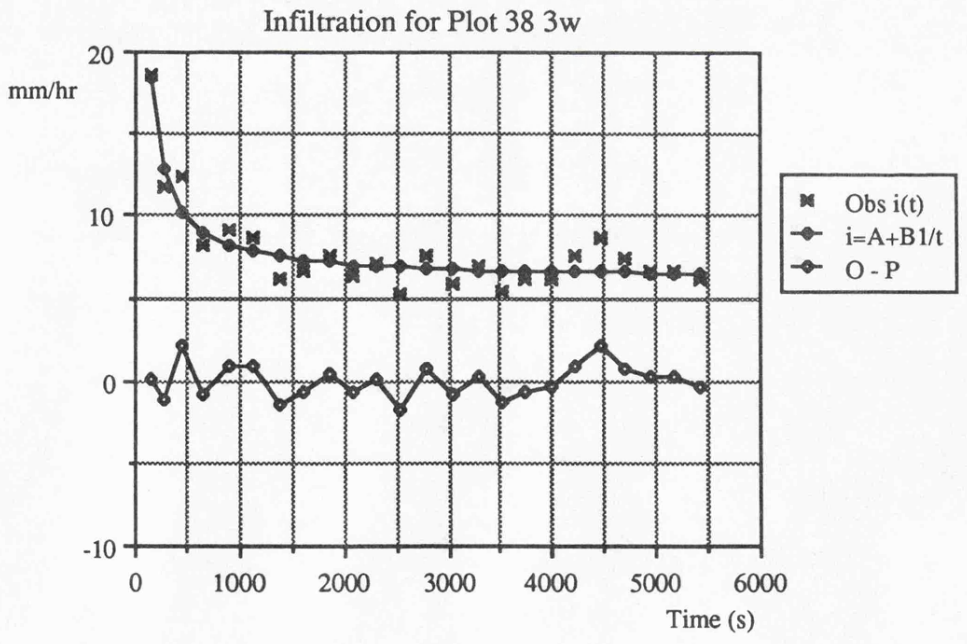

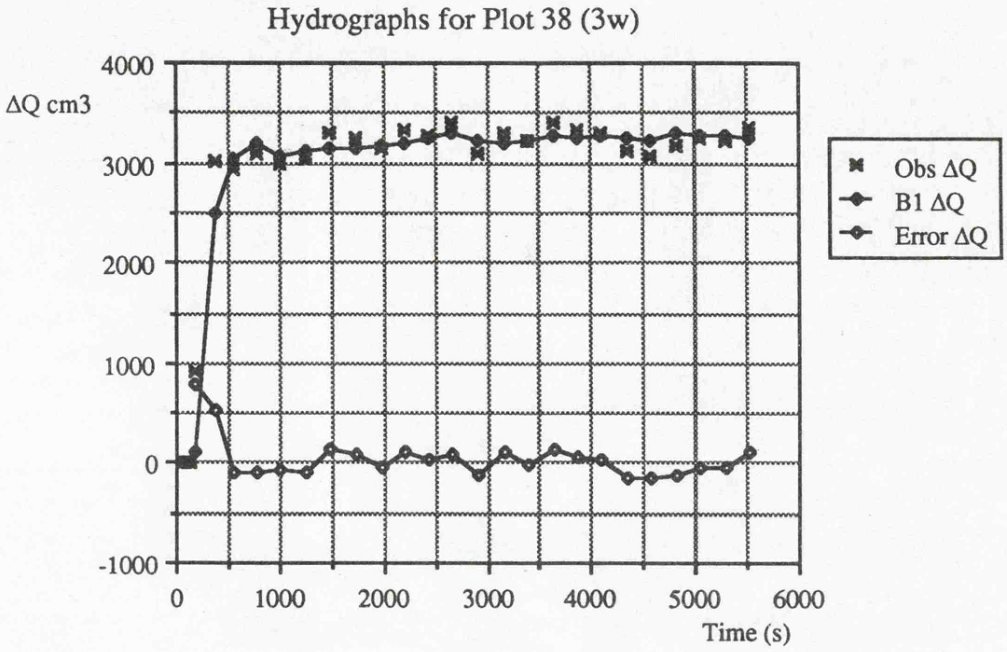

to5	Qin	WA	p	A	B2
5.91	21.505	16950	0.001269	0.000171	0.0065

Σt	Obs ΔQ	B2 ΔQ	Obs ΣQ	B2 ΣQ
115.0	0.000	426.533	0.000	426.533
186.0	905.000	1227.243	905.000	1653.775
366.0	3010.000	3355.275	3915.000	5009.051
546.0	2950.000	3428.781	6865.000	8437.832
780.0	3100.000	3504.062	9965.000	11941.894
1014.0	3000.000	3291.142	12965.000	15233.035
1250.0	3030.000	3301.373	15995.000	18534.408
1493.0	3300.000	3299.086	19295.000	21833.494
1737.0	3240.000	3276.197	22535.000	25109.691
1978.0	3140.000	3273.854	25675.000	28383.545
2208.0	3320.000	3286.059	28995.000	31669.604
2423.0	3280.000	3314.834	32275.000	34984.438
2665.0	3410.000	3386.875	35685.000	38371.313
2918.0	3100.000	3296.754	38785.000	41668.066
3160.0	3330.000	3259.316	42115.000	44927.383
3393.0	3230.000	3290.199	45345.000	48217.582
3628.0	3400.000	3316.289	48745.000	51533.871
3863.0	3330.000	3308.359	52075.000	54842.230
4102.0	3300.000	3315.902	55375.000	58158.133
4352.0	3120.000	3301.871	58495.000	61460.004
4579.0	3070.000	3262.609	61565.000	64722.613
4814.0	3180.000	3339.168	64745.000	68061.781
5052.0	3250.000	3319.570	67995.000	71381.352
5300.0	3220.000	3304.602	71215.000	74685.953
5531.0	3340.000	3268.828	74555.000	77954.781

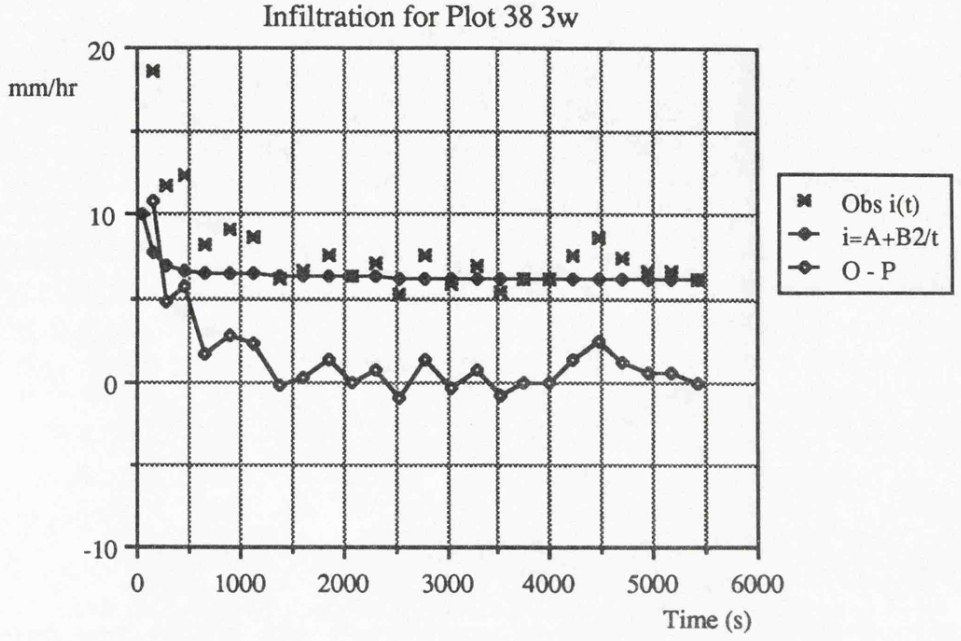
Infiltration for Plot 38 3w
mm/hr
20
10
0
-10
0
1000
2000
3000
4000
5000
6000
Time (s)
Obs i(t)
i=A+B2/t
O - P

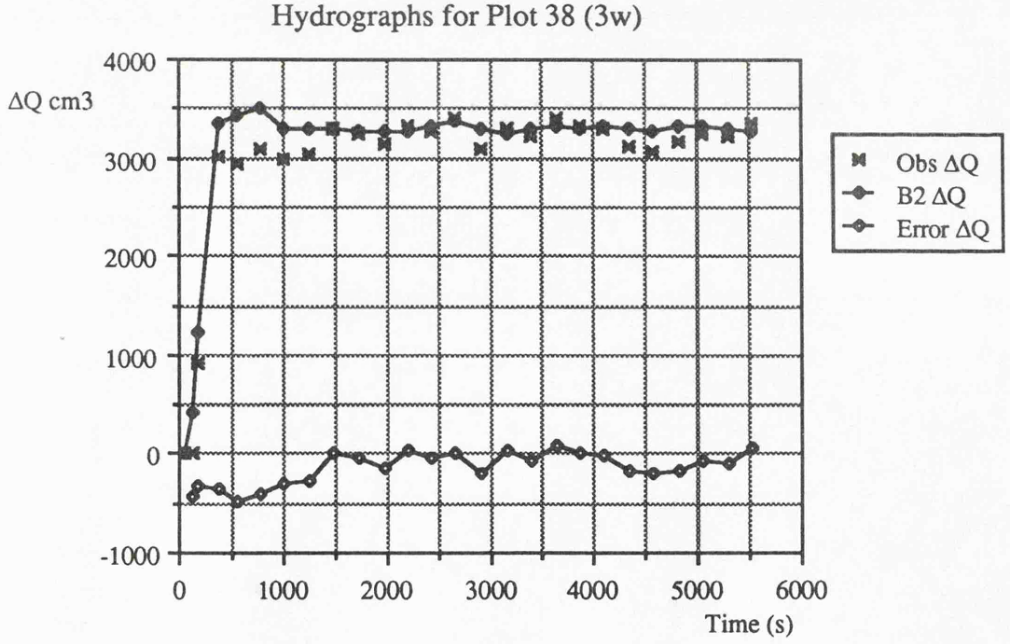
Hydrographs for Plot 38 (3w)
ΔQ cm3
4000
3000
2000
1000
0
-1000
0
1000
2000
3000
4000
5000
6000
Time (s)
Obs ΔQ
B2 ΔQ
Error ΔQ

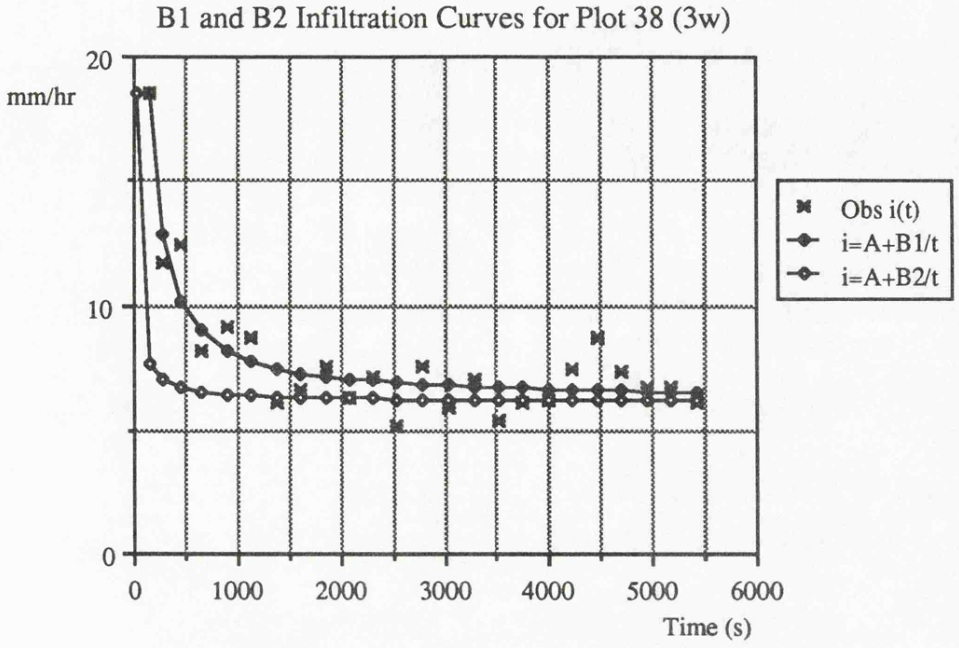
B1 and B2 Infiltration Curves for Plot 38 (3w)
mm/hr
20
10
0
0
1000
2000
3000
4000
5000
6000
Time (s)
Obs i(t)
i=A+B1/t
i=A+B2/t

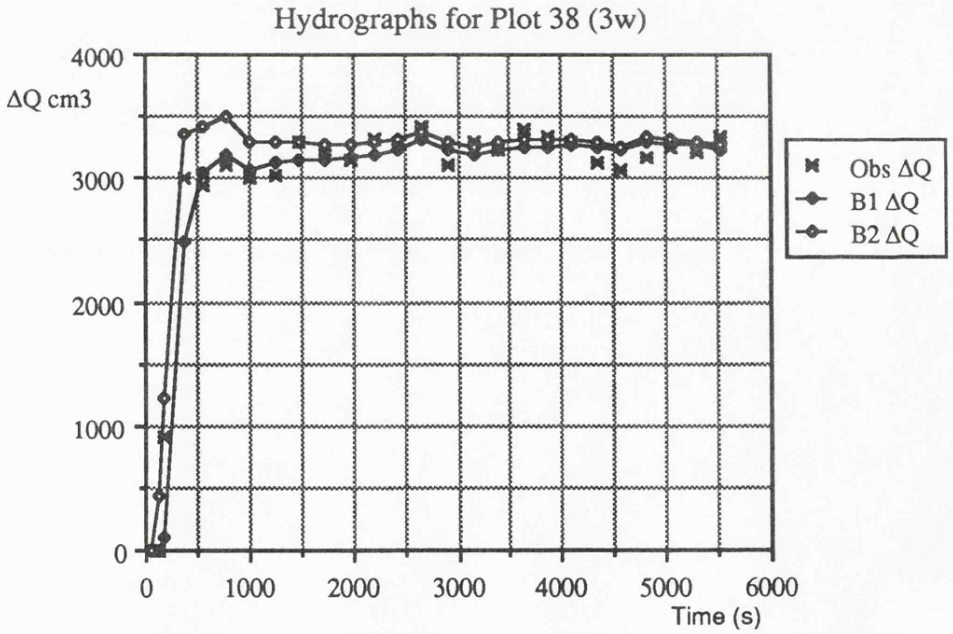
Hydrographs for Plot 38 (3w)
ΔQ cm3
4000
3000
2000
1000
0
0
1000
2000
3000
4000
5000
6000
Time (s)
Obs ΔQ
B1 ΔQ
B2 ΔQ

Appendix 5.1.10 Results from Plot 42 Unit 6w

A	B1	n	S	Δt	Δx
0.000193	0.082	0.22	0.0505	1.0	20.0
t	5	4	3	2	1
3951	100.0	86.5	85.5	97.0	110.5

Σt	Obs ΔQ	B1 ΔQ	Obs ΣQ	B1 ΣQ
66.0	0.000	0.000	0.000	0.000
228.0	1600.000	311.729	1600.000	311.729
477.0	3200.000	2774.863	4800.000	3086.591
742.0	3360.000	3144.004	8160.000	6230.595
1007.0	3350.000	3245.588	11510.000	9476.184
1269.0	3220.000	3307.655	14730.000	12783.839
1543.0	3400.000	3358.895	18130.000	16142.733
1825.0	3340.000	3358.962	21470.000	19501.695
2113.0	3220.000	3361.262	24690.000	22862.957
2403.0	3290.000	3365.084	27980.000	26228.041
2708.0	3260.000	3375.898	31240.000	29603.939
3017.0	3250.000	3349.693	34490.000	32953.633
3327.0	3470.000	3353.516	37960.000	36307.148
3638.0	3250.000	3351.059	41210.000	39658.207
3950.0	3380.000	3357.543	44590.000	43015.750

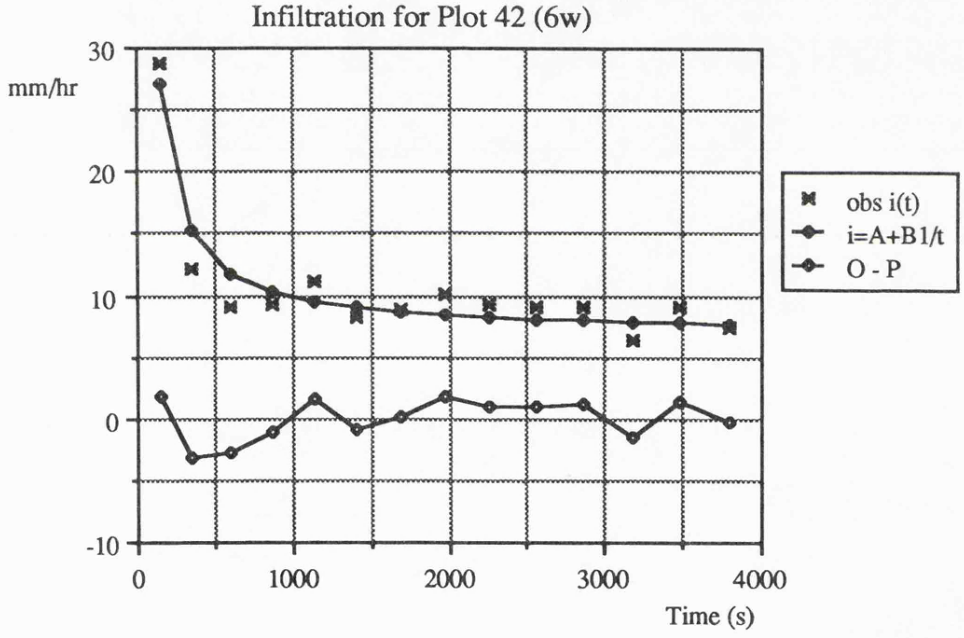

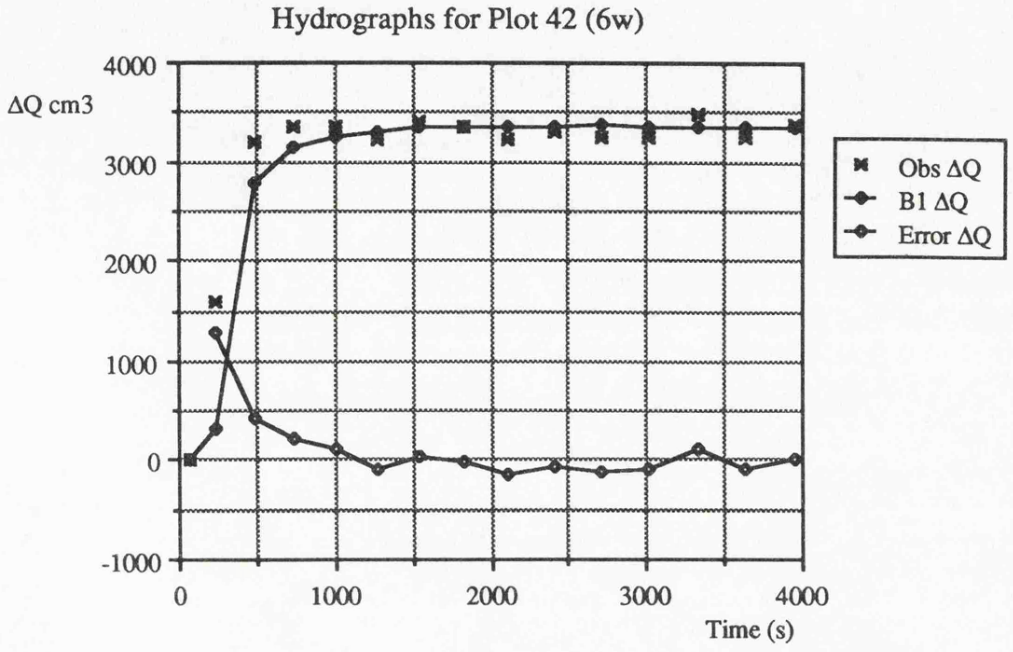

to5	Qin	WA	p	A	B2
9.56	17.544	9590	0.001829	0.000193	0.0156

Σt	Obs ΔQ	B2 ΔQ	Obs ΣQ	B2 ΣQ
66.0	0.000	0.000	0.000	0.000
228.0	1600.000	1744.842	1600.000	1744.842
477.0	3200.000	3473.907	4800.000	5218.750
742.0	3360.000	3480.773	8160.000	8699.522
1007.0	3350.000	3464.905	11510.000	12164.428
1269.0	3220.000	3468.797	14730.000	15633.225
1543.0	3400.000	3492.313	18130.000	19125.537
1825.0	3340.000	3472.232	21470.000	22597.770
2113.0	3220.000	3459.328	24690.000	26057.098
2403.0	3290.000	3450.629	27980.000	29507.727
2708.0	3260.000	3454.797	31240.000	32962.523
3017.0	3250.000	3420.969	34490.000	36383.492
3327.0	3470.000	3417.797	37960.000	39801.289
3638.0	3250.000	3409.602	41210.000	43210.891
3950.0	3380.000	3411.219	44590.000	46622.109

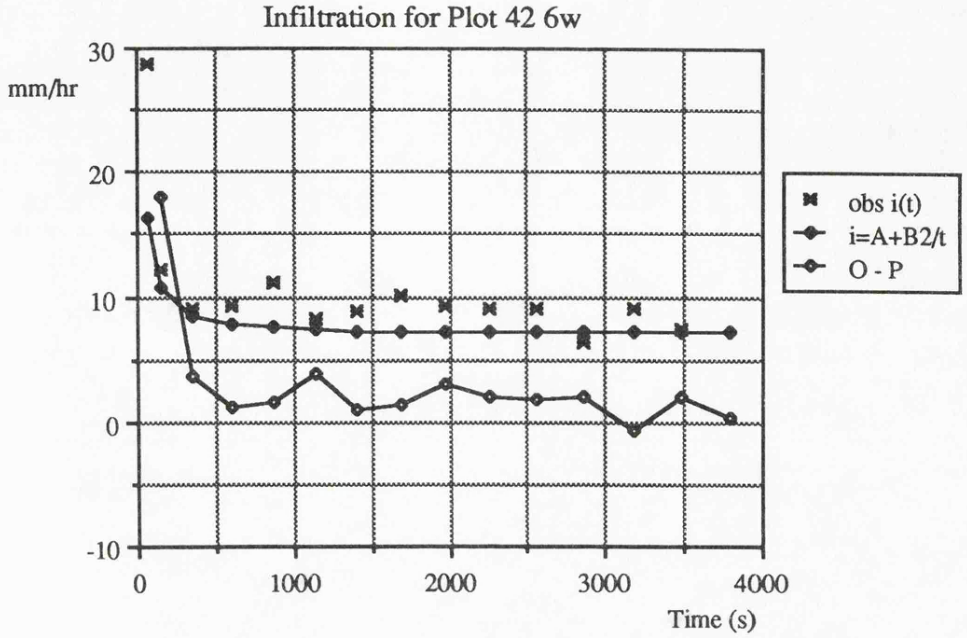
Infiltration for Plot 42 6w
mm/hr
30
20
10
0
-10
0
1000
2000
3000
4000
Time (s)
obs i(t)
i=A+B2/t
O - P

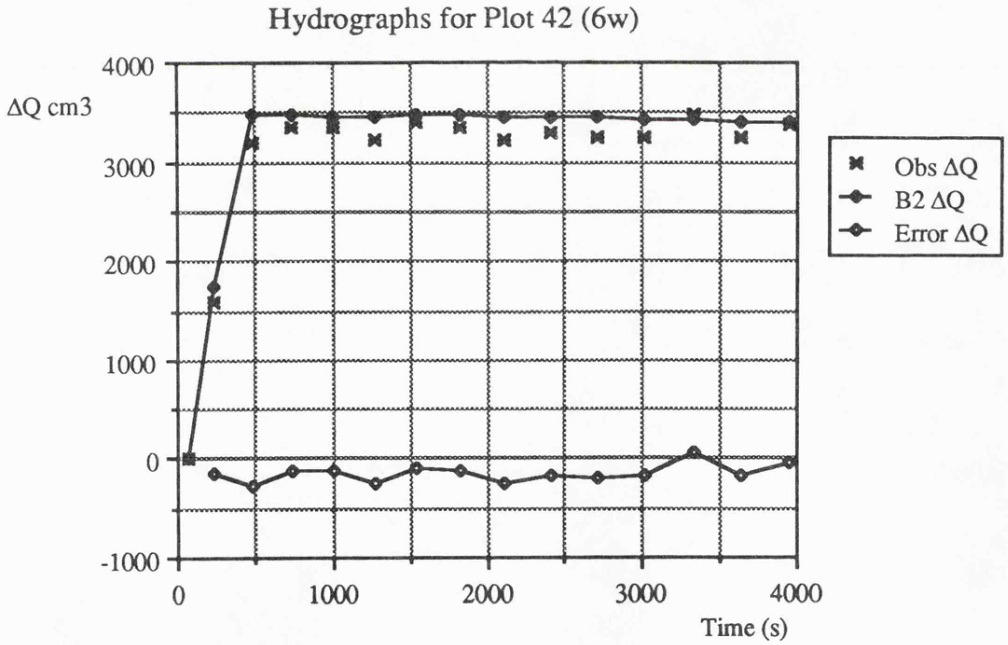
Hydrographs for Plot 42 (6w)
ΔQ cm3
4000
3000
2000
1000
0
-1000
0
1000
2000
3000
4000
Time (s)
Obs ΔQ
B2 ΔQ
Error ΔQ

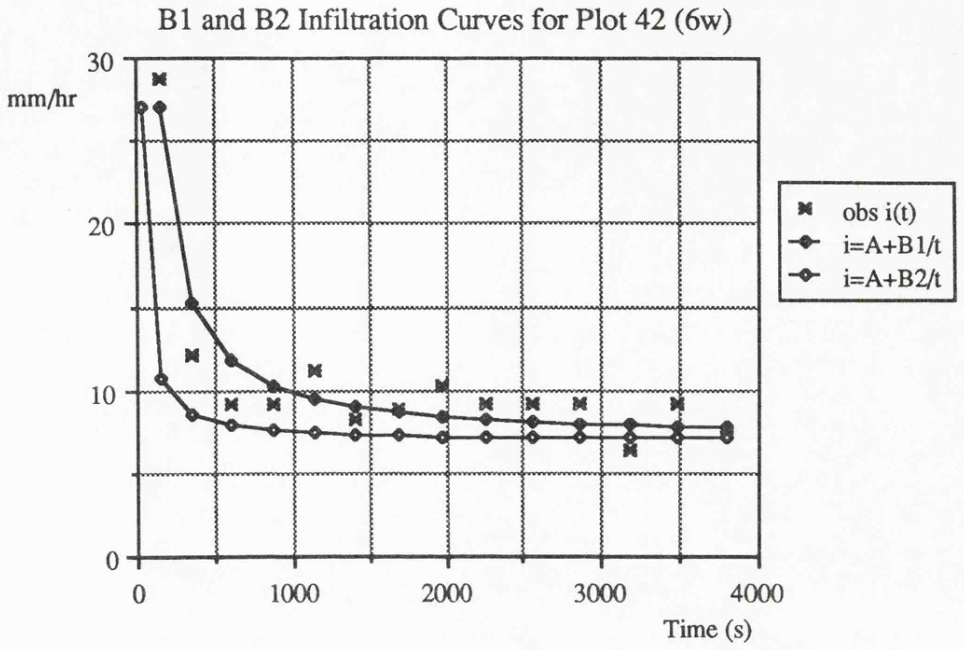
B1 and B2 Infiltration Curves for Plot 42 (6w)
mm/hr
30
20
10
0
0
1000
2000
3000
4000
Time (s)
obs i(t)
i=A+B1/t
i=A+B2/t

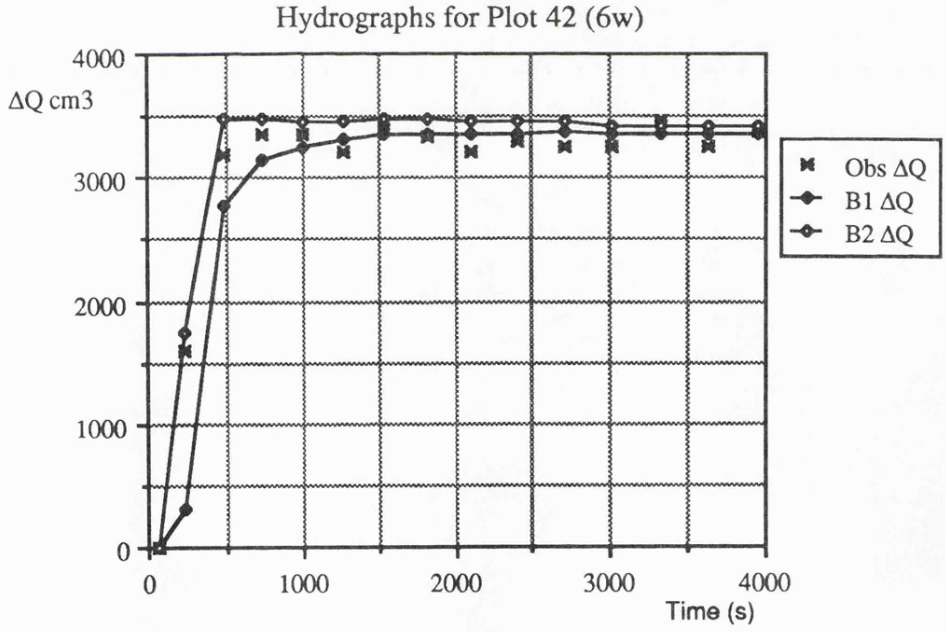
Hydrographs for Plot 42 (6w)
ΔQ cm3
4000
3000
2000
1000
0
0
1000
2000
3000
4000
Time (s)
Obs ΔQ
B1 ΔQ
B2 ΔQ

Appendix 5.1.11 Results from Plot 47 Unit 5w upper

A	B1	n	S	Δt	Δx
0.000381	0.191	0.25	0.0331	1.0	20.0

t	5	4	3	2	1
341	94.9	79.4	68.9	60.5	56.1
2212	100.1	100.1	100.1	100.1	100.1
4659	101.5	107.5	113.5	120.5	127.0

Σt	Obs ΔQ	B1 ΔQ	Obs ΣQ	B1 ΣQ
68.0	0.000	0.000	0.000	0.000
176.0	870.000	0.000	870.000	0.000
354.0	2330.000	1511.412	3200.000	1511.412
532.0	2730.000	2525.103	5930.000	4036.515
709.0	2780.000	2634.475	8710.000	6670.989
887.0	2820.000	2822.421	11530.000	9493.410
1067.0	2930.000	2924.629	14460.000	12418.039
1250.0	2770.000	2985.715	17230.000	15403.754
1433.0	2970.000	3016.266	20200.000	18420.020
1616.0	3030.000	3053.551	23230.000	21473.570
1798.0	3300.000	3083.721	26530.000	24557.291
1982.0	2970.000	3111.223	29500.000	27668.514
2160.0	2900.000	3103.145	32400.000	30771.658
2382.0	3020.000	3250.596	35420.000	34022.254
2600.0	2760.000	2834.332	38180.000	36856.586
2822.0	3020.000	2870.707	41200.000	39727.293
3047.0	2840.000	2863.629	44040.000	42590.922
3274.0	2760.000	2863.742	46800.000	45454.664
3502.0	2850.000	2863.488	49650.000	48318.152
3736.0	2880.000	2866.730	52530.000	51184.883
3968.0	2800.000	2844.801	55330.000	54029.684
4198.0	2820.000	2866.414	58150.000	56896.098
4421.0	2860.000	2879.141	61010.000	59775.238
4658.0	2860.000	2920.480	63870.000	62695.719

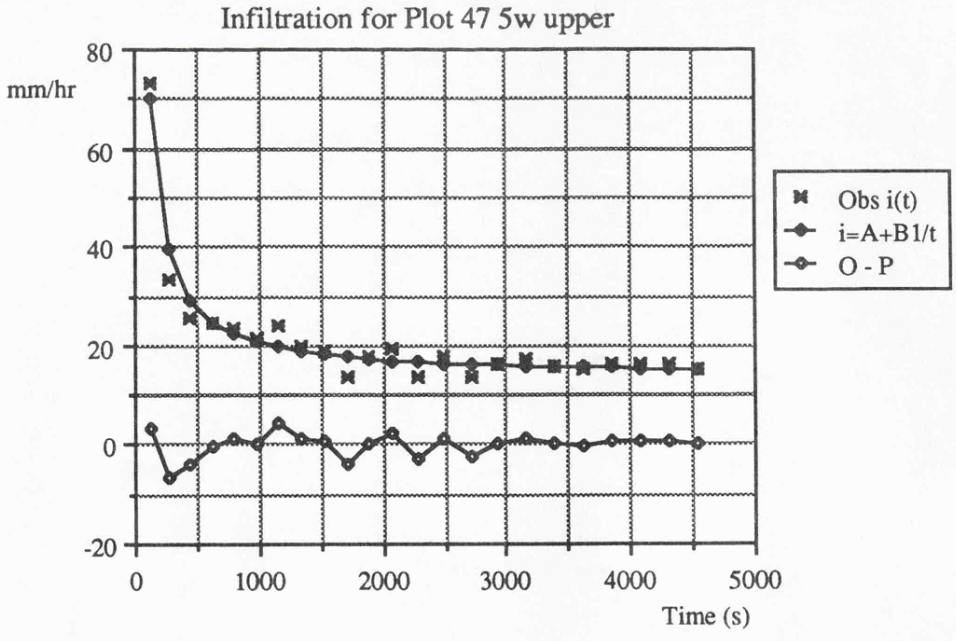

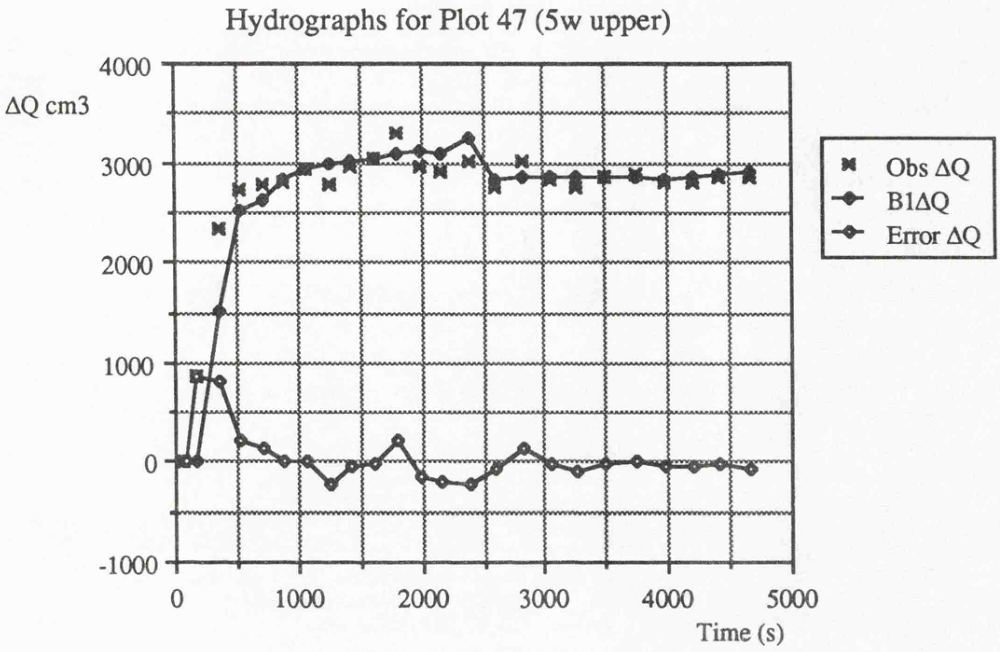

to5	Qin	WA	p	A	B2
16.45	22.727	7200	0.003156	0.000381	0.0457

Σt	Obs ΔQ	B2 ΔQ	Obs ΣQ	B2 ΣQ
68.0	0.000	0.000	0.000	0.000
176.0	870.000	892.590	870.000	892.590
354.0	2330.000	3368.304	3200.000	4260.895
532.0	2730.000	3369.885	5930.000	7630.779
709.0	2780.000	3168.509	8710.000	10799.288
887.0	2820.000	3212.438	11530.000	14011.726
1067.0	2930.000	3234.485	14460.000	17246.211
1250.0	2770.000	3244.572	17230.000	20490.783
1433.0	2970.000	3236.146	20200.000	23726.930
1616.0	3030.000	3244.471	23230.000	26971.400
1798.0	3300.000	3251.654	26530.000	30223.055
1982.0	2970.000	3263.074	29500.000	33486.129
2160.0	2900.000	3236.848	32400.000	36722.977
2382.0	3020.000	3414.578	35420.000	40137.555
2600.0	2760.000	2988.141	38180.000	43125.695
2822.0	3020.000	3013.473	41200.000	46139.168
3047.0	2840.000	2996.820	44040.000	49135.988
3274.0	2760.000	2988.121	46800.000	52124.109
3502.0	2850.000	2979.695	49650.000	55103.805
3736.0	2880.000	2977.840	52530.000	58081.645
3968.0	2800.000	2948.395	55330.000	61030.039
4198.0	2820.000	2963.121	58150.000	63993.160
4421.0	2860.000	2967.895	61010.000	66961.055
4658.0	2860.000	3009.367	63870.000	69970.422

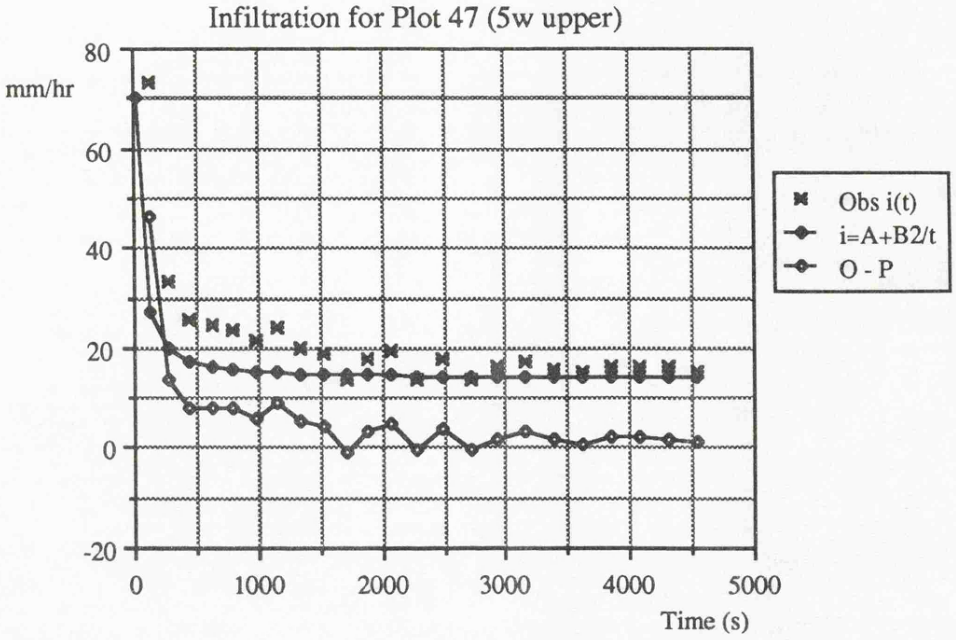
Infiltration for Plot 47 (5w upper)
mm/hr
80
60
40
20
0
-20
0
1000
2000
3000
4000
5000
Time (s)
Obs i(t)
i=A+B2/t
O - P

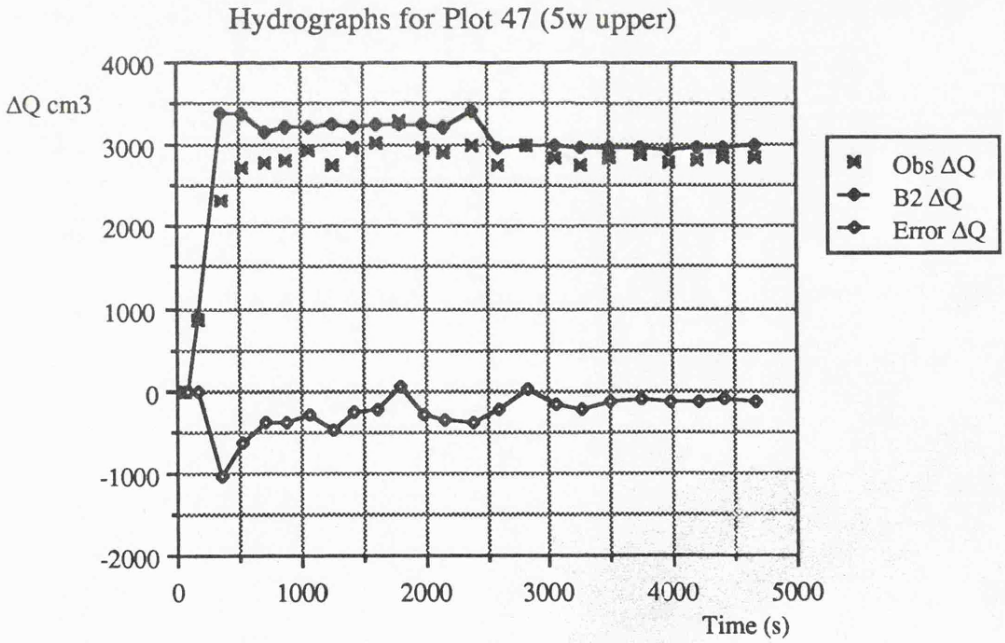
Hydrographs for Plot 47 (5w upper)
ΔQ cm3
4000
3000
2000
1000
0
-1000
-2000
0
1000
2000
3000
4000
5000
Time (s)
Obs ΔQ
B2 ΔQ
Error ΔQ

B1 and B2 Infiltration Curves for Plot 47 (5w upper)

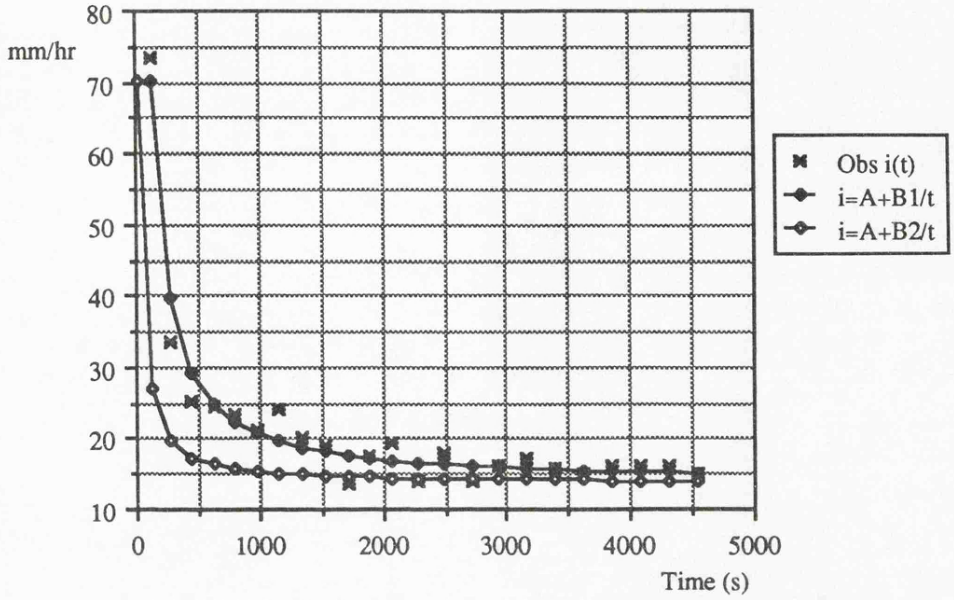

Hydrographs for Plot 47 (5w upper)

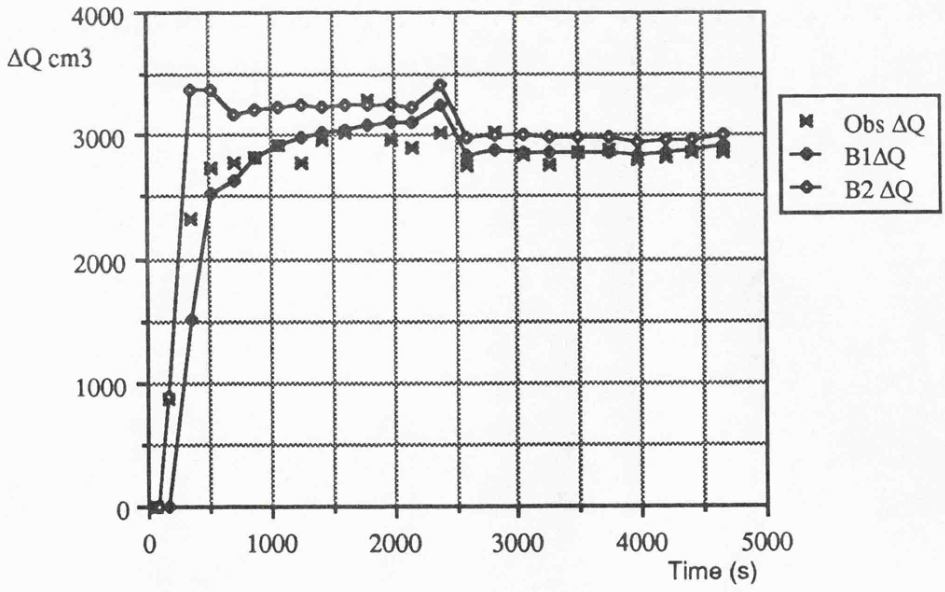

Appendix 5.2.1

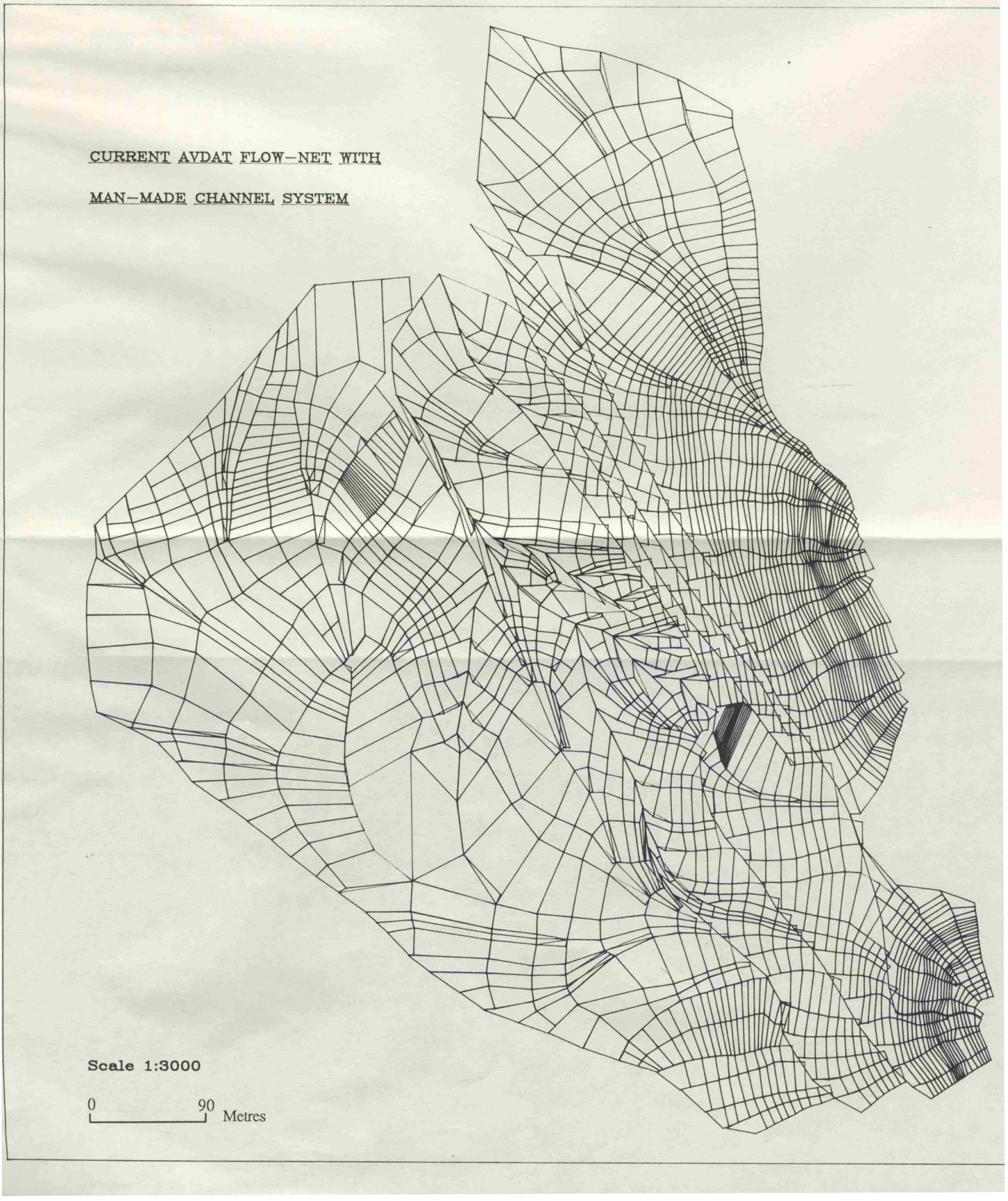

Appendix 5.2.2

AVDAT FLOW-NET WITHOUT

MAN-MADE CHANNEL SYSTEM

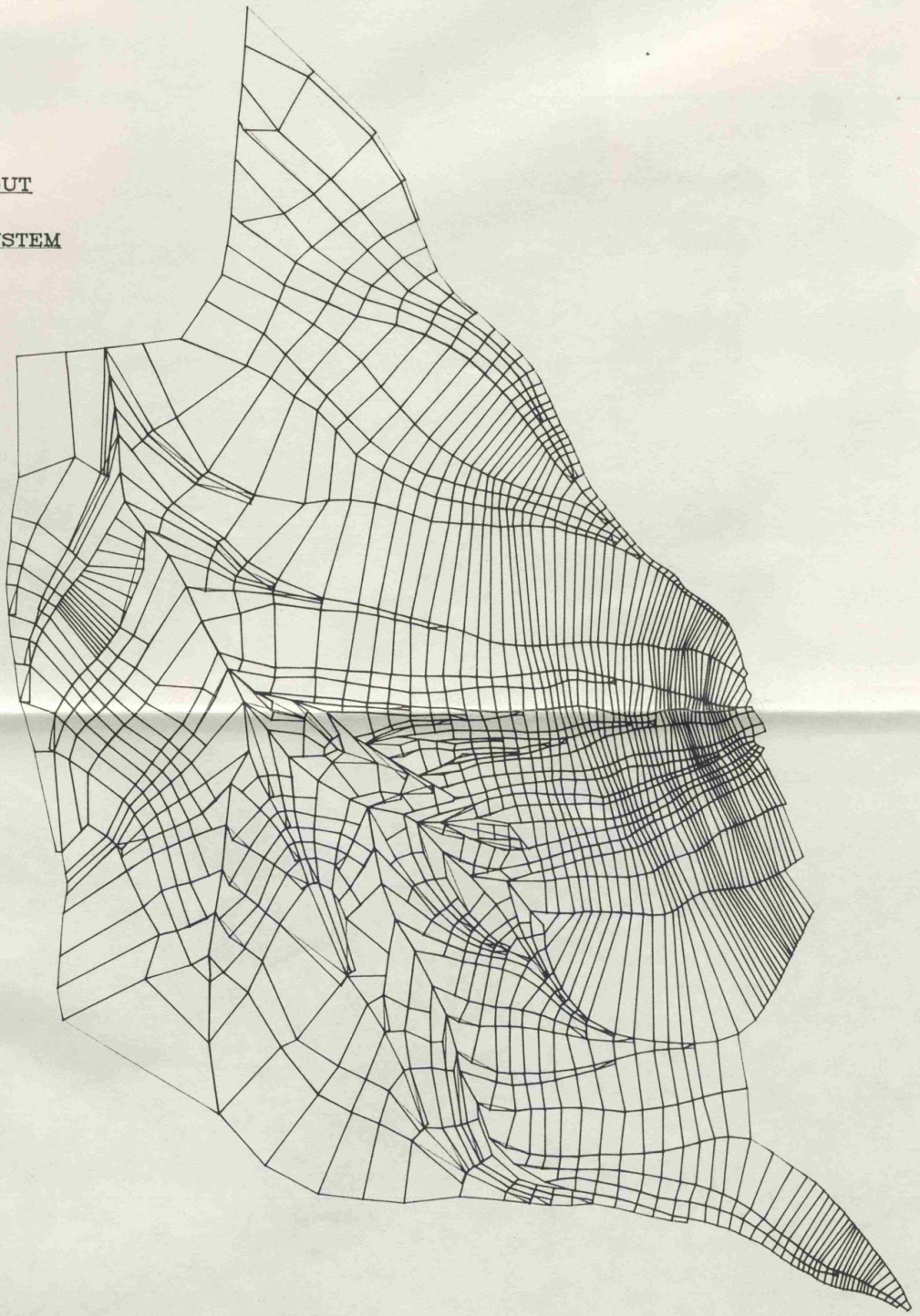

Scale 1:3000

0 90 Metres

Appendix 5.3.1



Appendix 5.3.2

AVDAT CATCHMENT WITH NATURAL

CHANNEL SYSTEM : UNIT DISTRIBUTION

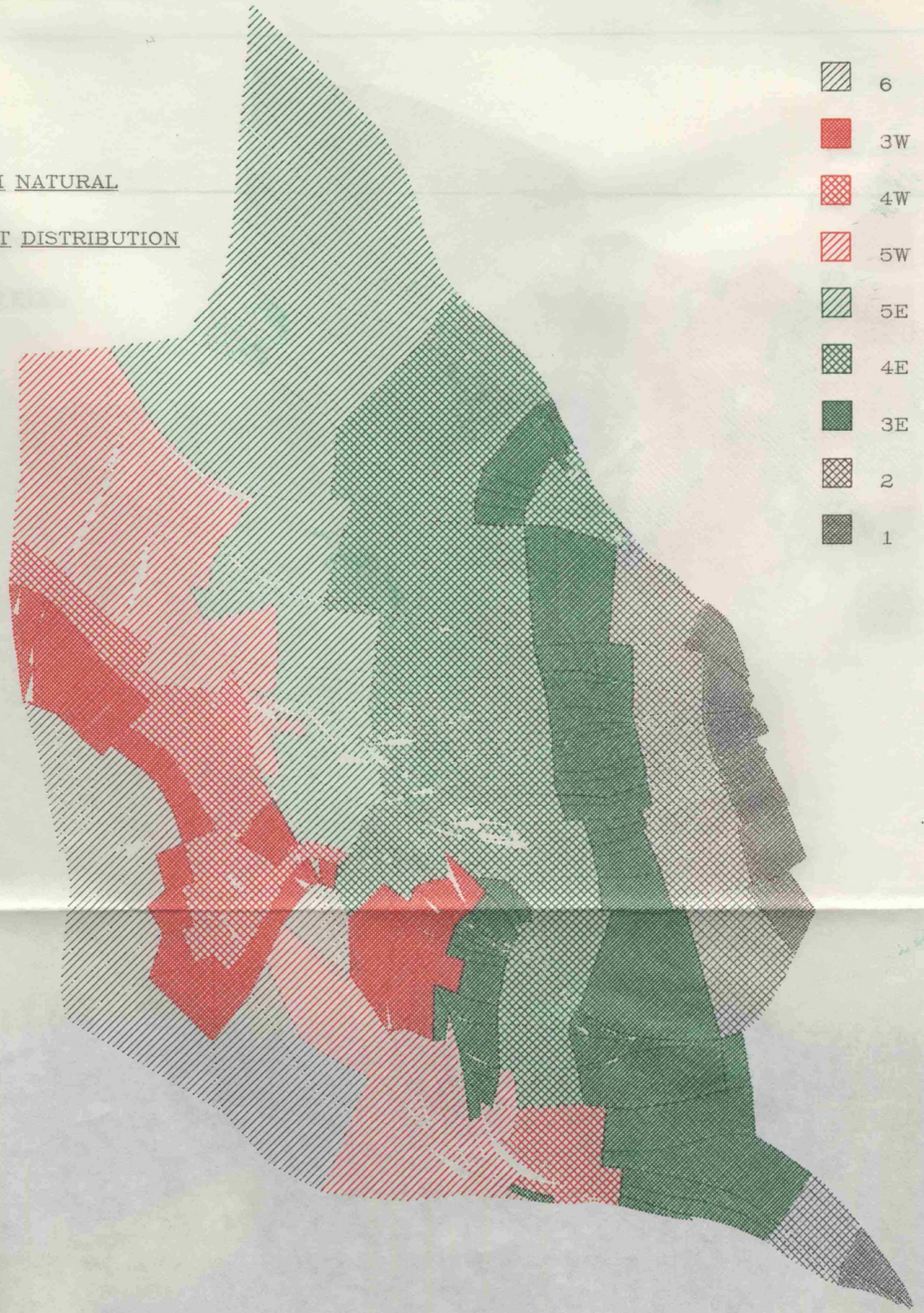

Scale 1:3000

Appendix 5.5

Appendix 5.4

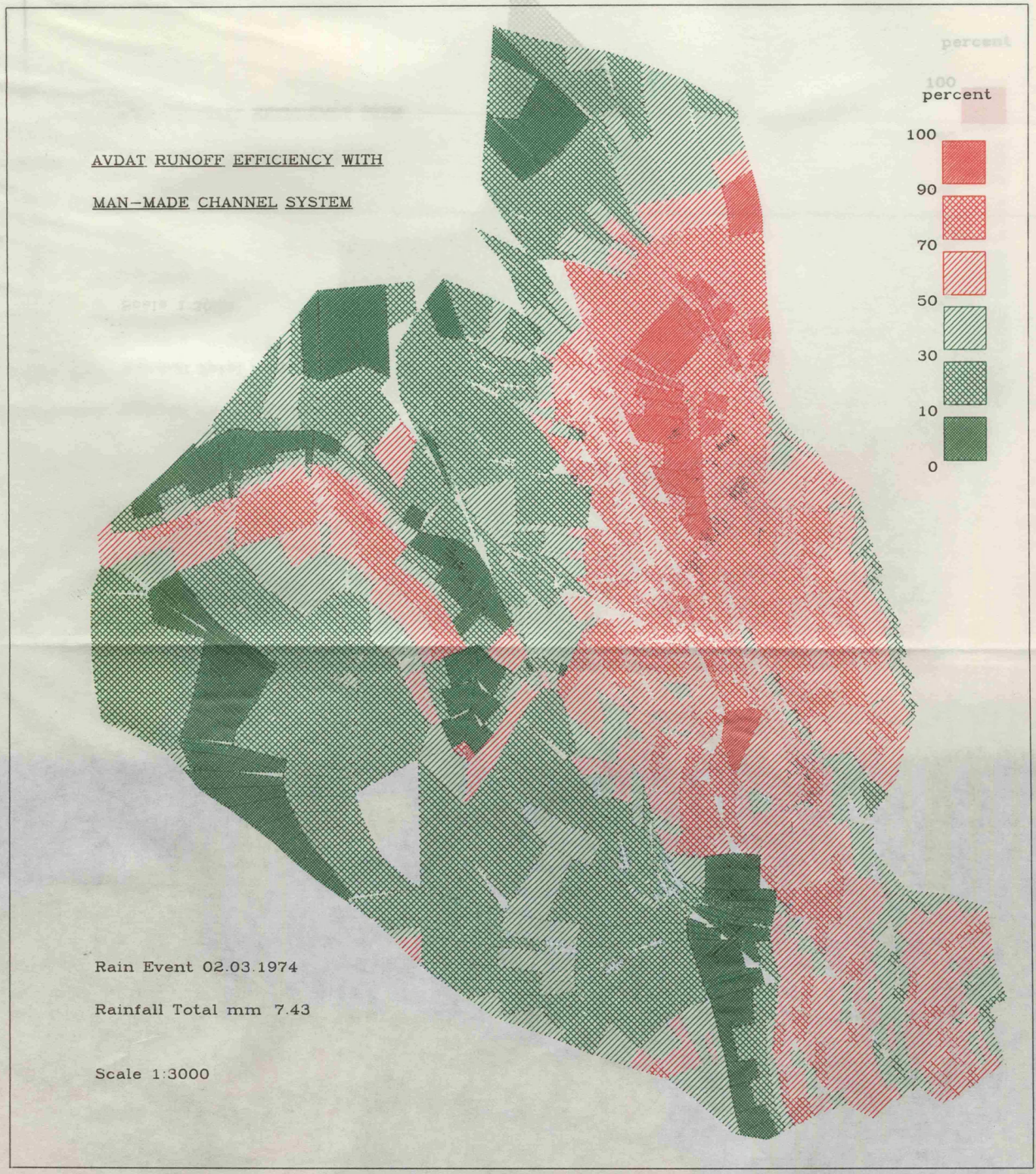

Appendix 5.5

AVDAT RUNOFF EFFICIENCY WITH

UNALTERED CHANNEL SYSTEM

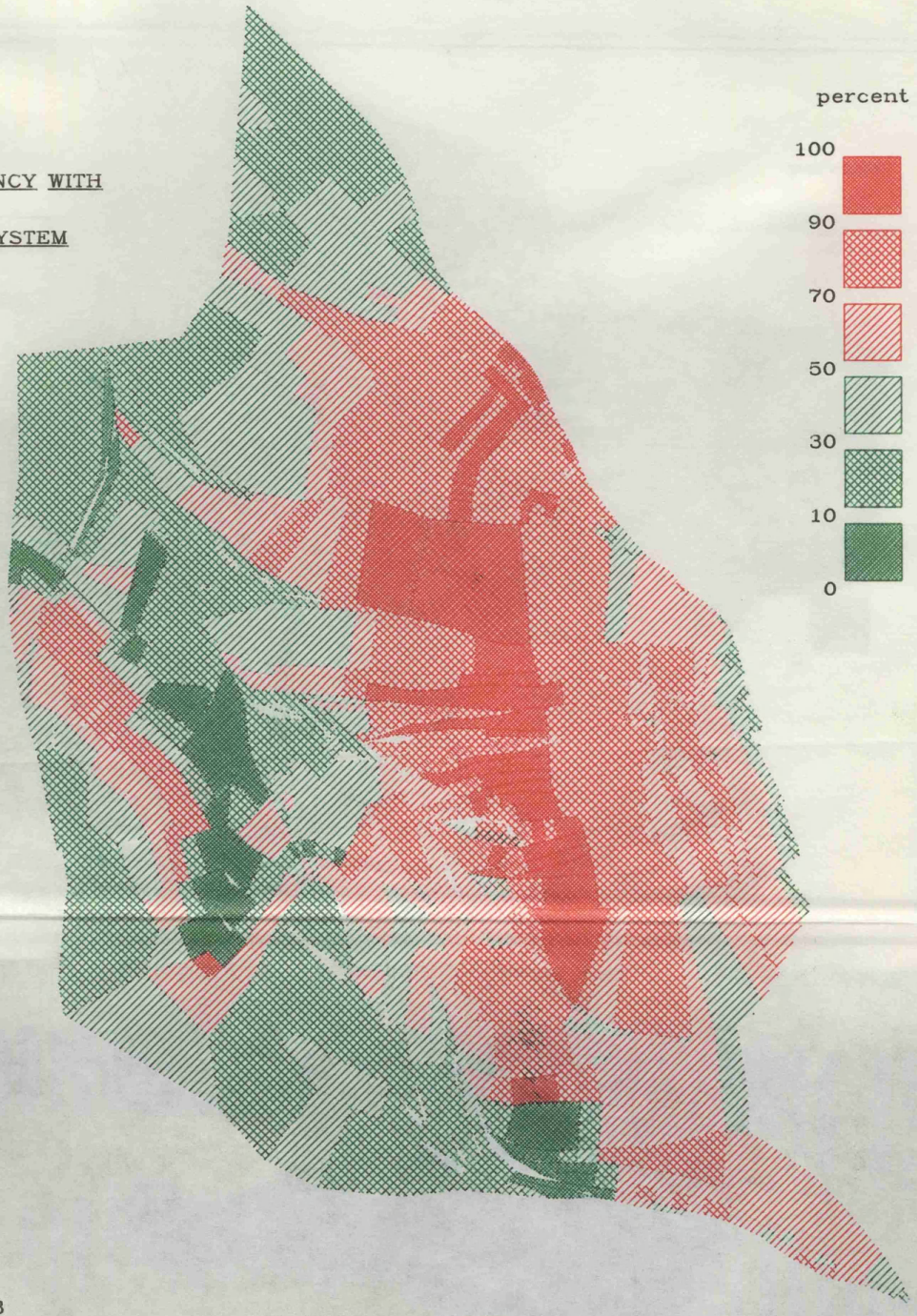

Rain Event 02.03.1974

Rainfall Total mm 7.43

Scale 1:3000

Appendix 5.6

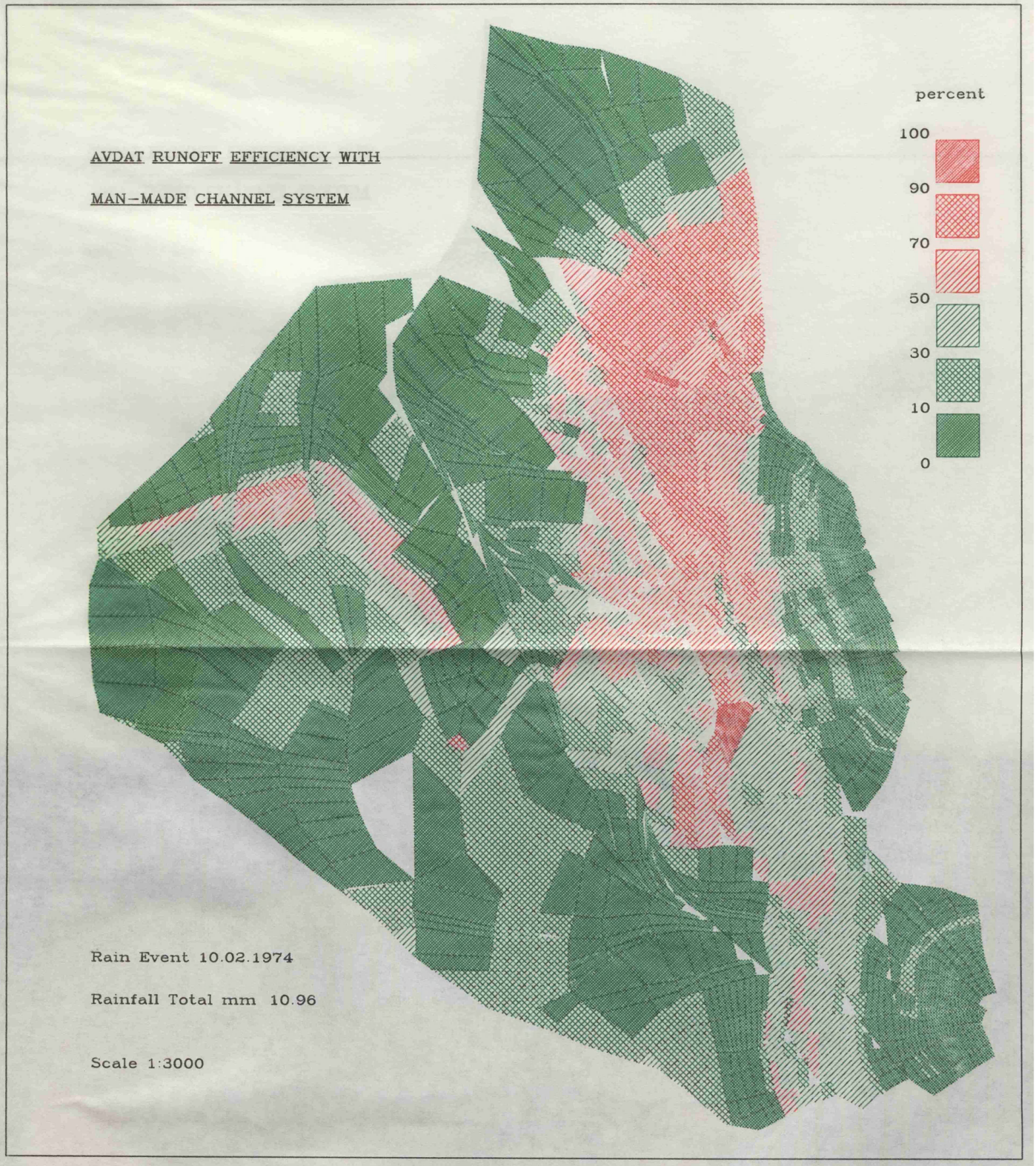
AVDAT RUNOFF EFFICIENCY WITH
MAN-MADE CHANNEL SYSTEM
percent
100
90
70
50
30
10
0
Rain Event 10.02.1974
Rainfall Total mm 10.96
Scale 1:3000

Appendix 5.7


AVDAT RUNOFF EFFICIENCY WITH
UNALTERED CHANNEL SYSTEM
percent
100
90
70
50
30
10
0
Rain Event 10.02.1974
Rainfall Total mm 10.96
Scale 1:3000